Derivation of human embryonic stem cells to study early development and genetic disease

Emma Stephenson
Department of Biochemical Engineering
University College London

A thesis submitted for the degree of
Doctor of Philosophy

2009

Declaration

I, Emma Louise Stephenson, confirm that the studies presented in this thesis were the unaided work of the author except for the following:

1. The culture of embryos until day 4 or 5 of development in preimplantation genetic diagnosis (PGD) cycles was carried out by the Guy's ACU embryology team. The embryos unsuitable for patient use were transferred to the research project under HFEA Research licences R0075 and R0133.

2. The collection of placentas for the work in Chapter 3 was in conjunction with Kate Spacey, a BSc student supervised by this author.

3. The single cell Fluidigm^{TM} PCR studies discussed in Chapter 4 were in collaboration with Dr. Fozia Chaudry from LGC, Teddington. The contribution to the work was equal but the experimental design and the results and discussion presented within were entirely the work of this author. The statistical analyses of the data were performed in collaboration with Dr. Stephen Ellison, also of LGC.

4. The neural differentiation study discussed in Chapter 5 was in collaboration with Dr. Nathalie Lefort from I-Stem, Evry, Paris. The contribution to the differentiation work was equal but the analysis and results presented within were independent and entirely the work of this author.

5. The microsatellite analyses to confirm ploidy of a cell line as presented in Chapter 5 were performed by Dr. Pamela Renwick from the Guy's Genetic Centre and PGD team, but interpreted by this author.

6. Statistical analysis was performed in collaboration with Paul Seed, Lecturer in Medical Statistics, King's College London.

Where any experimental work was outsourced the details are given in the thesis text.

Emma Louise Stephenson

Abstract

Stem cells are unique cells that have both the capacity for self-renewal and, depending on their origin, the ability to form at least one, and sometimes many, specialised cell types of all three embryonic germ lineages - germ cells (endoderm, mesoderm and ectoderm), extra-embryonic tissue and trophoblast. Since the derivation of the first human embryonic stem cell (hESC) line in 1998, there has been substantial interest in the potential of these cells both for regenerative medicine and cell therapy, and as disease models for monogenic disorders. Aside from the need to improve derivation efficiency and further the understanding of the basic biology of these cells, the ability to work with hESC opens up three broad research areas. The first is the development of clinical grade culture systems with the aim of producing cell lines suitable for subsequent manipulation for therapy. The second is the opportunity to use these cells as a tool to study the earliest determinative events in mammalian development, such as the origins of patterning in the mammalian embryo. The third is the use of hESCs carrying clinically relevant genetic mutations as models for disease research and therapeutic target identification.

The development of several methods of embryo manipulation tailored to the morphology of the blastocyst is described here, which resulted in the derivation of seven lines from four different procedures and provided the tools for subsequent research. Acknowledging that each laboratory in isolation is unlikely to derive sufficient lines to draw significant conclusions regarding manipulation methodology and culture parameters, an international collaboration was initiated with the aim of standardising the reporting of derivation and thus obtaining the maximum information from the generation of each new hESC line.

To address the need for the development of clinical grade culture systems, alternative feeder cells were assessed for their suitability in hESC culture and derivation. Modified human foreskin fibroblasts and human amniotic epithelial cells (hAECs) were investigated, as both cell types can be fully qualified and validated. Whilst both were able to support the culture of existing lines, only the hAECs showed promise in supporting derivation. In addition, analysis of in-house and commercially available media showed that neither were physiologically optimal for the growth of inner cell mass (ICM) cells or putative hESC, as metabolite concentrations were in excess and subsequent catabolite levels exceeded known toxic levels.

The timing and mechanisms establishing patterning and future polarity in the mammalian embryo remains a subject of intense debate. Here, the potential of single blastomeres to generate hESC was used as an assessment of pluripotency. The determination of the most appropriate day for attempting derivation was performed by assessing blastomere development and pluripotent marker expression, and the predicted success of derivation was considered in the light of division patterns. Putative stem-like cells were visible in several cultures. Furthermore, isolated blastomeres from two-, four-, and eight-cell embryos were analysed for the quantitative expression of multiple target genes known to be associated with lineage formation and the stem cell state. Analysis suggested that broad changes in gene expression were occurring with development stage. However, no consistent grouping structure for cells within embryos was observed, and no convincing pattern was seen when considering the individual embryo variance scores. Several approaches are discussed to differentiate between the biological and methodological variability in this experimental design.

The suitability of hESC as models for genetic disease was studied following the derivation of two lines carrying Huntington disease (HD). Subsequent differentiation using a stromal co-culture neural induction protocol resulted in the establishment of a stable, highly proliferative cell population which was simple to culture and bank. The cells were of

an astroglial phenotype, and therefore highly suited for subsequent studies regarding HD pathophysiology, as glial cells are severely affected in HD. During differentiation the CAG repeat size increased from 46 to 70, showing the salient feature of somatic instability of the huntingtin gene. Therefore this cell population provides a valuable tool in the study of disease pathogenesis and transmission.

Acknowledgements

I wish to extend sincere thanks to Professors Braude and Mason for guidance and encouragement throughout. Prof - I remain awe-struck at your capacity to be a perpetual source of inspiration, it has been such a privilege to work with you.

This tome is dedicated to my family. To my wonderful ma and paps, in heartfelt gratitude for a lifetime of support and a bottomless pit of encouragement. To my little brothers, for making me laugh and keeping it all in perspective. To my remarkable husband, for believing I could do it, and for keeping me sane while I got there.

'The life of man is an unrepeatable experiment. No placebos, no controls.'
Erwin Chargaff, 1978

Publications

1. Stephenson, E.L., P.R. Braude, and C. Mason. Proposal for a universal minimum information convention for the reporting on the derivation of human embryonic stem cell lines. Regenerative Medicine, 2006. 1(6): p. 739-750.

2. Stephenson, E.L., P.R. Braude, and C. Mason. International community consensus standard for reporting derivation of human embryonic stem cell lines. Regenerative Medicine, 2007. 2(4): p. 349-62.

3. Stephenson, E.L., C. Mason, and P.R. Braude. Preimplantation Genetic Diagnosis as a Source of Human Embryonic Stem Cells for Disease Research and Drug Discovery. BJOG, 2009. 116(2): p. 158-65.

4. Stephenson, E.L., P.R. Braude, and C. Mason. Embryonic Stem Cells: Derivation and Culture. Advances in Tissue Engineering (Imperial College Press).

5. Patel, M.J., E.L. Stephenson, and S. Minger. Organization and good aseptic technique in the human embryonic stem cell laboratory. Human Embryonic Stem Cells: The Practical Handbook (Wiley Press).

6. Franklin SB, Hunt C, Cornwell G, Peddie V, Desousa P, Livie M, Stephenson EL, Braude PR. hESCCO: development of good practice models for hES cell derivation. Regenerative Medicine, 2008. 3(1): p. 105-16.

Abbreviations

AEC	amniotic epithelial cell
AGP	astroglial progenitors
AT	acid Tyrode's
A-V	animal-vegetal axis
B	batch
BDNF	brain-derived neurotrophic factor
bFGF	basic fibroblast growth factor
BM	blastocyst medium
BRL	buffalo rat liver cell
BSA	bovine serum albumin
CM	cleavage medium
CM	conditioned medium
cT	cycle threshold
DMEM	Dulbecco's modified Eagle's medium
DMSO	dimethylsulphoxide
EB	embryoid bodies
ECC	embryonal carcinoma cell
ECM	extra-cellular matrix
EGC	embryonic germ cell
EGF	epidermal growth factor
em-ab	embryonic-abembryonic axis
EN	extraction negative control
EUTCD	European Union Tissue and Cells Directive
FACS	fluorescence activated cell sorting
FCS	fetal calf serum
FM	fertilisation medium
Fr	fresh embryos
Fz	frozen-thawed embryos
GEL	gelatin
GFP	green fluorescent protein
GMP	good manufacturing practice
HBSS	Hank's balanced salt solution
HD	Huntington disease
hESC	human embryonic stem cell

HFEA	Human Fertilisation and Embryology Authority
HFF	human foreskin fibroblasts
HTT	huntingtin protein
I	immunosurgical isolation
ICC	immunocytochemistry
ICM	inner cell mass
ICSI	intracytoplasmic sperm injection
IMDM	Iscove's modified Dulbecco's medium
iPS	induced pluripotent cell
IVF	*in vitro* fertilisation
KODMEM	knock-out DMEM
KOSR	(knock-out) serum replacement
L	laser isolation
LIF	leukaemia inhibitory factor
M	mechanical isolation
MEF	mouse embryonic fibroblasts
mESC	mouse embryonic stem cell
mHTT	mutant huntingtin protein
MMC	mitomycin C
NEAA	non-essential amino acids
P	passage
PAN	preamplification negative control
PBST	phosphate buffered saline with triton
PCA	principle component analysis
PFA	paraformaldehyde
PGC	primordial germ cell
PGD	preimplantation genetic diagnosis
PGH	preimplantation genetic haplotyping
POL	polyornithine-laminin
ROS	reactive oxygen species
RTN	reverse transcription negative control
SEP	sperm entry position
SNP	single nucleotide polymorphism
SPSS	synthetic protein serum substitute
TE	trophectoderm
UKSCB	UK Stem Cell Bank
W	whole plating

Contents

Chapter 1

Introduction

1.1 Stem cells and regenerative medicine

Stem cells are unique cells that have both the capacity for self-renewal and, depending on their origin, the ability to form at least one, and sometimes many, specialised cell types of all three embryonic germ lineages - germ cells (endoderm, mesoderm and ectoderm), extra-embryonic tissue and trophoblast. Embryonic stem cells derived from blastomeres of the cleavage stage embryo or the inner cell mass of preimplantation blastocysts can differentiate into cell types of all three lineages thus showing *totipotent* potential. However, until their contribution to all cell types of the human body is proven, they are, by definition, *pluripotent*. Embryonic germ cells from primordial germ cells of post-implantation embryos, and embryonal carcinoma cells from teratomas are also *pluripotent*. Additionally, induced pluripotent stem cells seem to have the same differentiative and proliferative capacity as embryonic stem cells. Embryonic stem cells *in vitro* appear to be immortal, proliferating indefinitely in an undifferentiated state. However embryonic cells *in vivo* lose this property as differentiation ensues with development and growth promoting signals change. By adulthood, the few remaining stem cells are dispersed throughout the body and are difficult to locate. However these cells seem able to continue to generate identical daughter cells and/or tissue cells at each division.

These residual pools of stem cells are suggested to be the source of tissue regeneration and repair that occurs in adults. Tissue-specific stem cells are present in multiple organs and systems of adult animals although they differ greatly in their ability to self-renew and differentiate. For example, spermatogonial stem cells in the testis are *unipotent* and produce only one type of differentiated cell - the spermatozoon.

In contrast, mesenchymal stem cells are *multipotent* and can produce adipocytes, osteoblasts, chondrocytes and myocytes in culture. However, unlike their embryonic counterparts, tissue-specific stem cells are not immortal, and show decreasing self-renewing capability with increasing age. This limitation has been associated with the inability to repair the damage that accumulates with aging, likely to be due to exhaustion of the stem cell pool or a consequence of inherited or acquired mutations throughout life that impede normal stem cell function. However, if these stem cells divide in response to environmental cues, such as following injury or disease manifestation, and should the daughter cells differentiate at a rapid rate, then identifying the number of parent stem cells would be virtually impossible; perhaps therefore estimations of adult stem cell populations may be lower than actually present.

Regenerative medicine is an emerging and rapidly evolving field of research, tissue engineering and therapeutics that aims to compensate for this inability of the body to repair itself beyond a critical level of damage. One definition states that regenerative medicine aims at 'repair, replacement or regeneration of cells, tissue or organs to restore impaired function' (Daar & Greenwood, 2007). Ultimately, the aim is to provide treatment for conditions where current therapies are inadequate. Therefore both tissue-specific and embryonic stem cells, with their differentiative capacity, are a key source material for regenerative medicine, and understanding their biology is imperative to fully exploit the potential of this field (Bajada *et al.*, 2008). Therapy could be via stimulation of the endogenous stem cell pool, or by introduction of exogenous stem cells to compensate for the effects of aging and/or disease.

1.1.1 Tissue-specific stem cells

The mechanisms of stem cell regulation in the adult are still largely undeciphered. However it is becoming clear that the specialised actions of stem cells are intimately linked with neighbouring differentiated cells and the extracellular matrix, which together form a supportive three-dimensional microenvironment or 'niche' (Lovell-Badge, 2001). The niche is thought to influence or control genes and properties that define 'stemness' of the stem cells - self-renewal or differentiation to committed cells. Stem cells may be regulated in niches because of their developmental history. Rather than evolve complex, specialised internal mechanisms and signals to control phenotype, stem cells might first have appeared when microenvironments developed

as niches which were able to sequester, preserve and control undifferentiated embryonic cells that already had the necessary cellular properties (Spradling *et al.*, 2001). Niches are proposed to operate in one of two basic ways; lineage niches, which retain the self-renewing daughter cell but release the differentiating daughter, and population niches, which either retain both self-renewing daughter cells or release both to differentiate. Niches may also modify their regulatory properties in response to changing conditions to ensure that stem cell activity parallels the need for particular differentiated cell types. Some pools of adult tissue-specific stem cells can be isolated and the cells used for therapy, although they are often difficult to locate and access, and once in culture the cells generally replicate only a finite number of times before senescence or transformation. Nevertheless, there are established clinical treatments and experimental evidence for function restoration with many types of tissue-specific stem cells from various niches, some examples of which are discussed.

Evidence for germline niche-based regulation in mammals comes from studies of spermatogenesis. In the testis, germ cell development is maintained by germline stem cells that lie in contact with Sertoli cells and the basement membrane of the seminiferous tubule. Sertoli cells are the only somatic cell in direct contact with germ cells, and as such constitute the primary cellular component of the germ cell niche - providing nutritional and structural support for spermatogenesis. As germ cells enter meiosis and begin to differentiate into sperm, they lose contact with the basement membrane and move towards the lumen of the seminiferous tubule, while maintaining their association with Sertoli cells (Dadoune, 2007). Disruption of this relationship can lead to sub- or in-fertility in the male. Germline niche restoration by Sertoli cell transplantation had been shown to rescue stem cells in the defective host microenvironment to allow spermatogenesis and the production of offspring from infertile animals (Kanatsu-Shinohara *et al.*, 2005).

Neural stem cells are present in various niches of the postnatal brain, including the hippocampus and the subventricular zone (Temple, 2001). These neurogenic niches are formed from endothelial cells, astroglia, ependymal cells, immature progeny of neural stem cells and mature neurons, and regulate different steps of adult neurogenesis in response to physiological and pathological stimulations. Neural stem cells can differentiate *in vitro* and *in vivo* into neurons, astrocytes and oligodendrocytes, and *in vivo* migrate to specific sites of damage (Gage, 2000). Grafts of mesencephalic

tissue containing fetal stem cells can survive for a long period in the human brain and have been shown to restore dopaminergic innervation to the striatum in patients with Parkinson's (Kordower *et al.*, 1995). Similarly, fetal stem cells have been shown to be effective in the treatment of Huntington disease (HD). HD patients have been grafted with human fetal neuroblasts into the right striatum then the left one year later. The impact on neurological, neuropsychological, neurophysiological, and psychiatric tests was assessed in the following year. Motor and cognitive functions were improved or maintained within the normal range in three of the five patients treated (Bachoud-Levi *et al.*, 2000). More than 100 HD patients are now involved in such trials throughout Europe.

Many different epithelial stem cells maintain various mammalian tissues such as skin, hair follicles, sebaceous glands and sweat glands. Hair follicles contain two zones of stem-like cells - matrix and bulge stem cells (Spradling *et al.*, 2001). The dermal papilla appears to be a key component of the follicular niche, and a source of signals that stimulate the activity of matrix stem cells. Hair follicles do not develop, persist or function without a dermal papilla. This niche activity has been exploited commercially. A Phase II clinical trial has been completed by Intercytex (www.intercytex.com) for ICX-TRC - an autologous hair regeneration therapy. A suspension of dermal papilla cells is used for the treatment of male pattern baldness and female diffuse alopecia in this therapy. These follicle stem cells seem also to have a high differentiative potential. Nestin, a marker for neural stem cells, is expressed in follicle stem cells and these cells have been shown to differentiate into neurons, glial cells, keratinocytes and smooth muscle cells *in vitro*. Hair-follicle stem cells implanted into the gap region of a severed sciatic nerve in the mouse have been shown to differentiate largely into Schwann cells and greatly enhance the rate of nerve regeneration and the restoration of nerve function (Hoffman, 2006). Follicle stem cells therefore hold promise for therapy as they are abundant, easily accessible and multipotent.

Populations of epithelial stem cells have been used in other approaches to cell therapy. Recently, end-stage bronchomalacia was treated successfully by the clinical transplantation of a tissue-engineered airway. Autologous epithelial and mesenchymal stem cell-derived chondrocytes were seeded onto a decellularised allogeneic donor tracheal scaffold and matured in a novel bioreactor system. This graft was then used

to replace the left main bronchus of the recipient, immediately providing a functional airway (Macchiarini *et al.*, 2008). The graft had a normal appearance and mechanical properties after a few months, and the patient had no anti-donor antibodies and did not need immunosuppressive drugs.

The first successful ophthalmic stem cell therapy for limbal epithelial stem cell failure was reported in two patients with severe alkali burns in the eye, with complete loss of the corneoscleral junction - the limbal stem cell niche (Pellegrini *et al.*, 1997). Limbal epithelial stem cells are essential for corneal maintenance; deficiencies lead to in-growth of conjunctival cells, neovascularisation of the corneal stroma and eventual corneal opacity and visual loss (Limb & Daniels, 2008). Autologous limbal epithelial stem cells for therapy were obtained from a small limbal biopsy of the unaffected eye and expanded in culture before being transplanted to the damaged eye. Both patients experienced improved vision for at least two years. A number of clinics have further developed this technique using a variety of different cell culture protocols and carrier systems for transplantation (Limb & Daniels, 2008). However, autologous limbal biopsy carries the risk of depleting the limbal stem cell population from the niche in the undamaged eye, and the supply of cadaveric tissue is not reliable. Therefore alternative cell sources are being investigated. Culturing embryonic stem cells on collagen IV using medium conditioned by limbal fibroblasts can result in the formation of terminally differentiated epithelial-like cells of the cornea (Ahmad *et al.*, 2007).

The physiological process of regeneration where remaining tissues organise themselves to replace a lost body part has long been recognised in lower vertebrates such as the phenomenon of limb regeneration in the newt (Brockes, 1997). The regenerative medicine field aims to translate the tremendous potential of stem cell biology to achieve regeneration in humans. However, if tissue-specific or embryonic stem cells are to be used to treat a wide variety of human diseases, then several formidable challenges will need to be overcome (Bongso *et al.*, 2008; Skottman *et al.*, 2006a). The substantial risks associated with unregulated therapies have been highlighted by the recent report describing a donor-derived brain tumor following fetal neural stem cell transplantation (Amariglio *et al.*, 2009). Clinical grade stem cells will be required in large quantities to be differentiated in a controlled and defined manner

to form homogeneous populations of cells that are histocompatible with an individual, and do not form tumours or differentiate inappropriately upon transplantation. These cells will then have to be delivered to the appropriate site in the body with the required combination of temporally and spatially controlled signals to encourage incorporation by the host. General approaches for cell delivery for therapy have so far involved the use of direct injection of single cell suspensions into target tissues, seeding cells into biodegradable scaffolds, using scaffolds as controlled release vehicles, or cell sheet engineering technology (Bianco & Robey, 2001; De Laporte & Shea, 2007; Yang *et al.*, 2006). Aside from clinical therapy, other important applications of stem cells include studying early human development, modelling disease, providing a platform for therapeutic target screening, and as tumorigenic models to study cancer and cancer stem cells.

1.1.1.1 Cancer stem cells

Increased understanding of the regulation of stem cell self-renewal has highlighted the similarities between stem cell proliferation and oncogenesis, and has suggested a stem cell origin for human cancers. Furthermore, evidence is accumulating which shows that many pathways classically associated with cancer also play key roles in regulating normal stem cell development (Taipale & Beachy, 2001). For example, the Wnt and Hedgehog (Hh) signalling pathways are known to direct growth and patterning during embryonic development, and these pathways are also implicated in the postembryonic regulation of constantly renewing epithelial stem cells - such as those of the skin and intestine. Studies showing that a high frequency of certain human cancers is associated with mutations that constitutively activate the Wnt and Hh pathways have implicated a pathogenic role for transcriptional responses in these pathways (Taipale & Beachy, 2001). This suggests that transformed somatic stem cells are a locus of tumour initiation and that expansion of this population may be the first step in the formation of at least some types of cancer. There is considerable evidence that certain types of leukaemia arise from accumulated mutations in haematopoietic stem cells (Reya *et al.*, 2001). In constantly renewing cells, there is a much greater opportunity for mutations to accumulate in individual stem cells than in most terminally differentiated mature cell types, as suggested by the exponential increase of cancer incidence with age. For example, cancer formation from

cells that persist throughout life is suggested by an increased incidence in adults of skin tumours like melanoma after a higher childhood exposure to a mutagenic agent such as ultraviolet radiation (Taipale & Beachy, 2001).

It has been shown for leukaemias and solid cancers that the cells are phenotypically heterogeneous and that only a small proportion of cells are clonogenic in culture and *in vivo*, which has profound implications for cancer therapy (Reya *et al.*, 2001). Although there are drugs available that can shrink metastatic tumours, the effects are usually transient, and often do not appreciably extend the life of patients (Lippman, 2000). These therapies may shrink tumours by eliminating mainly cells with limited proliferative potential. If tumours are initiated by rare cancer stem cells with indefinite proliferative potential that are less sensitive to these therapies, then they may remain viable after treatment and re-establish the tumour. By contrast, if therapies can be targeted against cancer stem cells, then they might be more effective, rendering the tumours unable to maintain themselves or grow. Elucidating the signalling pathways that are used by normal stem cells and neoplastic cells should facilitate both the use of normal stem cells for regenerative medicine, by understanding how to prevent tumorogenicity, and the identification of cancer stem cell targets for anticancer therapies.

1.1.2 Human embryonic stem cells

Human embryonic stem cells (hESC) are derived from inner cell mass cells of preimplantation blastocysts once isolated from the niche of the blastocoel, or from blastomeres of cleavage stage embryos, and have the potential to differentiate into any cell type of the three germ layers of ectoderm (epidermal tissues and nerves), mesoderm (muscle, bone, blood), and endoderm (liver, pancreas, gastrointestinal tract, lungs) (Thomson *et al.*, 1998). HESC might be considered as artefacts of culture, as they do not seem to exist in an identical form during *in vivo* embryonic development. Once derived *in vitro*, it is unlikely that these cells could develop into a viable fetus as the spatial and temporal signalling cues essential to normal *in vivo* development are lost, and because they may not retain the potential to contribute to extra-embryonic tissue. If transplanted *in vivo*, pluripotent hESC cells form a teratoma, not a fetus. These cells recapitulate many of the early developmental processes seen *in vivo* and are therefore a valuable tool for studying early mammalian development. Primitive

streak formation and neurogenesis are two of the earliest events that occur during gastrulation, and *in vitro*, hESC readily differentiate into neuroectodermal lineages under appropriate culture conditions (Cai & Grabel, 2007). Similarly, the heart is the first functional organ to develop *in vivo*, and hESC readily form spontaneously contracting cardiomyocytes *in vitro* (Van Laake *et al.*, 2005). In contrast, more complex cell structures that appear later in embryonic development, such as insulin-producing islets, have proven challenging to obtain via hESC differentiation. Whilst some success has been seen in producing cells that secrete insulin, so far the quantity of hormone produced is low, and insufficient to correct hyperglycemia when the cells are transplanted into streptozotocin-induced diabetic mice (Santana *et al.*, 2006).

The pluripotent state of hESC is maintained *in vitro* by a number of essential transcription factors that also play crucial roles in embryonic development. These include the homeodomain proteins POU class 5 homeobox 1 (OCT4/POU5F1) and Nanog homeobox (NANOG), and the SRY-related HMG-box (Sox)-containing protein SOX2. *SOX2* and *POU5F1* bind to the *NANOG* promoter, hence exerting some level of regulation (Rodda *et al.*, 2005). *NANOG*, *SOX2* and *POU5F1* together bind the promoter region and are assumed to regulate over 350 genes in hESC (Boyer *et al.*, 2005). *POU5F1* is detectable throughout murine and human oogenesis and preimplantation development (Cauffman *et al.*, 2005b; Hansis *et al.*, 2001; Kimber *et al.*, 2008; Rosner *et al.*, 1990) and is crucial to the maintenance of pluripotency in hESC (Bodnar *et al.*, 2004; Nichols *et al.*, 1998; Niwa *et al.*, 2000). Down-regulation of *NANOG* leads to significant down-regulation of *POU5F1* and loss of hESC cell-surface antigens (Hyslop *et al.*, 2005). *SOX2* transcripts have been detected from the four-cell stage onwards in human development (Kimber *et al.*, 2008) although in mice *Sox2* transcription begins at the late morula stage (Avilion *et al.*, 2003). Interestingly, a maternal component of *Sox2* has been implicated in establishing early cell fate decisions and patterning in murine development (Avilion *et al.*, 2003). *NANOG* transcripts have been detected in the pronucleate human embryo, and then from the eight-cell stage onwards (Kimber *et al.*, 2008). It appears later in the mouse at the morula stage (Dietrich & Hiiragi, 2007) and is expressed in both human and mouse ESC. Retroviral insertion of *POU5F1*, *SOX2*, Kruppel-like factor 4 (*KLF4*) and v-myc myelocytomatosis viral oncogene homolog (*C-MYC*) into human dermal fibroblasts (Takahashi *et al.*, 2007), or *POU5F1*, *SOX2*, *NANOG* and lin-28 homolog

(*LIN28*) into human fetal fibroblasts (Yu *et al.*, 2007), results in reprogrammed induced pluripotent stem (iPS) cells.

The expression of these transcription factors and the signals for self-renewal or differentiation are regulated, at least in part, by several extrinsic influences. These signals can originate from the feeder cells, fetal calf serum or be given by exogenous supplementation. The factors involved include basic fibroblast growth factor (bFGF), insulin-like growth factor and the heparin sulphate proteoglycans (Bendall *et al.*, 2007; Koivisto *et al.*, 2004; Levenstein *et al.*, 2008), activin A (Beattie *et al.*, 2005), Notch (Chiba, 2006; Zhang *et al.*, 2007) and the Wnt proteins (Villa-Diaz *et al.*, 2008). In addition studies have now shown that epigenetic mechanisms are vitally important to the pluripotent nature of hESC and that these mechanisms regulate differentiation (Surani, 2001). There are at least two critical periods during development when epigenetic reprogramming occurs; one during gametogenesis and another during the preimplantation embryonic stage (Reik *et al.*, 2001). The epigenetic signature of hESC appears to be unique and has been linked strongly to the global permissivity of gene expression and pluripotency in these cells (Atkinson & Armstrong, 2008).

Despite the potential of hESC for therapy, to date there have been no approved clinical trials for embryonic stem cell treatment in the UK and only one in the USA. The challenges to the use of hESC in therapy are similar to those for tissue-specific stem cells as discussed above, and include controlled differentiation, cell efficacy, immunogenicity, tumourigenicity, cell delivery systems and safety (Civin & Rao, 2006; De Sousa *et al.*, 2006; Gruen & Grabel, 2006; Unger *et al.*, 2008). There are clinics that offer embryonic and fetal stem cell treatment but these are based on unpublished protocols, offer no credible outcome data and lack appropriate regulation. Examples include the Embryonic Tissues Centre in the Ukraine (www.emcell.com) and Medra Incorporated in the Dominican Republic (www.medra.com). The Geron Corporation (www.geron.com) is the first company to begin fully approved, regulated clinical trials using hESC. The Food and Drug Administration (FDA) granted clearance of their Investigational New Drug (IND) application in January 2009, for a Phase I clinical trial of hESC-derived oligodendrocytes (GRNOPC1) in patients with acute spinal cord injury. Geron's second hESC product, GRNCM1, is a population

of cardiomyocytes which is intended for the treatment of patients with myocardial disease. These cells are currently in the large animal test phases.

1.2 The emergence of *in vitro* fertilisation

The success of clinical human *in vitro* fertilisation (IVF) sits on solid foundations of many years of animal research. The earliest reports of attempted *in vitro* fertilisation date to the 1930's, although most investigators then considered fertilisation to mean the penetration of the sperm into the cytoplasm of the oocyte, which in reality is only the beginning of the process. One of the earliest reports was in 1930 (Pincus, 1930). Tubal rabbit oocytes were obtained from does previously mated to vasectomised bucks and incubated with sperm obtained from the vas deferens of a donor buck. In two cases a spermatozoon was observed with its head partially in the zona and at right angles to the axis of the egg. The tail movements were described as being fairly vigorous, and the sperm head slowly entered the egg cytoplasm, the tail being left in the zona pellucida. Pincus admitted however that as the sperm head entered the cytoplasm it was practically impossible to observe it further due to the opacity of the egg cytoplasm. Furthermore, there was no significant difference in his other experiments between the proportion of cleaving oocytes/embryos that were collected after mating with vasectomised versus untreated controls, shedding some doubt on the validity of the results. In a later report pieces of oviduct were used to culture rabbit oocytes with sperm, 14 of 21 were 'fertilised', nine of which were polyspermic and five of which were penetrated by a single spermatozoon, although the second polar body was not observed in the timeframe of culture (Moricard, 1950). A year later it was reported that rabbit spermatozoa needed to reside for several hours in the female reproductive tract to acquire the ability to fertilise oocytes *in vivo* (Chang, 1951). This discovery that sperm must undergo a physiological change before they can fertilise was of critical importance for the subsequent success of *in vitro* fertilisation. The term *capacitation* was coined by Austin in a series of experiments examining the number of embryos present in excised rat fallopian tubes following normal copulation. By collecting the tubes at between 1 and 6 hours after copulation, it was demonstrated that less than 1% of the oocytes were fertilised in up to two hours, increasing to 98% after 6 hours (Austin, 1952). It is now known

that capacitation is a series of biochemical transformations which are regulated by the activation of intracellular signalling pathways that control the phosphorylation status of sperm proteins. The first event is cholesterol efflux leading to the elevation of intracellular calcium and bicarbonate leading to the production of cyclic-AMP, which activates protein kinase A to indirectly phosphorylate certain proteins on tyrosine (Urner & Sakkas, 2003). During capacitation, there is also an increase in the membrane-bound phospholipase C (PLC), the zeta isoform of which is implicated in the induction of calcium oscillations during oocyte activation (Swann *et al.*, 2004).

The evidence in early reports of successful *in vitro* fertilisation was based on histological examination of oocytes, the validity of which was questioned because of the ambiguity of cytological criteria (Chang, 1968). The first unequivocal evidence of *in vitro* fertilisation was the report that mammalian oocytes fertilised *in vitro* could develop normally following embryo transfer. Unfertilised rabbit oocytes were incubated with *in vivo* capacitated spermatozoa in autologous serum supplemented medium. Normal fertilisation and development was observed in around one fifth of oocytes with just under half of the embryos transferred to the uterus developing into live offspring (Chang, 1959). *In vitro* capacitation was first reported with hamster spermatozoa (Yanagimachi & Chang, 1963). Whilst the fertilisation rate was lower with epididymal sperm than *in vivo* capacitated sperm, the ability to induce capacitation *in vitro* opened up the possibility of human IVF with sperm collected from the male reproductive tract. *In vitro* fertilisation of mouse oocytes without oviduct co-culture was first achieved with uterine sperm (Whittingham, 1968). The resulting embryos were transferred to recipient females and some developed into normal fetuses until sacrifice on day 17 of development.

At the same time as work progressed on obtaining sperm capable of fertilising, attention was also focused on sourcing the mature oocytes needed for IVF. Whilst superovulation regimes or the excision and flushing of oviducts following mating were successful approaches in animal studies, sourcing mature human oocytes was more of a challenge. After careful consideration of culture conditions, the successful *in vitro* maturation of mouse, pig, cow, sheep, rhesus monkey and human oocytes provided another means to obtain mature embryos (Edwards, 1965). Collecting oocytes from human ovarian tissue samples, it was demonstrated that from germinal vesicle breakdown to first polar body extrusion required a maximum of 40-48 hours

in culture. However, whilst penetration of spermatozoa into the perivitelline space was observed, fertilisation did not occur in these oocytes.

In 1968 Robert Edwards met Patrick Steptoe at a London gathering of the Royal Society of Medicine. After further work on culture parameters and medium composition (particularly pH) the first *in vitro* fertilisation of *in vitro* matured human oocytes with ejaculated spermatozoa was reported (Edwards *et al.*, 1969). From 56 inseminated human oocytes, 34 matured *in vitro* and pronuclei were seen in seven. After fixation, the midpiece and tail of the fertilising spermatozoon was observed in three zygotes. The imminent publication of the results in Nature was announced on Valentine's day, a fact which may have exacerbated the immediate furore of international media activity. A view of the social and legal considerations raised by IVF treatment was published soon after (Edwards & Sharpe, 1971).

Their combined efforts then transferred to the clinical management of IVF cycles, and fertilising *in vivo* matured oocytes collected by laparoscopy from infertile women - a technique pioneered by Steptoe. Supporting *in vitro* cleavage of embryos to the 16-cell stage (Edwards *et al.*, 1970) and then development to the fully expanded blastocyst stage (Steptoe *et al.*, 1971) was achieved rapidly. Over about 6 years Robert Edwards and Patrick Steptoe aspirated and inseminated oocytes from more than 100 women, but with a single exception, none initiated a pregnancy. The exception was a tubal pregnancy that had to be terminated at 13 weeks gestation (Steptoe & Edwards, 1976). They were finally successful when they collected oocytes from a natural unstimulated cycle. In 1978 the August edition of The Lancet published a letter that heralded great change in the field of infertility; the first birth following IVF (Steptoe & Edwards, 1978). After the birth of Louise Brown, live births with IVF occurred in Australia in 1980, in the USA in 1981 (the first using human menopausal gonadotrophin stimulation) and in Sweden and France in 1982 (Cohen *et al.*, 2005). These breakthroughs were followed by the first births following intracytoplasmic sperm injection (ICSI) (Palermo *et al.*, 1992) and the development of clinical preimplantation genetic diagnosis (PGD) (Handyside *et al.*, 1990). The proof of principle for PGD had been reported in 1967 when the sex of rabbit blastocysts was determined by the fluorescent scoring of sex chromatin (Edwards & Gardner, 1967). PGD enables embryos to be tested for a specific genetic defect prior to implantation, designed as an alternative to prenatal diagnosis for fertile couples

carrying a genetic disorder (Braude *et al.*, 2002). Whilst the first UK IVF baby was from a natural cycle, the advent of successful super-ovulation stimulation regimes resulted in more embryos being created than used for immediate transfer to the patient. Those embryos could be used for research, donated to other couples, cryopreserved or discarded. As IVF became more widely available, the need for the cryopreservation of human embryos became apparent. Techniques were developed with the aims of avoiding the replacement of embryos in the event of hyperstimulation, and reducing the transfer of large numbers of embryos with the associated inherent risk of multiple birth. The first pregnancy from a cryopreserved day 3 embryo was reported in 1983, where 5 from 8 cells survived thaw and the embryo was transferred (Trounson & Mohr, 1983). Although the pregnancy ended in a miscarriage, frozen embryo transfers are now routine practice, and cryopreservation has had a huge impact on the cumulative pregnancy success from one oocyte retrieval.

In the 25 years following the first IVF birth, around 68,000 IVF babies were born in the UK, with an estimated 1 million worldwide (Pearson, 2003). The numbers continue to rise rapidly as diagnosis, treatment and follow-up care continue to be investigated and improved. As well as enabling the study of the earliest stages of human development for the first time, it is this great success story that laid the foundations for the field of hESC research. For any stem cell derivation group, the backing of a committed, driven and successful IVF clinic is paramount in order to obtain good quality, progressive embryos for research.

1.3 The emergence of human embryonic stem cell research

Pluripotent cell lines were first isolated not directly from embryos, but from teratocarcinomas. Teratocarcinomas are tumours that arise when embryos are transplanted to an extra-uterine site in a histocompatible host. *In situ* differentiation of these tumours results in teratomas. The stem cell lines that are isolated from teratomas are termed embryonal carcinoma cell (ECC) lines. The first report describing these cells showed that a single ECC injected intraperitoneally in turn gave rise to a teratocarcinoma containing a wide variety of differentiated tissues (Kleinsmith & Pierce, 1964). These cell lines have been used extensively as an *in vitro* model system for

studying the developing embryo as there are similarities both biochemically and in ultrastructure (Martin & Evans, 1975). In addition they are relatively easy to obtain in large numbers and to culture *in vitro*. The limitations to using ECC cells as a model of human development include a more limited differentiation capability when compared to 'true' ESC and a universal aneuploid karyotype.

The first report describing ESC obtained directly from embryos was in 1966, when Cole, Edwards and Paul described long-lived and stable cells obtained from either whole or dissected rabbit blastocysts (Cole *et al.*, 1966). Multiple medium and feeder layer combinations were tested and four embryo manipulations were used; disaggregated cleavage stage cells, cultures of whole blastocysts, explanted embryonic discs and disaggregated embryonic discs. Division was observed during the culture of cleavage stage cells but the clusters only gave rise to trophoblast-like outgrowths on further incubation. The embryonic disc cells required a surface layer of collagen to attach in culture, whereas when whole blastocysts were plated, the trophoblast cells migrated over the glass surface and the epiblast cells grew over the top. These epiblast cells generated colonies that displayed outgrowths containing blood islands, muscle, connective tissue, neurons, macrophages and other undefined tissues. The majority of the colonies degenerated 20-30 days after culture, some were maintained for over 40 days, and others were successfully passaged, although mostly trophoblastic cells reattached. Cell lines derived from the embryonic discs were fibroblast- or epithelial-like cells, and were successfully cultured for over 200 generations and remained euploid. One epithelial cell line expressed high alkaline phosphotase activity.

The culture of whole mouse blastocysts for up to two months revealed that multiple differentiated cells could be obtained from this species also (Sherman, 1975). The trophectoderm (TE) cells gave rise to a monolayer of trophoblasts, with cells resembling both ectoplacental cone cells and primary giant cells observed. The inner cell mass (ICM) cells developed into spherical, fluid-filled vesicles or egg cylinder-like structures which contained a variety of different cell types after two to four weeks of culture. Four cultures of blastocyst cells were continuously maintained *in vitro* for more than one year, although possibly of trophoblast origin. However the large majority of metaphases after this period showed a hypotetraploid chromosome content and none of the cell lines generated teratomas upon *in vivo* injection.

Development of the immunosurgery procedure for isolating the ICM of mouse blastocysts reduced the preparation of these structures to a simple and routine laboratory technique, enabling large numbers to be isolated for experimentation (Solter & Knowles, 1975). The first *in vitro* studies using this method showed that isolated ICMs could undergo an early differentiative step with the production of endoderm-like cells (Solter & Knowles, 1975). The ICMs were grown in modified Eagle's medium in plastic dishes without feeder or substrate support. Around half did not attach but formed embryoid bodies, the others attached and formed multicellular outgrowths. Subsequently it was demonstrated that some or all of these endoderm-like cells possessed plasminogen activator activity, as do midgestation parietal endoderm cells *in vivo* (Strickland *et al.*, 1976).

Further studies demonstrated that isolated mouse ICMs undergo a number of developmental steps morphologically similar to those which take place in intact blastocysts *in vitro* (Wiley *et al.*, 1978). Isolated ICMs were cultured in suspension for a variable number of days, before being fixed, sectioned and examined histologically. After two or three days of culture, the ICMs consisted of an outer layer of endoderm and an inner layer of ectoderm that had cavitated centrally. By six days of culture, a large proportion of ICMs had expanded into yolk-sac-like structures that subsequently produced capillaries containing blood cells (mesoderm). These results showed that all three germ layers could be obtained from isolated ICMs cultured *in vitro* without the continued presence of the TE. The use of a fibroblast feeder layer as a supportive co-culture system was described at around the same time, and was successfully used for the continuous growth of isolated ICMs for up to four weeks, producing a variety of differentiated cell types including keratin, nerve, beating muscle, fibroblasts and cartilage (Hogan & Tilly, 1977). The continued growth of undifferentiated cells was also attempted. Medium conditioned by both murine and non-murine feeder cells was shown to facilitate the spreading of ICM cells along a culture dish surface. The active factor in the medium enabling such migration was isolated but not identified (Atienza-Samols & Sherman, 1978).

Immortal mouse (m)ESC were established in culture after hormonal manipulation of mice to produce late stage blastocysts (Evans & Kaufman, 1981). Induction of diapause by ovariectomy at day 2.5 of pregnancy enables blastocysts to hatch but prevents implantation. A gradual increase in cell number occurs and primary

endoderm may be formed but no further development takes place. This procedure was used to produce sufficiently large numbers of ICM cells from each blastocyst. Whole blastocysts were plated in groups in tissue culture dishes, and ICM outgrowths were passaged onto inactivated immortalised mouse feeder (STO; single-minded gene, 6-thioguanine resistant, ouabain resistant) cells in medium supplemented with serum. Subsequent colonies were passaged every 2-3 days, had normal karyotype and formed teratomas upon injection into syngeneic mice.

In the same year, pluripotent mESC cell lines were also established following immunosurgical isolation of murine ICMs and culture on STO feeders in medium conditioned by a teratocarcinoma cell line (Martin, 1981). Diapause was not initiated, instead normal blastocysts were flushed from the uterus before implantation. The cell lines derived in this way had all the essential features of teratocarcinoma stem cells. Subclonal cultures derived from single ESC differentiated *in vitro* into a wide variety of cell types and formed teratomas when injected *in vivo*. The term *embryonic stem cell* was first coined in this paper to distinguish cells derived directly from embryos from *embryonal carcinoma cells* derived from teratocarcinomas.

Therefore mESC lines were successfully derived by two different methods by two different teams in the same year. In one, the use of conditioned medium provided proliferative signals to encourage normal isolated ICM cells to divide. In the other the embryos were manipulated *in vivo* to increase ICM cell number, and plated whole. Both used a feeder layer of STO fibroblasts to encourage undifferentiated growth. The ability to derive pluripotent mESC lines directly from an embryo circumvented the need for 'converting' an embryo to a tumour *in vivo*.

It was subsequently shown that the differentiation of mESC *in vitro* could be reversibly inhibited by leukaemia inhibitory factor (LIF) (Smith & Hooper, 1987). Furthermore LIF could substitute for the essential function of feeders and enabled the feeder-free derivation and propagation of germ-line competent mESC under simpler, more defined conditions (Nichols *et al.*, 1990). As mESC could contribute to functional germ cells in chimeras, this provided a powerful approach for introducing specific genetic changes into the mouse germ line through such manipulation (Bradley *et al.*, 1984). Long-term culture of mouse primordial germ cells (PGCs) was also achieved by culture with bFGF, LIF and steel factor on STO feeders (Matsui *et al.*, 1991; Resnick *et al.*, 1992). These pluripotent embryonic germ cells (EGC)

resembled both mESC and mECC, expressing both Ssea1 and alkaline phosphatase activity and germ-line transmission in experimentally produced chimeras.

Several early experiments highlighted the potential of ESC. The generation of the first chimeric mouse by injection of embryonic cells into the blastocoel showed that these cells could be incorporated into the host embryo and contribute to a number of tissues (Gardner, 1968). Donor murine cells carrying a colour marker and the T6 chromosome translocation were isolated following disaggregation of blastocysts and then injected into the blastocoel of albino mouse blastocysts of the same age. Mosaicism was confirmed by pigmentation of the iris, skin and coat in the offspring, and by pigmentation of the iris and presence of the T6 translocation in sacrificed fetuses. The therapeutic potential of ESC was demonstrated when the cells from entire mouse embryos at 6 or 7 days of development were shown to repopulate the haemopoietic system of lethally X-irradiated recipients (Hollands, 1987). Saline injected control mice died at approximately 12 days post-irradiation whereas 80% of grafted X-irradiated recipients survived and donor markers were found in each of them.

The first report of long term *in vitro* culture of human embryos described a trophoblast outgrowth from a whole blastocyst plated directly onto a culture dish in modified Earle's medium (Fishel *et al.*, 1984). These outgrowths survived for over 4 days before being fixed for analysis. Human chorionic gonadotrophin was detected in the drops used to culture the blastocyst. Further studies with whole human blastocyst culture generated cells with typical stem cell morphology, that were alkaline phosphatase positive, karyotypically normal and which could be maintained for 2 passages (Bongso *et al.*, 1994b). Using experience with embryo co-culture in IVF (Bongso *et al.*, 1989a,b, 1994a), pronuclear embryos were grown to the blastocyst stage and allowed to hatch on non-inactivated human fallopian tubal epithelial monolayers. Once cavitating blastocysts were formed the medium was changed from Medicult to Chang's medium supplemented with human LIF. When the blastocysts attached the ICM clumps were manually separated, partially disaggregated with trypsin and then plated directly onto tissue culture plastic. 19 from 21 embryos were able to produce ICM clumps that could be maintained through at least 2 subcultures without differentiation.

Pluripotent cell lines were derived from several non-rodent species around this time, including from the pig (Evans *et al.*, 1990), cow (Anderson *et al.*, 1992; Evans *et al.*, 1990), sheep (Piedrahita *et al.*, 1990) and also from the golden hamster (Doetschman *et al.*, 1988), although in general the developmental potential of the cell lines was poorly characterised. A pluripotent ESC line was then isolated from a rhesus monkey after immunosurgical isolation of the ICM and plating on mouse embryonic fibroblasts (MEFs) (Thomson *et al.*, 1995). The line expressed all the markers in common with human ECC (POU5F1, SSEA3, SSEA4, TRA1-60, TRA1-80), had a normal karyotype, generated teratomas upon injection into severe combined immunodeficient mice and at the time of reporting had been maintained in undifferentiated culture for over 12 months. LIF was not required for the derivation or undifferentiated growth of these primate ESC. As feeder-free human pluripotent cells differentiated despite the addition of LIF to the medium (Bongso *et al.*, 1994b), together these results suggested that the signalling required for maintenance of pluripotency was likely to be species-specific. Recent evidence suggests however that the embryonic stage at which cells are isolated may determine the subsequent characteristics of the cell population. Post-implantation epiblast-derived stem cells have been generated from mouse epiblast and shown to share patterns of gene expression and signalling responses with hESC, whilst being distinct from mESC (Brons *et al.*, 2007; Tesar *et al.*, 2007). These epiblast stem cells are therefore a valuable model system for determining whether the differences between mESC and hESC are due to species differences or diverse temporal origins.

Pluripotent stem cell lines were derived from human gonadal ridges and mesenteries containing PGCs in 1998 (Shamblott *et al.*, 1998). PGCs were cultured on mouse STO fibroblast feeder layers in the presence of human recombinant LIF, human recombinant bFGF, and forskolin. The cells expressed the typical panel of pluripotent markers, were morphologically similar to mESC and mEGC, maintained a normal karyotype, and demonstrated ability to differentiate into the three germ layers. In the same year hESC lines were derived from human blastocysts (Thomson *et al.*, 1998). The derivation method and characterisation studies were the same as for primate ESC. Five lines were derived from 14 isolated ICMs. From five lines in 1998, there is now anecdotal evidence of over 300 hESC lines worldwide (Abbott *et al.*, 2006).

Whilst it was shown in these early studies that hESC had the capacity to differentiate into derivatives of all three germ layers either *in vivo* or *in vitro*, such differentiation was spontaneous and unregulated. One early report considered the influence of growth factors on differentiation. Eight growth factors were tested on a hESC line to assess the ability of exogenous signals to regulate hESC differentiation (Schuldiner *et al.*, 2000). The cells were passaged from feeders to gelatin to remove feeder contamination, briefly aggregated as embryoid bodies and then dispersed as single cells and re-plated. The exogenous growth factors were then added. The cells expressed receptors for each of the growth factors. Whilst none of the eight growth factors tested directed completely uniform differentiation to one cell type, the factors encouraged differentiation into specific lineages. The three germ layers and eleven tissues were identified by molecular markers. This was the initial step toward attempting fully directed cell differentiation with hESC. It complemented similar work with adult stem cells, such as the use of specific media for directing the differentiation of mesenchymal stem cells, and determination of the surface markers to confirm the correct lineage had been established (Pittenger *et al.*, 1999).

1.4 Regulation of IVF and human embryo research in the UK

Whilst hailed as a scientific breakthrough, the birth of the first IVF baby also caused a backlash of moral indignation (Deech, 2008). To address this outcry, the British government set up an enquiry to consider IVF and embryo research that was led by Mary Warnock (now Baroness Warnock), in her capacity as a moral philosopher.

The Warnock Committee (1982-84) (Warnock, 1984) recommended the formation of a regulatory authority that had statutory control over fertility treatment, gamete and embryo storage and embryo research. It was advised that the authority should consist of lay members as well as clinicians, scientists, ethicists, legal experts and theologians (reviewed in Warnock (2007)). The report also recommended that research on human embryos should be regulated but permitted only up to 14 days after fertilisation. After this time the definitive germ layers begin to form, no twinning can take place and the primitive streak appears, constituting a single individual.

In 1985 based on the recommendations of the Warnock Report, the Medical Research Council and Royal College of Obstetricians and Gynaecologists established the Voluntary Licensing Authority as an approach to regulate human IVF until the introduction of government legislation. This became the Interim Licensing Authority and then the Human Fertilisation and Embryology Authority (HFEA) after the Human Fertilisation and Embryology (HFE) Act was passed by Parliament in 1990. The United Kingdom was the first country to consider and enforce legislation that covered human embryo research. Unlike the situation in other countries the HFE Act applies to all research and clinical practice regardless of whether the funding is public or from charities, foundations or private companies. The 1990 HFE Act specified that a research licence would not be granted unless the HFEA was satisfied that any proposed use of human embryos was essential for the research and that the research was necessary or desirable for the purposes specified in the Act. These purposes are:

To promote advances in the treatment of infertility

To increase knowledge about the causes of congenital disease

To increase knowledge about the causes of miscarriages

To develop more effective techniques of contraception

To develop methods for detecting the presence of gene or chromosome abnormalities in embryos before implantation.

Following votes in the House of Commons in 2000 then the House of Lords in 2001, and driven largely by the potential of hESC in regenerative therapy, the HFE Act was amended to include the HFE (Research Purposes) Regulations. This allowed research on embryos to be licensed for three additional purposes;

To increase knowledge about the development of embryos

To increase knowledge about serious disease

To enable such knowledge to be applied in the development of treatments to combat serious disease.

The Human Reproductive Cloning Act was also added in 2001 following a judicial review requested by the ProLife Alliance to clarify the scope of the HFE Act. This prohibited the uterine transfer of a human embryo created otherwise than by fertilisation.

In response to public demand the House of Lords established a committee to further review the need for embryonic (and adult) stem cell research. Following this review, in 2002 the House of Lords Select Committee on stem cell research was set up to oversee the formation of a UK Stem Cell Bank (UKSCB). The UKSCB was founded with the aim of minimising the number of cell lines that need to be derived and therefore the number of embryos used, and also to establish codes of practice for the use of hESC. Whilst it is a condition of the derivation licences granted by the HFEA that samples of all new lines must be deposited in the UKSCB, once derived, the use of hESC in research is no longer covered by the HFEA. As the cells do not have the moral status of human embryos the same regulation is not needed. Instead research is expected to follow guidelines issued by the UKSCB steering committee. The UKSCB is the first of its kind in the world. Master cell banks of quality-controlled and well characterised stocks of each deposited line are established and made freely availably to research groups. King's College London and the Roslin Institute were granted the first UK licences for hESC research in early 2002. Subsequently, King's College London deposited one of the first cell lines into the UKSCB coinciding with the official opening of the facility in May 2004.

Owing to rapid progress in science and to changes in legal and public opinion, the British Government recently proposed amendments to the 1990 Act in a new HFE Bill. The Bill incorporates major changes in the types of clinical practice and research that it will allow but is still based on the principles that were laid down in the original Act. The Bill legalises the creation of animal-human admixed embryos including cytoplasmic hybrids, 'true' hybrids, and transgenic human embryos as well as chimeric human embryos. The Bill will also allow the functionality of hESC-derived gametes to be tested by creating embryos. However, these gametes are currently defined as 'not permitted' and cannot be used clinically for reproductive purposes. The new Bill is designed to facilitate research but not necessarily its clinical application, especially when this is thought to be distant. Aspects of the Bill relevant to hESC research form only a small part, although one that is often strongly debated. The third reading of the HFE bill was voted upon and carried by a large majority in the House of Commons in October 2008. It now goes on to the statutes and the HFEA must decide how to implement it.

Further regulation relevant to IVF and stem cell research is the European Union Tissue and Cells Directive (EUTCD). This is made up of three Directives, the parent Directive (2004/23/EC) which provides the framework legislation and two technical directives (2006/17/EC and 2006/86/EC), which provide the detailed requirements of the EUTCD. These set standards of quality for donation, procurement, testing, processing, preservation, storage and distribution of human tissues and cells (Unger *et al.*, 2008). The directive became mandatory in 2007 and requires a stringent standard of quality for IVF laboratories and laboratories deriving stem cells intended for therapeutic use.

1.5 Embryo development I: Mechanics of blastocyst formation

During fertilisation, the entry of the spermatozoon into the oocyte initiates the development of the embryo. Activation of mammalian oocytes is characterised by a series of calcium oscillations that initiate shortly after gamete fusion and terminate with pronuclei formation (Schultz, 2005; Swann & Yu, 2008). The calcium release is thought to be triggered by the cytosolic sperm component phospholipase C zeta (Swann *et al.*, 2004). Meiosis is resumed in the oocyte as the metaphase spindle elongates and rotates on its axis during anaphase and telophase to result in the expulsion of the second polar body (Jones, 2005). Fertilisation is considered complete at syngamy when the male and female pronuclei fuse. If fertilisation has occurred in the ampulla, embryos begin their cleavage divisions as they move through the oviduct. Embryos are carried in oviductal fluid, the composition of which changes as the embryo travels and develops (Gardner *et al.*, 1996; Leese, 1988). In IVF, embryos progress through development in the laboratory, and the culture conditions and media should be designed to mimic the *in vivo* conditions as closely as possible in order to achieve good quality blastocysts by day 5-7 of development.

1.5.1 Early cleavage divisions

The initial phase of mammalian embryo development is a period during which cellular multiplication takes place in the absence of net growth. In the human the first cleavage can be expected 24-28 hours after fertilisation (Lundin *et al.*, 2001) and divides

the embryo into two morphologically equal cells. The second division is notable as the cleavage is asynchronous and the two cleavage planes most commonly lie at right angles to each other (Gardner, 2002). Successive divisions take place around every 24 hours. The fertilised embryo changes from a single, large and relatively inert cell to a number of small active cells. The nuclear to cytoplasm ratio of the blastomeres therefore declines, approaching that of somatic cells. The individual blastomeres of cleavage stage embryos are distinct, but in contact via microvilli (Nikas *et al.*, 1996). Initially, both turnover of energy substrates and synthetic activity are low. During the cleavage stages, many organelles assemble in the cytoplasm of the blastomeres and the metabolism of the embryo gradually becomes more complex (Gardner & Lane, 2002). Glycolysis and Kreb's cycle activity increase by orders of magnitude and diverse synthetic activity commences. Increasing macromolecular synthesis and the activation of the embryonic genome leads to the appearance of new RNA, DNA, protein, and polysaccharide molecules.

1.5.1.1 Activation of the embryonic genome

In amphibia, stored maternal transcripts have been shown to control the earliest stages of development in the embryo up to gastrulation. The first 12 cell divisions of *Xenopus laevis* embryos do not require embryonic gene transcription, such that these cell cycles are controlled at a post-transcriptional level using maternally inherited information (Duval *et al.*, 1990). In the mouse, cleavage to the two-cell stage is regulated largely if not exclusively at a post-transcriptional level (Flach *et al.*, 1982). The increase in synthesis of particular polypeptides at the early two-cell stage has been shown to be using maternal mRNAs synthesised before fertilisation (Braude *et al.*, 1979) and maternal genes are still active until at least the four-cell stage (Nothias *et al.*, 1995). Treatment of human embryos at various stages of development with transcription inhibitors demonstrated that the first two cleavage divisions occur normally, but that development beyond this stage is blocked (Braude *et al.*, 1988). Hence the major activation of the embryonic genome occurs around the four-cell stage in humans, with the loss of maternal transcripts occurring at around the same time as genome activation, but independently (Braude *et al.*, 1988). Embryonic genome activation is essential for the synthesis of new proteins and further cleavage, but cleavage arrest is not always indicative of failure of activation (Artley

et al., 1992). Furthermore, the transition to embryonic transcription could be dependent on karyokinesis rather than cytokinesis, with evidence of one-cell embryos demonstrating transcription-dependent protein synthesis, and after nuclear staining, multiple nuclear structures (Artley *et al.*, 1992).

1.5.2 Blastocyst development

There are two major morphogenetic events that mark the progression to the blastocyst stage; compaction and cavitation. Compaction starts around the 16-cell stage (the morula) with an increase in interblastomeric contacts. Gap junctions, adherens junctions, tight junctions and desmosomes form until the embryo appears as a uniform cellular mass with dense surface microvilli (Bloor *et al.*, 2002; Watson, 1992). Contacts and junctions are dynamic and change to accommodate the loss of coupling during mitosis. Blastomeres or fragments that are unable to form contacts or to communicate appropriately with other blastomeres, or are undergoing apoptosis are generally excluded from the developing embryo, often remaining in the zona pellucida after hatching (Hardy, 1999). Metabolism of the cells switches preferentially to glycolysis (Gardner & Lane, 2002).

Compaction represents the onset of the first morphologically visible cellular differentiation during mammalian development with polarisation of the cells of the morula (Johnson & Ziomek, 1981a; Johnson *et al.*, 1986). By the 16-32 cell stage there is a distinct outer (polar) and inner (apolar) layer. Polarisation of the outer cells is evident by the basal migration of the nucleus, lipid vesicles and mitochondria, the apical accumulation of actin bundles, endocytic vesicles, microvilli and the asymmetrical distribution of membrane proteins (Fleming & Pickering, 1985; Maro *et al.*, 1985). Once a cell has become polarised, the polar status of the progeny of the cell will depend on the orientation of the cleavage plane (Johnson & Ziomek, 1981b).

The development of a polarised transporting epithelium layer facilitates the formation of the epithelial junctional complex. Sodium/potassium (Na^+/K^+) ATPase pumps result in a sodium gradient and regulation of paracellular transport of chloride ions, which drives the osmotic accumulation of water across the epithelium into the nascent blastocoelic cavity resulting in expansion (Watson, 1992). The formation of a transporting epithelium is significant to metabolism, as the embryo becomes

capable of actively regulating its internal environment by controlling ionic gradients. The control of fluid leakage is achieved by the formation of the calcium-dependent cell adhesion molecule E-cadherin (Hyafil *et al.*, 1981; Watson *et al.*, 1999). Hence calcium-free medium can be used to dissociate junctions in compacted morulae and morulae cultured in such medium do not cavitate normally. For several hours after the formation of the blastocoel, these junctions are semi-permeable and this incomplete seal appears to be the reason why mammalian blastocysts are seen to expand and collapse in a pulsatile fashion (Massip *et al.*, 1982). As the blastocyst expands the zona pellucida is stretched and thins before hatching occurs. Implantation serine proteinase (*Isp*) genes in preimplantation murine embryos have been described, and *Isp1* and *Isp2* together form hetero-dimeric complex which is the active form of the enzyme strypsin, implicated as the hatching enzyme (Sharma *et al.*, 2006). When embryos were exposed to a synthetic inhibitor of *Isp*, hatching was almost completely inhibited. Hatching will also occur through a mechanically made hole following biopsy or assisted hatching.

1.6 Human embryo culture

Human embryo development is inherently variable, with a wide range of embryo quality and genetic integrity observed in IVF embryos (Balakier & Cadesky, 1997; Munne, 2006). For pregnancy, the selection of the highest quality embryo(s) maximises the chances of conception. Similarly, for research, this selection not only increases the chance of success of the experiment, but also adds strength to conclusions by excluding those embryos displaying signs of abnormal growth or development. An optimal human embryo developmental programme *in vitro* would expect division to 2 cells by late day 1 after insemination or injection followed by subsequent, albeit asynchronous divisions to 4 cells on day 2, 8 cells on day 3, 16-32 cells that show signs of early or complete compaction on day 4, and cavitation late on day 4 to day 5, to a fully expanded blastocyst from day 5-7. In order to achieve this ideal sequence, each and every aspect of *in vitro* culture should be examined and improved where possible. Factors that might need to be considered are: the culture medium chosen and the type of medium overlay, the culture vessels used, the incubation chamber and

gas composition, ambient air quality and the competence of the technicians. However the underlying constraint remains that it is not possible to make good quality embryos from poor quality gametes. Therefore patient health and fertility status in combination with *in vitro* culture parameters will determine success.

1.6.1 Media development

Whilst co-culture systems and undefined medium have been used in IVF (Bongso *et al.*, 1994b; Feng *et al.*, 1996; Menezo *et al.*, 1995; Wiemer *et al.*, 1995) the necessity for, and safety of, somatic cell support in embryo culture has been called into question (Bavister, 1992; Behr *et al.*, 1999; Van Blerkom, 1993). The inherent problems with such systems include the difficultly in providing optimum growth conditions for two disparate cell types and the use of serum which introduces variability into the system (Orsi & Reischl, 2007). The use of co-culture has since been abandoned in favour of defined medium which confers many benefits, among which are accurate batch to batch production for use in any laboratory, a defined composition that can be varied in a controlled manner, and absence of contaminants of unknown biological activity such as enzymes or growth factors.

One of the first uses of chemically defined medium as opposed to biological medium was in the culture of embryonic chick tissues (cited in Summers & Biggers (2003)). The culture of early mammalian embryos was studied mainly in the rabbit and the mouse (Whitten, 1956). Historically, two approaches have been used to alter the components of chemically defined media in the pursuit of the optimum composition - the back-to-nature approach (Gardner *et al.*, 1996) and empirical optimisation (Summers & Biggers, 2003).

The back-to-nature method is based on the logic that the concentrations of substances incorporated into the medium should approximate to those found at each stage *in vivo* as the embryo develops. The analysis of nanolitre quantities of oviductal and uterine fluids in the mouse (Harris *et al.*, 2005) and human (Gardner *et al.*, 1996; Leese, 1988; Tay *et al.*, 1997) showed that the mammalian embryo is exposed to differing metabolite concentrations as it passes along the oviduct to the uterus. The consideration of these conditions led to the development of complex sequential media designed to reflect the changing physiology of the human embryo as it develops *in vivo*, for example the G series (Jones *et al.*, 1998). The problem with this

approach is the difficultly in obtaining reproducible volumes of fluid from each stage of the female reproductive tract with which to make these measurements, and the possibility that embryos in culture may adapt and selectively utilise substrates that they require from the environment as long as the concentrations of the components are within tolerable ranges (Summers & Biggers, 2003). Empirical optimisation requires the concentration of each compound in a medium to be varied separately and the response of the embryo to be observed. The results are then used to estimate a concentration-response line, and the concentration selected for the medium is usually that which gives maximum response. However, the effects of each component in the medium may depend on the concentrations of all the others, and the maximum response is not necessarily the most natural. The mathematical model also becomes intractable when the number of components in the medium is greater than three. However, this method led to the establishment of successful simple media used by some centres for all stages of embryo development, initially with the formation of simplex optimisation medium (SOM) and then KSOM and finally KSOMaa (Erbach *et al.*, 1994).

There are now few simple, but several sequential media systems available commercially for use in IVF clinics. Unfortunately their constituents generally remain proprietary, raising concerns for the quality of science and safety of the products (Biggers, 2000). This leads to claims by manufacturers of the superior performance of their products which can only be ascertained by systematic comparison of different systems, rather than the detailed analysis of the components. Similarly, in human embryonic stem cell culture, proprietary media are available for research, but are based on general cell culture requirements rather than specific consideration of the needs of the embryos and putative stem cells.

1.6.2 Media composition

Much of the data regarding optimal combinations and concentrations of media components come from mouse studies. Results must be extrapolated to the human with caution as the mouse is not necessarily a good metabolic model for the human, being 4-5 times smaller and without the energy reserves of the human embryo. Nevertheless, important information on metabolite effects have been elucidated with mouse

studies, and this has formed the knowledge base on which the formulation of human IVF medium has been developed. The major media components are considered here, the effects of metabolites on embryo development are also discussed further in Chapter 4.

There is data to suggest that any media composition should be designed to promote embryo metabolism that is 'quiet' rather than active (Leese, 2002, 2003; Leese *et al.*, 1993, 2007). Upregulation of metabolism, whether induced *in vivo* or *in vitro*, is associated with a reduction in viability. This lead to the theory that embryos should develop optimally in the minimum concentrations of exogenous nutrients such that endogenous metabolism is not compromised. This is likely to lead embryos to utilise endogenous nutrients; something for which their size suggests that they have evolved to do - the egg is the largest cell in the female mammal and has plentiful energy reserves.

Carbohydrates

During murine embryonic development, pyruvate or oxaloacetate are essential for early cleavage divisions (Bavister, 1995), whereas lactate but not pyruvate is essential for supporting *in vitro* development of early hamster embryos. Whilst glucose is an effective substrate from the eight-cell stage onwards, mammalian cleavage embryos do not utilise glucose as an energy source to any great extent (Biggers *et al.*, 1967). Indeed in simple culture media, glucose is responsible for the retardation or developmental arrest of hamster and mouse embryos - the '2-cell block' (Quinn, 1995; Schini & Bavister, 1988b). Historically, glucose has been excluded from culture medium due to this observed toxicity when not balanced by the addition of other components. This may not fatally affect cleavage stage embryos, but the removal of glucose from a medium used for murine blastocyst culture results in a significant reduction in subsequent fetal development (Gardner & Lane, 1996). Not only is glucose present in oviduct and uterine fluids (Gardner *et al.*, 1996), but mouse embryos possess a specific glucose carrier from at least the 2-cell stage onwards (Gardner & Leese, 1988). Furthermore glucose is required not only for energy production, but is also essential for lipid, nucleic acid and triglycerol biosynthesis (Reitzer *et al.*, 1980). Glucose therefore becomes increasingly important once the embryonic genome is activated and biosynthetic levels increase. In the presence of suitable regulators such as amino acids, EDTA and vitamins, glucose does not impair development (Gardner

& Lane, 1996). Therefore to alleviate cleavage arrest by removing glucose from the culture medium is not only unphysiological but should be considered as an artefact (Gardner & Lane, 1997). Hence in sequential media, glucose is included at low levels initially but the concentration is increased in the medium for culture from the 8-cell stage when its inclusion is critical. At the time of implantation the environment around the blastocyst is relatively anoxic, hence glycolysis may be the only means of generating energy before angiogenesis in the endometrium is complete. A source of this glucose for glycolysis could be endogenous glycogen stores. Should the embryo have prematurely used such stores during development due to the absence of glucose in the culture medium, these embryos may have a reduced developmental capacity.

Amino acids

Early work which led to the formulation of media capable of supporting the development of mouse zygotes to the blastocyst stage was carried out with the insensitive F1 mouse strain and led researchers to believe that amino acids had no significant effect on embryo development (Biggers *et al.*, 1967; Whitten, 1956). For nearly twenty years following this work, amino acids were absent from culture media. The role of amino acids was reconsidered with the advent of human IVF and the attempts to optimise *in vitro* development. It has since been demonstrated that the intracellular pool of amino acids in embryos is affected by the medium used for culture (Van Winkle & Dickinson, 1995). Murine blastocysts that developed *in vitro* contained about six times more alanine and about one-sixth as much taurine as blastocysts that developed *in vivo*, but they contained about the same amounts of glycine and serine. Glutamine content increased nearly tenfold in embryos *in vivo* between the 2-cell and 4-8-cell stages whereas no such increase occurred *in vitro* unless supplied in the culture medium. An exposure as short as 5 min to medium lacking amino acids at the zygote stage results in a significant impairment of subsequent development (Gardner & Lane, 1996).

Work on golden hamster embryos demonstrated that specific amino acids (glutamine, isoleucine, methionine, phenylalanine, and taurine) were essential for development of the zygote past the 2- and 4-cell block in culture (Schini & Bavister, 1988a). The study of the amino acid content of preimplantation rabbit embryos and fluids of the reproductive tract showed that high levels of non-essential amino acids plus glutamine were present (Miller & Schultz, 1987). Non-essential amino acids

with glutamine alleviate the 2-cell block in CF1 mouse embryos (Gardner & Lane, 1996) and also decrease the time of the first three cleavage divisions and increase compaction of F1 mouse embryos *in vitro* (Lane & Gardner, 1997). A synergy between amino acids and EDTA has been demonstrated, with the combination giving high rates of development past the 2-cell block and subsequent blastocyst formation (Gardner & Lane, 1996). EDTA functions both as a chelator of toxic metal ions and inhibits premature utilisation of glycolysis by cleavage stage embryos. Therefore it must be removed from culture media after the 8-cell stage as inhibition of glycolysis from this point significantly reduces blastocyst formation (Gardner & Lane, 1996). Mouse oocytes and embryos possess specific transport mechanisms for amino acids throughout the preimplantation period. Murine blastocyst formation, blastocyst cell number and hatching rates are all significantly improved with the addition of all 20 amino acids, but further improved when culture medium is supplemented with just the non-essential group plus glutamine during cleavage stages (Gardner & Lane, 1993). This implies a possible detrimental effect of some of the essential amino acids or is possibly due to competition for specific transporters during the first cleavage divisions. However all 20 amino acids have been shown to be beneficial in later development to the blastocyst stage (Lane & Gardner, 1997). Fetal development after transfer of blastocysts was also significantly increased by culture with the essential amino acids from the 8-cell stage. This reflects the changing metabolic needs of the embryo at compaction.

Amino acids have now been proposed as amongst the most important regulators of mammalian preimplantation development and therefore a key constitution of culture media (Gardner & Lane, 1997). In sequential human IVF media the non-essential amino acids and glutamine are included for the cleavage stages, and then all 20 are incorporated from the 8-cell to blastocyst stage. However evidence suggests that human embryos, unlike those of the mouse and hamster, make no distinction between essential and non-essential amino acids (Houghton *et al.*, 2002). Furthermore, the turnover of only three amino acids (asparagine, glycine and leucine) has been significantly correlated with clinical pregnancy and live birth in the human (Brison *et al.*, 2004).

Amino acids are involved in many metabolic functions; as energy substrates, for protein synthesis, for intracellular pH regulation, as intracellular osmolytes and chela-

tors of embryo toxins such as heavy metals. However, amino acids are metabolised by the embryo and spontaneously break down in the culture medium particularly at 37°C to produce embryo-toxic amounts of ammonium. Mouse embryo cleavage rates slow after 72 hours unless the embryos are transferred to fresh medium, shown to be due to ammonium build-up (Gardner *et al.*, 1996). Ammonium has detrimental effects on embryo development, affecting metabolism, intracellular pH regulation, gene expression and imprinting. In IVF the build-up of ammonium is addressed by regularly moving embryos to fresh culture medium, but there is evidence to suggest that even overnight equilibration of dishes at 37°C before use can detrimentally affect embryo development (Bavister & Poole, 2005). During the derivation of human embryonic stem cells ammonium build-up causes a more difficult situation as the medium is exchanged infrequently, discussed further in Chapter 4.

Macromolecules

Serum contains growth factors and other potentially beneficial compounds such as chelators of heavy metals, can act as a pH buffer, and serve as a nutritive source. For these reasons serum has historically been included in embryo culture systems. However, serum also contains many peptides, proteins and other undefined molecules to which the embryo is never exposed *in vivo*. Oviduct and uterine fluids are not serum transudates, but specialised environments created by the transporting epithelium of the reproductive tract (Leese, 1988).

The use of whole serum in culture medium can adversely affect the development of embryos at several levels compared to the use of serum albumin only. In sheep embryos, whole serum has been shown to reduce blastocyst cell number, inhibit blastocoel formation, affect sequestration of lipid, perturb metabolism and result in abnormal mitochondrial ultrastructure and abnormally large offspring (Thompson *et al.*, 1995). Bovine embryos cultured in serum-supplemented medium have been shown to contain numerous cytoplasmic lipid droplets and immature mitochondria compared to those cultured in serum-free medium (Abe & Hoshi, 2003). Furthermore the survival and hatching rates of embryos produced in serum-free media were superior to those of embryos produced in the serum-supplemented medium after cryopreservation and thaw. Apart from the detrimental effects on embryo development, the inclusion of serum in culture medium makes it impossible to standardise culture

conditions, as each serum batch is a unique mixture of hormones, growth factors and metabolites.

The exact mechanisms by which serum deleteriously affects development remain to be resolved. However the role of growth factors in serum in inducing altered patterns of development cannot be overlooked. Secondary effects of serum could include a contribution to the ammonium load in medium, which can adversely affect embryo development as discussed. A synthetic protein serum substitute is now used in the culture of human embryos in clinical IVF.

Influence of culture volume and embryo grouping

It has been demonstrated that the culture of mouse embryos in reduced volumes of medium and/or in groups significantly increases blastocyst development rates and blastocyst cell number (Lane & Gardner, 1992; Paria & Dey, 1990; Quinn, 1995; Schini & Bavister, 1988a). The inferior development of singly cultured embryos can be markedly improved by the addition of epidermal growth factor or transforming growth factor to the culture medium, suggesting specific growth factors of embryonic and/or reproductive tract origin participate in preimplantation embryo development (Paria & Dey, 1990). Culture in large volumes dilutes autocrine factor(s) secreted by the embryos and adversely affects development. Culturing embryos in small volumes has also been shown to increase viability after transfer (Lane & Gardner, 1992).

1.6.3 Gas environment

In vivo, mammalian oocytes and embryos are exposed to significantly lower oxygen concentrations than contained in atmospheric air. Analysis of over 1000 human follicular fluid aspirates estimated the dissolved oxygen tension between 1.0 and 5.5% (cited in Gardner *et al.* (1996)). The value in the oviducts and uterine horns has been measured from 3 to 5%, and the mean intrauterine oxygen tension as 11.8% air saturation (Ottosen *et al.*, 2006). These conditions continue throughout gestation, such that the whole of organogenesis occurs at low oxygen tension. Low oxygen culture has been shown to enhance *in vitro* preimplantation embryo development in the mouse (Karagenc *et al.*, 2004), sheep and cow (Thompson *et al.*, 1990), goat (Batt *et al.*, 1991) and pig (Watson *et al.*, 1994). However in most IVF laboratories, gametes and embryos are cultured at 5% CO_2 in air (approximately 21% oxygen). Apart from the considerable cost of establishing low oxygen culture,

conflicting information in the literature regarding the benefits of such culture for human embryos has contributed to the reticence of IVF laboratories to switch to low oxygen culture. Although significantly improved morphological score on day 3 has been demonstrated following embryo culture in 5% oxygen, no significant difference in ongoing pregnancy rate was found (Bahceci *et al.*, 2005). Similarly no difference in pregnancy rates were observed whether embryos were cultured at atmospheric or 5% oxygen tension, although a significantly greater number of cells was seen in blastocysts in the low oxygen condition (Dumoulin *et al.*, 1999). Conversely, decreasing the dissolved oxygen tension during all phases of embryo production has been shown to increase blastocyst development and viability (Gardner *et al.*, 1999) and to increase pregnancy rates (Catt & Henman, 2000). More recently a large study of culture to the blastocyst stage in 5% oxygen tension compared with 19% concluded a better blastocyst outcome and significant improvement in pregnancy rates and live birth following low oxygen culture (Waldenstrom *et al.*, 2008).

The detrimental effects of high oxygen culture on mammalian embryo development are mediated through the action of reactive oxygen species (ROS), which are highly active electron acceptors. ROS are generated as a by-product of aerobic respiration during oxidative phosphorylation. Oxygen acts as the terminal electron acceptor in the mitochondrial electron transport chain, and this reduction of oxygen facilitates the conversion of adenosine diphosphate (ADP) to adenosine triphosphate (ATP), providing the cell with energy. ROS are formed during the intermediate steps of oxygen reduction; the superoxide anion radical, hydrogen peroxide and the hydroxyl radical corresponding to the steps of reduction by one, two or three electrons respectively (Burton *et al.*, 2003). The concentration of these molecules depends upon embryo metabolism and environmental oxygen tensions, the relative contribution to damage depending on the species, stage of development and culture conditions.

At physiological concentrations, ROS are involved in intracellular signalling, regulating homeostatic mechanisms and mediating stress responses. Human sperm capacitation induced by biological fluids and progesterone is associated with the production of ROS (de Lamirande *et al.*, 1998a). ROS scavengers reduce or totally prevent the acrosome reaction of capacitated spermatozoa (de Lamirande *et al.*, 1998b). However, an increase in the concentration of reactive oxygen or nitrogen

species beyond the ability of cellular defences to cope leads to indiscriminate damage to lipids, proteins and DNA, perturbation in cellular function and eventually apoptosis or necrosis. ROS induce lipid peroxidations with subsequent effects on cell division and metabolite transport. With oxidative stress the rates of protein disulphide bonds increase within cells, and as a consequence, inactivation of enzymes can occur, such as glyceraldehyde 3-phosphate dehydrogenase that catalyses the sixth step of glycolysis. ROS can also induce nuclear DNA strand breaks (Guerin *et al.*, 2001). As development proceeds, the sensitivity of the embryo to ROS damage decreases (Gardner & Lane, 2005; Karagenc *et al.*, 2004), such that the earliest stages of development - gametes and pre-compaction embryos - are most susceptible, corresponding to the *ex vivo* period of culture during IVF.

An increased production of hydrogen peroxide has been measured in *in vitro* cultured mouse embryos as compared to *in vivo* derived embryos (Goto *et al.*, 1993). Furthermore ROS production in murine (Goto *et al.*, 1993) and bovine (Nagao *et al.*, 1994) embryos increases during culture at atmospheric oxygen. ROS have been implicated in murine embryo arrest and abnormal development (Johnson & Nasr-Esfahani, 1994). A direct relationship between increased hydrogen peroxide levels and human embryo fragmentation has been observed (Yang *et al.*, 1998), with apoptosis occurring only in fragmented embryos, confirmed by the presence of apoptotic bodies and cytoplasmic condensation. ROS in semen have been associated with a reduction in sperm motility and decreased ability for oocyte fusion (Iwasaki & Gagnon, 1992). The two main sources of ROS in semen are the sperm themselves and infiltrated leukocytes. Furthermore, amine oxidases are released by dead spermatozoa and catalyse the formation of hydrogen peroxide. It has been suggested that the use of low oxygen culture may improve the competence of spermatozoa from oligozoospermic patients in IVF (Griveau *et al.*, 1998), and that short insemination times produce human embryos with significantly improved morphology (Quinn *et al.*, 1998). Metallic cations or excess glucose in culture media, ultraviolet light, amine oxidase in serum and uterine infection or inflammation are factors related to IVF procedures and can all contribute to the ROS load (Guerin *et al.*, 2001).

Mitochondrial DNA (mtDNA) is particularly vulnerable to ROS due to the proximity to the site of production of free radicals, the lack of histone protection (which normally quench ROS) and minimal repair mechanisms (Kowaltowski & Vercesi,

1999). One consequence of this damage is that cells shift from oxidative use of pyruvate in the full tricarboxylic acid cycle to use of the portion involving succinate and succinate dehydrogenase. Glutamine can serve as a substrate, via its conversion to 2-oxoglutarate through the action of glutamine transaminase. Thus, in cells subjected to ROS, an increased use of glutamine is observed. Another outcome of damage is a loss of the mitochondrial membrane potential and hence collapse of ATP synthesis. In addition, as mtDNA encodes for enzymes of the respiratory chain, mutations or deficiencies in the production of these enzymes due to free radical damage can lead to further electron leakage, hence compounding the injury. Mitochondrial structure and distribution in arrested mouse embryos is abnormal (Muggleton-Harris & Brown, 1988).

Of great concern are the observations that oxygen tensions are able to alter gene expression. Transcription factors such as nuclear factor κB ($NF\kappa B$), hypoxia-inducible factor (*Hif*)-1, -2 and -3 and the tumour suppressor factor p53 are all affected by free radical concentrations. $NF\kappa B$ is induced by hypoxia (Koong *et al.*, 1994) and knockout of the factor causes embryo lethality in mice (Beg *et al.*, 1995). The α subunit of the *Hif*-1, 2 and 3 is unstable under normoxia but is rapidly stabilised upon exposure to hypoxic conditions. Following heterodimerisation with the constitutively expressed β subunit, *Hif*s activate the transcription of a number of genes involved in maintaining oxygen homeostasis (Wenger, 2000). p53 interacts with *Hif*-1 to provide an alternative protein stabilisation pathway, thought to be involved in hyperglycaemic-induced apoptosis in mouse embryos (Moley & Mueckler, 2000).

Significant differences in gene expression in mouse embryos cultured to the blastocyst stage in 5% compared to 20% oxygen tension have been reported following gene expression array analysis (Gardner & Lane, 2005). Similarly, oxygen-sensitive gene expression in bovine embryos has been described (Harvey *et al.*, 2007a) with significantly lower levels of myotrophin and anaphase promoting complex 1 following culture at 20% compared to 2% oxygen tension. The *Hif*-2 regulated lactate dehydrogenase (Harvey *et al.*, 2007b) and glucose transporter (*Glut*) 1 (Harvey *et al.*, 2004) gene expression are also significantly increased at 2% oxygen tension, with both genes having important roles in embryo development. *Glut1* and *Glut3* along with vascular endothelial growth factor have been shown to be increased in murine

embryos by 2- to 4- fold following culture at 2% oxygen (Kind *et al.*, 2004). An increased cell number at the blastocyst stage, and a global gene expression profile more closely resembling *in vivo* controls has been described in the mouse at 5% oxygen culture compared to 20%, where marked perturbations in the global pattern were observed (Rinaudo *et al.*, 2006). The significance of alterations in gene expression is that the effects might be life-long and are potentially inheritable (De Rycke *et al.*, 2002; Maher *et al.*, 2003; Thompson *et al.*, 2002).

Mammalian embryos have some defence mechanisms against ROS damage, such as the synthesis of enzymes that catalyse the destruction of ROS, although differences exist between species. Transcripts for catalase, CuZn-containing superoxide dismutase (CuZn-SOD), Mn-SOD, glutathione peroxidase (GPX), and glutamylcysteine synthetase (GCS) have been detected in mouse embryos at all stages of development whereas preimplantation cow embryos expressed transcripts for catalase, CuZn-SOD and GPX but not Mn-SOD at any stage (Harvey *et al.*, 1995). These observations suggest that differences in gene expression may contribute to the variation in the ability of embryos of different species to develop *in vitro*. Culture of mouse pronuclear embryos in the presence of CuZn-SOD has been shown to overcome the two-cell block and significantly increase the blastulation rate to 45% when compared with the control rate of 4% without enzyme supplementation (Noda *et al.*, 1991). The addition of anti-SOD antibodies to the culture medium significantly reduced this effect. All these enzymes except for catalase have been detected in human oocytes (El Mouatassim *et al.*, 1999). Reduced glutathione appears to be the main non-enzymatic defence against ROS in embryos, by reducing the environment and also acting as the substrate for GPX (Takahashi *et al.*, 1993). However, the evidence discussed here strongly suggests that the detrimental effects of culture at atmospheric oxygen can overwhelm any defence systems of the mammalian embryo and that subsequent downstream effects manifest.

As for IVF embryo culture, routine stem cell culture is generally undertaken in atmospheric oxygen. Nevertheless hESCs have been shown to grow as well under 3% or 5% oxygen as at 21%, but with markedly reduced levels of spontaneous differentiation at low oxygen tensions (Ezashi *et al.*, 2005). Corroborating results have shown reduced spontaneous differentiation of hESCs, enhanced cell proliferation, and increased plating, freezing and thawing efficiency after maintenance in low oxygen

tension for more than 14 passages (personal communication O. Genbacev). A two-fold mechanism has been suggested, both a direct effect of hypoxia on the hESCs and a hypoxia-induced change in feeder secretory phenotype, with protein arrays showing a difference in the availability of growth factors depending on the oxygen tension. Oxygen tension of 2% has been shown to enhance hESC clonal recovery and significantly reduce the acquisition of spontaneous chromosomal abnormalities (Forsyth *et al.*, 2006). Fluorescence activated cell sorting (FACS) analysis demonstrated that the cells cultured at 2% oxygen were smaller and less complex than those at 21%, indicating a more undifferentiated state.

The combination of an appropriately designed medium reflecting the biology of development, and a suitable gas phase to minimise oxidative damage and mimic *in vivo* conditions has enabled the successful routine culture of human embryos to the blastocyst stage. This not only improves pregnancy rates even with single embryo transfer (Khalaf *et al.*, 2008) but also provides good quality, representative embryos for basic research.

1.7 Sources of embryos for research

The human Embryonic Stem Cell Coordinators' (hESCCO) network was founded in 2005 with a remit to establish a nationwide programme of cooperation in stem cell research that would benefit scientists, practitioners, and hopefully in the future, patients alike, with the creation and development of stem cell lines for research and therapy. The aim of the network is to ensure a thorough and standardised consenting procedure is in place across the country for patients considering donating to research, and to maximise the number of embryos available by identifying clinics that are willing to collaborate with the national stem cell programme, but conduct no in-house stem cell research (Franklin *et al.*, 2008). In formulating the consent forms, there was strict adherence to the Medical Research Council requirements for ensuring consent was fully informed, assuring the ethical provenance of the embryos used from the UK centres participating in this network. This is in stark contrast to the United States National Institutes of Health (NIH) lines. A recent review of the consent forms signed by those who donated embryos for the NIH-approved hESC lines highlighted several problems, questioning the ethical provenance of these lines (Streiffer, 2008). This is

of major concern considering the multitude of international laboratories that use or have used these lines for research. The use of cryopreserved embryos is associated with lesser ethical concerns than 'surplus' fresh embryos (Cornwell, 2006; Sjogren *et al.*, 2004; Stephenson *et al.*, 2009) and the endeavours of the hESCCO network maximise the availability of embryos from this source.

1.7.1 Use of embryos from routine IVF

Embryos used in the study of early development and stem cell research are usually donated by patients undergoing IVF procedures to alleviate infertility. In general these embryos are reported in derivation publications as being 'surplus' to the IVF cycle of the couple, deemed unsuitable for transfer or cryopreservation on day three of development, the most usual time transfer is undertaken (Chen *et al.*, 2005; Lerou *et al.*, 2008; Mitalipova *et al.*, 2003). However, morphology of the embryo on day 3 is not a particularly good indicator of developmental competence of the embryo (Hardarson *et al.*, 2003; Rijnders & Jansen, 1998) nor is it even a good predictor of developmental progression to the blastocyst stage (Graham *et al.*, 2000). Given that the requirement for efficient derivation of hESC is a progressive blastocyst with a visible ICM, embryos considered suitable for derivation attempts are blastocysts which are likely also to be suitable for transfer to patients in their pursuit of pregnancy, or for cryopreservation for their future use. Thus in this context, it is ethically questionable whether the use of 'surplus' embryos for stem cell derivation is in the best interest of the IVF patients trying to maximise their chances of pregnancy. The general shift towards single blastocyst transfer which not only carries excellent prospects for pregnancy (Khalaf *et al.*, 2008), but will address the epidemic of multiple pregnancy following IVF, adds credence to this moral stance. As increasing numbers of patients will choose or be offered extended culture to day 5, day 3 'surplus' embryos will no longer be available even for those research groups willing to use this source. Therefore, certainly in the UK, the ethical source of embryos for research is likely to shift to those embryos that have been cryopreserved for future use by the patients who then decide they no longer wish to use them in treatment, or to the use of embryos unsuitable for transfer following PGD for serious genetic disease. In other countries, legislation and funding conditions are in place that restrict the use of human embryos regardless of the source, reflecting fundamental objections by some

people to any embryo research (Alikani, 2007), although privately funded research using human embryos does occur.

1.7.2 Use of embryos from PGD

During PGD a representative cell is removed from an IVF generated embryo, and tested for a specific genetic defect prior to implantation. Only embryos found to be unaffected by the genetic disorder, or to be carriers without clinical consequences in the case of recessive diseases, are suitable for replacement into the patient, or for cryopreservation for their later use. Blastomeres are tested using either polymerase chain reaction (PCR) in single gene disorders, or fluorescence *in situ* hybridisation (FISH) for sex-linked diseases or translocations. The development of preimplantation haplotyping (PGH) as a universal method of amplifying and testing DNA from single cell biopsies has improved the reliability of the assay and eased the development process of tests for new disorders (Renwick *et al.*, 2006).

Embryos found unsuitable for replacement because they are at high risk of transmitting a genetic disorder would normally be discarded, despite often being of good progressive quality and capable of forming blastocysts. These blastocysts are suitable for stem cell derivation, and are free from the ethical difficulties associated with using 'surplus' embryos from patients seeking infertility treatment (Cornwell, 2006). For those individuals with a fundamental objection to embryo research however, these embryos are no less problematic.

1.7.2.1 Induced pluripotent stem cells

While the number of diseases able to be screened with PGD is ever growing, stem cell models of some late onset degenerative diseases such as Parkinsons, motor neurone disease or Alzheimers, for which no single predictive gene has been identified, will not be available through PGD. Successful reprogramming of human somatic cells into a pluripotent state would allow the creation of disease-specific stem cells for a huge range of human diseases. Furthermore, such technology would enable the production of patient-specific cells, which are required to fully exploit the application of stem cell therapy. The induction of pluripotent stem (iPS) cells from adult human fibroblasts by defined factors has been achieved (Takahashi *et al.*, 2007) and validated in multiple labs (Aoi *et al.*, 2008; Park *et al.*, 2008; Yu *et al.*, 2007).

Haematopoietic progenitors obtained *in vitro* from autologous iPS cells have been shown to rescue a humanised sickle cell anaemia mouse model (Hanna *et al.*, 2007). The proof of principle that iPS cells can be generated directly from elderly patients with the chronic disease amyotrophic lateral sclerosis using material that has been exposed to disease-causing agents for a life-time has been reported (Dimos *et al.*, 2008). Indeed, all of the advantages of using PGD hESC as disease models also apply to the use of iPS cells with the added attraction of a greater number of diseases, the easier availability of starting material, the use of samples from the diseased tissue and from donors in the age range when the disease occurs. However, there are serious drawbacks with the current methods of iPS production such as the use of a retrovirus for gene insertion and proto-oncogenes to encourage proliferation. In one study 20% of mice created by germline transmission of iPS cells developed tumours attributable to reactivation of *c-Myc* (Okita *et al.*, 2007). Although these are likely to be temporary issues, further studies are essential to determine whether human iPS cells can replace hESC in therapeutic applications.

1.8 Human embryonic stem cell derivation

The first method for establishing hESC lines was the use of immunosurgery to isolate the ICM by complement-mediated lysis of the TE cells (Solter & Knowles, 1975). Subsequently derivation has been achieved following isolation of the ICM mechanically with needles (Amit & Itskovitz-Eldor, 2002; Strom *et al.*, 2007) with a laser (Turetsky *et al.*, 2008) or following whole plating of the blastocyst (Findikli *et al.*, 2005; Heins *et al.*, 2004; Suss-Toby *et al.*, 2004) or morula (Strelchenko *et al.*, 2004) with subsequent isolation of cells with stem-like morphology. Methods to derive from apparently arrested embryos (Feki *et al.*, 2008; Gavrilov *et al.*, 2009; Zhang *et al.*, 2006), to increase ICM cell number before derivation (Stojkovic *et al.*, 2004) and to tailor derivation to the quality of the blastocyst (Kim *et al.*, 2005; Stephenson *et al.*, 2006) have been discussed. Further developments include the derivation from single eight-cell (Klimanskaya *et al.*, 2006) and four-cell (Feki *et al.*, 2008) blastomeres. In an attempt to circumvent research restrictions, mainly in the USA, methods to derive lines without the destruction of embryos have been developed.

These include genetically modifying mouse embryos to make implantation impossible (Meissner & Jaenisch, 2006), taking a single cell for derivation and culturing the parent embryo on to the blastocyst stage (Chung *et al.*, 2006; Klimanskaya *et al.*, 2006), using parthenogenetically activated oocytes (Revazova *et al.*, 2007) or triploid oocytes which have had pronuclear reduction, although many disagree with such tactics (Mertes *et al.*, 2006).

1.8.1 PGD and human embryonic stem cell derivation

Due to their fundamental attributes of unlimited expansion and pluripotency, the potential of hESCs with mutations significant to human disease has provoked substantial interest as an unlimited source of cells for study of the disease (Stephenson *et al.*, 2009). HESC lines have been derived with a number of monogenic disorders including cystic fibrosis (CF) (Pickering *et al.*, 2005), myotonic dystrophy type 1, Huntington disease (HD) (Mateizel *et al.*, 2006), adrenoleukodystrophy, fragile-X syndrome and thalassaemia (Verlinsky *et al.*, 2005).

The suitability of ESC as models has been validated for CAG repeat diseases, the most common of which is HD. Research has shown that mESC expressing long CAG motifs were able to differentiate into neurons, but were characterised by stunted neurite outgrowth, low efficiency of neuronal formation, and decreased survival during differentiation (Lorincz *et al.*, 2004). Similarly, the generation of a spinal muscular atrophy (SMA) cell-based assay provided a promising new primary cell source for assays of new therapeutics for neurodegenerative diseases (Wilson *et al.*, 2007). The generation of a pure population of lung alveolar epithelial type II cells derived from hESC for the study of CF has been reported (Wang *et al.*, 2007). HESC, particularly those carrying clinically relevant mutations, have also gained considerable interest from the biopharmaceutical sector (Gorba & Allsopp, 2003; McNeish, 2007). The current pharmaceutical discovery process is universally accepted as being time consuming and inefficient with an accompanying high financial burden. Improvements to the discovery phase of new compounds will come through the application of more appropriate, disease-orientated cellular screens, for both therapeutic target validation and optimisation of compounds following their discovery via high-throughput screens (HTS) (Ashton *et al.*, 2007). In HD studies, HTS have been designed to isolate compounds that inhibit stages of protein misfolding and aggregation, with

one identifying the benzothioazoles as a potentially interesting class of compounds in a anti-aggregation screen (Heiser *et al.*, 2002). Within the toxicological field ESC are already being utilized (Pouton & Haynes, 2007). HESC carrying known mutations will also be important for exploring pathophysiological effects produced by gene-dosage anomalies and how these might in the future be addressed to ameliorate the phenotype in conditions such as trisomy 21 (Peura *et al.*, 2008). In diseases with complex genetic pathology such as HD or Duchenne's muscular dystrophy (DMD), or those diseases with different causative mutations such as CF, several lines with different naturally occurring mutations/variations could be derived and their pathophysiology compared.

However it is important to address basic but crucial questions with regard to the use of hESC (or iPS cells) in disease research. Bearing in mind the late onset of diseases such as HD, it is essential to assess whether neurons and neuroprogenitors differentiated *in vitro* from HD-hESC faithfully express HD phenotypes. Similarly it needs to be confirmed that muscle cells differentiated *in vitro* from, for example, DMD-hESC faithfully express their phenotypes. Furthermore it must be established whether these differentiated cells are equivalent or superior to animal disease models, and whether they accelerate clinically-relevant drug discoveries. HESC from PGD embryos should represent an even more relevant model than genetically engineered ESC or animal models as the mutant protein is expressed in its normal physiological context and range of expression pattern (Stephenson *et al.*, 2009). Therefore the importance of the continued use of PGD embryos to generate lines carrying clinically relevant diseases should not be underestimated.

1.9 Human embryonic stem cell culture

The efficiency of hESC derivation and the suitability of the resultant cells for clinical application is dependent on the fundamental limitation of the quality of the embryo as well as the quality and specification of the culture system in which the cells are grown. Current culture systems most commonly rely on feeder cell support or the use of conditioned medium to maintain undifferentiated growth of hESC. Further consideration of the culture systems employed for hESC are discussed in Chapter 4.

1.9.1 Feeder cell systems

Primary MEF feeder cells (Thomson *et al.*, 1998), immortalised mouse fibroblasts (Choo *et al.*, 2006) or a fibroblast cell line (STO) (Park *et al.*, 2003) can support the undifferentiated growth of murine, bovine, primate, and human embryonic stem cells. However, animal pathogens or immunogenic molecules can be transferred from animal feeders to hESC which renders them unsuitable for therapy (Cobo *et al.*, 2005; Martin *et al.*, 2005). Primary MEFs senesce by passage 5 limiting the batch size available from one preparation. Alternatives such as human fetal muscle (Richards *et al.*, 2003), fetal skin (Richards *et al.*, 2003), human placental fibroblasts (Genbacev *et al.*, 2005) human adult fallopian tube epithelial cells (Richards *et al.*, 2003), human adult uterine endometrial cells (Lee *et al.*, 2005), human adult breast parenchymal cells (Lee *et al.*, 2004) and human neonatal foreskin (Hovatta *et al.*, 2003), have all been tried but all have associated problems of procurement, growth and validation, as well as varying success in maintaining undifferentiated growth of hESC. A report of xeno-free production of foreskin fibroblasts still included the use of human serum (Meng *et al.*, 2008). Feeder cells derived from hESC themselves have been grown, immortalised and used successfully in culture (Stojkovic *et al.*, 2005; Wang *et al.*, 2005; Xu *et al.*, 2004). However the suitability of this source is predicated on the production of a clinical grade hESC line with which to obtain such feeders. Proteomics and transcriptome profiling are being used to try to identify the factors in serum and secreted by feeders that support the derivation and propagation of hESC (Chin *et al.*, 2007; Kueh *et al.*, 2006; Prowse *et al.*, 2005; Skottman *et al.*, 2006b). Whilst a feeder-free derivation system is desirable, there has been limited success to date. BD Matrigel^{TM} has been used to culture hESC in a feeder-free environment but is a solubulised basement membrane preparation extracted from mouse sarcoma, and conditioned medium is required for undifferentiated growth (Xu *et al.*, 2001). Extracellular matrix components have been tested as culture surfaces but often prove inferior to traditional feeder culture (Amit *et al.*, 2004; Richards *et al.*, 2002). Clinical grade derivation of new hESC lines has been achieved with qualified fetal calf serum (Crook *et al.*, 2007). Many alternative feeder sources are tested by ability to support existing hESC lines not derivation of new hESC lines, although

the ultimate requirement for a culture system must be to support the growth of the inner cell mass onwards (Klimanskaya *et al.*, 2005).

1.9.2 Media composition

Original culture media for hESC derivation contained fetal calf serum (FCS), as well as conditioned medium from a variety of cell types. Due to the unreliability of serum batches and the unsuitability for clinical use, other media options have been investigated. Approaches to circumvent the use of animal serum and other animal-derived products are being developed with the aim of being able to create a true xeno-free culture system (Ellerstrom *et al.*, 2006; Hewitt *et al.*, 2007; Ludwig *et al.*, 2006; Mallon *et al.*, 2006; Rajala *et al.*, 2007). Knock-out serum replacement (KOSR) is a popular alternative to FCS, however it contains AlbuMAX™ which is a lipid-rich albumin fraction of bovine serum and bovine transferrin, and therefore, although better defined than FCS, is not xeno-free (Price *et al.*, 1998). Plasmanate® has been tested as another alternative (Klimanskaya *et al.*, 2005). A complete formulation of a defined medium successfully used to derive new hESC lines is available (Ludwig *et al.*, 2006). A comprehensive study of various xeno-free media concluded that none of those tested were as effective at culturing hESC as the conventional KOSR system (Rajala *et al.*, 2007). Several commercially available proprietary media which claim various levels of clinical suitability and efficacy are becoming available e.g. hEScGRO™ (Chemicon), StemPro® (Invitrogen) and mTeSR™ (Stem Cell Technologies). The use of animal enzymes for passaging is also a concern, not only as a xeno-component, but also as an agent in driving karyotypic change (Mitalipova *et al.*, 2005). Whilst manual passaging is labour-intensive and unsuitable for large scale culture, automated manual passaging may be an alternative (Joannides *et al.*, 2006).

Growth factors are an essential component of medium, particularly in the absence of serum. Basic fibroblast growth factor was identified as supportive to undifferentiated hESC growth (Koivisto *et al.*, 2004) even without conditioned medium (Xu *et al.*, 2005). Feeder-secreted heparin sulphate proteoglycans (HSPG) can stabilise bFGF and mediate binding of the growth factor to the hESC surface (Levenstein *et al.*, 2008). Although further supplements were needed to return the proliferation

rate to normal, activin A has been shown to maintain pluripotent growth in the absence of feeder layers or conditioned medium (Beattie *et al.*, 2005) through the induction of pluripotent gene expression (Xiao *et al.*, 2006). Brain-derived neurotrophic factor (BDNF), neurotrophin (NT)3 and NT4 also mediate hESC survival, and their addition to cell cultures improves clonal survival (Pyle *et al.*, 2006). Albumin-associated lipids stimulate hESC self-renewal (Garcia-Gonzalo & Belmonte, 2008) and the addition of Wnt1 promotes undifferentiated colony growth (Villa-Diaz *et al.*, 2008). As the signalling pathways maintaining hESC in an undifferentiated state are increasingly understood, exogenous supplementation of defined factors could circumvent the current need for undefined feeder or matrix co-culture systems.

1.9.3 Good manufacturing practice and clinical grade lines

The importance of complete validation of any stem cells destined for therapy cannot be underestimated. History demonstrates that infection from donated tissue is possible and devastating. The first case report documenting the transmission of HIV during blood transfusion appeared in 1983 (Ammann *et al.*, 1983). In 1988, 128 women were exposed to the hepatitis B virus via contaminated donor serum that had been added to IVF culture media. Seventy nine women were infected but no serious forms of hepatitis developed either in them or the children born from the treatment (Quint *et al.*, 1994). Prion diseases can also be transmitted via tissue and blood donation (Llewelyn *et al.*, 2004). The use of bovine serum in culture carries the risk of transmission of a number of bovine viruses including bovine polyomavirus, bovine adenovirus and rabies, as well as prion particles. Using murine feeder cells can transmit certain viruses shown to be capable of infecting humans such as Sendai virus, reovirus type 3 and lactic dehydrogenase virus (Cobo *et al.*, 2005). Unlike conventional donation where blood or tissue from one donor may be transplanted to two or three patients, the expansion of stem cell cultures could allow a single hESC line to be used for hundreds, if not thousands of patients. The risk of disease transmission from a single infected donor thus increases exponentially (Braude *et al.*, 2005).

Good manufacturing practice (GMP) is that part of quality assurance, already in use in the pharmaceutical industry, which ensures that products are consistently produced and controlled to the quality standards appropriate to their intended use and

as required by the product specification. GMP is concerned with both production and quality control and these standards are applied to clinical-grade hESC derivation and culture. GMP requires that production occurs in a cleanroom, which is a room in which the concentration of airborne particles is controlled, and which is constructed and used in a manner to minimise the introduction, generation, and retention of particles inside the room, and in which other relevant parameters, e.g. temperature, humidity, and pressure, are controlled as necessary (ISO standard 14644-1). GMP also requires traceability of all raw materials and also that every step of production follows validated standard operating procedures. It is also imperative to realise that clinical-grade lines are not the final product. Once cell lines have been established, validated scale-up, expansion and differentiation protocols will be required to generate a product that may be used for clinical trials. The use of hESC therapeutically must also conform to the standards of the Human Tissue Authority (HTA).

1.10 Embryo development II: Mechanisms of blastocyst formation

One of the fundamental questions in developmental biology is how a single cell - the fertilised oocyte - can give rise to embryos and then animals with distinct developmental axes; front, back, top and bottom. There is much controversy in the developmental literature about the timing of the origins of these axes in mammals. In lower vertebrates and invertebrates, developmental polarity is evident from the oocyte and cleavage stage embryos where unique protein domains, concentration gradients, and asymmetric protein distributions are the principle forces establishing the identity and fate of individual cells during early development. For example, the sea urchin is characterised by a strict oocyte polarity and invariant cell lineages (Davidson, 1989). When embryos are separated into animal and vegetal halves, the vegetal halves develop into complete animals, whereas the animal halves form blastula-like structures, and fail to undergo gastrulation.

Similarly, the cytoskeleton and organelles of ascidian eggs are organised along a pre-existing animal-vegetal (A-V) axis (Roegiers *et al.*, 1995). Fertilisation triggers a cortical contraction that causes the relocalisation of pre-existing cytoplasmic domains, which place cell fate determinants in specific areas of the zygote prior to

the first cell division. The initiation site and orientation of the cortical reaction is dependent on the sperm entry position.

In Drosophila, asymmetric RNA localisation is essential for patterning the embryo and partitioning the embryonic cytoplasm into future somatic and germline lineages (Steinhauer & Kalderon, 2006). This process begins in the oocyte, where key RNAs are restricted to specific cortical regions. Localization of specific mRNAs to the anterior and posterior regions of the oocyte establishes the anterior-posterior (A-P) and the dorsal-ventral (D-V) axis.

Conversely, early mammalian development is highly regulative and oocytes of eutherian mammals seemingly differ from those of virtually all other animals by having no obvious functional polarity. Consequently axis formation has historically been treated as being independent of any aspect of organisation of the oocyte. Instead, cell fate was assumed to be established with the first visible morphological evidence of polarity at the blastocyst stage, where the ICM and TE cells can be distinguished and the embryonic-abembryonic (em-ab) axis forms through the ICM (the regulative model). However, emerging evidence from diverse experiments brought this assumption into question and resulted in the proposal that the axes are present from the oocyte onwards, but are not fixed until the blastocyst stage (the prepatterning model).

Should the organisation of the oocyte or zygote be prepatterned, this leads to the possibility that the blastomeres formed from the first cleavage divisions could have qualitatively or quantitatively differential inheritance of determinants that could influence the fate of their progeny. Thus, early cleavage blastomeres may not be truly equivalent, but instead have a patterning bias that is still sufficiently adaptive to compensate for pertubations in development.

1.10.0.1 *In vivo* development of isolated blastomeres

Experience with farm and laboratory mammals has shown that application of embryo splitting, at whatever developmental stage it is performed, generally does not disturb ongoing embryo development. Split embryos have a smaller than normal number of cells present during early cleavage, but offspring are normal in size because regulation of cell number occurs after the time of blastocyst formation (Tarkowski, 1959).

The ability of isolated blastomeres, either singly or in pairs, from 2-, 4-, 8-, and 16-cell stage embryos to support term pregnancies and to produce genetically identical animals has been documented in the mouse (Papaioannou *et al.*, 1989), rat (Matsumoto *et al.*, 1989), pig (Saito & Niemann, 1991), horse (Allen & Pashen, 1984), sheep (Willadsen, 1979) and cow (Johnson *et al.*, 1995; Willadsen *et al.*, 1981).

The usual outcome in the production of monozygotic offspring is singletons or twins, such as the production of monozygotic twins following splitting of sheep two-cell embryos (Willadsen, 1979). There is however, one report of four identical calves being produced following the split of a four-cell bovine embryo into single blastomeres (Johnson *et al.*, 1995). The blastomeres, placed in donor zona pellucidae and co-cultured on bovine epithelial cells until gastrulation, were transferred in pairs and resulted in four genetically identical bulls as evidenced by genetic and mitochondrial fingerprinting. In contrast, whilst the successful implantation of all four single blastomeres from a four-cell mouse embryo has been reported, no full-term development resulted (Rossant, 1976). This could be explained by the small size of the resultant embryos, rather than inherent inability of the quarter blastocysts to develop to term. While pregnancies have been established following two-cell blastomere separation of Rhesus monkey embryos, only singleton offspring have resulted, regardless of whether split embryos were transferred together to the same recipient or separately to different recipient monkeys (Chan *et al.*, 2000; Mitalipov *et al.*, 2002).

Certainly it is known that human embryos are highly regulative, with successful compensation for loss of blastomeres seen on a daily basis in routine IVF. Normal term births are achieved following transfer of embryos sustaining cell death following thaw cycles, or loss of cell number following biopsy of one (or occasionally two) blastomere(s) for PGD. Indeed one case study is published describing normal ongoing pregnancy following the transfer of a day two embryo with only one cell intact following thaw (Veiga *et al.*, 1987) with subsequent term birth of a healthy male infant (A. Veiga, personal communication).

This astounding regulative ability has been used as the cornerstone of the argument that the early blastomeres of mammalian embryos are identical, with no specification of cell fate. However, accumulating observations that were difficult to

reconcile with a model of initially naive blastomeres required a reassessment of this assertion.

1.10.0.2 Models of establishment of polarity

After compaction, the mammalian embryo starts to form the blastocoel cavity, and morphologically recognisable differentiation to ICM or TE cells takes place. The localisation of the ICM to one side of this cavity marks the first appearance of the em-ab axis. Therefore this differentiation into ICM or TE is closely linked to the specification of the blastocyst em-ab axis. Three main hypotheses have been put forward to explain the differentiation of fate by seemingly naive blastomeres.

The 'inside-outside' theory (Tarkowski & Wroblewska, 1967) suggested that the fate of the blastomeres depended on their position within the morula, in which the inside and outside cells exist in different conditions. The outside cells become flattened and form predecessors of the TE while the inside cells develop in a micro-environment created by the outside cells and in this environment become the precursors to the ICM. This hypothesis accounts for the observation that when isolated mouse four- and eight-cell blastomeres are cultured on, they usually form trophoblastic vesicles. Presumably, given the reduction in cell number, there is insufficient cellular mass to enclose inner cells and provide the environment for ICM formation. However the influence of the blastocoel microenvironment on development was investigated by injecting eight-cell and morula stage embryos into the blastocoel of giant chimeric blastocysts (Pedersen & Spindle, 1980). Two-thirds of the donor embryos that were injected developed into morphologically normal blastocysts, despite being within the host blastocoel, showing that the constituents of the blastocoel did not alter early morphological development. Furthermore the inner cells of a morula have been shown to form both ICM and TE, whereas the outer cells form TE only (Fleming, 1987). Subsequent observation that the outer cells become polarised due to their location led to an alternative theory - the polarisation hypothesis.

The polarisation hypothesis (Johnson & Ziomek, 1981a) expanded on grounds laid by the inside-outside theory to consider the initiation of polarity of individual blastomeres at the eight cell stage. Each blastomere undergoes major reorganisation in which it becomes structurally and functionally polarised, induction of which is influenced by cell contact (Ziomek & Johnson, 1980), and polarity is conserved

during division of the blastomere. Subsequent divisions of these blastomeres are either meridional, generating identical daughter cells, or equatorial, thus producing daughter cells of two distinct populations as a result of inheritance of distinctive regions of the cytoplasm and membrane, termed polar (TE) and apolar (ICM) as shown in Figure 1.1. Various supporting experimental data exist, including cell surface distribution of microvilli (Nikas *et al.*, 1996), the influence of cell contact on orientation of division (Pickering *et al.*, 1988), the cue to initiate polarisation (Pratt *et al.*, 1982), the influence of division order (Surani & Barton, 1984) and the effect of intercellular contacts (Garbutt *et al.*, 1987).

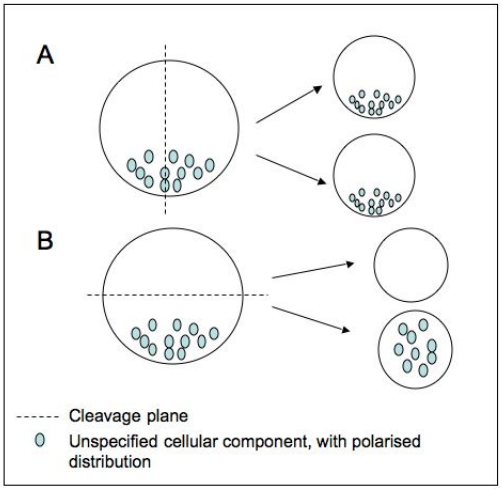

Figure 1.1: Schematic to illustrate the generation of polar or apolar cells from the division of a polarised blastomere. (A) Meridional division of a polar blastomere generates two identical polar daughter cells inheriting the same polarised distribution of the cytoplasm. (B) Equatorial division of a polar blastomere generates two apolar cells with differential inheritance of the polarised cytoplasm.

Both the inside-outside and polarisation theories attributed the differentiation to ICM or TE as being a response to environmental cues during development. However, the theories did not address the formation of the em-ab axis, namely why the ICM and blastocoel cavity form at opposite poles. While the early theories considered the diversification of individual blastomeres, they did not encompass the organisation of the embryo as a whole.

The cleavage-driven theory (Edwards & Beard, 1997; Gardner, 2001; Piotrowska & Zernicka-Goetz, 2001), was proposed to accommodate a hypothesis of how overall

patterning of the embryo arises. The theory suggests that the lineage fate of a cell is decided before cell positioning, polarisation or morula formation, and is determined by the earliest cleavage planes. Thus the first cleavage separates the zygote into halves that have different destinies, and differing composition or behaviour of blastomeres along the future axes of the embryo results in the overall polarised form of the blastocyst. The theory does not therefore preclude the influence of the environment to direct blastomere differentiation into ICM or TE, as the em-ab boundary is proposed to lie deep within the ICM and therefore each blastomere is expected typically to form both ICM and TE derivatives. Whilst there is accepted experimental verification of the polarisation theory for the formation of TE or ICM fate, there is a divide between biologists who argue for the cleavage-driven theory and hence that prepatterning exists from the zygote, and those that argue for the regulative model of development where the first axis of polarity forms at the blastocyst stage. The underlying mechanisms responsible for the development of morphologically apolar oocytes to overtly polar blastocysts is unclear. However, a multitude of elaborate and tenacious experiments have been designed to address this issue.

1.10.1 Mammalian oocyte polarity

1.10.1.1 Oocyte axes

A decisive experiment that called into question the regulative model was the demonstration that the early blastocyst is bilaterally symmetrical (Gardner, 1997). It was suggested that the long axis of symmetry was predicted by the A-V axis of the zygote, with the animal pole defined by the second polar body as an enduring marker. As well as being aligned to the A-V axis, the long axis of symmetry was orthogonal to the em-ab axis, which bisects the ICM and opposing mural TE, as shown in Figure 1.2. The majority of second polar bodies that survive intact to the early blastocyst stage therefore lie at the em-ab junction. This led to the suggestion that the specification of the axes of the blastocyst depended on the spatial patterning of the zygote.

By marking sites in the embryo with oil drops in the zona pellucida, and culturing free, gel-embedded or zona-thinned two-cell embryos to the blastocyst stage, subsequent results from the same laboratory suggested that the em-ab axis of the blastocyst and its plane of bilateral symmetry are also normally orthogonal to the

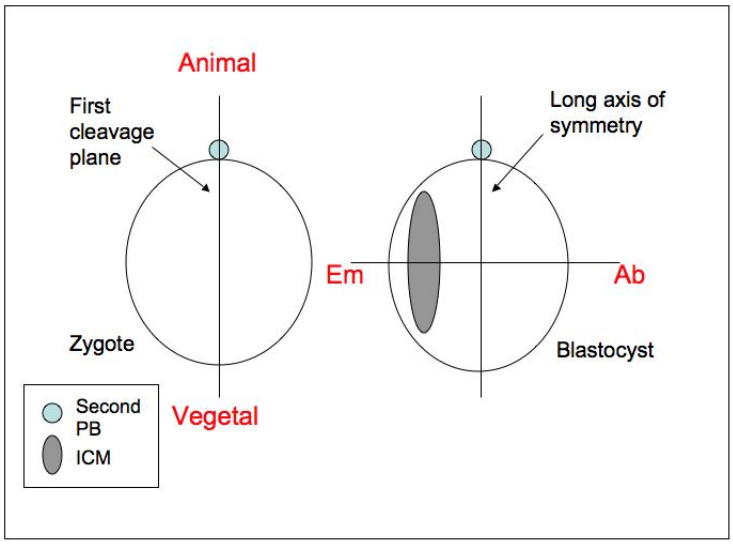

Figure 1.2: Schematic of the axes described in mammalian zygotes and blastocysts. The long axis of symmetry of the blastocyst maps onto the first cleavage plane, which itself is parallel to the A-V axis. The em-ab axis and bilateral plane are orthogonal to the plane of first cleavage.

plane of first cleavage (Gardner, 2001). As the long axis of symmetry maps to the A-V axis, these results further indicated that the axes of the blastocyst are already specified by the onset of cleavage. Furthermore the axes of the blastocyst have been implicated in establishing those of the fetus by a series of experiments using mRNA encoding an enduring marker to track the progeny of the ICM into the post-implantation visceral endoderm (Weber *et al.*, 1999). The visceral endoderm cells that originated near the second polar body were found distally in the egg cylinder, whereas those opposite the second polar body were found proximally. This raised the suggestion that the bilateral symmetry of the blastocyst, therefore by implication the axes of the zygote predict the proximodistal axis and hence polarity of the later conceptus.

Fundamental supporting evidence to the morphological studies regarding zygote axes would be the elucidation of any determinants, essential for development, that are distributed asymmetrically or along a concentration axis within the ooplasm. Following several unsuccessful or disputable attempts to visualise such gradients (reviewed in Edwards & Beard (1997)), an asymmetric distribution of the cytokine leptin and the signalling molecule STAT3 to the animal pole of the mouse and human

egg was reported (Antczak & Van Blerkom, 1997). Further work by these researchers suggested the polarised distribution of several other proteins in the human oocyte and embryo, including the growth factors TGFβ2 and VEGF, growth factor receptors c-KIT and EGF-R and apoptosis-associated proteins BCL-X and BAX (Antczak & Van Blerkom, 1999).

These suggestions appeared inconsistent with published reports that removal of either the animal or vegetal pole of the murine oocyte, or the creation of chimeras composed of either only animal or vegetal 8-cell blastomeres (all defined in relation to the second polar body) resulted in live, fertile offspring (Ciemerych *et al.*, 2000; ZernickaGoetz, 1998). This could be interpreted as implying that the bilateral symmetry of the blastocyst is independent of axial information in the ooctye. However the authors concluded that while the A-V axis of the murine oocyte predicts the polarity of the em-ab axis in the blastocyst, if determinants of polarity are localised uniquely to the animal or vegetal poles of the oocyte, they are not absolutely required for development. However, there could also be a morphogenetic gradient in the oocyte which relies on the relative not absolute concentration of a morphogen. In this way, a gradient would still exist after removal of one pole. These experiments are also a clear demonstration of the regulative capabilities of mammalian embryos, which enable normal development patterns to resume following perturbation.

Taken together these experiments suggest that even if the definitive axes of development only become irreversible at implantation, the axes of polarity can be traced back to the zygote, with perturbations in development being overcome by the regulative capability of the early embryo. This, therefore, aligns mammalian development with that of some other vertebrates. As a substantial minority of oocytes and embryos in each experiment did not conform to the predicted model, and until these are shown to be incompatible with development, it seems that any oocyte organization is facilitatory rather than determinative for future polar axes. However, these early experiments incited a flurry of responses rejecting the conclusions and asserting that no early patterning in the oocyte or cleavage embryo exists.

1.10.1.2 First cleavage division

The second polar body was used as a stationary marker of the animal pole in several early studies (Gardner, 1997, 2001; Plusa *et al.*, 2002), but the validity of this has

been called into question (Hiiragi & Solter, 2004; Kurotaki *et al.*, 2007; Motosugi *et al.*, 2005). Using time-lapse recording of the first cleavage in murine embryos, it has been stated that the second polar body does not mark a stationary animal pole, but instead moves towards the cleavage furrow in half of the embryos studied (Hiiragi & Solter, 2004). It should be noted that half of the original cohort of embryos was excluded from analysis as movement of the second polar body could not be clearly determined from the videos. Some studies not only concluded that the second polar body is mobile on the surface of the embryo, but that the embryos rotated within the zona (Kurotaki *et al.*, 2007; Motosugi *et al.*, 2005). From these experiments, the authors concluded that the first cleavage plane is not predetermined in the oocyte, and that an A-V axis does not exist. However, the robust validation in early studies is difficult to refute, as it has been shown that the second polar body remains physically tethered to its site of production and therefore marks the animal pole of the zygote for as long as it survives (Gardner, 1997).

1.10.1.3 Pronuclear apposition

Instead, it has been suggested that the first cleavage of the mouse zygote is defined by the topology of the two apposing pronuclei (Hiiragi & Solter, 2004). In 18 from 25 embryos in this study, the cleavage plane was defined by the two apposing pronuclei, which also bisected the shortest arc between the second polar body and the sperm entry position. Further experiments where the male pronucleus was removed and replaced with a male or female pronucleus at the opposite side of the zygote (thereby creating a new topology between the pronuclei) showed that the cleavage plane still occurred through the apposition of these pronuclei, and suggested that the sperm does not play a part in specification. A further experiment with a small cohort of embryos was also alluded to, in which parthenogenetically activated embryos also conformed to this model.

However, in a directly contradictory report, such patterns of cleavage as described above were seen only in selected groups of embryos that had been chemically treated before analysis, or had undergone a shape change such that the pronuclei lay on the long axis of the zygote. Instead, in elegant time-lapse observations of the first cleavage on multiple focal planes, in over 60% of zygotes the two pronuclei were aligned with the second polar body and the cleavage furrow formed within 30° of

this plane (Plusa *et al.*, 2005). The authors suggest the previous conclusion that the first cleavage does not relate to the second polar body could be due to the analysis of only those embryos in which the pronuclei lay on the same focal plane, after half the embryos had been discarded.

1.10.1.4 Sperm entry position

The relevance and influence of the sperm entry position (SEP) is perhaps the most contentious of the theories proposed for the determination of polarity, causing disagreements even between groups that advocate the prepatterning theory. It has been proposed that the SEP predicts the plane of initial cleavage (and therefore by implication the blastocyst axes), and that the blastomere inheriting the SEP at cleavage acquires a division advantage and contributes preferentially to the embryonic region of the blastocyst (Piotrowska & Zernicka-Goetz, 2001). This agrees with evidence from other species for a role of the sperm in axis formation as discussed. However, this conclusion was refuted in a series of experiments showing that the use of phytohaemagglutinin (or similar) to mark the SEP was invalid, as lectin-based markers did not bind to the fertilisation cone, rather they did bind strongly to the zona (Davies & Gardner, 2002). By labelling the anterior end of the sperm tail (AnT) with an oil drop in the zona, or observing it directly, it was demonstrated that the AnT remained associated with the midpiece. The group then mapped the angle of departure of the AnT from the centre of the cleavage plane and concluded that there was no correlation between sperm entry and first cleavage. A response followed in the same year showing that direct sperm labelling, rather than marking the fertilisation cone with a bead, showed an even more precise correlation with first cleavage, rising from 60% to 88% of embryos (Plusa *et al.*, 2002). However, time-lapse recordings of the second cleavage concluded that the blastomere inheriting the SEP divided first in only half the embryos studied (Motosugi *et al.*, 2005). In addition, the development of diploid parthenogenetic embryos through gastrulation, or artificial digynic zygotes to the blastocyst (Hiiragi & Solter, 2004) suggests that any role of the sperm in axis formation is perhaps dispensable. If there is a need for the sperm in specification of the cleavage plane, it is not known whether the signal must be long-lasting (persisting to the formation of the cleavage furrow) or transient (to initiate downstream events).

However, experiments in which mixing of clonal descendants occurred following removal of the SEP region after pronuclear migration is interpreted as suggesting an enduring influence of the spermatozoa (Piotrowska & Zernicka-Goetz, 2002). Furthermore when studying the development of parthenogenetic embryos, in contrast to fertilised oocytes, there was no tendency for the two-cell blastomeres to follow different fates throughout development (Piotrowska & Zernicka-Goetz, 2002). This was interpreted as indicating that in normal development, fertilisation is one contributing factor in initiating embryonic patterning.

1.10.1.5 Bilateral symmetry

In an elegant series of experiments, the bilateral plane of symmetry of mouse zygotes was marked by spaced oil drops in the zona, and rotation of the zygotes within the perivitelline space prevented by the injection of alginate. Subsequent monitoring of development to the blastocyst stage demonstrated that the first cleavage was almost invariably orthogonal to the bilateral plane of symmetry, and further confirmed that the em-ab axis of the blastocyst aligned with this plane of symmetry (Gardner & Davies, 2006). The first cleavage was more variable with respect to the A-V axis than to the bilateral plane of symmetry. The removal of the zona did not change this relationship, arguing against the mechanical constraint of the zona dictating cleavage and axes formation (see below). That the bilateral plane of the blastocyst was consistently aligned with that of the zygote strengthened the case for the existence of prepatterning from the zygote stage.

1.10.1.6 Zona pellucida shape

It has been argued that when the zona is ellipsoidal rather than spherical, it provides sufficient mechanical restraint to force the em-ab axis of the blastocyst to align with its greatest diameter, thus the em-ab axis is not specified until blastulation (Motosugi *et al.*, 2005). Furthermore, from studies using time-lapse imaging of transgenic mouse embryos it has been asserted that the first cleavage plane and em-ab axis of the blastocyst aligns relative to the ellipsoidal shape of the zona (Kurotaki *et al.*, 2007). The results also describe continuous movement of the embryo within the zona pellucida, which slows at the morula stage, leading to the conclusion that there is not a fixed axis or a characteristic cleavage pattern in early development.

In direct contradiction of these results however, it has been shown that cells lying under the lesser zona diameter map consistently towards the equatorial region of the blastocyst, significantly more frequently than randomly labelled cells (Gardner, 2007). This occurred regardless of whether the zona was left intact, was softened, or removed altogether. The non-random mapping of cells following zona removal questions whether it can play any role in specifying cleavage.

1.10.1.7 Actual cleavage

One study suggested that the first cleavage itself predicted the blastocyst axis, such that the em-ab axis specification occurs with respect to the first cleavage plane whether or not it passes through the A-V axis (Plusa *et al.*, 2005). By artificially elongating embryos as described above, it was shown by non-invasive lineage tracing with lipophilic dyes that even when first cleavage occurred along the short axis, the progeny of the resulting two cell blastomeres tended to populate either the embryonic or abembryonic parts of the blastocyst, such that in 17 out of 20 blastomeres, two or fewer cells crossed the em-ab boundary. One interpretation of this experiment would be that the A-V axis of the oocyte plays no part in the specification of future polarity, but further studies are needed to determine whether the developmental properties of the individual blastomeres are altered by forcing cleavage to occur orthogonally to the A-V axis.

1.10.2 Early cleavage and blastocyst axes

The emerging evidence to suggest that axes exist in the oocyte and that first cleavage may specify two differing populations of cells led to the investigation of subsequent cleavage and the identity of the progeny. The second cleavage divisions can either be meridional (M)(as the first cleavage) or equatorial (E) (orthogonal to first cleavage), typically producing a tetrahedral four-cell embryo with six intercellular contacts. It has been shown that while any combination of division is possible, sequential M and E divisions are most common (Gardner, 2002). By gelating the perivitelline space it was determined that the second division was not meridional following rotation of the blastomere through 90° as in the rabbit, but was truly (approximately) equatorial. However, the rate of non-tetrahedral cell conformation was too high to conclude that regular cleavage is an absolute prerequisite for development. While it has been shown

that the progeny of one two-cell blastomere contributes to the ICM and polar TE and the other to the mural TE (Piotrowska & Zernicka-Goetz, 2001), the boundary between progeny was not strictly orthogonal to the em-ab axis of the blastocyst. However, this is explained by the conformation of the regular tetrahedral four cell embryo. The cell inheriting the vegetal portion of the cytoplasm after an equatorial division overlies the vegetal pole asymmetrically rather than being away to one side (Gardner, 2002), therefore distorts the original plane of first cleavage, and progeny are expected to span the boundary zone of the blastocyst.

Therefore a typical meridional first cleavage produces two nearly identical daughters, each inheriting the full A-V axis. The second equatorial division produces one daughter inheriting mostly animal cytoplasm, and one inheriting mostly vegetal. Should a (yet unknown) determinant be involved in cell fate, it is conceivable that a gradient of such a factor along the A-V axis would be differentially inherited by these three categories of blastomeres as a result of their composition of different axial levels of the zygote, as shown in Figure 1.3. It must be noted however that whilst the second cell cycle results in a regular tetrahedral embryo in more than two-thirds of embryos, leading to partitioning of the cytoplasm in regard to the A-V axis, there is a possibility that there are developmental asymmetries orthogonal to this axis (Gardner, 2002).

Isolated sister pairs of the meridional or equatorial divisions in the mouse embryo gave comparable rates of normal development through gastrulation (Gardner, 2002). However these combinations resulted in all levels of the A-V axis being represented and therefore theoretically the pairs were not deficient in any determinant. However, chimera studies have extended this work to consider the developmental potential of each category of blastomere, and concluded that while all four cells can have full developmental potential, they differ in their individual developmental properties according to their origin (Piotrowska-Nitsche *et al.*, 2005). Chimeras were constructed of only either; blastomeres inheriting animal cytoplasm (animal chimera), blastomeres inheriting vegetal cytoplasm (vegetal chimera) or blastomeres inheriting the full A-V axis (meridional chimera). Normal live offspring were seen from between 69-85% of meridional chimeras, whereas most vegetal chimeras died after implantation, with only a 30% offspring rate. Animal chimeras showed an

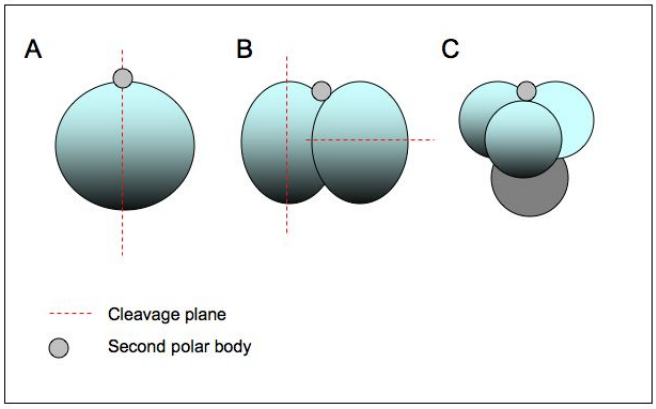

Figure 1.3: Schematic representation of the formation of a tetrahedral four-cell embryo. (A) One cell zygote with asymmetric distribution of unspecified determinants as shown by a blue-grey colour gradient along the A-V axis. (B) A meridional first cleavage produces two identical daughter cells each inheriting the full axis. (C) One meridional and one equatorial second cleavage results in a tetrahedral four-cell embryo with three cell types. Both the progeny of the meridional division inherit the full axis (blue-grey), whereas the equatorial division produces one daughter inheriting only the animal pole (blue) and one inheriting only the vegetal pole (grey).

intermediate survival. Furthermore, in general those chimeras made from later dividing blastomeres had lower survival than those made from the earlier dividing sister cell, attributed to a reduced proliferative capacity and inherent differences in potential. Despite this demonstration of predetermined fate, the regulative capacity of the blastomeres was also considered, and it was shown that when a vegetal cell was surrounded by cells of random origins it contributed to a variety of embryonic lineages, in contrast to the failure of development of vegetal chimeras.

Using lineage tracing experiments it has been concluded that the first cell to complete the second cleavage contributes more progeny to the portion of the ICM likely to become epiblast and the polar TE compared with the later dividing cell, which contributes preferentially to the mural TE and the portion of the ICM that also gives rise to the primitive endoderm (Piotrowska & Zernicka-Goetz, 2001). The mechanism behind this segregation is unclear, but possibly due to the earlier initiation of a developmental programme by the earlier dividing cell (Piotrowska & Zernicka-Goetz, 2001), an advantage bestowed by the inheritance of the SEP (Piotrowska & Zernicka-Goetz, 2001), or as a consequence of more extensive intercellular contacts (Surani & Barton, 1984). However, the conclusion of an opposing study was that the em-ab axis is independent of early cell lineage. By tracing the marked nuclei from transgenic mice backwards from the blastocyst stage cell lineage maps were constructed which showed that all of the descendants of two-cell blastomeres, and 84% of four-cell blastomeres contributed to both embryonic and abembryonic regions in the blastocyst (Kurotaki *et al.*, 2007).

1.10.2.1 Blastocoel formation

The ICM and blastocoel cavity lie at either end of the em-ab axis, therefore the mechanism of formation of the cavity is crucial in establishing this axis. One hypothesis is that the pattern of conservative and differentiative divisions from the eight-cell stage influence the cavity position and hence the em-ab axis. At the morula, the inner cells consist of those that are generated from the division of other inner cells, and those that are generated from the differentiative division of outer cells. These associations may be of different strengths, and therefore a cavity may form where the connections are weakest between inner and outer cells (Plusa *et al.*, 2005). There would be a tendency for this to be adjacent to regions in which the outer cells had recently

divided predominantly symmetrically, and not attached to inner cells. Therefore it is irrelevant where or in how many places the blastocoel originates, but the location of the final position that marks the abembryonic pole (Zernicka-Goetz, 2005).

However, opposing experiments conclude that the blastocoel is not formed in a predefined manner at the abembryonic pole, but originates in multiple points and finally coalesces at one end of the long axis of the zona due to differential pressure imposed by the glycoprotein coat (Motosugi *et al.*, 2005). Using serial confocal scanning they first showed that the origin of these multiple fluid-filled vesicles did not occur within just one of the clonal areas from two-cell descendants. Then by artificially elongating two-cell embryos it was observed that the cavity was forced to form at one end of the long axis of the zona, although this model does not account for the positioning of blastocoel opposite the ICM in non-manipulated or spherical embryos. Despite disagreeing on the mechanism, both groups agree that the cavity develops as a function of differences between cells or parts of cells, not as a response to a determinative signal.

1.10.2.2 Further studies

There are many methodological uncertainties that contribute to the ongoing discrepancies in results from different research groups. The use of fluorescent beads, fluorescent dyes, chemical manipulation such as the use of cytochalasin, recording methods such as confocal microscopy or time lapse, immobilisation of oocytes or embryos, appropriate controls, method of results analysis and strain of mouse used have all come under fire in the ongoing polarity debate (Hiiragi *et al.*, 2006). Certainly alternative interpretations are offered for some observations (Johnson, 2003). Until the various groups exactly replicate the protocols of others, the conflict of result interpretation may not be resolved. The definitive experiment would be to identify a gene or protein, like those already identified in the frog or fly embryos, that clearly marks the fate of different early embryonic cells. If a gene is found to be expressed in a specific region of the oocyte or in one early blastomere and not the others - and if removing the gene interrupts development - then prepatterning is proven. Until then, these elegant and carefully designed experiments will continue to shed both light and uncertainty on the polarity debate.

Some molecular experiments have been attempted with human embryos, although doubts over the methodology limits the value of the results. For example, the identification of polarised distribution of leptin and signal transducer and activator of transcription 3 (STAT3) in the oocyte (Antczak & Van Blerkom, 1997) led to the investigation of expression in the later embryo. As a consequence of the orientation of the cleavage planes, these proteins became allocated preferentially to specific blastomeres, such that by the 8-cell stage there appeared populations of leptin/STAT3 rich and poor cells, and subsequently to the cells of the TE rather than cells of the ICM (Antczak & Van Blerkom, 1997). For unequivocal confirmation, the experiments should have been repeated with the orientation of the embryos inverted to control for technical bias due to changing intensity of the laser reaching the far surface of the embryos. Further molecular studies are discussed in Chapter 5.

No definitive conclusions can be made at this juncture regarding the origin, timing and influence of axes of polarity in the oocyte and early cleavage stage embryos. Certainly there appears highly persuasive evidence regarding the non-randomness of the first developmental divisions making it very difficult to discard the prepatterning theory. The existence of axes in early development is reflected in the conservation of numerous other developmental pathways shared between mammalian and non-mammalian species. However, the mechanisms underlying the establishment of these axes, and even elucidating how essential they are for normal development, remains controversial. The possibility is that there is a pattern, but that it is not determinant. Instead it could be thought of as a set of influences that steer normal development, but that are sufficiently flexible and regulative to compensate for (sometimes major) perturbations and still allow normal development to proceed in the majority of cases.

Whilst many of the experiments discussed using murine embryos are unrepeatable in humans given the number of embryos required, there are studies that need to be done and can be done with human material. There has been no systematic study of lineage-specific gene expression in single human early cleavage embryos with the aim of analysing whether differences in expression exist between sister blastomeres. Furthermore, whilst chimeric proof of pluripotency after manipulation is clearly not possible in humans, the ability of all sister single blastomeres to generate stem cell lines would offer convincing proof of retained pluripotency or at least plasticity.

Chapter 2

General Methods

2.1 Human embryo culture

2.1.1 Oocyte collection and fertilisation

A standard long protocol was used to induce ovulation and controlled timing of oocyte retrieval (Khalaf *et al.*, 2000). Pituitary supression was achieved with buserelin nasal spray (Suprefact; Shire, Andover, UK), followed by ovarian stimulation with between 150 and 450 IU daily of recombinant human FSH (r-hFSH; Gonal-F, Serono Pharmaceuticals Ltd, Feltham, Middx, UK) for the first 10-12 days. 10,000 IU of human chorionic gonadotrophin (hCG) was administered to trigger ovulation when adequate follicular development had been demonstrated by transvaginal ultrasonography and there were at least three follicles greater than 18 mm in diameter. Transvaginal oocyte retrieval was performed 35 h later. Intracytoplasmic sperm injection (ICSI) was used when the spermatozoa were of poor quality, otherwise standard *in vitro* fertilisation (IVF) was used.

2.1.2 Culture of human embryos

Following oocyte and sperm collection, with or without ICSI, gametes were incubated overnight in Quinn's Advantage™ Fertilization Medium (FM). The following morning bi-pronucleate stage embryos were transferred to Quinn's Advantage™ Cleavage Medium (CM) for culture until day 3 of development. For further culture to the blastocyst stage, embryos were transferred on day 3 into Quinn's Advantage™ Blastocyst Medium (BM) until day 5-7 of development. All media were supplemented with 10% synthetic protein serum substitute (SPSS). FM was used at 0.5

mL volumes in 4 well Nunc plates (BioTipp, Belfast, County Antrim, Ireland). CM and BM were used as 20-40 μL drops under tissue culture grade sterile oil, in 35 mm Falcon dishes (Becton Dickinson, BD Biosciences, Oxford Science Park, Oxford, UK) or 60 mm Corning dishes (Corning Life Sciences, Acton, MA, USA). All media and supplements were from Sage BioPharma, CooperSurgical Inc. Trumbull, CT, USA. All dishes were prepared a minimum of 6 hours before use and equilibrated at 37°C, in 5% CO_2 in air, or in 6% CO_2, 5% O_2, 89% N_2. All manipulation was carried out in a Class II or laminar flow hood on a heated microscope stage, unless otherwise specified. Between each transfer to a sequential medium, either during culture, manipulation or freeze/thaw, thorough wash steps were performed. The sequential medium was expelled over the embryos, so that when the embryos were aspirated for transfer they were suspended in the medium for the next stage of culture. The pipette was then rinsed and the embryos washed around the edge of the well/in the wash microdrop before being placed in the centre/culture microdrop for incubation. All cleavage stage embryos were graded according to the criteria of Bolton *et al.* (1989) where the highest quality embryos are assigned grade 4, and the lowest, grade 1. Blastocysts were graded using the grading system in Stephenson *et al.* (2007).

2.1.2.1 Cryopreservation of cleavage stage embryos

Embryos were cryopreserved on day 1, 2 or 3 after fertilisation using Quinn's Advantage Embryo Freeze kit (Sage, Cooper Surgical). All solutions were at room temperature (RT). Embryos were placed for 5 min in each of 0.5 M propanediol (PPD), 1.0 M PPD, then 1.5 M PPD/0.1 M sucrose solution. During this final 5 min, the embryos were loaded into cryostraws (BioSystems, IMV Technologies, L'Aigle cedex, France) with the medium containing the embryos aspirated into the straws between air bubbles. A pre-programmed Cryologic controlled rate freezer (Cryologic PL, Australia) was used to cool the embryos from 37°C to -6°C at 2°C/min. Manual seeding was performed at -6°C, after which the embryos were held at this temperature for 10 min before being cooled to -35°C at 0.3°C/min. The straws were placed into liquid nitrogen for long-term storage.

2.1.2.2 Cryopreservation of blastocysts

Blastocysts were cryopreserved on day 5 or 6 after fertilisation using Quinn's Advantage Blastocyst Freeze kit (Sage, Cooper Surgical). All solutions were at RT. Blastocysts were placed in freeze diluent for 5 min and then transferred to 5% glycerol freezing medium for 10 min, followed by 10 min in 9% glycerol/0.2 M sucrose freezing medium. During this final 10 min, the blastocysts were loaded into cryostraws and the controlled rate freeze and storage performed exactly as described for cleavage stage embryos.

2.1.2.3 Thawing of cleavage stage embryos and blastocysts

Cleavage stage embryos and blastocysts were thawed using Quinn's Advantage Thaw kit (Sage, Cooper Surgical). All solutions were at RT. Each cryostraw was removed from liquid nitrogen and held in air for 40 s before being immersed in a sterile water bath at 30°C until the medium reached liquid phase. The contents of the straw were then expelled into a culture dish and the embryos transferred to 0.5 M sucrose thawing medium for 10 min. This was followed by 10 min each in 0.2 M sucrose thawing medium and thaw diluent solution before transfer to a pre-equilibrated dish of the appropriate culture medium. A 2-3 h recovery period was allowed after each thaw before further manipulation.

2.2 Cell culture

2.2.1 Isolation of primary mouse embryonic fibroblasts

All cell culture was at 37°C in 5% CO_2 in air. All manipulation was carried out in a class II or laminar flow hood on a heated microscope stage, unless otherwise specified. Appropriate media components were combined, filtered through 0.22 μm polyethersulphone (PES) sterile filter (Corning) and stored at 4°C for a maximum of 14 days.

Day 12.5 uterine horns were obtained from Swiss MF1 mice and placed in a culture dish containing pre-warmed phosphate buffered saline (PBS; Gibco Invitrogen Corporation, Carlsbad, CA, USA) supplemented with 50 U/mL penicillin and 50 μg/mL streptomycin (pen/strep; Autogen Bioclear UK Ltd., Calne, UK). Using sterile dissection implements the embryos were removed from the embryonic sac and

the placenta and membranes extracted and discarded. The embryonic hindbrain and liver were removed and the remaining tissue washed three times in PBS plus pen/strep. This was repeated for the remaining embryos, and all the tissue collected together. Using scissors or a scalpel the tissue was thoroughly minced, then incubated in a centrifuge tube (Corning) at 37°C in 2 mL 0.25% trypsinEDTA (Gibco Invitrogen) for 10-20 min. The solution was vortexed vigorously and then quenched with Dulbecco's Modified Eagle's Medium (DMEM; no pyruvate, high-glucose formulation, with L-glutamine, Gibco Invitrogen) supplemented with 10% fetal calf serum (FCS; Autogen Bioclear) before centrifuging at 1000 xg for 10 min. One T75 flask (Corning) per embryo was prepared by coating with 0.1% gelatin (Sigma Aldrich Co Ltd, Dorset, UK) in PBS for 5 min, aspirating off the excess and allowing to air dry before adding 7 mL DMEM containing 10% FCS, 4 mM L-glutamine (Gibco Invitrogen) and 2% pen/strep (DMEM/FCS). Following centrifugation, the supernatant was removed and placed in a T225 flask (Corning). DMEM/FCS was added to the pellet at 2 mL per embryo and the pellet re-suspended. 2 mL of this solution was aliquoted into each T75 flask. The flasks were incubated until the cells reached approximately 90% confluence, on average after two days. These primary mouse embryonic fibroblasts (MEFs) were then cryopreserved exactly as in section 2.2.2.2. One vial was thawed, expanded and used for sterility and mycoplasma testing. The remaining vials were expanded as necessary to passage 3 before being inactivated as in section 2.2.3.

2.2.2 Culture of mouse embryonic fibroblasts

A vial of the desired batch and passage number of MEFs was thawed rapidly in a 37°C water bath and the suspension added in a centrifuge tube to 5 mL MEF media, consisting of DMEM, 10% FCS, 4 mM L-glutamine, 1% non-essential amino acid (NEAA; Gibco Invitrogen) and 0.1 mM β-mercaptoethanol (Gibco Invitrogen). The cells were centrifuged at 1000 xg for 5 min. The supernatant was discarded and the pellet re-suspended in 1 mL MEF media. T75 flasks were prepared by coating with 0.1% gelatin for 5 min, aspirating off the excess and allowing to air dry before adding 7 mL MEF media. The MEF suspension was added to the flask and incubated at 37°C until 70-80% confluent.

2.2.2.1 Passaging of mouse embryonic fibroblasts

To passage a MEF culture, the MEF medium was aspirated from the flask, the cells were washed with PBS and then incubated at 37°C for 3-4 min in 3 mL trypsin. The flask was physically agitated to detach the cells and the enzyme quenched with 6 mL MEF medium. The cell suspension was then centrifuged at 1000 xg for 5 minutes, the supernatant removed and the pellet re-suspended in 3 mL MEF media. Three T75 flasks were prepared with gelatin and MEF medium as before. 1 mL of the MEF suspension was added to each flask and these were incubated at 37°C until 70-80% confluency was reached and then used as required. MEFs were generally used at P3 when preparing feeder layers.

2.2.2.2 Cryopreservation of mouse embryonic fibroblasts

MEF cultures were cryopreserved when the flask reached 70-80% confluency. The MEF medium was aspirated from the flask, the cells were washed with PBS and then incubated at 37°C for 3-4 min in 3 mL trypsin. The flask was agitated to detach the cells and the enzyme quenched with 6 mL MEF medium. The cell suspension was then centrifuged at 1000 xg for 5 min, the supernatant removed and the pellet re-suspended in 5 ml MEF media. 900 μL aliquots of the cell suspension were placed in labelled cryovials (Corning) to which 100 μL dimethylsulphoxide (DMSO; VWR International, Lutterworth, Leicestershire, UK) was added. The vials were placed overnight at -80°C then placed in liquid nitrogen for long-term storage.

2.2.3 Preparation of mouse embryonic fibroblast feeder layers

MEF media was aspirated from a 70-80% confluent T75 flask of P3 MEFs and 7 mL of a 10 μ0g/ml dilution of mitomycin C (MMC; Sigma Aldrich) in MEF media was added to the cells for 2-3 h at 37°C. The cells were then washed with PBS and incubated in 3 mL trypsin for 3-4 min. The cells were detached from the bottom of the flask by physical agitation and the trypsin solution was quenched with 6 mL MEF medium. The suspension was aspirated from the flask and placed in a 15 mL tube then centrifuged at 1000 xg for 5 min. The supernatant was discarded and the pellet re-suspended in 5 mL MEF media.

The feeder layers were prepared in 4-well Nunc plates. 0.5 mL of 0.1% gelatin was added to each well for 5 min then the excess aspirated and the wells air dried. The cell number in the suspension was counted using a haemocytometer, and the volume of cell suspension required for the desired feeder concentration was calculated and aliquoted into each well, which was then made up to 500 μL with MEF media. The plates were incubated overnight before use, then the MEF medium was exchanged for the specific medium used for the subsequent cell culture. The plates were used up to five days after preparing for passaging established cell lines and up to three days for derivation attempts and newly derived cell lines.

2.2.4 Preparation of buffalo rat liver cell conditioned medium

A vial of buffalo rat liver (BRL) cells (kindly donated by Dr. Paul Sharpe, Craniofacial Development Department, King's College London) was thawed rapidly in a 37°C water bath and the suspension added in a centrifuge tube to 5 mL BRL medium comprising of DMEM (high glucose with Glutamax^{TM}), 20% FCS, 4 mM L-glutamine, 1% NEAA stock and 0.1 mM β-mercaptoethanol. The cells were centrifuged at 1000 xg for 5 min. The supernatant was discarded and the pellet re-suspended in 1 mL BRL media. The cell suspension was then added to 30 mL BRL media in T225 flasks. BRL cells were grown at 5% CO_2 in air to 70-80% confluency typically over 48 h and the conditioned medium (CM) collected and stored at -80°C.

After the BRL CM was collected the cells were washed with PBS and then incubated at 37°C for 3-4 min in 5 mL trypsin. The flask was agitated to detach the cells and the enzyme quenched with 10 mL BRL medium. The cell suspension was then centrifuged at 1000 xg for 5 min, the supernatant removed and the pellet re-suspended in 3 mL BRL medium. 1 mL of the cell suspension was then added to 30 mL BRL media in T225 flasks for culture. BRL cells were cryopreserved exactly as MEFs, except BRL medium was used to re-suspend the cell pellet.

2.3 Human embryonic stem cell culture

All cell culture was at 37°C and in 5% CO_2 in air or in 6% CO_2, 5% O_2, 89% N_2. All manipulation was carried out in a Class II or laminar flow hood on a heated microscope stage, unless otherwise specified. Appropriate media components

were combined, filtered through 0.22 μm PES sterile filter and stored at 4°C for a maximum of 14 days.

2.3.1 Human embryonic stem cell culture medium

Culture of human embryonic stem cells (hESC) was either in hESC CM comprised of 3 parts BRL CM and 2 parts BRL medium (section 2.2.4) with 8 ng/mL basic fibroblast growth factor (bFGF; PeproTech Inc., Rocky Hill, NJ, USA) supplemented fresh to each equilibrated aliquot, or in Knock Out Serum Replacement (KOSR; Gibco Invitrogen) medium. KOSR comprised of Knock-Out DMEM (KODMEM; Gibco Invitrogen) with 20% KOSR, 4 mM L-glutamine, 1% NEAA stock, 0.1 mM β-mercaptoethanol and 8 ng/mL bFGF supplemented fresh to each equilibrated aliquot. The medium used for each experiment is specified in each section.

The media on hESC cultures was exchanged on alternate days. Sufficient medium for exchange of all cultures was placed in a culture dish and equilibrated at 37°C for a minimum of 30 min and a maximum of 3 h before use. The medium was then supplemented with the bFGF and used to feed the cells. The spent medium was either stored at -80°C for future analysis, or discarded.

2.3.2 Passaging of human embryonic stem cells

Sterile glass pipettes (Hunter Scientific Ltd., Saffron Walden,Essex, UK) were heated in an ethanol flame, pulled to a small diameter then broken to create a hooked end. Colonies were selected for passage when under rapid mitogenic proliferation and before evident differentiation. The edges of the colonies selected for passaging were scored using the pipettes and cut into appropriate sized pieces depending on the behaviour of the individual cell line. The colony pieces were then transferred to a fresh MEF plate and incubated for 48 h. Culture medium was then exchanged as standard.

2.3.3 Vitrification of human embryonic stem cells

For vitrification, hESC colonies were prepared as for passaging, but the pieces cut to twice the size. All solutions were equilibrated prior to use, and made fresh each

time. The prepared colony pieces were washed through and then placed in ES-HEPES holding solution consisting of the DMEM base of the culture medium used with 20% FCS and 2% of 1 M HEPES (Gibco Invitrogen). 4-6 pieces at a time were transferred to 10% vitrification solution for 1 min, then to 20% vitrification solution for 25 s. The components of the solutions are given in Table 2.1. During the 25 s step the pieces were aspirated in a minimum of solution and expelled onto an inverted culture dish lid in a drop. This drop was aspirated into a vitrification straw (LEC Instruments, Australia) using capillary action, held horizontally with sterile forceps and plunged into liquid nitrogen. This was repeated for the remaining colony pieces, and the straws were then placed in a 5 mL cryovial which was labelled with the cell line identifiers and stored in liquid nitrogen.

Table 2.1: Formulation of hESC cryopreservation medium. The sucrose was dissolved at 37°C in 6 mL ES-HEPES. This was made up to 8 mL with ES-HEPES and the FCS added. Ethylene glycol and sucrose were from Sigma Aldrich.

1M sucrose solution	
Sucrose	3.42 g
ES-HEPES solution	8.0 mL
FCS	2.0 mL
10% vitrification solution	(v/v)
ES-HEPES solution	80%
Ethylene glycol	10%
DMSO	10%
20% vitrification solution	(v/v)
ES-HEPES solution	30%
1M sucrose solution	30%
Ethylene glycol	20%
DMSO	20%

2.3.4 Thawing of human embryonic stem cells

The tip of the vitrification straw was placed directly into either hESC CM or KOSR immediately after removal from liquid nitrogen. The thawing medium normally flowed out of the straw but if necessary the expulsion of the colonies could be aided by inserting a Gilson tip into the top of the straw and expelling. The colonies were

washed gently through two further wells of medium and then transferred to prepared MEF plates.

2.3.5 Microbiological analysis

Samples of all cell cultures and media were routinely tested for mycoplasma contamination. This was outsourced to Surrey Diagnostics (Surrey Diagnostics, Cranleigh, Surrey). If microbial contamination was suspected, samples of all cultures and media were sent to the Microbiology Department of Guy's Hospital. The samples were inoculated on blood and chocolate agar at 36°C for 48 h to assess for growth of any general bacteria, and on Sabouraud's agar at 36°C for 72 h to assess for growth of any yeast or fungal agents. Any colonial growths were subject to identification techniques in an attempt to speciate the isolate and suggest probable sources.

2.4 Embryo and single blastomere analysis techniques

2.4.1 Immunocytochemistry

Embryos and blastomeres were fixed for 10 min at RT in 4% paraformaldehyde (PFA) then washed through four drops of PBS supplemented with 1% bovine serum albumin (BSA; Sigma Aldrich). 4% PFA was always made fresh and in a fume hood. 1 g of PFA (Sigma-Aldrich) was added to 20 mL PBS in a glass bottle with a stirring bar. 4.5 μL of sodium hydroxide (NaOH; Sigma Aldrich) was added and the bottle placed on a magnetic hot plate for 15 min with stirring. 2-2.5 μL hydrochloric acid (HCl; VWR) was added until the pH was 7.0, as assessed with the Corning pH meter 240. 5 mL PBS was added, the solution filtered through a 0.22 μm Whatman syringe filter (Sigma Aldrich) and placed at 4°C for 20 min before use. The fixed cells were stored in PBS at 4°C until prepared for immunofluorescence.

Fixed cells were washed through four drops of PBS with 0.1% triton X-100 and 1% BSA (PBST; Sigma Aldrich) and then incubated in 0.5% PBST for 30 min at RT with occasional agitation. After washing in 0.1% PBST the cells were placed in 10% FCS in 0.1% PBST blocking solution for 1 h at RT. This blocking solution was used to dilute the primary antibodies. Primary antibodies used were POU5F1-iA and NANOG, details of which are given in Table 2.2. Fluorescein isothiocyanate (FITC)

anti-mouse secondary (emission wavelength 520 nm) and Cyanine3 (Cy3) anti-rabbit secondary (emission wavelength 570 nm) were used to allow simultaneous double staining. The embryos and blastomeres were incubated in the primary antibodies overnight at 4°C.

Following incubation the cells were washed through 4 drops of 0.1% PBST then incubated in 0.1% PBST for 30 min at RT. Secondary antibodies were diluted in 0.1% PBST at 1:300. The cells were incubated in the secondary antibody combinations for 1 hr in the dark at RT, then washed through 4 drops of 0.1% PBST. Embryos and blastomeres were then mounted in a 1 μL drop of softmount Vectashield plus 4',6-diamidino-2-phenylindole (DAPI; Vector Laboratories, Burlingame, CA, USA) onto a coverslip dish (MatTek Corporation, Ashland, MA, USA). Images were captured by a Perkin Elmer Ultraview ERS confocal microscope using the Ultraview Suite software version 3.0.

2.4.2 Single cell dynamic polymerase chain reaction

The Applied Biosystems (ABI; Foster City, CA, USA) TaqMan® PreAmp Cells-to-CT™ kit was used to preamplify target cDNA from single blastomeres, which was subsequently analysed with the Biomark™ Fluidigm® Dynamic Quantitative (q)PCR platform. The data were analysed by mixed-effects modelling and principle component analysis as detailed in Chapter 5. All statistical analysis was performed in R version 2.8. Mixed-effects modelling used the nlme or lme4 packages, depending on whether random effects were purely nested or were crossed.

2.4.2.1 Reverse transcription to cDNA

Pronuclear or day 2 embryos were thawed as described in section 2.1.2.3, and cultured to the desired stage for disaggregation which was performed as in section 5.2.1.3. All reagents used subsequently were provided in the Cells-to-cT kit.

Single blastomeres were transferred to eppendorf tubes (Eppendorf UK Limited, Cambridge, UK) containing 50 μL lysis solution which contained DNase and reagents to inactivate endogenous RNases and incubated at RT for 5 min. 5 μL stop solution was then added and mixed thoroughly before incubation at RT for 2 min, then the samples were placed on dry ice for transport to the molecular laboratory. A minimum

of three extraction negative (EN) controls were also prepared in exactly the same way but without addition of a blastomere.

The entire cell lysate was reversed transcribed (RT) to synthesise cDNA. A master mix was made and vortexed before use. For each sample plus one spare, 75 μL 2x RT buffer, 7.5 μL 20x RT enzyme mix and 12.5 μL nuclease-free water were mixed. The quantities of the reagents were scaled up from the manufacturers protocol so that 95 μL of the mastermix was added directly to the whole 55 μL lysate to minimise loss of template. Triplicate reverse transcription negative (RTN) controls were also prepared each time by substituting the RT enzyme mix for nuclease-free water. The samples were vortexed gently, and then centrifuged briefly at 1000 rpm for 2 min to collect all the contents at the bottom of the vessel. Unamplified cDNA was generated by incubation at 37°C for 60 min, 95°C for 5 min and then cooling to 4°C indefinitely, using a PTC-100 Thermal Cycler (MJ Research, Global Medical Instrumentation Inc., Minnesota, USA).

2.4.2.2 Preamplification of cDNA targets

The preamplification step was used to increase the abundance of 24 specific cDNA targets for subsequent gene expression analysis. Validated TaqMan gene expression assays were selected. Each assay was a ready-to-use 20x mixture of specific PCR primers and TaqMan probes designed so that any combination of assays could be run in the same thermal cycling conditions for preamplification. The assays were thawed immediately prior to use, vortexed and centrifuged briefly.

A master mix was made for the preamplification reaction. For each sample plus one spare, 25 μL of TaqMan preAmp master mix was added to 12.5 μL 0.2x pooled assay mix. The pooled assays were diluted to 0.2x by the addition of the appropriate volume of 1x TE buffer. Details of the selected assays used are given in Table 5.1 in Chapter 5. 12.5 μL of cDNA sample was added to each 37.5 μL master mix aliquot and the samples vortexed gently then centrifuged briefly. Triplicate preamplification negative (PAN) controls were also prepared each time by substituting the cDNA template for nuclease-free water.

Preamplification of the selected targets was achieved by a 95°C incubation for 10 min and then 14 cycles of 95°C for 15 secs and 60°C for 4 min. Upon completion, the preamplified samples were placed immediately on ice.

2.4.2.3 Fluidigm dynamic qPCR

The Fluidigm dynamic chip was primed with the injection of control line fluid into the accumulator ports on both sides of the chip according to the manufacturer protocol. The chip was then placed into the Integrated Fluidic Circuit (IFC) controller and the priming programme executed.

The assays were prepared in a 96 well plate. 3 μL of Fluidigm DA assay loading reagent was placed in each well of lanes 7-12. To each appropriate well 3 μL of a 20x assay was added. The 24 assays were always run in duplicate therefore filling the 48 wells of the dynamic chip.

The preamplified cDNA sample reaction mixes were prepared in lanes 1-6 of the 96 well plate. A mastermix of 3 μL TaqMan universal mastermix and 0.3 μL Fluidigm DA sample loading reagent per sample plus five spare was prepared, vortexed, and 3.3 μL added to each well of lanes 1-6. To each appropriate well 2.7 μL of cDNA or control sample was added. EN, RTN and PAN were always included on each chip run. Nuclease-free water was always added to well D4 as this was used as a reference well by the Fluidigm platform.

A multichannel pipette was used to mix and then aliquot 5 μL of either sample or assay to the appropriate wells on the primed dynamic chip. The chip was then replaced into the IFC controller and the loading programme executed.

The loaded chip was then placed in the Fluidigm machine to run the qPCR reaction. The reaction profile was a 50°C incubation for 2 min, a 95°C incubation for 10 min and then 40 cycles of 15 s at 95°C and 60 s at 60°C, followed by cooling to 4°C indefinitely. A passive ROX reference was used in the reaction to normalise the fluorescence values. Analysis of the results was with the Biomark Real-Time PCR software version 2.0.6.

2.5 Cell analysis techniques

2.5.1 Immunocytochemistry

The culture medium was removed from the cells to be fixed, and the wells washed twice with PBS. 4% formaldehyde solution (PFA; Sigma-Aldrich, a 1:9 dilution in PBS of the 37% stock solution) was placed on the cells for 10 min at RT. The fixative

was removed and the cells washed twice with PBS, then stored in PBS at 4°C until use.

For immunocytochemistry (ICC) to detect surface membrane targets, the cells were first blocked by incubation in 1% BSA in PBS for 30 min at RT. For nuclear or cytoplasmic targets, the cells were blocked and permeabilised by incubation in a 1:1 solution of 1% BSA and 0.25% PBST for 30 min at RT. Primary antibodies were diluted in the these same solutions depending on target localisation, and placed on the cells overnight at 4°C. Once the primary antibody solutions were removed, the cells were washed in PBS three times for 5 min each. The secondary antibodies were diluted in 1% BSA and incubated with the cells for 1 h at RT in the dark. The washing was repeated as before, except that in the second 5 min wash, 0.1 μg/mL DAPI (Sigma Aldrich) was added to counterstain the cell nuclei. Visualisation of cell staining was performed either with a Nikon TE2000 inverted microscope and images captured using the SimplePCI software or with a Nikon Eclipse TE2000-U using NIS-Elements software version 2.30.

The markers for pluripotency characterisation used were as detailed in Table 2.2. The appropriate secondary antibodies used were FITC or tetramethylrhodamine isothiocyanate (TRITC, emmission wavelength 576 nm) conjugated anti-mouse or anti-rabbit, all from Molecular Probes (Invitrogen) and used at a 1 in 300 dilution.

Table 2.2: Primary antibodies used for pluripotency characterisation. POU5F1 also known as OCT4, -iA is the pluripotent isotype, SSEA: stage specific embryonic antigen, TRA: trafalgar antibodies. Santa Cruz: Santa Cruz Biotechnology, Inc., CA. USA; Abcam: Abcam PLC, Cambridge, UK; DSHB: The Developmental Studies Hybridoma Bank, Iowa City, IA, USA; Chemicon: Chemicon, Millipore, Billerica, MA, USA.

Name	**Isotype**	**Clone**	**Company**	**Dilution**
POU5F1-iA	Mouse IgG2b	C-10	Santa Cruz	1 in 250
NANOG	Rabbit IgG	Polyclonal	Abcam	1 in 200
SSEA1	Mouse IgM	SSEA1	DSHB	1 in 100
SSEA3	Rat IgM	SSEA3	DSHB	1 in 100
SSEA4	Mouse IgG3	SSEA4	DSHB	1 in 100
TRA1-60	Mouse IgM	TRA1-81	Chemicon	1 in 200
TRA1-81	Mouse IgM	TRA1-60	Chemicon	1 in 200

2.5.2 Molecular analysis

The cells for analysis were washed twice in PBS. Whole colonies of hESC were cut with a pulled glass pipette and placed in an eppendorf tube with a minimum amount of PBS carry-over. MEFs alone were also collected each time as a negative control.

2.5.2.1 RNA extraction

Total RNA was isolated using the RNeasy kit (Qiagen Ltd, Crawley, UK) as per the manufacturer instructions, and all solutions were provided in the kit. The nuclear content of the cells was first released by lysis of the cells by addition of 350 μL buffer RLT, then the lysate was homogenised by passing a minimum of 5 times through a 20 gauge needle (0.9 mm diameter). 350 μL of 70% ethanol was added to each sample and mixed by pipetting to precipitate the DNA and RNA. The sample was then transferred to a RNeasy mini spin column and centrifuged at 13,000 rpm for 15 s. The flow-through was discarded as the RNA remained within the membrane. The membrane was then washed by the addition of first 700 μL buffer RW1 and then 500 μL buffer RPE to the spin column and centrifugation at 13,000 rpm for 15 s. 500 μL buffer RPE was then added again and the column centrifuged at 13,000 rpm for 2 min to dry the membrane and ensure no ethanol was carried over. The membrane was then placed into a RNase-free eppendorf tube and 30 μL RNase-free water was expelled directly onto the membrane. The column was centrifuged at 13,000 rpm for 1 min to elute the RNA from the membrane. The isolated total RNA was placed on ice for immediate use or stored at -80°C for future use.

2.5.2.2 cDNA synthesis

Complementary (c)DNA was synthesised from total RNA samples using avian myeloblastosis virus reverse transcriptase (AMV RT; Promega UK, Southampton, UK). RNasin plus (Promega) was used to inhibit any RNase activity.

A master mix was made and vortexed before use. For each sample plus a spare, 1 μL of 10 mM dNTPs, 1 μL of oligo(dT)18 and 1 μL of random(dN)10 (all from Promega) were mixed. 3 μL of the master mix was mixed with 11 μL of the RNA samples. The samples were then heated to 70°C for 5 min to reduce secondary RNA structure then immediately placed on ice.

For the reverse transcription, for each sample plus a spare, 4 μL 5x AMV RT buffer (Promega) and 1 μL RNasin were mixed on ice. 5 μL of the master mix was added to each sample tube and mixed by pipetting, then 2 μL of this mix removed for the AMV RT negative control to ensure against genomic DNA contamination. 1 μL of AMV RT was then added to all the positive samples. The samples were then incubated at 37°C for 10 min, 42°C for 30 min and then 52°C for 20 min followed by heat inactivation of AMV RT at 80°C for 10 min. The cDNA samples were diluted 5-fold with diethyl pyrocarbonate-treated DNase- RNase-free UltraPURE^{TM} water (dH_2O; Gibco Invitrogen). The negative control samples were diluted 10-fold with dH_2O. The samples were used immediately in PCR reactions or stored at -20°C for future use.

2.5.2.3 Polymerase chain reaction

With the exception of βactin (kindly donated by the Molecular Biology Department, King's College London), primer sequences were from published reports from this group and primers were from Sigma-Aldrich, provided as a powder. Stock solutions of 100 μM were prepared by dissolving the powders in the appropriate volume of dH_2O as specified by the supplied data sheet. Working solutions of 10 μM were then prepared by a 10-fold dilution in dH_2O and stored at -20°C.

A master mix was made on ice and vortexed before use. For each sample plus a spare, 4 μL 5x GoTaq coloured buffer, 2 μL 2 mM dNTPs, 2 μL 10 μM F-primer, 2 μL 10 μM R-primer, 9 μL dH_2O and 0.2 μL 5 μg/μL GoTaq DNA polymerase were mixed (except for primers, all from Promega).

1 μL cDNA template or negative control was added to 19 μL of the master mix. All polymerase chain reaction (PCR) conditions were as follows: 2 min incubation at 95°C, 35-40 cycles of denaturation at 95°C for 40 s, annealing at 58-60°C for 30 s and extension at 74°C for 60 s, then a 5 min incubation at 74°C before indefinite storage at 4°C. Details for each primer used for pluripotency analysis are given in Table 2.3.

2.5.2.4 Product visualisation

A 50x stock solution of tris acetate EDTA (TAE) buffer was prepared by adding 242 g tris base (VWR) to 57.1 mL of glacial acetic acid (Fisher Scientific, Pittsburgh,

Table 2.3: Primers used for pluripotent analysis of hESC. The primers and annealing temperature of *POU5F1* were designed to exclude the detection of pseudogenes. Temp: annealing temperature, Size: predicted product size in base pairs.

Target	Sense/Antisense primer	Temp (°C)	Size
ACTB	5-GAG CAC AGA GCC TCG CCT TTG C-3 5-GGA TCT TCA TGA GGT AGT CAG TCA GG-3	58	520
POU5F1	5-GGA GGT ATT CAG CCA AAC-3 5-CTT AAT CCC AAA AAC CCT GG-3	58	650
SOX2	5-CCC CCG GCG GCA ATA GCA-3 5-TCG GCG CCG GGG AGA TAC AT-3	60	448

PA, USA) and 100 mL of 0.5 M EDTA pH 8.0 (Fisher Scientific), then diluted to 10x working solution with distilled water as needed.

A 1.5% agarose gel was prepared by adding 0.75 g of agarose (Fisher Scientific) to 50 mL of 10x TAE and then heating the mixture in a microwave for approximately 2 min until it boiled and the agarose was completely dissolved. After allowing the solution to cool to approximately 40°C, 0.5 μg/mL ethidium bromide (Promega) was added. The gel solution was poured into a tray with an appropriate size comb; any bubbles were removed using a Gilson tip and the gel was left to solidify for approximately 30 min.

The solidified gel was placed in a tank and submerged in TAE buffer, and 10 μL of each sample was loaded. pBluescript II SK$^+$-Hpa II digest ladder (kindly donated by the Molecular Biology Department, KCL) was added at either end of the samples. The gel was run at 80 V for approximately 45 min or until the ladder bands were sufficiently separated. The gel was visualised using a Uvitec transilluminator (Uvitec, Cambridge, UK).

2.5.2.5 Extraction of genomic DNA

Genomic (g)DNA was extracted from hESC using the Illustra tissue and cells genomicPrep Mini Spin Kit (GE Healthcare Amersham, UK) according to the manufacturers instructions. All solutions were provided in the kit.

Whole colonies of hESC were washed with PBS and collected into a centrifuge tube. Cells were centrifuged at 13,500 rpm for 1 min to collect a pellet and the

supernatant discarded. 100 μL of lysis solution 1 was added and the cells resuspended by pipetting followed by vortexing for 15 s. 10 μL of 20 mg/mL proteinase K was then added and vortexing repeated for 15 s. The sample was incubated at 56°C for 15 min followed by 70°C for 2 min. Cells were centrifuged briefly to bring the contents to the bottom of the tube. 5 μL of 20 mg/mL of RNase A was then added and the sample incubated at RT for 15 min followed by the addition of 500 μL of lysis solution 2 and incubation at RT for 10 min. The sample was then placed in a spin column and centrifuged at 11,000 rpm for 1 min and the flow-through discarded. 500 μL of lysis solution 2 was added and the column was centrifuged at 11,000 rpm for 1 min and the flow-through discarded. The second wash step was performed by addition of 500 μL wash buffer and centrifugation at 11,000 rpm for 3 min. The column was then transferred to a fresh centrifuge tube and 20 μL elution buffer pre-warmed to 70°C added directly onto the membrane and incubated at RT for 1 min. The column was then centrifuged at 11,000 rpm for 1 min to collect the purified gDNA. The gDNA was stored at -20°C until use.

2.5.3 Karyotype analysis

Karyotype analysis of hESC was outside the clinical load of the cytogenetic department and was therefore outsourced to The Doctor's Laboratory (TDL) a clinical pathology accredited laboratory. The following protocol for analysis is summarised from that supplied by TDL.

2.5.3.1 Suspension harvest

The cells were incubated in colcemid (Sigma-Aldrich) at 20 μL/mL of hESC media for 20 min and then washed with PBS before incubation in 3 mL trypsin/EDTA (Sigma-Aldrich) for 3 min. The detached cells were mixed with 3 mL of 1:12 solution of fetal bovine serum:H_2O, then incubated at 37°C for 25 min before being pre-fixed with 5 drops of fresh cool fixative of 3:1 methanol:glacial acetic acid (VWR). The suspension was then centrifuged for 10 min at 1500 rpm, the resulting supernatant discarded and the cells pellet loosened. The cells were then re-fixed and re-centrifuged exactly as described twice further before re-suspension of the pellet in a minimal volume of fixative solution.

2.5.3.2 Preparation of the slides

40 μL of the cell suspensions were applied just below the frosted end of a wet, washed slide, which was then tilted to allow the suspension to run slowly down the surface, and air dried.

2.5.3.3 G banding

The slides were aged in a drying oven at 92°C for 40 min or 63°C overnight before being rinsed in PBS for 5 min. The slides were then treated with 1 in 50 dilution of trypsin in PBS for a critical time dependent on cell sample. The trypsin was quenched with a PBS solution containing serum before being stained with 3:1 leishman/giemsa (Merck, Whitehouse Station, NJ, USA) (2.5 mL in 47.5 mL pH 6.8 buffer) and rinsed briefly in purified water, gently blotted dry, and mounted with coverslips.

2.5.3.4 Analysis

Slides were analysed by conventional bright field microscopy, examined with oil immersion 1000x high power objective with reference to ISCN2005. A minimum of 10, but if possible, 20 metaphase spreads were examined for each analysis. A typical metaphase was digitised and stored using a Cytovision image analysing system.

2.5.4 Fluorescence activated cell sorting

The BD Fluorescence Activated Cell Sorting (FACS) Calibur (BD Biosciences; Becton, Dickinson and Company, Oxford, UK) was used to analyse various cell surface marker expression profiles of hESC. Dishes of human foreskin fibroblast (HFF) feeders with 80-90% confluent hESC, or HFF alone, were washed briefly with PBS before trypsin was added for approximately 5 min. The enzyme was quenched and the sample centrifuged at 1000 xg for 3 min. The supernatant was discarded and the cell pellet resuspended in 100-200 μL culture medium depending on cell number. The majority of the antibodies used for analysis were conjugated with a fluorescent secondary so the staining was only one step. The details of the antibodies used for all experiments are given in Table 2.4. The conjugated antibody or appropriate isotype control was added to the cell suspension at the correct dilution and incubated at 4°C in the dark for 30 min. 500 μL PBS was added and the sample centrifuged at

1000 xg for 3 min. For unconjugated antibodies, the incubation and wash steps were repeated with the secondary antibody. The supernatant was discarded and the cells resuspended in 100-200 μL of culture medium before immediate analysis. Isotype controls and/or HFF only samples were used to define the gates of positive cells. The results were analysed with the BD CellQuest^{TM} software version 3.3.

Table 2.4: Details of antibodies used for all FACS analysis performed. NCAM: neural cell adhesion molecule, CD: cluster of differentiation, HLA: human leukocyte antigen, KRT: keratin, HNK: human neural crest, PE: phycoerythrin. e-Bioscience, San Diego, CA, USA. a-m; anti mouse, sec; secondary if unconjugated, used at 1 in 500.

Name	Isotype	Fluorochrome	Clone	Company	Dilution
NCAM	mouse IgG1	PE	B159	BD	1 in 10
SSEA1	mouse IgM	FITC	HI198	BD	1 in 10
SSEA4	mouse IgG3	PE	MC-813-70	e-Bioscience	1 in 50
CD73	mouse IgG1	PE	AD2	BD	1 in 10
CD9	mouse IgG1	FITC	M-L13	BD	1 in 10
CD30	mouse IgG1	PE a-m IgG1 (sec)	Ber-H2	SantaCruz	1 in 20
CD45	mouse IgG1	FITC	HI30	BD	1 in 10
HLAabc	mouse IgG1	PE	G46-2.6	BD	1 in 10
KRT18	mouse IgG1	alexa 488 a-m IgG1 (sec)	CK2	Chemicon	1 in 20
HNK1	mouse IgM	FITC	NK-1	BD	1 in 10
p75	mouse IgG1	PE	C40-1457	BD	1 in 10

2.5.4.1 Cell cycle analysis

Analysis of hESC cycling was performed by FACS analysis. A dish of HFF feeders with 80-90% confluent hESC cells and HFF alone was prepared as described in section 2.5.4 and a cell count performed. It was essential to obtain a complete single cell suspension and to perform an accurate count so that the proportion of the reagents could be accurately calculated.

Care was taken to ensure analysis of single cells, as two diploid cells aggregated together in the G1 phase of the cell cycle could be mistaken as one cell in G2/M. Aggregates and simultaneously read events were unavoidable during the acquisition part of cell cycle analysis, despite careful and appropriate sample preparation. The approach to maintain the fidelity of the data was to exclude these non-single cells

from later analysis. Usually only the height (maximum fluorescence emission FL2-H) was recorded for FACS analysis. However FL2-H gave no information about singularity and could not be used for accurate cell cycle analysis. Pulse width (FL2-W) was indicative of particle transit time. Single cells would have a smaller pulse width compared to cells that had aggregated. The area (FL2-A) gave total cell fluorescence and was the parameter selected for DNA analysis. Plotting FL2-A against FL2-W was therefore used to distinguish between single cells and aggregates. Single cells had similar pulse width (transit time) values. Aggregates had larger width values and could be easily seen on the plot to the right of the single cell region. Single cells were then gated and an FL2-A histogram drawn and formatted to show only the events inside of the single cell region.

For 500,000 cells, a total reaction volume of 500 μL was required, consisting of 0.5 μL saponin (Sigma Aldrich) for permeabilisation, 1 mg/mL RNAse, 10 μg/mL propidium iodide (PI; Sigma Aldrich) for DNA labelling with the balance as the cell suspension volume. The reaction was incubated at 4°C overnight and analysed the following day. Control cycles were run where the PI concentrations were doubled to ensure that the results remained consistent, and PI was not limiting or exaggerating the data.

2.5.5 CAG repeat analysis

When cell lines were derived from embryos diagnosed as affected by Huntington disease (HD) the disease status and length of CAG repeat was confirmed in the hESC, in collaboration with the Guy's PGD team.

2.5.5.1 Cell lysis

A small clump of hESC was placed in calcium and magnesium free media (Sage BioPharma) and disaggregated with pipetting to single cells before being washed through a poly vinyl pyrrolidone (PVP; Research Instruments Ltd, Cornwall, UK) solution of concentration 5 mg PVP/mL PBS.

Eppendorf tubes were prepared containing 2.5 μL of NaOH/dithiothreitol (DTT; Sigma Aldrich) lysis buffer. Lysis buffer was prepared by diluting a 3 M stock of pH 5.2 sodium acetate (NaAc; Sigma Aldrich) to 0.01 M in dH_2O. 250 mg of DTT powder was added to 1.62 mL 0.01 M NaAc to make a DTT mix. 4 g of NaOH was

added to 10 mL dH_2O to make 1 M solution. 500 μL 1 M NaOH (final concentration 200 mM) was added to 125 μL 1 M DTT mix (final concentration 50 mM) in 1.875 mL dH_2O and sterile filtered to form the lysis buffer. Aliquots were stored at -20°C.

Single or multiple cells were added to the lysis buffer, along with control buccal samples and an RTN without cell addition. The solutions were covered in mineral oil (Sigma Aldrich) and lysed on a DNA Engine PCT 200 PCR block (MJ Research) at 65°C for 10 min, then cooled to 4°C. The samples were then neutralised by pipetting 2.5 μL of 200 mM Tricine (Sigma Aldrich) under the oil layer into the sample volume. Tricine was prepared by diluting 1 g in 27.9 mL dH_2O to give a 200 mM solution. Aliquots were stored at -20°C.

2.5.5.2 Polymerase chain reaction profile

A master mix was prepared on ice and vortexed before use. For each sample plus a spare, 10.95 μL dH_2O, 2.5 μL of 27.5 mM magnesium chloride buffer, 2.5 μL deaza dNTPs (Promega), 1.0 μL of 50 μM HD1 forward primer, 1.0μL of 50 μM HD3-5 reverse primer, 1.25 μL DMSO and 0.8 μL Taq DNA polymerase enzyme were mixed. The buffer and enzyme were from an Expand Long Template PCR System kit (Roche Pharmaceuticals, Nutley, NJ, USA). HD1 forward primer sequence: 5'-GGCCTTCGAGTCCCTCAAGTCCTTC-3', HD3-5 reverse primer sequence: 5'-GGCGGTGGCGGCTGTTGCTGCTGCT-3'. Both primers were from ABI.

20 μL of the master mix was added to each sample under the oil layer giving a final sample volume of 25 μL. The PCR was run using a Percol Elmer 9700 or GRI DYAD DNA engine (MJ Research) using the Brussels 38 HD programme. The PCR profile was a initial 5 min incubation at 95°C followed by 35 cycles of 30 s at 95°C and 90 s at 68°C, finished by a 5 min incubation at 72°C and cooling to 4°C indefinitely.

2.5.5.3 CAG fragment analysis

An ABI Prism 3100 was to analyse the CAG fragment sizes. The processing software used was Gene Scan Analysis 2, and results were analysed with Genotyper 2.5.

A master mix was prepared for 16 wells of a 96 well plate as required by the machine, by adding 6 μL ladder LIZ-500 (GeneScan 500) to 260 μL formamide (Sigma Aldrich; to denature the DNA to single strands). The master mix was vortexed then

15 μL added to each of the 16 wells. 3 μL of sample template was then added. The plate was placed in a 100°C hot block for 2.5 min before being quenched in a water bath at RT and loaded into the Prism 3100. Ten second injections were performed with the G-5 dye matched to the LIZ-500. Electrofluorograms were generated by the Genotyper 2.5 program.

2.5.6 Western blot analysis

HESC were washed in PBS, manually cut, pooled in an eppendorf tube and centrifuged at 13,000 rpm for 2 min. The entire volume of PBS was removed from the cell pellet and the dry pellet snap frozen at -80°C until use. A control sample of HFF cells was also collected.

2.5.6.1 Cell lysis

Two lysis buffers were used, the details of which are given in Tables 2.5 and 2.6. All except the last three components of each buffer were combined and placed on a roller for 5 min. 10 mL aliquots were made and stored at -20°C until use. The final three components were added to a 10 mL aliquot and this was placed on a roller until the protease inhibitor tablet had dissolved. The buffer was then kept on ice.

The cell lysate was prepared by adding approximately two volumes of either RIPA or KCl buffer directly onto the thawed cell pellets. The pellet was then agitated until the solution was opaque. If the solution was too thick then further buffer was added. The cells were then snap frozen on ice and left for 20 min to ensure lysis of the cells and release of the proteins.

During the 20 min incubation the cell samples were sonicated using a Jencons VibraCell set at 80 Hz and located in a cold room at 4°C. The cells were pulsed with the sonicator for between 5 and 10 s total to ensure complete shear of genomic DNA. The cell sample was then centrifuged at 4°C for 15 min at 13,000 rpm. The supernatant was collected and the pellet was discarded. The centrifugation was repeated and the supernatant placed on ice.

2.5.6.2 Protein quantification

The quantity of protein extracted from the cell samples was quantified using the Bi-Cinchoninic Acid (BCA; Thermo Fisher Scientific, Waltham, MA, USA) assay.

Table 2.5: RIPA buffer reagents. NaCl: sodium chloride, SDS: sodium dodecyl sulphate, Tris: tris(hydroxymethyl) aminomethane, PMSF: phenylmethylsulphonyl fluoride. Protease inhibitor cocktail from Roche Diagnostics, Indianapolis, IN, USA; PMSF from Fluka, Sigma Aldrich; all other reagents from Sigma Aldrich.

Reagent	**Volume for 50 mL**	**Final concentration**
5 M NaCl	1.5 mL	150 mM
Igepal	500 μL	1%
Deoxycholate	0.25 g	0.5%
10% SDS	50 μL	0.1%
1 M Tris HCl pH 8.0	2.5 mL	50 mM
H_2O	45.45 mL	
β-mercaptoethanol	3.5 μL	1 mM
1 mM PMSF	5 μL	
500 mM DTT	5 μL	
Protease inhibitor cocktail	1 tablet	

Table 2.6: KCl buffer reagents. KCl: potassium chloride, EDTA: ethylenediaminetetraacetic acid. KCl, glycerol and EDTA from Sigma Aldrich.

Reagent	**Volume for 50 mL**	**Final concentration**
1 M KCl	7.5 mL	150 mM
Glycerol	5 mL	10%
0.5 M EDTA	500 μL	5 mM
1 M Tris HCl pH 8.0	2.5 mL	50 mM
H_2O	34.5 mL	
0.1 M PMSF	2 μL	
0.1 M DTT	2 μL	
Protease inhibitor cocktail	1 tablet	

The solutions were provided in the BCA kit and the standards for the assay were prepared as shown in Table 2.7

Table 2.7: BCA standards preparation.

Tube	**Volume of water (μL)**	**Volume of BSA (μL)**
1	100	0
4	98	2
8	96	4
16	92	8
32	84	16

Sample tubes were prepared by adding 1 μL of each protein lysate to 99 μL of water. BCA reagents A and B were mixed in a 50(A):1(B) ratio to make sufficient reagent to add 900 μL to each standard and each sample. Once added and mixed, the standards and samples were incubated at 37°C for 10 min. A biophotometer (Eppendorf) with a BCA programme was used to record the optical density of each solution. The average of the standards was used to calculate the protein concentration and to determine the loading volume for the gel. The volume of lysate needed to provide the required total protein was calculated and samples diluted as necessary to allow the same loading volume. An equal volume of 2x loading buffer (National Diagnostics, Atlanta, Georgia, USA) was added. 20 μL prestained protein marker (broad range, Cell Signalling Technology Inc. Danvers, MA, USA) was added to a separate tube. All samples were denatured for 5 min at 95°C before loading onto a gel. The ladder had bands from 6.5 kDa to 175 kDa, so the gel could be run until the final band reached the end of the gel and the mutant Huntingtin protein would be above this final band. The remaining quantified protein samples were stored at -80°C until use.

2.5.6.3 SDS Polyacrylamide gel electrophoresis

Mutant Huntingtin protein is approximately 350 kDa, therefore a low percentage gel coupled with a long running time was necessary to visualise the band. BioRad gel plates were cleaned with water and then ethanol and then assembled appropriately before making the gels.

For an 8% resolving gel, 2.67 mL Protogel (National Diagnostics) and 2.60 mL Protogel resolving buffer (National Diagnostics) were added to 4.62 mL millipore water. 100 μL 10% ammonium persulphate (APS; Sigma Aldrich) and 10 μL N,N,N,N -Tetramethyl-Ethylenediamine (TEMED; Sigma Aldrich) were then added, mixed quickly and the gel solution loaded immediately between the gel plates and allowed to set. Water saturated butanol was added to the set level to ensure the top of the gel set evenly, and removed when the gel was solidified.

For the stacking gel, 0.65 mL Protogel and 1.25 mL Protogel stacking buffer (National Diagnostics) were added to 3 mL millipore water. 50 μL 10% APS and 10 μL TEMED were then added, mixed quickly and poured on top of the resolving gel. An appropriate size comb was inserted immediately and the gel allowed to set. The stacking gel functioned to ensure all the samples entered the resolving gel at the same time so that any separation was purely by weight not by the time the gel was run. A 10 well comb was selected to allow a larger sample volume to be loaded. Once the stacking gel had set the comb was removed. The gel apparatus was then transferred to a tank and the running buffer poured into the central cavity until the overflow covered the electrodes. Gel running buffer was prepared by adding 100 mL of the 10x stock solution of 0.25 M tris and 1.92 M glycine (National Diagnostics) in 1% SDS running buffer (National Diagnostics) to 900 mL millipore water to give a 1x solution. Gels were run at 150 V for 2-6 h.

2.5.6.4 Sample transfer and visualisation

Transfer buffer was prepared as a 10x stock solution by adding 14 g glycine and 30 g of tris to 1 L of millipore water. 1x working solutions were prepared by adding 100 mL of 10x stock and 200 mL methanol to 700 mL water.

10 cm x 8 cm pieces of nitrocellulose membrane and Whatman filter paper were prepared and soaked in 200 mL of transfer buffer, along with the sponges used in the transfer cassette apparatus. The transfer holders were prepared in the loading buffer. After each layer was added the surface was gently smoothed to remove any air bubbles. A sponge was placed in the holder followed by a piece of Whatman paper. A dry piece of filter paper was used to adhere to the gel and remove it from the glass holders once these had been gently separated with a slider. The gel and paper were then added to the holder, followed by the nitrocellulose membrane and

two further layers of Whatman paper and the second piece of sponge. The holder was closed and secured and placed in the transfer cassette. An ice cube tray was added and the tank filled with transfer buffer. The transfer gel was run for 2 h at 120 V.

After running, the apparatus was disassembled and the membrane was rinsed twice in PBS and then incubated overnight on a shaker platform at 4°C in 5% milk powder in PBS for blocking. Following a further rinse the membrane was incubated for 90 min at RT in the primary antibody. 4 mL of primary antibody at the appropriate dilution in 0.01% tween20 PBS was added to a 50 mL Falcon tube. The details of the primary antibodies are given in Table 2.8. The membrane was then washed 4 times in PBS and 0.2% tween20 for 10 min on a shaker. The appropriate secondary antibody conjugated to horse radish peroxidase (HRP; Dako, Glostrup, Denmark) was prepared at 1:5000 in 2% milk solution in PBS. The membrane was incubated in a tray with the secondary for 1 h at RT before being washed as before. The membrane was then further washed twice in PBS.

An equal volume of enhanced chemiluminescence detecting reagents (EC; GE Healthcare Amersham, UK) were mixed and used to blot the protein side of the membrane for 1 min. The liquid was drained and the membrane placed in a saran wrap. The membrane was exposed to film (GE Healthcare) for 3-10 min before being read with a Compact X4 Automatic X-ray Film Processor (Xograph Imaging Systems Ltd, Gloucestershire, UK).

Table 2.8: Antibodies used for wild-type and mutant huntingtin detection by western blot

Antibody	Company	Species	Clone	Detection	Concentration
2166	Chemicon	Mouse IgG	1HU-4C8	N terminal htt	1 in 1000
S830	KCL	Goat IgG	Polyclonal	CAG expansion	1 in 5000
MW1	Novartis	Mouse IgG	Polyclonal	Mutant PolyQ	1 in 1000

2.5.7 Cryopreservation-thaw

An important part of characterisation was to ensure that the hESC lines could successfully be vitrified and thawed. Until this was confirmed the line was not suitable

for submission to the UKSCB. At each passage from 5 (exact passage number dependent on behaviour of the line) several colonies were vitrified as in section 2.3.3 and then thawed as in section 2.3.4. If the colonies attached, proliferated and showed normal behaviour on propagation, as many colonies as possible were cryopreserved at each subsequent passage to form a bank, aliquots of which were deposited in the UKSCB.

2.6 Media analysis techniques

Samples of media were analysed using a NOVA BioProfile® 400 metabolite analyzer (Nova Biomedical, Waltham, MA, USA) which could simultaneously measure the levels of glutamine, glutamate, glucose, lactate, sodium ions (Na^+), potassium ions (K^+), ammonium ions ($NH_4{}^+$), as well as pCO_2, pO_2, osmolality and pH. Due to the need for frozen storage of samples, and a known defined culture environment, the pCO_2, pO_2 and pH measurements were discarded.

The NOVA 400 software possessed an automated calibration protocol and measured via two methods. Potentiometric electrodes that developed a voltage proportionate to the concentration of charged ions were used for the measurement of $NH_4{}^+$, Na^+ and K^+. Ampherometric electrodes that had immobilized enzymes in the membranes to generate a current proportional to the substrate were used for the measurement of glucose, lactate, glutamine and glutamate. In order to ensure that reduction of enzyme activity with time or other fluctuations did not affect the readings, the same sample was analysed at the beginning and end of the sample set. As long as any differences in readings were within the accuracy range given in the manufacturer instructions the efficiency of the machine was deemed sufficient.

2.6.1 Medium collection

Samples of each batch of hES CM and KOSR medium were collected fresh at the time of formulation. Also collected was the base BRL medium before addition of the CM component. The samples were centrifuged briefly to remove any debris, and stored at -80°C until analysis. 10 samples were collected for KOSR and 15 for hESC CM.

To collect samples of the proliferating feeder conditioned medium, a single vial of both the HFF and MEF feeders was thawed, and the cells expanded by a 1:2 split every 2 days at the same time of the day. Samples of feeder CM were collected from the flasks of HFF and MEF cells every 48 h, just before the cells were split. For the duration of the experiment the fibroblasts were fed with a single batch of feeder medium and all culture and passage was performed exactly as in section 2.2.2. In this way, the sample collection exactly mimicked routine collection of CM used for experimentation. The feeder CM was centrifuged briefly to remove any cell debris, and stored at -80°C until analysis. 15 samples were collected for each feeder type and compared to a control sample of the base feeder medium without exposure to cells.

To collect samples from inactivated feeders with or without hESC, inactivated HFF and MEF feeders were plated exactly as for routine passaging as described in section 2.2.3. In order to have 10 triplicate measurements, 30 wells of each were prepared. As the NOVA required a minimum of 1.5 mL for analysis and each well contained 500 μL, the triplicate samples were pooled, resulting in 10 samples per condition. The following day, the feeder medium was removed, the cells washed once with PBS and KOSR added. After 24 h the medium was collected, pooled, centrifuged briefly and stored at -80°C. The cells were fed with fresh KOSR, which was collected in exactly the same way after 48 h. To assess the effect of hESC on metabolite levels, 10 colonies of hESC of comparable size were added to each feeder well. The medium was again collected at 24 h and 48 h after plating the cells. In total, 10 samples from each of the 4 conditions were collected and the metabolite levels compared.

Chapter 3

Derivation of human embryonic stem cell lines

3.1 Introduction

The establishment rate of human embryonic stem cell (hESC) lines is quoted as anything between 2% and 40%, although most commonly around 20% (Findikli *et al.*, 2005; Lysdahl *et al.*, 2006; Stephenson *et al.*, 2006). The low establishment rate is accompanied by a low reported frequency of chromosomally aberrant cell lines (Hanson & Caisander, 2005). This combination suggests that selection occurs, not only during development to the blastocyst stage, but also during the establishment of hESC lines, given that derivation rates even fall short of positive pregnancy test rates with IVF. This selection could have origins in the quality of the embryo, and also be driven by sub-optimal manipulation or culture conditions during derivation and early propagation of hESC. It has been speculated that only a small fraction of ICM cells give rise to the hESC line by activation and proliferation of a few founder cells (Sjogren *et al.*, 2004), thus the quality parameters used in IVF may not be directly applicable to predicting derivation outcome (Stephenson *et al.*, 2006).

Clearly, early culture conditions may have a profound effect on the success of derivation; the feeder cells used, the medium employed and the gas phase of culture could all influence the outcome. These factors are considered in Chapter 4. It is also likely that the technique, either the method to isolate the ICM or the direct culture of the intact blastocyst, may have an effect on derivation success. Whilst immunosurgery was the only reported technique for several years, a comparison between this and plating the intact blastocyst concluded that the efficiency was higher

with whole plating (Sjogren *et al.*, 2004). This led to the suggestion that healthy TE cells may be as beneficial to hESC establishment as they are in implantation, perhaps by secreting mitogenic factors.

There is now anecdotal evidence of over 300 lines worldwide (Abbott *et al.*, 2006). However, current reporting of derivation is variable and incomplete, a fact which creates hurdles for the derivation community (Stephenson *et al.*, 2007, 2006), and may contribute to the low derivation rates reported as a factor of poor communication of results. Efficiency of derivation with any method cannot accurately be compared using published reports; as such, the most suitable plating method, developmental day of use, or culture conditions cannot be ascertained. Certainly the basis of the vast range of reported efficiencies cannot be unravelled until it is clear whether the efficiency is reported per embryo, per blastocyst or per ICM, and equally importantly, the grade of the blastocysts used.

3.1.1 Aims

The aim of this work was to develop several alternative hESC derivation methods such that each attempt could be tailored to the morphology of the blastocyst in order to try and improve derivation rates. There then could be a reasonable expectation of hESC line generation from each suitable embryo entering the research programme - particularly important with the infrequent acquisition of embryos carrying clinically significant genetic mutations. When this work started, the only established derivation methods were immunosurgery and whole plating. Whilst immunosurgery was used initially to prove competence with manipulation and culture skills, it is likely to preclude any hESC from clinical application as it involves the use of xeno products. Hence, once competence had been proven with this approach, subsequently it was abandoned as a useful methodology. Instead, the use of mechanical and laser ICM isolation and whole plating was investigated. Both isolation methods still left residual mural TE and intact polar TE, thereby potentially retaining the beneficial effects of TE signalling whilst minimising the risk of TE overgrowth.

Accurate records of each and every embryo used, along with developmental information and the quality of the blastocysts manipulated were kept, with the aim to calculate true efficiencies of derivation. As individual derivation laboratories do not each process sufficient embryos to draw meaningful conclusions in isolation, and

experience with derivation of hESC lines and long-term culture is still limited, the establishment of an international collaboration to address these questions was attempted.

3.2 Method development

3.2.1 Development of derivation techniques

Several derivation methods were tried, tailored to the different morphology of the blastocysts, in order to maximise the efficiency of derivation. This would ensure best use of the embryos donated to research. Along with this was the need to develop techniques for derivation suitable for eventual clinical use of the cells. Statistical analysis was carried out using Stata, version 9.2 (StataCorp, College Station, Texas, USA). Quantitative data are presented as mean ± standard deviation. Chi-squared analysis was used to determine significant differences between groups. All results were considered significant at $p<0.05$. Kappa analysis was used to determine observer agreement between groups.

3.2.1.1 Immunosurgical isolation of the inner cell mass

Three hESC lines (KCL001, 002, 003-CF1) had been derived previously by others at Guy's ACU using immunosurgery. Therefore initial attempts at derivation were with immunosurgery using the same protocol in order to prove personal competence with established methods, and to gain necessary experience with the morphology and appearance of early hESC before undertaking experiments to develop novel derivation methods that were compatible with GMP standards.

Blastocysts were considered for immunosurgery on day 5, 6 or 7 of development depending on morphology. A substantial ICM was essential as immunosurgery is an invasive procedure, and small ICMs tended to be damaged or destroyed during the process. Small aliquots of protease, rabbit anti-human serum and guinea-pig complement (all from Sigma Aldrich) were stored at -20°C. Solutions were pre-equilibrated prior to use.

Blastocysts with an intact zona pellucida were incubated in 0.5% protease solution under constant observation and gentle pipetting. Once the zona had thinned and expanded away from the TE the blastocysts were washed twice in blastocyst

medium. Zona-free blastocysts were incubated in rabbit anti-human serum for 20 min at 37°C, then washed three times in blastocyst medium. The final incubation was for 10-30 min in guinea-pig complement, under frequent observations, until the TE cells swelled with bubble-like 'blebs'. When the complement reaction was complete, the cells were washed three times in hES CM. The collapsed blastocysts were aspirated and expelled several times with decreasing diameter pipettes until the majority of the lysed TE cells were removed. The isolated ICMs were then transferred to pre-prepared feeder plates (section 2.2.3) and left undisturbed for 48 h. Subsequently one half of the medium was exchanged on alternate days and photographic and written records of growth kept. The spent medium was collected and stored at -20°C for future analysis. Cultures were kept for a minimum of 15 days before discarding unless only degenerate cells were visible. Any cultures with stem-like cells visible were expanded as in section 2.3. Unsuccessful dishes for discard were flooded with 70% ethanol, rinsed with water and placed in clinical waste.

3.2.1.2 Mechanical isolation of the inner cell mass

Blastocysts were considered for mechanical isolation when there was a distinct ICM, and used on day 6 or 7 depending on morphology. Day 5 blastocysts were generally not used for mechanical attempts, as they had not expanded sufficiently and therefore the risk of damage to the ICM was too great.

If the blastocysts had not yet hatched the zona was removed as for immunosurgery. For initial attempts at mechanical isolation, a dish was prepared with five 30 μL drops of pre-equilibrated hESC CM without oil overlay. Blastocysts were washed through four of these drops, changing the transfer pipette each time to eliminate oil carry-over from the original culture dish. A Gilson tip was used to pull a channel out from the side of the fifth drop. The use of multiple drops was important as preliminary experiments without these wash steps demonstrated that the presence of oil prevented the formation of a channel. The blastocysts were placed in this drop then gently pushed into the channel until they became flattened due to the minute volume of medium as shown by the schematic in Figure 3.1. From this point manipulations had to be carried out extremely swiftly to avoid evaporation of the medium and subsequent lysis of the blastocyst. Initially a feather scalpel (Feather Safety Razor Co., Ltd, Osaka, Japan) was used for isolation attempts. However,

a single implement was not straightforward, as the blastocysts could still rotate to some extent despite the volume restrictions. In general, very little TE was removed in these experiments. The protocol was modified to incorporate a pair of needles with the aim of stabilising the blastocyst for manipulation. Using BD Microfine-100 Insulin needles (BD Biosciences) the TE cells were gently cut away from the ICM, then the channel flooded with medium. The portion of the blastocyst containing the ICM was washed through two drops of hESC CM and then transferred to pre-prepared feeder plates. Occasionally slivers of plastic attached to the cells if use of the needles damaged the culture dish. These were removed if deemed safe to do so, otherwise they were left in the culture.

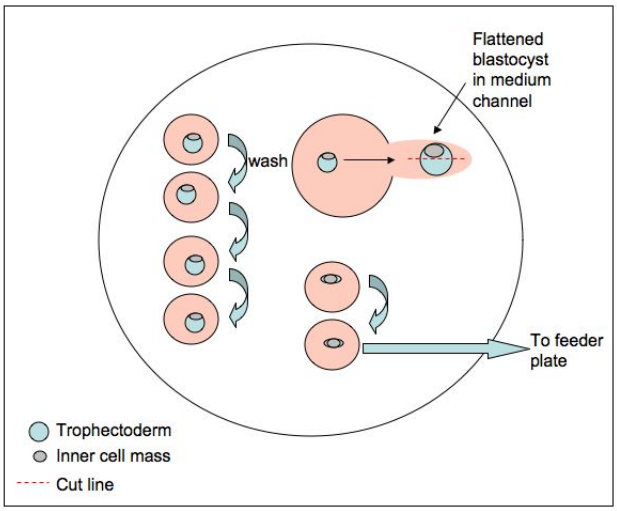

Figure 3.1: Schematic to illustrate the mechanical method of ICM isolation. Blastocysts were washed through drops to remove any oil carry-over and TE removed once the blastocyst was flattened in a drawn-out channel. The ICM and residual TE was washed before being transferred to a feeder layer.

Although successful derivation was achieved with this protocol, osmotic shock was a concern, both from rapid changes in osmolality of the medium following evaporation and subsequent intracellular perturbations in the cells of the blastocyst. In fact lysis of the ICM and TE was observed on more than one occasion when difficulty in manipulation resulted in delayed flooding of the channel with medium. Modifications were therefore developed to optimise this method. In later attempts, the zona was removed as described, but the blastocysts were manipulated in the original culture

drop under oil. Using a Gilson tip, the medium forming the drop containing the blastocyst was aspirated from under the oil until only a surface layer remained and the blastocyst was spread against the bottom of the dish. This medium was added to a neighbouring drop in the same dish. The needles were then used to cut as close as possible to the ICM, with accuracy facilitated by the reduced time pressure. Once the isolation was completed, medium was aspirated from the neighbouring drop and used to re-form the original culture drop. The advantage to this modification was the elimination of the possibility of evaporation of the medium and ensuing damage to the blastocyst, as well as the better maintenance of pH under oil. However, it was essential that the portion of the blastocyst containing the ICM was attached to the bottom of the dish before re-flooding the drop, as in some initial experiments, the ICM became trapped at the medium-oil interface at the apex of the drop, and it was not possible to retrieve it for plating. It was a very simple matter to use the tip of the needle to secure a few remaining TE cells to the bottom of the dish, such that blastocyst portion remained at the bottom of the drop when re-flooding and could be released by pipetting, prior to being washed through two drops of hESC CM and plated. Following isolation and plating with this method, culture, medium exchange and disposal was exactly as for immunosurgery.

3.2.1.3 Laser isolation of the inner cell mass

Blastocysts were considered for laser isolation on any day of development when there was a distinct ICM, but specifically if the blastocyst was in the process of hatching and the ICM was contained within the extruded area. Although mechanical manipulation had proven successful, occasional damage was caused to the ICM and a more delicate and accurate method was required for ICM isolation for those blastocysts with appropriate morphology. Furthermore a number of volatile organic compounds detrimental to embryo development have been shown to be emitted by disposable plastic petri dishes, including styrene, ethyl-benzene and benzaldehyde (Gilligan *et al.*, 1997). Scraping the surface of the dishes during mechanical isolation risked the release of these compounds.

Manipulation was carried out in biopsy dishes (BD Biosciences) with microdrops of HEPES-buffered medium under oil. The blastocyst was secured with a holding pipette (The Pipette Company; TPC, Thebarton, South Australia) at the region of

the zona opposite the ICM , and a biopsy needle (TPC) prepared to aspirate the hatched area. Using a Saturn Active laser (Research Instruments; RI, Falmouth, Cornwall, UK) and Cronus software (RI), the appropriate time pulse for the laser was selected to avoid damage to the ICM but remove as many TE cells as possible. Laser pulses were directed at the TE cell junctions adjacent to the ICM cells but outside of the safety circle, as shown in Figure 3.9b. At this point both the hatched and zona-contained cavities tended to collapse, so the biopsy needle was used to secure the hatched cells and pull them gently away from the main body of the blastocyst. The laser firing was repeated as appropriate whilst gently retracting the biopsy needle until the two sections separated. If this was unsuccessful, the plate was removed from the micromanipulation rig and two hand-held pipettes used to apply stronger suction to separate the portions. The cellular area containing the ICM was then washed though two drops of hESC CM and transferred to pre-prepared feeder plates. Subsequent culture and medium exchange was exactly as for immunosurgically prepared ICMs.

3.2.1.4 Whole plating of blastocysts

Blastocysts were considered for whole plating when of poor quality or when those that collapsed in culture did not re-expand in an appropriate time-frame. If the blastocysts had not yet hatched the zona was removed with protease as for immunosurgery. The blastocysts were then washed through two drops of hESC CM and transferred to pre-prepared feeder plates. Culture and medium exchange was exactly as described for the other methods. Once the blastocysts had attached, mechanical isolation of cells displaying stem cell-like morphology was performed before a total of 14 days in culture. If no cells of interest could be identified by this time, and therefore isolation was not possible, the cultures were discarded as described for the other methods.

3.2.2 Development of a standard for reporting derivation

3.2.2.1 Data collection

There are a number of universally agreed key steps required to successfully initiate, develop and maintain a biological standard (Brazma *et al.*, 2001; Brooksbank &

Quackenbush, 2006; Field & Sansone, 2006). In forming a proposed standard for the reporting of derivation these steps (1-6 below) were followed closely.

1. *Identify the scope of the information to be included in the standard*

In order to identify the scope of the proposed biological standard an extensive review was performed of all the derivation literature available, focusing on what information was included in the reports. For example it was determined whether or not groups reported if the embryos used were fresh or frozen, the total number of embryos allocated to the research, and the quality of blastocysts used in derivation attempts. The full review is shown in Tables 3.1 and 3.2.

2. *Develop a framework for the information that is clear and easy to use*

The framework for the information was developed in two parts: a grading system for the blastocysts used in derivation attempts and a table of metadata categories for the required information. Based on existing clinical embryology grading systems, but tailored to hESC derivation, a grading system was presented with detailed grades for the extent of expansion and ICM quality, and more basic categories for the TE. To facilitate the use of the system, photographic examples of the ICM grades were also given, particularly to aid those scientists attempting derivation with a cell culture rather than embryological background. The grading system and examples are shown in Figure 3.2.

The aim of the metadata categories included in the system was to maximise the information from each derivation attempt. In addition, as very few stem cell laboratories process enough embryos to draw meaningful conclusions in isolation, international collaboration and sharing of results was needed. Based on the literature review, consultation with a small group of embryologists and personal experience, a minimum information dataset for inclusion in all reports of derivation was compiled and the categories grouped into *essential* or *desirable*. The full list is shown in Table 3.3

3. *Make the draft specification freely available to all interested parties*

The draft proposal was published in the Medline-listed journal Regenerative Medicine as a free-of-charge open access download. In addition, to ensure widespread distribution, a substantial number of copies were posted to derivation groups and distributed at national/international conferences, including in Europe, Asia, Australia and North America.

Table 3.1: Summary of the literature review with respect to the data categories included. Fr; fresh, Fz, frozen, Used; number of embryos used, Blast; number developing to blastocyst, Suitable; suitable for use, Medium; embryo culture medium used. Surplus; deemed surplus to the IVF cycle as not suitable for freezing, donated; donated gametes, PGD; affected embryos from a PGD cycle.

Group	**Fr/Fz**	**Used**	**Blast**	**Suitable**	**Medium**
Thomson et al, 1998	Not specified	36	20	14	Vitrolife
Reubinoff et al, 2000	Fresh (donated)	Not reported	4	4	Not specified
Lanzendorf et al, 2001	Fresh	110	50	40	Vitrolife
Amit et al, 2002	Frozen	Donated at blastocyst	5	Not reported	Not reported
Park et al, 2003	Frozen	Not reported	Not reported	32	Vitrolife
Pickering et al, 2003	Fresh (PGD)	44	24	24	Vitrolife
Pickering et al, 2003	Frozen	14	8	8	Vitrolife
Mitalipova et al, 2003	Fresh (surplus)	Donated at blastocyst	19	19	Not reported
Hovatta et al, 2003	Fresh (surplus)	Donated at blastocyst	5	5	Vitrolife
Heins et al, 2004	Fresh	Not reported	Not reported	Not reported	Not specified
Kim et al, 2004	Frozen	Not reported	Not reported	19	Vitrolife
Stojkovic et al, 2004	Fresh (donated)	11	7	7	G1, G2.3, BRL
Cowan et al, 2004	Frozen	286 embryos, 58 blastocysts	Not reported	Not reported	Not reported
Pickering et al, 2005	Fresh (PGD)	2	1	1	Vitrolife
Kim et al, 2005	Frozen	Not reported	47	47	Vitrolife
Inzunza et al, 2005	Fresh and frozen	Donated at blastocyst	37	37	Medicult
Chen et al, 2005	Fresh (surplus)	130	19	19	Vitrolife
Findikli et al, 2005	Fresh (surplus)	Donated at blastocyst	20	15	Not reported
Findikli et al, 2005	Fresh (5 surplus, 6 PGD)	Donated at blastocyst	11	11	Not reported
Lysdahl et al, 2006	Fresh (surplus)	198	24	24	Medicult
Ludwig et al, 2006	Frozen	Not reported	Not reported	5	Vitrolife

Table 3.2: Summary of the literature review continued. Quality; blastocyst quality, ICM; number of ICMs isolated, Colonies; number of stem-like colonies, Lines; number of lines.

Group	**Quality**	**ICM**	**Colonies**	**Lines**	**Efficiency**
Thomson et al, 1998	Not reported	14	Not reported	5	
Reubinoff et al, 2000	Not reported	4	Not reported	2	
Lanzendorf et al, 2001	Reported when successful	18	Not reported	3	
Amit et al, 2002	Not reported	Not clear	Not reported	3	43% (per blast used)
Park et al, 2003	Not reported	30	10	3	10% (per blast used)
Pickering et al, 2003	Reported	16	7	2	5% (per embryo)
Pickering et al, 2003	Reported	8	3	1	7% (per embryo)
Mitalipova et al, 2003	Reported	Not reported	8	4	
Hovatta et al, 2003	Reported	5	2	2	
Heins et al, 2004	Reported when successful	Not reported	Not reported	6	
Kim et al, 2004	Not reported	16	12	9	47% (per blast used)
Stojkovic et al, 2004	Hatching info	7	3	1	
Cowan et al, 2004	Reported when successful	97	Not reported	17	
Pickering et al, 2005	Reported	1	1	1	
Kim et al, 2005	Reported for ICM	Whole/partial culture	Not reported	13	28% (per blast)
Inzunza et al, 2005	Reported when successful	Not reported	12	12	
Chen et al, 2005	Reported	10	5	2	
Findikli et al, 2005	Reported	12	4	2	27% (colonies per blast)
Findikli et al, 2005	Not reported	Whole culture	5	5	46% (per blast)
Lysdahl et al, 2006	ICM size reported	23	Not reported	4	2% (per embryo)
Ludwig et al, 2006	Not reported	5	Not reported	2	

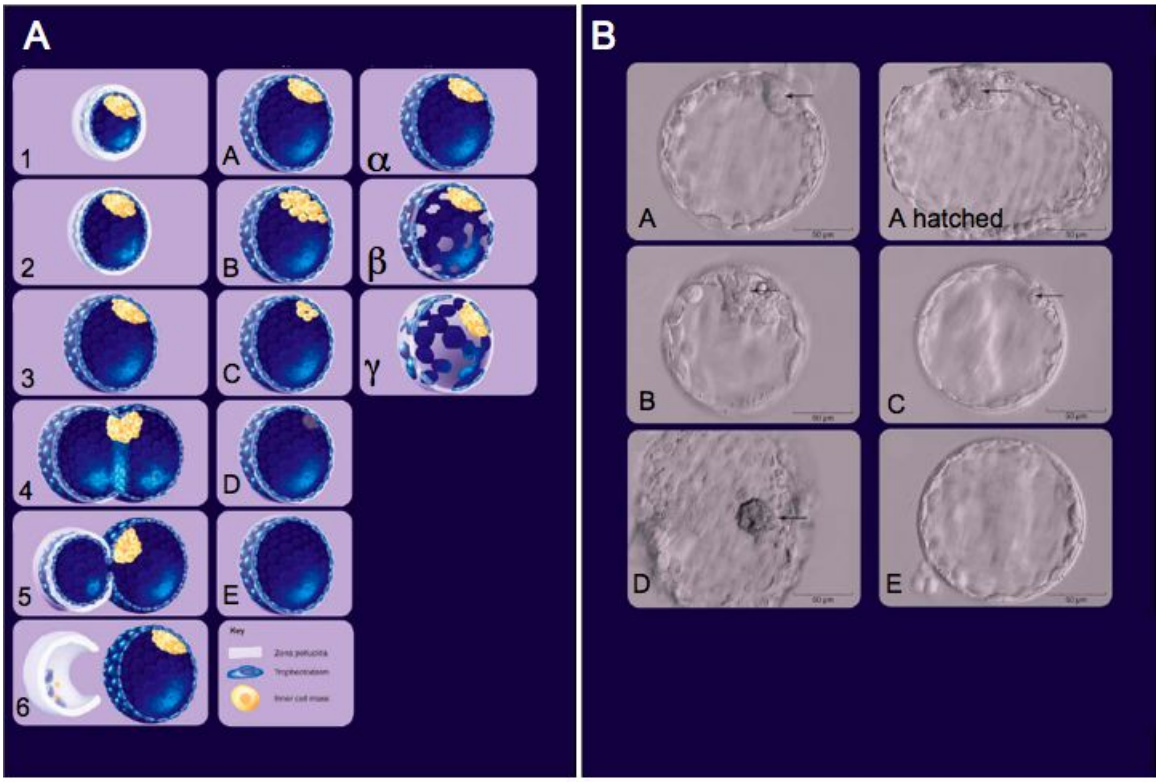

Figure 3.2: Classification system for blastocysts used for hESC derivation (A) Schematic representation of (1-6) Expansion status (A-E) ICM appearance and (α-γ) TE appearance. (B) Photographic images of ICM grades, ICM indicated by an arrow.

Table 3.3: Categories for inclusion in the standards proposal, thought to be *essential* or *desirable* for collection. ECM: extracellular matrix

Essential
Total number of embryos allocated to the research project
Stage of embryos used
Number of embryos allocated at the cleavage stage developing to blastocyst
Number of blastocysts suitable for use
Day of development of blastocysts used
Grade of all blastocysts used
Number of ICMs placed on feeder layer/ECM
Method used to isolate ICMs
Number of ICMs that attach to feeder layer/ECM
Number of days until appearance of stem cell-like outgrowth
Number of stem cell-like colonies that arrest in early culture
Number of hESC lines established
Known disease if PGD
Proprietary IVF medium used
Gas phase employed
Desirable
Source of embryos if fresh
Hatched naturally or method of zona removal
Karyotype

4. *Develop a consensus with the community*

The editorial contained several requests for feedback on the proposed minimum information convention. However to maximise the response rate, the manuscript and a questionnaire consisting of multiple-choice questions regarding the data and fields for free-text comments were distributed to all identified derivation teams. Participants were requested to categorise the MI data as *essential*, *desirable*, or *not required* in publications regarding hESC derivation. In addition they were asked specific questions regarding the need for a standard in this field. Several rounds of follow-up contact ensured that as many responses as possible were obtained.

5. *Circulate widely the agreed protocol to all interested parties*

The results from the community consultation were again published in Regenerative Medicine as a free of charge open-access download. Included in the supplementary information was a data collection form. The publication, grading system and data collection form were distributed widely to derivation teams and also circulated to stem cell banks, standards agencies, networks who had specific interest in developing standards, and to regulatory authorities.

6. *Standards are an ongoing process and care must be taken to ensure they remain relevant and up-to-date*

This step is of paramount importance in order to ensure that the standard does not quickly become out-of-date and obsolete. The goal is to use the standard as a means of gathering derivation data from community and feedback regarding included categories. This information will then form a multi-author publication which the derivation community can use as a benchmark for future work.

3.2.2.2 Method of data analysis

1. Response to the consensus

Respondents classified each proposed dataset as *essential*, *desirable* or *not required* in publications regarding hESC derivation. The initial analysis was by vote count and percentage calculation. In collaboration with a statistician a linear weighting system was devised for the data. The response *essential* was weighted as +3, *desirable* as +1, *not required* as -1. This enabled the data categories to be placed in rank order. The responses to the specific questions were counted and presented in percentage form.

2. Validation of grading system

When observer reliability studies involve categorical data in which the response variable can be classified into multivariate categories, the measurement of observer agreement can be assessed by kappa statistics (Landis & Koch, 1977). This can be interpreted as a measure for expressing the extent to which the observed amount of agreement among raters exceeds what would be expected if all the raters made their ratings completely randomly. The kappa-statistic measure of agreement is scaled to 0 when the amount of agreement is as expected by chance, and 1 when there is perfect agreement. For intermediate values, Landis and Koch suggest the following interpretations as shown in Table 3.4

Table 3.4: Strength of observer agreement based on kappa values.

Kappa statistic	**Strength of agreement**
Below 0.00	Poor
0.00-0.20	Slight
0.21-0.40	Fair
0.41-0.60	Moderate
0.61-0.80	Substantial
0.81-1.00	Almost perfect

Ten experienced embryologists independently and anonymously graded 20 photographs of blastocysts using the grading system published in the standards manuscript. Each participant was shown the same 20 pictures using the same computer, and were given as much time and as many repeat viewings as required in one sitting.

Taking into account that is it more difficult to view pictures and not actual samples, particularly for expanded blastocysts where it was not always possible to focus on the TE and ICM, it was agreed with the statistical consultant prior to analysis that the minimum kappa value acceptable for validation of the system was *moderate* (between 0.41 and 0.60).

3.3 Results

3.3.1 Obtaining research embryos

Between January 2006 and June 2008, 467 cryopreserved research embryos were imported through the hESCCO network to the Guy's hospital stem cell programme, from 13 clinics nationwide. In addition to this, 115 cryopreserved embryos were donated from Guy's ACU patients, and 548 fresh embryos declared as unsuitable for transfer following PGD were also donated to the stem cell programme. For comparison, during 2005 a total of 85 frozen embryos were obtained, which serves to highlight the success of the hESCCO venture.

3.3.2 Use of research embryos

A total of 549 embryos were thawed for research from 13 clinics between January 2006 and June 2008. 155 of these had been frozen on day 1, 225 on day 2, 125 on day 3 and 44 on day 5. Each embryo was thawed exactly as in section 2.1.2.3, with survival defined as 50% or greater cells remaining intact following the procedure, or in the case of pronuclear embryos, intact membrane and normal cytoplasm. Figure 3.3 details the survival of each embryo stage and the proportion of thawed embryos which continued to develop defined as further appropriate cleavage or re-expansion of the blastocoel cavity. Additionally, the proportion of thawed embryos developing successfully to enable use for research is shown.

There was no significant difference between the survival rates of each embryo stage (chi-squared, 3 degrees of freedom, p=0.833). There was however a significant difference between the rates of continued development (p=0.017) but not use (p=0.061). Day 5 embryos demonstrated significantly lower continued development compared with day 1 (p=0.005) and day 2 (p=0.016), although not compared to day 3 (p=0.135)

To see whether the originating clinic was related to thaw outcome, the survival, development and use of all embryos thawed was calculated per clinic. The results are shown in Figure 3.4. Any clinics from which fewer than ten embryos were thawed were excluded. Overall, those clinics that provided embryos with a good survival rate also had a high rate of continued development and use for research, and vice versa for those clinics with a low survival rate.

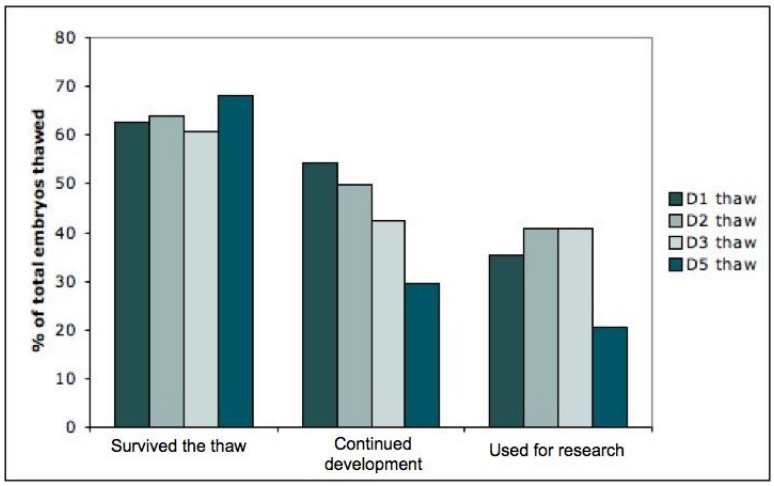

Figure 3.3: Outcome of thawing by survival, continued development and use for research segregated by stage of cryopreservation. Survival defined as cellular survival of at least 50%, continuation of development defined as subsequent appropriate cleavage or re-expansion of blastocoel cavity.

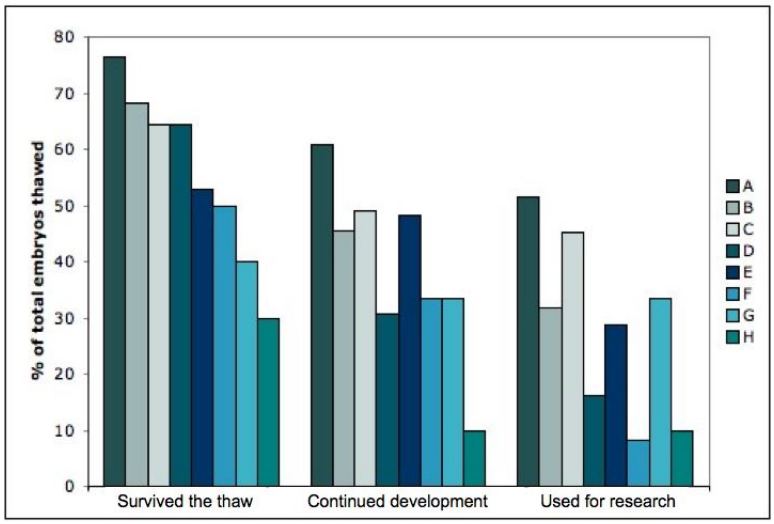

Figure 3.4: Survival, continued development and use of thawed embryos of all stages segregated by clinic of origin A-H.

3.3.3 Derivation of hESC lines

Before any manipulations were performed on the blastocysts used in derivation attempts, comprehensive details were recorded in both written and photographic form, which included the number of embryos donated by each patient, the number developing to blastocyst, the number of those suitable for use and the method used. In total 7 hESC lines were derived numbered KCL004 to KCL010. When a hESC line was established, routine characterisation was performed, including karyotype and marker expression. The methods are detailed in section 2.5, and representative examples of the results are described within.

3.3.3.1 Derivation of KCL004

The initial method attempted to derive hESC lines was immunosurgery. This required a period of practise with the method, as there were several areas that seemed critical to success.

All *manipulations of blastocysts* without a zona had to be done with extreme care, as excessive shear could cause the blastocoel to collapse thus lowering the efficiency of the complement reaction due to reduced cellular surface area for antigen binding. This made it more difficult to remove sufficient TE cells and increased the risk of damage to the ICM from vigorous pipetting. ICMs were isolated from some collapsed blastocysts, but with much more difficultly.

The *size of the pipettes* used was critical in the success of obtaining viable ICMs. A pipette was required with an internal diameter slightly greater than that of the ICM, but smaller than the TE diameter. During the initial use of the procedure some ICMs were damaged due to use of suboptimal pipettes. Subsequently, no attachment occurred and the cells degenerated, not being visible by two or three days after plating. It was essential that pipetting of the ICMs at this step was gentle, as they had a tendency to stick to the inner surface of the pipette and were then lost from culture.

The *timing and extent of the complement reaction* with each individual blastocyst was variable and something determined only by experience. Bubble-like blebs formed almost immediately once the blastocyst was placed in the solution, which indicated that the TE cells were undergoing lysis. However when isolation of the ICM was

attempted after this short time, it was not successful. A minimum of 10 minutes was deemed a sufficient time for the reaction to occur, and then the extent of blebbing was considered before removing the embryo from the complement solution. The vast majority of the ICMs attached by 24 hours after plating onto MEFs, unless obviously damaged by the immunosurgical procedure. The extent and morphology of any resulting outgrowth was blastocyst-dependent, each attempt differed in both timing and appearance of any cell proliferation.

KCL004 was derived from one of a pair of embryos cryopreserved on day 2 of development. They both thawed intact with 4/4 cells viable. The following day embryo one had divided to nine cells, embryo two had reached six cells. By day six both had developed to expanded blastocysts. The blastocysts were both graded as 3Aα (Stephenson *et al.*, 2007). Immunosurgery was performed successfully on day 6 of development (Figure 3.5C), with both ICMs appearing healthy and undamaged by the procedure. The ICMs were plated into the same well of MEF feeders from batch seven at passage four (B7 P4), at 21% dissolved oxygen tension. As the feeders appeared sparse at the time of plating, further MEFs were inactivated and added to the well later on the same day. By two days after plating both ICMs had attached and spread, the ICM cells having pushed the feeders to the edge of the colony. By three days after plating the two areas of cellular proliferation had merged, with the feeders pushed to the edge of the large colony. By this time a small number of cells with large nuclei and prominent nucleoli were visible. By day five after attachment however, there were areas of differentiation visible, although cells with prominent nuclei (stem cell-like cells) were still present. Freshly inactivated MEFs were added as necessary. Over the following days the cell colonies appeared to arrest, the culture appeared to become degenerate such that by 10-12 days after plating the derivation attempt appeared unsuccessful. However, on day 14 after attachment, a putative stem cell-like colony became evident (Figure 3.5G). The cells rapidly proliferated and were passaged for the first time 15 days after attachment of the ICMs. The colony was manually cut into 4 pieces, 3 were transferred to a fresh MEF plate and the fourth left in the original culture dish. All 4 colonies had re-attached within 24 hours. The culture was expanded rapidly by manual passaging, and colonies vitrified when sufficient cells were available. Figure 3.5 details the early morphology of the embryos and hESC colonies.

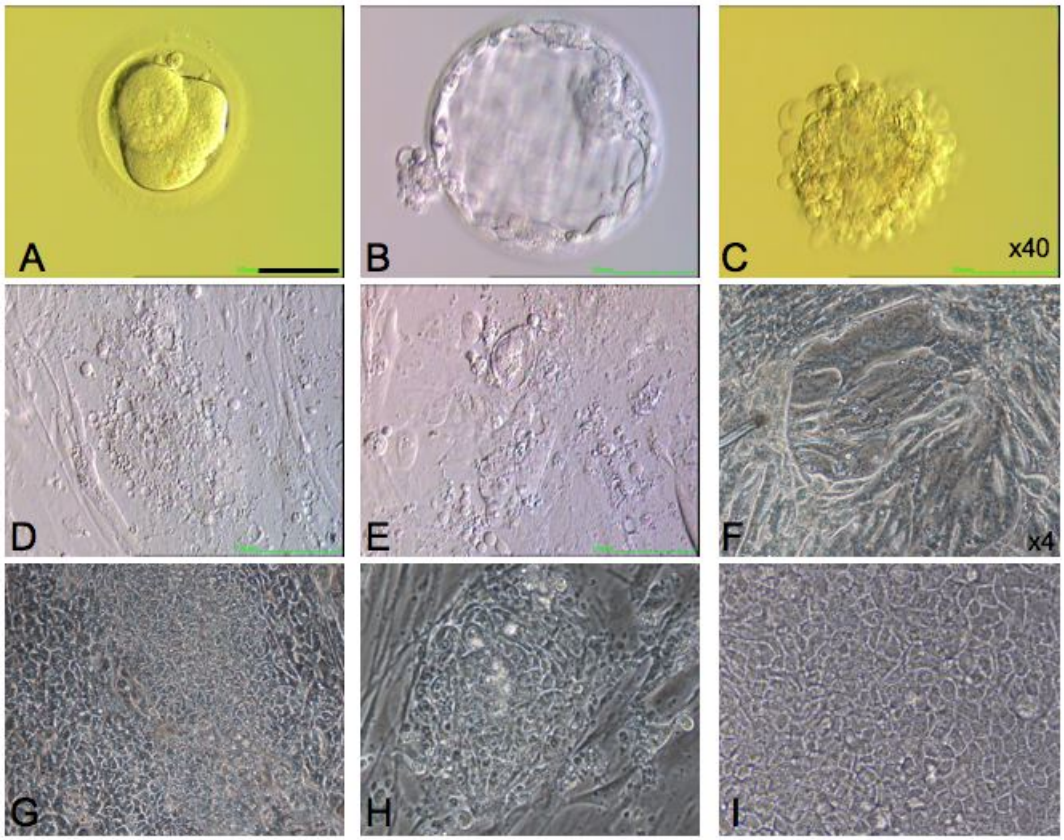

Figure 3.5: Embryo morphology and early culture of KCL004. (A) One of the 4 cell embryos on D2. (B) Same embryo as an expanded blastocyst on D6. (C) Blastocyst during immunosurgery, the lysing TE cells could be seen as blebs at the edge. (D) Culture D2 after plating the ICM. (E) D4 after plating. (F) D8 after plating, some degenerate areas were visible. (G) D14 after plating, stem-like cells were visible. (H) Passage 1, day 1. (I) Re-growth from original colony. All images at x20 objective unless otherwise indicated. Scale bar indicates 50 μm at x20 objective.

The cells became contaminated from an unknown source at P2. At first due to inexperience with cell culture, the altered appearance of the colonies (increased cell debris, retarded cell growth) was assumed to be a problem with culture on old MEFs. However, the contamination soon became evident when the medium became turbid and the colour changed due to altered pH. The cells were treated with 2% pen/strep in combination with 0.05 mg/mL gentamycin (Gibco Invitrogen) for seven days. The antibiotics appeared to successfully clear the infection and the cells seemed to recover. The colonies were maintained until P7 with initial characterisation and continued vitrification when enough cells were obtained. However from P7 any attempts at passaging were unsuccessful, the colonies generally did not attach, and if they did, they did not proliferate. The fresh culture was discarded and several attempts were made to thaw earlier passages of KCL004. Unfortunately these attempts were not successful and the cell line remained in cryopreserved storage with the hope that the development of superior thawing conditions and experience might enable the cells to be thawed from the 12 remaining straws at a later date.

3.3.3.2 Derivation of KCL005-HD1

KCL005-HD1 was also derived using immunosurgery. The embryo was donated for research on day four following an affected diagnosis for Huntington disease (HD) with 48 CAG repeats and therefore unsuitable for embryo transfer. The blastocyst was used on day six of development and graded as 5Aβ (Figure 3.6B). Immunosurgery was performed successfully on the blastocyst, although the ICM appeared slightly damaged by the procedure, possibly due to a suboptimal pipette diameter used to remove residual TE. The ICM was plated onto B3 P3 MEF feeders at 5% oxygen tension. By day two after plating the ICM had attached and was beginning spread into culture (Figure 3.6D). By three days after plating the ICM had spread, but there was no evidence of significant proliferation and the ICM cells had not yet pushed the feeders to the edge of the colony. The cells continued to sit on top of the feeders and slowly proliferate such that the colony became dense and elongated rather than flatten onto the dish as observed with KCL004 (Figure 3.6F). Cells with large nuclei and prominent nucleoli were observed throughout the culture period. By day 11 the colony had begun to flatten and stem-like cells were observed at the edges of the colony. Inactivated MEFs were added to the culture on day 12 as the original MEFs

were beginning to detach and curl up in suspension. By day 15 a convincing stem cell-like colony was observed. The colony was passaged onto fresh feeders as a single piece as it was too small to cut into sections. The piece re-attached by the next day but as a solid button (Figure 3.6H). However by 48 hours after passage the cells had migrated from the central button and spread as a colony. The culture was expanded by manual passaging, and colonies vitrified when sufficient cells were available. At P2 cells were analysed to confirm Huntington's status, as described in section 2.5.5. Figure 3.6 details the early morphology of the embryo and colony.

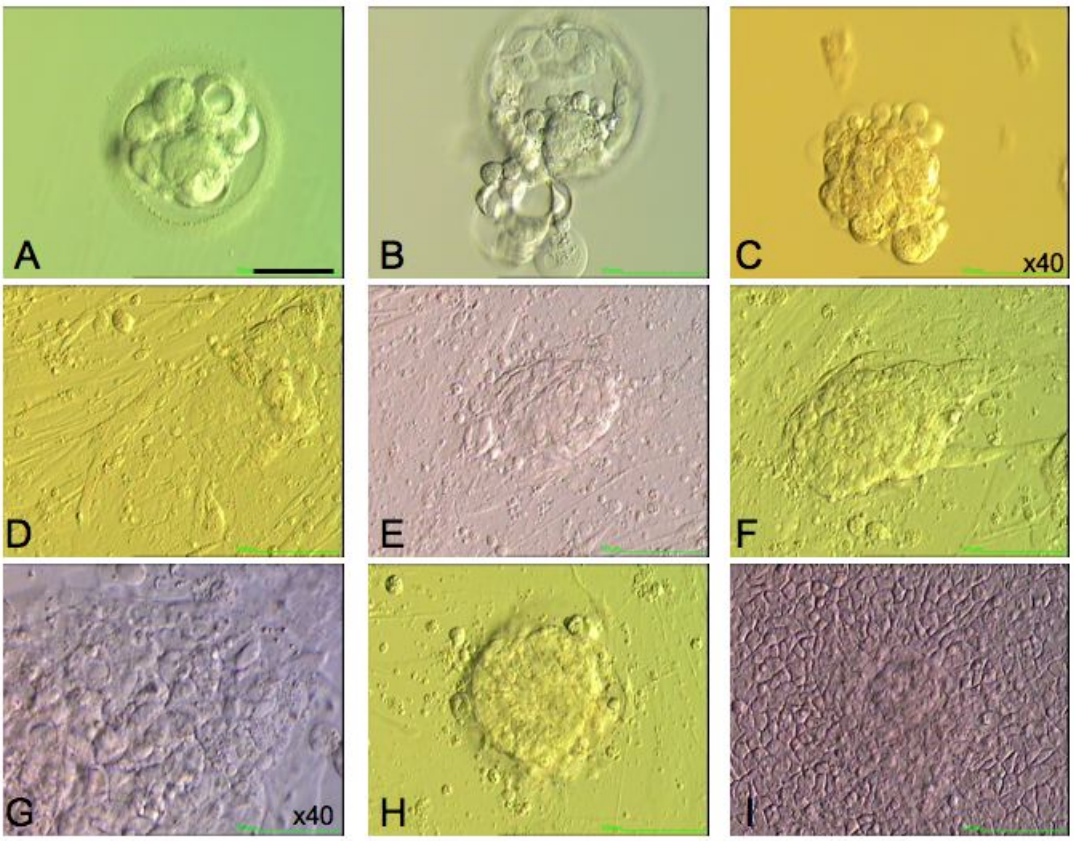

Figure 3.6: Embryo morphology and early culture of KCL005. (A) Embryo on D4, not yet compacted. (B) Embryo on D6 as a hatching blastocyst. (C) Blastocyst during immunosurgery (D) Culture D2 after plating the ICM. (E) D4 after plating. (F) D5 after plating. (G) D9 after plating. (H) Passage 1, day 1. (I) Passage 1, day 3. All images at x20 objective unless otherwise indicated. Scale bar indicates 50 μm at x20 objective.

The colonies became contaminated at P5 due to a infected MEF batch obtained from a collaborating research laboratory. The cells arrested in culture and were

unable to be passaged any further. The fresh culture was discarded and several attempts were made to thaw earlier passages of KCL005-HD1. Unfortunately these attempts were not successful and the cell line remained in cryopreserved storage. Several straws were deposited in the UK Stem Cell Bank (UKSCB). The staff have attempted to thaw and culture these samples, but without success.

3.3.3.3 Derivation of KCL006

KCL006 was derived using mechanical isolation with the channel method. The embryo was obtained on day four following an inconclusive diagnosis for HD and therefore unsuitable for transfer. However, subsequent re-running of the single blastomere PCR sample for confirmation of diagnosis determined the embryo as unaffected with the disorder. The blastocyst was used on day seven of development and graded as 6Bα. Mechanical isolation was performed successfully obtaining a healthy ICM that was plated on B7 P3 feeders at 5% oxygen tension. LIF was exchanged for 8 ng/mL bFGF in the medium. The ICM had attached by two days after plating (Figure 3.7B), and the cells proceeded to proliferate over the following days such that by four days after plating, stem cell-like cells were visible with the typical cobblestone morphology seen in monolayer culture (Figure 3.7C). By seven days after attachment a convincing putative stem cell colony was evident in culture. However, there was a crescent of differentiated or TE cells visible on the edge of the colony. The concern was that these cells would proliferate and overtake the culture, or secrete factors into the milieu that would prevent the stem-like cells from propagating. Therefore eight days after attachment as many of the differentiated cells as possible were gently removed without damaging the stem-like colony with a fine pulled glass pipette. The removal of the cells was successful and the putative colony continued to proliferate. By day 14 (Figure 3.7E) after attachment the colony was large enough to passage, it was cut into two pieces and one piece plated onto fresh B7 P3 MEFs. The colonies grew as a monolayer (Figure 3.7H) which made passaging more difficult as it was easy to damage the cells whilst trying to lift them from the bottom of the dish. However, the culture was expanded rapidly by manual passaging, and colonies vitrified when sufficient cells were available. Once a sufficient cryopreserved stock was achieved, all of the remaining colonies were vitrified as the cells were not needed at that time for experimentation. Figure 3.7 details the early morphology of the embryo and colonies.

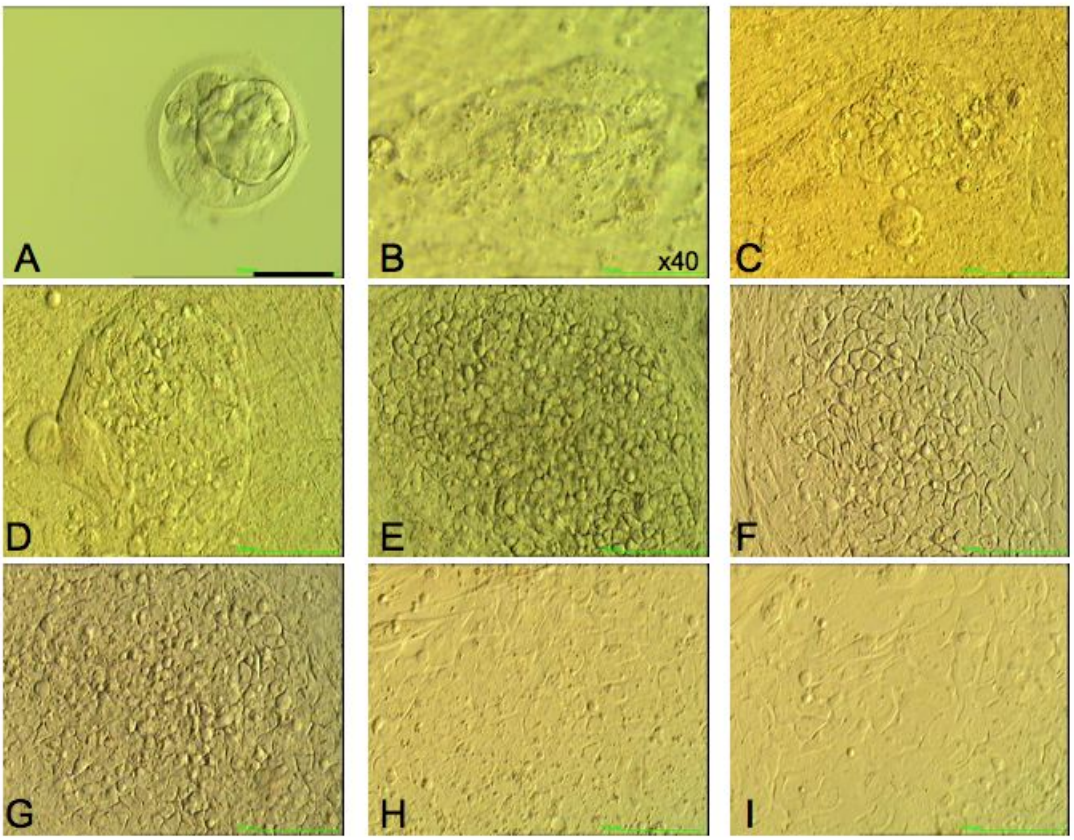

Figure 3.7: Embryo morphology and early culture of KCL006. (A) Poor quality blastocyst on day 5 which subsequently expanded with a good quality ICM on day 7. (B) Culture D2 after plating the ICM. (C) D5 after plating. (D) D8 after plating. (E) D14 after plating. (F) Passage 1, day 2. (G) Regrowth from original colony. (H) Passage 1, day 12, monolayer culture. (I) Passage 2. All images at x20 objective unless otherwise indicated. Scale bar indicates 50 μm at x20 objective.

3.3.3.4 Derivation of KCL007

KCL007 was also derived using mechanical isolation, but with the microdrop method. The embryo was obtained on day five following a 50% risk diagnosis from exclusion testing for HD. This line was unsuitable for banking in the UKSCB as the HD status was unknown and could not be investigated, due to the patient not wishing to know their disease status. This was agreed with the steering committee of the UKSCB, and the cells placed in cryopreserved storage in case the patient decided in the future to determine their disease status, at which point the cell line status could also be investigated.

The blastocyst was used on day seven of development and graded as 6Bα (Figure 3.8C). The ICM was particularly expanded measuring approximately 78x65 μm. Mechanical isolation was performed successfully obtaining a healthy ICM that was plated on B7 P3 feeders at 5% oxygen tension. By two days after plating, the ICM appeared slightly degenerate, and by three days after plating a large differentiated area was evident (Figure 3.8D). The culture did not show potential morphologically until ten days after attachment, where although there were still degenerate cells around the edge of the colony, a small area of monolayer stem-like cells was visible which had pushed the feeder cells away (Figure 3.8E). This area continued to proliferate and by 13 days after ICM isolation a convincing stem cell-like colony was visible. By day 15 after attachment the colony was large enough to passage, it was cut into two pieces and one piece plated onto fresh B7 P3 MEFs (Figure 3.8G). The culture was expanded rapidly by manual passaging, and colonies vitrified when sufficient cells were available. Once a sufficient cryopreserved stock was achieved, all of the remaining colonies were vitrified as discussed. Figure 3.8 details the early morphology of the embryo and colonies.

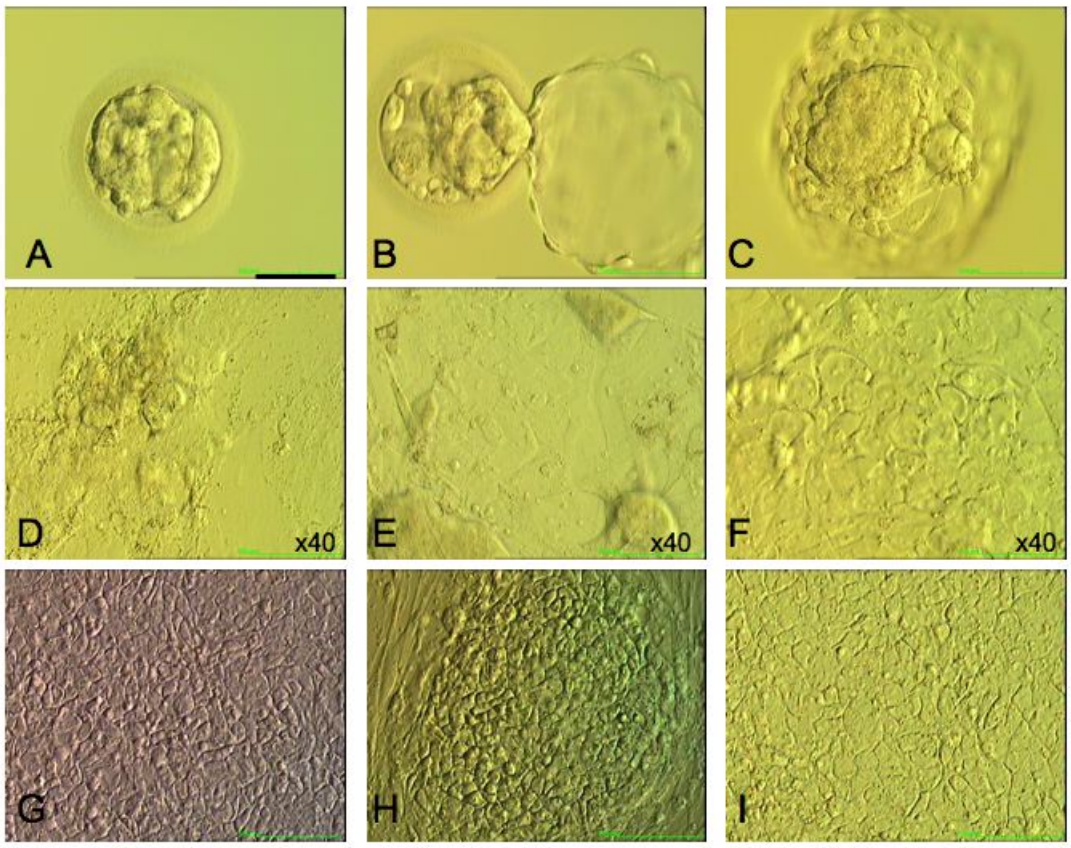

Figure 3.8: Embryo morphology and early culture of KCL007. (A) Poor quality unexpanded day 5 embryo, excluded cells were visible. (B) Hatching blastocyst on day 6, possible ICM at the zona opening. (C) Hatched blastocyst on day 7 with unusually large ICM. (D) Culture D3 after plating the ICM, large differentiated area visible. (E) D10 after plating, a monolayer of stem-like cells was visible. (F) D12 after plating. (G) D15 after plating. (H) Passage 1, day 2. (I) Passage 4. All images at x20 objective unless otherwise indicated. Scale bar indicates 50 μm at x20 objective.

3.3.3.5 Derivation of KCL008-HD2

KCL008-HD2 was derived using laser isolation of the ICM cells. The embryo was obtained on day four following an affected diagnosis for HD with 46 CAG repeats. The blastocyst was used on day five of development and graded as 5Aβ (Figure 3.9A). Several 550 μs or 800 μs pulses were directed at the TE cells at the site of the zona opening (Figure 3.9B). Lysis of the cells was visible, and gentle pulling of the micropipettes successfully separated the ICM cells with minimal surrounding TE (Figure 3.9C). The remaining TE was retained in culture for observation. The ICM portion was plated onto B5 P3 MEF feeders at 5% oxygen tension. The ICM had attached by day two after plating but was surrounded by residual TE cells (Figure 3.9D). The rest of the TE retained in culture had re-expanded and completed hatching. By day four after plating significant proliferation of the ICM cells was evident with a dense core of stem-like cells visible. The following day further inactivated MEFs were added to the culture. Proliferation was still evident until day six after plating. However there was an adverse change to the culture by day eight. The TE appeared to undergo a rapid expansion to form terminally differentiated giant cells, which had overgrown the stem-like mass of cells (Figure 3.9F). Insulin needles were used to cut out the central mass of stem-like cells and the isolated colony was placed at a distance in the same well. Six hours following the manipulation the ICM cells had reattached but appeared dense and of poor morphological quality. Over the next 48 hours there was no significant change in the appearance of the colony, with no obvious spreading of the colony nor visible proliferation. By day 13 after the original plating and five days after the re-attachment there was a change in shape of the colony. The MEFs had been pushed to the edge and a small number of cells with stem cell-like appearance were visible having grown out of the dense core of cells. This area continued to proliferate such that by 15 days after the original attachment a convincing stem cell-like colony was observed. By day 19 after attachment the colony was large enough to passage, it was cut into two pieces and one piece was plated onto fresh B7 P3 MEFs (Figure 3.9I). The cells adhered tightly to each other and the MEFs, which made the initial passage difficult. Although the colony that was moved to a new dish attached, it did not propagate and degenerated in culture, possibly due to carry over of differentiated cells or damage during passaging. How-

ever the re-growth from the original colony enabled the culture to be propagated. Figure 3.9 details the early morphology of the embryo and colonies.

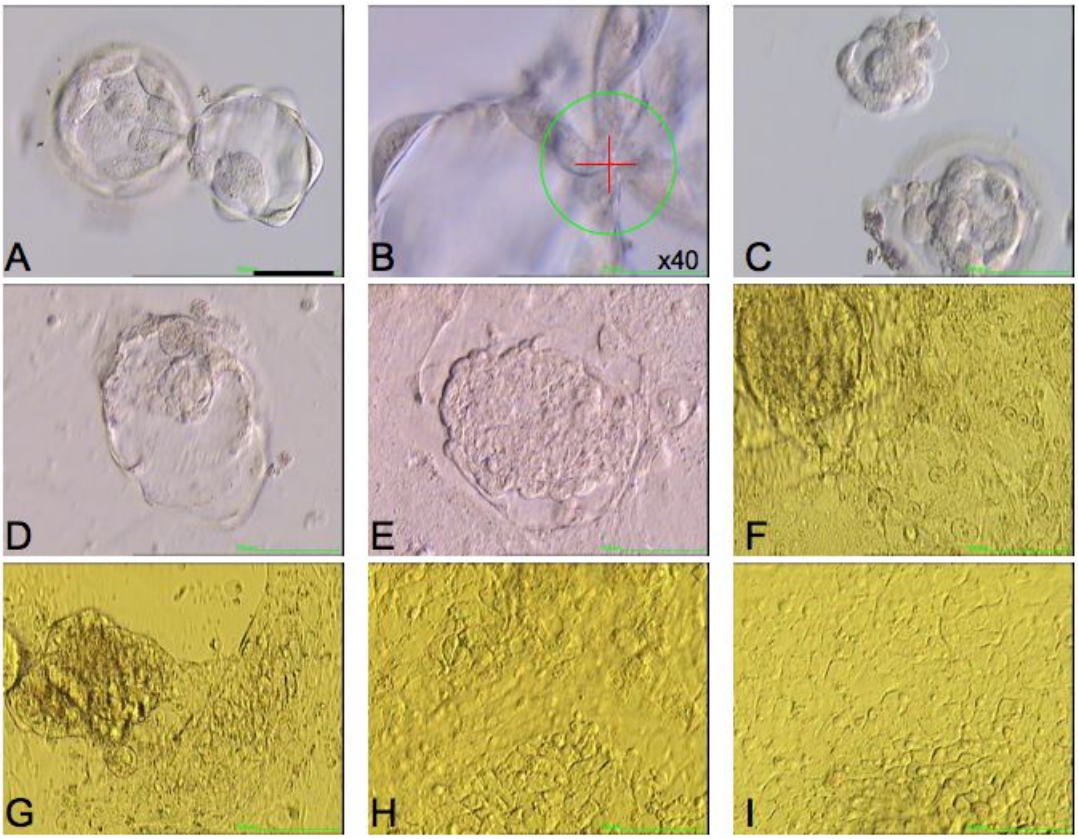

Figure 3.9: Embryo morphology and early culture of KCL008. (A) Hatching blastocyst on D5, the ICM could be seen in the hatched portion. (B) Magnified image of the zona pellucida opening with the laser target and safety circle overlaid to show the position of the laser pulses aimed the TE cells. (C) The separated ICM with residual TE after laser isolation. (D) Culture D2 after plating the ICM, the attached ICM and flattened TE cells could be seen. (E) D5 after plating, the ICM area had proliferated. (F) D7 after plating, terminally differentiated TE cells were visible. (G) Passage 1, day 5, a small area of stem-like cells to the right of the central button was seen. (H) Passage 1, day 9. (I) Passage 2. All images at x20 objective unless otherwise indicated. Scale bar indicates 50 μm at x20 objective.

For the first 10-15 passages the cells were extremely difficult to culture. The attachment of passaged pieces was poor, with only approximately 30-50% of pieces attaching and growing. To overcome this the size of pieces cut was varied to try to obtain the optimum size. Colonies were passaged into 250 μL medium instead of the normal 500 μL to prevent the colony pieces from remaining in suspension as they were pressed onto the feeders by the reduced volume of medium. The concentration

of bFGF was increased to 16 ng/mL in an attempt to keep the cells undifferentiated during the slow growth of colonies. On two occasions the cells entered a replication crisis when left in the hands of a technician during unavoidable absence from the laboratory and it took approximately eight weeks to recover the cultures each time. Colonies were vitrified when sufficient cells were available, but significant fragmentation of the pieces during cryopreservation reduced the chances of post-thaw survival. By passage 15 the cells seemed to have stabilised and adapted to culture sufficiently, particularly when transferred into KOSR medium. A sufficient bank of cells was then cryopreserved and full characterisation performed. At P2 cells were analysed to confirm Huntington's status (section 2.5.5).

3.3.3.6 Derivation of KCL009-trans1

KCL009-trans1 was derived by whole plating of the blastocyst. The couple that donated the blastocyst presented with the male patient having a karyotype of 46XY, t(7;12)(q31;p13.1), a balanced reciprocal translocation between the long arm of chromosome 7 and the short arm of chromosome 12. Carriers of reciprocal translocations will produce sperm or eggs of which a significant number will carry unbalanced forms of the translocation (Mackie Ogilvie & Scriven, 2004). The embryo was obtained on day six as was unsuitable for replacement following analysis with PGD. It was graded on day six as 5Cβ (Figure 3.10A). The blastocyst had not completely hatched, and the zona was removed with gentle pipetting of the embryo, before plating on B5 P3 MEF feeders at 5% oxygen tension. By three days after plating the blastocyst was attached and had spread flat in culture (Figure 3.10B). There were a few cells with prominent nuclei present, but the culture also contained dense TE and differentiated cells. By day five after plating the differentiated cells had begun to overgrow the stem-like cells, and therefore insulin needles were used to carefully cut around the cells of interest and the colony was placed in a distant area of the same well. This disaggregated area had re-attached within 24 hours (Figure 3.10D) with some proliferation evident in the following days. The concentration of bFGF was increased to 16 ng/mL in the medium when it appeared that some of the cells in the culture were differentiating. By day 11 after plating, a small number of cobblestone stem-like cells were visible at the periphery of the colony, but overall the culture appeared insubstantial (Figure 3.10F). It was not until 18 days after plating that the cells had

grown into a convincing colony. On day 19 after plating the colony was large enough to passage, it was cut into 2 pieces but both were kept in the same well, just placed at a distance from the original outgrowth (Figure 3.10H). The cells were expanded by manual passaging and colonies were vitrified when sufficient cells were available. However, as with KCL008-HD2, on two occasions the cells entered a replication crisis when left in the hands of a technician during absence from the laboratory. A sufficient bank of cells was eventually cryopreserved, and full characterisation performed. Figure 3.10 details the early morphology of the embryo and colonies.

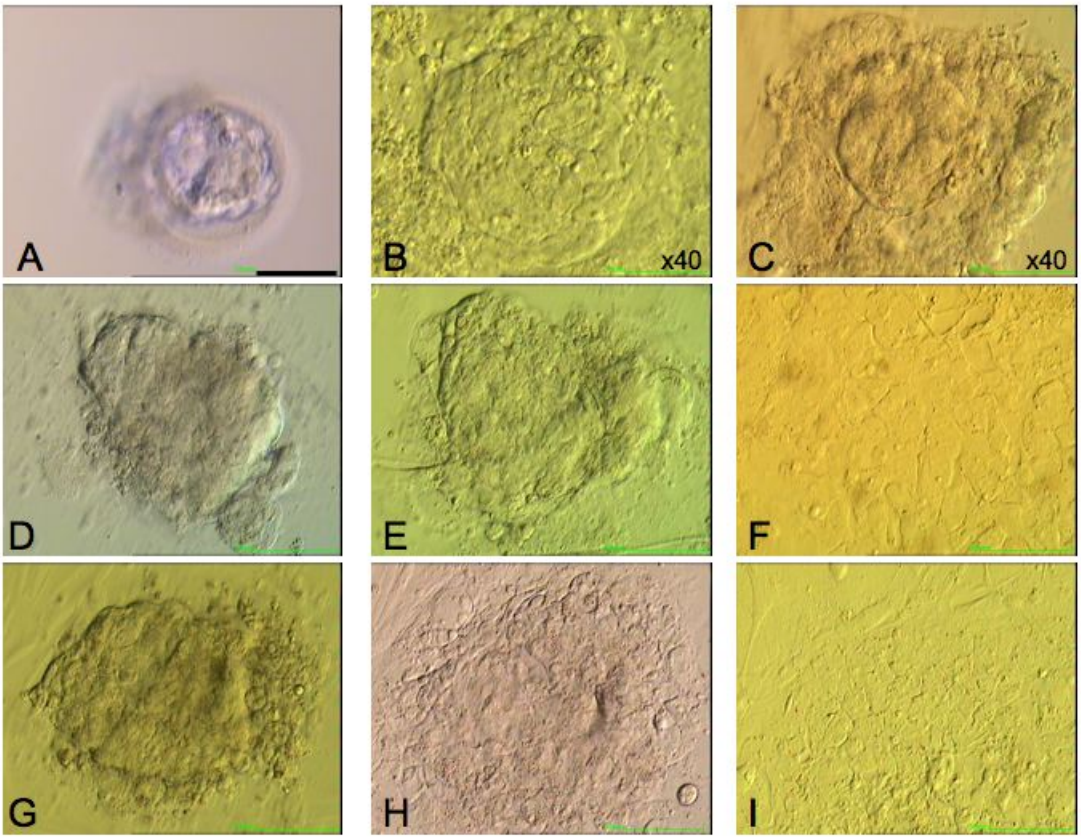

Figure 3.10: Embryo morphology and early culture of KCL009. (A) Hatching blastocyst on D9, only a very poor ICM could be seen. (B) Culture D3 after plating the whole blastocyst, ICM-like cells were visible. (C) Isolation of the ICM-like cells on D5 after plating. (D) Passage 1, day 1, reattachment of ICM-like cells. (E) Passage 1, day 2, cells beginning to spread (F) Passage 1, day 11, monolayer outgrowth (G) Passage 2, day 1. (H) Passage 2, day 2. (I) Passage 2, day 12, monolayer of cells. All images at x20 objective unless otherwise indicated. Scale bar indicates 50 μm at x20 objective.

3.3.3.7 Derivation of KCL010

KCL010 was derived using the whole plating technique. The embryo was obtained on day five following a 50% risk diagnosis from exclusion testing for HD, exactly as KCL007. The blastocyst was used on day five of development and graded as 5Bβ (Figure 3.11A). Despite the good quality of the ICM, there were very few TE cells and the blastocyst had not expanded, therefore mechanical isolation was not a suitable approach, with the high ICM to TE ratio favouring the use of whole plating rather than manipulation. Following zona removal with protease, the blastocyst was plated on B3 P4 feeders at 5% oxygen tension. The blastocyst had attached by day one after plating, although the expanded TE was evident (Figure 3.11B). By day three, the blastocyst had attached fully and spread into a cell colony, although no ICM-like cells were visible. By day six after plating a cluster of stem-like cells were visible, surrounded by cells with a differentiated morphology (Figure 3.11D). Upon the attempt to dissect out the stem-like cells, it became clear that they were encased by differentiating TE. Therefore a slit was made along one side of the cell cluster and the TE peeled completely away with the use of a glass pipette. The stem-like cells were transferred to fresh feeders (Figure 3.11E). Once a sufficient cryopreserved stock was achieved, all of the remaining colonies were vitrified as, as discussed for KCL007, these cells could not be banked or distributed at that time. Figure 3.11 details the early morphology of the embryo and colonies.

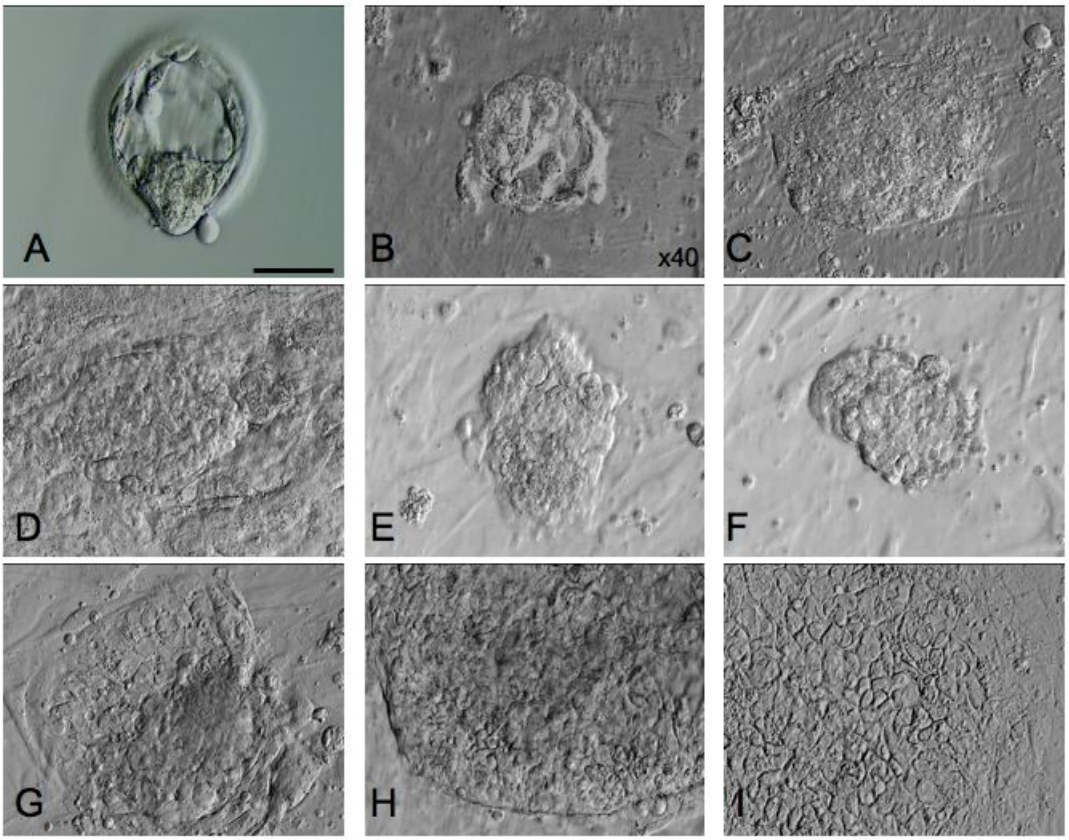

Figure 3.11: Embryo morphology and early culture of KCL010. (A) D5 blastocyst, beginning to hatch. (B) Culture D1 after plating the whole blastocyst. (C) D2 after plating. (D) D6 after plating, cells with stem-like morphology were seen. (E) Stem-like cells following mechanical isolation on D6. (F) Passage 1, day 1, cells had reattached. (G) Passage 1, day 2, outgrowth of central button of cells. (H) Passage 1, day 5. (I) Passage 2. All images at x20 objective unless otherwise indicated. Scale bar indicates 50 μm at x20 objective.

3.3.3.8 Summary of derivation

The total number of fresh and frozen embryos and details of development to blastocyst, derivation attempts and outcome is summarised in Table 3.5.

Table 3.5: Summary of all the fresh and frozen embryos used in derivation attempts. Thaw; frozen embryos thawed, Surv; survived, Fr; fresh embryos donated, Blast; developed to blastocyst stage, Used; suitable for derivation attempt, ICM; ICM isolated, Att; ICM attached to feeder layer, Lines; number hESC line established, ID; identifying name. Fr; fresh, Fz; frozen, I; immunosurgery, M; mechanical, L; laser, W; whole, na; not applicable.

Method	Thaw	Surv	Fr	Blast	Used	ICM	Att	Lines	ID
Fr - I	na	na	61	19	10	8	5	1	KCL005-HD1
Fz - I	87	55	na	28	23	23	15	1	KCL004
Fr - M	na	na	112	32	18	17	15	2	KCL006, 007
Fz - M	34	17	na	11	9	8	5	0	
Fr - L	na	na	2	2	2	2	2	1	KCL008-HD2
Fr - W	na	na	129	65	50	na	48	2	KCL009, 010
Fz - W	21	11	na	5	5	na	4	0	
Total	142	83	304	162	117	58	94	7	

The additional information specific to each line deemed *essential* when reporting derivation is shown in Table 3.6.

3.3.4 Efficiency

A total of seven hESC lines were established between January 2006 and June 2008. Two of the lines carried HD, one carried a translocation, two were at 50% risk of HD and two were wild-type lines with no known genetic mutation. Four derivation methods were developed so that the manipulation used was tailored to the quality and morphology of each individual blastocyst. Table 3.7 details each and every embryo used, the 'intention to derive', and the efficiency of derivation based on method for both fresh and frozen embryos.

Table 3.8 details the efficiency overall per method, regardless if either fresh or frozen embryos were used.

In order to correlate the quality of the blastocyst and outcome of derivation attempts, the efficiency of derivation was calculated based on ICM grade as defined

Table 3.6: Summary of derivation information for each line as per the consensus metadata categories; stage of embryos used, day of blastocyst use, grade of blastocyst, method used to isolate ICM, number of days until appearance of stem-like cells, genetic disorder if PGD embryo, proprietary IVF medium used, gas phase for incubation, source of embryos if fresh, method of zona (ZP) removal, karyotype, deposited in the UKSCB. Immuno; immunosurgery, Mech; mechanical, na; not applicable, NYD; not yet done.

Category	**KCL004**	**KCL005**	**KCL006**	**KCL007**	**KCL008**	**KCL009**	**KCL010**
Stage	Blastocyst						
Day	D6	D6	D7	D7	D5	D6	D5
Grade	3Aα	5Aβ	6Bα	6Bα	5Aβ	5Cβ	5Bβ
Method	Immuno	Immuno	Mech	Mech	Laser	Whole	Whole
Days	14	11	7	13	4	11	6
Disorder	na	HD	na	HD exclusion	HD	7;12 translocation	HD exclusion
IVF medium	Quinn's Advantage Fertilisation, Cleavage and Blastocyst media						
Gas	6% CO_2 in air	Certified premixed gas at 6% CO_2, 5% O_2, balance N_2 in MINC					
Source	Frozen	PGD	PGD	PGD	PGD	PGD	PGD
ZP removal	Protease	Protease	Hatched	Hatched	Hatched	Pipetting	Protease
Karyotype	46XY	NYD	NYD	NYD	68,XXY, -6	7;12 trans (Figure 3.12)	NYD
UKSCB	Yes	Yes	Pending	No	Yes	Yes	No

Table 3.7: Efficiency of each derivation method used for fresh and frozen embryos per embryo donated if fresh (Fresh column) and embryo thawed (Thawed column) if frozen, then per embryo reaching the blastocyst stage, per blastocyst used, per ICM obtained and per ICM that attached to the feeder layer. Fr; fresh, Fz; frozen, I; immunosurgery, M; mechanical, L; laser, W; whole, na; not applicable.

Method	**Lines**	**Fresh**	**Thawed**	**Blast**	**Used**	**ICM**	**Attach**
Fr - I	1	1/61	na	1/19	1/10	1/8	1/5
Fz - I	1	na	1/87	1/28	1/23	1/23	1/15
Fr - M	2	2/112	na	2/32	2/18	2/17	2/15
Fz - M	0	na	0/34	0/11	0/9	0/8	0/5
Fr - L	1	1/2	na	1/2	1/2	1/2	1/2
Fr - W	2	2/129	na	2/65	2/50	na	2/48
Fz - W	0	na	0/21	0/5	0/5	na	0/4
Total	7	6/304	1/142	7/162	7/117	7/58	7/94

Table 3.8: Efficiency of each derivation method overall per embryo donated plus thawed, then per embryo reaching the blastocyst stage, per blastocyst used, per ICM obtained and per ICM that attached to the feeder layer.

Method	**Lines**	**Donated**	**Blast**	**Used**	**ICM**	**Attach**
Immunosurgery	2	2/148	2/47	2/33	2/31	2/20
Mechanical	2	2/146	2/43	2/27	2/25	2/20
Laser	1	1/2	1/2	1/2	1/2	1/2
Whole	2	2/150	2/70	2/55	na	2/52

by the published derivation standard. This is detailed in Table 3.9.

Table 3.9: Efficiency of derivation for blastocysts from both fresh and frozen embryos per ICM grade.

Grade of ICM	Blastocysts	Lines	Efficiency (%)
FRESH			
A	8	2	25
B	13	3	23
C	23	1	4
D	12	0	0
E	26	0	0
FROZEN			
A	9	1	11
B	9	0	0
C	3	0	0
D	6	0	0
E	4	0	0
TOTAL			
A	17	3	18
B	22	3	14
C	26	1	4
D	18	0	0
E	30	0	0

3.3.5 Contamination control

The initial arrangement for hESC culture was a collaboration with a non-clinical research laboratory. The preparation of feeders and medium occurred in this laboratory then were transported to Guy's. Cleaning protocols in this facility consisted of regular surface cleaning with 70% ethanol, routine aseptic technique for tissue culture and the wearing of clean overalls, gloves and a facemask for bench work. However, the laboratory air was unfiltered and up to 15 people at one time were using one incubator and two culture hoods. Stocks of feeders, cells and media regularly showed signs of contamination, likely to be from poor tissue culture techniques and recurring mycoplasma infection. No service agreement was in place with a microbiological laboratory to identify the contamination, instead the cultures were treated with antibiotics if a contamination was suspected.

The loss of fresh cultures of new lines due to contamination was unacceptable, and measures were taken to eliminate the risk as far as possible. Firstly, all derivation and early culture of lines was contained to the derivation laboratory at Guy's until large frozen stocks were established. Therefore all culture, passaging and feeding was performed personally, including feeder preparation and medium production. All reagents were ordered separately so that nothing was shared with any other lab.

Contract arrangements were made with the microbiology department of Guy's hospital for analysis of media if any contamination or infection was suspected. The nature of the samples was discussed and the most suitable analysis to perform agreed (section 2.3.5). Very infrequent bacterial contamination of isolated culture wells was observed, identified as most likely to be skin contamination with staphylococcus strains. The requirement for protective clothing was increased following this result to include sterile sleeves as well as gloves, hat and facemask to minimise the risk of skin contamination. On one occasion a fungal aspergillus strain was detected, and further sample analysis confirmed the source as the water bath in the bottom of the incubator. All removable sections of the incubator were autoclaved and a deep clean of the incubator body performed. The antifungal agent Aquaguard 1 (Biological Industries, Haemek, Israel) was added to the water bath, and further samples sent after these measures to confirm the fungus had been eradicated.

A contract for outsourced routine mycoplasma testing was established with an accredited laboratory (section 2.3.5), and samples of every culture and medium in use sent for analysis monthly. Any cells or cell products imported from other laboratories were screened for mycoplasma before use, and withdrawal of any antibiotics or antifungal agents from imported cultures was performed to enable early identification of any contamination. All new feeder batches were extensively tested before use.

These measures, in combination with stringent sterile tissue culture techniques, were successful in maintaining the sterility of the cell cultures. Immediate disposal of any wells displaying signs of contamination (following sample collection for microbiological testing) prevented any spread between cultures. The anticipation is that the move to new clean laboratory facilities and instigation of GMP protocols will further eliminate problems with culture contamination due to the strict controls and maintenance of air quality in the laboratory.

3.3.6 Characterisation of hESC lines

3.3.6.1 Karyotype

Karyotype analysis was outside of routine clinical NHS duties and was therefore outsourced to an accredited laboratory (section 2.5.3). KCL004 was shown to be normal 46,XY karyotype by cytogenetic analysis as shown in Figure 3.12. Two attempts to obtain a cytogenetic karyotype of KCL008-HD2 were unsuccessful, as no mitoses were obtained by the laboratory. A third attempt with more optimised cell colonies revealed a karyotype of 68,XXY, -6. This is discussed in detail in Chapter 6.

The karyotype of the embryo that gave rise to KCL009-trans1 was 46,XX,der(7) t(7;12)(q31.1;p13.1)pat. This meant that the embryo had a 7,der(7),12,12 complement for chromosomes 7 and 12, with monosomy for 7q31.1 to 7q ter and trisomy for 12p13.1 to 7p ter. Two attempts to karyotype KCL009-trans1 were unsuccessful, but the third gave an unexpected result, as three separate karyotypes were observed: (i) 46XX,del(7)(q22q32)[9], (ii) 46XX,del(1)(q10),del(7)(q22q32)[1] and (iii) 46XX,del(7)(q22q32),del(9)(q11)[1], as shown in Figure 3.12. However the deletions of the long arm of chromosome 1 in (ii) and 9 in (iii) began at heterochromatic breakpoints - areas rich in repeat lengths of chromatin. Breaks in these regions are common artefacts of preparation techniques. As these karyotypes were only found in a single cell of the preparation it was likely that the deletions occurred during processing rather than representing a true karyotypic change. All 11 cells analysed had a karyotype which contained del(7)(q22q32), suggesting a deleted chromosome 7 rather than a derivative. However, when not specifically looking for a translocation, and using standard G banding, it is conceivable that a derivative chromosome could be mistaken for a deletion. It is more than likely that the true karyotype of the cell line was 46,XX,der(7)t(7;12)(q31.1;p13.1)pat, the same as the embryo diagnosis. Karyotype of the remaining lines was not completed, as either propagation of the lines was not successful, or because they were from exclusion cases and in cryopreserved storage only.

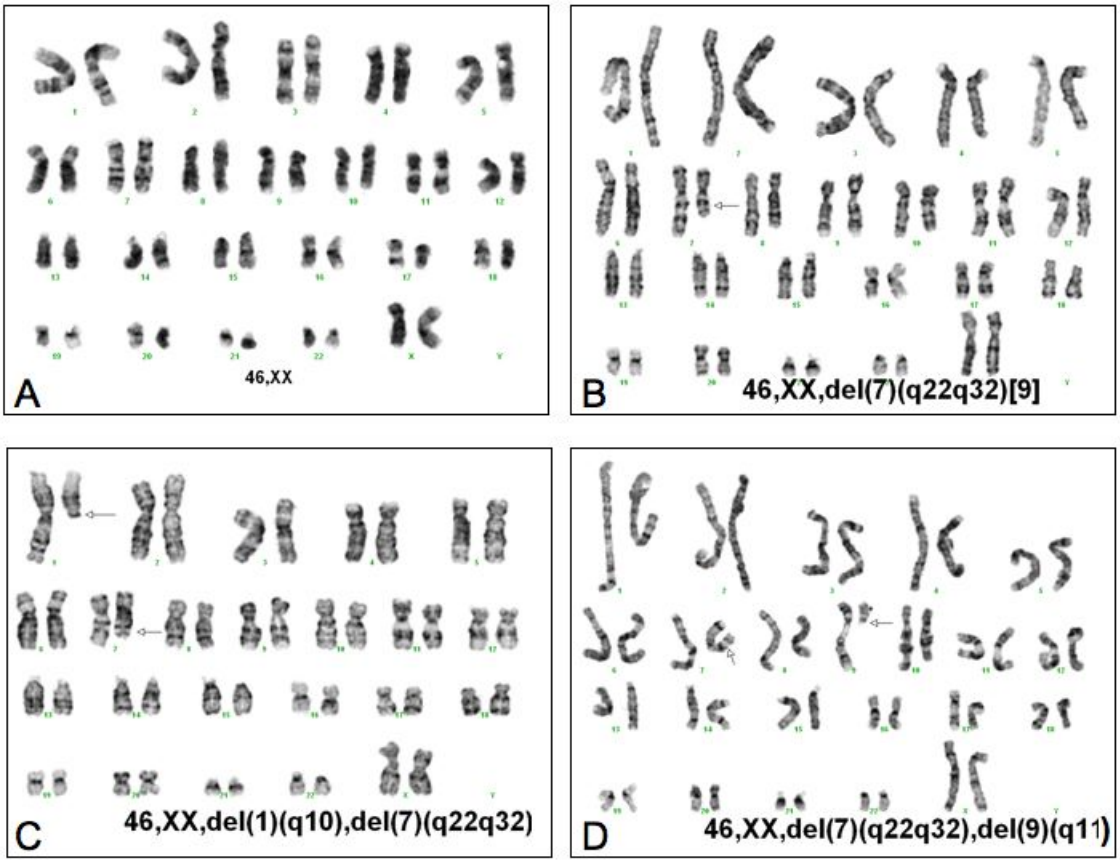

Figure 3.12: Cytogenetic karyotypes of (A) KCL004 (B-D) KCL009-trans1

3.3.6.2 Pluripotency

Immunohistochemical analysis for markers of pluripotency was completed for cell lines KCL004, KCL008-HD2 and KCL009-trans1. These lines expressed all the standard markers OCT4/POU5F1, NANOG, SSEA3, SSEA4, TRA1-60 and TRA1-81 and were negative for SSEA1. Figure 3.13 shows representative examples of the cell line results when grown on MEFs. The remaining cell colonies have not yet been characterised, therefore should be considered outgrowths or putative lines until this is completed.

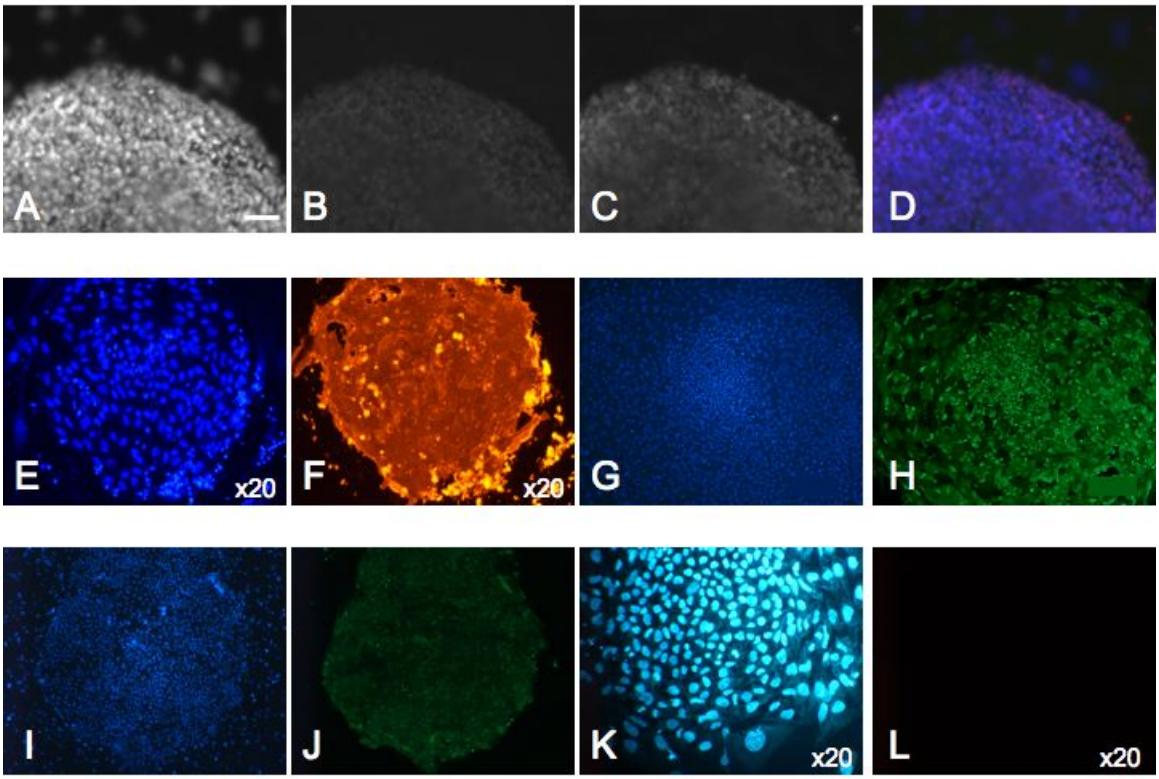

Figure 3.13: Immunocytochemical analysis of pluripotent marker expression. Images are representative of all cell lines tested. A-F KCL008 stained for (A) DAPI (B) NANOG (C) POU5F1 (D) Merged image of A-C, (E) DAPI, (F) SSEA4. G-H KCL004 stained for (G) DAPI, (H) TRA1-60. I-J KCL009 stained for (I) DAPI, (J) TRA1-81. K-L KCL008 stained for (K) DAPI, (L) SSEA1. All images at x10 objective unless otherwise indicated. Scale bar indicates 100 μm at x10 objective.

PCR analysis for pluripotency genes was performed for KCL008-HD2 and KCL009-trans1. βactin (*ACTB*), *POU5F1*, and *SOX2* expression was investigated by the use

of published primers from previous work in this laboratory. Representative results are shown in Figure 3.14. A low-level contamination was seen in one RT negative sample for *SOX2*, likely to be carry over during the PCR process. Multiple bands were visible for *POU5F1* suggesting DNA contamination or pseudogene or isoform detection. Initially the conditions for the PCR reaction were altered but this did not change the outcome. More optimal primers would be necessary to obtain 'perfect' gels; however the results were sufficient to prove expression of these pluripotent markers in the cell lines analysed.

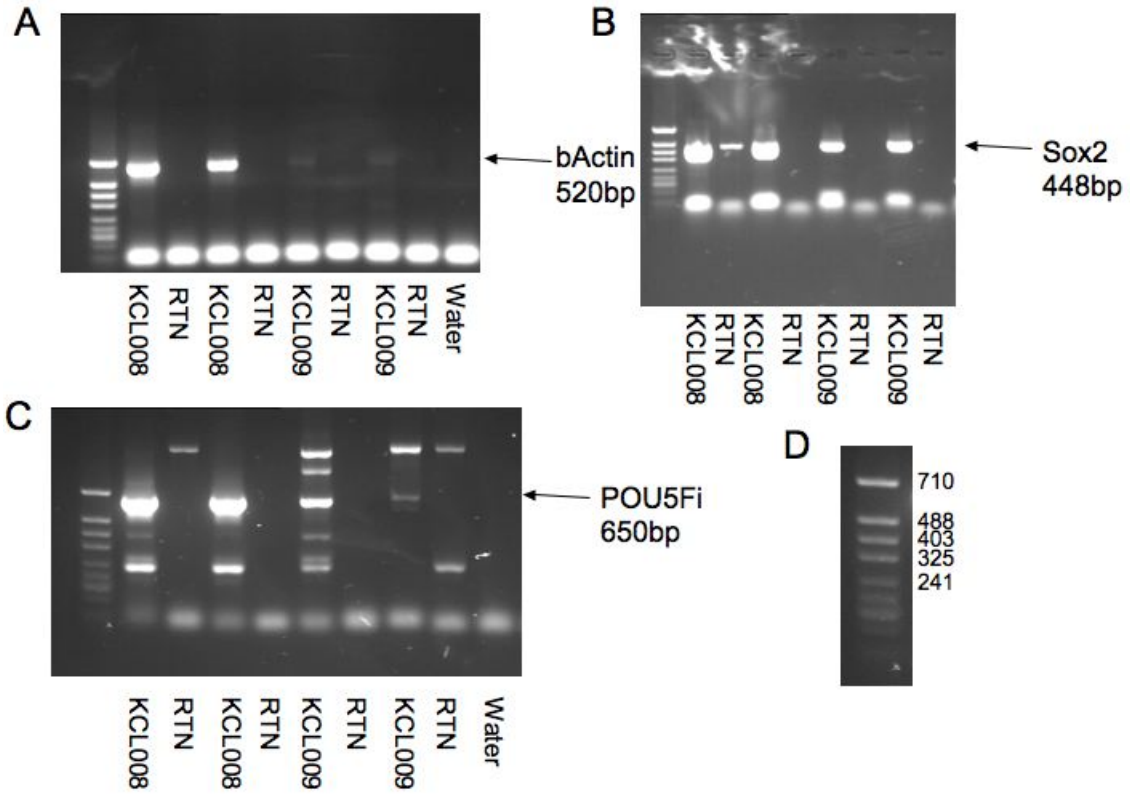

Figure 3.14: PCR analysis for the expression of (A) *ACTB*, (B) *SOX2* and (C) *POU5F1* in both KCL008-HD2 and KCL009-trans1. (D) Band sizes for the pBluescript II SK$^+$-Hpa II ladder. RTN: reverse transcription negative sample.

3.3.6.3 Freeze-thaw

Successful freeze-thaw of the colonies is a mandatory test before cell lines can be deposited in the UKSCB. This was attempted at P5 and P10 for KCL008-HD2 and KCL009-trans1. Both passages were successfully thawed for KCL009-trans1,

but, although P5 KCL008-HD2 cells survived the thawing procedure, the colonies differentiated almost immediately after attaching to the feeder layer. In contrast, thawing of P10 cells was successful, with subsequent propagation of morphologically normal, undifferentiated cells. Subsequent successful thaw of P2 cells was achieved when thawing into KOSR rather than hESC CM.

3.3.7 Standards data

3.3.7.1 Consensus response

From the 40 groups targeted with this survey, 31 responses were received. The count of votes placed all but one of the datasets in the *essential* series; the exception - the number of days until the appearance of stem-like cells - had been classified as *desirable*. None of the datasets were considered as *not required*. Following the linear weighting, the rank order of the datasets was plotted as shown in Table 3.10.

Table 3.10: Rank order of datasets following weighting

Dataset for collection	**Rank**
Number of hESC lines established	1
Method used to isolate ICMs	2
Known genetic disorder (if PGD)	3
Day of development of blastocysts used	4
Stage of embryos used	4
Number of ICMs placed on feeder layer/ECM	6
Source of embryos if fresh	7
Number of blastocysts suitable for use	7
Gas phase employed	9
Grade of all blastocysts used	9
Proprietary IVF medium used	9
Number of embryos allocated at the cleavage stage developing to blastocyst	12
Total number of embryos allocated to the research project	13
Karyotype	14
Number of ICMs that attach to feeder layer/ECM	15
Hatched naturally or method of zona removal	16
Number of stem cell-like colonies that arrest in early culture	17
Number of days until appearance of stem cell-like outgrowth	18

Of the respondents, 28/31 agreed that a universal standard for reporting deriva-

tion was *essential*, 27/31 of these would adopt the standard, and 23/31 agreed to provide data for central analysis.

3.3.7.2 Validation

The average experience of the ten embryologists who participated in the grading validation was 6.1 ± 2.8 years.

Kappa analysis of the expansion status, TE appearance and ICM appearance assigned by the embryologists to each of the 20 images is shown in Table 3.11. Each of the components of the grading scheme achieved at least the minimum 'moderate' agreement (between 0.41 and 0.60).

Table 3.11: Kappa values calculated from 200 grades (10 embryologists, 20 pictures) of Expansion Status, Inner Cell Mass Grade and Trophectoderm Grade.

Expansion Status	Kappa
1	0.77
2	0.68
3	0.66
4	0.65
5	0.77
6	0.87
Combined	**0.74**
Inner Cell Mass Grade	Kappa
A	0.51
B	0.33
C	0.65
D	0.73
E	0.37
Combined	**0.53**
Trophectoderm Grade	Kappa
α	0.55
β	0.28
γ	0.60
Combined	**0.47**

Since the grade of the ICM had been deemed the most important variable when considering derivation attempts, the categories for ICM appearance were combined. This revealed which grades were least consistent between the observers. This then

highlighted where the grading system could be improved, either with better photographic examples or more detailed explanation of the salient features of each grade. The kappa analysis was re-run, firstly combining grades A and B, and secondly also combining C and E. The results are shown in Table 3.12. The combination of grades A and B significantly improved the agreement to 'substantial'. Combining C and E did not significantly increase the agreement further.

Table 3.12: Kappa values for ICM grades when grade A and B were combined and grades C and E were also combined.

Inner Cell Mass Grade	Kappa
A+B	0.82
C	0.65
D	0.73
E	0.37
Combined	**0.71**
A+B	0.82
C+E	0.65
D	0.73
Combined	**0.74**

3.3.7.3 Data collection

Collection will continue until sufficient data are available for significant conclusions. Tables 3.13 and 3.14 summarise the responses received so far from external clinics for central analysis of data, the numbers 1-8 indicating separate responses. When asked to define 'established' for a hESC line, the majority of responses included; morphology, positive pluripotency markers (SSEA4, TRA-1-60, TRA-1-81, POU5F1, NANOG), *in vitro* differentiation into three germ layer derivatives and more than 15 passages in culture without change in growth rate or morphology.

Table 3.13: Summary of derivation information from responses to the data collection as per the consensus metadata categories; Number of fresh (Fr) embryos donated, number used, number of frozen (Fz) embryos thawed, number used, stage of embryos used, day of blastocyst use, number of embryos developing to blastocyst, number used, grade of blastocysts, method used to isolate the ICM, number of ICMs placed on feeders, feeder type, number of ICMs that attached, number of days until appearance of stem-like cells, number of putative stem cell lines which arrested in early culture, number of lines established, genetic disorder if PGD embryo, proprietary IVF medium used, gas phase for incubation for embryos (E) and hESC (ES), source of embryos if fresh, method of zona removal, karyotype. Immuno; immunosurgery, Mech; mechanical, HFF; human foreskin fibroblasts, AT; Acidified Tyrode's.

Category	**Lab 1**	**Lab 2**	**Lab 3**	**Lab4**
Fr donated	354	50		
Fr used	304	50		
Fz thawed	N/A	2	18	34
Fz used	N/A	2	5	34
Stage	Blastocyst	Blastocyst	Blastocyst	Blastocyst
Day	D5-8	D5-7	D5	D6
Blastocyst	32	52	4	4
Used	21	52	4	4
Grade	6Aα to 3Cβ	ICM:A:26	3:3Aα	1:3Bα, 2:3Aα
		B:10, C:1, U:15	1:1Aβ	3:3Bβ, 4:2Bβ
Method	Mech or acid	Immuno or whole	Whole	Whole
Feeder	8	52	4	4
Type	MEF	MEF	HFF	HFF
Attached	8	52	3	4
Days	7 to 10	7 to 14	17 to 21	14 to 17
Stem	5	Unknown	0	0
Lines	2	20	3	2
Disorder	N/A	N/A	N/A	N/A
IVF medium	Medicult	Vitrolife	Vitrolife	Vitrolife
Gas - E	5% CO_2, 21% O_2	5% CO_2, 21% O_2	5% CO_2, 8% O_2	5% CO_2, 8% O_2
Gas - ES	5% CO_2, 21% O_2	5% CO_2, 21% O_2	5% CO_2, 8% O_2	5% CO_2, 8% O_2
Source	Unsuitable for use	Unsuitable for use	N/A	N/A
Zona removal	AT	Pronase	AT	AT
Karyotype	Unknown	7: 46XX, 8: 46XY	2: 46XX	2: 46XY
		2: 47XX+13	1: 46XX-10+20	
		2: XXX, 1: XXY		

Table 3.14: Standard table continued. Chr abn; chromosomal abnormality.

Category	**Lab 5**	**Lab 6**	**Lab 7**	**Lab 8**
Fr donated		17		
Fr used		16		
Fz thawed	36		27	23
Fz used	35		23	23
Stage	Blastocyst	Blastocyst	Blast - like	Blast - like
Day	D6	D6	D6	D6
Blastocyst	11	3	8	11
Used	11	3	8	11
Grade	2:3Aα, 3:2Aβ	4Aβ, 6Aβ	N/A	N/A
	3:2Bβ, 3:1Cβ	1Aγ		
Method	Whole	Whole	Whole	Whole
Feeder	11	3	8	11
Type	HFF	HFF	HFF	hESC-derived
Attached	11	3	8	11
Days	15 to 17	14	17	12 to13
Stem	Unknown	Unknown	Unknown	Unknown
Lines	4	2	1	2
Disorder	N/A	Chr abn	N/A	N/A
IVF medium	Vitrolife	Vitrolife	Vitrolife	Vitrolife
Gas - E	5% CO_2, 8% O_2	5% CO_2, 8% O_2	5% CO_2, 20% O_2	5% CO_2, 20% O_2
Gas - ES	5% CO_2, 8% O_2	5% CO_2, 8% O_2	5% CO_2, 20% O_2	5% CO_2, 20% O_2
Source	N/A	PGD	N/A	N/A
Zona removal	AT	AT	AT	AT
Karyotype	2: 46XY	2: 46XX	1: 46,XX	1: 46XX, 1: 46XY
	1: 47XY+12/46XY			
	1: 69XXY			

3.4 Discussion

The aim of this part of the work was to develop derivation methods tailored to the quality of the blastocyst, and to obtain transparent information regarding the efficiencies of derivation with respect to manipulation techniques and embryo quality.

3.4.1 Embryo Use

This is the first time that a large cohort of cryopreserved embryos at different stages and from multiple clinics has been thawed by one person using one method. The variability of technician skill is therefore eliminated at the thaw step and allows valid comparison of post-thaw survival and development between clinics. In addition, as the embryos were kept in culture rather than being transferred to patients, longer-term monitoring of *in vitro* development was possible.

There are two main reasons why variability may be observed; the criteria used for selecting suitable embryos for cryopreservation may differ and there may be differences between the in-house cryopreservation techniques used in clinics. When outcome was compared by clinic, the survival rates ranged from 77% to 30% (median 60%), continued appropriate development from 61% to 10% (median 46%) and use for research from 51% to 8% (median 32%). A general trend was maintained, such that those clinics providing embryos that had a poor thaw outcome also showed poor continued development and a low rate of use. These figures suggest underlying differences between clinics either in selection or cryopreservation of embryos. There could also be multiple minor differences in techniques used during culture that accumulate to have a significant effect on embryo viability. The decision on selection criteria is a balance between maximising cumulative pregnancy chances, but not offering false hope to patients by cryopreserving embryos which are unlikely to survive the freeze-thaw process. There may also be a financial imperative as the vast majority of patients in the UK, whether NHS-funded, self-funded or private have to cover the cost of cryopreservation themselves, and this is a means to generate profit. It seems unlikely that a difference in thaw survival from 77% to 30% can be due only to variations in technique. This is because all clinics providing embryos to Guy's were asked to provide cryopreservation information and all used commercially available proprietary freezing media, and similar iterations of a slow-rate freezing

protocol. Therefore it is likely that the selection of embryos for cryopreservation was the most significant variable between laboratories. Future comparisons could include analysing the pregnancy rate for populations of patients from these clinics to see if this is reflected in the thaw survival.

When the thaw outcome based on the stage of cryopreservation was considered, there was no significant difference in thaw survival between stages. However, continued appropriate development of the embryo stages ranged from 54% for day 1 thaws to 30% for day 5 thaws. There was no difference between the development of day 1 and day 2 thawed embryos but blastocysts thawed on day 5 had a significantly lower rate of continued development compared to day 1 and day 2 thaws. Day 3 development was intermediate. Defining survival following thaw and monitoring of subsequent development (not quality) for cleavage stage embryos is straightforward, as it simply involves counting the number of cells each day and relating that to the number appropriate for the age of the embryo. Whilst by no means robust, the likelihood of further development of thawed cleavage embryos can be inferred from the peri-thaw morphology. However, applying these criteria to blastocyst thawing is more difficult, since blastocysts are in a collapsed state during the thawing process and potentially for several hours after. Thus the assessment of the proportion of viable cells is subjective and can only be roughly estimated. In order to continue with development, the blastocoel must re-expand and cell division resume. This is difficult to predict from the peri-thaw outcome. Whilst mindful of the small number of blastocysts thawed compared to cleavage embryos, this difficulty with assessing survival may explain the subsequent sharp drop in blastocyst numbers at the next stages of development. From 68% survival, only 30% of blastocysts re-expanded and only 21% developed to be suitable for use. This unexpected discrepancy may be due to either the initial estimate of survival being artificially elevated due to the difficulty with assessing cell number, or that the prognosis for blastocyst development is poor following cryopreservation. The latter reason is unlikely given the success of single embryo transfer in this and other laboratories (Criniti *et al.*, 2005; Khalaf *et al.*, 2008) with clear evidence of the superior embryo selection when pregnancy is the end point. However the thawing results imply that an appropriate window of time should be determined and allowed between thaw and transfer, during which re-expansion can be expected, in order to confidently select progressive blastocysts for

transfer. Collection of thaw data is continuing, and will be re-analysed at a suitable time point when comparable numbers of cleavage stage and blastocysts have been thawed. The effect of poor development from blastocyst thaw on clinic-specific outcome can be discounted, as far fewer blastocysts were thawed compared to cleavage stage. In addition, the majority were thawed from the two clinics with the highest overall survival and development rates.

3.4.2 Derivation

In total 7 hESC lines were derived using four methods tailored to the morphology of the blastocyst. Each of the derivations was distinctive. Although the stage and morphology of each blastocyst were generally similar in each attempt, the behaviour of the colonies was unpredictable; colony morphology and development was different with each attempt. Day 5, 6 and 7 blastocysts were used successfully, and the number of days until appearance of stem-like cells varied from 4 to 14. Five new hESC lines were derived without LIF but with the addition of bFGF, confirming the suitability of bFGF as a supportive factor for derivation and undifferentiated culture. This also questions the usefulness, if any, of LIF for derivation of human lines as noted by others (Daheron *et al.*, 2004). Replication arrest was seen in two lines which had been contaminated from an undetermined source. Following this, procedures were implemented to minimise repeat incidences. Routine characterisation analyses were performed on three lines, all of which displayed appropriate marker expression and survived cryopreservation - thaw cycles. The remaining lines were not fully characterised either because of poor thaw survival with current techniques, or because they were not suitable for banking. From the seven lines, four are at various stages of the deposition process with the UKSCB, one is pending submission and two are unsuitable for banking due to their HD exclusion status.

Several methods were established with the aim of working towards a GMP compatible culture system. The development of alternative methods to isolate the ICM or stem-like cells was a step towards this as it eliminated the need for animal serum components used in immunosurgery. In addition, establishing that murine LIF was not required for derivation, and the substitution for trypsin by recombinant TryplE^{TM} Express in the culture of feeders also reduced the exposure of hESC to xeno products. Whilst the change to KOSR medium did not eliminate all animal components

for routine culture, the more defined serum replacement (SR) component is substantially better than batches of FCS previously in use. The establishment of Standard Operating Procedures (SOPs) and the recording of the lot numbers of all consumables and media components used, was a start to the processes required for clinical grade qualification with respect to the full traceability of every aspect of the cell line culture. Further culture adaptations towards GMP suitability are discussed in Chapter 4.

3.4.3 Efficiency of derivation

Nearly 60% of frozen cleavage embryos survived thaw, of which more than half developed to the blastocyst stage, and 45% were used for one of the 4 derivation methods. Of the 304 fresh cleavage embryos donated, nearly 40% reached the blastocyst stage and 26% were manipulated and used. If a blastocyst was not used it was due to a high proportion of the cells considered degenerate. Of the 162 blastocysts obtained overall, 72% were suitable for use; an ICM was obtained from 36% and a further 34% were plated whole. 58% of the total blastocysts or ICMs attached to the feeder layer, and seven lines resulted.

The method of plating resulted in differing efficiencies. Whilst the efficiency per embryo donated was effectively the same (less than 2% for immunosurgery, mechanical or whole), the efficiency per plated ICM or blastocyst varied with the type of subsequent manipulation, which was selected depending on blastocyst morphology. Efficiency was 7% for immunosurgery, 8% for mechanical and 4% for whole plating. The data for laser is not yet comparable because of very low embryo numbers.

Table 3.9 shows that, as with implantation and clinical pregnancy rates, there was an association between quality of the ICM and derivation efficiency. Use of grade A ICMs resulted in the highest derivation efficiency; 25% from fresh blastocysts and 11% from frozen blastocysts. Grade B ICMs were also capable of giving rise to lines, with an efficiency of 23% from fresh blastocysts, although no success from frozen blastocysts. A poor efficiency was obtained from fresh blastocysts with grade C ICMs (4%) but no derivation success from grade D or E ICMs. When considering clinical pregnancy rates following single blastocyst transfer, the derivation rates seem low, but as yet there has been no comparison reported. Blastocyst score has been shown to effect implantation and pregnancy rates (Gardner *et al.*, 2000) but two or

more blastocysts were replaced and efficiency calculated per blastocyst transferred so direct comparisons cannot be made.

No two hESC lines seem identical in either pluripotent marker expression, transcriptional profiling, genetic stability or epigenetic stability (Allegrucci & Young, 2007; Skottman *et al.*, 2005); a better understanding of the quality of the starting material may help to elucidate some of these differences. It is clear that a good quality product cannot be made from poor quality starting materials. Just as pregnancy rates are lower with poor quality blastocysts, so derivation rates may be. However, the number of lines derived in this work is insufficient in isolation to draw conclusions. It may also be that if poor quality blastocysts do generate hESC lines, they are also of poor quality. Now that a number of derivation protocols have been established and proven successful, attention must be turned to making good quality lines, and establishing characterisation methods to validate this. For example, the mitochondrial number and function within stem cells should be considered in order to assess the efficiency of cellular metabolism and the quality of the cells (Cho *et al.*, 2006; Lonergan *et al.*, 2007).

The numbers of lines generated from each derivation clinic is still too small to ascertain significance in isolation for any of the variables in the culture systems. Therefore in order to obtain the maximum information from each embryo used it is important that data regarding derivation attempts is pooled and shared. Up to September 2008, 38 lines have been accessioned to the UKSCB from UK clinics. Table 3.15 details the number of lines at each stage. When deposition paperwork has been completed but the cell line is not yet received by the UKSCB it is *accepted*. A line is *accessioned* when it is received into the Bank. Following thorough quality control and cell characterisation studies, pre-master, master and distribution cell banks are generated and the cell line is *released*. Once released, with appropriate paperwork, the lines become *available* for distribution. Only the UK data have been included in this instance, as it is not a condition of derivation licences outside of the UK to deposit each line in the UKSCB, and therefore the proportion of lines submitted from international clinics is not known.

Table 3.15: Number of UK-derived lines at the various stages of deposition to the UKSCB as of September 2008. NYB: Not yet banked (if known).

Clinic	Available	Released	Accessioned	Accepted	NYB	Total
King's College	1	2	3	1	3	10
Sheffield	7		2			9
Newcastle	1	5	3			9
Nottingham	2					2
Roslin		4	1	1		6
Edinburgh			4			4
Manchester				1	1	2

3.4.4 Characterisation

As there is no definitive marker for stem cell identity, a panel of markers has been developed and accepted by the community to demonstrate likely pluripotency of hESC lines. The UKSCB is currently validating semi-quantitative cell surface staining and transcription factor protocols and developing a characterisation strategy for 'research' and 'clinical grade' cell lines. KCL004, KCL008-HD2 and KCL009-trans1 demonstrated appropriate expression of pluripotent markers, were karyotyped and were successfully thawed at early passage.

The ability of hESC to differentiate into cells from all three germ layers is also part of routine characterisation. The differentiation capability of KCL008-HD2 is discussed in Chapter 6. Differentiation studies were not performed with the other lines. The studies are time consuming and a strain on resources and as all characterisation tests are re-run by the UKSCB on accession, only pluripotency assays were performed on the other lines. Further characterisation studies performed by the UKSCB include validating comparative genome hybridisation microarray analysis as an alternative to conventional karyotyping and identifying a test regime for adventitious agents.

3.4.5 Standards data

The response from the community agreed with the proposed need for international dissemination of results and collaboration in order to progress the derivation field as efficiently as possible. All but one of the categories proposed were voted as

essential for recording in these early days of research and development, with the final category of number of days until appearance of stem-like cells deemed *desirable* for collection. In future modifications of the standard, it may be more useful to allocate the categories on a continuous scale rather than a discrete scale for more precise ranking.

Within the feedback generated, participants discussed the importance of including all the metadata suggested. For example, the number of embryos used allows comparisons between protocols, feedback to the IVF clinics on their culture systems, and more accurate calculation of the efficiency of methods used. It may be the case that an efficiency for each grade can be established. This will provide accurate information about the number of embryos needed to fulfill GMP need once derivation in clean rooms to a clinical grade is commonplace.

3.4.5.1 Standards validation

Many years of clinical IVF experience has allowed grading systems for blastocysts to be established judged by pregnancy outcome. However the criteria for stem cell derivation may be different. The possibility of a subset of founder cells within the ICM (Cauffman *et al.*, 2009), and the role of TE cells in derivation should be considered. Genotype may be as, or more, influential on the outcome of derivation, but until this information is reported these interactions may remain elusive. Furthermore, morphological assessment is not the only approach for embryo selection - the metabolic activity of the embryo may also be a key predictor, with a 'quiet' metabolism suggestive of a good prognosis (discussed further in Chapter 4).

From the validation of the grading system performed by ten embryologists, each component achieved the minimum inter-observer agreement of 0.41-0.60, a 'moderate' level. Therefore the system was deemed valid for use for grading blastocysts for derivation attempts. Kappa analysis was not to determine whether the grades assigned were correct, but that the embryologists agreed on the grade of each component for each image.

There was 'substantial' agreement for expansion status, both for each individual grade and the overall agreement (kappa of 0.73). While both alpha and gamma grades for TE achieved a 'moderate' agreement by the embryologists, there was some confusion over the beta grade, which only reached a 'fair' agreement. There

was 'moderate' agreement overall for the TE appearance. There was 'moderate' agreement for ICM appearance (kappa of 0.53). As the overall kappa value increased to within the 'substantial' range (0.71) when A (cells compacted, tightly adhered, indistinguishable as individual cells) and B (less compacted, loosely adhered, some visible as individual cells) were combined, this suggests that the observers were disagreeing between these grades when looking at the pictures. Combining C and E further increased the kappa value (0.74) but not significantly. Therefore, in future planned revisions of the standard once data collection is complete, the aim is to include clearer, or more, photographic examples, and to provide a more detailed description of each grade, particularly so that those scientists without an embryological background will be able to grade accurately. These modifications are needed in order to make the grades as meaningful as possible, and therefore to extract the most accurate data from pooled reports.

As those scientists grading blastocysts for derivation will be looking at actual samples, not pictures, and therefore able to focus throughout the planes of the blastocysts, and rotate if necessary to see each cell component, it is expected that the agreement will be greater than in this assessment. In addition, the culture of human embryos to the blastocyst stage as a routine part of clinical IVF is only a recent development, and common in only a few clinics. As the use of blastocyst culture and day 5 transfer becomes the norm experience will improve, and it is likely that agreement when grading will do likewise.

3.4.5.2 Data collection

Derivation data has been submitted up to September 2008 by eight clinics for central analysis, including information about 36 hESC lines derived from 559 donated fresh or frozen embryos. Blastocysts at day 5-8 and of a range of grades were used, with the main plating methods being immunosurgery or whole culture. Stem-like cells were first seen in culture from between 7 and 21 days. 22 of the lines were derived on MEFs, 12 on HFF and 2 on hESC-derived fibroblasts. 25 lines were derived under 5% CO_2 in air, the remaining were at 5% CO_2 and 8% O_2. Of the 34 lines for which karyotype was reported, 8 were abnormal. Whilst the data received so far is insufficient to draw conclusions (36 lines represents only approximately 10%

of the total lines known of), data collection continues, with the hope of providing a derivation 'baseline' to maximise future embryo use.

Whether as a result of the standards publications or not, a number of recent reports have included far more data than early papers, detailing each embryo used and the outcome for each derivation attempt (Feki *et al.*, 2008; Strom *et al.*, 2007; Turetsky *et al.*, 2008). Furthermore, the standard has been incorporated as part of the efforts of the European Human Embryonic Stem Cell Registry (hESCreg; www.hescreg.eu), which aims to provide freely accessible information on existing hESC lines, their derivation, molecular characteristics, use and quality (Borstlap *et al.*, 2008). The hESCreg also recognises that there is little coordination of hESC line derivation, and comparative information on the characteristics and quality of these cells is sparse. The collection of such data is difficult, however the integration of this derivation standard with other initiatives under the hESCreg should lead to a common and internationally accepted central reference.

Chapter 4

Optimisation of hESC culture conditions

4.1 Introduction

The main parameters when considering hESC culture are three-fold; the gas phase composition, the media used and the feeder system employed. The analysis of whether alternative forms of these parameters are acceptable must be in the light of successful embryo and hESC culture and qualification under GMP. Each of these factors will influence the efficiency of derivation. The effect of oxygen tension on embryo development and stem cell culture is discussed in Chapter 1. The limitations of embryo quality on derivation success is discussed in Chapter 3. The studies discussed here focused on the medium composition and the feeder cell type with the aim to improve the derivation and culture of hESC.

4.1.1 Derivation medium

The culture medium used for the growth and propagation of the first King's College hESC lines relied upon conditioning of a base medium with Buffalo rat liver (BRL) cells. BRL cells are a liver epithelial and parenchyma-like cell line. This line has been used extensively in co-culture or as a source of conditioned medium (CM) to support the development of mammalian pre-implantation embryos and the growth of ESC. BRL cell co-culture or CM was first used on mouse one-cell embryos to overcome the 2-cell block *in vitro* (Hu *et al.*, 1998). It was subsequently shown to confer benefit to the development of bovine (Funston *et al.*, 1997; Vansteenbrugge *et al.*, 1994), and

human (Hu *et al.*, 1998; Stojkovic *et al.*, 2004) embryos, and to maintain undifferentiated growth of mESC in culture (Smith & Hooper, 1987). Further investigation revealed that the cell line produced relatively high levels of insulin-like growth factor II, transforming growth factor 13, leukemia inhibitory factor (LIF), stem cell factor (Funston *et al.*, 1997) and colony stimulating factor (Barmat *et al.*, 1997).

The principle factor produced by BRL cells which supported undifferentiated growth of mESC was identified as LIF (Smith & Hooper, 1987). Activation of signal transducer and activator of transcription 3 (STAT3) via LIF receptor signalling appears sufficient for maintenance of mESC pluripotency. LIF is expressed by endometrial and placental tissue during the uterine secretory phase in humans, and plays a role in uterine function during pregnancy (Kojima *et al.*, 1994). This suggests that BRL cells might also be able to support later stage embryo development. The addition of human LIF to culture medium has been shown to enhance the proliferation of human blastocysts showing poor development with low cell numbers (Mitalipova *et al.*, 2003). Based on these reports of the beneficial effects of BRL cells, BRL CM was used in early attempts to derive hESC lines. Successful derivation with the use of BRL CM has been reported (Pickering *et al.*, 2003, 2005; Stojkovic *et al.*, 2004). However, human LIF is unable to maintain the pluripotent state of hESCs despite functional activation of the LIF-STAT3 signalling pathway (Daheron *et al.*, 2004). It is likely that other growth factors present in the BRL CM were responsible for the successful derivation of those early hESC lines. Since the use of BRL CM would be unacceptable for culture of cells destined for clinical use, alternative media are required.

BRL CM is not the only type of conditioned medium that has been used in hESC culture. Medium conditioned by both murine and human feeders has been used extensively in attempts to culture hESC in a feeder-free environment (Choo *et al.*, 2006; Xu *et al.*, 2001), on human feeders (Richards *et al.*, 2002) and in autogenic systems (Xu *et al.*, 2004). Whilst published reports discuss the issues arising from xeno-contamination, little, if any consideration has been given to the components of the milieu provided by the CM and the effect this may have on experimental outcomes.

4.1.2 Alternative feeder cell types

The feeder cells used for the growth and propagation of the first King's College hESC lines were MEFs derived from Swiss MF1 mice. The priority for this part of the work was to validate a human source of feeder cells suitable for hESC derivation and culture. The use of human feeders is not without concern regarding viral or infectious agent transmission (Cobo *et al.*, 2005; Stacey *et al.*, 2006). However, appropriately screened, qualified human feeder cells are currently the best possible support for clinical-grade hESC (Unger *et al.*, 2008) until feeder-free, fully-defined systems become available.

4.1.2.1 Amniotic epithelial cells as feeders

Human placentas are routinely discarded following birth. They may be a useful, readily available, non-controversial and clean source of tissue for feeder cells for hESC derivation and culture, as long as the donating patients have been screened in accordance with current GMP and EUTCD standards. Placental tissue expresses a low level of major histocompatibility complex antigens and is involved in modulating fetal tolerance (Parolini *et al.*, 2008). This may prove beneficial if placental tissue is approved as a feeder type for the culture of hESC for clinical use. The amniotic epithelium of the placenta is an uninterrupted single layer of flat, cuboidal and columnar epithelial cells in contact with amniotic fluid. Under certain high density culture conditions amniotic epithelial cells (AEC) form spheroid structures that retain stem cell characteristics such as expression of OCT4/POU5F1 and NANOG (Miki *et al.*, 2005).

Amniotic epithelial cells have been used as a feeder source for maintaining primate embryonic stem cells (Miyamoto *et al.*, 2004) and human limbal epithelial stem cells (Chen *et al.*, 2007), and are able to support the differentiation of adult neural stem cells towards specialized tissues (Meng *et al.*, 2007; Ueno *et al.*, 2006). AECs have proved superior to cell-free matrices for primate ESC culture (Miyamoto *et al.*, 2004) but have yet to be tested as a feeder source for hESC derivation and culture. As the embryo develops in close contact with extraembyonic membranes *in vivo*, placental amnion may replicate the stem cell niche *in vitro*. AECs were assessed here as feeder cells for hESC derivation and culture.

4.1.2.2 Human foreskin fibroblasts expressing basic fibroblast growth factor as feeders

Fibroblast growth factor (FGF) was originally identified in extracts of pituitary and brain that stimulated the growth of 3T3 cells (Armelin, 1973; Gospodarowicz, 1974). During embryonic development FGFs have diverse roles in regulating cell proliferation, migration and differentiation (Rifkin & Moscatelli, 1989). HESCs express bFGF receptors (Xu *et al.*, 2005) and bFGF is able to maintain undifferentiated growth of hESCs in the absence of conditioned medium (Levenstein *et al.*, 2006; Xu *et al.*, 2005). The action, at least in part, is through modulating the expression of transforming growth factor beta (Greber *et al.*, 2007). bFGF and insulin-like growth factor have been described as cooperatively establishing the stem cell niche (Bendall *et al.*, 2007).

The FGF family are very labile proteins, sensitive to extreme pH, temperature and proteases (Wolff *et al.*, 1996). Daily supplementation with exogenous bFGF appears sufficient to support the undifferentiated growth of established hESC, but for derivation of new lines the culture regime differs. Medium exchange is less frequent and therefore little, if any, bFGF is likely to remain between medium exchanges. bFGF-expressing germ layer derived fibroblast cells have been used for the culture of existing hESC lines (Saxena *et al.*, 2008; Unger *et al.*, 2009). Such cells provide a continuous source of bFGF for the maintenance of pluripotency, but were not validated for the derivation of new lines. Human foreskin fibroblasts (HFF) expressing bFGF were assessed here as feeder cells for hESC derivation and culture.

4.1.3 Aims

The next phase of development towards entirely xeno-free derivation and maintenance of hESCs would be; the combination of mechanical or laser isolation of the ICM, use of human feeder cells derived and cultured in defined xeno-free medium, and the use of defined xeno-free culture medium in hESC culture. To that end, BRL CM and a commercially available culture medium were analysed along with feeder conditioned medium. The suitability of human AECs and HFFs as feeder layers in the culture of existing hESCs and the derivation of new lines was also investigated.

4.2 Method development

4.2.1 Growth of mouse embryonic fibroblasts

Before moving the culture of hESC to 5% oxygen, the growth of MEFs was assessed in this condition. MEFs were thawed, expanded, and plated as described in section 2.2.2. To select the initial concentration for the growth analysis, wells were plated at 1, 2, 3, 4 and 5x10^4 cells/well and cultured for 5 days. The optimum concentration was selected such that the cells on day 5 were not over-confluent.

Twenty wells at the selected concentration were prepared. On each of 5 days, 4 wells were fixed and the nuclei stained with DAPI (section 2.5.1). The number of nuclei in 5 random fields of view were counted for each of the 4 wells, and the average of the 20 counts taken. The percentage cumulative growth was plotted by calculating the average cell number each day as a percentage of the number of cells plated on day one.

4.2.2 Analysis of derivation medium

4.2.2.1 Human embryonic stem cell culture medium

Batch-to-batch stability of BRL CM and the commercially available knock-out serum replacement (KOSR) was evaluated by measuring the levels of metabolic substrates and by-products. Freshly made samples from 15 batches of hESC CM and 10 batches of KOSR were collected and stored at -80°C until analysis. A different batch was defined as the use of a different vial of BRL cells or a different batch of SR. Analysis was performed on the NOVA Bioprofile® 400 exactly as in section 2.6. Morphological and immunocytochemical analysis of hESC grown for a minimum of 10 passages in KOSR was performed to ensure hESC maintained a stem cell profile in the commercial medium (section 2.5).

4.2.2.2 Analysis of feeder conditioned medium

Representative samples of CM from MEF and HFF feeder cells were collected following routine culture for CM preparation. Therefore cell counts were not performed to plate equal numbers in each culture vessel, but instead thawed vials and subsequent pellets on passage were split equally between flasks. Feeders were passaged 1 in 3 every 48 h. At this time the CM was collected, centrifuged at 1000 xg for 2 min to

remove cell debris and stored at -80°C until analysis. 15 samples were collected from each cell type. Triplicate samples of the base medium without conditioning were also collected as a control. Analysis was performed on the NOVA Bioprofile.

4.2.3 Isolation of amniotic epithelial cells

Human placentas were obtained with prior informed consent (National Research Ethics Service (NRES) approval reference 08/H0802/7) from healthy women undergoing uncomplicated elective caesarean deliveries at St Thomas' Hospital. Only those patients negative for HTLV-I, HIV and hepatitis B and C were approached. Placentas were washed in sterile saline at the birth suite before being transported to the Department of Women's Health. All subsequent manipulations were performed in a sterile class II cabinet or a laminar flow hood. Culture was at 5% CO_2 in air at 37°C.

Before beginning manipulations each placenta was photographed and measured. The placentas were placed cord side up on a sterile sheet, and the cord cut close to the surface and discarded. The amnion surface was then cut into quadrants through the cord stump using a sterile scalpel. The amnion membrane was gently separated from the chorion, from medial to lateral. The membrane pieces were washed through several changes of Hank's balanced salt solution (HBSS; Gibco Invitrogen) to remove any blood, then placed in HBSS on ice to transfer to the stem cell laboratory at Guy's Hospital. The remaining placental tissue was double bagged and placed in clinical waste for incineration.

The AEC isolation method was modified from two published reports (Miki *et al.*, 2005; Miyamoto *et al.*, 2004). Four culture conditions were compared to select the one most suited to the isolation and growth of AEC. For the initial digest of the membrane the samples were placed in equal volumes of 0.25% trypsinEDTA and incubated at 37°C for 30 min. The samples were then washed thoroughly in HBSS and incubated in 10 mL of 0.05% collagenase type I (Gibco Invitrogen) for 30 min at 37°C to release the AECs. At the end of the incubation the samples were quenched with 15 mL of 90% Iscove's Modified Dulbecco's Medium (IMDM; Gibco Invitrogen) with 10% FCS, before being strained through a 100 μm cell strainer (Corning) to remove any undigested tissue. The cell suspension was centrifuged at 1000 xg for 5 min, the supernatant removed and the separate AEC pellets combined. Viability of

the cell sample and total cell number obtained were assessed by trypan blue (Sigma Aldrich) count on a haemocytometer.

4.2.3.1 Validation of culture conditions

The cell pellets were initially placed in one of four culture conditions on gelatin-coated T25 flasks. Condition 1 was simple medium consisting of IMDM, 10% FCS and 2% pen/strep. Condition 2 comprised simple medium supplemented with 10 ng/mL epidermal growth factor (EGF; Sigma Aldrich). Condition 3 was enriched medium consisting of IMDM, 10% FCS, 4 mM L-glutamine, 1% NEAA and 2% pen/strep. Condition 4 comprised enriched medium supplemented with 10 ng/mL EGF. Pen/strep supplementation was withdrawn over the initial expansion. Media was exchanged every 48 h with EGF added fresh to each batch. The initial media exchanges required an additional wash in PBS to remove residual blood cells. Statistical analysis was carried out using Stata, version 9.2 (StataCorp, College Station, Texas, USA). Linear regression was used to determine significant differences in growth rates in the conditions.

To validate the isolation procedure, the supernatants were collected following both the trypsinisation and centrifugation steps and a cell count performed to ensure no cells were lost during this process. A sample from each amnion was cryopreserved and then thawed to assess viability after thaw and percentage attachment after plating.

Growth curves were initiated in each condition to compare the four culture media. $4x10^4$ cells/cm^2 were plated in 12 dishes for each condition. At two-day intervals three dishes were trypsinised and cell counts performed. The medium on the remaining dishes was exchanged. The number of unattached cells in each condition at the first medium exchange was counted to assess the impact of cell attachment on the subsequent growth rate.

The media samples collected at each exchange were analysed in order to confirm that none of the conditions were growth limiting due to loss of metabolic substrate or accumulation of toxic by-products. Throughout the isolation and culture, morphological characteristics of the AECs were monitored and documented photographically.

Once the best culture method was chosen, FCS was exchanged for synthetic protein serum substitute (SPSS), and trypsin for TryplE Express to remove the

animal components from the culture system. One half of an amnion was cultured in enriched medium with EGF, the other half was cultured in enriched medium with EGF but with substitution of FCS for SPSS. As SPSS is used in human embryo culture this added no further components to the culture.

4.2.3.2 Pathogen testing

AEC samples from each placenta were submitted to the Microbiology department at Guy's Hospital and to Surrey Diagnostics for routine microbiological screening and mycoplasma testing respectively. Negative viral status for HIV, HTLV and hepatitis B and C was predetermined by selecting only serum-negative donors.

4.2.3.3 Characterisation of amniotic epithelial cells

The purity of the AEC was assessed after three passages using immunocytochemistry and FACS analysis (section 2.5). The presence of antigens for cytokeratin (KRT; indicative of epithelial cells), CD45 (universal marker for nucleated blood cells) and POU5F1 (indicative of pluripotent cells) was analysed.

4.2.3.4 Preparation of feeder plates

Confluent flasks of AECs were inactivated and plated exactly as for MEFs (section 2.2.3). Efficacy of the inactivation time for this cell type was assessed by negative staining for KI67 (strictly associated with cell proliferation). For determination of appropriate cell density for hESC culture, feeders were initially prepared at $2.6\text{x}10^4$, $3.9\text{x}10^4$ and $5.3\text{x}10^4$ cells/cm^2. The densities chosen were for coverage of the culture vessel surface and were based on the relative size of AECs to MEFs.

4.2.3.5 Evaluation of AECs as feeders

Undifferentiated, subconfluent colonies of hESC were manually dissociated and transferred onto prepared AEC feeder layers. Equivalent colonies were plated onto MEFs as a comparison. After five days in culture, several plates were fixed and processed for immunocytochemistry. The remaining hESC were passaged onto freshly prepared AEC plates as required. The morphological characteristics of the colonies were noted and documented photographically. After 3 months of continuous culture

on AEC, several plates of hESC were fixed and routine characterisation performed for pluripotency markers.

4.2.3.6 Derivation of new human embryonic stem cell lines

Cryopreserved embryos were thawed exactly as in section 2.1.2.3 and derivation attempted by either mechanical isolation or whole plating exactly as described in section 3.2.1. The feeder layer was the only variable, the technique and medium used were identical to successful derivations on MEFs. Therefore ten blastocysts with grade A ICM was set as the preliminary limit for derivation attempts, as this was within the efficiencies set by derivation on MEFs (2 lines from 8 fresh grade A ICMs, 1 line from 9 frozen grade A ICMs). Embryos came from three donors to ensure any failure to derive was not due to the use of a single unsuitable donor.

4.2.4 Production of human foreskin fibroblasts expressing fibroblast growth factor

A novel line of human feeders was investigated in collaboration with the Department of Gynaecology and Obstetrics at the Medical School of the University of Geneva. At the Medical School, by lentiviral transduction and cre-lox recombination, HFF were modified to secrete human modified bFGF and express a green fluorescent protein (GFP) selection marker. A fibroblast line was established through subsequent subculture and manual selection for fluorescent cells. A HFF sample was acquired from the Medical School for validation at passage 12, subsequent thawing, culture, expansion and banking was performed exactly as for MEFs, described in section 2.2.3.

4.2.4.1 Pathogen testing

HFFs were received in medium containing pen/strep, gentamicin, amphotericin B and Fungizone. These supplements were withdrawn from the culture and cell and medium samples submitted regularly to the Microbiology department and to Surrey Diagnostics for routine microbiological screening and mycoplasma testing respectively.

4.2.4.2 Characterisation of HFF

Positive GFP expression was confirmed at regular intervals, and preceding each cryopreservation. The concentration of bFGF secreted by the HFFs was 300 ng/ml of bFGF from 400,000 irradiated cells, the equivalent of approximately 0.75 pg bFGF/cell .

4.2.4.3 Preparation of feeder plates

Confluent flasks of HFFs were inactivated and plated exactly as in section 2.2.3. KI67 expression was used to test the efficacy of the inactivation time for this cell type. For determination of appropriate cell density for hESC culture, feeders were initially prepared at $1.1x10^4$, $2.1x10^4$ and $4.2x10^4$ cells/cm^2. The densities chosen were based on the relative size of HFF to MEFs.

4.2.4.4 Evaluation of HFF as feeders

Undifferentiated, subconfluent colonies of hESC were dissociated manually and transferred onto prepared HFF plates and MEF plates as a control. The morphological characteristics of the colonies were recorded and documented photographically. Plates of hESC were fixed after 3 months of continuous culture on HFF, and maintenance of a pluripotent phenotype confirmed by routine characterisation. The derivation of new hESC lines on HFF was attempted exactly as for AECs.

4.3 Results

4.3.1 Growth of mouse embryonic fibroblasts in 5% oxygen

From the preliminary growth investigation, $1x10^4$ cells/well was selected to compare growth. Figure 4.1 shows the percentage of cumulative growth of MEFs over 5 days in 21% vs 5% oxygen tension. There was no difference in growth rates between these conditions and therefore subsequent embryo and hESC culture was performed at 5% oxygen.

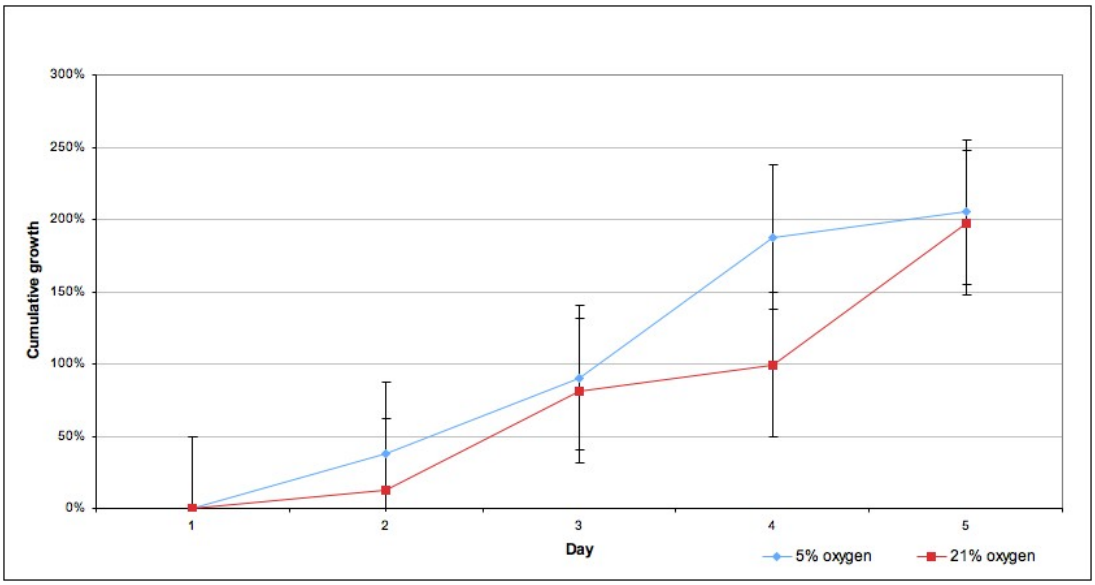

Figure 4.1: Cumulative growth of mouse embryonic fibroblasts in 5% and 21% oxygen tension.

4.3.2 Analysis of culture medium

4.3.2.1 Human embryonic stem cell medium

Simultaneous measurement of the levels of glutamine, glutamate, glucose, osmolality, lactate, ammonium, Na^+, and K^+ of different batches of hESC CM and KOSR are shown in Figures 4.2 and 4.3.

The change in medium for hESC culture to KOSR was successful. Attachment following passage was equal to that of hESC CM. Initially cells appeared granular in KOSR compared to the sister colony pieces remaining in hESC CM, but after 3-5 passages the morphology returned to normal. Colonies grew on top of the feeders rather than pushing them to the side, and tended to form multiple layers as opposed to the monolayer observed with hESC CM. Passaging was facilitated in KOSR, as the colony pieces could be gently knocked off from the top of the parent colony, rather than the cutting and delicate scraping required in hESC CM. Differentiation following long-term culture without passage occurred mainly at the colony borders, with occasional differentiated or necrotic cells being observed in the centre of the colony. At high magnification, the individual cells retained the classic morphology, that of a cobblestone appearance, high nucleus to cytoplasm ratio and prominent nucleoli. Immunocytochemical analysis confirmed continued pluripotent status of

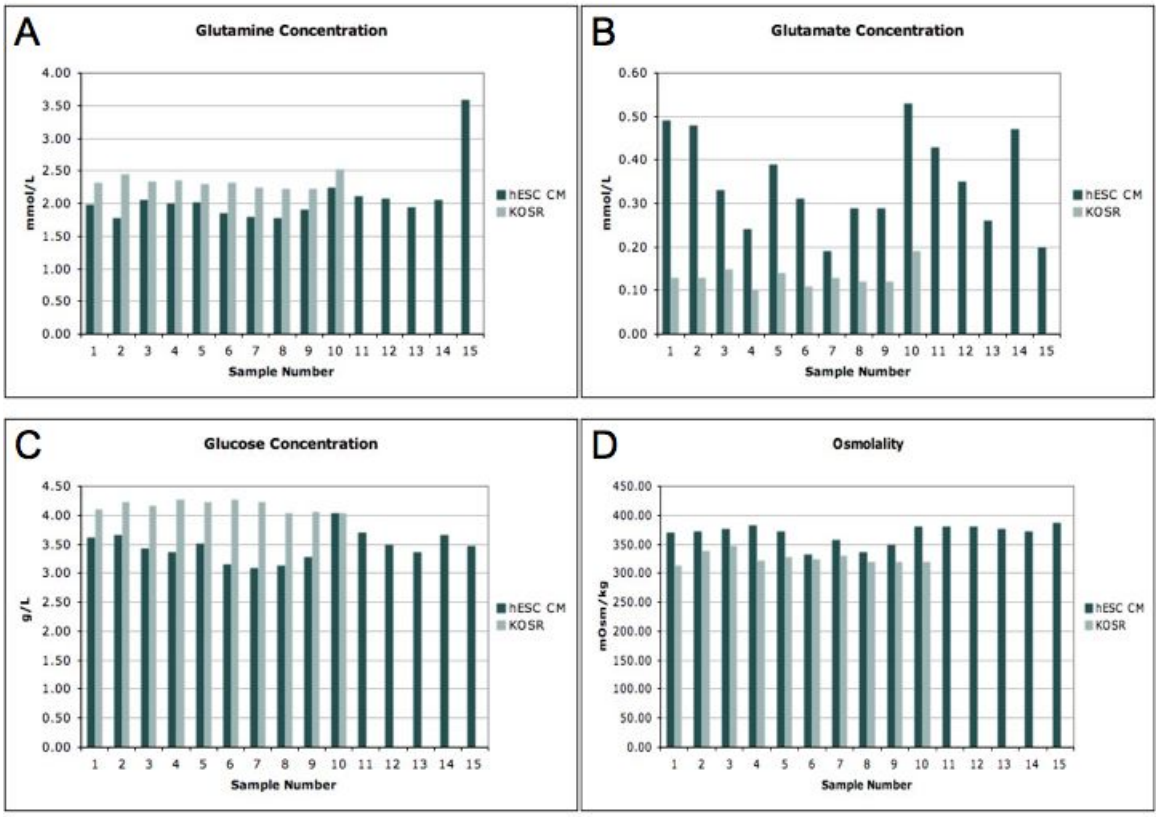

Figure 4.2: Levels of (A) glutamine (B) glutamate (C) glucose (D) osmolality in batches of hESC CM and KOSR.

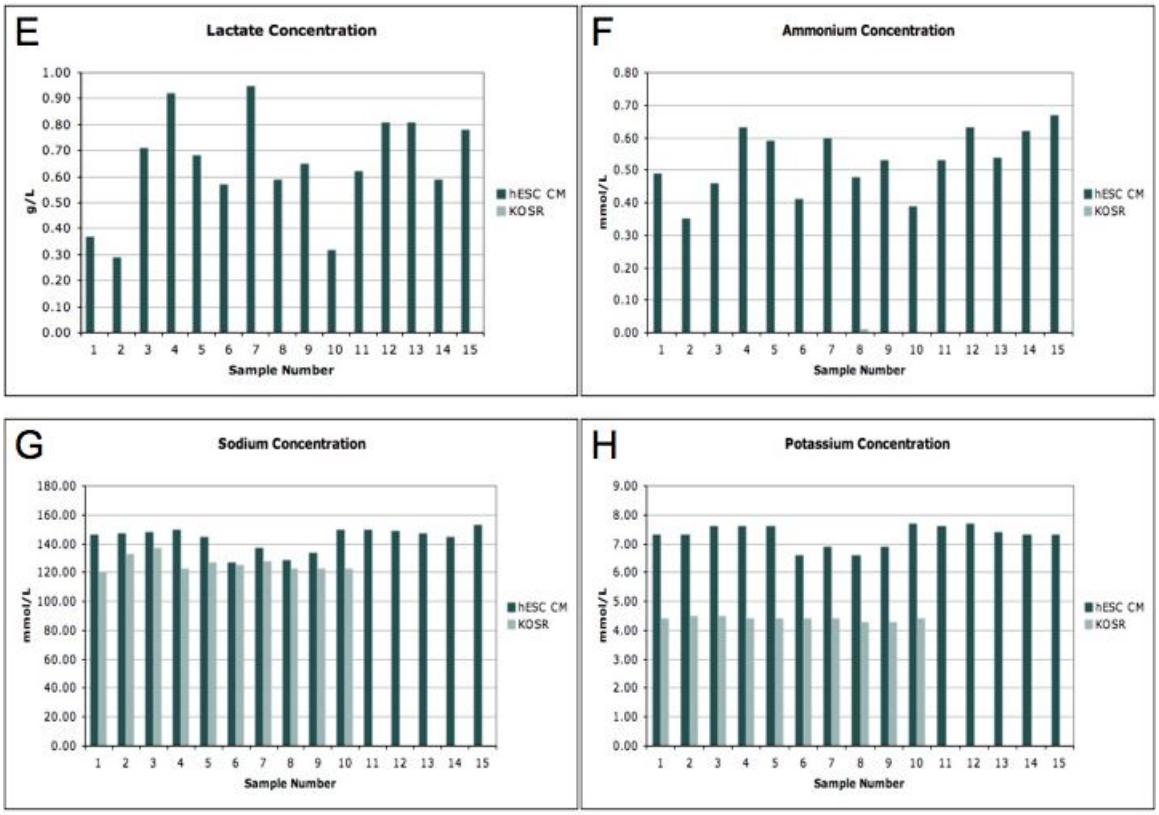

Figure 4.3: Levels of (E) lactate (F) ammonium (G) Na^+ (H) K^+ in batches of hESC CM and KOSR.

the hESC after a minimum of 10 passages in KOSR. Representative images are shown in Figure 4.15.

4.3.2.2 Feeder conditioned medium

Simultaneous measurement of the levels of glutamine, glutamate, glucose, osmolality, lactate, ammonium, Na^+, K^+ of different batches of MEF CM and HFF CM are shown in Figures 4.4 and 4.5.

Table 4.1 compares the levels of metabolites and catabolites in the CM and KOSR samples with published reports of the levels found in human serum, blastocoel fluid, and the data available regarding toxic concentrations in cell culture and embryo development.

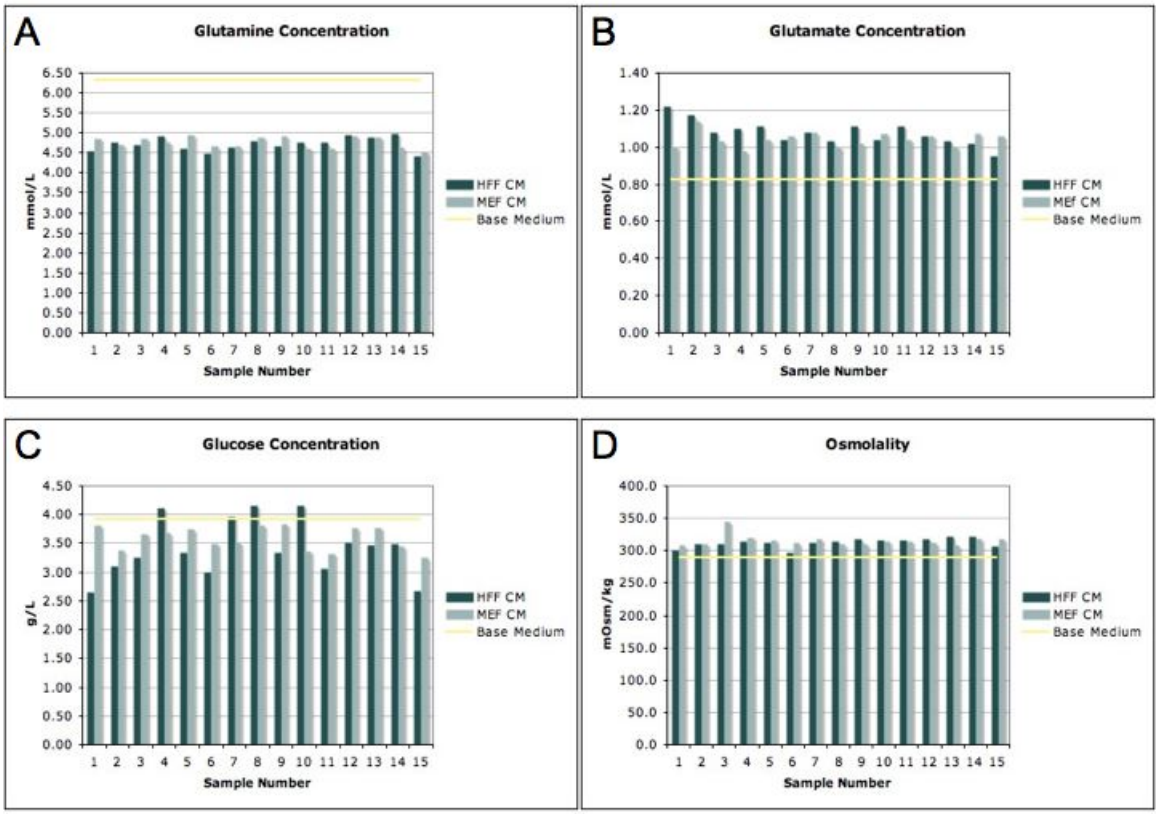

Figure 4.4: Levels of (A) glutamine (B) glutamate (C) glucose (D) osmolality in batches of MEF CM and HFF CM.

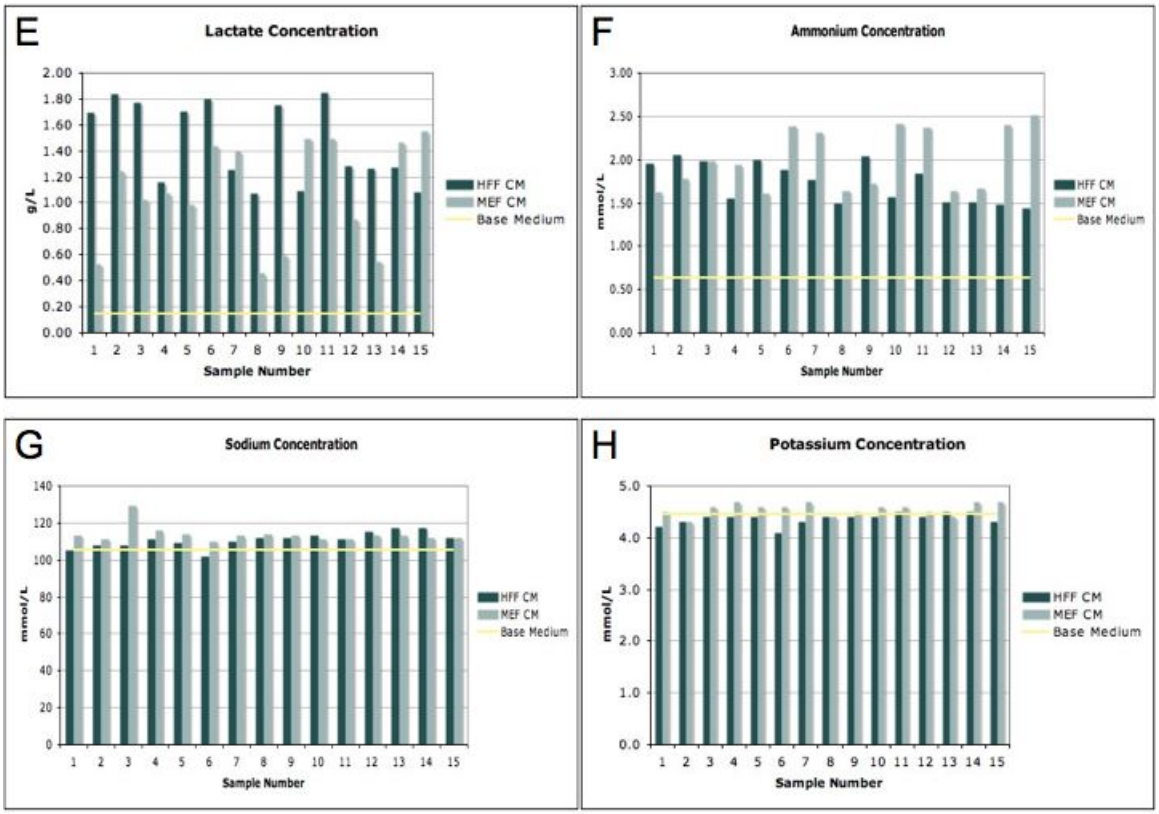

Figure 4.5: Levels of (E) lactate (F) ammonium (G) Na^+ (H) K^+ in batches of MEF CM and HFF CM.

Table 4.1: Levels of metabolites and catabolites found in the media used in ICM and hESC culture, compared with human serum and blastocoel fluids. Toxic levels in culture are included if known. Gln; glutamine (mmol/L), Glt; glutamate (mmol/L), Glu; glucose (g/L), Na^+; sodium ions (mmol/L), K^+; potassium ions (mmol/L), Lac; lactate (g/L), Amm; ammonium (mmol/L), Osm; osmolality (mOsm/kg).

Substance	**Gln**	**Glt**	**Glu**	**Na^+**	**K^+**	**Lac**	**Amm**	**Osm**
KOSR	2.33	0.13	4.16	126	4.4	0.00	0.00	326
BRL CM	2.08	0.35	3.47	144	7.3	0.64	0.53	368
MEF CM	4.75	1.04	3.59	114	4.6	1.08	2.00	316
HFF CM	4.72	1.08	3.42	111	4.4	1.46	1.74	313
Serum (approx)	0.57	0.06	0.90	130	4.6	0.07	0.04	290
Blastocoel fluid			0.11	167	32.6	0.20		
Toxic - cell culture						1.8 - 2.7	2.0 - 3.0	
Toxic - embryo							0.08	

4.3.3 Establishment of alternative feeder systems

4.3.3.1 Isolation of amniotic epithelial cells

NRES approval was sought for the project in January 2008. The application was returned for revision in early February 2008 and approval granted in late February. In total 8 couples were approached regarding placental donation, of which 6 consented. Of the two couples that declined, one cited reasons as religious and one as cultural (the placenta was to be buried).

Five of the six placentas were collected. For placenta 0801 the incorrect cell type was isolated, likely to be chorion, and insufficient cells were obtained for culture. Placenta 0804 was not collected as the caesarean was rescheduled. AECs collected from placenta 0806 were contaminated with a fungus, possibly as a result of culture or isolation technique. The cells were discarded the day after collection. Placentas 0802, 0803 and 0805 were obtained, and AEC isolated successfully. 2.3×10^6 cells were isolated from 0802, 13.2×10^6 cells from 0803 and 2.6×10^6 from 0805. The surface area of the amnion membrane of 0803 measured 267 cm^2 whilst 0805 measured 408 cm^2 corresponding to 4.9×10^4 cells/cm^2 and 6.4×10^3 cells/cm^2 respectively.

4.3.3.2 Validation of amniotic epithelial cell culture conditions

At the completion of the isolation procedure 90% of the AECs were viable as assessed by trypan blue exclusion. Initial validation of the procedure confirmed that no cells were found in the supernatant following trypsin digestion; subsequent to this the supernatant was discarded. Just over 2% of the isolated cells remained in the supernatant following collagenase incubation; increasing the centrifugation step to 10 minutes reduced this to under 2%. Viable cell counts before and after a freeze-thaw cycle showed that only 5% of AECs lysed during the procedure. 85% of these cells attached following plating, confirming that the cells were suitably robust for banking.

Confluent cultures were achieved 6-8 days after plating all the cells from one amnion into a T75 flask. Evaluation of glucose, ammonium and lactate concentration over 48 hours for three media exchanges revealed that the average loss of glucose was 10%, with 3.8 g/L remaining in the medium. Similarly, the average lactate production was 1.05 mmol/L and average ammonium accumulation was 1.58 mmol/L.

The growth of AECs was heavily density dependent, with little, if any, proliferation at low densities. 2.1x10^4 cells/cm^2 were plated for the initial growth curve comparison. The first count on day two showed fewer than half the cells had attached, and no further proliferation was observed over the following 6 days. When plating concentration was doubled (4.2x10^4 cells/cm^2), the culture was confluent in six days in the EGF-supplemented conditions, and in eight days for the non-supplemented cultures. To assess whether there was significant difference in the growth rates between the conditions, linear regression was used to estimate the daily rate of cell growth in each medium as a percentage. Cell counts were log-transformed, and Normality confirmed by distributional plots. Censored values due to dishes becoming confluent were considered as being censored at the largest observed value, and interval regression used (Amemiya, 1973). As all dishes were seeded from the same cell suspension, a single initial concentration was assumed. There was a significant increase in cell growth of 10% in the enriched condition compared to the simple condition ($p<0.0001$, 95% confidence interval (CI) 1.081-1.126). There was also a significant increase in cell growth of 10% when the media were supplemented with EGF ($p<0.0001$, CI 1.077-1.128). There was no evidence of interaction between the enriched and enriched plus EGF conditions, instead a simple additive effect was observed. Figure 4.6 shows an example of AEC morphology. Figure 4.7 details the growth curve results.

The spent medium from the day 2 growth curves was collected to assess the attachment of the cells in each condition. Table 4.2 details the attachment.

Table 4.2: Percentage of cells attached by 48 h after plating in the four test culture conditions. Cells; cells plated, Un; unattached, Att; attached.

Medium	**Cells (x10^4)**	**Un (x10^4)**	**Att (x10^4)**	**% attached**
Simple	4	0.5	3.5	88
Enriched	4	0.4	3.6	90
Simple EGF	4	0.3	3.7	93
Enriched EGF	4	0.1	3.9	98

Considering the outcome of the preliminary experiments, enriched medium supplemented with 10 ng/mL EGF was used for all subsequent culture.

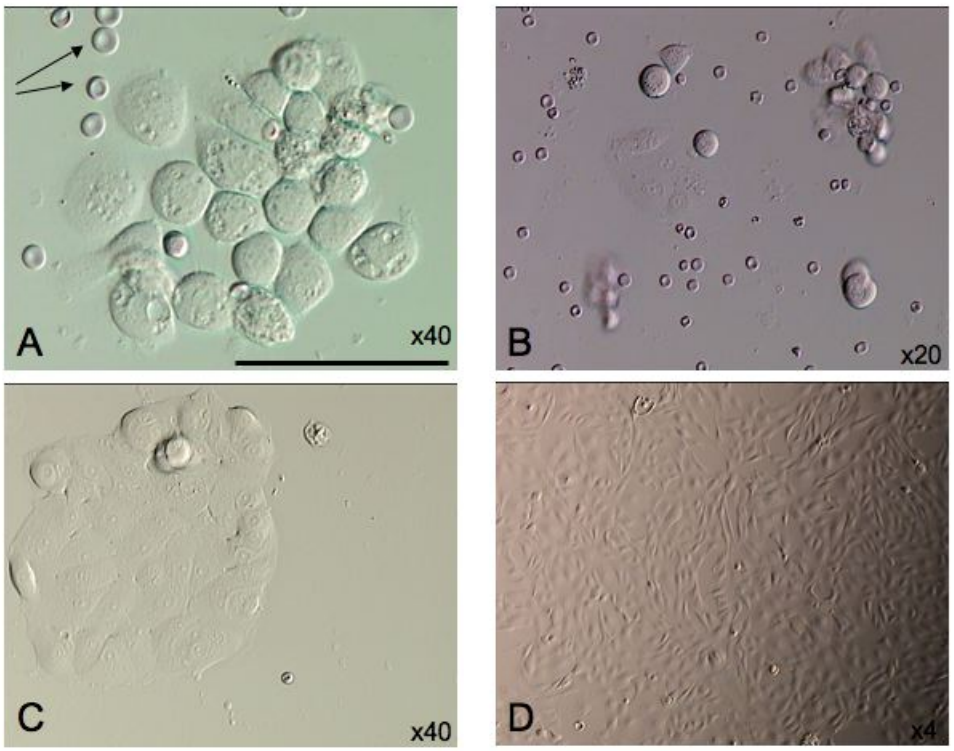

Figure 4.6: Morphology of AECs in the enriched medium with EGF supplementation (A) Day 1 after plating, the cells are rounded having not yet flattened and spread on the flask surface. Residual red blood cells can be seen (arrows). (B) Day 2 after plating, some cells were beginning to flatten while others remained rounded. (C) Day 3 after plating, the majority of cells flattened to form colonies. AECS remained circular rather than extended as fibroblasts. (D) Day 7 after plating, a confluent layer of AECs. Scale bar indicates 50 μm at x40 objective.

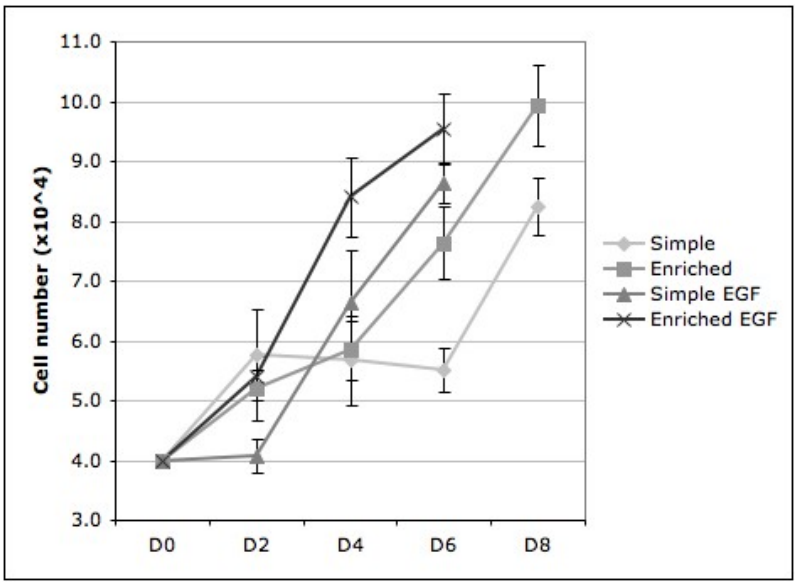

Figure 4.7: Growth characteristics of AECs in the different culture conditions. EGF; epidermal growth factor.

4.3.3.3 Human foreskin fibroblasts

The protocols and conditions for HFF culture were very straightforward. Enriched medium without any supplementation was used, and the cells were expanded in gelatin-coated T225 flasks. The cells grew very rapidly, when the cultures were split one flask into 6 they were confluent 36-48 h later. A large bank of cells was cryopreserved from a single starting vial, at between 13 and 16 passages.

4.3.3.4 Removal of animal components of the culture system

Figure 4.8 shows the morphology and growth of placenta 0805 after 6 days of culture in medium supplemented by either FCS or SPSS.

The use of TryplE Express was equally successful as trypsin in detaching the cells from the flask for passaging, with all cells released within 5 min using either enzyme.

4.3.3.5 Pathogen testing

Placentas 0802, 0803 and 0805 screened negative for microbacterial and mycoplasma contamination. The first and last vial frozen in the HFF cell bank were tested and were also negative. All cells originated from the same first vial so this showed the cells had remained sterile during the scale-up procedure.

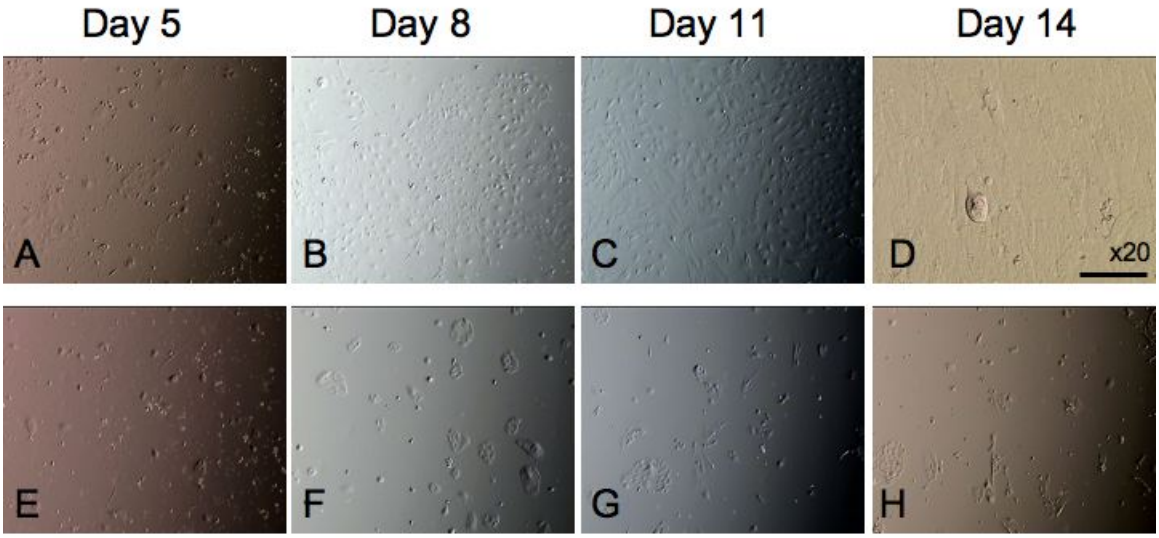

Figure 4.8: Cultures of AECs in FCS (A-D) and SPSS (E-H) at 5, 8, 11 and 14 days after plating at the same density. By day 11 the FCS cultures were confluent, and by day 14 they were over-confluent and had lost their typical rounded morphology. In contrast, negligible growth was observed in SPSS for the duration of culture. All images at x4 objective unless indicated otherwise. Scale bar indicates 50 μm at x20 objective.

4.3.3.6 Characterisation of feeders

The positive GFP status of the HFF was confirmed at regular intervals by FACS analysis and fluorescence as shown in Figure 4.9.

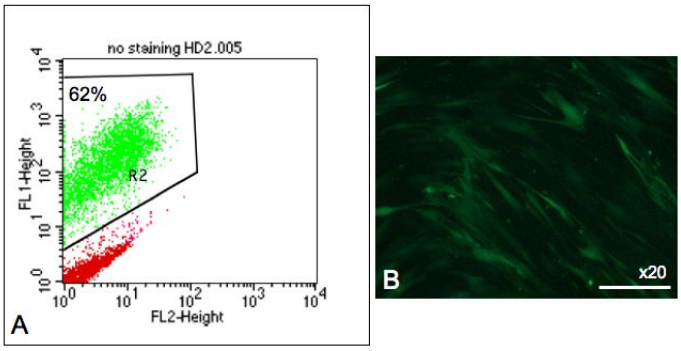

Figure 4.9: Characterisation of HFF. (A) FACS analysis of hESC on HFF with no antibody staining. Over 60% of the cells were GFP positive and therefore HFF feeders. (B) Fluorescent image showing uniform expression of GFP. Scale bar indicates 50 μm.

Epithelial origin of AECs was confirmed by positive staining for KRT5 and 14. This proved lack of contamination by other cell types during the isolation procedure, such as by amniotic mesenchymal fibroblasts. The cultures were negative for CD45 proving the cells were not of haematopoietic origin. Whilst the AECs stained negatively for POU5F1, they were positive for SSEA4 and the TRA antigens and were negative for SSEA1. The TRA 1-60 and TRA 1-81 positive cells were solitary and present throughout the surface of amniotic membrane without a specific pattern of distribution, whereas SSEA4 was positive on all amniotic epithelial cells. HFF did not show positive staining for any of the pluripotency markers. The AEC results are shown in Figure 4.10.

4.3.4 Evaluation of AEC and HFF as hESC feeders

A 2 hour incubation with MMC was sufficient for inactivation of the AECs. This was shown by negative staining for KI67 whilst hESC colonies cultured on the cells

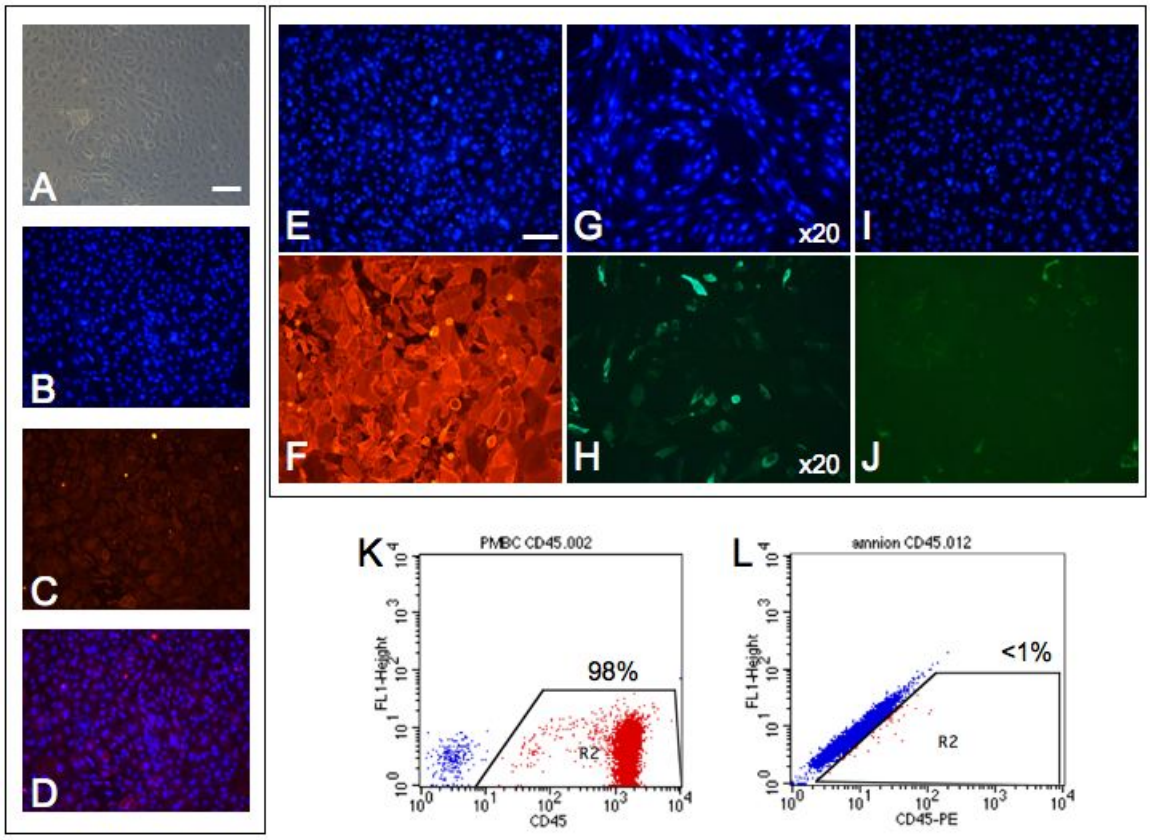

Figure 4.10: Characterisation of AECs. Cells were positive for KRT5 and 14, shown in (A-D). (A) Bright field. (B) DAPI. (C) KRT5,14. (D) Merged image. AECs also strongly expressed SSEA4 (E) DAPI, (F) SSEA4, and weakly expressed TRA1-60 (G) DAPI, (H) TRA1-60. Occasional cells were weakly positive for TRA1-81 (I) DAPI, (J) TRA1-81. (K) Positive control for CD45, peripheral blood mononuclear cells. (L) AECs were negative for CD45. All images at x10 objective unless indicated otherwise. Scale bar indicates 50 μm at x10 objective in each panel.

were positive for the proliferation marker. HFF cells required 3 h inactivation as there was a small population of cells positive for KI67 after 2 hours. The expression of KI67 after inactivation times are shown in Figure 4.11.

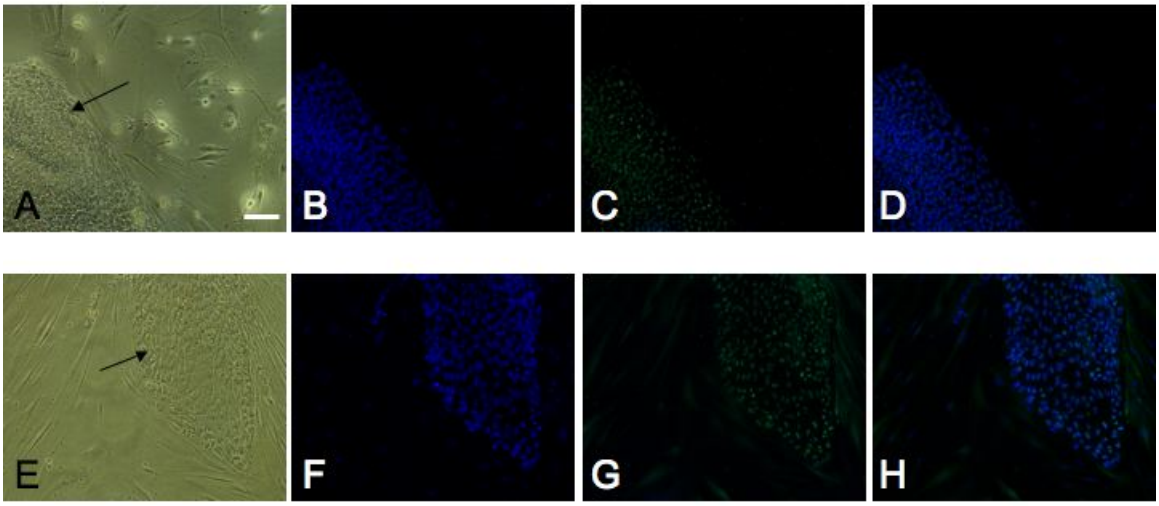

Figure 4.11: A colony of hESC cultures on AECs (A-D) and HFFs (E-F). (A,E) Bright field, arrow indicates hESC colony. (B,F) DAPI. (C,G) KI67, staining visible in the nuclei of hESC but not in the nuclei of feeders. (D,H) Merged images. All images at x10 objective. Scale bar indicates 50 μm.

Three test densities were used to determine a suitable cell density for feeder plates and assessed by initial hESC colony attachment and growth. Although some colonies attached in all three conditions, the subsequent growth was variable. At 2.6x10^4 cells/cm^2 the support from the AECs appeared inadequate, with the hESCs either differentiating or lifting off from the feeders and degenerating in suspension by 6 days after passage. At 5.3x10^4 cells/cm^2, although some colonies attached, they remained as a solid clump, and did not spread out over the feeder layer, ultimately differentiating. However, at 3.9x10^4 cell/cm^2 some colonies attached, spread flat and exhibited normal growth at this first passage, such that the colonies required passag-

ing after 5-7 days. Some of these initial colonies were fixed for immunocytochemical analysis. In an identical approach the most appropriate cell density of HFFs was selected as $2.6x10^4$ cells/cm^2. The morphology of these initial colonies on HFFs is shown in Figure 4.12 and on AECs is demonstrated in Figure 4.13. All subsequent feeder layers were prepared at these densities.

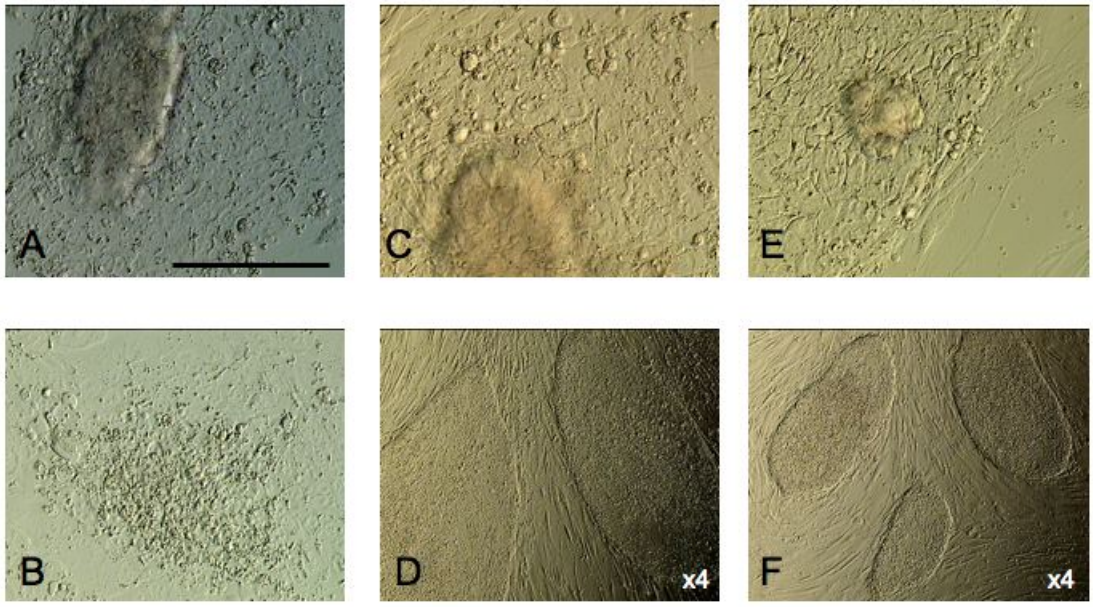

Figure 4.12: hESC colonies passaged onto HFF feeders at (A,B) $2.1x10^4$ cells/cm^2, (A) day 1 after passage (B) day 3 after passage. (C,D) $2.6x10^4$ cells/cm^2, (C) day 1 after passage (D) day 6 after passage. (E,F) $3.2x10^4$ cells/cm^2, (E) day 1 after passage (F) day 4 after passage. All images at x40 objective unless otherwise indicated. Scale bar indicates 50 μm at x40 objective.

Once a suitable density had been determined, feeder layers were prepared for the culture of hESC. On AEC although the growth of colonies that attached exhibited similar morphology and characteristics to those of MEFs, the attachment rate was very low for the first 6 passages. A 90-100% attachment rate would be expected from manual passage of good quality, proliferating, sub-confluent colonies onto MEFs. The rate of attachment to the AECs was sometimes as low as 10%. At passage 4 there

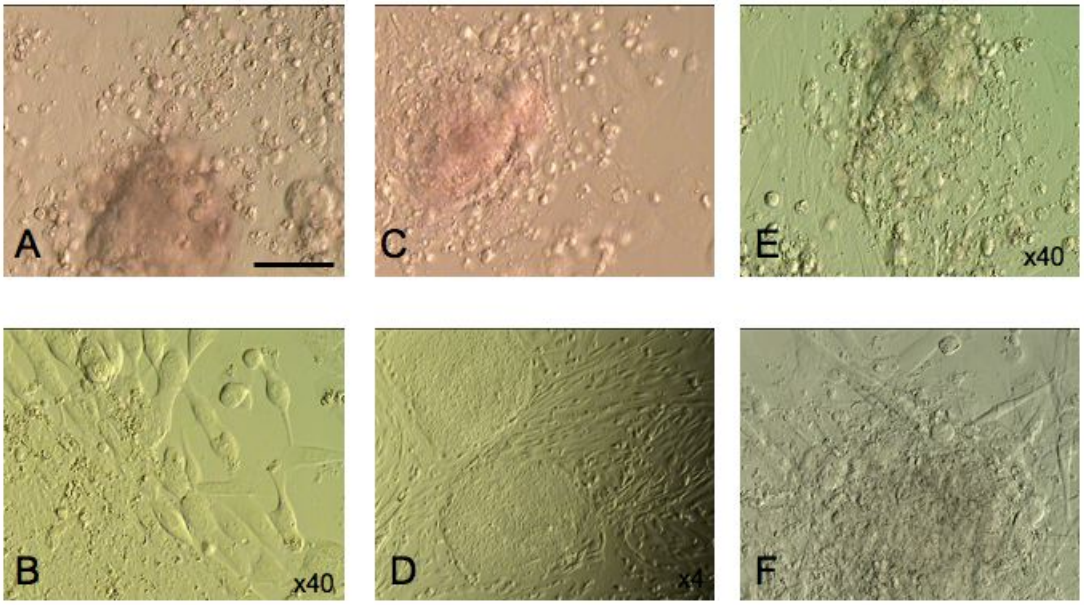

Figure 4.13: hESC colonies passaged onto AEC feeders at (A,B) 2.6x10^4 cells/cm^2, (A) day 1 after passage (B) day 6 after passage. (C,D) 3.9x10^4 cells/cm^2, (C) day 1 after passage (D) day 6 after passage. (E,F) 5.3x10^4 cells/cm^2, (E) day 1 after passage (F) day 3 after passage. All images at x20 objective unless otherwise indicated. Scale bar indicates 50 μm at x20 objective.

was only one colony growing on AEC from all of the original passaged plates. The colonies showed the typical granular morphology of adapting cells, but were otherwise normal in appearance as shown in Figure 4.14. The only subtle difference was at the edges of the hESC colonies where the boundaries on AECs were not as sharp or defined as on MEFs. Adaptation seemed to occur after approximately 7 passages, from which point onwards the attachment improved to above 70% and passage was required every 5-7 days. After 3 months in culture on AECs (10 passages), hESC growth was indistinguishable from colonies cultured on MEFs and characterisation was performed.

The hESC adapted rapidly to the HFFs, although the colony passage size needed to be slightly larger than for MEFs for the first few passages. Attachment and growth rates were indistinguishable from culture on MEFs. For the first few passages the cells had a typical granular morphology of adapting cells, but otherwise the morphology of the cells was normal. In general, colonies of HFF had one of 2 shapes. Whilst some were round, the majority were long, thin and angular as shown in Figure 4.14. This was because the HFFs grew in whorls rather than as dispersed cells like MEFs and AECs. This has been noted by other investigators for a variety of human fibroblast cells (Genbacev *et al.*, 2005; Richards *et al.*, 2002). The rapid proliferation of the HFF and the successful adaptation of the hESC enabled the culture to be expanded rapidly. Feeders were initially made in 4 well plates, but culture was soon expanded to 3 cm and then 6 cm dishes, greatly facilitating scale-up of cells needed for some experiments.

At both passage 1 and 10 on AECs, and passage 5 and 15 on HFFs, hESC expressed all the universally agreed markers of self-renewal and pluripotency. The cells were positive for POUF51, SSEA4, TRA1-60 and TRA1-81 with negative staining for SSEA1 as shown in Figure 4.15. Representative images on MEFs are shown in Figure 3.13.

AECs appeared to reach senescence at P5 in culture, beyond which no significant growth was observed. Cultures were kept for over four weeks before being discarded. In contrast, HFF were used at between passage 15-17 and showed no signs of senescence.

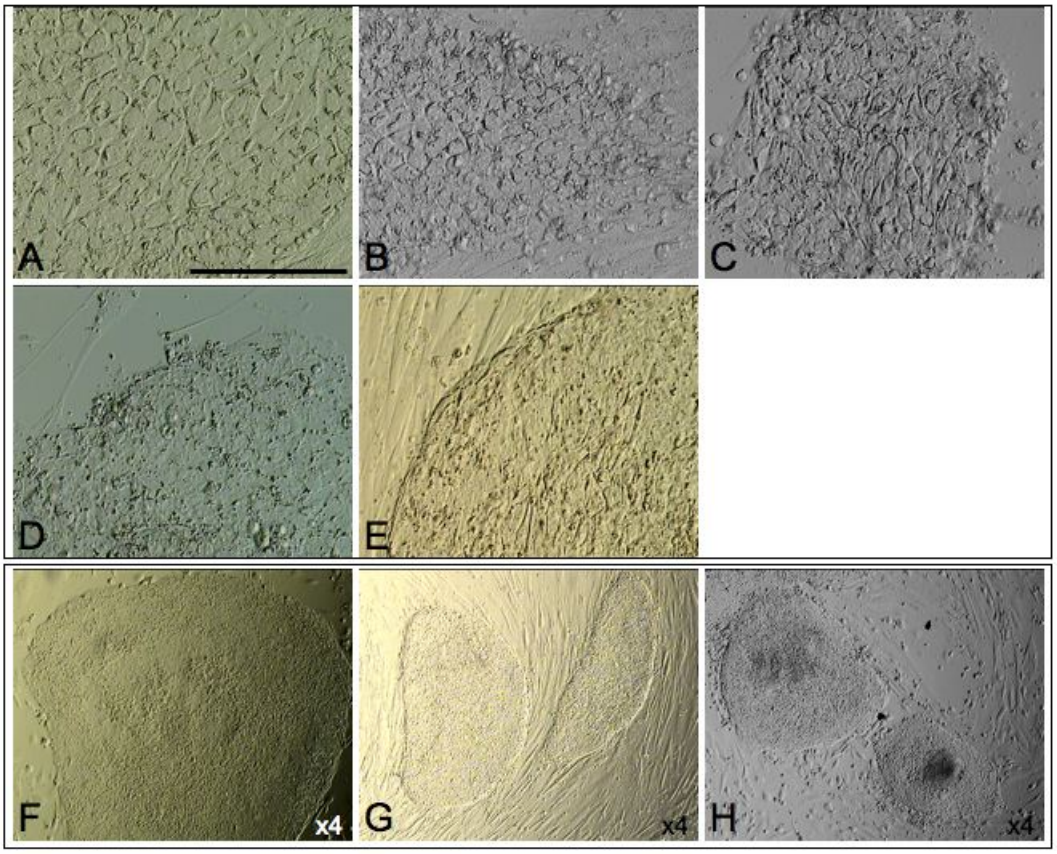

Figure 4.14: Morphology of hESC on various feeders. (A-C) hESC on AECs, (A) P1, (B) P3 and (C) P7. Although granular in early culture, by P7 the cells appeared adapted with normal growth and morphology. (D,E) hESC on HFF, (D) P1 and (E) P3. The hESC adapted rapidly showing normal morphology and growth by P3, although granular cells were visible earlier in culture. Comparison of morphology of hESC colonies grown on (F) MEFs (G) HFF and (H) AECs. Note the round shape of colonies on AEC and HFF compared with the long, angular shape on HFF cells. All images at x40 objective unless otherwise indicated. Scale bar indicates 50 μm at x40 objective.

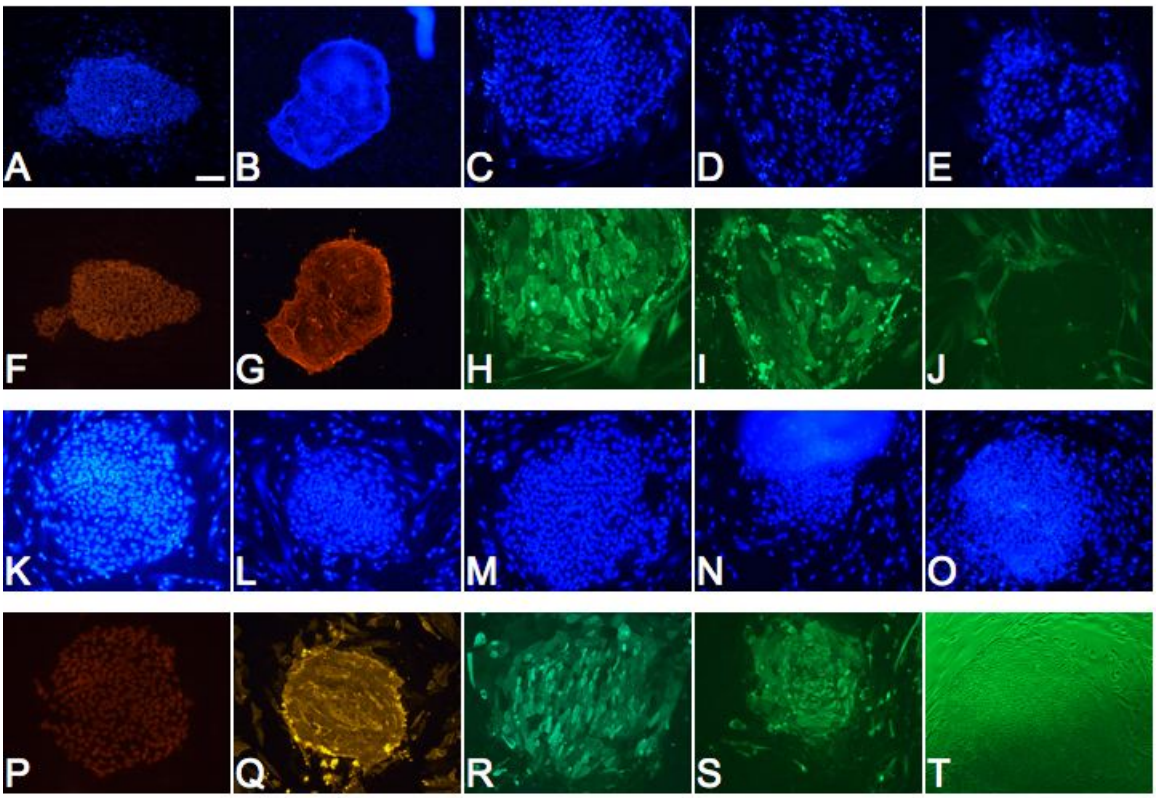

Figure 4.15: Characterisation of hESC on HFF (A-J) and AEC (K-T). HFF and AECs support the growth of the hESC lines in an undifferentiated state, as demonstrated by expression of markers of pluripotency. (A-E and K-O) DAPI images of colonies and feeders. (F,P) POU5F1, (G,Q) SSEA4, (H,R) TRA1-60, (I,S) TRA1-81, (J,T) SSEA1. Note that the green appearance of the HFF is due to GFP transfection not positive staining for the markers. All images at x10 objective. Scale bar indicates 50 μm.

4.3.5 Derivation of new hESC lines

Ten progressive day 5-8 blastocysts with a visible ICM were used for derivation attempts on HFF feeders. Mechanical isolation of the ICM was used for 7 blastocysts, and three were plated whole onto the feeders. All ten ICM/blastocysts had attached to the feeders by 48 h after plating, and spread out on top of the feeders. However, all ten cultures differentiated rapidly by 2 or 3 days after plating, and no ICM or stem-like cells were observed at any point. The exception was blastocyst number 2, but still the cells were not of convincing stem-like morphology. Upon differentiation, giant cells were visible, and the cells were very granular. Therefore no cells could be passaged, and all cultures were discarded after 15 d of observation. Figure 4.16 shows examples of the rapid differentiation of the cultures. No further attempts were made to derive lines, as the continued use of embryos in a system where no pluripotent cell morphology had been observed could not be justified.

Ten progressive day 5-7 blastocysts with a visible ICM were used for derivation attempts on AEC feeders. Mechanical isolation of the ICM was used for 5 blastocysts, and five were plated whole onto the feeders. All ten ICM / blastocysts attached to the feeders by 48 h after plating, and spread out on top of the feeders. Initial morphology appeared hopeful, with seven cultures containing cells with typical 'cobblestone' morphology and prominent nucleoli. However, in three of these cultures, the TE cells overgrew any cells of interest and the cultures rapidly differentiated. It appeared from these initial experiments that the AEC were equally supportive to TE as ICM proliferation. In subsequent derivation attempts, as much TE was removed as possible in mechanical manipulations, or, more successfully, the whole blastocyst was plated and then the TE cut completely away once the blastocyst had attached. To encourage undifferentiated growth the concentration of bFGF was increased to 24 ng/mL. In two further attempts there was no continued growth of any cells, and the colonies subsequently differentiated. One cell culture proliferated sufficiently to be passaged to fresh feeder layers, but no further growth was observed and the cells differentiated over the following days. Examples of these cultures are given in Figure 4.17.

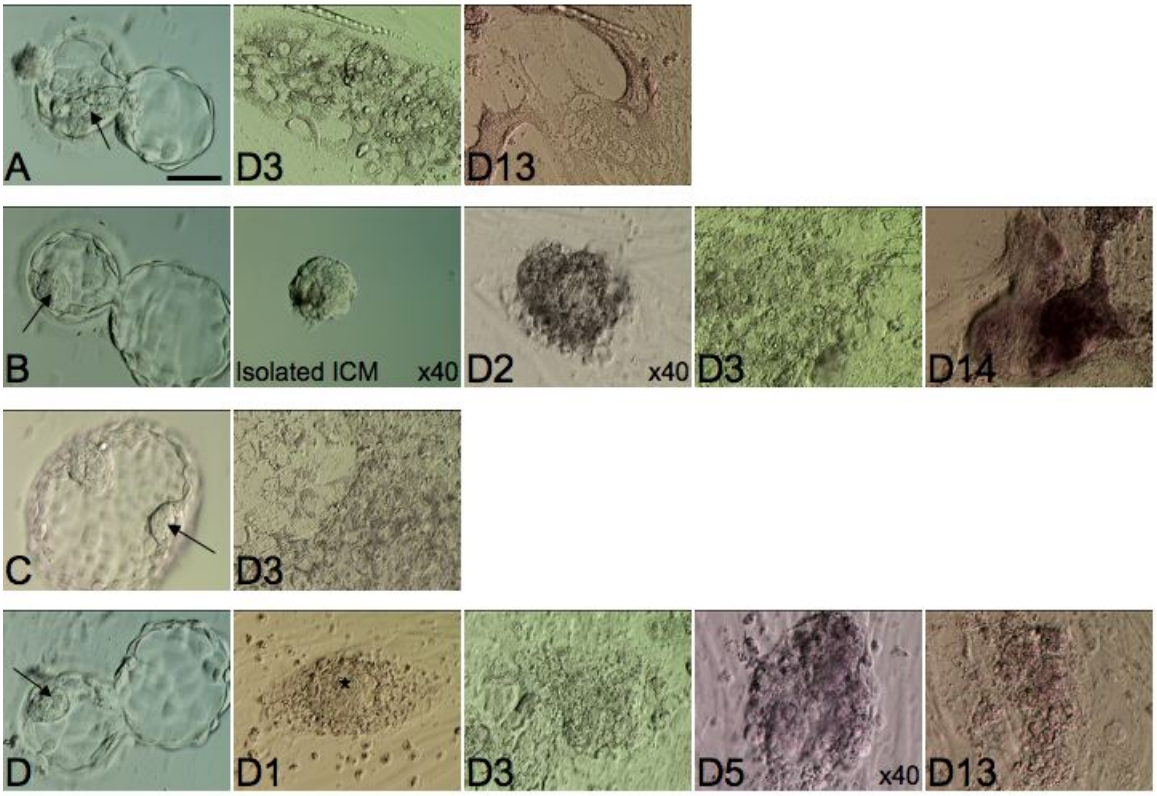

Figure 4.16: Examples of embryos used for derivation attempts on HFF. Blastocysts at D5 (B) D6 (A,D) and D7 (C) of development, all with good quality ICM (arrows). All cells rapidly differentiated and degenerated by D3-D14 of culture. The only culture which displayed ICM-like cells was (D) on D1, where a dense cluster of cells was visible (star) but this also differentiated by D13. All images at x20 objective unless otherwise indicated. Scale bar indicates 50 μm at x20 objective.

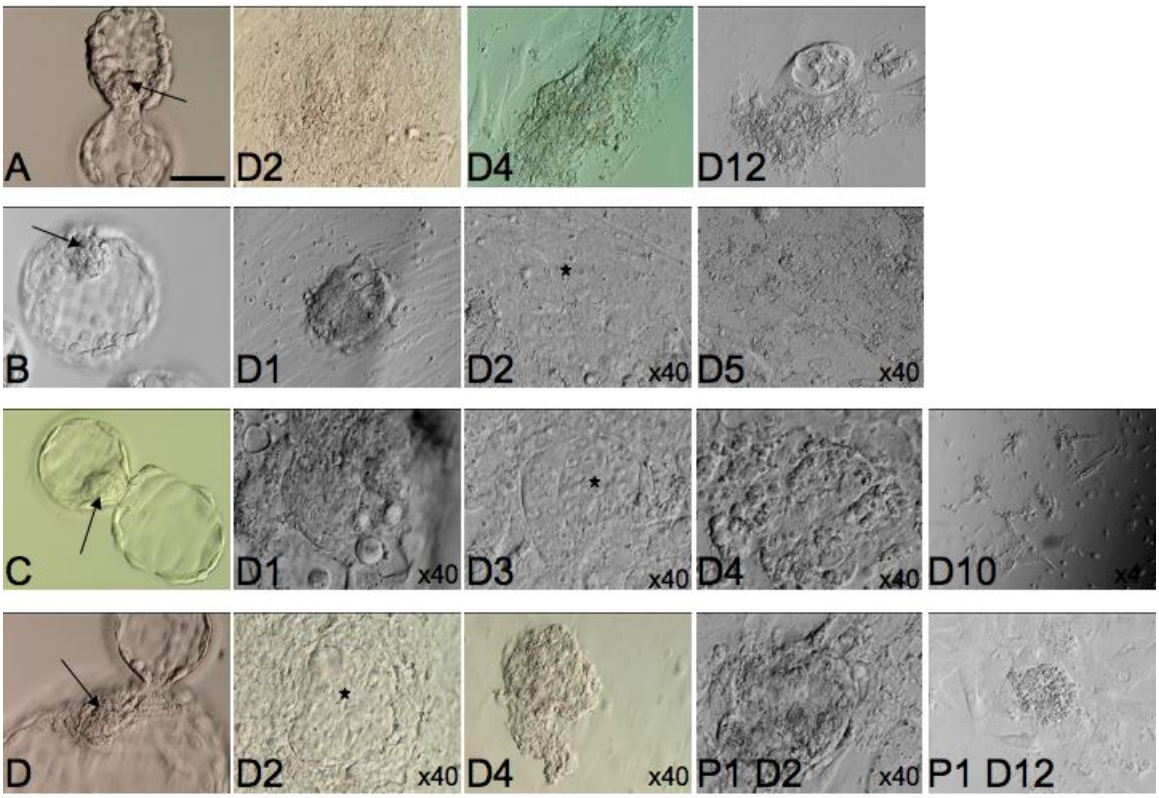

Figure 4.17: Examples of embryos used for derivation attempts on AEC. Blastocysts at D6 (B,C,D) and D7 (A) of development, all with good quality ICM (arrows). No cells of stem-like morphology were seen from embryo A, which differentiated and degenerated by D12. Stem-like cells could be seen in all other cultures as indicated by the stars. However, none were able to be propagated beyond P1. All images at x20 objective unless otherwise indicated. Scale bar indicates 50 μm at x20 objective.

On the ninth attempt, a day 5 blastocyst graded as 2Bβ was plated whole onto AEC feeders. After 24 h the blastocyst was still in suspension having further expanded, so the blastocoele was pierced with a needle to deflate the blastocyst and encourage attachment. In a further 24 h the blastocyst had attached and spread, and ICM/stem-like cells were visible. Incisions were made around this cell clump, and the TE cut and peeled away as far as possible. The following day, the cell clump had proliferated, but was growing upwards and becoming more dense, rather than spreading out. Close inspection revealed than some residual TE cells were enclosing the cell culture and preventing it from spreading. Approximately one quarter of the colony was cut and moved to a proximal place in the dish. The following day the passaged portion had attached and displayed stem-like morphology, and the parent

colony had proliferated and spread. The colony boundary was not defined, just as observed when culturing existing lines on AECs. The following day the parent colony was passaged onto fresh feeders, and continued to proliferate with an undifferentiated morphology over the subsequent days. The stem-like cells were maintained in culture until passage three, when differentiation occurred and the proliferating colony could not be rescued. Figure 4.18 details the early morphology of the stem-like colony. Table 4.3 details the embryo use for all derivation attempts.

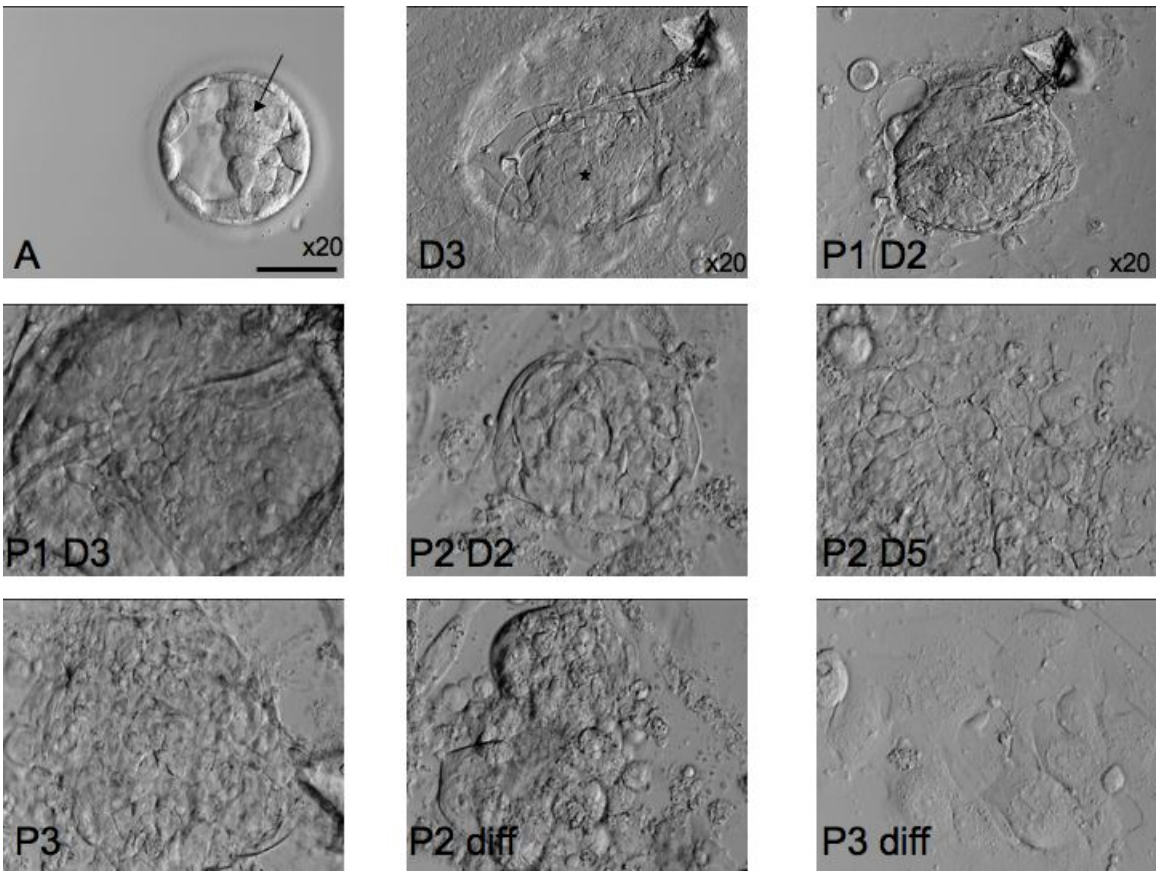

Figure 4.18: The morphology of the stem-like colony on AECs during early culture. (A) D5 blastocyst graded as 2Bα, arrow indicates the ICM. At day 3 after plating, the expanded TE cells were visible, but the ICM cells had proliferated (star). Stem-like cells were visible throughout culture until P3, when proliferation ceased and the cells differentiated. All images at x40 objective unless otherwise indicated. Scale bar indicates 50 μm at x20 objective.

Table 4.3: Summary of the use of embryos for derivation attempts on AEC and HFF. Mech; mechanical ICM isolation, diff; differentiation.

Embryo	Grade	Day	Method	Feeder	Attach	Stem	Outcome
1	5Bβ	6	Whole	HFF	Yes	No	Rapid diff
2	5Aα	6	Mech	HFF	Yes	Yes	Rapid diff
3	5Aα	5	Mech	HFF	Yes	No	Rapid diff
4	2Bγ	6	Whole	HFF	Yes	No	Rapid diff
5	5Cβ	6	Mech	HFF	Yes	No	Rapid diff
6	6Cα	6	Mech	HFF	Yes	No	Rapid diff
7	5Bβ	6	Mech	HFF	Yes	No	Rapid diff
8	6Aα	7	Whole	HFF	Yes	No	Rapid diff
9	6Cβ	6	Mech	HFF	Yes	No	Rapid diff
10	6Bβ	8	Mech	HFF	Yes	No	Rapid diff
1	5Bβ	6	Mech	AEC	Yes	Yes	TE overgrowth, diff
2	5Aβ	6	Mech	AEC	Yes	No	No further growth, diff
3	6Cβ	7	Whole	AEC	Yes	No	Rapid diff
4	3Bα	7	Whole	AEC	Yes	Yes	P1, no further growth
5	3Aα	6	Mech	AEC	Yes	Yes	TE overgrowth, diff
6	3Bβ	7	Mech	AEC	Yes	Yes	No further growth, diff
7	4Bβ	6	Mech	AEC	Yes	Yes	TE overgrowth, diff
8	3Cα	7	Whole	AEC	Yes	Yes	No further growth, diff
9	2Bα	5	Whole	AEC	Yes	Yes	P3, no further growth
10	4Bβ	7	Whole	AEC	Yes	No	TE overgrowth, diff

4.4 Discussion

4.4.1 Analysis of culture medium

4.4.1.1 hESC culture medium

The variation in levels of glucose, glutamine, glutamate, lactate, ammonium, sodium ions, potassium ions and osmolality between the 10 batches of KOSR was negligible. Substrate levels were high, with just over 2 mmol/L glutamine, 0.15 mmol/L glutamate and just over 4 g/L glucose. No lactate or ammonium was present in any of the batches, confirming that these components had been removed from the serum replacement fraction.

In contrast, there was pronounced variability in the levels of substrates between the different batches of hESC CM. Glutamine levels varied from 1.75 to 3.5 mmol/L, glutamate oscillated between 0.2 and 0.5 mmol/L and glucose levels varied from 3 to 4 g/L. One result of such elevated substrate levels was the production of toxic by-products. The minimum lactate level in hESC CM was just under 0.3 g/L, while the maximum value peaked three-fold higher at 0.9 g/L. Similarly, the lowest level of ammonium recorded was just under 0.4 mmol/L, while the maximum level peaked at just under 0.7 mmol/L. Both sodium ion and potassium ion levels were elevated compared to KOSR, at around 140 mmol/L and 7.25 mmol/L respectively. The osmolality of the medium was also raised, averaging at 370 mOsm/kg.

4.4.1.2 Analysis of feeder conditioned medium

In a similar outcome to the BRL-conditioned hESC medium, there was significant variability in measured levels of substrates in the MEF and HFF conditioned medium. Approximately 2 mmol/L of glutamine was utilised by the metabolising cells, with a production of between 0.2-0.4 mmol/L glutamate, resulting in levels in the CM of between 0.9-1.2 mmol/L. Variable catabolism of glucose was evident, with levels between 2.5-4.0 g/L. The levels of lactate and ammonium were even higher in CM from the feeder cells, with lactate the range a four-fold difference from around 0.4-1.5 g/L in MEF CM and just under a two-fold difference of 1-1.8 g/L in HFF CM. Ammonium concentrations peaked at 2.5 mmol/L in MEF CM, and reached 2.0 mmol/L in HFF CM. Levels of sodium ions, potassium ions and the osmolality of the media were fairly consistent, with osmolality averaging at around 315 mOsm/kg

for both cell types, the slight elevation from the base medium is likely to be due to evaporation of medium over time, as the cultures were not under oil.

4.4.2 Effect of metabolite concentrations on cell cultures

Lactate excretion is due to incomplete oxidation of glucose by the glycolytic pathway. The end product of this pathway is pyruvate, which is transformed to lactate in order to maintain the oxidative status of the cell. Lactate can also be formed from sugars other than glucose, and from glutamine. The toxic action of lactate is probably due to the effect on pH and osmolarity of the culture medium, although only occurs at relatively high concentrations of greater than 1.8-2.7 g/L (Hassell *et al.*, 1991). The concentration of lactate in the feeder CM peaked at 1.8 g/L. If this CM is used to culture hESC in experiments, it is more than likely that lactate will exceed toxic concentrations.

Ammonia release by cells is due to amino acid metabolism, mainly that of glutamine. The L isomer of glutamine is routinely added to culture media to stimulate growth. Glutamine is chemically labile in cell culture media, especially at 37°C; consequently chemical decomposition of glutamine also contributes to the soluble ammonium levels. Accumulation of ammonium ions to concentrations of 2-3 mmol/L has been shown to significantly inhibit the growth of cells in culture (Butler & Spier, 1984). The concentration of ammonium in the feeder CM peaked at 2.5 mmol/L, therefore the levels of ammonium in some CM batches already exceeded toxic levels before being used further to culture hESC.

The variation in levels of metabolic by-products in batches of CM raises issues for interpreting experimental results. For example, were batches 5 and 15 of MEF CM used when comparing the effect of different variables on the growth of hESC, an inferior outcome may result from batch 15. This may not necessarily be due to the effect of the variable, but because the hESC were exposed to levels of ammonium in excess of those shown to be toxic in cell culture. Poorly defined culture medium has the potential to cause considerable experimental error and variations in culture artefacts over time. A key recommendation from the inaugural meeting of the International Stem Cell Initiative (ISCI; (Andrews *et al.*, 2005) was to develop a fully defined generic medium that could be used throughout the field and would provide a rational foundation for experimentation.

It is unrealistic to suggest that use of CM in these early stages of research and development should be avoided, as currently for many protocols there is no satisfactory alternative. However, measures can be taken to minimise the variation. Large pooled batches of CM could be collected so that the same batch is used for the span of the experiment. Although limiting the volumes obtainable, CM could be collected from inactivated, rather than proliferating feeder cells, when excretion of ammonium and lactate is reduced. Less convenient than purchasing commercially available formulations, but ultimately the most physiological approach, would be to develop modified medium with appropriate substrate concentrations for the cell type.

4.4.3 Effect of metabolite concentrations on embryos during derivation

Exposure of ruminant and rodent preimplantation embryos to ammonium results in reduced intracellular pH, altered amino acid metabolism (Orsi & Leese, 2004), depressed oxidative phosphorylation (Lane & Gardner, 2003), altered developmental kinetics, fetal retardation, exenchephaly (Lane & Gardner, 1994) and decreased blastocyst cell number (Gardner & Lane, 1993). A significant reduction in blastocyst cell number was observed at an ammonium concentration of 75 μmol/L. Altering intracellular pH disrupts development in preimplantation hamster embryos, in part due to disruption of mitochondrial organisation (Squirrell *et al.*, 2001). Data suggest that a 'quiet' metabolism during early development is consistent with successful embryo development (Leese *et al.*, 2007). Exposure to external stresses in culture may compromise cell viability. Energy will be expended in an attempt to accommodate repair processes and manifest in an active metabolism. Free plasma levels of glutamine and glutamate in human plasma measure at 0.57 mmol/L and 0.06 mmol/L respectively (Bergstrom *et al.*, 1974), far lower for example, than the 2.3 mmol/L and 0.1 mmol/L in KOSR. L-glutamine acts as an organic osmolyte and significantly protects the embryo from hypertonic conditions when added to the medium, and therefore this consideration should be balanced against ammonium production due to breakdown of this amino acid.

The history of the use of glucose in embryo culture medium is long and contradictory (Summers & Biggers, 2003) (and discussed further in Chapter 1). The observation that glucose and phosphate caused arrest of 2-cell hamster embryos

(Schini & Bavister, 1988b) had a major impact on the subsequent design of culture media. Evidence now exists to suggest that the stage of embryo cultured and the background composition of the medium used influences whether glucose inhibits development. For example it was determined using mouse embryos that pyruvate is the preferred source of energy in mature oocytes and zygotes, but that by the 8-cell stage glucose becomes the preferred source (Leese & Barton, 1984). Similarly, the uptake of glucose relative to pyruvate increases after the 8-cell stage in human development (Leese *et al.*, 1993) although pyruvate consumption remains high. However, whilst glucose is consumed by isolated mouse ICMs (Hewitson & Leese, 1993), high concentrations of glucose are known to inhibit ICM development in the rat (De Hertogh *et al.*, 1991) and hamster (Seshagiri & Bavister, 1991). Enhanced glycolysis inhibits respiratory activity. Increasing concentrations of glucose accelerates glycolysis which results in the production of appreciable amounts of ATP through substrate-level phosphorylation. This reduces the need for oxidative phosphorylation through the tricarboxylic acid cycle and the electron transport chain and therefore decreases oxygen consumption (the Crabtree effect). As oxidative phosphorylation provides the predominant source of ATP in the developing embryo this may be one reason for the damaging effects of high glucose.

In vivo most mammalian cells are bathed in extracellular fluid of almost constant osmolarity. In the artificial environment of *in vitro* culture, embryonic cells have to avoid excessive alterations of cell volume that jeopardize structural integrity and constancy of intracellular milieu. Alterations of cell volume and volume regulatory mechanisms participate in a wide variety of cellular functions including epithelial transport, metabolism, excitation, hormone release, migration, cell proliferation, and cell death (Summers & Biggers, 2003). When the osmolality exceeds 290 mOsm/kg the development of mouse embryos is severely impaired, at osmolality below 230 mOsm/kg development is not affected. However, hypoosmotic conditions cause spermatozoa to swell which can lead to plasma membrane rupture (Jeyendran *et al.*, 1992). HESC have been shown to proliferate optimally at 350 mOsm/kg (Ludwig *et al.*, 2006). In the process of hESC derivation, there seem to be two distinct osmotic environments needed for embryo and stem cell growth. Embryonic development is optimum at 284±2 mOsm/kg while stem cell culture is optimum at 350 mOsm/kg

- which impairs embryo development. How continuity is achieved between these requirements needs to be considered. The osmotic shock induced to the embryo or ICM when placed directly into KOSR or CM for derivation may contribute to the current low derivation efficiency. The osmolality was around 315 mOsm/kg at the lowest level in all media tested.

The analysis of concentrations of components in hESC CM confirmed that the use of BRL CM in derivation attempts was unacceptable when the aim was to optimise the use of every embryo entering the derivation programme. The variability and elevated levels of metabolites and catabolites within the media can only be deleterious to the fragile cluster of ICM cells trying to proliferate in an already suboptimal environment. In addition, the use of an animal cell line for the production of CM raises similar issues as the use of animal feeder layers in culture, namely the transmission of xeno-pathogens to the human cells and the risk of immunological rejection. The design of a medium that minimises the stress that is inevitably imposed on blastocysts/isolated ICMs during derivation must be an aim for the improvement of hESC derivation efficiences.

4.4.4 Design of derivation medium

Reports emerging at the initiation of this work cited the successful use of the commercially available KOSR in the culture of hESC lines (Cowan *et al.*, 2004; Inzunza *et al.*, 2005; Koivisto *et al.*, 2004; Skottman *et al.*, 2006a) and derivation of new lines in this medium (Genbacev *et al.*, 2005; Inzunza *et al.*, 2005). Whilst still containing a fraction of bovine serum, serum replacement is far more defined than using batches of FCS. KOSR proved to be superior to hESC CM in terms of batch stability and concentration of catabolites. It was also successfully used for the culture of existing hESC lines, and proved superior to hESC CM in thawing early passage cells. However it is not necessarily optimum or appropriate for early blastocyst growth. Considering the composition of KOSR it is evident that scant attention has been paid to the requirements of the blastocyst/ICM in developing commercial culture media.

As hESC are derived from the ICM of preimplantation blastocysts, it would seem prudent when trying to design derivation medium to consider the *in vivo* niche within which the ICM develops. The blastocoel fluid forms the microenvironment of the

ICM and its composition is controlled by the TE cells. The Na^+ and K^+ concentrations in blastocoel fluid of *in vivo* produced mouse blastocysts has been measured at 167 mmol/L and 32.6 mmol/L respectively (Borland *et al.*, 1977). Lactate concentration in blastocoel fluid was measured as 2.22 mmol/L and glucose concentration was found to be 0.59 mmol/L when *in vitro* matured murine blastocysts were incubated in medium with levels of metabolic substrates close to those found in oviduct fluid (Brison *et al.*, 1993). In excess external lactate and glucose however, the concentrations in the blastocoel reached 14.6 mmol/L lactate and 2.30 mmol/L glucose. Lactate is accumulated in the blastocoel cavity to high concentrations, probably as a result of its excretion by the cells of the TE and the ICM during glycolysis. The media available commercially for the growth of stem cells provide glucose and glutamine far in excess of physiological concentrations, such that the inevitable outcome is accumulation of ammonium (from glutamine degradation and cell metabolism) and lactate (from incomplete oxidation of glucose and cell metabolism).

To minimise the build-up of ammonium and lactate in culture, medium should be exchanged regularly. This may be detrimental in early derivation stages when conditioning of the medium is likely to be important, and therefore other approaches should be considered. Most of the ammonium accumulating in mammalian cell culture is derived from deamination of glutamine to glutamate catalysed by glutaminase. Substitution of glutamate for glutamine, or other amino acids, would ameliorate this problem. The turnover of only three amino acids (asparagine, glycine and leucine) in human embryos has been significantly correlated with clinical pregnancy and live birth (Brison *et al.*, 2004). Therefore supplementation of the entire spectrum of non-essential amino acids in culture medium may not be necessary for derivation. Alternatively, the excess formation of ammonium due to glutamine catabolism could be reduced by limiting glutamine and potentially glucose provision to just that actually required by the feeders and hESC. A system for removal of ammonium from culture media by *in situ* enzymatic conversion to glutamate has been suggested as another means of reducing ammonium toxicity (Lane & Gardner, 1995). However this method is only effective to the point of equilibrium between glutamate and ammonium.

Defining the microenvironment to which the cells of the ICM are exposed could indicate ideal culture components for use in the very early days of derivation, al-

though it is acknowledged that this is complicated by the requirements of the feeder cells used for hESC derivation. Indeed neglect of the specific requirements of somatic cells in co-culture can result in the loss of their *in vivo* morphological and functional properties, such as absorption, transcytosis and secretion. This may impact on their embryotrophic properties (Orsi & Reischl, 2007). Therefore in a co-culture system both cell types must be considered, although focus on the embryo in the early stages may be beneficial to derivation efficiency.

The composition of KODMEM and KOSR is proprietary, and the only information available in the public domain is that neither contain L-glutamine, the glucose concentration in KODMEM is 4 g/L and that KOSR is a defined, serum-free formulation. Future work will aim to develop an alternative medium for derivation of hESC lines based on physiological principles and the minimum need of substrates for both the embryo and the feeder system, optimising the conditions for the early days of hESC derivation and thus increasing the chances of obtaining a line from each embryo used. This work is already underway for the culture of existing lines in the International Stem Cell Initiative (ISCI) phase two study. Four research laboratories are comparing 10 defined media in order to select three for testing by the whole consortium. Continuing development of novel media, supplements and substrates is also ongoing in many laboratories, such as those involved in ESTOOLS - the largest grouping of hESC researchers in Europe. The collaboration involves 21 academic and commercial research teams spanning 10 countries, with a focus to develop the tools, techniques and expertise necessary for eventual medical, pharmaceutical and bioindustrial applications of hESC research. Focussing on the development of medium specifically for derivation would complement such existing studies.

4.4.5 Alternative feeder systems

Three cultures of AECs were established and characterised including; multiple freeze-thaw cycles, appropriate marker expression and successful use as a feeder layer to support the undifferentiated growth of hESC. The surface area of the 0803 amnion membrane measured 267 cm^2 ($4.9x10^4$ cells/cm^2) and 0805 measured 408 cm^2 ($6.4x10^3$ cells/cm^2). Whilst no conclusions can be drawn from only two cell counts, an association between small placentas and increased efficiency of placental nutrient

transport has been suggested (Sibley *et al.*, 1997) which may account for the higher cell yield from the smaller membrane.

The culture of HFFs was straightforward with the use of the same protocols as for MEFs.

4.4.6 Validation of culture conditions

Initial attachment of the AECs seemed to take up to 48 hours, beyond which no further attachment was evident and subsequent media exchange removed any non-viable cells from suspension. Confluent cultures were obtained 6-8 days after plating. Whilst consistent with published results (Miyamoto *et al.*, 2004), this was significantly longer than for MEFs which were confluent in 2 days. The growth of AECs was heavily density dependent, with little, if any, proliferation at low densities. This has been noted by other researchers (Parolini *et al.*, 2008). Therefore consideration regarding passaging regimes and split ratios was important. HFFs proliferated very rapidly and became confluent overnight.

Significantly greater growth rates were observed for AECs in enriched medium versus simple, and also with the addition of EGF. Higher attachment rates were also observed in enriched and supplemented media. Enriched plus EGF was therefore the most favorable condition and used for all subsequent culture. No significant depletion of metabolites from the medium were observed, therefore substrates were not rate limiting. EGF may function as a regulatory factor in the migration of epithelial cells and in the mobility of their cell membranes (Keski-Oja *et al.*, 1981). This may explain the superior attachment in supplemented conditions, and therefore more rapid expansion of cells. Further optimisation would be necessary to determine the most suitable concentration of the growth factor.

4.4.7 Removal of animal components from the culture system

Once a successful culture system was established for AECs, SPSS was substituted for FCS. SPSS is used in human embryo culture during clinical IVF and therefore introduces nothing new to the culture of hESC. However the attachment and growth of the cells in SPSS was negligible. As the growth of AECs was dependent on density, poor attachment could have prevented further growth in this condition. Therefore,

an AEC sample was plated in FCS, but at the first feed SPSS was exchanged for FCS. As in the first attempt, no significant further growth was observed during 16 days of culture. The AECs are likely to require a cocktail of growth factors for proliferation as do differentiated adult cells. These are not provided in SPSS which is optimised for embryo growth that requires little, if any, growth factor supplementation. Determining the exact growth factor combination required by the AECs may still enable a synthetic serum substitute to be used.

The derivation of clinical grade lines has been reported (Crook *et al.*, 2007), but KOSR and FCS were used in various stages of culture. Although these components were qualified to GMP standards it remains to be seen if culture can be achieved without any trace of xeno material. In the light of the data available showing incorporation of non-human sialic acid by hESC cultured with animal products (Martin *et al.*, 2005), these clinical grade cells could be rejected if transplanted, therefore a complete xeno-free system is required.

4.4.8 Pathogen testing

All placentas placed into long term culture were negative for microbacteria and mycoplasma. It has been suggested that collection of placentas from caesarean sections may be preferable to placentas following vaginal delivery as the latter have a higher occurrence of bacterial infection (Parolini *et al.*, 2008). The HFF also screened negative for microbacterial and mycoplasma contamination.

4.4.9 Characterisation of feeders

The immunocytochemical profile of the AECs was consistent with published characterisation of this cell type (Parolini *et al.*, 2008). The negative result for CD45 ruled out blood contamination while positive expression of KRT5,14 corroborated the origin of the cells as epithelial. A stem cell population has been reported within the amnion and amniotic fluid (De Coppi *et al.*, 2007; Miki *et al.*, 2005). The expression of POU5F1 and NANOG was enriched in cells maintained over the basal layer of more differentiated cells (Miki *et al.*, 2005). That style of culture system was not employed in this instance and the AECs were consistently negative for POU5F1.

The expression of other pluripotent markers on the AECs is in accordance with published reports (Miki *et al.*, 2007; Parolini *et al.*, 2008). While some placenta

tissues are derived from trophectoderm, amniotic epithelia are derived from the pluripotent epiblast. It is reasonable to speculate as AECs retain pluripotent stem cell characteristics when cultured in a particular three-layer system (Miki *et al.*, 2005), that when cultured as feeders, they may also express some pluripotent markers. The seemingly random pattern of TRA1-61 and TRA1-80 positive cells suggested that they did not reside in specific stem cell niches (as clusters of positive cells would suggest). Rather AECs seemed to express a residual epiblast phenotype. The SSEA4 antibody may react to a wide-range of epiblast-derived stem cells. The absence of POU5F1 eliminates confusion between the AECs and the hESC colonies in co-culture.

The GFP status of the HFF cells was beneficial for FACS analysis, as the feeders could be completely excluded when hESC were stained with a TRITC or PE fluorophore.

4.4.10 Evaluation of amniotic epithelial cells and foreskin fibroblasts as suitable feeder layers

Overgrowth of feeders due to inadequate inactivation is unfavorable for hESC cultures, and would be particularly detrimental in the early stages of derivation. Therefore the time required for complete inactivation of the two feeder types was determined; 2 hours for AEC and 3 hours for HFF.

AECs appeared to reach senescence in culture at P5. Beyond this no significant growth was observed even though the cells were kept in culture for four weeks. Reports of senescence range from 2-6 passages (Parolini *et al.*, 2008). MEFs also senesce by P5 and this limits the size of bank of these cell types. In contrast, HFF were used at between passage 15-17 and showed no signs of senescence. The advantage to this behaviour is the ability to create a very large cell bank from one batch of starting material, which can then be used for long-term culture. However, the suitability of genetically modified cells as feeders for the culture of hESC for use in clinical therapy is questionable.

AECs and HFFs were used successfully to culture existing hESCs in a pluripotent state for at least 3 months, or approximately 10-15 passages. The hESC expressed appropriate pluripotent markers after this time. Not all human cell types share

this property (Genbacev *et al.*, 2005; Richards *et al.*, 2003). However, successful derivation of new hESC lines is the definitive test for a novel feeder system.

4.4.11 Derivation of new lines

All 10 blastocysts used for derivation attached to the AEC feeder layer. Seven formed outgrowths containing ICM/stem-like cells. Two could be passaged, and one formed a putative hESC culture although it arrested at passage 3. Derivation attempts will continue on AECs due to the early success with this cell type, and the advantages these cells could offer over MEFs and HFF feeders.

As the embryo develops in close contact with extraembyonic membranes *in vivo*, it was thought that placental amnion might replicate the stem cell niche *in vitro*. The decision to proliferate and self-renew or differentiate is governed to a great extent *in vivo* by the microenvironment in which stem cells reside. The concept of a stem cell niche originated in the haematopoiesis field (Adams, 2008). Compared with somatic cells, little is known currently about the specialised microenvironment that gives rise to the transient stem cell population of the early stage human embryo. Contact with the extracellular matrix and with other cells is a mechanism for sensing the microenvironment and making decisions that govern cell fate. The ability of AEC to support the growth of hESC in an undifferentiated state for at least 10 passages in serum replacement, rather than serum, suggests that the cells secrete supportive proteins into the culture milieu. Preserved amniotic membrane has been shown to express mRNA for a number of growth factors and growth factor receptors including EGF, bFGF, transforming growth factor alpha (TGF-α), TGF-β, TGF-β2 and TGF-β3 (Koizumi *et al.*, 2000). Of these, bFGF and TGF-β have been implicated in the maintenance of the pluripotent stem cell state (Greber *et al.*, 2007). In addition, AEC express no major histocompatibility complex (MHC) class II and fewer MHC class I molecules, and acute immune rejection does not occur after the transplantation of human amniotic epithelial cells (Akle *et al.*, 1981). This may prove a great advantage when considering strategies to produce hESC for clinical use.

HFF were comparable to MEFs as feeders for existing hESC. As a culture system they are superior given their robust proliferation and late senescence. However, it was not possible in this instance to derive novel lines in this system, on these particular

cells. The reason for this is not known for certain, as other foreskin fibroblast lines have been used successfully to derive more than 30 lines (Hovatta *et al.*, 2003). It is possible that the passage number used is critical to success. A similar observation has been made with MEFs. The expression profile of secreted factors in CM from a supportive and non-supportive MEF line has been assessed (Chin *et al.*, 2007). Thirteen proteins were found to be downregulated in the non-supportive MEFs, of which 4 were soluble factors related to growth stimulation and/or differentiation and 3 were membrane-associated or related to the extracellular matrix. Therefore differences in conditioning by human feeders of the same cell type but different donors may be responsible for the variation in support to derivation and culture of hESC. One further possibility with the HFF analysed here is the high level of bFGF secretion by these cells. At the cell density used for culture bFGF secretion was approximately 300 ng/mL. Whilst addition of bFGF is beneficial in maintaining undifferentiated growth, generally 4-16 ng/mL is used. bFGF is involved in multiple signalling pathways, for example, concentrations equal to or above 20 ng/mL are used in neural differentiation protocols (Hong *et al.*, 2008; Ying & Smith, 2003). During the early days of derivation it is possible that signals from the HFF may have caused the ICM cells to differentiate and therefore lose their pluripotent and self-renewing phenotype. However, it seems that the microenvironment created is conducive to self-renewal and robust proliferation of established hESC lines. Whilst the HFF provided an excellent culture system for expansion of hESC for experimentation, and as a research tool they have many potential applications, they failed to support derivation. This, combined with the genetic modification of these cells, is likely to render them unsuitable for future clinical application.

The important but often overlooked point highlighted by these results is that it is not sufficient to validate a culture system solely by growth of existing hESC. These cells seem rather indifferent and sufficiently robust to grow on a variety of feeders. Validation of a new system requires derivation of a new line, maintenance for at least 10 passages, and fully characterisation. As demonstrated, both AECs and HFFs supported the undifferentiated and pluripotent growth of existing hESC lines, but only AECs were able to sustain growth of the embryo and early stem-like cells. When selecting a feeder system, not only must suitability for derivation be proven but other considerations should include the ability to document full provenance of

the cell type and the capacity of the cells to grow without serum. As a summary, Table 4.4 compares the main features of the three feeder systems investigated and their suitability for use as clinical grade feeders.

Table 4.4: Main features of MEF, AEC and HFF culture systems. Isolation; ease of obtaining primary tissue, Validation; likelihood of validation for clinical use, Cell density; density required for culture of hESC, in cells/cm^2, Derivation; derivation of new hESC lines, blast; blastocysts, GM; genetically modified (immortalised).

Consideration	**MEF**	**AEC**	**bFGF-HFF**
Isolation	Moderate	Simple (discarded tissue)	Difficult
Validation	Unlikely	Probable (donor screening)	Unlikely
Senescence passage	P5	P5	>P17
Supplementation	None	EGF	None
Time to confluence	2d	6-8d	1d
Cell density	2.6x10^4	3.9x10^4	2.1x10^4
Supportive to hESCs	Yes	Yes	Yes
Derivation	Yes	Most likely	No
Efficiency	7 lines, 39 blast	1 P3 culture, 10 blast	0 lines, 10 blast
Other	Xeno-product	Immunoprivileged	GM

Chapter 5

Assessment of pluripotency and patterning in single human blastomeres

Current research focuses on the potential uses of stem cells in medicine and how they can provide effective treatment for a range of diseases. This approach has resulted in the field of medical practice called regenerative medicine. To attain the promises of regenerative medicine, it is necessary to fully understand the biology and properties of stem cells, achieve their successful differentiation into functional tissues, overcome the barriers related to immune responses after administration, and assess any oncogenic properties that limit their use. The availability of human stem cells not only raises hope for cell replacement therapies, but also provides a system for understanding the mechanisms of embryonic development and disease progression.

5.1 Introduction

The mechanisms that establish patterning and lineage decisions in the mammalian embryo are a subject of fierce debate. Whether there are axes present in the oocyte that influence future polarity, or whether the blastomeres of early embryos are naive, has been studied in a great many elegant and often tenacious experiments with mouse embryos (Chapter 1). Whilst molecular studies have been attempted with single blastomeres, as yet there has been no report of a molecular bias with respect to multiple lineage markers in individual cells of the same embryo. The pluripotent capacity of single non-human mammalian blastomeres has been investigated by the production of live offspring as discussed in section 1.10.0.1. Considering that this

approach cannot be taken with human material, currently the most robust assessment of pluripotency in human blastomeres is to ascertain the potential of these cells to generate hESC.

5.1.1 Molecular studies

One theoretical interpretation of the cleavage hypothesis is that the two blastomeres inheriting the full animal-vegetal (A-V) axis at the second cleavage are precursors of the ICM, the blastomere inheriting mostly animal cytoplasm gives rise to the TE and the blastomere inheriting mostly vegetal cytoplasm is the precursor to the germline (Edwards & Beard, 1997). Whilst not so prescriptive, experimental work has shown that differential inheritance of cytoplasm from the A-V axis occurs due to meridional or equatorial divisions of the 2-cell embryo (Gardner, 2002), and the progeny of one two-cell blastomere contributes to the ICM and polar TE and the other to the mural TE (Piotrowska & Zernicka-Goetz, 2001). There are several studies addressing the molecular basis of this differentiation.

The existence of a single TE precursor cell at the human 4-cell stage has been reported following the identification of *βhCG* mRNA in only one of the four blastomeres (Hansis *et al.*, 2002). Negative correlation between *βhCG* and *POU5F1* was then demonstrated (Hansis *et al.*, 2004), suggesting a role for *βhCG* in early cell allocation. It must be noted however that only abnormally developing human embryos were investigated. The measurement of *POU5F1* expression in individual blastomeres showed that at the 4-5 cell stage the majority, but not all, of the blastomeres were positive for this pluripotency marker. Expression fell to about one third of cells at the 7-10 cell stage (Hansis *et al.*, 2001). In a subsequent study using morphologically normal diploid embryos, variability of protein expression within embryos and between embryos of the same stage was observed, but all four cells were positive for POU5F1 in some 4-cell embryos (Cauffman *et al.*, 2005b). The analysis of POU5F1 expression is complicated by the presence of two isoforms, only one of which identifies, but not exclusively, pluripotent cells (Cauffman *et al.*, 2006). Caudal type homeobox 2 (Cdx2) has been proposed as a TE marker in murine development. Studies have proposed that *Cdx2* mRNA is localised in the oocyte and becomes exclusively segregated into one of the two cell blastomeres at division (Deb *et al.*, 2006). One 2-cell contributed solely to the ICM and the other solely to the

TE. This contradicts observations from both the regulative and prepatterning groups and therefore warrants further attention.

In normal development each blastomere of the 8-cell embryo acquires clear apical and basolateral domains - the initiation of cellular polarity. Polarity is retained during division to 16 cells so that depending on the orientation of division with respect to the polar axis, either two polar cells (conservative division) or one polar and one apolar cell (differentiative division) result. Whether a blastomere undergoes one or the other forms of division seems to be influenced by the partitioning defective (Par) proteins in murine development. These proteins were originally identified in model organisms as regulators of polarity. Both Par3 and its complex with atypical protein kinase C adopt a polarised localisation from the 8-cell stage onwards; manipulating these proteins re-directs cell positioning and consequently influences cell fate (Plusa *et al.*, 2005).

Epigenetic factors also seem to play a role in early lineage segregation. H3 methylation is maximal in the blastomeres at the 4-cell stage that contribute progeny to the ICM and polar TE in the mouse (Torres-Padilla *et al.*, 2007), suggesting some level of epigenetic control of lineage determination. Overexpression of H3 methyltransferase in individual blastomeres can cause an upregulation of *Nanog* and *Sox2* and direct the fate of the cells to ICM.

Whilst the timing and expression of lineage markers has been investigated in whole human embryos (Kimber *et al.*, 2008), there has as yet been no systematic analysis of normal, progressive single human blastomeres. The definitive evidence of patterning would be to identify a single gene or protein that clearly marks the fate of different early embryonic cells, like those already identified in the frog or fly embryos. Analysing multiple markers of ICM, TE and germ line might be one means to assess whether there appears a bias within a cell to a particular lineage.

5.1.2 Derivation of stem cells from single blastomeres

The derivation of hESC from single human blastomeres is the most robust method currently available to assess pluripotent status. Derivation from all the individual cells of the 2-, 4- and 8-cell embryo would need to be attempted in order to address cell fate questions. Derivation of mESC from single biopsied 8-cell blastomeres has been reported (Chung *et al.*, 2006). Using a co-culture method with established

mESC lines, 5 lines were generated from 125 blastomeres (4% derivation efficiency). Subsequently a more efficient method was described, generating lines from 2-, 4- and 8-cell blastomeres with an average efficiency of 60%, 30% and 15% respectively (Wakayama *et al.*, 2007). The reduction in efficiency reflected loss of pluripotency with cell age. In a smaller subset of experiments this group considered the ability of each cell within an embryo to give rise to a mESC line. Successful derivation from both 2-cell blastomeres was demonstrated, but not from all four or all eight. However, the number of embryos was small and the overall derivation rate far lower than that described for biopsied cells, perhaps indicating technical problems with isolating all the blastomeres.

Derivation attempts specifically from all sister blastomeres of mouse embryos has been reported. From 2-cell blastomeres both cells outgrew in 60% of cultures, and only one cell outgrew in 25%. From 4-cell blastomeres all four cells outgrew in 6%, three cells in 6%, two cells in 22% and one cell in 44% of attempts. mESC lines were only established from individual 2-cell blastomeres (Lorthongpanich *et al.*, 2008), with 4 lines from 72 blastomeres. However, a strain of mouse known to be particularly difficult to derive from was used. This complicates the interpretation of the study with respect to pluripotency of individual blastomeres, while highlighting the difficulty of comparing results from different mouse strains and extrapolating mouse results to the human.

Unsuccessful derivation of hESC from conjoined pairs of sister 8-cell blastomeres was first reported (Fong *et al.*, 2006). Blastomere-derived cell aggregates were grown, however after these structures were placed on MEFs, they failed to develop past the initial formation of a small colony of hES-like cells. The hESC medium used by this group contained fetal bovine serum but no basic fibroblast growth factor (bFGF). Undefined components of serum can promote differentiation, and bFGF supports the undifferentiated growth of hESC. The culture medium used in these experiments may therefore explain why the hESC did not proliferate past initial outgrowths.

This was followed by a report of the derivation of two lines from 91 single 8-cell blastomeres (2% efficiency) (Klimanskaya *et al.*, 2006). A green fluorescent protein (GFP)-expressing hESC line was used for co-culture with the blastomeres. Given the failure to produce viable offspring or derive mESC from four-cell mouse blastomeres, it is somewhat surprising that successful derivation from a human 8-cell

blastomere has been achieved. It suggests that the effect of co-culture with an existing hESC line may have proffered an advantage to the cell over and above its intrinsic potential. Given the premise for the experiment was political not scientific, these research avenues were overlooked. However, further work from the group reported the generation of hESC with a higher efficiency using co-culture, and also one hESC from a single 8-cell blastomere without co-culture (Chung *et al.*, 2008). The addition of laminin to the culture medium was identified as the basis for the enhanced efficiency and the success without co-culture. This supplement appeared to depolarise existing hESC inducing them to form a more ICM-like phenotype. It also induced the formation of ICM-like rather than trophoblastic outgrowths from single blastomeres. Interestingly, laminin is known to influence the distribution of cadherins, and E-cadherin redistribution to the inner surface of blastomeres is a key event in early polarisation (Johnson *et al.*, 1986). To maximise the potential of an eight-cell blastomere to generate a hESC line, polarisation must be suppressed or reversed. Should polarisation proceed, subsequent divisions must be differentiative to generate the maximum number of apolar inner cells (Johnson, 2008). The increased efficiency with the addition of laminin suggests that polarisation was altered in these cultures by this supplementation.

5.1.3 Aims

The demonstration that individual blastomeres can generate pluripotent hESC would provide a robust assessment of the potential of these cells. According to the cleavage-driven hypothesis, the potential of individual cells may differ from the 4-cell stage onwards due to asymmetric inheritance of cytoplasm from along the A-V axis. Therefore the aim of these experiments was to attempt derivation of hESC from all blastomeres of the 4-cell embryo. Given the paucity of molecular studies to investigate lineage marker expression in single human blastomeres, the aim was also to validate a single cell PCR approach and use it to assess a panel of markers for ICM, TE and germline.

5.2 Method Development

The study of isolated blastomeres requires robust manipulation techniques such that the cells retain viability and the ability to continue development. Inevitably the loss of the protective features of the zona pellucida and absence of cell-cell communication could have had a detrimental effect on the cells. Thus, the objective was to select an appropriate method for disaggregation, to optimise culture, and to investigate pluripotency, derivation potential and lineage-specific gene expression in single human blastomeres.

5.2.1 Embryo Manipulation

5.2.1.1 Day 3 embryos

All embryos cryopreserved on day 1, 2 or 3 were thawed exactly as in section 2.1.2.3. Disaggregation initially was attempted at the 8-cell stage of development. Following thawing, day 3 embryos were incubated for a minimum of 2 hours for complete equilibration and day 2 embryos were cultured overnight. For disaggregation, embryos were incubated in warmed calcium and magnesium-free HEPES for approximately 5 min or until any visible signs of compaction were reversed. The embryos were exposed to acidified Tyrode's (AT) solution at pH 3.0 until thinning of the zona was evident. The zona-free cells were washed through four drops of culture medium with gentle aspiration and expulsion to remove the remaining zona layer and disaggregate the individual blastomeres. Pulled and polished glass capillaries with decreasing diameters were used if normal handling pipettes were not successful. The separated blastomeres were cultured in individual 10 μl microdrops of blastocyst medium for the desired number of days before being fixed for immunocytochemistry (section 2.4.1) or plated for derivation attempts (section 5.2.3).

5.2.1.2 Day 2 embryos

Several alterations were made to the method following the first disaggregation attempts to try to improve the rate of survival and development of the cells. Previously embryos were first exposed to calcium and magnesium-free HEPES following the methods used for embryo biopsy. However, on several occasions after zona removal

the embryos had to be returned to this medium to enable disaggregation, prolonging the exposure of the embryos to sub-optimal conditions. The order of drops was therefore reversed so that embryos were first briefly exposed to AT. The pH of the AT used was changed from pH 3.0 to pH 2.5 which dissolved the zona more rapidly and reduced the time of exposure. A pipette primed with culture medium containing 10% SPSS was used to flood the AT drop as soon as the zona had dissolved, to inactivate the acid by buffering the solution. It was also useful to coat the inside of the pipette with protein-containing medium as the zona-free embryos tended to be sticky. Only then were the embryos incubated in calcium and magnesium-free HEPES supplemented with 10% SPSS for approximately 5 min before being disaggregated, and then washed and cultured exactly as before.

5.2.1.3 Day 1 embryos

The thaw of day 1 pronuclear embryos not only allowed a minimum of 12 h of culture before disaggregation, but also addressed the problem of embryos thawing with not all cells intact. Protease was used to remove the zona after its successful use during immunosurgery. Late day 1 or day 2 embryos were placed in 0.5% solution of protease in DMEM under constant observation until the zona was seen to thin and expand away from the blastomeres. The drop was then flooded with cleavage medium with 10% SPSS. Embryos were washed through 2 wells of this medium before being transferred to calcium magnesium free medium supplemented with 10% SPSS. Modified pipettes were made by pulling a glass capillary to a wider diameter and then polishing just the tip to be slightly wider than the diameter of the zona-free embryos. This way the only point the embryos were subject to slight pressure was on passage through the tip, once in the bore of the pipette the embryos were not mechanically stressed. The separated blastomeres were then washed through two drops of cleavage medium before being returned to the original culture drop. In each drop approximately 300 μm diameter indents in the base of the culture dish were made using a chimera tool (BLS; Biological Laboratory Equipment, Maintenance and Service Ltd., Budapest, Hungary). One indent was made for each blastomere of the same embryo, such that the blastomeres were cultured together but unable to come into physical contact.

5.2.2 Single cell immunocytochemistry

Immunocytochemistry was carried exactly as in section 2.4.1. Primary antibodies used were NANOG and POU5F1-iA as detailed in Table 2.2. The epitope of POU5F1-iA corresponds to amino acids 1-134 and therefore recognised POU5F1-iA only, not the POU5F1-iB isotope. POU5F1-iA is the only isotope shown to be associated with pluripotency (Cauffman *et al.*, 2006). Positive and negative controls were included in each experiment. In positive controls, regular IVF embryos were stained. In negative controls, the primary antibodies were replaced with isotype controls (Sigma Aldrich) at the same concentration. Reactions were also performed omitting the primary antibodies. Cell numbers were recorded by counting total DAPI-stained nuclei, and the proportion of NANOG or POU5F1 positive cells calculated.

5.2.3 Derivation from single blastomeres

5.2.3.1 Medium selection and exchange

To determine the most suitable period for media conditioning, KOSR was incubated for 24 h and 48 h on inactivated MEF and HFF, and then assessed with the NOVA BioProfiler (section 2.6). Ten hESC colony pieces were then added to each well and the incubation repeated. Samples were centrifuged to remove cell debris and then stored at -20°C until analysis. For the control samples, aliquots of KOSR were stored without incubation, and KOSR alone and under oil was incubated for 24 h and 48 h before collection and storage.

5.2.3.2 Preparation of microdrop feeder layers

On the day of embryo disaggregation, 20 μL drops of gelatin were placed in a culture dish for a minimum of 5 min. These were then aspirated and 2.6x10^4 cells/cm^2 inactivated MEF feeders plated on each gelatin base. The cell drops were submerged in mineral oil and incubated overnight. The following day the MEF medium was exchanged for 20 μL KOSR and again incubated overnight. Just prior to plating the blastomeres, the medium was replaced with conditioned KOSR supplemented with 8 ng/mL bFGF and 2.5 μg/mL laminin. 10 μL of medium was exchanged for conditioned KOSR every day. Daily photographic records were maintained.

5.2.3.3 Embryo manipulation

Pronuclear stage embryos were thawed and cultured overnight. Those that had reached the four-cell stage within an appropriate timeframe were selected for derivation attempts. These were disaggregated as described above. The individual blastomeres were placed in microwells in microdrops of cleavage medium for a further 24 h. The following day (D2+1) the blastomeres were examined and scored for morphology. The blastomere cultures were transferred to microwells in microdrops of blastocyst medium for a further 24 h culture. On D2+2 the blastomeres were again examined and scored. The inferred sequence of division was assessed, with division defined as broadly orthogonal or broadly parallel to the plane of polarity, as shown in detail in Figure 5.3. A second embryologist also scored the clusters, but from photographic images. Clinical constraints prevented concurrent observation, and the intention for minimum culture disruption precluded the removal of the cultures from incubation more than once per day. When identical scores were given and the divisions fell unambiguously into one of the categories the cells were included in the analysis. The cell cultures were plated individually into the MEF feeder microdrops. The cultures were left undisturbed for 48 h, after which they were photographed at 24 h intervals, and 10 μL of spent medium replaced daily. After 7 days of culture, the feeding schedule was determined by culture morphology and growth, with the concentration of growth factors and serum altered as deemed appropriate.

5.2.4 Gene expression analysis by single cell PCR

5.2.4.1 Embryo selection

Pronuclear or day 2 embryos were thawed and cultured for 12 h, 24 h or 48 h to obtain viable and progressive 2-, 4- or 8- cell embryos. Those that had developed appropriately within these timeframes and were grade 4 or 3 (Bolton *et al.*, 1989) were disaggregated as in section 5.2.1.3. The single blastomeres were placed in lysis buffer at room temperature (section 2.4.2.1) and stop solution added after between 5 and 20 min. Lysates were stored immediately at -80°C until processing. Some embryos that divided following thaw but had not developed normally were used for reverse transcription negative (RTN) controls and collected in the same way. Whole

day 6 blastocysts were also collected as positive controls for the gene assays. Multiple donors were used for each embryo stage to control against any patient-specific effects.

5.2.4.2 Gene target selection

Gene targets identified as known early markers of lineage were selected. Markers were chosen for the ICM/stem cell lineage, TE, germ line, early transcriptional pathways, as well as the six genes originally used to generate iPS cells and five housekeeping genes. In total, 24 gene targets were selected, the details of which are shown in Table 5.1. Example references discussing the expression and function of the genes are included.

The Biomark™ Fluidigm® dynamic chip PCR platform was used for analysis, with preamplification of target cDNA using the ABI Taqman® Preamplification Cells-to-cT kit (section 2.4.2.2).

5.2.4.3 Detection threshold

As the Fluidigm platform was being used for the first time for single cell experiments, preliminary detection tests were performed on both the 'gold-standard' ABI 7900 HT and the Fluidigm. The detection threshold dynamic range of both platforms is 15-30 cycles, below which insufficient target is generated for detection, and above which the reagents begin to become limiting. Before using human embryonic material, the validity of the preamplification kit for single cell detection was tested with a fibroblast dilution. A confluent T175 flask of fibroblasts was trypinised, the cell number counted, the cells centrifuged, and the pellet resuspended in lysis buffer. The volume of buffer was calculated to give a suspension of 10,000 cells per microlitre. This suspension was serially diluted 1 in 10 to give the equivalent of 1,000, 100, 10 and 1 cell per microlitre. cDNA was generated from these samples and target cDNA for *ACTB*, *B2M* and *GAPDH* preamplified before qPCR was performed on the ABI 7900 HT. Per sample the reaction mixture consisted of 25 μL Taqman 2x gene expression buffer, 2.5 μL Taqman 20x target primers and probe (section 2.4.2.2) and 10 μL nuclease free water. 37.5 μL aliquots of reaction mix were placed in a 96 well plate and 12.5 μL of preamplified cDNA added. Cycling conditions were a 95°C incubation for 10 min, 40 cycles of 95°C for 15 s and 60°C for 60 s, before cooling to 4°C indefinitely. Following this, non-preamplified and preamplified cDNA

Table 5.1: Gene targets for single blastomere PCR analysis. pluri; ICM/stem lineage, germ; germline, TE; trophectoderm lineage, hsk; housekeeping gene.

Symbol	**Name**	**Assay ID**	**Indication**	**Reference**
POU5F1	POU class 5 homeobox 1	Hs01895061-u1	pluri/iPS	Cauffman *et al.* (2005b)
NANOG	Nanog	NM-024865	pluri/iPS	Hyslop *et al.* (2005)
SOX2	SRY (sex determining region Y) box 2	Hs00415716-m1	pluri/germ/iPS	Rodda *et al.* (2005)
REX1	Zinc finger protein 42	Hs01036059-m1	pluri	Rogers *et al.* (1991)
KLF4	Kruppel like factor 4	Hs00358836-m1	pluri/iPS	Takahashi *et al.* (2007)
LIN28	Lin28	NM-024674	pluri/iPS	Yu *et al.* (2007)
FGF2	Fibroblast growth factor 2	Hs00266645-m1	pluri	Rifkin & Moscatelli (1989)
NOTCH1	Notch1	Hs01062014-m1	pluri	Chiba (2006)
GATA6	GATA binding protein 6	Hs00934682-m1	pluri	Koutsourakis *et al.* (1999)
C-MYC	Avian myelocytomatosis viral oncogene	Hs99999003-m1	iPS	Takahashi *et al.* (2007)
LEPTIN	Leptin	Hs00174877-m1	TE	Antczak et al. (1997)
hCGβ	Human chorionic gonadotropin β	NM-033043	TE	Ohlsson *et al.* (1989)
ERK1/MAPK	Mitogen activated protein kinase 3	Hs00946872-m1	TE	Wang *et al.* (2004)
ZO1/TJP1	Zonular occludens 1	Hs00543824-m1	TE	Sheth *et al.* (1997)
OCLN	Occludin	Hs00170162-m1	TE	Ghassemifar *et al.* (2003)
CLDN1	Claudin1	Hs00221623-m1	TE	Ghassemifar *et al.* (2003)
CDX2	Caudal type homeobox 2	Hs00230919-m1	TE	Ralston & Rossant (2005)
DAZL	Deleted in azoospermia like	Hs01058897-m1	germ	Cauffman *et al.* (2005b)
TBN/TAF8	Taube Nuss	Hs00373267-m1	ICM survival	Voss *et al.* (2000)
HPRT	Hypoxanthine phosphoriboseyl transferase 1	Hs01003267-m1	hsk	Mamo *et al.* (2007)
GAPDH	Glyceraldehyde-3-phosphate dehydrogenase	NM-002046.3	hsk	Jeong *et al.* (2005)
ACTB	βactin	NM-001101.2	hsk	Jeong *et al.* (2005)
B2M	β2 microglobulin	NM-004048.2	hsk	Mamo *et al.* (2007)
CHUK	Conserved helix-loop-helix ubiquitous kinase	Hs00989503-m1	hsk	Falco *et al.* (2006)

from single blastomeres was run on both machines to ensure the signal fell within the detection range.

5.3 Results

5.3.1 Embryo manipulation

5.3.1.1 Day 3 disaggregation

A total of 23 day 2 and day 3 embryos were thawed for preliminary disaggregation experiments on day 3. Of a possible 153 blastomeres from these embryos, 109 (71%) survived the thaw process. 85 (78%) isolated blastomeres were intact following disaggregation. Over a third of these blastomeres completed first cleavage by D3+1, with almost a fifth having initiated compaction. 40% had begun cavitation by D3+2. The summary of each stage of development is shown in Table 5.2.

Table 5.2: Summary of development of all embryos disaggregated on D3. Numbers in brackets indicate the outcome as a percentage of total blastomeres obtained.

Number embryos	23
Total blastomeres available	153
Total blastomeres survived thaw	109
Total blastomeres obtained	85
Number cleaved D3+1	31 (37)
Number compacted D3+1	15 (18)
Number cavitated D3+1	4 (5)
Number initial cleavage D3+2	29 (34)
Number further division D3+2	28 (33)
Number compacted D3+2	11 (13)
Number cavitated D3+2	35 (41)
Number fully expanded ('mini blastocyst')	9 (11)
Number clusters 10+ cells but no cavitation	2 (2)

Overall only 3 (13%) 8-cell embryos survived thaw or culture fully intact; in only two were all 8 blastomeres isolated. Of those, one embryo gave rise to 6 'mini blastocysts', one uncompacted 4 cell cluster and 1 arrested single blastomere. From the other embryo, two blastomeres arrested at 1 cell, 5 arrested after the first division to 2 cells and the remaining blastomere arrested at 3 cells.

5.3.1.2 Day 2 disaggregation

A total of 43 day 2 embryos were thawed for the preliminary disaggregation experiments from day 2 embryos. Of a possible 163 blastomeres from these embryos, 139 (85%) survived the thaw process. 81 (58%) isolated blastomeres were intact following disaggregation. Over half of these blastomeres completed first cleavage by D2+1, with around a quarter having initiated compaction by D2+2. One fifth had begun cavitation by D2+3. Of the 21 cell clusters kept in culture until D2+4, 12 had degenerated. The summary of each stage of development is shown in Table 5.3.

Table 5.3: Summary of development of all embryos disaggregated on D2. Numbers in brackets indicate the outcome as a percentage of total blastomeres obtained

Number embryos	43
Total blastomeres available	163
Total blastomeres survived thaw	139
Total blastomeres obtained	81
Number cleaved D2+1	44 (54)
Number initial cleavage D2+2	16 (20)
Number further division D2+2	38 (47)
Number compacted D2+2	22 (27)
Number cavitated D2+2	4 (5)
Number compacted D2+3	13 (16)
Number cavitated D2+3	17 (21)
Number fully expanded ('mini blastocyst')	19 (24)
Number clusters 10+ cells but no cavitation	4 (5)

For D2 disaggregations 30 (70%) 4 cell embryos were intact following thaw. All four blastomeres were isolated from only 4 (13%). Of those, 1 embryo gave rise to 3 'mini blastocysts' and one cluster with a minimum of 15 cells, which was compacted but had not cavitated. The second embryo again gave rise to 3 'mini blastocysts' but one blastomere arrested following an initial cell division. From the third embryo all four blastomeres arrested at the one-cell stage. From the final embryo, 2 cells arrested at the single cell stage, one blastomere divided to 5 cells and one to 4 cells, with the latter cluster beginning the compaction process.

5.3.1.3 Day 2 disaggregation from day 1 thaws

From 26 thawed pronuclear embryos, 101 from a possible 104 (97%) individual blastomeres were collected on day 2. 83 (81%) completed the first cellular division to at least 2 cells by D2+1. Of these blastomeres, 62 (61%) had divided further by D2+2, of which over half had compacted, just as expected for D4 whole embryos. In fact, 5 blastomeres (5%) showed signs of cavitation, with either small blastocoel spaces visible or the appearance of a cavitation plane within the compacted cell cluster. Of the 40 blastomeres destined for fixation on D2+3, 31 cleaved further from D2+2 to D2+3. 16 of these were compacted, and 18 had cavitated, either with blastocoel spaces, or having formed 'mini blastocysts'. This disaggregation method resulted in significantly improved survival and development rates and was used for all subsequent experiments. Table 5.4 summarises the development of the blastomeres to either D2+2 or D2+3.

Table 5.4: Summary of development of all embryos disaggregated on D2 following thaw on D1. Numbers in brackets indicate the outcome as a percentage of total blastomeres obtained for D2+2, or as a percentage of those kept in culture for D2+3.

Number PN embryos	26
Total blastomeres on D2	104
Total blastomeres obtained	101
Number cleaved D2+1	83 (82)
Number initial cleavage D2+2	14 (14)
Number further division D2+2	62 (61)
Number compacted D2+2	35 (35)
Number cavitated D2+2	5 (5)
Number cultured to D2+3	40
Number further division D2+3	31 (78)
Number compacted D2+3	16 (40)
Number cavitated D2+3	18 (45)

From the 26 embryos used, 19 reached the endpoint of either plating or fixation with all 4 blastomeres intact and having completed at least one cleavage division. The behaviour of the blastomeres from the same embryo was variable and no definite pattern could be seen. However, all four blastomeres did not cavitate from any of the embryos. It was not possible to determine the reason from this experiment.

Failed cavitation may have resulted from inadequacy of developmental *competence* as a result of manipulation, or lack of developmental *potential* if blastomere fate was predetermined. Analysis of the expression of epithelial intercellular junction genes such as zonula occluden protein 1 (ZO-1) may distinguish between these reasons. Figures 5.1 and 5.2 show two examples of isolated sister blastomere development.

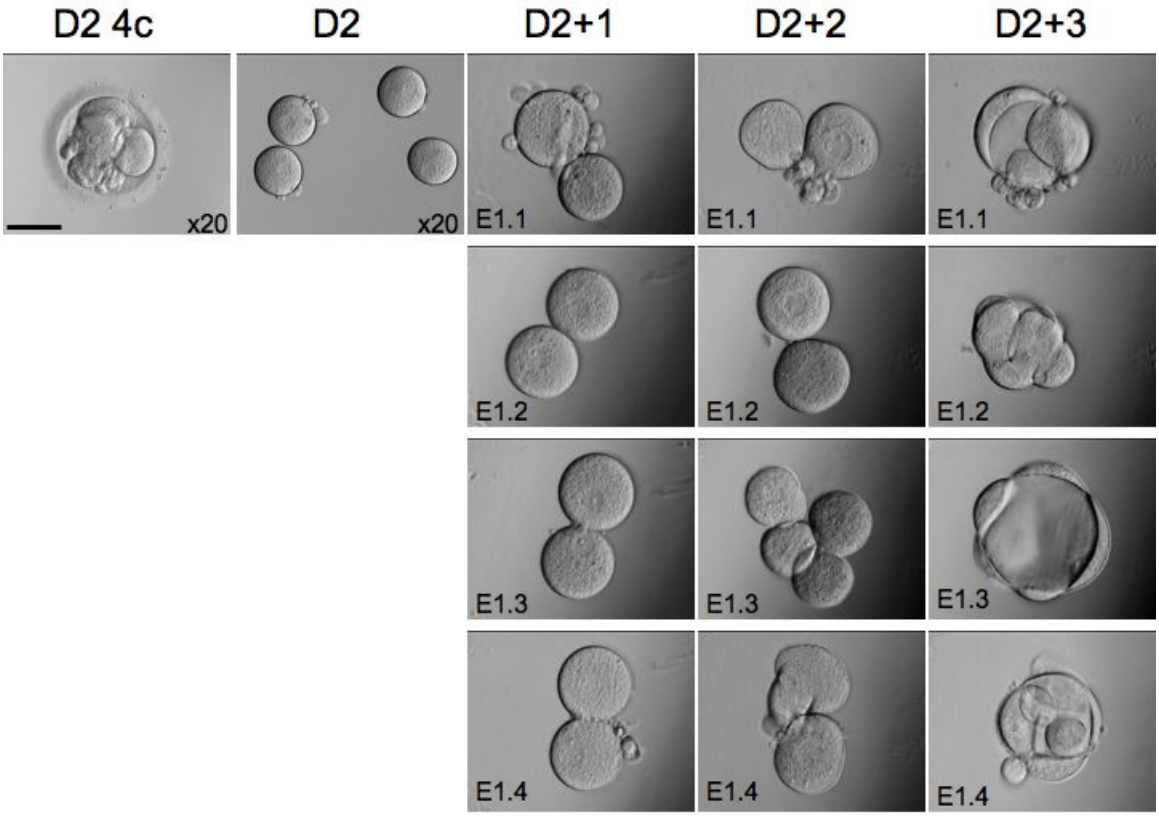

Figure 5.1: Development of individual blastomeres from a disaggregated day 2 embryo. Note the differing morphology of the sister blastomeres. Whilst all cells divided by D2+1 none had compacted by D2+2. By D2+3 E1.1 and E1.4 had initiated cavitation, E1.3 was cavitated and expanded whereas E1.2 had only reached compaction. All images at x40 objective unless otherwise indicated. Scale bar indicates 50 μm at x20 objective.

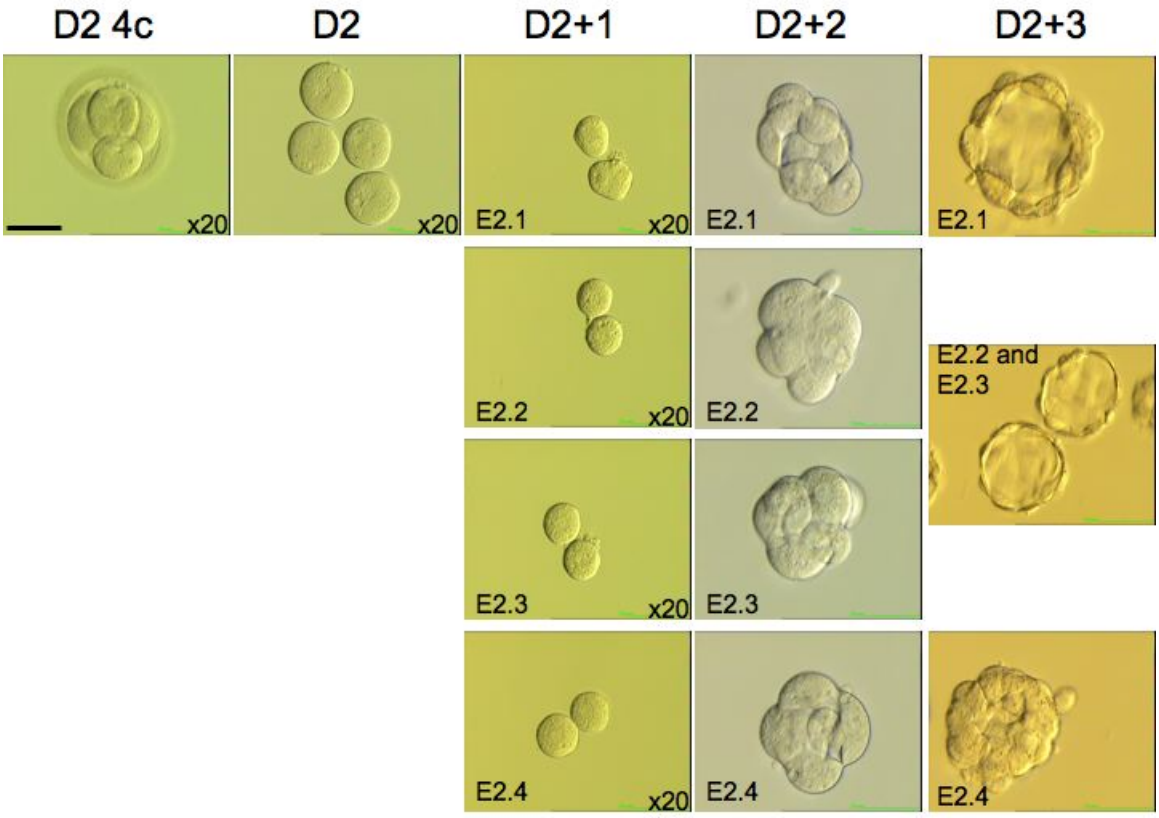

Figure 5.2: Development of individual blastomeres from a disaggregated day 2 embryo. Initial morphology was similar, with all sister blastomeres dividing to two cells by D2+1 and completing further division and compaction by D2+2. However, only three of the cell cultures had cavitated by D2+3. All images at x40 objective unless otherwise indicated. Scale bar indicates 50 μm at x20 objective.

Even from these two examples the variable development is clear. The sister E2 blastomere cultures had high cell numbers and developed into 'mini morulae' and 'mini blastocysts' that closely resembled that of whole embryo culture, only of approximately one quarter size. However the sister E1 blastomere cultures had low cell numbers, with only E1.3 showing further development on D2+2, but without compaction. Whilst cavitation was evident in three of the sister blastomeres, only E1.3 approached anything similar to the structures seen from E2. Nevertheless, overall the development of the isolated blastomeres was remarkable.

5.3.2 Division pattern

Each blastomere pair was scored for morphology and thereby for the inferred sequence of division by two independent embryologists 48 h after disaggregation. Division was defined as broadly orthogonal or broadly parallel to the plane of contact (Pickering *et al.*, 1988). The number of analysed clusters in each category and example images of the cells are shown in Figure 5.3. The long axis of polarity lies orthogonal to the plane of apposition in cell pairs, as shown by the dotted line. If the first division is orthogonal (conservative), two polar (white) cells are generated. If it is parallel (differentiative), one polar and one apolar cell (grey) results. At the second division three outcomes are possible depending on orientation of division; a cell cluster containing no apolar cells, a conformation with one apolar cell, or a cluster with two apolar cells. Not all cell clusters were able to be included in the analysis as the morphology was indeterminate. Examples of such clusters are shown in Figure 5.4.

Of the 125 single blastomere divisions analysed from all disaggregation experiments, only 19 were unequivocally assigned to a category by both viewers. Of the remaining, 10 were four cells but unclassifiable, 7 because of a 3D structure. Twenty-four had completed more than 2 cell cycles and therefore consisted of more than four cells on D2+2, and 72 consisted of only 2 or 3 cells, 13 of which had begun compaction.

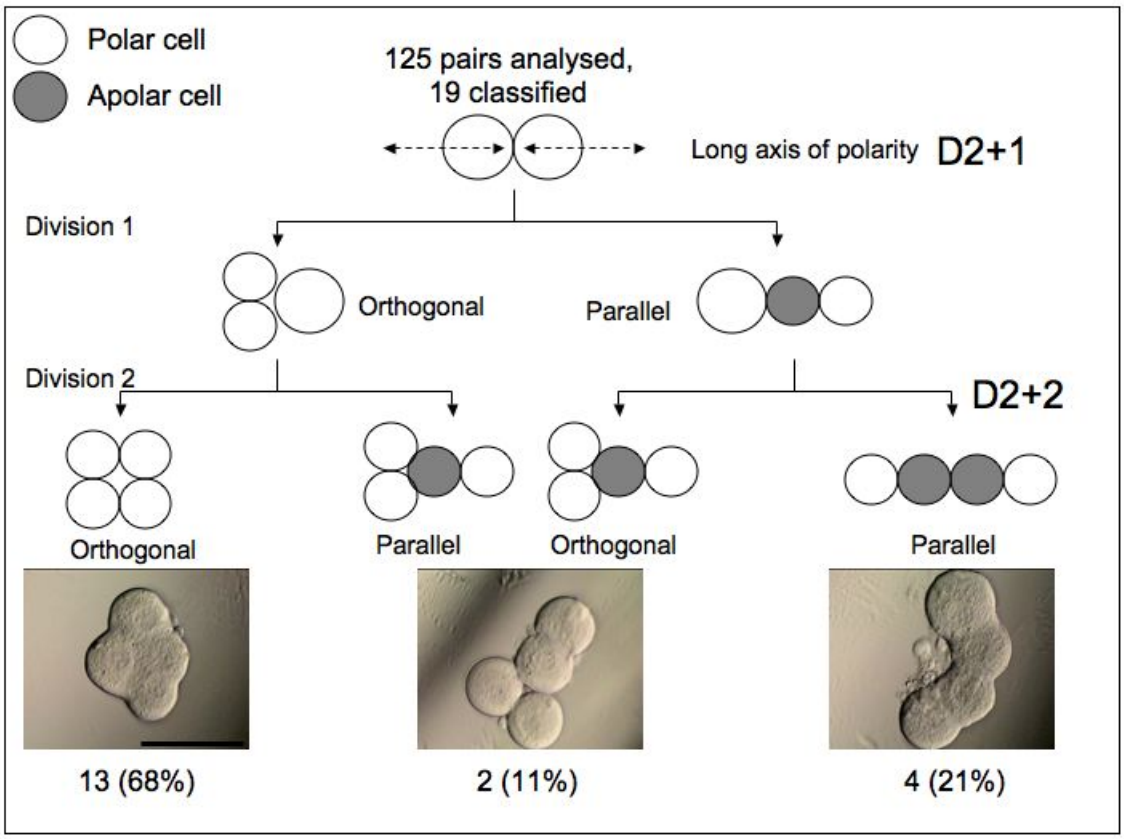

Figure 5.3: Schematic adapted from Pickering *et al.* (1988), demonstrating the possible sequences of division in the first two cell cycles of isolated blastomeres. The number of cell clusters scored and the percentage in each category of division orientation is shown. Representative examples of cell clusters observed are shown below each category. Images at x40 objective. Scale bar represents 50 μm.

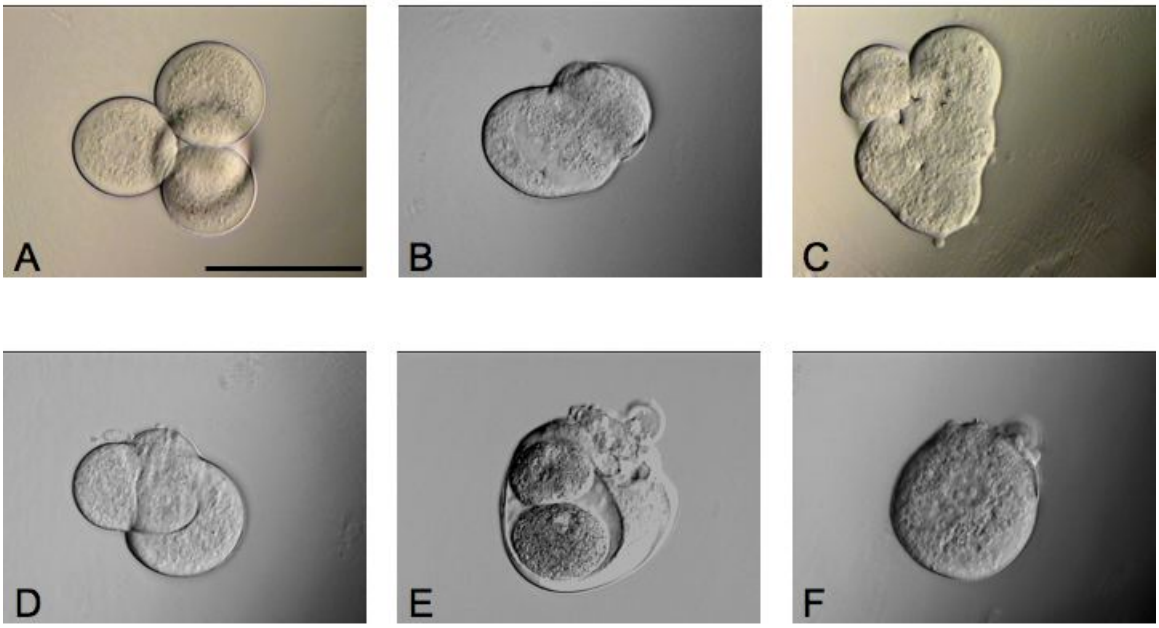

Figure 5.4: Inability to assign cell clusters to a category of division orientation was due variable development to D2+2. (A) Cells forming a 3D structure despite absence of zona pellucida, (B-E) undeterminable morphology, with greater than one round of cell division the preceding 24 h seen in (C), (F) nuclear division in the absence of cellular division. All images at x40 objective. Scale bar represents 50 μm.

5.3.3 Pluripotent marker expression

Six pronuclear embryos providing 24 individual blastomeres on D2 were used for immunocytochemical analysis of pluripotency markers. Of those 24 cells, 22 either compacted or reached cavitation, the remaining two arrested at the cellular stage following the first cell division.

The average cell number for D2+2 and D2+3 was 6.5 and 12.2 respectively, although the range of cell numbers on D2+3 was greater as shown in Figure 5.5. Whilst an increased cell number at the time of plating is likely to be an advantage for derivation attempts, this must be balanced against the pluripotent status of the cell clusters. Therefore marker expression was also analysed to assess the proportion of cells positive for POU5F1-iA and NANOG.

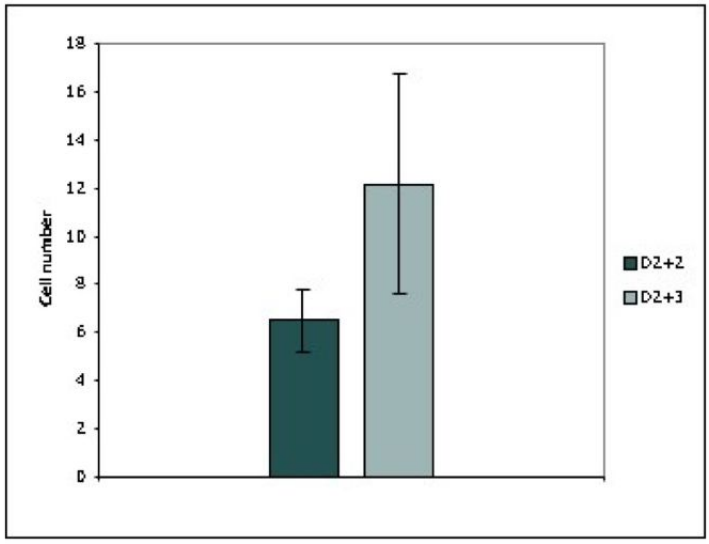

Figure 5.5: Average cell number of cell clusters from single blastomeres disaggregated on D2 and cultured to either D2+2 or D2+3. The maximum cell number at D2+2 was 8, and at D2+3 was 21. Error bars represent ±1 standard deviation.

All of the cells on D2+2 were compacted but not yet cavitating. The average percentage of POU5F1-iA positive cells at this stage was over 90%, but no cells were positive for NANOG. At D2+3, almost two-thirds of the cells were positive for POU5F1-iA but only 1% were positive for NANOG. These results are summarised in Figure 5.6. At D2+2 half of the cell clusters had all cells positive for POU5F1-iA, which fell to 15% by D2+3. In no set of sister blastomeres did all four resulting clusters consist of cells all positive for POU5F1-iA.

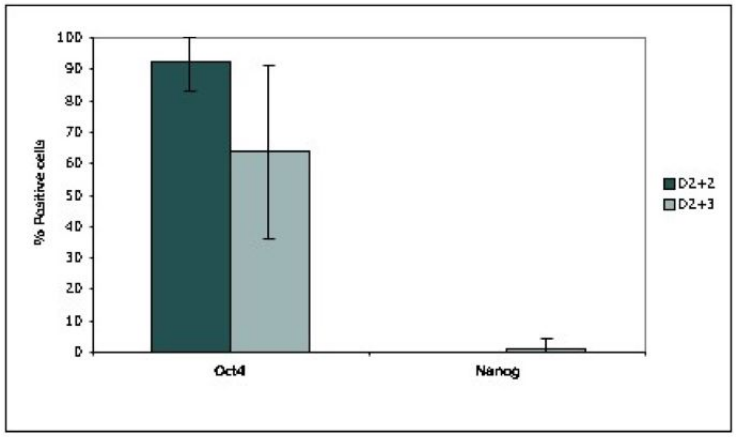

Figure 5.6: Average number of cells positive for POU5F1-iA and NANOG on D2+2 and D2+3. The error bars represent ±1 standard deviation.

Figures 5.7 and 5.8 show representative examples of the blastomere clusters stained for POU5F1-iA and NANOG on D2+2 and D2+3. Figure 5.9 shows representative controls performed alongside the blastomeres.

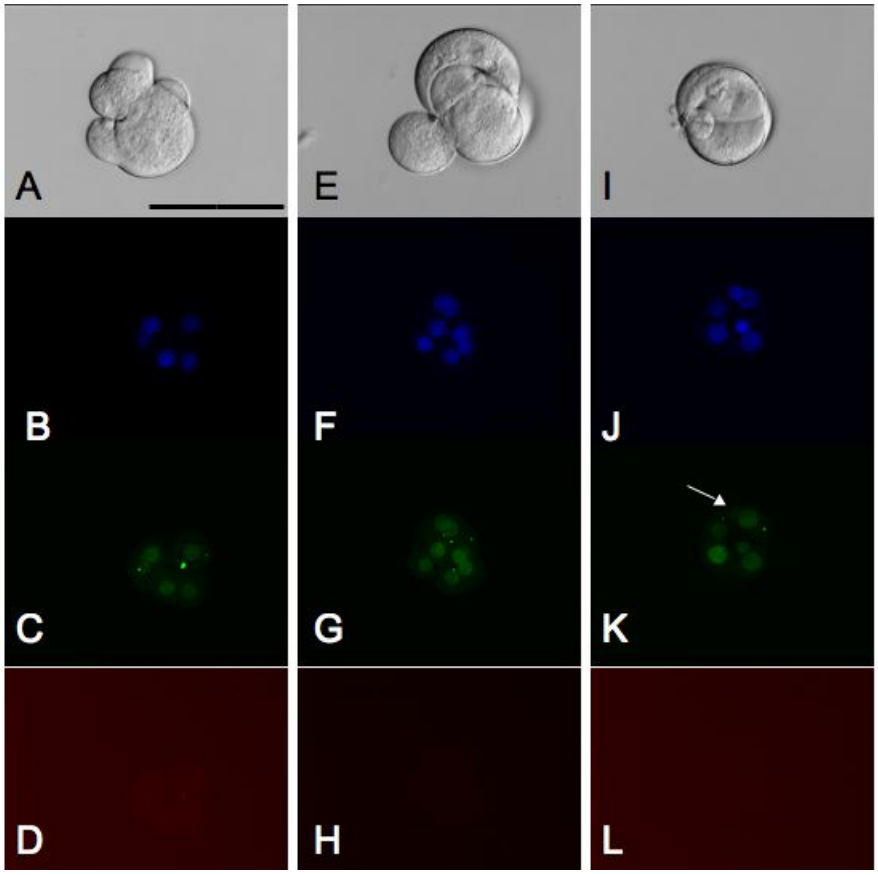

Figure 5.7: D2+2 blastomere cell clusters stained for DAPI (blue), POU5F1-iA (green) and NANOG (red). The arrow in K indicates loss of POU5F1-iA expression in one cell. Cell numbers; A-D five, E-H seven, I-L six. All images at x40 objective. Scale bar indicates 50 μm.

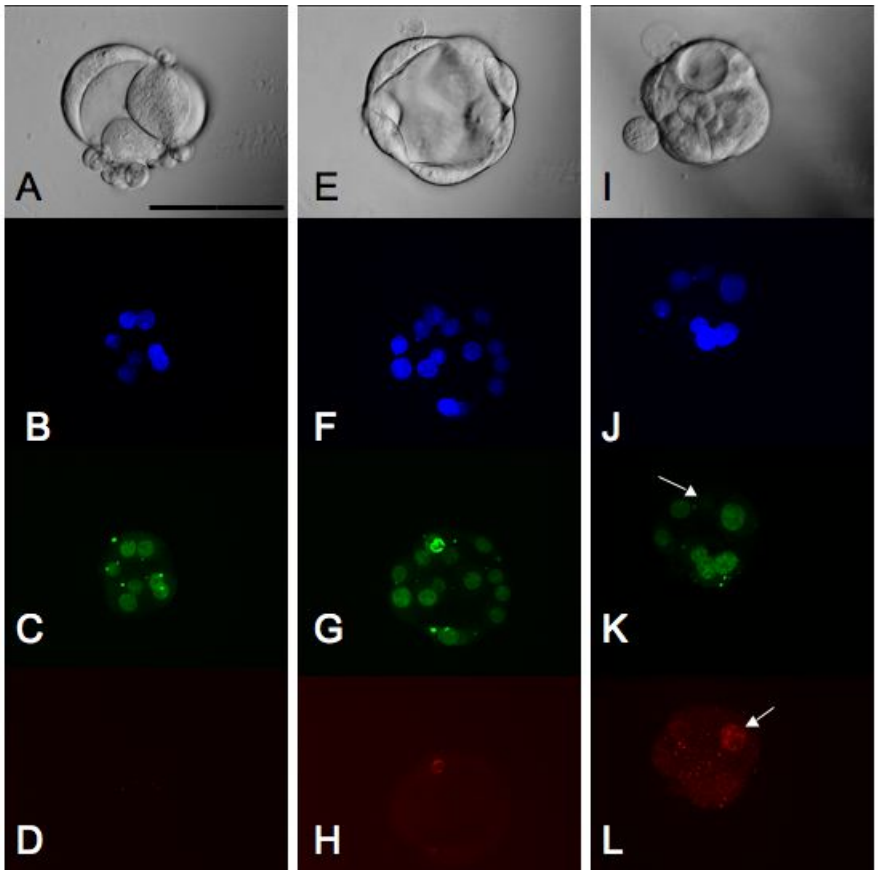

Figure 5.8: D2+3 blastomere cell clusters stained for DAPI (blue), POU5F1-iA (green) and NANOG (red). The arrow in K indicates loss of POU5F1-iA expression in one cell. The arrow in L indicates a NANOG positive cell. Cell numbers; A-D seven, E-H thirteen, I-L seven. All images at x40 objective. Scale bar indicates 50 μm.

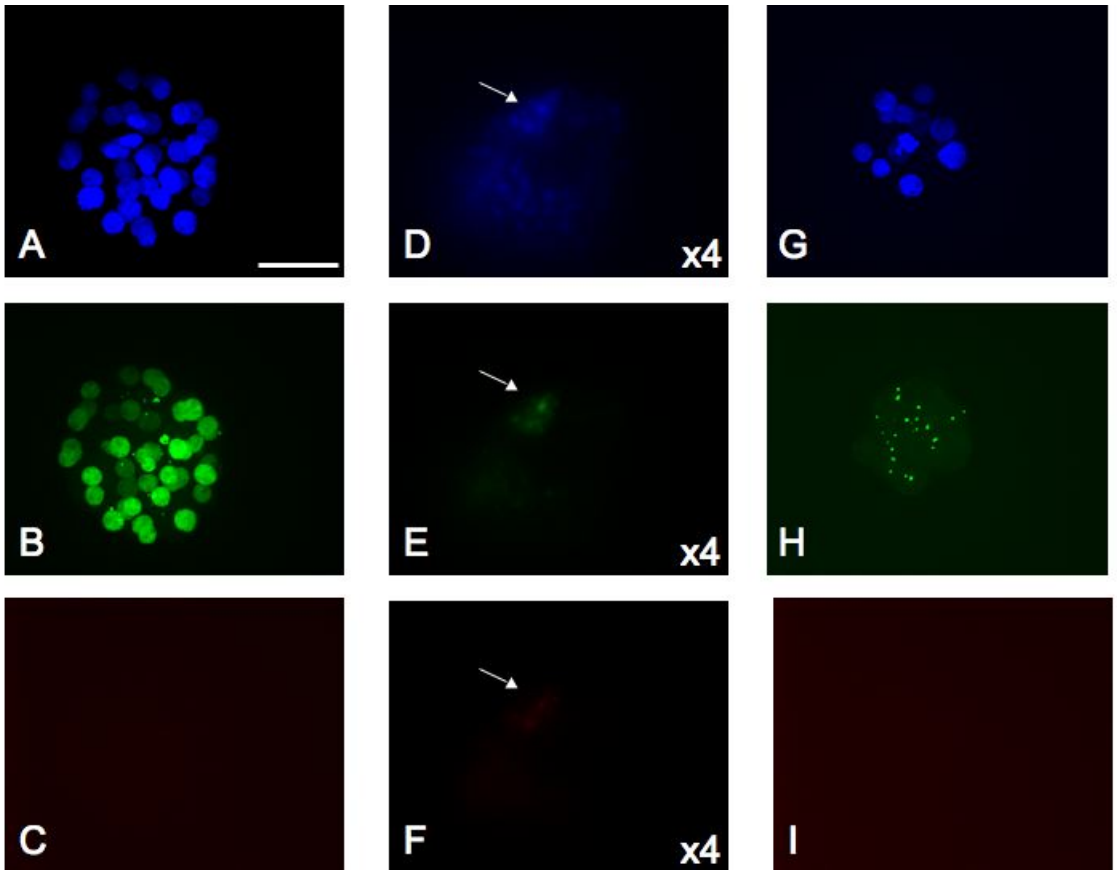

Figure 5.9: A-C D4 control morula positive for POU5F1-iA but not NANOG. D-F D6 control blastocyst with cells positive for both POU5F1-iA and NANOG in the ICM (arrows). G-I D4 negative control with secondary antibody only. DAPI (blue), POU5F1-iA (green) and NANOG (red). All images at x20 objective unless otherwise indicated. Scale bar indicates 50 μm at x20 objective.

5.3.4 Preliminary plating experiments

In the preliminary derivation experiments, day 3 embryos were disaggregated and the individual blastomeres plated directly onto MEF feeder layers in hESC CM. A total of seven embryos were used following day 1, 2 or 3 thaw, providing a potential 42 blastomeres by day 3. 30 (71%) blastomeres were obtained following disaggregation and plated into MEF microdrops. 16 (53%) cells completed one round of division to produce at least 2 cells by day 1 after plating, but only one cell pair had attached to the feeder layer. By day 2 after plating, 4 cell clusters were attached. The first had compacted and contained at least 2 cells. The second was at least four cells and had compacted, and was beginning the cavitation process. The third was at least four cells and had compacted. The final was at least five cells but had not yet initiated compaction. The majority of the cell clusters displayed multiple blebs extruding from the cell surface. The cells were kept in culture but they rapidly degenerated with no further development over the following 4-5 days. Figure 5.10 shows examples of the blastomere development and Table 5.5 summarises the outcome of the plating experiments.

Table 5.5: Summary of development of all embryos disaggregated on day 3 and immediately plated on MEF feeder layers. Numbers in brackets indicate the outcome as a percentage of total blastomeres obtained.

Number embryos	7
Total blastomeres available	42
Total blastomeres obtained	30
Number cleaved D1 after plating	16 (53)
Number attached D1 after plating	1 (3)
Number further cleaved D2 after plating	12 (40)
Number attached D2 after plating	4 (13)
Number viable D3 after plating	6 (20)
Number viable D5 after plating	0
Number with stem-like cells	0
Number cultures passaged	0
Number lines	0

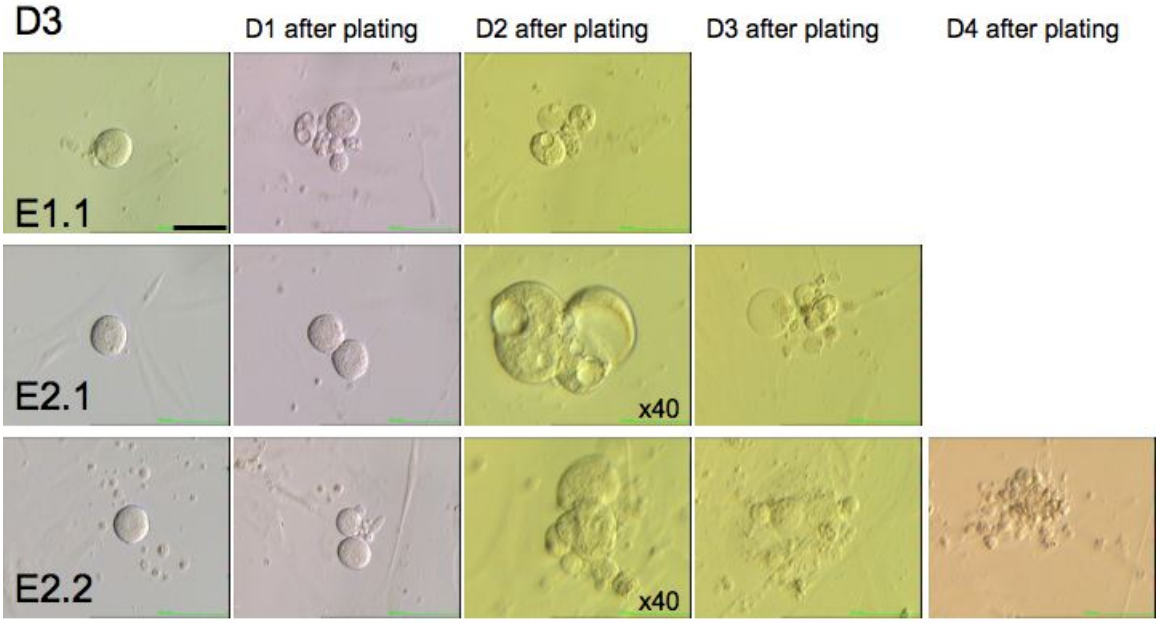

Figure 5.10: Disaggregated D3 blastomeres plated immediately onto MEF feeder layers. E1.1 had divided and fragmented by D1 after plating, and the cells had begun to degenerate by D2. E2.1 and 2.2 both divided to 2 cells the day following plating, and both showed signs of further development by D2 after plating. However, despite attaching to the feeder layer, both were degenerate by D4 after plating. All images at x20 objective unless indicated otherwise. Scale bar indicates 50 μm at x20 objective.

5.3.5 Medium and feeding regime

The culture requirements for derivation attempts with single blastomeres was thought to be potentially more complex than for whole embryo/ICM cultures. Before plating the blastomere clusters were likely to be more sensitive to culture parameters than whole embryos due to loss of the protective functions of the zona. In addition the reduced cell number and altered cell-cell interactions necessitated proliferation support. From previous work (Chapter 4) is was shown that a culture system utilising conditioned medium from proliferative feeder cells was likely to be unsuitable for derivation from whole embryos due to high concentrations of metabolic by-products. Therefore it was not recommended for single cell attempts either. However, it was thought that extra encouragement may be needed for the transition of the single cell through the ICM stage and ultimately to hESC (Klimanskaya *et al.*, 2006), and so the use of conditioned medium from hESC colonies growing on inactivated feeders was investigated.

The substrate concentrations remained in excess throughout the time periods measured. The lowest level of glucose recorded was 3.8 g/L in the 48 h HFF condition. The minimum level of glutamine was 2.1 mmol/L following 24 h culture on MEF and 48 h on HFF.

On both MEF and HFF feeders the levels of ammonium increased from around 0.22 mmol/L after 24 h to approximately 0.34 mmol/L after 48 h culture. Lactate production was variable, detected between 0-0.9 g/L with an average of 0.46 g/L after 48 h on MEF with hESC, but in no other condition on MEF. On HFF, lactate was detected at an average of 0.54 g/L after 48 h both with and without hESC. Figure 5.11 details the levels of these by-products in each condition.

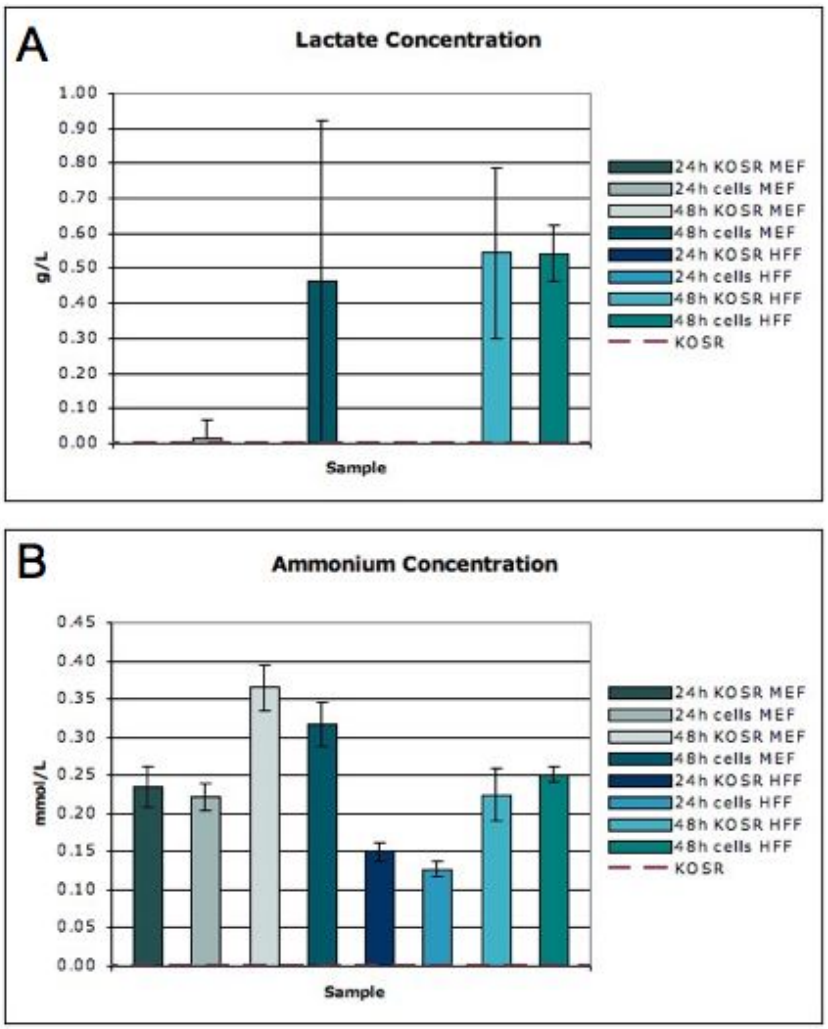

Figure 5.11: The concentrations of (A) lactate and (B) ammonium in each of the measured conditions. Error bars ± 1 s.d.

5.3.6 Derivation of hESC from single blastomeres

For single cell derivation attempts, 21 pronuclear stage embryos from three different patients were thawed, of which 15 (71%) survived the thawing process. Eleven of the 15 (73%) embryos had reached the 4 cell stage 24 h after thaw, although of varying quality. One further embryo had five cells by this point. Two of the cells were significantly smaller and highly likely to be sister blastomeres, and were therefore cultured together. Table 5.6 details the embryo quality and single blastomere development of each embryo used.

Table 5.6: Details of embryos used for single blastomere derivation attempts

Patient	Embryo number	Number of cells	Grade	Blastomeres obtained
A	1	4	3	4
A	2	4	3 upper	4
A	3	4	3 upper	4
A	4	4	3	4
B	5	4	3	4
B	6	4	2	4
C	7	4	3	4
C	8	4	3 lower	4
C	9	4	3 upper	4
C	10	4	4	3
C	11	5	3 lower	5
C	12	4	2	4

Following disaggregation, the single blastomeres were cultured in the same drop in microwells for 48 h to D2+2. On D2+2 the cell clusters were plated onto MEFs in microdrops. Tables 5.7 and 5.8 detail the development of each cell cluster following plating.

Two days after plating, 24 (51%) blastomere clusters had attached to the feeder layer, and a further 5 (11%) had attached by three days. During subsequent culture, 11 (23%) blastomere clusters outgrew to form clusters where cells of stem-like morphology were visible. Six (13%) reached at least 7 days in culture whilst still displaying potential but then arrested with no further proliferation. Four of these colonies containing stem-like cells were from the same embryo. Examples from the early cultures displaying stem-like potential are given in Figure 5.12.

Table 5.7: Details of embryos used for single blastomere derivation attempts. Emb; embryo number, Blm; blastomere number, D2+1; day 1 after disaggregation, D2+2; day D2 after disaggregation, D2; day 2 after plating the cell clusters onto feeders, D3; day 3 after plating, D4-9; day 4-9 after plating. +b; blebs visible, att; attached to feeders, spr; cells spread flat in culture, comp; compacted, cav; cavitated, ab; abnormal, nuc; nuclei, stem; stem cell like cells visible, D/D; differentiated or degenerate.

Emb	**Blm**	**D2+1**	**D2+2**	**D2**	**D3**	**D4-9**	**Outcome**
1	1	2c	4c	att and spr			D/D
	2	2c +frag	4c	att not spr			D/D
	3	2c	4c	att and spr			D/D
	4	2c	4c	att not spr		Stem	D/D
2	1	2c	4c	not att	not att		D/D
	2	2c +b	2c	att and spr			D/D
	3	2c	3c	not att	att and spr		D/D
	4	2c +b	4c	att and spr			D/D
3	1	2c	4c comp	att and spr			D/D
	2	2c	4c comp	att and spr			D/D
	3	2c +b	4c comp	att and spr		Stem	D/D
	4	2c	3-4c comp	att and spr		Stem	D/D
4	1	2c	2c	not att	not att		D/D
	2	2c	2c	not att	not att		D/D
	3	2c	3c	not att	att not spr		D/D
	4	2c	4c comp	not att	att not spr		D/D
5	1	4c	5c comp	att and spr		Stem	D/D
	2	4c	5c comp	att not spr		Stem	D/D
	3	4c	6c comp	att not spr			D/D
	4	2c +b	2c +b	att not spr			D/D
6	1	2c +b	3-4c	not att	not att		D/D
	2	2c	4c	not att	not att		D/D
	3	2c ab cells	1c multi nuc	not att	not att		D/D
	4	2-3c +b	1c multi nuc	not att	not att		D/D

Table 5.8: Details of embryos continued

Emb	Blm	D2+1	D2+2	D2	D3	D4-9	Outcome
7	1	2c	3c (4 nuclei)	att and spr		Stem	P1
	2	2c	6+c comp	att and spr		Stem	D/D
	3	2c	4+c comp	att and spr		Stem	D/D
	4	2c	4+c comp	att not spr		Stem	P2
8	1	1c ab	2c	not att	not att		D/D
	2	4c	4c	not att	not att		D/D
	3	3c	3c	not att	not att		D/D
	4	2c	2c	not att	not att		D/D
9	1	2c	2c	not att	not att		D/D
	2	1c +b	2c	not att	not att		D/D
	3	2c uneven	2c	att not spr			D/D
	4	2c +b	2c	att not spr			D/D
10	1	4c ab	5+c comp	not att	not att		D/D
	2	3c ab	4+c comp	att and spr		Stem	D/D
	3	2c	4+c comp, cav	att and spr		Stem	P3
	4	1c degen					D/D
11	1	1c	2c +b	not att	not att		D/D
	2	2c	1c cav plane	not att	att and spr		D/D
	3	2c ab cells	2c	att not spr			D/D
	4+5	2c comp	1c	not att	att and spr		D/D
12	1	2c ab cells	2c comp	not att	not att		D/D
	2	2c ab cells	3c but degen				D/D
	3	2c	4c cav	not att	not att		D/D
	4	2c +b	5+c comp, cav	att and spr			D/D

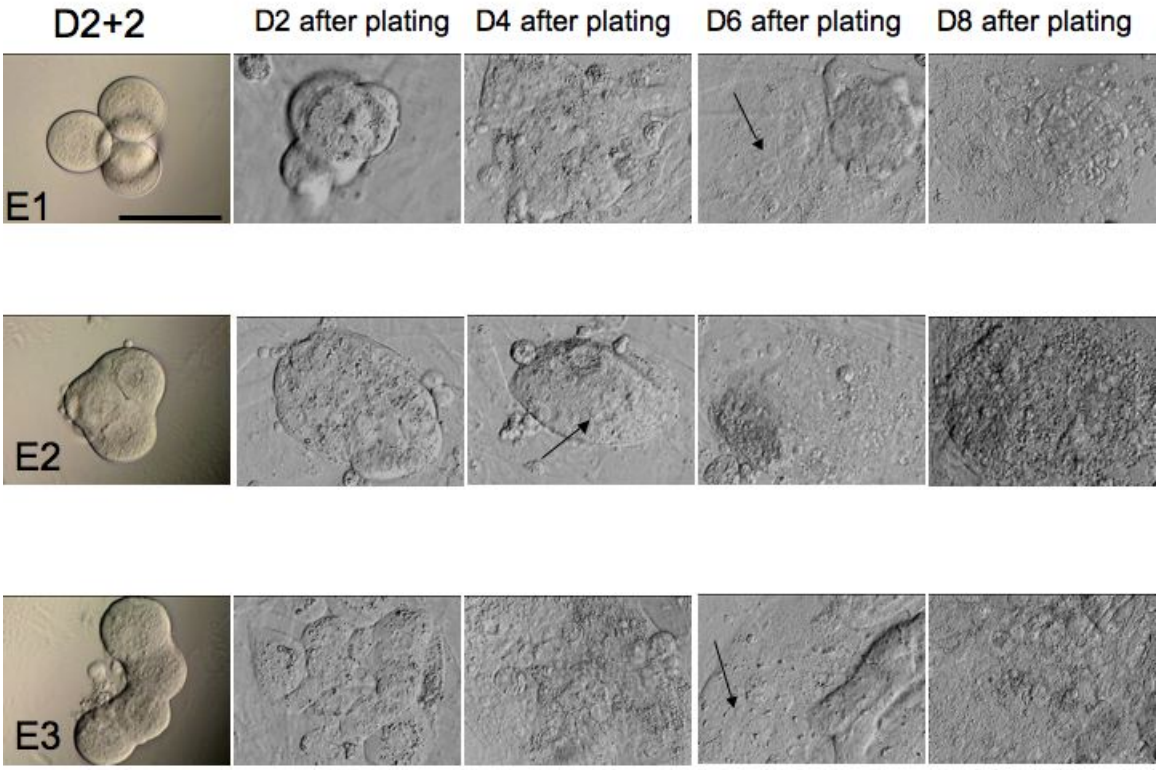

Figure 5.12: Examples of blastomere cultures during derivation attempts. Each culture contained cells with stem-like morphology (indicated by arrows) but subsequently either differentiated or arrested and finally degenerated despite addition of mitogens to the culture. All images at x40 objective. Scale bar indicates 50 μm.

Three cultures proliferated sufficiently to be passaged onto fresh MEF feeder layers in microdrops. Two cultures were passaged 7 days after plating and one after 9 days. All three colonies re-attached onto the fresh feeders. The first (E1.1) did not resume proliferation and no attached cells were visible at day 5 after passage. The second colony (E1.2) proliferated and pushed the MEFs to the edge of the colony, and was passaged again. However the re-attached colony grew as a monolayer and subsequently differentiated. Culture of this colony was abandoned 15 days after the first passage. The third colony (E2) showed robust proliferation, and was split into 2 pieces and passaged to P2. Only one of the pieces maintained undifferentiated morphology, and was subsequently split into 2 pieces and passaged to P3. However, proliferation arrest occurred after the third passage, and 23 days later the colony contained only differentiated or degenerate cells and the culture was discarded. The complete culture profile of these three blastomeres are shown in Figures 5.13, 5.14 and 5.15.

A summary of all the derivation attempts, from whole embryo to culture outcome, is given in Table 5.9.

Table 5.9: Summary of development of all single blastomere derivation attempts. Numbers in brackets indicate the outcome as a percentage of total blastomeres obtained.

Number embryos	12
Total blastomeres	49
Blastomeres obtained	48
Number cleaved D2+1	44 (92)
Number initial cleavage D2+2	3 (6)
Number further division D2+2	29 (60)
Number compacted D2+2	18 (38)
Number cavitated D2+2	3 (6)
Number attached D2 after plating	24 (50)
Number attached D3 after plating	5 (10)
Number with stem-like cells	11 (23)
Number cultures passaged	3 (6)
Number lines	0

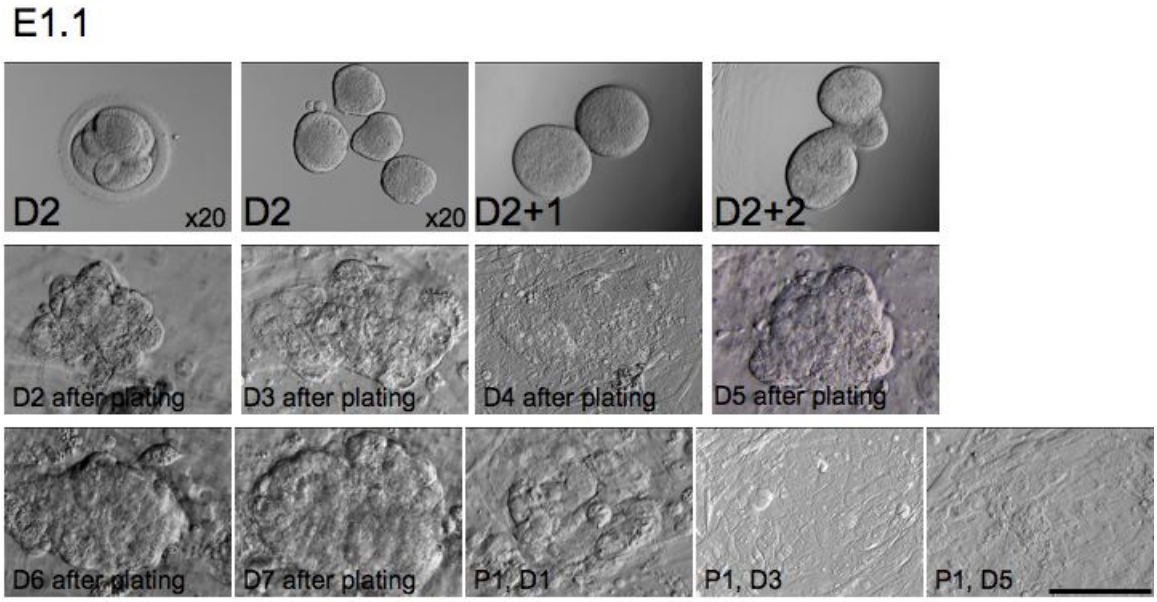

Figure 5.13: E1.1 divided by D2+1 to give two cells, and further developed by D2+2 when at least four nuclei were visible, likely to be a result of two parallel divisions. The cells attached by day 2 after plating, and robust proliferation was observed from day 5 to 7. However, following passage no further growth was observed, and by 5 days no stem-like cells were visible. All images at x40 objective unless otherwise indicated. Scale bar indicates 50 μm at x40 objective.

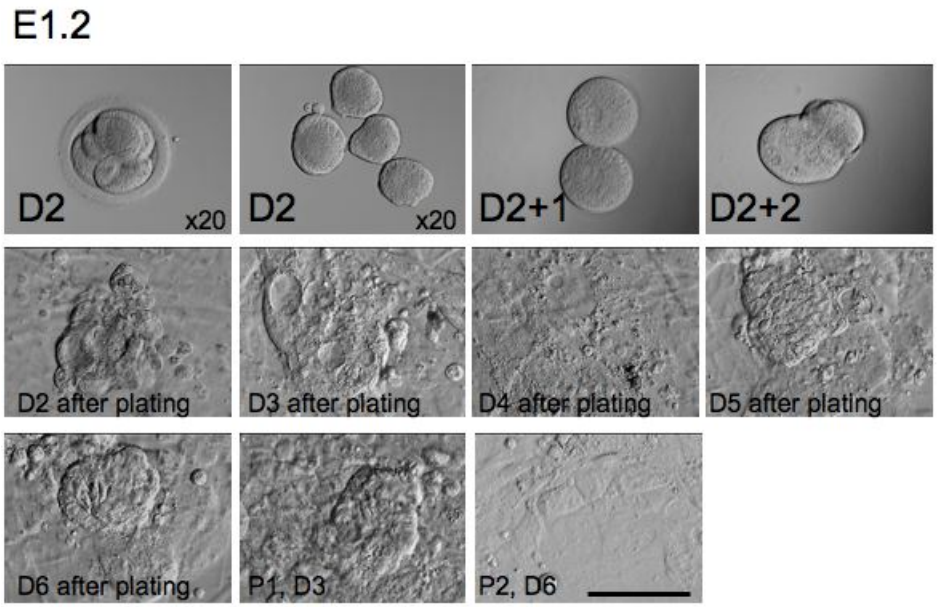

Figure 5.14: E1.2 divided by D2+1 to give two cells, and further developed by D2+2 when at least five nuclei were visible. The cell cluster was compacted but the pattern of division was undeterminable. The cells attached by day 2 after plating, and robust proliferation was observed from day 5. Passage of the colony was successful to P1, and the cells proliferated rapidly. However, when the colony was cut and passaged to P2, the cells flattened and differentiated, and no further culture was possible. All images at x40 objective unless otherwise indicated. Scale bar indicates 50 μm at x40 objective.

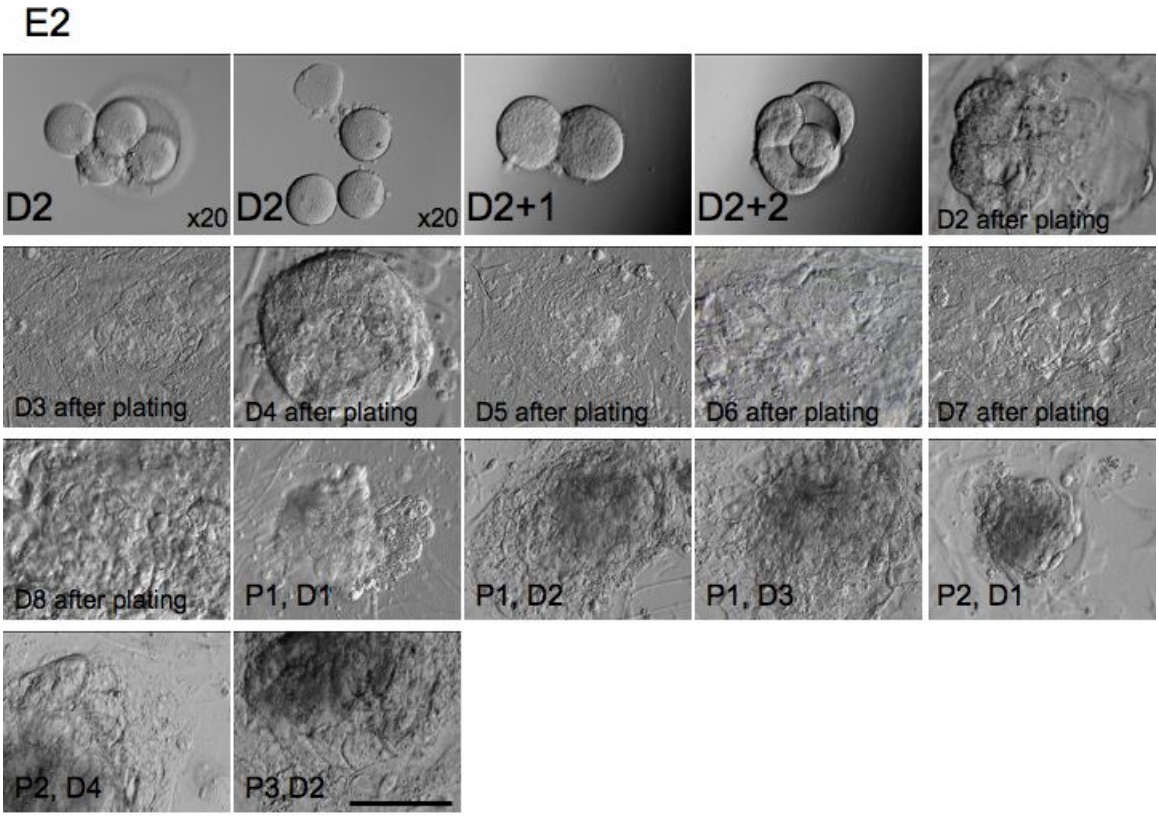

Figure 5.15: E2 divided by D2+1 to give two cells, and further developed by D2+2 when at least five nuclei were visible. The cell cluster had already initiated cavitation but the pattern of division was undeterminable. The cells attached by day 2 after plating, flattened on day 3, underwent robust proliferation by day 4, then re-flattened by day 5. Passage of the colony was successful to P1 and then P2. However, when the colony was cut and passaged to P3, the cells arrested, and no further culture was possible. All images at x40 objective unless otherwise indicated. Scale bar indicates 50 μm at x40 objective.

5.3.7 Gene expression analysis by single cell PCR

For single cell gene analysis, 86 pronucleate or day 2 embryos from 13 different donors were thawed. Of these, 24 were disaggregated and used for analysis, and a further 8 were used as RTN controls. Eight 2-cell, seven 4-cell, one 7-cell, two 8-cell and two blastocysts were collected. In addition two compacting 8-cell and two 7-cell embryos were collected, which were not developing optimally but were still stored for future analysis. The details of the embryos used are shown in Table 5.10. Each individual cell or whole blastocyst was assayed a minimum of three times against each target gene, generating approximately 20,000 data points for analysis.

5.3.7.1 Method validation

The suitability of the preamplification kit and the ability of the platform to detect single cell cDNA levels was assessed using a fibroblast dilution and single blastomeres from two-cell embryos. Figure 5.16 shows that the detection of the equivalent of a single fibroblast cell of preamplified cDNA was possible. Threshold cycles (cT) of approximately 27, 28 and 24 were generated for *ACTB*, *B2M* and *GAPDH* respectively, all within the 15-30 cycle dynamic range.

The detection of embryonic material was then assessed. Figure 5.17 shows representative plots that confirmed it was possible to detect preamplified cDNA from a single blastomere with both the ABI and Fluidigm, with cTs of around 20 for all targets. However, it was not possible to accurately detect non-preamplified targets. With the ABI, the amplification plots all had cT values of above 30, therefore beyond the accurate detection threshold, and the Fluidigm showed no amplification.

To aim to account for biological variability, replicates of each embryo stage were collected for analysis. None of the negative control reactions amplified during the PCR step. The extraction negative controls ensured there was no contamination of the reverse transcription, PCR reagents or consumables with extraneous DNA. The RTN controls confirmed that the template for the PCR was cDNA, and not genomic DNA. Although the TaqMan Gene Assays were selected on the basis that they spanned an exon-exon junction and so should not amplify genomic DNA, the RTN control was included for completeness. The preamplification negative control again ensured there was no contamination with extraneous DNA.

Table 5.10: Details of embryos used for single blastomere gene analysis using the Fluidigm dynamic PCR platform

Embryo	Cell number	Grade	Use	Comments
1	2	3 lower	Gene analysis	
2	2	4 lower	Gene analysis	
3	2	4 lower	Gene analysis	
4	2	3	Gene analysis	One cell with 4PN
5	2	3	Gene analysis	
6	2	3	Gene analysis	
7	2	3 upper	Gene analysis	
8	2	3 upper	Gene analysis	
9	4	3 lower	Gene analysis	
10	4	3 upper	Gene analysis	
11	4	3	Gene analysis	
12	4	3	Gene analysis	4 cell 26h post thaw
13	4	3 upper	Gene analysis	
14	4	4	Gene analysis	
15	4	3 lower	Gene analysis	
16	8	3 lower	Gene analysis	
17	8	3 upper	Gene analysis	
18	8	3 upper	Stored for future analysis	Compacted
19	8	3	Stored for future analysis	Compacted
20	7	3	Gene analysis	Slow cleavage
21	7	3	Stored for future analysis	Slow cleavage
22	7	3 upper	Stored for future analysis	Slow cleavage
23	blastocyst	6Cβ	Positive control	Low cell number
24	blastocyst	6Aα	Positive control	
25	3	n/a	RTN	
26	2	n/a	RTN	
27	4	n/a	RTN	
28	2	n/a	RTN	
29	4	n/a	RTN	
30	3	n/a	RTN	
31	4	n/a	RTN	
32	4	n/a	RTN	

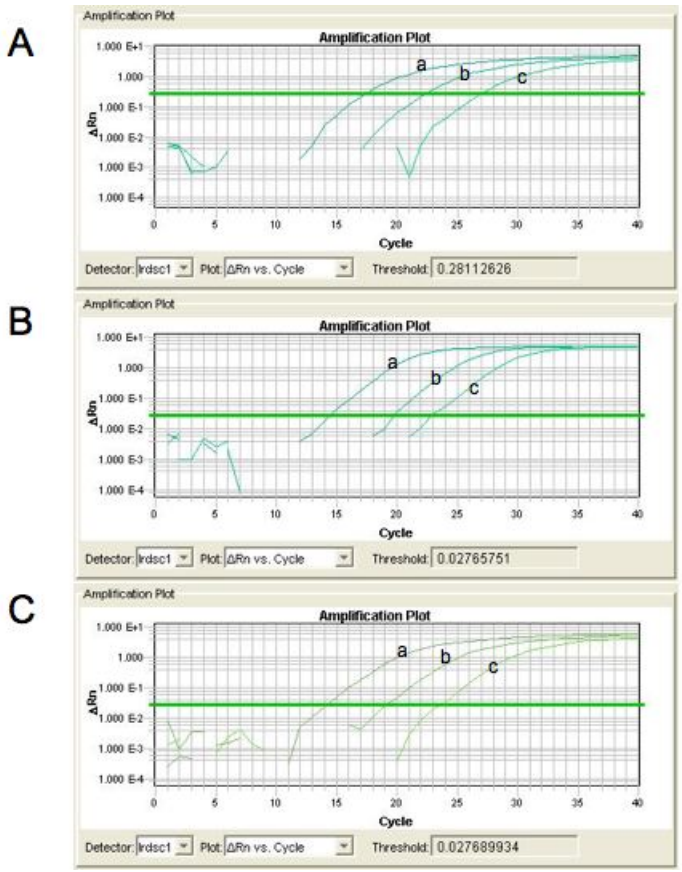

Figure 5.16: Amplification plots from the ABI using fibroblast cDNA dilutions equivalent to (a) 10,000 cells (b) 100 cells and (c) 1 cell assayed for (A) *ACTB* (B) *B2M* (C) *GAPDH*.

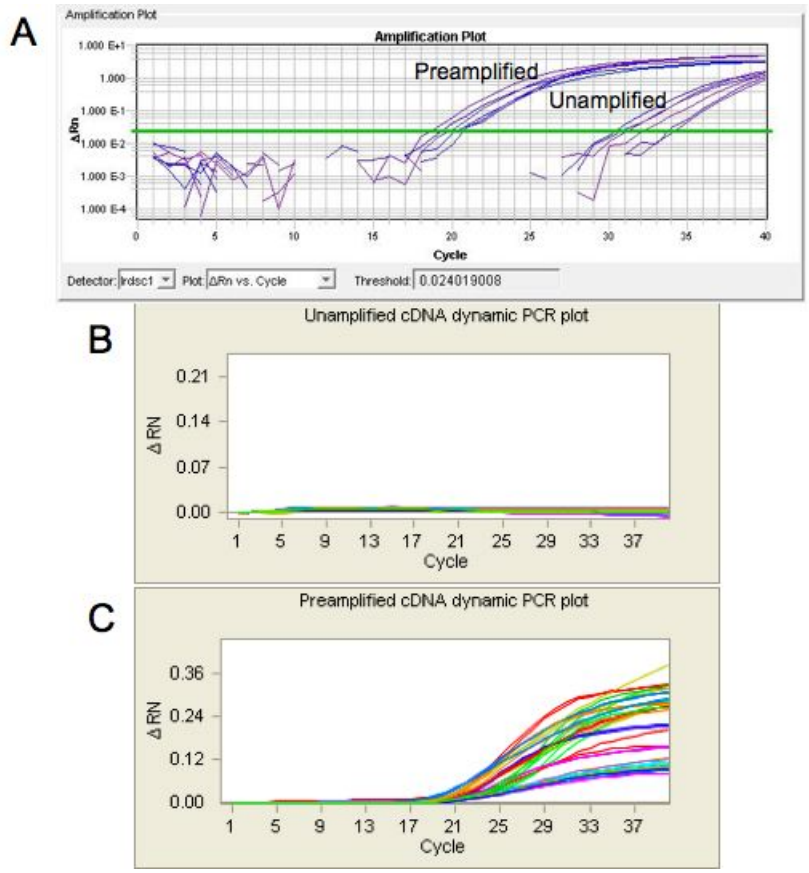

Figure 5.17: Amplification plots showing that it was not possible to detect target blastomere cDNA without a preamplification step. (A) Preamplified and non-preamplified cDNA from a single blastomere run on the ABI against the housekeeping genes. (B) Non-preamplified blastomere cDNA and (C) preamplified blastomere cDNA run on the Fluidigm against all 24 target genes. deltaRN: normalised to the internal passive fluorescence reference ROX.

RT-PCR with real-time detection of amplification products is a robust and quantitative way to measure mRNA levels in biological samples. Whilst the Biomark literature stated that the platform was optimised for reliable detection from single cells, both the platform and the preamplification kit were new on the market. No literature was available detailing the use of this combination for a single cell application, although successful use of the Fluidigm platform for tissue samples has been reported (Spurgeon *et al.*, 2008). Therefore thorough technical validation of each step of the PCR method was needed due to the sensitivity of detection required to accurately analyse single cells and the determination of significantly different expression levels.

As cell lysis to cDNA generation all occurred in a single tube from a single extraction with no sample splitting, validation of these initial steps was not possible. Confirmation that the preamplification step was linear was addressed, to rule that differences in threshold values between samples/genes were not due to relative abundance changes during this step. Datasheets provided from ABI using universal reference RNA showed a linear relationship between cT values for non-preamplified versus preamplified samples, with less than a two-fold change for over 99% of samples. A repeat of this validation was attempted for the embryo samples. As it was known that target cDNA could not be detected from non-preamplified single blastomere samples (Figure 5.17), cDNA from whole blastocysts was used. Detection from non-preamplified cDNA was still not possible as shown in Figure 5.18. Therefore the limits of sensitivity of the Fluidigm system precluded this assessment with the embryo samples.

To attempt to assess this another way, the preamplification step was run with one single blastomere sample probed for three housekeeping targets; *ACTB*, *GAPDH* and *CHUK*. 1 μl of sample was removed after the completion of each of the 14 amplification cycles and cDNA levels quantified using a Nanodrop® ND-1000 (Thermo Scientific, Wilmington, USA). Assuming no bias was introduced by the preamplification, a linear increase in cDNA quantity was expected, and therefore the ratios of the genes should have remained constant. However, the measurements showed no apparent change in cDNA levels, as detailed in Table 5.11. As the preamplification step was designed to only amplify target cDNA amplicons, the sensitivity of the nanodrop did not allow such small changes in concentration to be determined

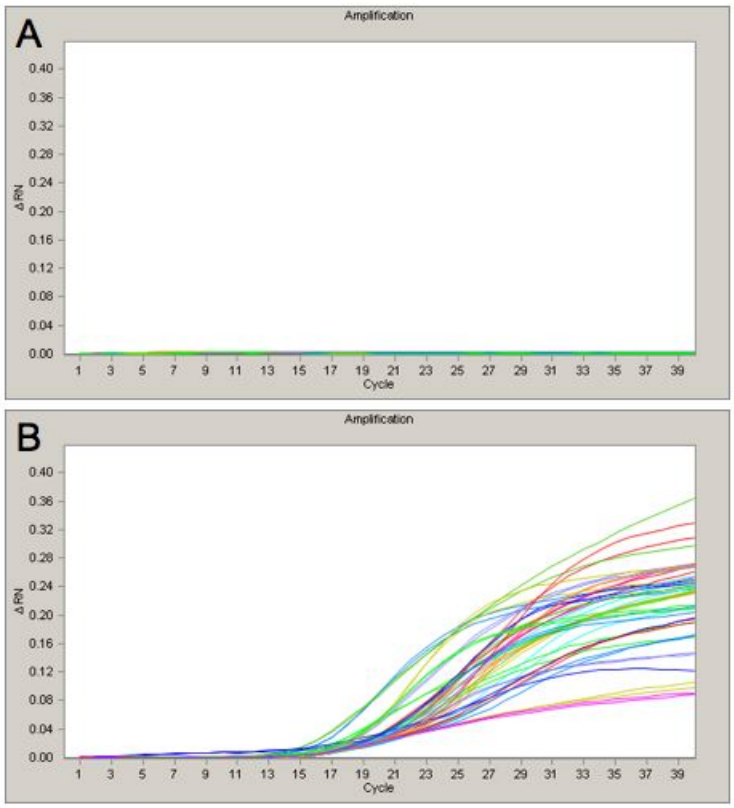

Figure 5.18: Amplification plots showing that it was not possible to detect any target blastocyst cDNA without a preamplification step. (A) Non-preamplified blastocyst cDNA, no amplification occurred. (B) Preamplified blastocyst cDNA, robust amplification was seen. The cT values were approximately 17 for the targets, as compared to approximately 20 for the single blastomere, reflecting the onset of embryonic transcription at the 4-8 cell stage.

above the background of endogenous cDNA and single strand components of the preamplification mastermix. Therefore, the detection levels of the available equipment precluded the validation of the preamplification step and the information from the ABI datasheets was accepted in the validation.

Table 5.11: cDNA quantity as measured by the nanodrop after each cycle of preamplification. Any increase in cDNA targets was not detectable above noise resulting from endogenous cDNA and single strand components of the reagents.

Cycle Number	***GAPDH*** **ng/ul**	***ACTB*** **ng/ul**	***CHUK*** **ng/ul**
1	1674.1	1363.1	1545.3
2	1478.3	1715.6	1495.6
3	1495.8	1392.8	1491.1
4	1449.0	1688.6	1505.0
5	1438.6	1505.5	1484.0
6	1522.4	1465.9	1496.2
7	1470.9	1546.5	1523.5
8	1478.9	1499.2	1509.5
9	1482.1	1519.4	1506.0
10	1491.9	1491.5	1544.5
11	1480.3	1477.1	1524.7
12	1483.9	1479.4	1538.8
13	1485.7	1488.4	1506.6
14	1524.1	1514.2	1546.1

5.3.7.2 Data collection

Eight chips were run for data collection. One chip included highly replicated observations on one gene for 4 samples for chip performance evaluation. The remaining chips included data for 24 genes, each observed in duplicate on each chip.

A failed amplification with no detectable fluorescence resulted in cT values of '999' which were excluded from the statistical analysis rather than treated as censored observations. Validity of this approach was confirmed with several considerations. Firstly, each of the 999 points showed no amplification curve, and were therefore marked as failures by the quality control algorithm in the Fluidigm software. Secondly, the distribution of cT values for the majority of genes was otherwise approximately symmetric and far from the maximum cycle number, indicating that the failures were not due to low DNA content within the typical population. Finally,

while the failure rate was clearly variable from one chip to the next, it was less variable from one treatment condition to the next giving little cause to expect serious bias from removal of failed reactions. The failure rate represented by the proportion of successes is shown in Figure 5.19 per chip, Figure 5.20 per developmental stage and Figure 5.21 per gene.

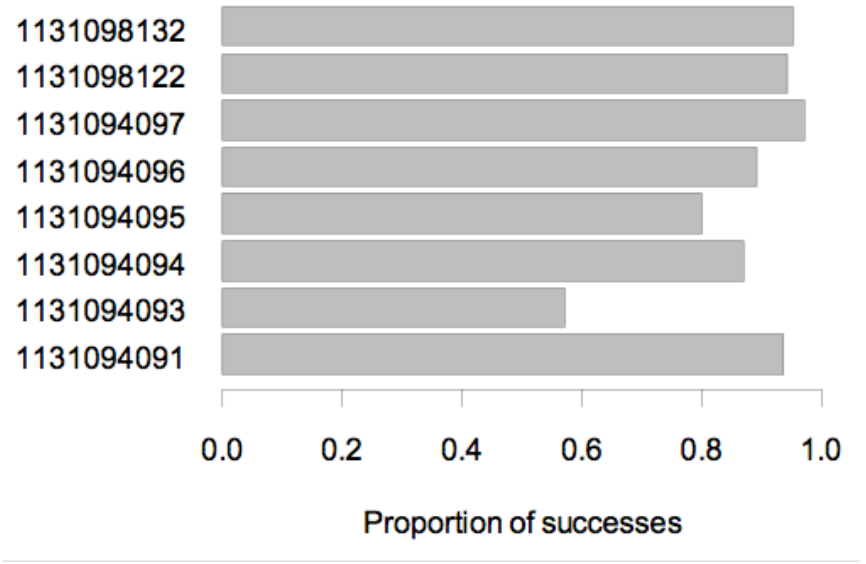

Figure 5.19: Proportion of successful amplification reactions per chip.

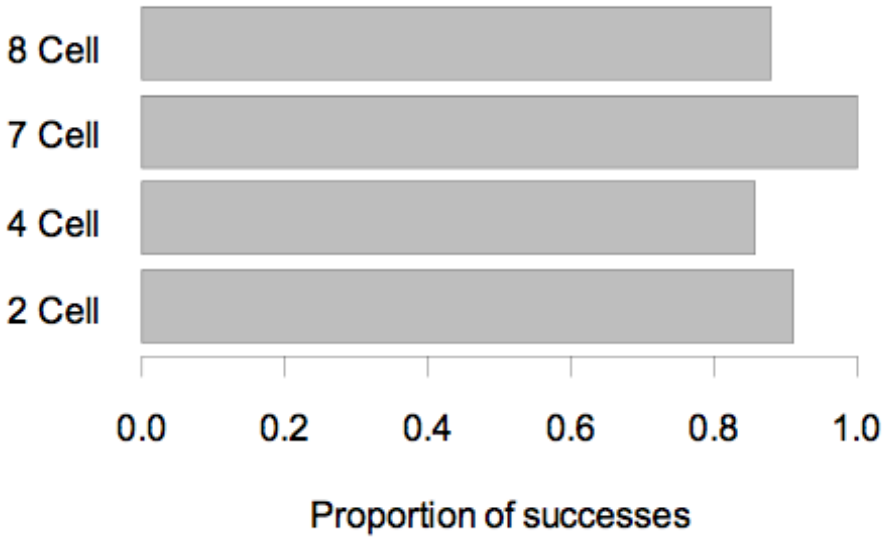

Figure 5.20: Proportion of successful amplification reactions per developmental stage of the embryo.

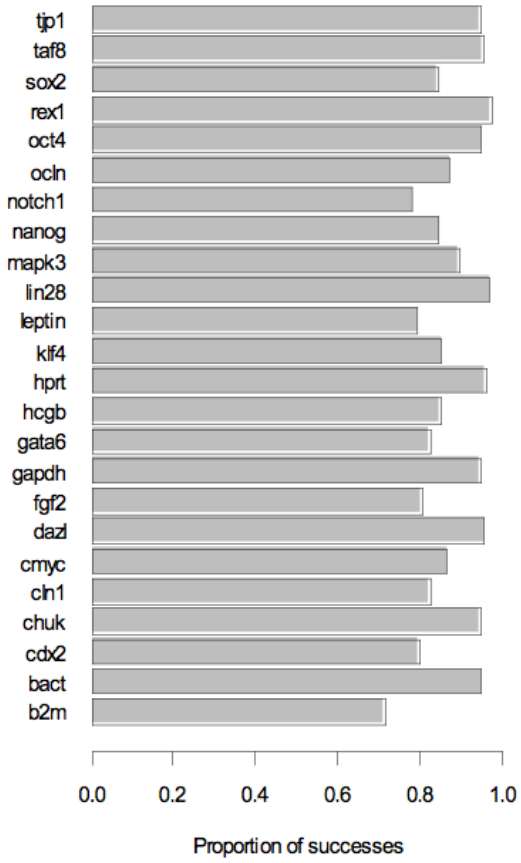

Figure 5.21: Proportion of successful amplification reactions per gene.

5.3.7.3 Data analysis of a single chip

The chip with high levels of replication of *GAPDH* against only four cell samples was assessed to provide an indication of within-chip variance. Figure 5.22 shows the cT values by location. In general, cT values were consistent for a given sample, with no visible evidence of trends across the chip. However, there was an indication of column, and perhaps also row, effects, visible as regular 'banding' across the chip. Failures appeared most often in whole rows or columns, possibly corresponding to mechanical failures in well loading during the Integrated Fluidic Circuit (IFC) controller steps. Possible outliers could be seen by colour anomalies, such as the well at row 24, column 2 in Figure 5.22. The water sample at row 22 shows high cT values indicating apparently successful amplification. However, the water row was a requirement as a loading reference rather than as a control.

For subsequent analysis of single-chip performance, rows 20, 22 (water), 25, 26, and 44 and column 30, all of which showed visibly anomalous results in Figure 5.22, were removed prior to analysis. Remaining outliers identified on the basis of extreme linear model residuals (Row 5 column 1, Row 23, column 2, coinciding with those identified by colour inspection) were also removed.

Analysis of variance (ANOVA) was applied as a preliminary check on the sizes of the different effects. The model assumed *row* nested in *sample* (cell), *sample* nested in *embryo* and *column* as a main effect only. The resulting ANOVA table is shown as Table 5.12. As all effects were random and some were nested, simple comparisons of mean squares with the residual term was not appropriate except for the row and column effects. The F statistics and corresponding p-values were therefore recalculated as follows: embryo was compared with sample mean square, sample was compared with the row mean square, and all others were compared to the residual mean square.

Analysis of the data revealed a small residual mean square, which corresponded to a residual standard deviation of approximately 0.2 cycles. However, the row and column mean squares were substantially larger, implying that these effects were important in explaining the variation between technical replicates. The corresponding p-values indicated that the row and column effects were very strongly significant.

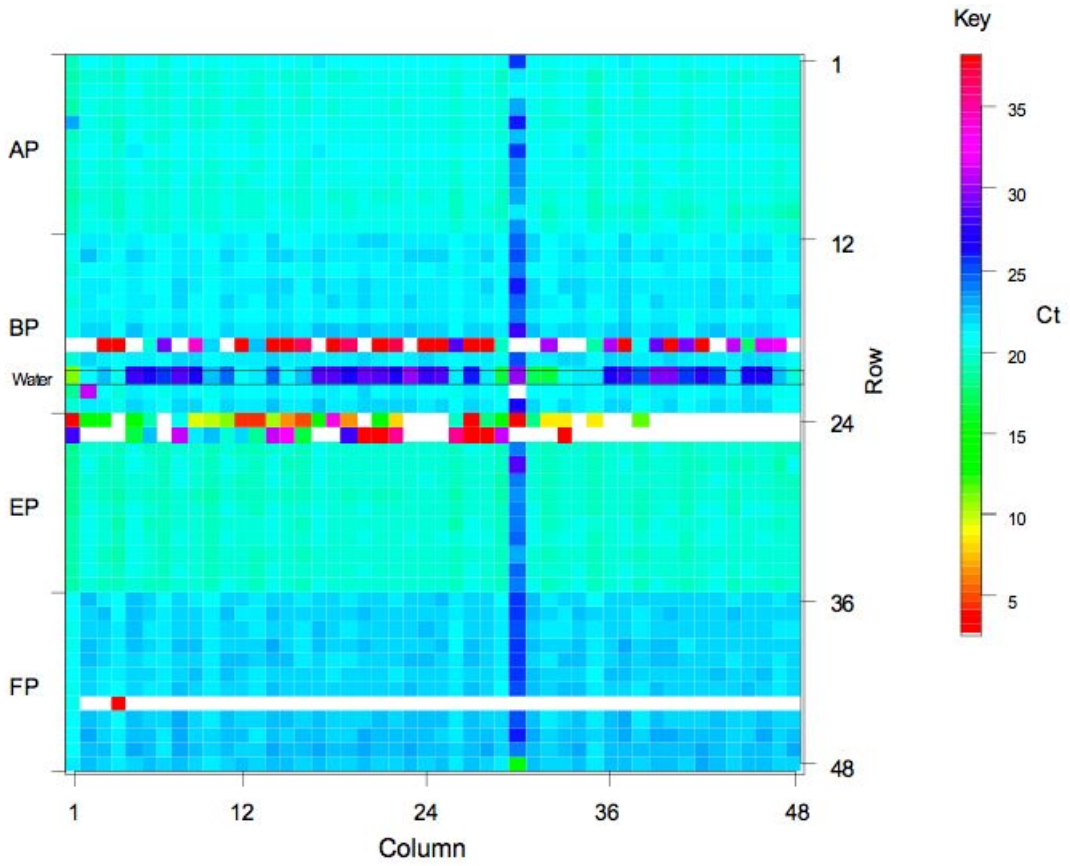

Figure 5.22: Replicated *GAPDH* assay. Colours show observed cT on four test samples (AP, BP, EP, FP), each a single cell. AP and BP were two cells from a single two-cell embryo; EP and FP two cells from a single two-cell embryo from a different donor. Rows correspond to sample aliquots; columns to the column ID for the chip. White squares indicate missing values (usually due to amplification failure). A water sample was included at the position shown.

Table 5.12: ANOVA table for the replicated *GAPDH* assay. Df; degrees of freedom, Sum Sq; sum of the squares, Mn Sq; mean square, NS; not significant, VSS; very strongly significant.

Effect	**Df**	**Sum Sq**	**Mn Sq**	**F value**	***p* value**	**Significance**
Embryo	1	14.5	14.52	0.02	0.9	NS
Embryo:Sample	2	1388.7	694.35	346.21	<2x10e-16	VSS
Embryo:Sample:Row	39	78.2	2.01	69.6	<2x10e-16	VSS
Column	46	209.1	4.55	157.74	<2x10e-16	VSS
Residuals	1930	55.6	0.03			

The embryo mean square was much smaller than the sample mean square and therefore did not contribute significantly to the variance; the associated p-value shows no statistically significant effect for embryo in this experiment. However, there was a very large sample mean square, again very strongly significant, indicating that the between-cell variation was probably a dominant effect.

Since all the effects were random, variance components are appropriate measures of the relative sizes of the effects. Variance components were estimated using mixed effects modelling. The model assumed *row* nested within *sample*, and *sample* nested in *embryo*; column was included as a main effect only, and was crossed with embryo, row and sample. Outliers identified above were omitted. Modelling used restricted maximum likelihood estimation to provide reliable variance estimates. The variance components for the replicated *GAPDH* assay are plotted in Figure 5.23. The sample (cell) effect was clearly the largest. Row and column effects, with standard deviations of 0.21 and 0.33 cycles respectively, were broadly similar to the residual term at 0.17 cycles, and the embryo effect was negligible.

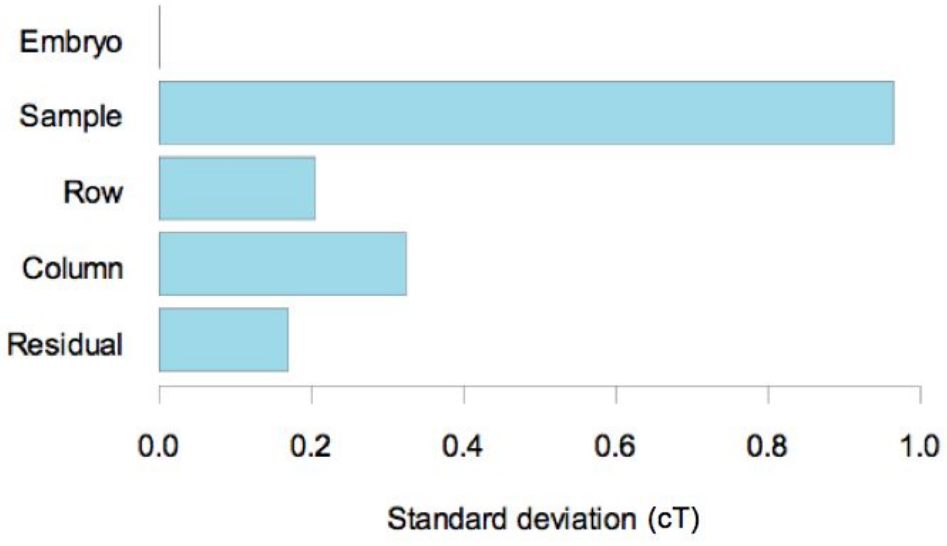

Figure 5.23: Variance components extracted by restricted maximum likelihood estimation and expressed as standard deviations in units of cycles.

5.3.7.4 Data analysis of multiple chips

Following analysis of within-chip variance, the complete data set from the seven multi-gene assay arrays was analysed by chip and by developmental stage. Figure 5.24 shows the assay data by gene and chip number. Figure 5.25 shows the assay data by gene and developmental stage.

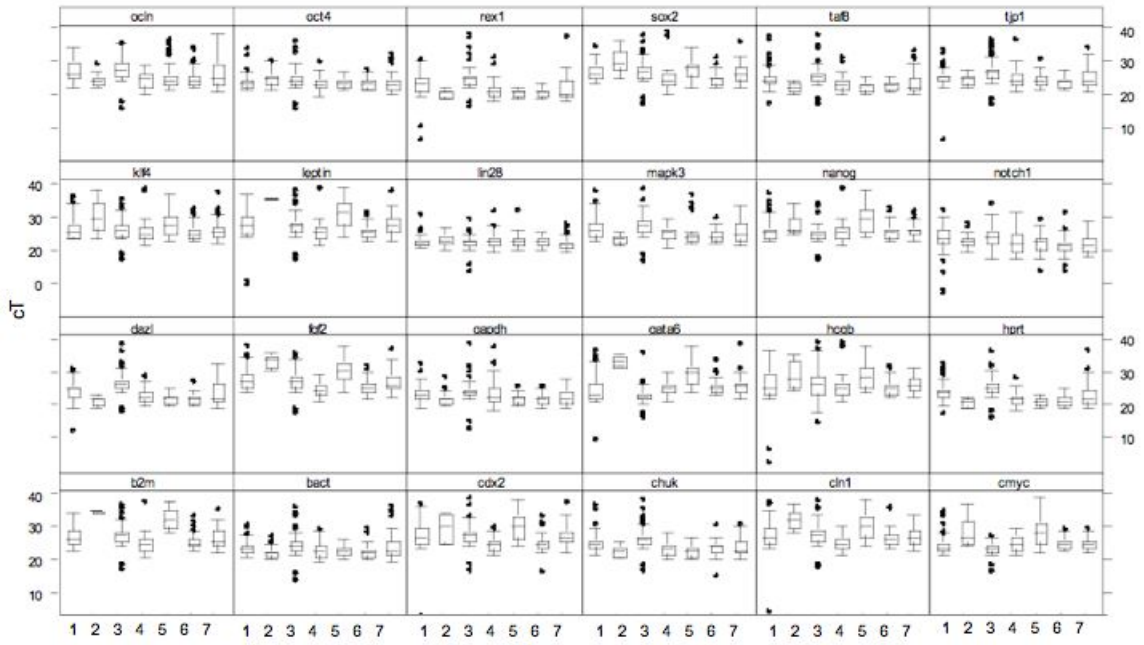

Figure 5.24: Multi-gene assay data by chip and gene. The figure shows cT response for all chips plotted by gene (y-axis) and chip number (x-axis).

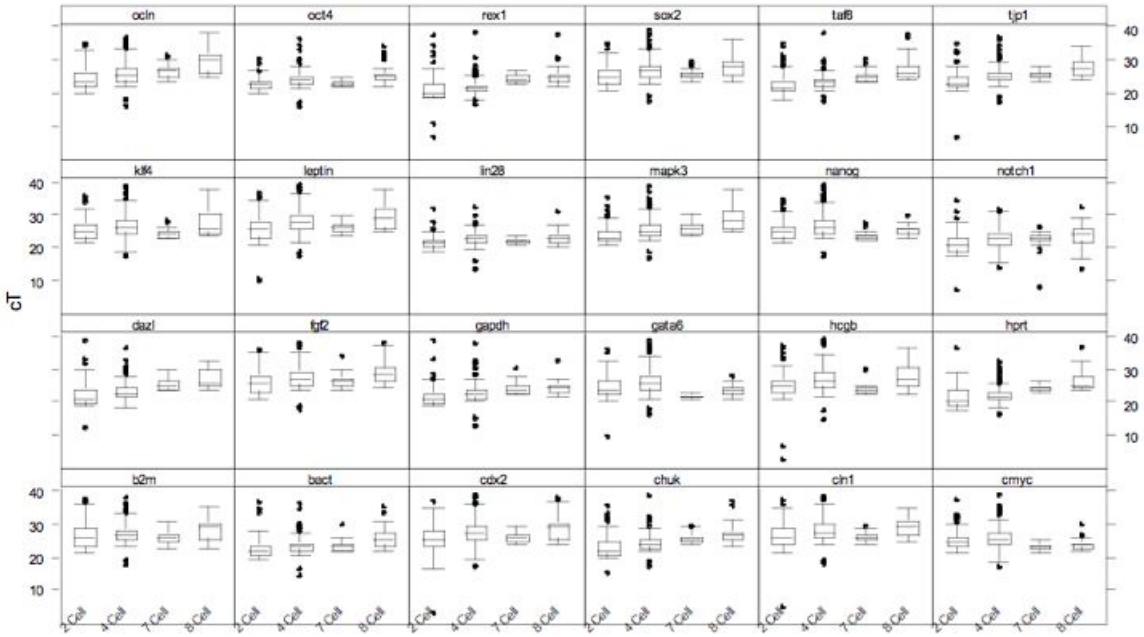

Figure 5.25: Multi-gene assay data by development stage of the embryo and gene. The figure shows cT response for all chips plotted by gene (y-axis) and development stage (x-axis).

Contributions to dispersion across multiple chips were assessed by mixed effects modelling using restricted maximum likelihood estimation. The model took development stage as a fixed effect, chip as a random effect, and treated donor, embryo and cell as nested random effects. The variance components for each gene are listed in Table 5.13, expressed as standard deviation in cT response. The median of the variance components is included to provide an indication of relative importance.

Table 5.13 shows that donor and embryo effects were small or negligible for most of the genes studied. The dominant effects were, in approximately decreasing order of importance, residual variance, between-chip variance then between-cell variance. Some genes showed high residual variance due to outliers, but the impact was modest; variance components did not change relative order on eliminating extreme values.

Comparison with the single-chip data in section 5.3.7.3 revealed substantially greater within-chip standard deviation (based on the median residual standard deviation of 2.3) for the multiple-chip experiment than for the single-chip experiment, for which the within-chip residual standard deviation was found to be approximately 0.2 cycles.

Table 5.13: Variance components by gene expressed as standard deviation for cT response. Cell was considered nested within embryo, in turn nested in donor. Chip was partly crossed with donor/embryo/cell; all cells appear on at least two chips but not all cells appear on all chips. For all the genes listed, group sizes were: Cell: 67; Embryo: 18; Donor: 8; Chip: 7 except for *B2M*, for which only 66 cells showed valid cT. The total numbers of individual observations for each gene is listed in the final column of the table. The median standard deviation is included to provide an indication of relative importance.

Gene	**Cell**	**Embryo**	**Donor**	**Chip**	**Residual**	**Number**
B2M	1.2	0	0	3.4	2.7	322
ACTB	0.9	0	0	0.8	2.3	428
CDX2	1.6	0	0	2.4	3	359
CHUK	0.8	0	0.4	1.4	2	427
CLN1	1.2	0	0	2.7	2.9	371
CMYC	0.9	0.9	0.5	2	2.1	390
DAZL	0.9	0	0	1.9	1.8	431
FGF2	1.3	0	0	3.4	2.5	362
GAPDH	0.9	0	0	1	2.2	410
GATA6	0.9	0.8	0.5	3.4	2.4	371
HCGb	1.6	0	0	1.6	3.3	383
HPRT	1	0	0.4	1.7	1.7	433
KLF4	1.3	0	0.7	1.9	2.8	385
LEPTIN	1.4	0	0	2.8	3.1	358
LIN28	0.9	0.5	0.5	0.4	1.5	437
MAPK	1.6	0	0	1.1	2.3	404
NANOG	1	0	0.1	1.8	2.6	382
NOTCH1	1.1	0	0	0.9	3	352
OCLN	1.7	0.6	0.4	0.9	2.7	393
OCT4	1	0	0.7	0.6	1.7	428
REX1	0.8	0	0.3	1.8	2	438
SOX2	0.9	0	0	2	2.6	380
TAF8	1.2	0	0.9	1.2	1.8	430
TJP1	0.8	0	0.5	1.2	2.2	427
Median	1	0	0.1	1.7	2.3	

5.3.7.5 Gene expression changes with development

Tests for the significance of development stage effects were complicated by two issues. First, the presence of crossed random effects influenced the estimation of p-values from models; p-values for complex, unbalanced random-effects models can be unreliable and may be optimistic. Second, cells for the later developmental stage (7/8 cell) were run on only two chips. This made it necessary to allow for the random chip effect in comparisons involving the 7/8-cell stage to avoid confusing chance chip effects with the effects of development stage on measured cT. The following strategy was therefore adopted. First, the significance of changes in cT with developmental stage was assessed for the 2-cell and 4-cell chips. Since all the cells from the 2-cell and 4-cell stage were studied on all of five chips the 2/4-cell experiment could be treated approximately as a blocked experiment with chip as the blocking factor. The analysis used mixed effects modelling with *donor*, *embryo* and *cell* as nested random effects; and *chip*, *gene* and *developmental stage* as fixed effects, with a gene:development stage interaction included. Array 1131094093 was excluded as having a high failure rate, though reanalysis including this array made no practical difference to the results. The initial analysis for differences between the 2-cell and 4-cell stage therefore used arrays 1131094094-7. The resulting analysis of deviance is shown in Table 5.14. The data showed that all the main effects were very strongly significant, while the interaction term was marginally significant. The implication is that while there was a marked change in cT in development stage across all genes, there was only marginal indication of differential change between the 2-cell and 4-cell development stages.

Table 5.14: Significance of effects on cT at the 2- and 4- cell stage analysed as a mixed-effects model. numDF; degrees of freedom for the fixed effect, denDF; density degrees of freedom for the random effect against which the fixed effect is tested.

Effect	**numDF**	**denDF**	**F-value**	***p*-value**
Chip	3	5526	127.22	<0.0001
Gene	23	5526	89.17	<0.0001
Devstage	1	9	29.13	0.0004
Gene:Devstage	23	5526	1.5	0.0602

The 2/4-cell analysis was followed up by analysis of the whole data set, covering the 2-, 4- and 7/8-cell stages. Since the 7/8-cell samples were run on only two chips, this necessitated analysis using a mixed effects model with chip treated as a random effect (treatment as a fixed effect does not affect significance of other effects in a blocked experiment as above, as all important comparisons are made within each chip). The resulting analysis of deviance is shown in Table 5.15.

Table 5.15: Analysis of deviance for a mixed-effects model for all developmental stages, in which chip, gene and development stage (Devstage) were taken as fixed effects, and chip, donor, embryo and cell as random effects with the latter nested in the order donor/embryo/cell.

Effect	**DF**	**Sum Sq**	**Mean Sq**	**F-value**
Devstage	3	172.6	57.5	7.9
Gene	23	29363.9	1276.7	174.3
Devstage:Gene	69	5123.7	74.3	10.1

The table does not include an indication of significance, because the distribution of the calculated F-value is not well understood, and the degrees of freedom for the associated random effects also unclear. However, the analysis includes seven arrays and the between-chip effect is generally larger than donor or embryo effects. Taking 6 degrees of freedom for the F-value denominator degrees of freedom returns a p-value of 0.004 for F=10.14 and 69 degrees of freedom for the numerator. Provisionally, therefore, there was significant differential expression across the range of development stages.

Profile changes were examined using principal components analysis (PCA). PCA is an exploratory technique which is effective for identifying clustering or other structure in data sets. In the present context, principal components represented changes in gene expression profile, so objects close together in PC space had similar expression profile and objects far apart had different profiles.

Initial studies showed that PCA results were dominated by the comparatively strong between-chip and cell variances. The data were accordingly standardised (normalised) by chip by subtracting the median for the chip and dividing by the median absolute deviation estimate of standard deviation (to minimise outlier effects on standardisation). The data were then reduced by taking cell medians across

chips, again to minimise outlier impact, and PCA applied to the resulting median cT for each gene and cell. The scree plot in Figure 5.26 shows that the first two principal components (PC1 and PC2) accounted for approximately three quarters of the variance. The results were subsequently compared with PCA using data standardised by housekeeping genes only, with no material change to the PCA results.

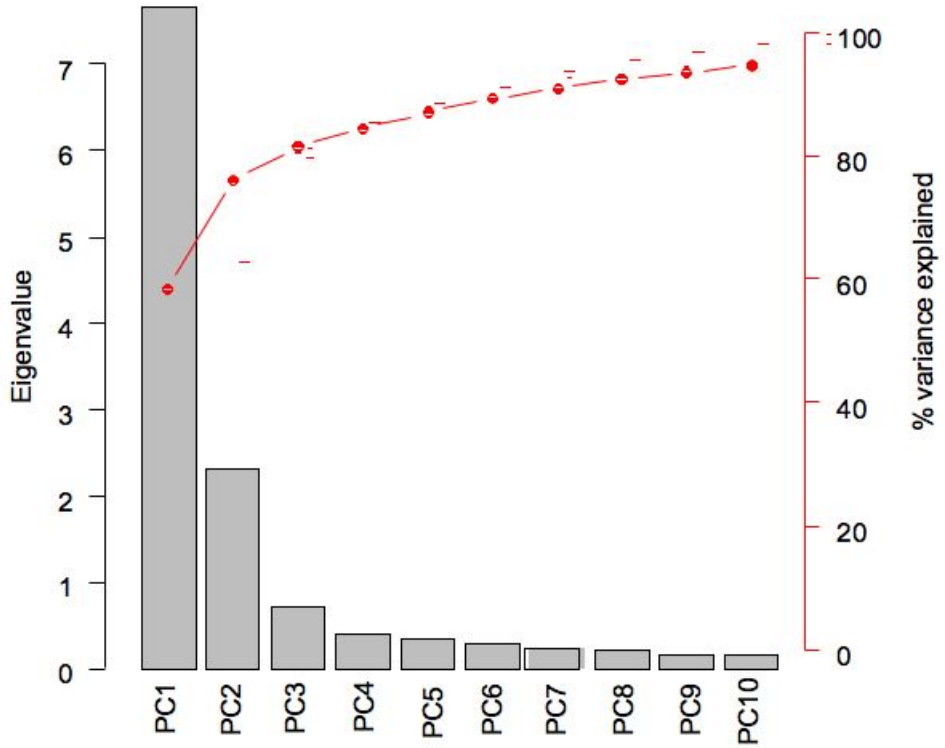

Figure 5.26: Scree plot showing that the first two principle components (PC1 and PC2) accounted for approximately three quarters of the variance of the entire data set standardised by chip.

Figure 5.27 shows a biplot of individual cell scores on PC1 and PC2, together with the direction of changes in cT for each gene (arrows). Cells are labelled according to development stage.

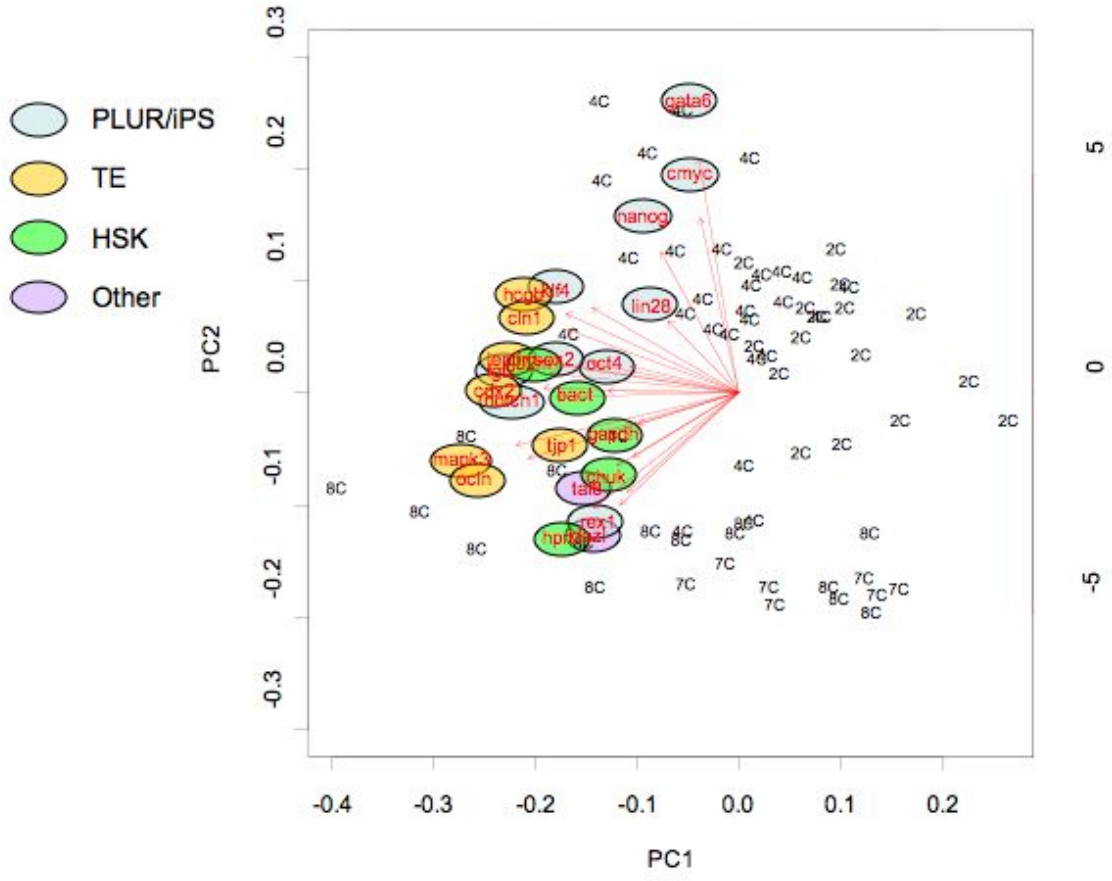

Figure 5.27: Scores for the first two principal components for individual cells (labelled by developmental stage). Arrows show the direction of changes in cT for each gene in PC coordinates. Coloured ellipses denote nominal gene function as shown in the key.

The loadings plots for the PCA analysis are shown in Figure 5.28. These show clearly that in PC1, essentially all the genes changed cT value together (and negatively with increasing PC1); PC2, by contrast, shows strong differences in expression between genes. PC1 was therefore associated with an overall change in cT response; PC2 with differential changes.

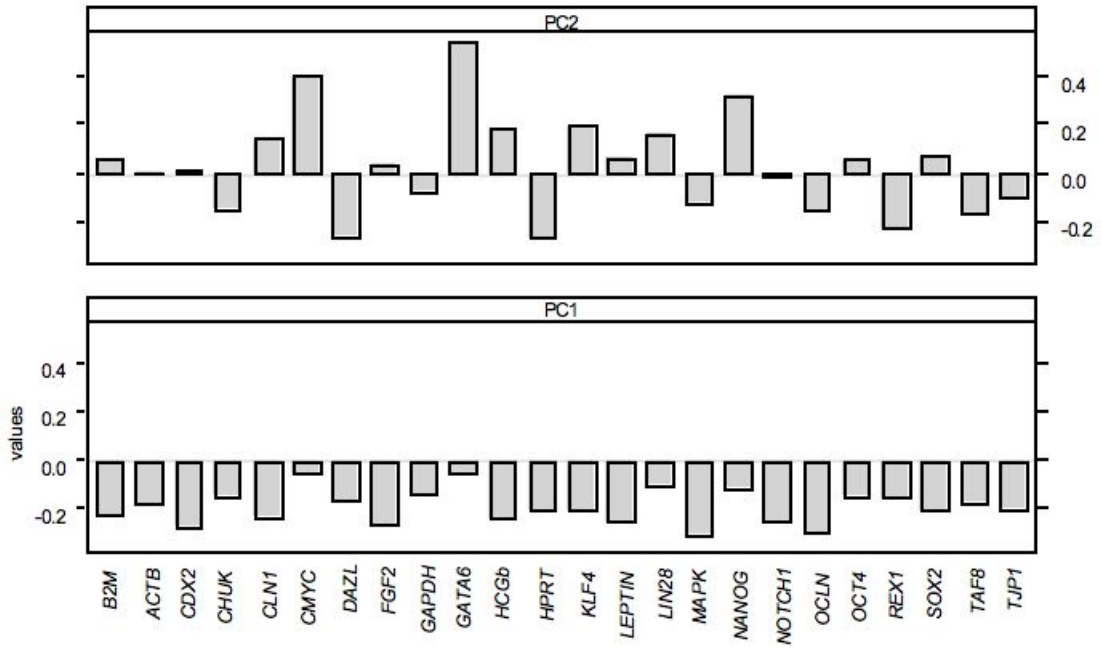

Figure 5.28: Principle components analysis loadings for PC1 and PC2. PC1 was associated with an overall change in cT response, whereas PC2 was related to differential changes.

In order to assess between-cell differences by embryo, systematic profile groupings within embryos were analysed. Plots of principal components scores for cells in each embryo are shown in Figures 5.29 and 5.30. No consistent grouping structure was evident for either of the first two principal components. This was essentially as expected given that residual variation was at least as large as between-cell variation; random effects on individual cell cT responses may therefore mask underlying structure of the same order of magnitude.

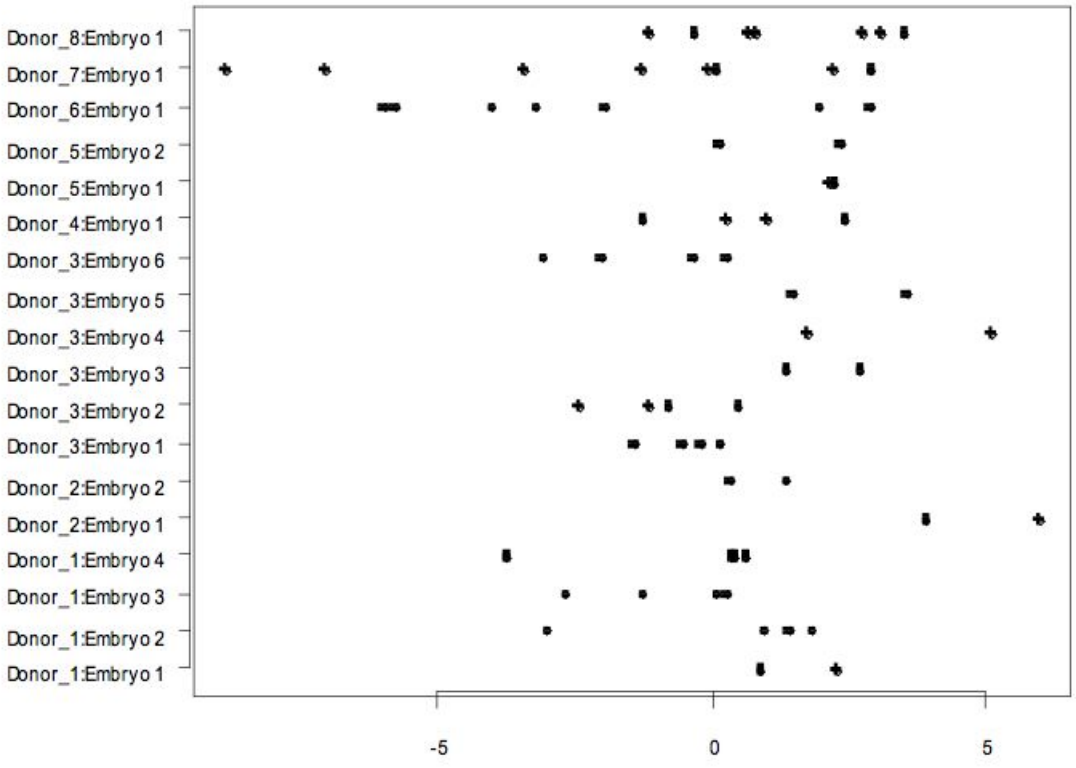

Figure 5.29: Principle component scores for individual cells grouped by embryo for PC1.

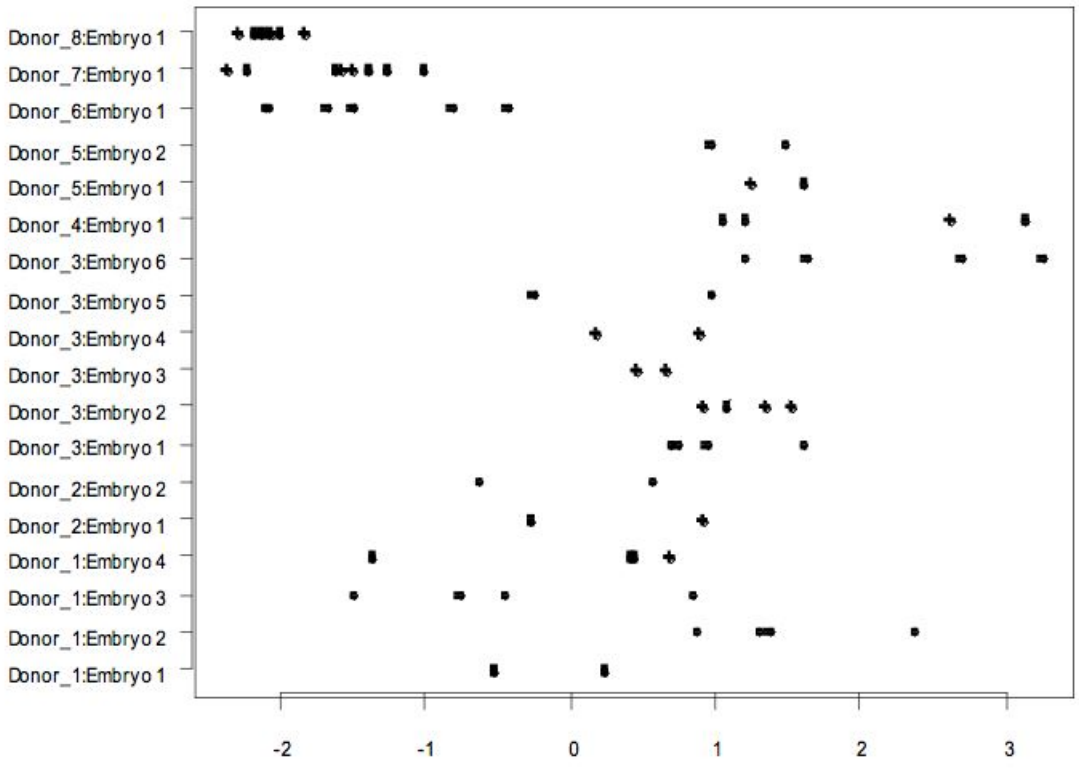

Figure 5.30: Principle component scores for individual cells grouped by embryo for PC2.

The individual variance scores for the embryos were calculated in order to see if there was any suggestion that the variance increased with developmental stage. These are shown in Table 5.16. The 2- and 4-cell embryos all showed variances broadly between 0-5, whilst the 8-cell embryos had variance scores of 13 and 18, indicating that between-cell differentiation of the target gene expression had taken place by this developmental stage. However, as the 7-cell sample had a variance of 3, and only two 8-cell embryos were analysed, no firm conclusions could be drawn at this stage.

Table 5.16: PC1 variance scores per embryo

Sample	**Cell number**	**Variance**
Donor 8 Embryo 1	7	3.25
Donor 7 Embryo 1	8	17.88
Donor 6 Embryo 1	8	12.51
Donor 5 Embryo 2	2	2.51
Donor 5 Embryo 1	2	0.01
Donor 4 Embryo 1	4	2.37
Donor 3 Embryo 6	4	2.35
Donor 3 Embryo 5	2	2.18
Donor 3 Embryo 4	2	5.57
Donor 3 Embryo 3	2	0.88
Donor 3 Embryo 2	4	1.45
Donor 3 Embryo 1	4	0.44
Donor 2 Embryo 2	2	0.53
Donor 2 Embryo 1	2	2.05
Donor 1 Embryo 4	4	4.45
Donor 1 Embryo 3	4	1.84
Donor 1 Embryo 2	4	4.97
Donor 1 Embryo 1	2	0.94

5.4 Discussion

Optimal human embryo development *in vitro* has been established as reaching the mid-stage of development to 2 cells by 31-35 hours post insemination, 4 cells by 47-51 hours, 8 cells by 63-67 hours, 16-32 cells that compact 78-99 hours post insemination and cavitation to blastocyst with over 100 cells by 110-116 hours (Edwards & Brody, 1995). However, the point at which preimplantation cells lose their totipotent potential is still unknown. The regulative capacity of early embryos enables overtly normal development following perturbations in organisation such as cell loss. Whether patterning information is intrinsic to the oocyte, zygote or a result of sperm entry, it has been suggested that partitioning of this information during typical cleavage results in three distinct types of blastomere (Edwards & Beard, 1997; Gardner, 2002). The significance of the differential inheritance can be assessed both by testing the developmental potential of the individual blastomeres and by investigating the gene expression profile at each division. Disaggregating early cleavage blastomeres and culturing each one individually, whilst inevitably placing some degree of duress on the cells, allows each cell to be studied in isolation. Understanding totipotency during development will have a great impact on the current knowledge of development, the derivation of hESC, and cell loss by fragmentation, cryopreservation, and PGD.

5.4.1 Isolated blastomere development

Thawing pronuclear stage embryos, culturing for the required time, using protease to remove the zona and gentle pipetting in calcium and magnesium-free HEPES proved a robust method to obtain viable individual blastomeres for study. One report describes an approximate 46% development rate to 8 or more cells on day 3, 34% compaction rate on day 4 and a 44% cavitation rate on day 5 (Van Landuyt *et al.*, 2005). The data are not directly comparable as embryos for the experiments presented here were selected on the day of disaggregation and therefore likely to be of an overall higher quality than a non-selected group. A general judgment however reveals that the capacity for overtly normal timed development of single isolated blastomeres was as least as good as that for unselected whole IVF embryos.

The development of each blastomere was tracked so that the behaviour of sister cells could be compared. Not all four sister cells always continued development *in*

vitro, either not dividing, not compacting, or not forming blastocyst-like structures. The arrest of blastomeres at each stage could be due to damage by manipulation, the probable transient stress caused by zona removal and disaggregation, or the absence of any protective function that the zona might perform during development, particularly from sub-optimal components of the culture system (Fleming *et al.*, 1987). In addition, impaired development could also be due to the loss of normal cell-cell signalling, particularly as the majority of divisions resulted in 2D cell clusters before compaction and then progressed three-dimensionally, whereas normal development proceeds in 3D due to the confines of the zona. Culturing the single cells in donor zona pellucidas might increase the developmental success of these cells, as shown in mouse experiments (Illmensee *et al.*, 2006).

A number of blastomeres completed the mechanics of development, i.e. they compacted or cavitated, but with severely reduced cell numbers. In some cases cavitation could be seen in a 2-cell blastomere cluster on D2+3, when further cell division had failed. In mouse embryos cleavage at the 2- or 4- cell stage can be artificially arrested for a number of hours by several agents, such as cytochalasin D or colcemid. Cytokinesis does not resume when the agent is removed, but the embryos compact and then cavitate with the same timing as untreated embryos to form blastocyst-like vesicles consisting of only two or four highly polyploid cells (Pratt *et al.*, 1981). This is suggestive of the existence of an 'embryological clock' that regulates development by time rather than the number of cell divisions. Monitoring the passing of time has been suggested to be by either cyclic or sequential mechanisms linked to various features of the cell cycle - a 'clock', or linear increases or decreases in a factor - a 'hourglass' (Johnson & Day, 2000). Cyclic oscillations in K^+ channel activity, which parallel cell cycle and circadian rhythms, have been suggested as involved in the timing mechanism (Day *et al.*, 2001). The isolation of the blastomeres did not interfere with division timing, suggesting that each individual cell has a mechanism for monitoring the timing of development, rather than some master cell control. Similarly zygotic genome activation has been shown to be regulated by time following fertilisation rather than by progression through the cell cycle in the mouse (Poueymirou & Schultz, 1987). Failure of genome activation was therefore unlikely to occur solely due to blastomere isolation. The cleavage arrest observed in

some clusters was therefore not necessarily a result of failure to initiate embryonic transcription.

Some cells showed evidence of nuclear division in the absence of cellular division, with the appearance of two nuclei on D2+1 in a one-cell blastomere. As polyploid cells can be generated following artificial cleavage arrest (Pratt *et al.*, 1981; Surani *et al.*, 1980) cyto- and karyo-kinesis can occur independently of each other. In the absence of cell division or normal intercellular interactions, DNA can be replicated with the same timing as in normal embryos. Whether it was damage to the cytoskeleton of these cells during manipulations, loss of cell signalling, or reduced developmental competence that caused division to fail is unknown. These cells did not resume development nor attach to the feeder layer and eventually degenerated in culture. The simple explanation for some cellular arrest could be that the results presented here reflect normal *in vitro* development as observed in the IVF laboratory, in that not all embryos are of good quality or progressive, with only around 14% of IVF embryos developing into top quality blastocysts by day 5 (Van Landuyt *et al.*, 2005).

5.4.2 Isolated blastomere potential

In normal development each blastomere of the eight cell embryo acquires clear apical and basolateral domains. Polarity is retained during division to 16 cells so that depending on the orientation of division with respect to the polar axis, either two polar cells (conservative division) or one polar and one apolar cell (differentiative division) result (Figure 5.3). Which way a blastomere divides is not determined randomly since in mice early dividing cells tend more frequently to divide differentiatively, and hence contribute proportionately more cells to the ICM than later dividing cells as a consequence of their more extensive intercellular contacts (Surani & Barton, 1984). Later dividing cells divide conservatively more frequently, and therefore the ratio of polar cell (TE) to apolar cells (ICM) is maintained (Fleming, 1987). The correlation with division type and polarity has been shown to be in excess of 80% as defined by surface microvilli distribution (Pickering *et al.*, 1988). Subsequently the *intercellular* components of compaction (cell flattening, increase in intercellular contact and the formation of epithelial cell junctions) are primarily associated with formation of the fluid transport system and blastocoel generation (Watson, 1992). The *intracellular* component of polarisation is associated with directing lineage segregation to TE and

ICM (Johnson & Ziomek, 1981b). These components of compaction can be dissociated from each other (Pratt *et al.*, 1982), and form a hierarchy of sensitivity to external influence, of which polarisation is the least disturbed by any treatment.

Disaggregation clearly affects cell-cell apposition as the number of cells in the clusters is reduced from that of normal embryo development. This in turn is likely to affect flattening and junctional formation, and ultimately cavitation. Polarisation on the other hand, is likely to occur, albeit not necessarily as normal (Pratt *et al.*, 1982). Indeed, when mouse 4-cell blastomeres are isolated and cultured individually to pairs, the polar region of the cell surface is approximately twice that of intact embryos (Pickering *et al.*, 1988) presumably arising from a lack of intercellular contacts. A consequent lower incidence of differentiative divisions from isolated pairs of cells could be predicted, as the greater the region of polarity, the more likely that a division, however orientated, will bisect it. This would result in cell clusters with fewer numbers of apolar cells - the future ICM. In order to assess whether reduced differentiative division occurred from isolated single blastomeres, the pattern of division was monitored and scored if unambiguous. For hESC derivation, it was hypothesised that those single blastomeres that completed two rounds of differentiative division to produce the maximum apolar cells would have the highest potential for successful derivation.

When the division patterns of isolated pairs of mouse blastomeres were analysed, 95% of divisions were unambiguous (Pickering *et al.*, 1988). The division of human cells was far less consistent, a category was only assigned for 19 blastomere pairs (15%). As predicted, only 4/19 of these cell clusters had completed two rounds of differentiative divisions to give rise to the maximum apolar cell content, whilst 13/19 completed two conservative divisions to produce only polar cells. Further analysis is needed given the high rate of ambiguous divisions. Nevertheless this is likely to have had an effect on the derivation outcome.

Lack of developmental potential could also have contributed to the failure of derivation. As well as assessing the morphology of development, expression of lineage-specific markers was analysed. Initially a TE lineage marker in concert with an ICM marker was desired for the staining experiments. In mice, Cdx2 is expressed in the nascent TE from the late morula stage and is tightly restricted to the TE lineage, especially in its proliferating population (Beck *et al.*, 1995). Cdx2 is initially

co-expressed with Pou5f1 and they form a complex for the reciprocal repression of their target genes in ES cells (Niwa *et al.*, 2005). The association of Pou5f1 with the pluripotent cell type has been well established in the mouse (Pesce & Scholer, 2001; Yeom *et al.*, 1996). During the pre-implantation period, a residual cytoplasmic maternal Pou5f1 expression is found in unfertilised oocytes and in subsequent cleavage stages (Palmieri *et al.*, 1994). Embryonic Pou5f1 expression is initiated at the 4-8 cell stage and is concomitant with an abundant expression in the nuclei of all blastomeres. At initiation of blastocyst formation, Pou5f1 is down-regulated in the TE and becomes restricted to the ICM (Mitalipov *et al.*, 2003) where it is required for the maintenance of the pluripotent state (Nichols *et al.*, 1998).

However, in human development the story is not so clear. Human oocytes and cleavage stage embryos reveal a variable POU5F1 expression pattern with a pure cytoplasmic localisation of the protein. During compaction, the variability in expression is reduced, indicating embryonic POU5F1 expression. The protein appears in the nucleus implying biological activity (Cauffman *et al.*, 2005b). In blastocysts, POU5F1 transcripts and proteins are present in the ICM and the TE revealing that it is not restricted to pluripotent cells (Cauffman *et al.*, 2005b; Hansis *et al.*, 2000; Huntriss *et al.*, 2004). However, subsequent work has discriminated between the POU5F1-iA and -iB isoforms, and shown that the stemness properties are attributed to the -iA isoform only as this is expressed by hESC (Cauffman *et al.*, 2006). Despite this distinction, POU5F1-iA positive cells could still be seen in the TE, implying that this isoform cannot sustain pluripotency alone, but probably functions in concert with other factors. In addition the ICM cells of human blastocysts, unlike those of mice, retain the ability to generate TE cells, as hESC can differentiate down this lineage either spontaneously through embryoid body formation or following the addition of bone morphogenetic protein 4 (Xu *et al.*, 2002). CDX2 transcripts are not detected in humans until the blastocyst stage (Kimber *et al.*, 2008), and therefore this marker is expressed too late in development for this experiment. Leptin and STAT3 have been shown to be expressed at higher levels in the TE than ICM (Antczak & Van Blerkom, 1997), but were used as markers of polarity rather than of lineage. Functional markers of TE such as CLDN1, OCLN and ZO-1 can be visualised from the blastocyst stage, but are generally variable and weak in the human, and dependent on blastocyst quality (Ghassemifar *et al.*, 2003; Sheth *et al.*, 1997).

A definitive marker pair for both the ICM and TE could not therefore be identified for early day 4 and 5 human blastomere derived cell clusters. Instead two markers indicative, although not completely exclusive to, the ICM lineage were used; POU5F1-iA and NANOG (Van de Velde *et al.*, 2008). *NANOG* transcripts have been detected in the pronucleate human embryo, and then from the eight-cell stage onwards (Kimber *et al.*, 2008), although the protein is not detectable until the blastocyst. NANOG is expressed in both human and mouse ESC and down-regulation leads to significant down-regulation of POU5F1 and loss of hESC cell-surface antigens (Hyslop *et al.*, 2005). Whilst expression was not expected in the D2+2 clusters it was possible that some cells might have been positive for this marker by D2+3.

Low expression of NANOG was seen at D2+3; only 2 cells were positive in total. This is reflected by whole embryo data when NANOG expression is most evident in the ICM of expanded day 6 blastocysts (Hyslop *et al.*, 2005). However, the greater loss of POU5F1-iA by this stage as compared to D2+2 suggested an overall loss of stem cell potential. While D2+2 clusters had an average of only 6.5 cells compared to 12.2 at D2+3, 50% of the D2+2 clusters consisted of cells all positive for POU5F1-iA compared to only 15% at D2+3. It was therefore decided to plate the cell clusters onto MEFs and therefore into conditions conducive to derivation at the earlier stage of D2+2.

5.4.3 Medium selection and exchange

KOSR conditioned by 24 h or 48 h contact with both MEF and HFF feeders, with and without hESC was analysed to determine the most suitable conditioned medium (CM) for single cell derivation attempts. Regardless of feeder type, the presence of cells, or the time in incubation, the levels of substrate remained in excess in the collected CM. The lactate and ammonium levels displayed a time-dependent relationship which was not affected by the presence of hESC colonies. When the cell conditions were averaged, there was an 50% increase in ammonium concentration from 24 h to 48 h culture on MEFs; from 0.23 mmol/L to 0.34 mmol/L. There was an even more marked difference on HFFs, with a greater than 70% increase from 0.14 mmol/L to 0.24 mmol/L. There was minute or no detection of lactate at 24 h for both feeders. On MEFs, there was also no lactate produced after 48 h of feeders alone, whereas 0.46 g/L was present when the hESC colonies were added.

On HFFs after 48 h culture, the lactate concentration had reached 0.54 g/L with and without hESC colonies. Based on these observations, CM was collected after 24 h incubation on MEF feeders, and a pooled batch created for use for all the derivation attempts. A further consideration in the feeder type choice was that ten derivation attempts on HFF had failed (section 4.3.5) and therefore the feeders were not validated for derivation, compared with seven lines successfully established on MEFs. As the reason for collecting CM was to obtain the unidentified factors secreted by the feeders that induce stem cell development from the ICM, the use of HFF feeders was judged to be inappropriate. In order to minimise the effect of toxic build-up but to maximise conditioning in derivation attempts, medium was prepared which was 50% fresh KOSR, 50% 24 h conditioned KOSR from MEF with hESC. This was used in all single cell derivation attempts. 50% of the medium in the microdrops was changed daily for the first 7 days, beyond which the feeding regime was tailored to the morphology of the cell culture.

Osmolality increased 2% from 326 mOsm/kg in KOSR, to 334 mOsm/kg after 24 h on MEFs with hESC colonies, and to 348 mOsm/kg (6% increase) after 48 h. Similar increases were observed on HFF and hESC colonies after 24 h and 48 h respectively. This rise could be attributed to evaporation, as it was generally not observed when KOSR was placed under oil. However it is not feasible to culture hESC under oil in wells due to the need for frequent media exchange, and the risk that oil would attach to the cells upon contact as the media was aspirated from under the layer. However evaporation of culture medium is a serious consideration when preparing microdrop dishes. 4 μL drops in air at 22°C have been shown to evaporate at 99 nl/min, resulting in 5% change in volume over 2 min and an increase in osmolarity of 5%, from 288 to 302 mOsm (personal communication, H. Leese). For this reason, each microdrop dish was prepared individually by adding the medium aliquots and covering them in oil immediately before preparing the next dish. It may be noteworthy that the common practice in IVF labs of distributing all the microdrops for the total number of dishes needed and then adding oil to them all at the end may be having a detrimental effect on *in vitro* culture of embryos.

The levels of substrates available in KOSR can be compared with the only published report where a medium has been designed for hESC derivation and culture and the formulation made freely available with the publication (Ludwig *et al.*, 2006).

In this medium, designated TeSR1, glucose was added at 2.5 g/L compared to 4.2 g/L in KOSR. TeSR1 contained 2.1 mmol/L L-glutamine, comparable to the 2.3 mmol/L in KOSR. No glutamate supplementation was made in TeSR1 compared to 0.13 mmol/L in KOSR. Furthermore, the optimum osmolality was determined experimentally as 350 mOsmol compared to 284±2 mOsmol for optimum embryo development, and measured on average at 326 mOsm/kg in KOSR. Compared to the use of KOSR, the lower glucose level in TeSR1 will reduce the lactate production during incubation, and the lack of glutamate and lower glutamine concentration will reduce the build-up of ammonium. However, these substrate levels are still far in excess of the estimated need of the ICM when placed directly in culture. There is a need for optimisation of the medium used for the first few days of derivation, when the cells are still considered embryonic. From derivation experiences, the earliest appearance of stem-cell like cells in the derivation of seven new lines was four days after plating, but the latest was fourteen. It could be argued that before the appearance of these cells, the culture conditions need to be optimised with the ICM in mind, and a gradual change to the higher substrate concentration/higher osmolality with time. The proliferation, and therefore need for metabolic substrates of newly-derived stem cells is far lower than when the line is established. From experience, passages 1 to 2 to 3 can be as far apart as 10 days each, and therefore there is no concern that with the feeding strategies commonly employed substrates would be limiting.

With the requirement for GMP grade facilities and cell culture consumables, it would be prudent to combine the search for xeno-free culture supplements with the optimisation of medium for derivation. The time, effort, and specialised manpower required to correctly run GMP facilities has led those with experience to comment that only those embryos with the greatest potential should be entered into the derivation program (personal communication, A. Coleman). In addition, the need is to produce high-quality hESC lines, not just any hESC lines. Clearly derivation efficiency is not solely about embryo quality, but also culture conditions and highlights the need for further consideration of the medium used.

5.4.4 Single blastomere derivation

Successful derivation of hESC lines from single blastomeres of 8-cell human embryos has been reported (Klimanskaya *et al.*, 2006). Whilst technically laudable, the

motives for the work were political, and therefore important scientific questions were overlooked. The developmental interest with the experiment is whether all eight cells are capable of forming pluripotent hESC, or whether some are already committed to a multipotent fate.

Taking isolated blastomere development into consideration the inherent chances of derivation from four-cell blastomeres is possibly lower than those from eight-cell embryos. Upon disaggregation, eight-cell blastomeres are likely to have an established polarity, which is then stable. Therefore, whilst subsequent manipulation may affect intercellular compaction and the ability of the clusters to cavitate may be compromised, segregation to produce both polar and apolar cells should proceed. In contrast, disaggregated four-cell blastomeres have not yet established polarity, and hence do so in the artificial environment of clonal culture. As discussed, this can result in abnormal polarisation, and a greater proportion of conservative divisions and hence fewer apolar cells destined to become ICM. As the efficiency of single eight-cell derivation was 2% (Klimanskaya *et al.*, 2006), it is not unreasonable that from 48 attempts described here, a line has not yet been established. However, the culture of stem-like cells to P3 is certainly encouraging, and efforts will continue with this approach.

Initial plating experiments in which the isolated blastomeres were placed immediately onto feeder layers were unsuccessful, with only 13% of cultures attaching, all of which had degenerated by day 5 after plating. In contrast, when the blastomeres were kept in sequential culture until D2+2 and then plated, 60% of the cell cultures attached, 23% produced outgrowths with stem-like cells visible, and 6% proliferated sufficiently to be passaged. Four of these colonies containing stem-like cells were from the same embryo, suggesting, but by no means proving, that all cells at the four cell stage have pluripotent potential. Of the eleven cultures with stem-like cells, one cell culture was assumed to have completed two conservative divisions following isolation and three appeared to have completed two differentiative divisions. Of the remaining, five clusters consisted of greater than four cells, and the final two were four cells but unclassifiable. Whilst the number cultures was low, the results imply that differentiative divisions may enhance derivation potential, as well as the plating of higher cell numbers.

While undertaking these experiments, a report was published confirming that single blastomeres from a 4-cell human embryo could develop autonomously into blastocyst-like vesicles one quarter the size of regular blastocysts (Van de Velde *et al.*, 2008). In one from six disaggregated embryos, all four blastomeres formed blastocyst structures by day six of development that contained cells positive for nanog. Subsequently the same group successfully derived two hESC lines from isolated four cell blastomeres, although one was karyotypically abnormal (Van de Velde *et al.* 2008, manuscript under revision). One of the lines was generated from a cell that underwent two differentiative divisions producing a linear arrangement of cells (Van de Velde, personal communication). The morphology of the other blastomere at D2+2 was unknown. The methods used by this group were similar to those presented here, although four well plates were used rather than microwells. The group attribute their success, at least in part, to the use of fresh donated gametes to produce top quality cleavage embryos for the derivation attempts. Subsequently, a hESC line from a single blastomere of a cryopreserved embryo was reported (Feki *et al.*, 2008). These successes prove that derivation is possible, but until hESC lines are derived from all four blastomeres, no conclusions can be drawn that all cells are equally pluripotent or plastic. Any potential factor(s) relating to lineage decisions and derivation potential that could become differentially distributed during early cleavage divisions should not necessarily be thought of as determinant however. This is because blastomere fate remains flexible and development is regulative in the cleavage stages.

5.4.5 Single blastomere gene expression

Taking the cleavage-driven hypothesis to the extreme as described by Edwards & Beard (1997), the two-cell blastomeres resulting from meridional division of the zygote should be identical. Should the second round of cleavage produce two ICM, one TE and one germline precursor, localisation of the earliest lineage markers should be observed. Therefore a high level of pluripotent markers should be seen in two from four cells, a low level in one cell and a probable intermediate level in the fourth and so on. Certainly this clear-cut description is an over-simplification, but was the basis for investigation into gene expression in the 2- 4- and 8- cell embryos. Whilst global gene expression profiling studies by microarray have been reported for both mouse

(Hamatani *et al.*, 2004, 2006) and human (Adjaye *et al.*, 2005) whole embryos, gene profiling with single cells has not been reported.

Only good quality, progressive and appropriately developing embryos were used in the study, in an attempt to assess gene expression in normal embryos. The morphology of the embryo can be an indicator of developmental capacity, with post-meiotic abnormalities associated with an increase in dysmorphism leading to delayed development, multinucleation, fragmentation and uneven cell size (Munne, 2006), therefore such embryos were excluded. Eight 2-cell, seven 4-cell, one 7-cell and two 8-cell embryos were disaggregated to 67 individual cells and assessed for expression of genes associated with lineage decisions in early development.

In previous publications, some of these targets have not been detected at early cleavage stages (Kimber *et al.*, 2008). In order to address this, unamplified cDNA from cleavage stage blastomeres or whole blastocysts was run on a chip in parallel with the same samples following preamplification. No detection was seen for any targets without the preamplification step, which could explain the failure to detect these targets in early stage embryos. Therefore at the single cell level preamplification is required at least with this platform to detect both low and high abundance targets.

The distribution of amplification failures across chips, genes and developmental stage was checked to assess the possibility of selection bias. Given the large number of observations, it was not surprising to find that the variation in proportion of failures was very strongly significant (chi-squared test, $p<$2x10e-16 for all three cases). The variation across chips was particularly affected by a single comparatively poor chip (1131094093). It was also found that amplification failure rate tended to rise with increasing mean cT across genes, likely to be due to the presence of less target cDNA in these samples. The effect was less pronounced after removal of the poorest chip (chip 1131094093). Correlation between removal rate and response potentially raises the possibility of selection bias; specifically, changes in mean cT due to selective removal of observations which would, if successful, have exhibited high cT. Censoring due to low levels of cDNA will tend to *decrease* mean cT by removing values higher than the censoring threshold. The result would be to reduce the significance of comparisons based on cT. Selection bias in this instance is therefore unlikely to lead to spurious significant differences in cT; rather, it would tend to lead

to reduced apparent significance. These considerations led to the '999' failed results to be removed from further analysis.

The analysis of the highly replicated single-gene chip revealed that the sample effect was highly significant but the embryo effect was insignificant. This was initially encouraging, as it indicated that there was more variance between cells of the same embryo than between different embryos. With human embryos being notoriously variable in morphology and behaviour, this result implied that it may be possible to use biological replicates to extract meaningful data. However, the row and column effects were also strongly significant. The implication of row- or column-wise failure for future statistical analysis is that identification of anomalous rows and columns is likely to be at least as important as individual outlier identification. From an experimental design point of view, a modest probability of clearly identifiable row- or column-wise failure can be accepted, as clear failures can be identified, removed and repeated as necessary. The appearance of anomalies like column 30 in Figure 5.22, none of which are marked as failures, is more difficult to address, suggesting that replication might be prudent to avoid misclassifying a single sample. As all samples were replicated within and across chips this issue was addressed. However the experimental design was not truly balanced, as not all samples appeared on all chips, and the genes were always loaded in the same order, and therefore the same columns. Failures and anomalies that can affect whole rows and columns as well as occasional single wells may question the suitability of this instrument in the application to single cell experimentation when the quantity of starting material and generated cDNA is limited.

The multi-gene chips showed substantially larger within-chip variance than the replicated *GAPDH* chip. In approximately decreasing order of size, the effects on cT dispersion were residual variance, between-chip variance then between-cell variance. This may simply be due to the fact that it is far easier to load a highly replicated rather than a heterogeneous chip. There were very strongly significant differences in cT response between different genes and between development stages after controlling for chip effects indicating differentiation of the samples.

This was further analysed by principal component analysis (PCA). PCA is a common technique using mathematical algorithms to find patterns in data of high dimension where simple x,y,z graphical representation is not possible (Ringner, 2008).

It reduces the dimensionality of the data while retaining most of the variation of the data set by identifying directions - principle components - along which the variation in the data is maximal. The principle components are linear combinations of the original variables; in this case for each cell the variables were the cT values of the 24 genes. It is possible to use components that, for example, correlate with a genotype of interest or to use enough components to include most of the variation in the data. Once PCA reveals the gradients of the data, a biological interpretation is needed to explain them. With this data set, the first two principle components accounted for over three quarters of the variation, and subsequent analysis was based on these components.

PCA is designed to identify directions with the largest variation and not necessarily the directions relevant for separating classes of samples. Nevertheless although there was substantial overlap, cells from the different development stages clustered naturally in three largely separate areas, indicating shared gene profiles within stage. Genes with similar functionality also tended to cluster; all the housekeeping genes were in the same quadrant, as were the TE genes. Pluripotency genes showed closely associated changes in cT except for *REX1*. PC1 was largely associated with a general decrease in cT (increase in product) (Figure 5.27), broadly related to the gradient from 2/4-cell to 7/8-cell. PC2 was associated with increase in cT (decrease in product) of some genes, especially *GATA6*, *CMYC* and *NANOG*. *Gata6* is expressed in the ICM of murine blastocysts (Koutsourakis *et al.*, 1999) and is essential for survival past the blastocyst stage. Reciprocal inhibition of *Gata6* and *Nanog* is thought to establish cell fate in mouse development, determining the divergence of the primitive endoderm and epiblast lineages (Ralston & Rossant, 2005). Retroviral insertion of *C-MYC* along with *POU5F1*, *SOX2*, and *KLF4* into human dermal fibroblasts has been shown to reprogramme the cells into a pluripotent state (Takahashi *et al.*, 2007). PC2 was also associated with a decrease in cT of some genes for example, *HPRT*, *DAZL* and *REX1*. *DAZL* is thought to function in the development of primordial germ cells, and expression has been demonstrated throughout preimplantation human development and in hESC (Cauffman *et al.*, 2005a). It shows a quality-dependent expression in blastocysts, which may imply other functions for *DAZL* beyond germ cell development. *HPRT* is X-linked housekeeping gene involved in purine salvage, constitutively expressed in all cells and tissues (Taylor

et al., 2001). Some genes showed no significant change on either the 2- to 4-cell gradient or the 2/4-cell to 7/8-cell gradient, such as *MAPK* and *OCLN*. The MAPK pathway is the major mitogenic pathway in preimplantation mouse embryos. Mapk protein has been detected in trophoblasts in E3.5 embryos when it is involved in mediating growth factor signals (Wang *et al.*, 2004). Components of MAPK pathways are present throughout the whole of mammalian preimplantation development (reviewed in (Zhang *et al.*, 2007)). *OCLN* is associated with tight junction formation, expressed ubiquitously thoughout human preimplantation development (Ghassemifar *et al.*, 2003), although it appeared susceptible to failure of detection indicating low levels of expression. The significance of expression by function cannot be analysed at this point due to the experimental limitations, but further studies could focus on those genes that show developmental changes rather than those that remain relatively constant.

These observations, taken together and considering the apparent statistical significance of gene/development stage interaction by mixed effects modelling, implied that broad changes in gene expression profile were occurring with development stage. The primary difference between 2- and 4-cell developmental stages was a general increase in cT (decrease in transcript) with moderate association with pluripotency genes. The transition from maternal to embryonic control is known to occur during the third mitotic cell division (Braude *et al.*, 1988). In general, mature oocytes contain sufficient maternal transcripts to support development through the first two cell cycles. At the time of the third cell cycle, these transcripts are down-regulated and/or degraded and specific embryonic mRNAs are synthesised. This process is not necessarily synchronised in each cell of an embryo, although transcripts present after the eight cell stage are assumed to be encoded by the embryonic genome. The general decrease in transcript levels from the 2- to 4-cell stage can therefore be explained by the halving of cytoplasm during division before the initiation of embryonic transcription. The 7/8-cell stage was chiefly distinguished from the 2- and 4-cell stages by higher cT for housekeeping genes and lower cT for pluripotency genes, indicating novel transcription of these latter factors. The 7/8-cell group was also strung out along the TE direction. *REX1* expression did not appear to be associated with other pluripotency genes. *REX1* shows highly-specific expression in mouse and human ESC (Eiges *et al.*, 2001; Rogers *et al.*, 1991) and as such is one of the most

commonly used markers in characterisation. However, recent studies suggest that *REX1* function is dispensable for both the maintenance of pluripotency in ES cells and the development of embryos (Masui *et al.*, 2008), therefore should perhaps be regarded just as a marker of pluripotency without functional significance.

However, no consistent grouping structure for cells within embryos was observed in the PCA plot, and no convincing pattern was seen when considering the individual embryo variance scores. Whilst the sample effect was significant, it was not clear whether this was truly due to differentiation of the cells or due to experimental error. The between-chip, row and column effects precluded any firm conclusions being drawn regarding within-embryo differential expression of lineage-associated genes. Given that the lysis to cDNA generation cannot be replicated within a sample, only the later steps of the method can be improved. The biological vs. methodological variability could be addressed by increasing the number of embryos in the experiment. Given that the embryo effect was insignificant, using a larger group of human embryos should be suitable, although clearly using murine embryos would be an easier way of increasing the sample set. If murine cleavage embryos are 'more' differentiated than human this would also facilitate the detection of differences between cells. Furthermore, whole embryos of a particular developmental stage could be compared just as for the individual cells. If the variance decreases between the whole samples, this may imply that the observed individual cell sample variance is true biological variability, assuming that the detection of the individual cell cDNA levels was not limiting. Higher replication per chip would address the chip-to-chip variability. From this experiment a smaller group of genes of interest that showed a change in expression with developmental stage could be selected, and therefore fewer genes with more replicates per chip used. These approaches should enable conclusions to be drawn regarding whether or not the Fluidigm platform is sufficiently sensitive for the study of single mammalian blastomeres during the early stages of development.

Chapter 6

Human embryonic stem cells as disease-in-a-dish models

6.1 Introduction

The potential of hESCs with clinically relevant mutations has generated substantial interest, as the cells offer an unlimited source of material to study the mechanisms of genetic diseases (Stephenson *et al.*, 2009). A line derived from an embryo containing the HD expansion (KCL008-HD2) was used to generate a neuronal population of cells with the aim of studying pathologic features of the disease. This addressed the question of whether hESC are suitable as 'disease-in-a-dish' models for research.

6.1.1 Huntington disease

The classic description of HD was by George Huntington in 1872 (Huntington, 1872). HD is an late-onset autosomal dominant, lethal, progressive neurodegenerative condition characterised by irrepressible motor disturbance, cognitive decline and progressive dementia (Martin & Gusella, 1986; THsDCR, 1993). It affects around 1 in 10,000 individuals of European descent.

Cloning of the HD gene (THsDCR, 1993) has led to rapid advances in understanding of the molecular events underlying the disease. The HD gene mutation is a CAG repeat expansion that results in long stretches of polyglutamine in the encoded protein Huntingtin (HTT). HTT is a large scaffold protein involved in many cellular functions. Wild-type HTT is ubiquitously expressed therefore the expression profile does not account for the characteristic pattern of neuropathology found in the brains of HD patients. The disease does not manifest below 35 CAG repeats,

incomplete penetrance is observed between 36-39 repeats and patients with, as well as without the disease have been described, and above 40 the disease is fully penetrant, showing the typical features of the disorder. The vast majority of adult onset cases have expansions ranging from 40 to 55 repeats; expansions of 70 and above are uncommon and invariably cause the juvenile onset form of the disease. Very few cases have been described with a repeat length exceeding 100 (Davies *et al.*, 1997). An association between apolipoprotein E (APOE) and age of onset of HD has been reported. Whilst length of CAG repeat is the most significant predictor of onset age, APOE$\epsilon 2\epsilon 3$ genotype is associated with significantly earlier age of onset in males than in females (Kehoe *et al.*, 1999). APOE genotype is known to also influence onset age in Alzheimer's.

The mutant protein misfolds and aggregates to form intranuclear inclusions, which are typically, but not exclusively found in those brain regions that are predominantly affected by the disease. Full-length HTT may be cleaved to form a N-terminal fragment containing the glutamine repeat. This fragment is more toxic and more prone to aggregation compared to the full-length protein. The mutation predominately acts by imparting a gain-of-function to the mutant HTT protein, although loss-of-function of wild-type HTT may also contribute to the disease process (Cattaneo *et al.*, 2001). Neuronal dysfunction and degeneration affects many brain regions including the striatum, cortex and hypothalamus. Diffuse, severe atrophy of the striatum is the pathologic hallmark of HD. Medium sized spiny striatal neurons containing gamma amino butyric acid (GABA) are extremely vulnerable (Watase & Zoghbi, 2003). Brain atrophy progresses after the clinical onset of HD with the intensity and rate of progression more pronounced in patients with larger expanded CAG repeat sequences (Ruocco *et al.*, 2008). The early symptoms include slight, uncontrollable muscular movements, stumbling and clumsiness, lack of concentration and short-term memory lapses. Almost all patients exhibit neuropsychiatric symptoms as the disease progresses, the most prevalent being dysphoria, agitation, irritability, apathy, and anxiety (Paulsen *et al.*, 2001). Reviews of psychiatric symptoms in HD have suggested that depression, apathy, aggression, and disinhibition are common, with suicide rates over four times those of the general population (Di Maio *et al.*, 1993). Subclinical obsessive compulsive symptoms (checking, cleanliness, compulsive

rituals, hoarding, and pathologic impulses) are present in pre-HD patients compared to controls (Beglinger *et al.*, 2008).

It is not only in the genetic sense that HD is a family disease. As the average age at onset of symptoms is between 35 and 45 years, HD begins when childbearing, child-rearing, and career development are all significant (Vamos *et al.*, 2007). There may be many members affected in one family unit and also in the extended family. There may be inter-sibling envy, regret and guilt if not all siblings inherit the disease. Marked family pathology in terms of low cohesion and expressiveness and high levels of conflict have been reported (Vamos *et al.*, 2007). Genetically unaffected spouses are likely to be almost equally affected by the illness in terms of concerns for the future and the future of subsequent generations, including the ability to function as a carer and a parent. The genetic implications of HD, coupled with the lack of a cure or reliable treatment to ameliorate the disease, means that avoidance is one of the main coping strategies deployed by carers. Secrecy about the disease is manifest in HD families (Lowit & van Teijlingen, 2005).

6.1.2 Models for Huntington disease

There are several approaches to develop models for human disease. Primary cultures of relevant cell types can be isolated from patients, but are generally difficult to obtain. Samples obtained post mortem only represent a single point in the disease and are commonly advanced disease stages; pre-symptomatic or early stage specimens are rare. There is a limited range of tissues from which primary cells can be obtained and the replication span of the cells can be brief before senescence is reached or before unwanted transformation occurs.

Alternatively, genetically engineered animals are used to generate research models, the most popular of which is the mouse model. Knock-in models have varying lengths of CAG repeats inserted into the mouse HD gene (hdh) (Shelbourne *et al.*, 1999). Transgenic models can have a mutated version of an N-terminal fragment of the human HD gene (Mangiarini *et al.*, 1996) or full length human cDNA (Reddy *et al.*, 1998). In transgenic models, the age of onset and progression of the disease can be manipulated by changing the size of the repeat or transgene expression level (Bates & Hockly, 2003) but the transgene integrates randomly into the mouse genome, which may have unwanted downstream effects. In knock-in models, the

CAG repeat is inserted into the correct place in the genome so models the disease more precisely, but manipulation of age of onset and progression of disease is limited to the size of the CAG repeat and breeding pairings.

Key insights into HD pathogenesis have resulted from the use of mouse models. For example, R6/2 mice transgenic for exon 1 of the human HD gene were used to show that pronounced neuronal intranuclear inclusions develop in the brains of the animals prior to developing a neurological phenotype. These inclusions contained HTT and ubiquitin proteins, thus implicating mutant HTT aggregation as a neuropathological hallmark of HD (Davies *et al.*, 1997). Similarly, transcription dysregulation was identified as an early event in disease onset by studying striatal gene expression changes in the R6/2 model (Luthi-Carter *et al.*, 2000).

However, the extent to which mouse models fully replicate the molecular pathogenesis of HD is unknown. Many of these models do not faithfully represent the abnormal phenotype as manifested in humans (Watase & Zoghbi, 2003), and therapeutic achievement in animal models is not always successfully repeated in human studies. This is partly due to inherent species differences and also to the difficulty in identifying comparable outcome measures (Ferrante *et al.*, 2002; THsDCR, 2001). Therefore it has been recommended that a compound of interest should show efficacy in two different mouse models in two different laboratories before being considered for clinical trials (Bates & Hockly, 2003). The use of transgenic mice which overexpress HD gene fragments dramatically shortens the time to symptom onset and development of disease pathology, but conversely the pathologic specificity is decreased (Menalled & Chesselet, 2002). These considerations have led to a search for alternative, but complementary disease models for HD.

6.1.3 Embryonic stem cells as disease models

Embryonic stem cells carrying genetic disease are an alternative disease model. With the fundamental attributes of pluripotency and self-renewal, they hold promise for an unlimited supply of cells with which to study the mechanisms and development of the disease. This is on the proviso that robust and reproducible protocols are developed. MESC expressing long CAG motifs are able to differentiate into neurons, but are characterised by stunted neurite outgrowth, low efficiency of neuronal forma-

tion, decreased survival during differentiation and redistribution of polyQ containing proteins (Lorincz *et al.*, 2004).

As a model of disease progression, naturally occurring mutations in hESC from PGD embryos represent a far more relevant model than genetically engineered mESC as the mutant protein is expressed in its normal physiological context and range of expression pattern. HESC models may not be identical to differentiated adult cells *in vivo*, but nor do they need to be; their phenotypes will be close enough to provide much improved pharmacological models. However, it is important to address basic but crucial questions with regard to the use of hESC in disease research. Bearing in mind the late onset of diseases such as HD, it is essential to assess whether neural progenitors and neurons differentiated *in vitro* from HD-hESCs faithfully express the HD phenotype as assayed by cell-based analyses, transcriptomics, and proteomics. The judgement can then be made as to whether these cells are equivalent or superior to animal models. If superior, this may reduce the need for whole-animal experiments. It then remains to be seen whether such cells accelerate clinically relevant drug discoveries, while reducing toxicity, since the initial screen is performed with human (rather than typically rodent) cells.

6.1.4 Neuronal differentiation protocols

Protocols for producing neuronal derivatives from ESC were initially designed for mESC and subsequently modified for application to hESC. Six main differentiation pathways have been used with varying success; retinoic acid (RA) induction, conditioned medium (CM) induction, serum-free embryoid body selection, stromal co-culture, low density clonal neurosphere and monolayer serum-free induction (reviewed in Cai & Grabel (2007)).

Stromal cell culture approaches are based on attempts to recapitulate the stem cell niche. When combined with serum removal and low density plating it has proven successful with mESC. Neuronal markers such as neural cell adhesion molecule (NCAM) and nestin (NES) have been reported after one week in culture (Barberi *et al.*, 2003; Kawasaki *et al.*, 2000). Advantages of this protocol include; the requirement for relatively low ESC numbers for initiation, induction of a relatively pure neuronal population, and the absence of an undefined EB step. In collaboration with I-Stem, Evry, Paris, a mouse stromal co-culture protocol (Barberi *et al.*, 2003;

Perrier *et al.*, 2004) was modified and used in attempts to induce neuronal differentiation in the HD-carrying human ESC line, KCL008-HD2. The pre-adipocytic mesenchymal murine bone marrow-derived stromal feeder cell line *MS-5* was kindly donated by I-Stem.

6.1.5 Aims

Preimplantation genetic diagnosis provides a novel source of embryos for hESC research that carry clinically relevant genetic disorders (Stephenson *et al.*, 2009). Donation of these these embryos does not compromise patient treatment in any way. In addition these embryos may be superior to those donated from IVF programmes since most patients are fertile and undergoing IVF purely to prevent disease transmission. The aim of this work was to develop a relevant population of cells for HD investigation, and so test the hypothesis that hESC can be used as alternative models in genetic disease research.

6.2 Method Development

6.2.1 Embryo culture and derivation

KCL008-HD2 was used throughout the neuronal differentiation study. The details of the methods for derivation and characterisation of this line are given in sections 3.3.3.5 and 3.3.6 respectively.

6.2.2 Repeat analysis

The length of the CAG repeat of the mutant *HTT* gene was monitored throughout the study. The length was determined just after derivation, upon initiation of the differentiation protocol and once a stable precursor population had been obtained. The method used was exactly as described in section 2.5.5.

6.2.3 Cytogenetic and molecular karyotype

Cytogenetic and single nucleotide polymorphism (SNP) analysis did not fall under routine NHS clinical load and were therefore outsourced to suitable laboratories. Cytogenetic analysis was performed by TDL (section 2.5.3). SNP analysis was outsourced to the biotechnology company Integragen. The service offered highly

multiplexed SNP genotyping assays processed in an automated, production-scale environment based on the Illumina high-throughput BeadArray™ platform technology (Illumina Inc., San Diego, CA, USA). Genotyping was performed by Integragen using a HumanHap300 chip containing 318,237 SNPs hybridised to 750 ng of genomic DNA (Simon-Sanchez *et al.*, 2007). Genomic DNA was extracted as described in section 2.5.2.5. KCL008-HD2, at passages 2-4 and 12-14, and a control line at passage 90 with known diploid karyotype (VUB05-HD) were analysed together.

6.2.4 Microsatellite analysis

Microsatellite analysis of the PGD products from the biopsied cell and the parents, and subsequent analysis of KCL008-HD2 and human foreskin fibroblasts (HFF) was performed by Guy's ACU PGD scientists according to their published quantitative fluorescence PCR protocol (Mann *et al.*, 2004). In the procedure the chromosome markers were co-amplified in one multiplex PCR assay. PCR products were analysed on 310 and 3100 capillary based genetic analysers (Applied Biosystems, Foster City, CA, USA). Genotyper version 2.5 was used for sizing and labelling alleles.

6.2.5 Pre-differentiation characterisation

Several steps were taken before initiating the differentiation protocol. In preparation for the cell numbers required in the differentiation protocol, routine culture of KCL008-HD2 on HFF feeders was expanded gradually, first into 3 cm and then into 6 cm dishes (BD Biosciences). KCL001 was used as a control cell line throughout. MS-5 cells were expanded to form a bank exactly as described for MEF cells (section 2.2.2). In order to establish baseline expression of both pluripotency and differentiation markers KCL008-HD2 cells were fully characterised by FACS analysis (section 2.5.4) and immunocytochemistry (ICC) (section 2.5.1). Negative controls were performed with each experiment by omitting the primary antibody or using isotype controls. The antibodies used for all FACS and ICC analysis are either in Table 2.4, section 2.5.4 or Table 2.2, section 2.5.1, or shown here in Table 6.1.

6.2.6 Neural induction

MS-5 cell feeders were plated at $2.6\text{x}10^4$ cells/cm^2 following mitomycinC inactivation. hESC were manually cut into pieces as for routine passaging, and a maximum of five

Table 6.1: Primary antibodies used for characterisation. SOX2; SRY-related HMG-box-2, NES; nestin, TUJ1; β III tubulin, GFAP; Glial Fibrillary Acidic Protein, MSI1; musashi-1, PAX6; Paired box-6, MAP2; Microtubule Associated Protein-2, AFP; α Fetal Protein. Dako; Dako Denmark A/S, Glostrup, Denmark.

Name	Isotype	Clone	Company	Dilution
SOX2	Mouse IgG	mAbcam 23960	Abcam	1 in 200
NES	Rabbit IgG	Polyclonal	Chemicon	1 in 250
TUJ1	Mouse IgG2a	TUJ1	Covance	1 in 500
GFAP	Rabbit IgG	Polyclonal	Dako	1 in 200
MSI1	Rabbit IgG	Polyclonal	Chemicon	1 in 200
PAX6	Rabbit IgG	Polyclonal	Santa Cruz	1 in 200
MAP2	Mouse IgG1	HM-2	Sigma	1 in 500
Brachyury	Mouse IgG2a	4G7	Chemicon	1 in 200
AFP	Mouse IgM	167H.4	Chemicon	1 in 200

colony pieces plated per 3 cm dish or 15 pieces per 6 cm dish. The cells were cultured in KSR medium on these stromal feeders for 14 days. KSR medium consisted of KODMEM with 15% KOSR, 1% NEAA, 4 mM L-glutamine, with no growth factor supplementation. Medium was exchanged every two or three days, and photographic records kept to document the differentiation. Wild-type hESC line KCL001 was also cultured in parallel.

At day 14 after plating onto MS-5 feeders, the medium was exchanged for N2 comprising DMEM F12 with Glutamax (Gibco Invitrogen) and 1% N2 supplement (Gibco Invitogen). 20 ng/mL brain-derived neurotrophic factor (BDNF; R&D Systems, Minneapolis, MN, USA) was added fresh to each medium aliquot at exchange. The hESC remained on the MS-5 feeders in N2 medium for a further seven days, with medium exchange every two or three days.

After 21 d on MS-5 the hESC colonies were manually passaged into pieces approximately 1.5 times the size of routine passaging and placed into one of three conditions. The dishes were coated in one of two ways; with polyornithine-laminin (POL) or gelatin (Gel). For POL conditions, culture dishes were incubated with 15 μg/mL polyornithine (Sigma Aldrich) in PBS for a minimum of 4 h at 37°C. The dishes were washed twice with PBS and then 1 μg/mL laminin (Sigma Aldrich) in PBS added for a minimum of 1 h at 37°C. Gel plates were prepared by adding 0.1% gelatin for a minimum of 5 min at RT.

In the first condition the hESC were passaged onto POL dishes and remained in N2 medium supplemented with BDNF. In the second, the hESC were passaged onto POL dishes and the medium exchanged for N2B27, a 50:50 composition of DMEM F12 with Glutamax and Neuralbasal medium (Gibco Invitrogen) with 1% N2 and 2% B27 supplementation. At each medium exchange the medium aliquots were supplemented with 20 ng/mL BDNF, 10 ng/mL epidermal growth factor (EGF; R&D Systems) and 10 ng/mL bFGF. In the third condition the cells were passaged onto Gel dishes in N2B27 with the same supplementation as before. From then on, the dishes were passaged with 0.25% trypsin when confluent, until no further growth was seen or the cells were used for FACS analysis, ICC or cryopreserved to form a bank. Cells that were successfully passaged several times were cryopreserved and thawed exactly as for MEFs (section 2.2.2) to assess post-thaw viability. CAG repeat (section 2.5.5) and western blot (section 2.5.6) analyses were performed when stable populations of cells were obtained. The experimental protocol is summarised in Figure 6.1.

6.2.7 Characterisation of differentiated cells

6.2.7.1 Growth rate

One vial of P4 KCL008-HD2 and KCL001 cells on POL in N2B27 was thawed, and $1x10^5$ cells plated in 3 dishes exactly as for routine culture. At each passage the cell number was counted in triplicate for each cell line, for each dish. For both cell lines three dishes were then re-plated for the next passage and cell count. The total cell number at each passage was calculated by averaging the cell counts and multiplying by the theoretical total number of dishes had all the cells been plated.

6.2.7.2 Marker expression

FACS analysis was performed at each step of the protocol to monitor differentiation. ICC was used once a stable cell population was generated to identify the cell type obtained. Cell cycle analysis was performed exactly as in section 2.5.4.1 to assess the chromosome content of KCL008-HD2, and compared with HFF cells as a control.

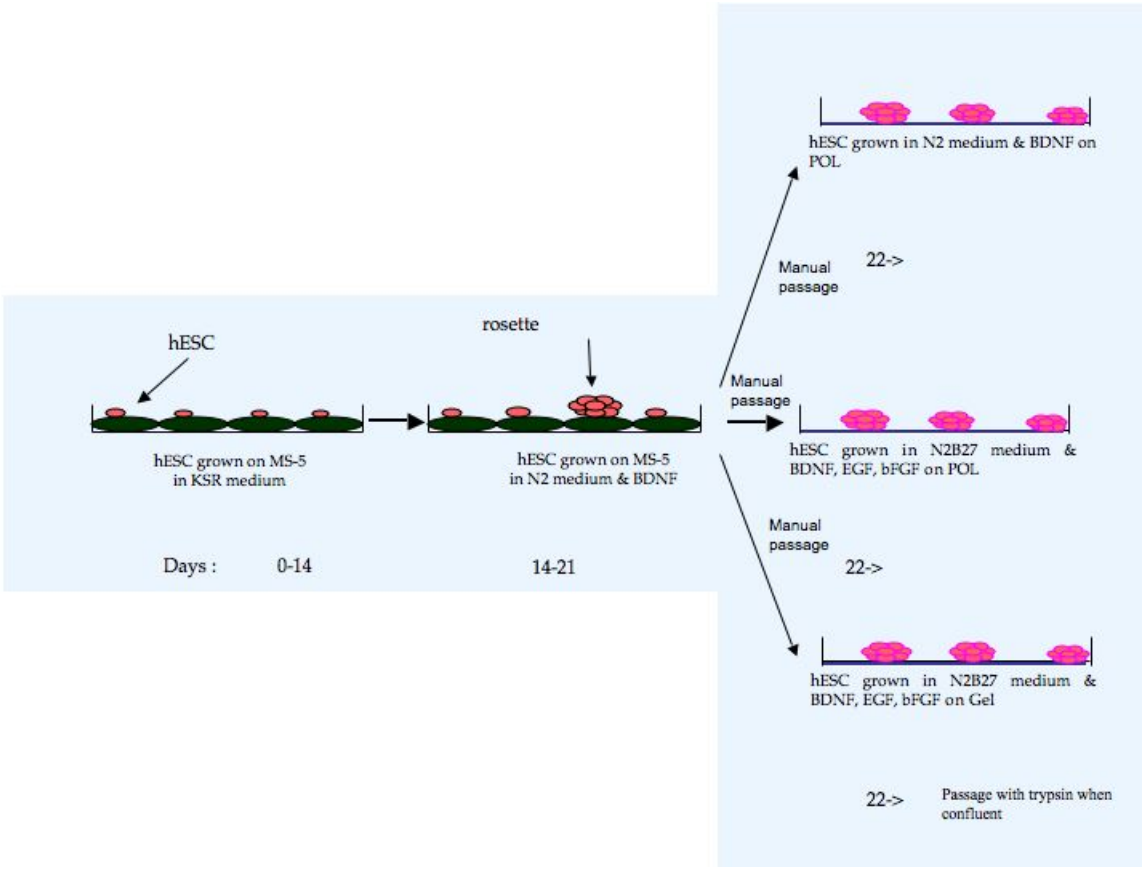

Figure 6.1: Summary of the differentiation stromal cell co-culture protocol, with the three conditions tested after the co-culture period.

6.2.7.3 Protein analysis

Western blots were run with KCL008-HD2 cells both when undifferentiated and once the cells had been differentiated into neural precursors. Each time HFF feeders were used as negative control cells, and immunoprecipiate of full length mutant HTT from the transgenic R6/2 hdh mouse model (150 CAG repeats) used as the positive control (kindly donated by C. Landles, Medical and Molecular Genetics Department, King's College). The protein content of the cells was isolated as in section 2.5.6.1 and stored at -80°C until use. The gels were set up and the samples prepared and run as in section 2.5.6.3. Immunohistochemical analysis to detect the HTT protein was performed exactly as in section 2.5.6.4.

6.2.8 Neuronal and astrocytic differentiation

Differentiation of the neural precursors to neurons was attempted by low-density plating and mitogen withdrawal. In preliminary experiments, the cells were plated in POL coated dishes at 100, 500, 1000, 2000, 3000, 4000 and 5000 cells/cm^2. Culture was in N2B27 medium, but without BDNF, FGF2 or EGF supplementation, and with medium exchange every 2-3 days. At day 7 the concentration of the cells was inspected. At 100 cells/cm^2 growth was negligible, but at 2000 cells/cm^2 and above, the cultures were confluent, or over-confluent, with increasing proportions of cells lifting off into suspension. As the differentiation step was a minimum of 14 day protocol, 500 cells/cm^2 was selected for neuronal differentiation. Differentiated KCL008-HD2 and KCL001 were plated in triplicate in these conditions at both P4 and P12. After 14 and 28 days in neuronal differentiation conditions, the cells were fixed and stained for MSI1, MAP2, PAX6, TUJ1 and NES.

To induce astrocytic differentiation, P4 cells were plated in triplicate at 500 cells/cm^2 in N2B27 medium without growth factor supplementation, but with 20% fetal calf serum (FCS). After 7 days in astrocytic differentiation conditions, the cells were fixed and stained as before.

6.3 Results

6.3.1 Derivation and early culture

The embryo used for the derivation of KCL008-HD2 was donated with informed consent by a 39-year-old woman undergoing IVF/PGD. In the treatment cycle, five oocytes were collected, of which four were mature and suitable for injection; one germinal vesicle oocyte was discarded. Sperm parameters were normal, with 32% normal forms, 20 million per mL density, and good to fair progression. At the time of ICSI, embryo one (E1, subsequently KCL008-HD2) was at metaphase II, with a large fragmented polar body, a thick zona and dark granular cytoplasm. No break of the membrane was observed on aspiration during ICSI. At fertilisation check E1 had two visible pronuclei although they appeared faint. On day 2 E1 was 4 cells and grade 3, but with uneven cell size. At biopsy on day 3, E1 was an eight cell graded as 3. Although not conclusive, two structures resembling polar bodies were visible within the ZP as shown in Figure 6.2.

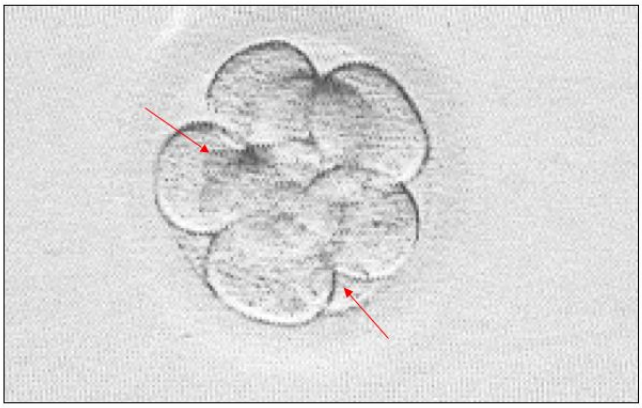

Figure 6.2: Morphology of E1 on day 3 just prior to biopsy. Two structures that were possibly polar bodies could be seen (arrows). Original image at x20 objective.

E1 was diagnosed as carrying the HD expansion following preimplantation genetic haplotyping (PGH) microsatellite analysis. Microsatellites are highly variable tandemly repeated sequences commonly used for mapping, linkage analysis and to trace inheritance patterns. The repeating unit is generally 1 to 4 nucleotides long

and variation in the number of repeats affects the overall length of the microsatellite. When being used as a diagnostic tool as in PGH, the specific number of repeats in a given microsatellite is not important, but rather the difference in the number of repeats between alleles, allowing the origin of the allele to be tracked. Following diagnosis for HD the embryo was unsuitable for transfer to the patient. The embryo compacted late on day 4, and was used for derivation on day 5 when it had developed to a hatching blastocyst. The derivation of KCL008-HD2 is detailed in section 3.3.3.5.

Early culture of the line proved difficult. The colonies proliferated slowly, and showed very poor attachment following passage. Culture was therefore restricted to 4-well plates, with reduced medium volume to aid attachment. 2.5 μg/mL laminin and 16 ng/mL bFGF were added to encourage attachment and undifferentiated growth. Replication crisis occurred several times, when only one or two undifferentiated colonies would remain, and of necessity attempts to expand were cautious. Transfer of the line to KOSR improved cell survival and attachment, and following adaptation to HFF feeders, routine culture methods could be used from approximately passage 15.

6.3.2 CAG repeat analysis at derivation

At the first passage of each HD line, single hESCs were collected and analysed to confirm the disease inheritance. Electrofluorograms generated from the Huntington's assay were used to calculate the number of repeats in each allele for each HD cell line. The peak size was measured using the Genotyper 2.5 programme software. The size of the primers (37 base pairs) was subtracted from the peak size, and the result divided by three to give the number of CAG repeat units. The longer the repeat size, the more likely it was to manifest a 'hedgehog' effect in the electrofluorograms, due to the Taq polymerase slipping while reading the template and therefore producing additional smaller peaks. In these cases, the average of similar peaks was taken and used to calculate the expansion size. The electrofluorograms for KCL005-HD1 and KCL008-HD2 are shown in Figure 6.3.

The analysis of KCL005-HD1 confirmed that the cell line carried the expanded *HTT* gene. One allele had a peak size of 92.5 base pairs, therefore the repeat length of the gene was 18, corresponding to the normal allele inherited from the paternal

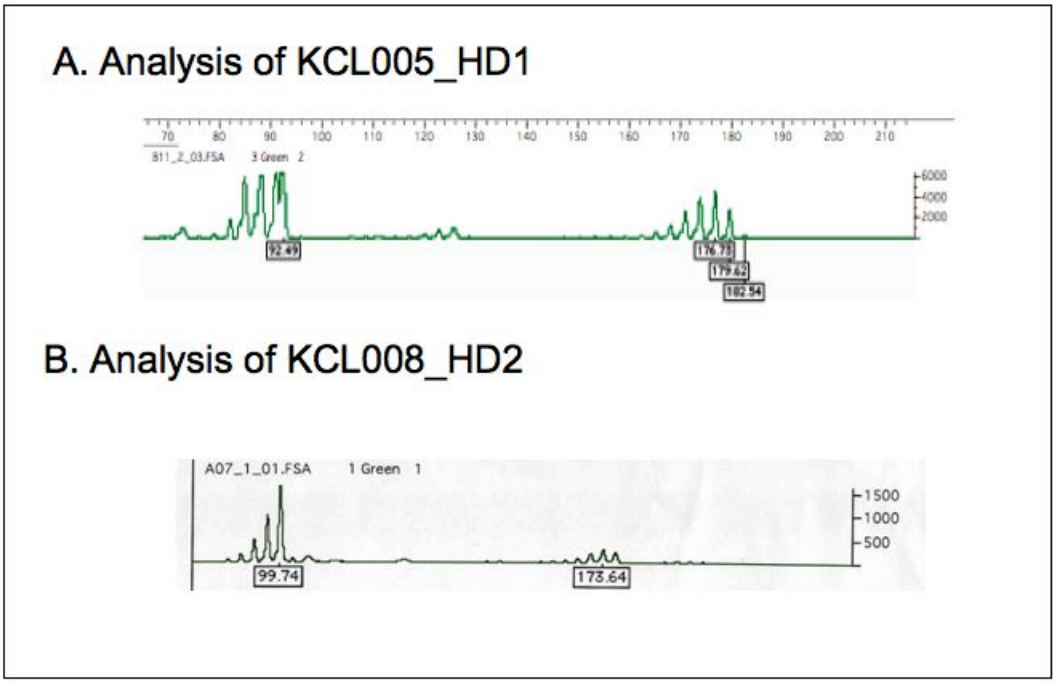

Figure 6.3: Electrofluorograms generated for CAG repeat analysis of (A) KCL005-HD1 and (B) KCL008-HD2

side. The maternal allele had an average peak size of 178.5 base pairs, therefore a repeat length of 47. Both the buccal and negative controls were appropriate, with the buccal samples giving a repeat length of 17 as expected, and no peak in the negative control.

The analysis of KCL008-HD2 confirmed that the cell line carried the HD expansion. One allele had an average peak size of 92.8 base pairs, therefore a repeat length of 21, corresponding to the normal allele inherited from the maternal side. The paternal allele had an average peak size of 173.6 base pairs, therefore a repeat length of 46. The repeat length was 44 in the male patient, and therefore an elongation of the repeat by 2 units had occurred. Paternal inheritance of the *HTT* gene is unstable and increases in repeat length through generations are not uncommon. Both the buccal and negative controls showed the appropriate outcome.

6.3.3 Cytogenetic and molecular karyotype

Cytogenetic karyotyping suggested that the chromosomal content of KCL008-HD2 was abnormal at 68,XXY,-6 as shown in Figure 6.4.

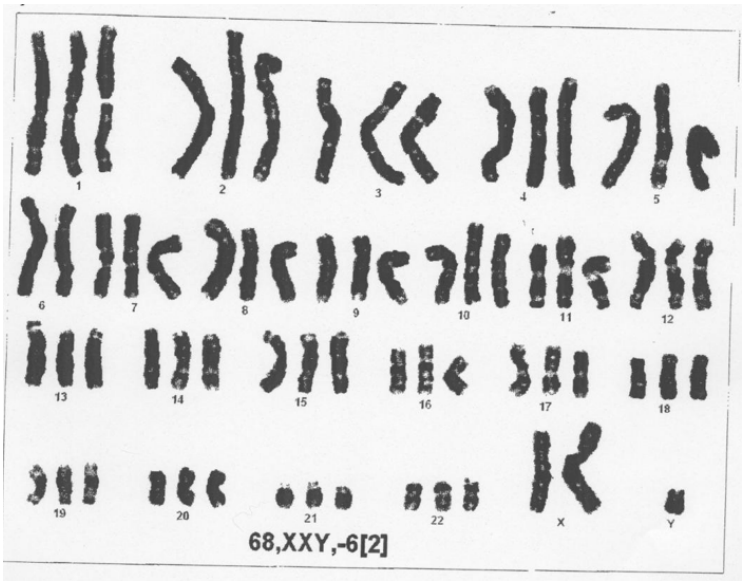

Figure 6.4: Cytogenetic karyotype of KCL008-HD2, showing abnormal chromosomal content of 68,XXY,-6 from two cell metaphases.

However, despite three separate attempts at karyotyping, only the third produced any result. Disappointingly, only two mitoses were suitable for analysis from approximately 50 colonies. Furthermore the karyotype of two cells analysed appeared to

disagree with the original microsatellite analysis of the biopsied cell. Although PGH is not designed to specifically detect aneuploidy, the analysis of the biopsied blastomere indicated normal chromosome content, with only ever one (due to drop-out or a non-informative marker) or two alleles present, never three, as shown in Figure 6.5.

Maternal markers - unaffected parent		
D4S3360	277	281
D4S2936	196	196
D4S3038	308	326
D4S43	262	266
D4S1614	177	179
D4S127	217	221
D4S126	227	229
HD (CGG)n	16	21
I1SCAHD	289	297
D4S3034	237	239
D4S412	303	311
D4S3023	196	200
D4S2925	198	198

Paternal markers - affected parent		
D4S3360	281	275
D4S2936	196	200
D4S3038	322	310
D4S43	260	260
D4S1614	177	181
D4S127	221	223
D4S126	227	233
HD (CGG)n	44	18
I1SCAHD	291	287
D4S3034	227	235
D4S412	303	313
D4S3023	194	194
D4S2925	200	200

Embryo markers - affected		
D4S3360	277	281
D4S2936	196	196
D4S3038	322	326
D4S43	262	
D4S1614	179	
D4S127	221	221
D4S126	227	227
HD (CGG)n		
I1SCAHD	289	
D4S3034	237	
D4S412	303	303
D4S3023	194	200
D4S2925	198	200

Figure 6.5: PGH results for chromosome 4 from both parents and the biopsied blastomere. The size of the microsatellites for both alleles are shown. The affected paternal allele is shaded green, and the corresponding markers found in the biopsied cell are also shaded. There are only ever zero, one or two marker results, which indicated a maximum of two alleles.

In the light of these results, it became necessary to confirm the karyotype of KCL008-HD2, and as an alternative to cytogenetic means single nucleotide polymorphism (SNP) analysis was attempted. SNPs are single-base pair variations in the DNA sequence and represent by far the most common source of genetic variation. The human genome is thought to contain over 10 million SNPs, about one in every 300 bases. SNP genotyping is the process of determining which point mutations

are present in the copies of a gene in a human (or model organism) genome.

Biallelic SNPs were used for the analysis, therefore only two bases are detected with each probe. Hence, if the two bases in question were A and T, the combinations possible at each SNP position in diploid cells would be AA, AT, TT. Therefore for heterozygous SNPs the expected ratio of allele 2 to allele 1 would be 50% (AT and TA). For any homozygous regions, the frequencies would lie at either 0% (AA) or 100% (TT). For a male line, no heterozygous bands should be visible in the X or Y analysis. For a female line, the majority of SNPs on the X chromosome are likely to be heterozygous, therefore a band at 50% frequency would be expected. Figure 6.6 shows the analysis of the diploid HD-derived male line, VUB05-HD, where the vast majority of hybridised SNPs were heterozygous and formed a band at 50% frequency, with no band visible in either sex chromosome.

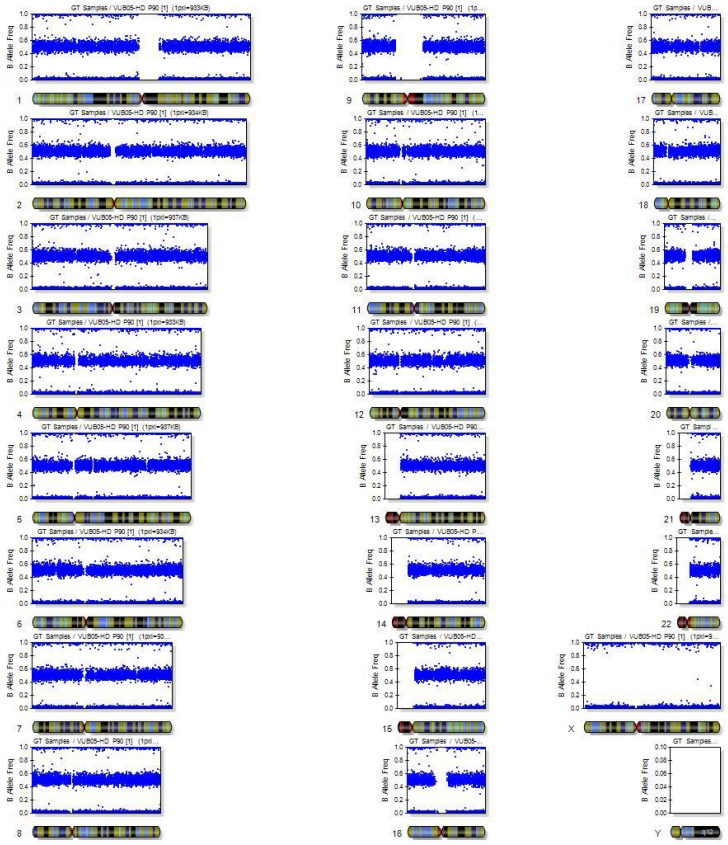

Figure 6.6: SNP analysis of the control line VUB at passage 90. The vast majority of SNP were heterozygous, showing as one band at 50% ratio of allele 2 to allele 1.

However, for triploid samples, the possible combination of bases becomes AAA,

AAT, ATT, TTT. Therefore the outcome ratios of allele 2 to allele 1 would be 0% (AAA), 33% (AAT), 67% (ATT) or 100% (TTT). The SNP analysis for KCL008-HD2 showed heterozygous regions at 33% and 67% for each somatic chromosome apart from 6, which showed only a heterozygous band at 50%. Hence this confirmed the triploid status of the cells (apart from chromosome 6) and substantiated the cytogenetic results. The analysis also showed a large area of homozygosity in the X chromosome. This could either be explained by a paternal diploid contribution if the parents were related, or a maternal diploid contribution with crossing over during meiosis. Figure 6.7 details the SNP analysis of KCL008-HD2.

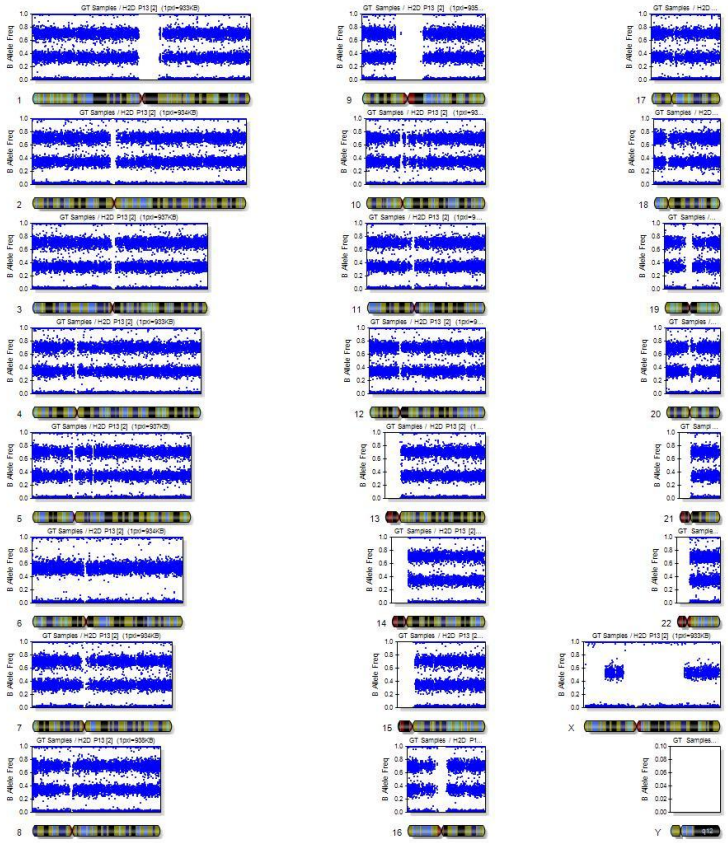

Figure 6.7: SNP analysis of KCL008-HD2 at passage 2-4. The triploid karyotype is confirmed by bands at the 33% and 66% allele ratios. The exception is chromosome 6 which is diploid.

With the inheritance of an extra set of chromosomes by KCL008-HD2, the possible mechanisms giving rise to triploidy were considered. Non-mosaic triploidy can arise from either the combination of one maternal and two paternal chromosome

sets (diandry) or one paternal and two maternal sets (digyny). Table 6.2 details the possible combinations at fertilisation.

Table 6.2: Details of the possible events at fertilisation, the resulting number of visible pronuclei and the parental genetic contribution. Pronuclei; number visible at fertilisation, Maternal; maternal component, Paternal; paternal component.

Event	**Pronuclei**	**Maternal**	**Paternal**
Normal fertilisation	2	n	n
Diandry - two haploid sperm	3	n	2n
Diandry - one diploid sperm	2	n	2n
Digyny - nondisjunction at meiosis I	2 or 3	2n	n
Digyny - nondisjunction at meiosis II	2 or 3	2n	n
Digyny - diploid (giant) oocyte	2 or 3	2n	n
Digyny - endoreduplication	2	2n	n

The presence of a third pronucleus is normally clearly seen at fertilisation check, an example is given in Figure 6.8. Similarly 'giant' oocytes are clearly abnormal and are generally discarded (Furuya *et al.*, 2005; Rosenbusch *et al.*, 2002). Therefore it was unlikely that the mechanism giving rise to the triploidy was either fertilisation by two haploid sperm or fertilisation of a 'giant' oocyte. To determine the origin of the triploid inheritance pattern of the cell line further investigation was performed by microsatellite analysis.

6.3.4 Microsatellite analysis of ploidy

To determine the mechanism of triploidy in the cell line, the original PGH products from the parents and the biopsied cell, and genomic DNA extracted from KCL008-HD2 hESC were compared. HFF feeders were also analysed to ensure no feeder contamination was present or to account for the presence of any anomalous alleles. Panels of microsatellite markers were used for chromosomes 13, 18, 21, X and Y, the results are shown in Figure 6.9. In addition, chromosome 6 was investigated to determine which copy was absent, the results are shown in Figure 6.10.

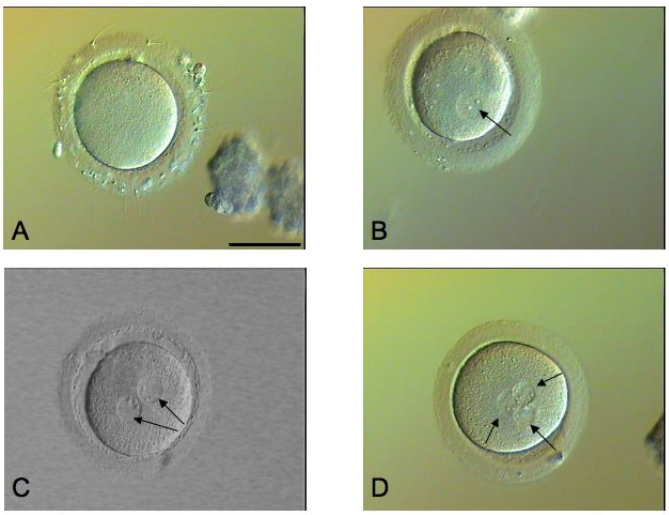

Figure 6.8: Images of fertilised oocytes with arrows indicating: (A) No pronuclei (B) one pronucleus (C) two pronuclei (D) three pronuclei. All images at x20 objective. Scale bar indicates 50 μm.

For the parental samples, 6 of the 13 sex chromosome, and 5 of the 16 somatic chromosome markers were fully informative. However for the biopsied cell, none of the sex chromosomes were conclusive. For all markers except one, none or only one allele was detected. This was likely to be due to allele drop out or homozygosity. The only locus where two alleles were detected (AMEL) was for a non-informative marker from the parents. Similarly the cell line was inconclusive. At the only locus where two alleles were detected for an informative marker (DXS7423), one microsatellite size was shared with the feeder cells. Whilst there was generally very little evidence for feeder contamination in the samples, this prevented a firm conclusion regarding inheritance, although it was suggestive of maternal diploid content.

The somatic chromosome analysis confirmed the inheritance as maternal diploid. For KCL008-HD2, informative microsatellite sizes were detected with markers D13S634, D13S325 and D18S386, where inheritance of both maternal chromosome copies and a single paternal copy were detected (grey boxes). Therefore the cell line carried one mutant copy of *HTT* from the father, and two normal copies from the mother. Analysis of chromosome six confirmed that the cell line carried one copy from each parent, with the loss of the second maternal copy occurring at an undetermined point in development.

Chromosome	Marker	Maternal donor	Paternal donor	Biopsied Cell	KCL008_HD2	HFF feeders
SEX	DXS6803	140/148	145		140	140
	DXS981	243/247	246		246	242
	DXS6807	332/344	332	344	344	319/331
Y	DXS1187	149/153	149		149/153	152
	DXS1283E	317/329	313		329	317
	DXS6809	408/412	420		408	424
	DXS7423	372/376	388	376	372/376	376
	DXYS267	257/269	257/265	257	257/269	257/269
	DXYS218	384	384/388	384	384	372/380
	HPRT	287/291	295		287/291	287
	AMEL	105	105/110	105/110	105/110	
	SRY		246	246	246	246
Y	YDYS448		348	348	348	353
13	D13S634	401/405	409/416	416	401/405/416	403/411
	D13S325	285/290	294/298	290/294	285/290/294	281/298
	D13S305	446/454	446/450	450/454	446/446/454	429/450
	D13S628	453	453/457	457	453/457	457
	D13S252	279/299	279/299	279	279/279	275/295
18	D18S535	490	466/482	490	482/490	474
	D18S391	218/226	218/226	218/226	218/226	218/228
	D18S386	384/390	367/376	367	367/384/390	356/375
	D18S978	211/215	207/215	215	207/215	215/220
	D18S390	371	368/380		371/380	360/371
	D18S819	412	412	412	412/412	400/412
21	D21S1435	185	185/189	185	185/185	189/193
	D21S11	249	249/260	249/260	249/260	245
	D21S1437	327/335	331/339	335/339	335/339	315/319
	D21S1411	309/333	309/325	333	309/325/333	300/313
	D21S1409	187/199	183/195	187	183/187	187/195

Figure 6.9: Microsatellite results for 27 markers on the PGH product from the biopsied blastomere, the donors, KCL008-HD2 hESC line and HFF feeders. The markers are shown grouped for sexing, chromosomes 13, 18 and 21. A blue box indicates an informative marker, a purple box indicates a suggestive result for the biopsied cell and a grey box indicates a conclusive result for the cell line.

Marker	Maternal donor	Paternal donor	Biopsied Cell	KCL008_HD2
D6S1714	154/158	158	154	154/158
D6S452	215/223	223	223	223
D6S498	195/210	199/203	199/210	199/210
D6S1956	286/298	286		286
D6S1960	235/239	243	239	239/243
D6S438	329/333	329/334	333/334	333/334

Figure 6.10: Microsatellite analysis showing inheritance of one copy of chromosome 6 from the father and one from the mother. The second maternal copy is absent. A blue box indicates an informative marker, a purple box indicates a conclusive result for the biopsied cell and a grey box indicates a conclusive result for the cell line.

For the single biopsied blastomere, the results were not so clear. From the 16 somatic markers used, none or one allele only was detected in 11. For the remaining five markers two alleles were detected, but three were at non-informative loci. The last two markers (D13S325, D21S1437) showed normal diploid inheritance of one chromosome from each parent - consistent with both the original PGH result and the two pronuclei visible at fertilisation. Given the high drop-out rate it was not possible to conclude that the biopsied cell was truly diploid, therefore further microsatellite analysis was performed. The panel of markers chosen previously were disease specific, clustered closely together and mostly distal on each chromosome. Therefore recombination could have reduced the number of informative alleles, and the subsequent failure to detect triploidy in the single biopsied blastomere.

A panel of markers on chromosome one was consequently selected as they were concentrated around the centromere and therefore loss of heterozygous markers through recombination was unlikely. The results are shown in Figure 6.11. Of the total of 6 chromosome one markers, 3 were fully informative for the parental samples, of which two were conclusive for the cell line, with two maternal and one paternal alleles present. For the single cell, marker D1S2885, despite paternal dropout, conclusively showed two maternal alleles for chromosome 1, confirming diploid maternal inheritance in the single cell and therefore the triploid status. Marker D1S495 was also suggestive of diploid maternal inheritance, but allele drop out in the paternal parental sample prevented an unequivocal conclusion.

Marker	Maternal donor	Paternal donor	Biopsied Cell	KCL008_HD2
D1S1656	187/210	179/206	187	187/206/210
D1S2655	239/243	237/245	243	243/245
D1S2700	313/340	295	313	295/313/340
D1S495	189/202	187	189/202	187/189/202
D1S2885	313/329	323/327	313/329	313/323/329
D1S2830	269/288	288/296		269/288

Figure 6.11: Microsatellite analysis for 6 markers for chromosome one on the PGH product from the biopsied blastomere, the donors and KCL008-HD2 hESC line. A blue box indicates an informative marker, a dark purple box indicates a conclusive result for the single cell, a light purple box is suggestive. A grey box indicates a conclusive result for the cell line.

Taken together, these results confirmed that the cell extracted for biopsy was triploid (with the exception of chromosome six), an identical karyotype to the cell

line generated from the embryo.

6.3.5 Pre-differentiation characterisation

Pre-differentiation characterisation confirmed that undifferentiated KCL008-HD2 cells were positive for POU5F1, SSEA3 and 4, TRA1-61 and 1-80, as shown by immunocytochemistry in Figure 6.12.

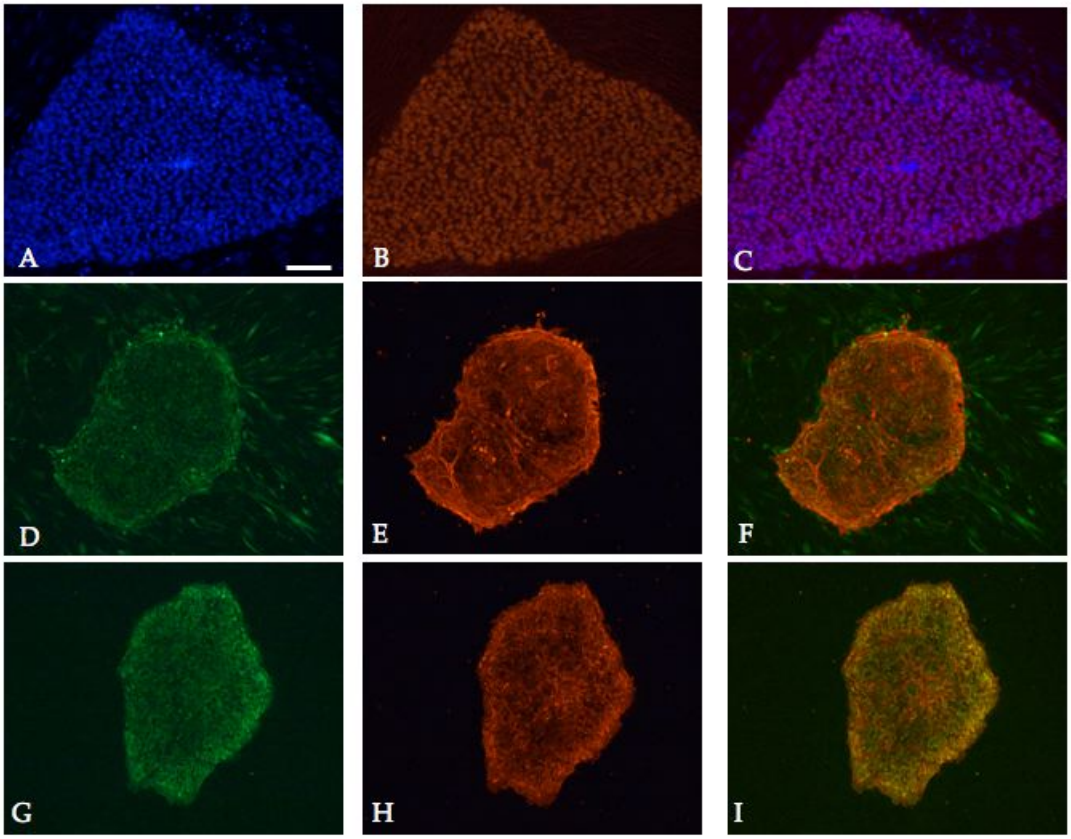

Figure 6.12: Predifferentiation characterisation of KCL008-HD2 showing positive expression for the common pluripotency markers: (A) DAPI, (B) POU5F1 (C) Merged imaged; (D) TRA1-60 (E) SSEA4 (F) Merged image; (G) TRA1-81 (H) SSEA4 (I) Merged image. All images at x10 objective. Scale bar indicates 50 μm.

Further quantitative analysis by FACS confirmed 97% of cells were positive for CD9, over 80% of GFP negative cells stained positive for SSEA4, and all cells were negative for SSEA1. Although the majority of cell samples were negative for NCAM, occasionally a small sub population of cells were positive. The intensity of the staining was always low in these samples. These results are shown in Figure 6.13.

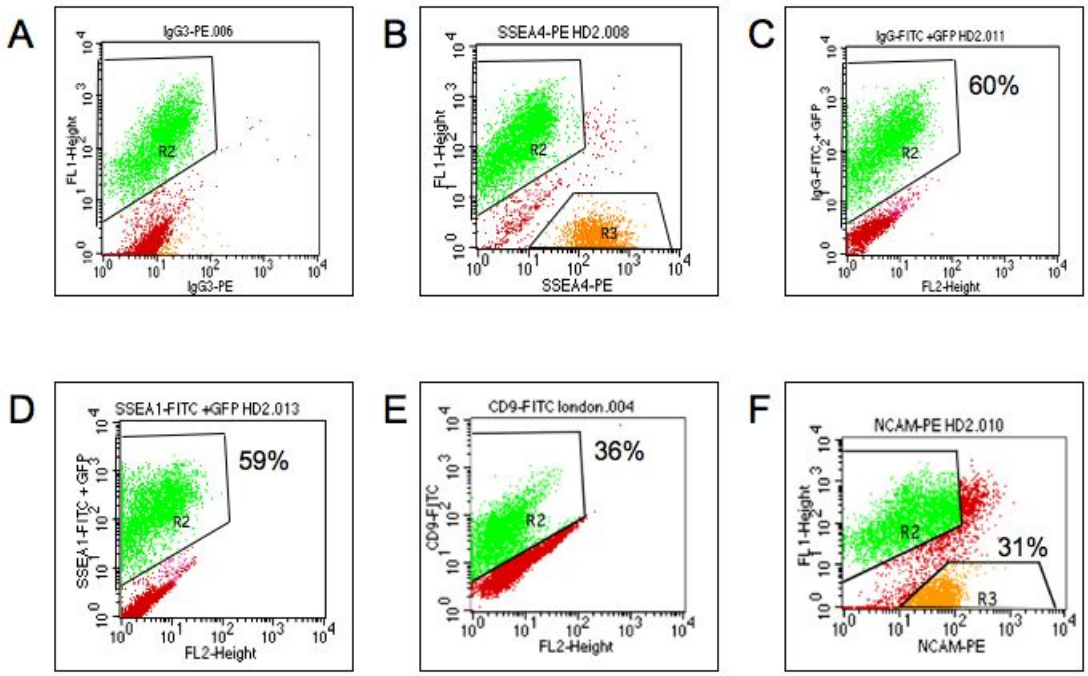

Figure 6.13: Predifferentiation characterisation of KCL008-HD2 showing quantitative analysis of the pluripotency markers SSEA4 and CD9 and the differentiation marker SSEA1. (A) Control sample of HFF and KCL008-HD2 without staining showing that 60% of the sample was FITC positive corresponding to the GFP feeders (B) The same sample stained for SSEA4-PE, showing 60% GFP positive feeders and over 80% of the GFP negative cells positive for SSEA4 (C) HFF feeders stained for SSEA1-FITC with around 60% of the sample positive (D) Sample of HFF and KCL008-HD2 stained for SSEA1-FITC. As again around 60% of the sample was positive, therefore the KCL008-HD2 cells were negative for SSEA1. (E) Around 36% of the undifferentiated cell culture was positive for CD9, the remaining likely to be feeders, which were negative in the control. (F) Some sub-populations of undifferentiated cells were positive for NCAM, but the surface level expression was low.

The undifferentiated colonies were also negative for NES, MAP2, PAX6 and SSEA1 as shown in Figure 6.14. As the HFF feeders used were GFP positive, it was possible to exclude them from analysis when the antibodies were conjugated with a red fluorochrome (cy3 or PE). However, when the fluorochrome used was green (FITC) the percentage of positive cells was calculated by comparing with the result from HFF alone.

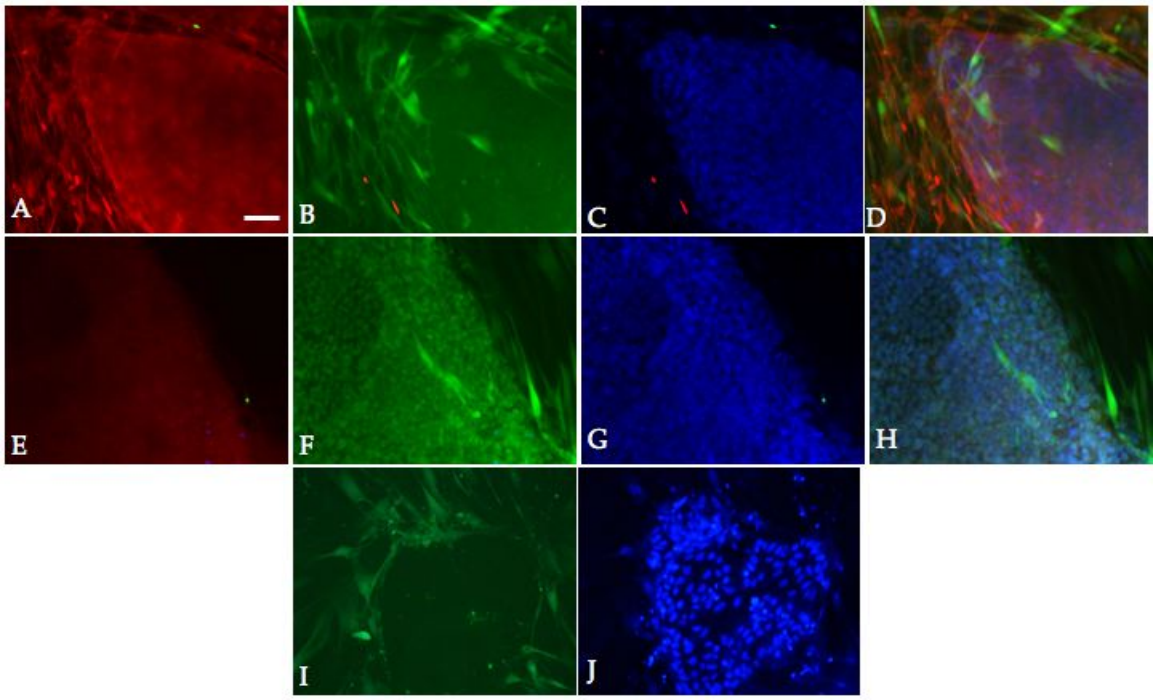

Figure 6.14: Predifferentiation characterisation of KCL008-HD2 showing negative expression for the common neural markers: (C,G,J) DAPI; (A) NES, (B) MAP2, (D) Merged image; (E) PAX6, (F) positive expression of POU5F1-iA, (H) Merged image; (I) the differentiation marker SSEA1. All images at x10 objective. Scale bar indicates 50 μm.

6.3.6 Neural induction

The differentiation protocol was initiated at seven time points consisting of 19 experiments with KCL008-HD2 and 7 experiments with KCL001. The hESC were plated in small pieces and with only a few pieces per dish to encourage low density growth

and to minimise cell-cell interactions and intercellular signalling. The two hESC lines behaved differently in the early stages, as shown in Figure 6.15.

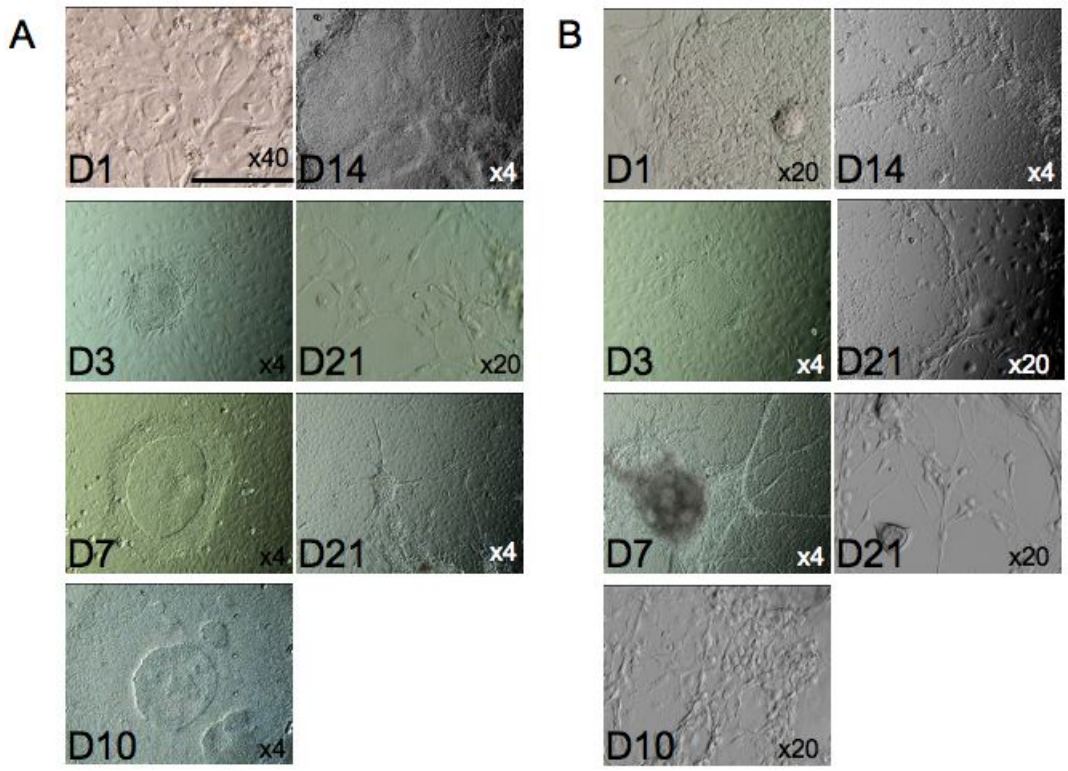

Figure 6.15: Morphology of (A) KCL008-HD2 and (B) KCL001 during the stromal co-culture period of the induction protocol from D1 to D21. Scale bar indicates 50 μm at x40 objective.

KCL008-HD2 routinely showed robust proliferation, forming dense colonies that differentiated initially in the centre, and then in additional pockets throughout the colony. The colonies were very large by day 14 when the medium was changed to N2. By day 21, a few cells with potentially neural morphology could be seen, but most of the cultures were so dense it was not possible to discern cell type. KCL001 also showed robust proliferation, but did not form dense colonies. Instead very large colonies only a few cells thick were observed, and individual cells with long processes of possible neural morphology could be seen as early as 10 days on MS-5. Whether this distinction was due to inherent behavioural characteristics of different cell lines, or due to the effect of the triploidy or mutant *HTT* gene could not be established

from the two lines used in this analysis. This could be investigated in the future with the use of multiple normal and mutant lines.

An increase in NCAM positive cells was seen during this early induction stage. With KCL008-HD2 around one fifth of cells were positive at day 14 which rose to over half at day 21. A concomitant decrease in SSEA4 expression from around 70% to 30% was observed at the same time points, as shown in Figure 6.16. With KCL001, NCAM expression increased from around 45% to 55% from day 14 to 21, with a simultaneous decrease in SSEA4 expression from 40% to 10%.

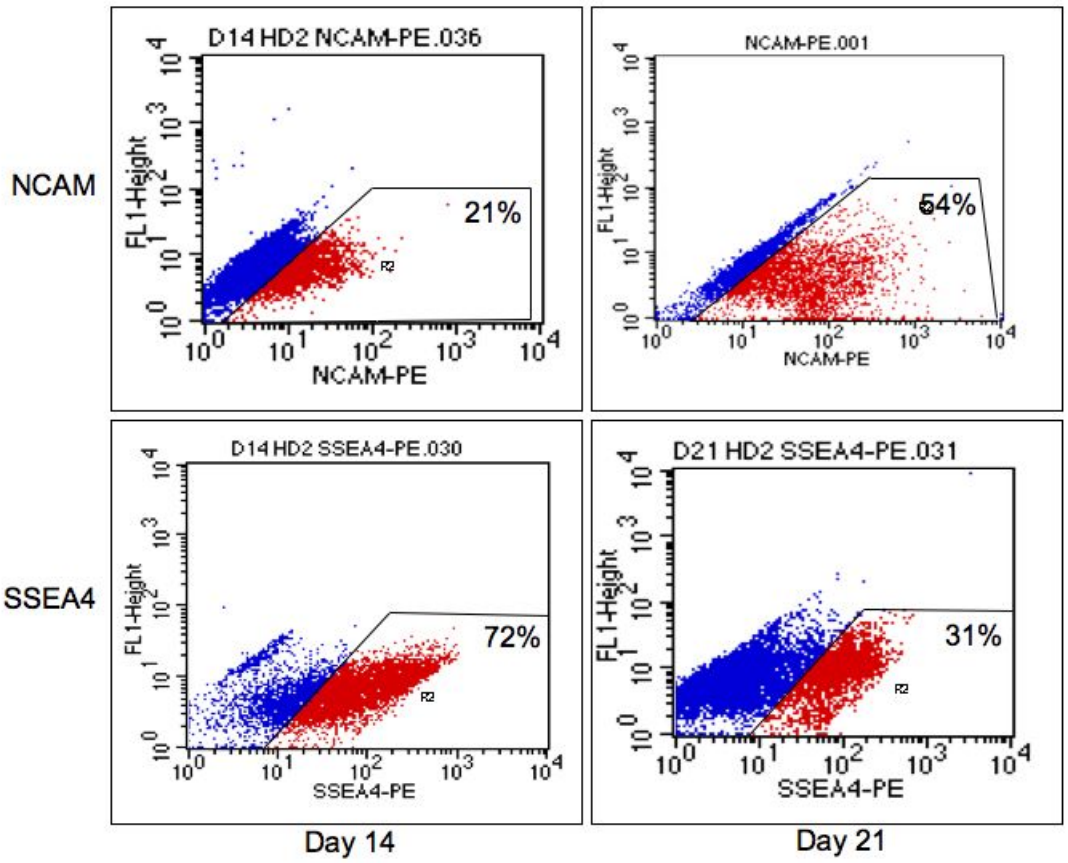

Figure 6.16: FACS analysis of KCL008-HD2 cells during the stromal co-culture period to assess NCAM and SSEA4 expression levels. A concomitant increase in NCAM and decrease in SSEA4 expression from day 14 to 21 was observed.

6.3.6.1 N2 medium on a POL surface

For both cell lines excellent attachment on initial passage to the POL surface was observed, although a wide range of cell morphology was seen, as shown in Figure 6.17. Despite the variable morphology, almost half of the cells were NCAM positive and less

than 3% were CD73 positive. This ruled out mesenchymal induction. Proliferation was poor, and in each of the replicate experiments for both cell lines there was extremely low attachment by P2. The cells therefore became low density cultures regardless of plating density. This resulted in replication arrest, and culture of these cells was not achieved beyond P2.

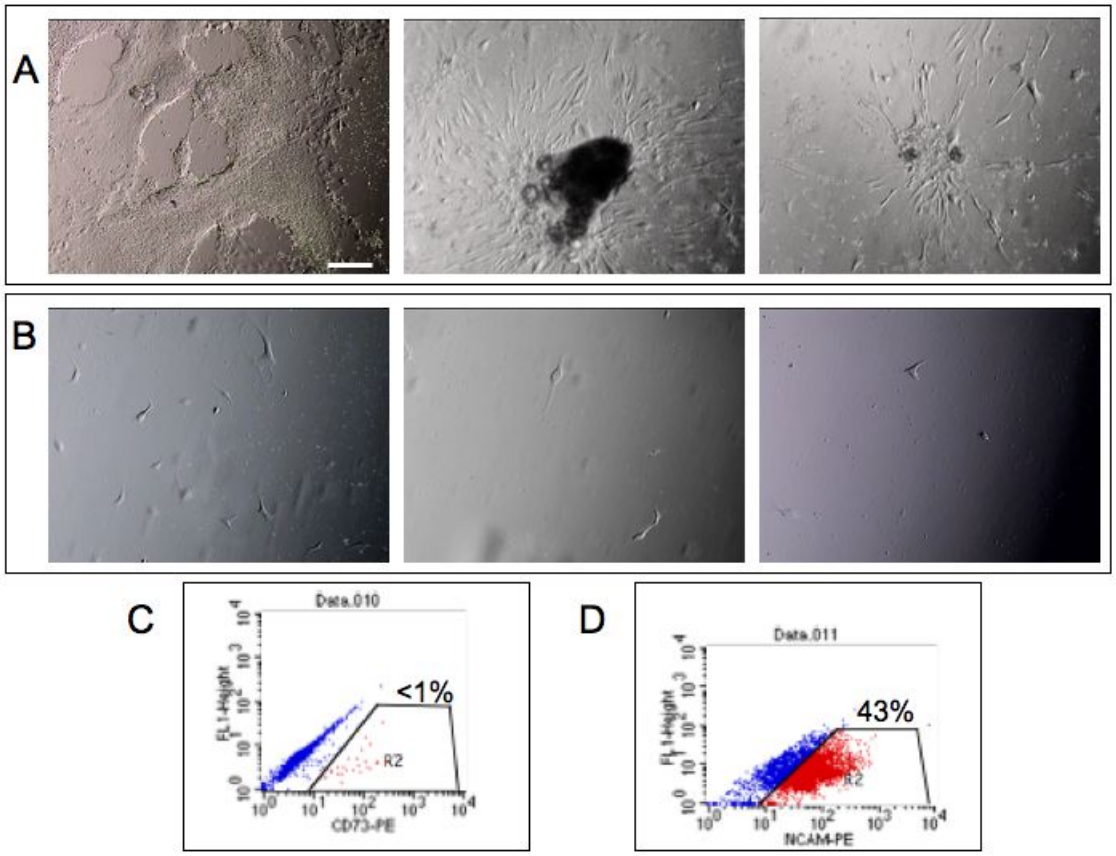

Figure 6.17: Examples of typical KCL008-HD2 culture morphology on POL in N2 medium at (A) P1 and (B) P2, commonly only two or three cells were visible in a low magnification field of view. All images at x4 objective. Scale bar indicates 100 μm. (C) FACS analysis at P1 showing (C) low CD73 expression and (D) moderate NCAM expression, implying differentiation of the cells to the neural lineage, but loss of proliferation prevented the continued culture of the cells.

6.3.6.2 N2B27 medium on a Gel surface

Initial attachment in the gelatin condition was variable. Generally small cell clusters proliferated and spread on the gelatin surface, although a high level of cell death was evident. Subsequent passage to P2 and P3 was possible. Increasing homogeneity

of cell morphology was seen and around one third of the cells were positive for NCAM at P1. However, attachment was poor, and further attempts at passage were unsuccessful. Figure 6.18 shows typical KCL008-HD2 cell morphology at P1-3.

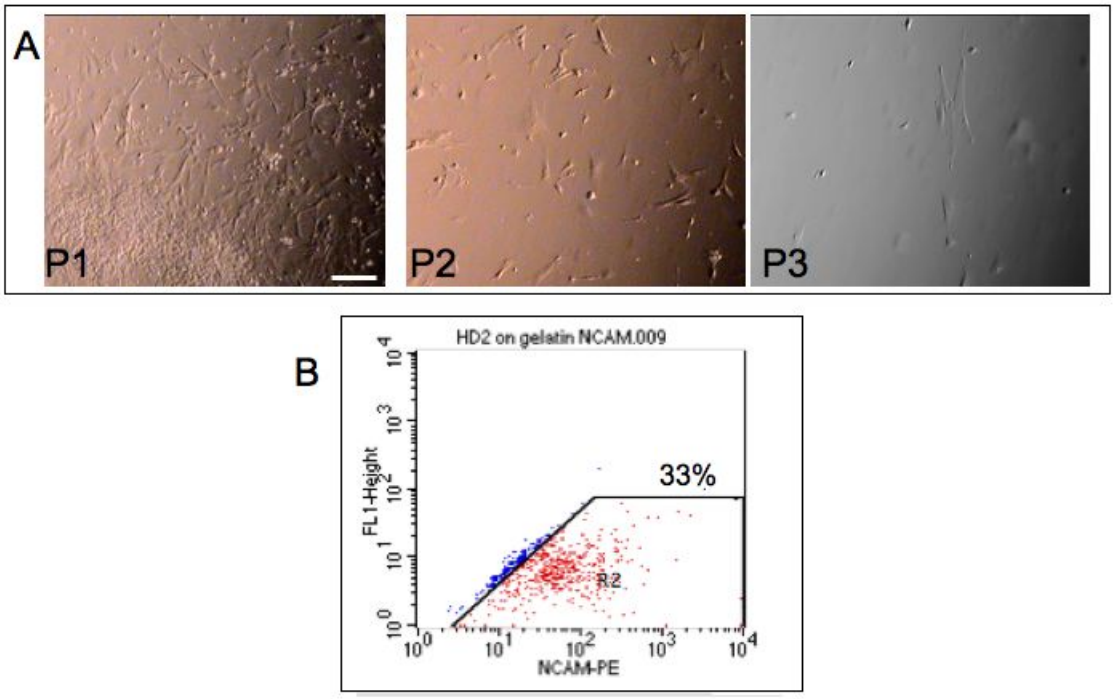

Figure 6.18: Examples of typical KCL008-HD2 culture morphology on gelatin in N2B27 medium at (A) P1, P2 and P3, with reduced attachment at each passage. All images at x4 objective. Scale bar indicates 100 μm. (B) FACS analysis showing moderate NCAM expression at P1, suggesting differentiation of the cells to the neural lineage, but loss of proliferation prevented the continued culture of the cells.

6.3.6.3 N2B27 medium on a POL surface

Initial attachment and proliferation of the cells plated on POL in N2B27 was robust and rapid. Diverse cell morphology was observed in early culture as shown in Figure 6.19. The morphology could be characterised broadly into four types, (A) attachment of EB-like clumps with subsequent diverse outgrowth (B) cells with non-neural morphology (C) low density cell attachment, some process extension (D) high density attachment of cells with neural-like morphology and long cellular processes.

Cells with non-neural morphology were used for differentiation experiments for other lineages.

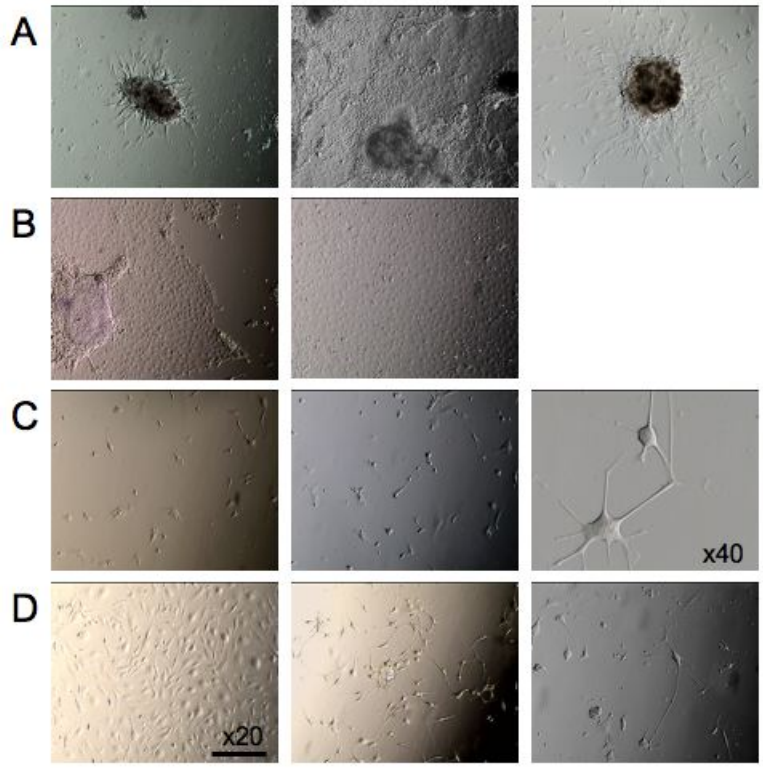

Figure 6.19: Examples of diverse culture morphology of P1 KCL008-HD2 cells on POL in N2B27 medium, broadly grouped into four categories (A-D), see text for descriptions. All images at x4 objective unless otherwise indicated. Scale bar indicates 50 μm at x20 objective.

The population of neural-like cells became more homogeneous with subsequent passage. By P4 for KCL001 and P5 for KCL008-HD2 one distinct cell type had emerged. The population was identical in morphology for both cell lines and is shown for KCL008-HD2 in Figure 6.20. The proliferation of the cells was highly dependent on cell density, with low-density cultures arresting and no further passage possible. Following this observation, split ratios were kept low, the first one to ten passages were split 1:2 or 1:3. By P10 passage was required daily and the ratio was increased. Several vials were cryopreserved at regular intervals following a successful freeze-thaw cycle, with the method exactly as for MEFs.

Of the 13 experiments with KCL008-HD2 in N2B27 medium on POL dishes, two

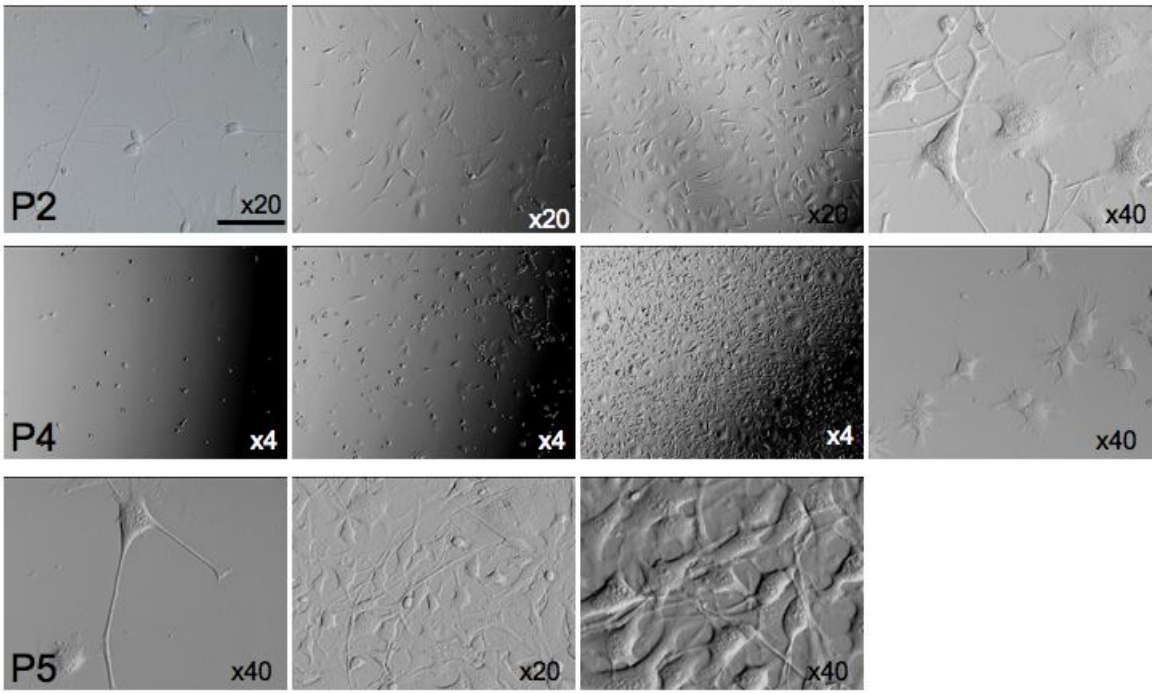

Figure 6.20: Examples of KCL008-HD2 cell culture morphology at P2, 4 and 5 on POL in N2B27 medium. By P5 a homogeneous population of cells was obtained, showing robust proliferation and survival following cryopreservation. Scale bar indicates 50 μm at x20 objective.

resulted in a stable cell line with the characteristics of robust proliferation, very high homogeneity by P3, ability to be passaged between a 1:5 and 1:10 ratio, and excellent freeze-thaw survival. These cells were extensively characterised to confirm neural lineage. Comments regarding efficiency of the differentiation protocol cannot be made as refinements to the details of the protocol were made throughout. For example plating density and split ratios were changed between and within experiments. As hESC show poor low density/clonal survival, passage of undifferentiated cells onto MS-5 feeders was initially performed as for routine culture. However, clonal or low density passage onto stromal co-culture systems has been shown to be key for reliable differentiation (Barberi *et al.*, 2003; Kawasaki *et al.*, 2000). Therefore in later experiments, the colonies were cut into the smallest pieces possible still enabling attachment and proliferation. The proliferation of the neural stem-like cells was extremely density dependent, with robust propagation only achieved initially at high density passage. In some experiments, there was either insufficient cell number to passage at high density, or the split ratio was too high too early in the induction phase. These low density cells stained positive for the neural precursor marker NES as demonstrated in Figure 6.21. However, no further growth was evident, the the cells did not assume neural-like morphology. The two experiments where neural lines were established were initiated with the plating of very small colony pieces, and passage at high density until the line was established, thereafter split ratios could be increased to between 1:5 and 1:10.

6.3.7 Characterisation of differentiated cells

6.3.7.1 Growth rate

Passage 4 KCL008-HD2 and KCL001 cells were cultured for 22 days which included six passages. The initial plating number for the growth analysis was $1x10^5$ cells in a 6 cm dish. From a single dish of KCL008-HD2 around $6.0x10^8$ cells were obtained - a 6000-fold increase in cell number in just over three weeks. Similarly for KCL001, around $8.8x10^8$ cells were obtained - a 8800-fold increase. The growth curves are shown in Figure 6.22.

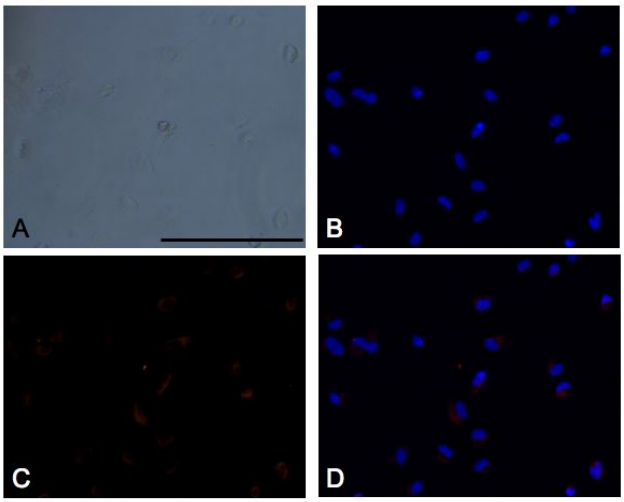

Figure 6.21: Examples of a low proliferative population of cells positive for nestin. (A) Bright field (B) DAPI stained nuclei (C) Cytoplasmic nestin staining (D) Merged image. All images at x40 objective. Scale bar indicates 50 μm.

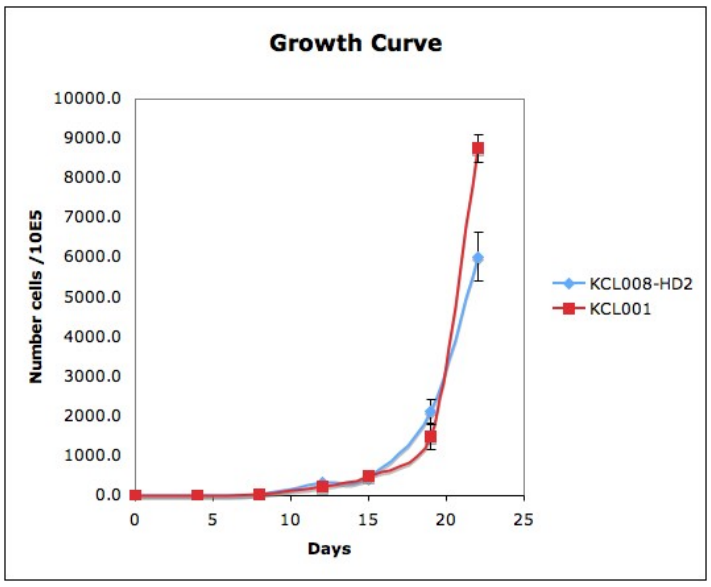

Figure 6.22: Expansion curve of KCL008-HD2 and KCL001 derived neural precursor cells for six passages (P4 to P10) with initial plating number of 1x10^5 cells in a single 6 cm culture dish.

6.3.7.2 Marker expression

Despite the initial morphological heterogeneity, NCAM expression was consistently high on POL in N2B27 conditions. At P1 and P3 NCAM positive KCL008-HD2 cells exceeded 80% and 90% of the population respectively. Less than 5% CD73 positive cells were consistently observed. SSEA4 expression had decreased to around 3% by P3. Results for KCL008-HD2 are shown in Figure 6.23. Occasionally cell populations were assessed throughout the various experiments which were positive for non-neural markers or negative for NCAM. For example, at the end of 21 d on MS-5 one cell population expressed NCAM at only 7%, compared over 50% as shown previously. In a further cell population, over 80% of cells were positive for the epithelial marker K18. In general however, proliferating populations showed high levels of NCAM and appropriate expression of other markers.

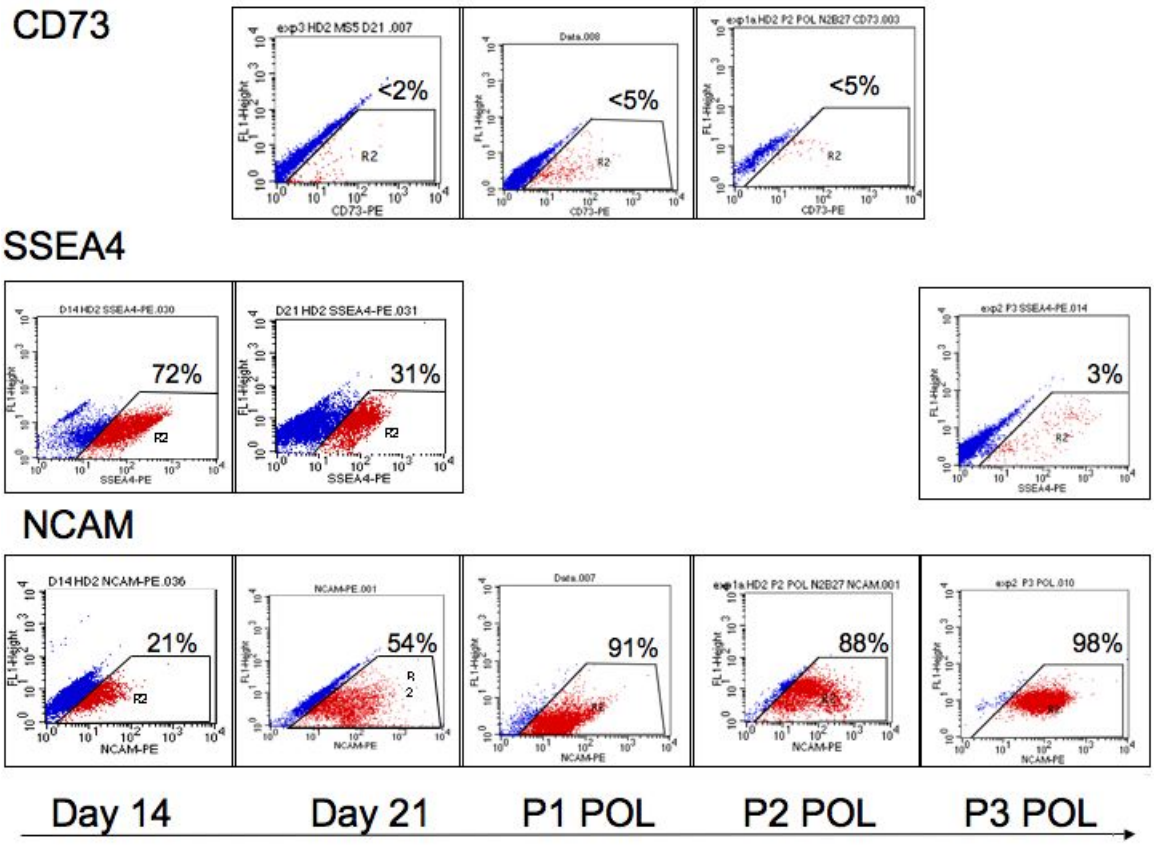

Figure 6.23: FACS analysis showing the gradual acquisition of the neural surface marker NCAM during neural induction, with concomitant decrease in the pluripotent marker SSEA4. The consistent low expression of CD73 confirmed mesenchymal induction had not occurred.

Thorough characterisation was performed on the cells once stable proliferation was established. Positive staining for NES, SOX2 and MSI1 confirmed the neural lineage of the cells. The proliferative phenotype was reflected in the high proportion of cells that were positive for KI67. FACS analysis confirmed positive expression of CD9. This characterisation for KCL008-HD2 cells is shown in Figure 6.24.

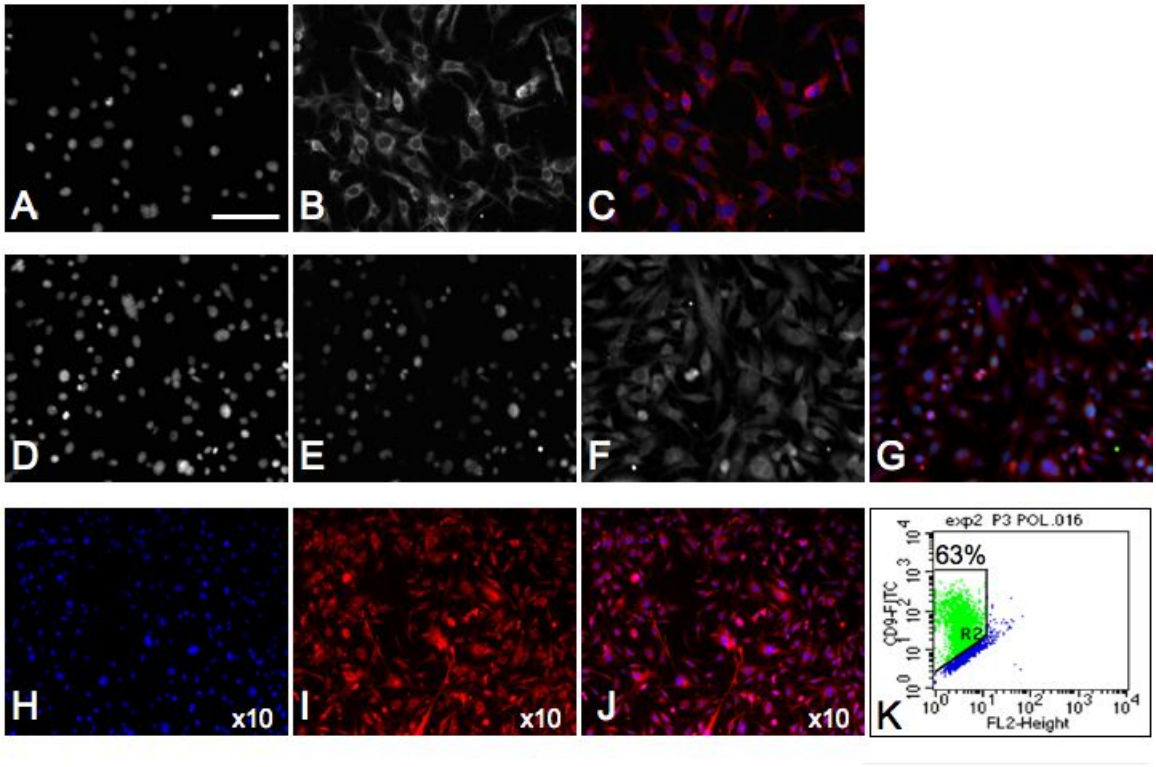

Figure 6.24: Differentiation of KCL008-HD2 cells to the neural lineage was evidenced by positive expression of (A-C) NES, (D-G) MSI1 and KI67 (H-J) SOX2 and (K) CD9. (A,D,H) DAPI nuclei, (B) NES, (C) merged image. (E) KI67, (F) MSI1, (G) merged image. (I) SOX2, (J) merged image. All images at x20 objective unless otherwise indicated. Scale bar indicates 50 μm at x20 objective.

The differentiated cells were negative for POU5F1, confirming loss of pluripotent status. Negative expression of cytokeratins 5,14 and 18 ruled out epidermal induction. Mesodermal differentiation was excluded by negative staining for brachyury and mesenchymal differentiation by negative expression of CD73. Induction into the endoderm lineage was ruled out by negative staining for AFP. Surprisingly, levels of SSEA1 did not appear to be expressed in the time frame of the experiment. At P3 on

POL the level of SSEA1 was below 1%. This questions the routine use of this marker for characterisation of differentiation. Negative expression of HNK-1 and P75 ruled out the differentiation to neural crest cells. This characterisation is shown in Figure 6.25.

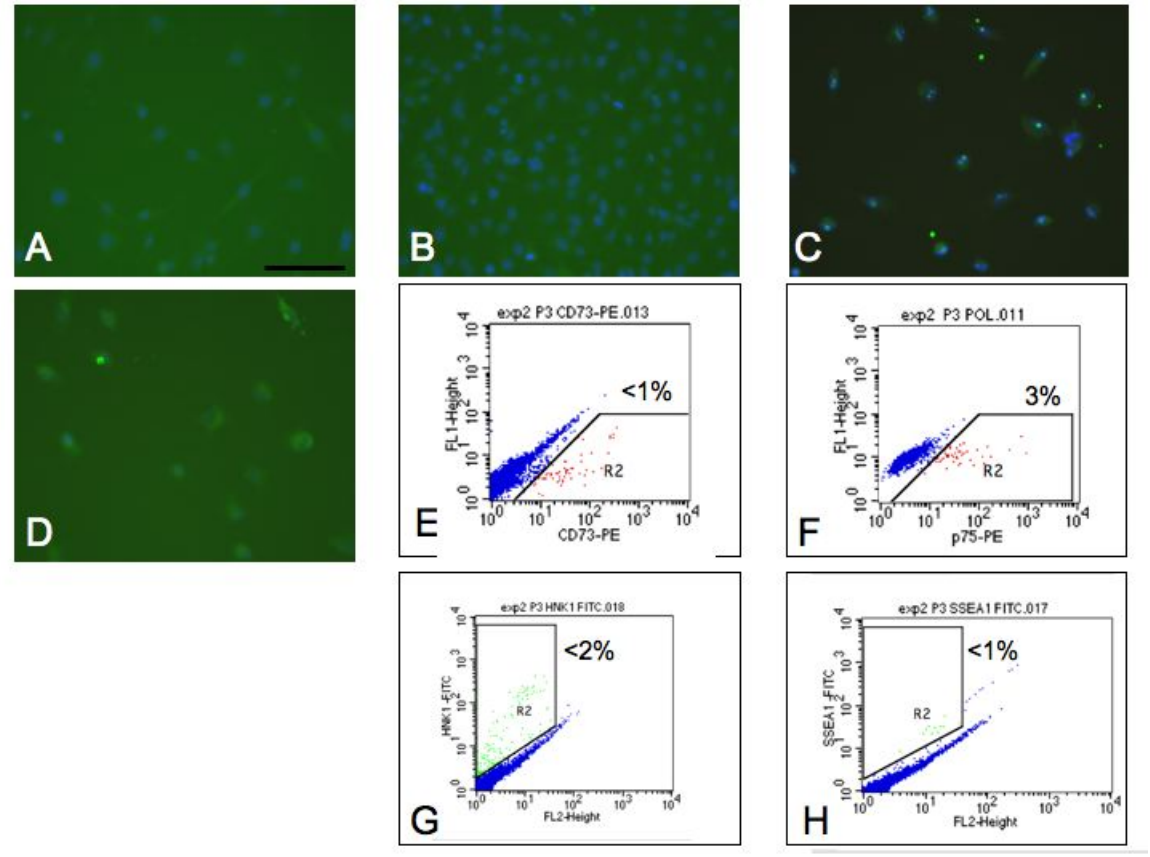

Figure 6.25: Loss of pluripotency of KCL008-HD2 cells was shown by negative expression of (A) POU5F1-iA and differentiation to non-neural lineages was ruled out by negative expression of (B) KRT5, 14 (C) brachyury (D) AFP (E) CD73 (F) P75 (G) HNK-1. (H) SSEA1 expression was not induced in the timeframe of culture. All images at x20 objective. Scale bar indicates 50 μm.

6.3.7.3 Cell cycle

In the interval between receiving the cytogenetic karyotype and waiting for the SNP analysis to be completed, cell cycle analysis of the KCL008-HD2 cells was performed. This was in the attempt to confirm the triploid chromosome content of the cells as suggested by the cytogenetic karyotype. Analysis of the replication state of a population of cells can be achieved by FACS following fluorescence labelling of the

nuclear DNA. In a diploid population, quiescent and G1 cells will have one copy of DNA (2n) and will therefore have 1x fluorescence intensity. Cells in G2/M phase of the cell cycle will have two copies of DNA (4n) and accordingly will have 2x intensity. Since the cells in S phase are synthesising DNA they will have fluorescence values between the 1x and 2x populations. In a triploid population, the 1x and 2x peaks correspond to 3n and 6n chromosomes respectively. Cell cycle analysis was performed for KCL008-HD2 exactly as described in section 2.5.4.1. HFF were used as a euploid control.

Initially the aim was to gate out the HFF feeders dues to their GFP expression. However, the permeabilisation step affected detection of GFP and gating was not possible. Therefore, the HFF cells were analysed alone, and then KCL008-HD2 cells on HFF feeders were examined. Figure 6.26 shows the results of the analysis.

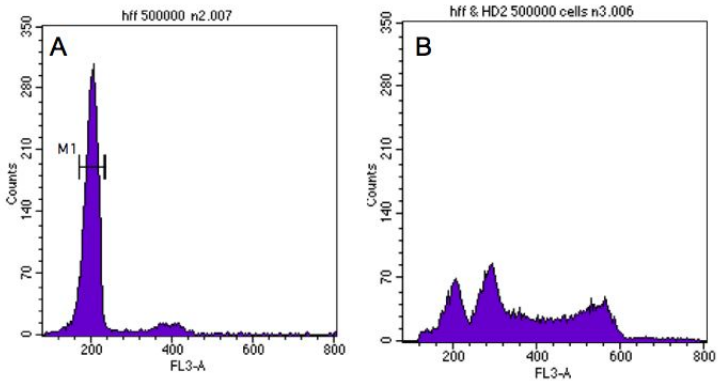

Figure 6.26: FACS analysis of cell cycle characteristics of (A) HFF (B) KCL008-HD2 and HFF.

Analysis of HFF feeders showed a peak at 2n and 4n as expected. From a total of 500,000 analysed cells, over 300,000 were quiescent or in G1 with a corresponding 2n complement. This is likely to be due to contact inhibition by neighbouring cells when the culture is grown to confluence. The HFF were harvested for analysis prior to passage and therefore were almost fully confluent. Despite this, a small peak of approximately 150,000 cells contained a 4n content corresponding to the G2/M phase. The remaining cells were assumed to be between the two peaks in S phase.

No further peaks were visible. The analysis of a total of 500,000 KCL008-HD2 cells and HFF together displayed three peaks. Approximately 70,000 HFF were found to be in the G1 phase at 2n intensity, but the 4n peak could not be distinguished. As KCL008-HD2 cells in S phase would lie between 3n and 6n, it was likely that they were masking the 4n peak. However, this peak could be inferred from the HFF alone analysis. Approximately 100,000 KCL008-HD2 cells were in G1 or the quiescent phase with a chromosome content between that of 2n and 4n. Approximately 40,000 cells contained a 6n content corresponding to G2/M. The peak was not exactly at twice the area of the 3n peak. This could be because there were insufficient cells at the 6n stage to form a true peak above background noise in the experiment. Modifications to the protocol, the number of cells analysed and the isolation method failed to produce a more accurate result.

6.3.7.4 CD30 expression

The early culture of KCL008-HD2 was difficult (with poor attachment and proliferation arrest) but the line appeared to successfully adapt to culture by P10. Therefore it was investigated whether the cells were chromosomally unstable having undergone spontaneous transformation. CD30 is a member of the tumor necrosis factor superfamily which has been identified as a marker for transformed hESC (Herszfeld *et al.*, 2006). It is expressed on transformed but not normal undifferentiated hESC. CD30 expression is associated with a protective mechanism against apoptosis. Each sample of undifferentiated KCL008-HD2 cells was split and stained for SSEA4 and CD30. A comparison sample of KCL001 was also analysed. The HFF feeders were gated out of the analysis by GFP expression, and 100,000 events collected in the hESC gate only. The results are shown in Figure 6.27.

Approximately 85% of KCL008-HD2 cells were positive for SSEA4, confirming the undifferentiated status of the majority of the cells at the time of analysis. Less than 5% of the cells were positive for CD30. The KCL008-HD2 cells, despite being triploid, were neither transformed nor had acquired growth or anti-apoptotic advantages through the mechanisms associated with CD30 expression. It might be that three copies of those genes controlling cell division and pluripotency could confer some advantage to the cells and enable culture adaptation despite the HD and triploid status. 65% of KCL001 cells were positive for SSEA4 but almost half of

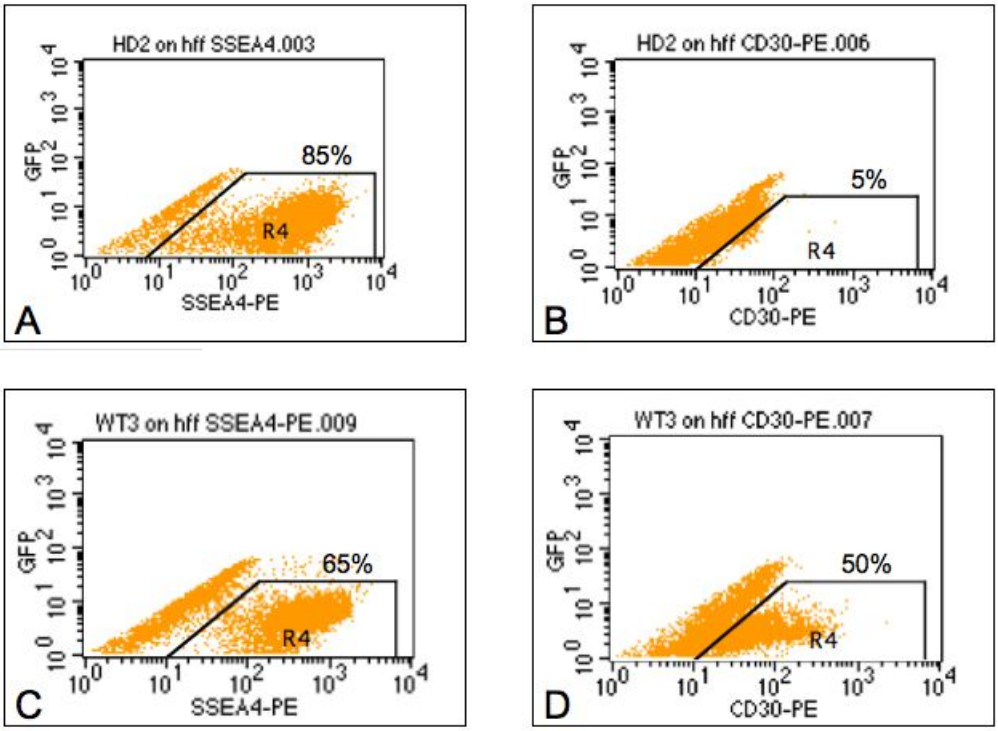

Figure 6.27: FACS analysis of hESC after gating out of feeders the GFP expression. (A) SSEA4 expression on KCL008-HD2 cells (B) CD30 expression on KCL008-HD2 cells (C) SSEA4 expression on KCL001 cells (D) CD30 expression on KCL001 cells.

these cells were also positive for CD30. This was unexpected as it suggested that approximately half of the KCL001 cell population was transformed, despite normal cytogenetic karyotype at a similar passage to that used for the analysis. However, it is highly likely that G-banding is not sensitive enough to pick up minor deletions or duplications that may contribute to a transformed phenotype (Pera, 2004). Therefore, SNP and CGH analysis is planned with this cell line to confirm or question the validity of CD30 as a marker of transformed cells.

6.3.8 CAG repeat analysis

The CAG repeat analysis was performed on the undifferentiated KCL008-HD2 cells just prior to neural induction, and also on P12 POL cells at the end of the protocol. The undifferentiated cells had the same CAG repeat unit sizes as at derivation, with the maternal allele carrying 18 repeats and the paternal with 46 repeats. While the normal allele was unchanged following differentiation, the mutant repeat length had increased from 46 to approximately 70 CAG repeats. The trace is shown in Figure 6.28.

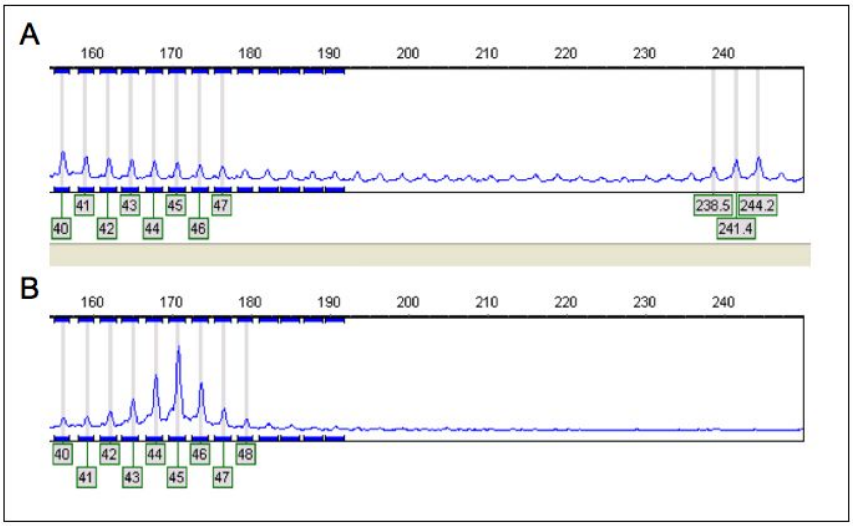

Figure 6.28: CAG repeat analysis of KCL008-HD2 at P12 on POL, enlarged from the whole trace. (A) The size of the peak was around 244 bases, corresponding to a repeat size of approximately 70 CAG repeats. (B) A control sample with 45 repeats.

6.3.9 Protein analysis

Western blot analyses of KCL008-HD2 cell lysates were performed to confirm the translation of the paternally inherited mutant *HTT* gene into mutant protein. For each immunodetection, the samples were run in triplicate and the gels were probed with each of the three antibodies - 2166, S830 and MW1 (section 2.5.6.4).

Several early attempts were unsuccessful. For experiment one, undifferentiated KCL008-HD2 cells were used with HFF as the negative control. The concentration of protein in the cell lysates is shown in Table 6.3, and a total of 20 μg of protein was loaded in to the gel wells. The lysates were made in RIPA buffer. The gel was not run for long enough to separate the HTT protein and no bands were visible on the exposed film for the test samples. Mutant HTT is a very large protein, with a molecular weight of around 350 kDa. The gel needed to be run for much longer than the normal 2-3 h which is sufficient for the majority of other proteins.

In experiment two, the same samples were run on the gel for 5-6 h, but again no bands were visible on the exposed film. The cell lysates were prepared again but in KCl buffer. This was recommended by staff at the Medical and Molecular Genetics laboratory at King's College as potentially better for running western blots for mutant HTT.

In experiment three, both undifferentiated KCL008-HD2 and the differentiated neural cells were used to make lysates in KCl buffer, with HFF as the negative control. The concentration of protein in the cell lysates is shown in Table 6.3. A total of 20 μg of protein was loaded into the wells, and the gel was run for 5-6 h. Again, no bands were visible in the test lanes on the exposed film. It was possible that if the cells were only expressing low levels of HTT, loading 20 μg of protein might not be sufficient for detection. A larger culture of cells was grown for protein extraction. An over-confluent T75 flask of KCL008-HD2 neural progenitors was used and the lysates were made in KCl buffer. The concentration of protein in the cell lysates is shown in Table 6.3. A total of 50 μg of protein was loaded into the gel wells. Once again, nothing was seen on the exposed film. A reversible Ponceau red stain confirmed there was protein present however. The final step was to use fresh batches of antibodies for the immunodetection, and to run the gel for 3-4 h to enable bands of other proteins/mutant HTT fragments to be seen. The final attempt was

successful in detecting normal HTT with the 2166 antibody in both the KCL008-HD2 cells and the HFF feeders, as well as the positive control. Mutant HTT was detected in the KCL008-HD2 cells and the positive control using the MW1 antibody. The western blot traces are shown in Figure 6.29.

Table 6.3: Concentration (conc.) of protein in all the lysates made from undifferentiated (HD2) and differentiated (AGP) KCL008-HD2 and the HFF feeder cells.

RIPA buffer								
Standard μg/uL	0	4	8	16	32	mean	HD2	HFF
Optical Density (OD)	0	0.097	0.168	0.318	0.596		0.057	0.089
OD/Standard μg/uL	0	0.024	0.021	0.019	0.019	0.021		
Protein conc. μg/uL							2.7	4.2
KCl buffer								
Standard μg/uL	0	2	4	8		mean	HD2	AGP
Optical Density (OD)	0	0.05	0.09	0.16			0.077	0.216
OD/Standard μg/uL	0	0.025	0.0225	0.02		0.0225		
Protein conc. μg/uL							3.4	9.6
KCl buffer								
Standard μg/uL	0	4	8	16	32	mean	AGP	HFF
Optical Density (OD)	0	0.085	0.165	0.312	0.573		1.061	0.281
OD/Standard μg/uL	0	0.021	0.021	0.0195	0.018	0.0199		
Protein conc. μg/uL							53.3	14.1

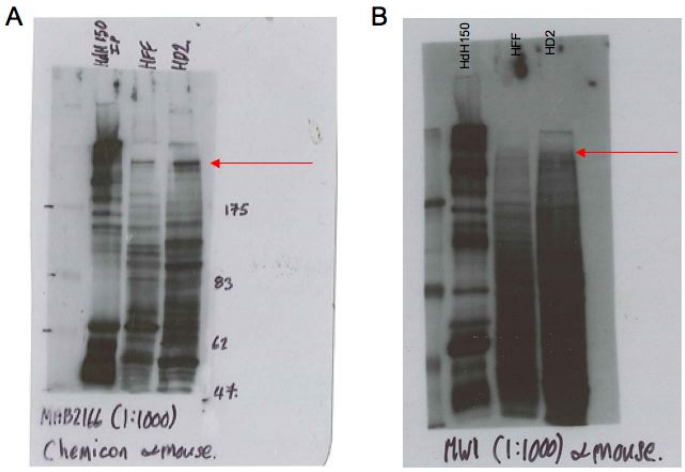

Figure 6.29: Western blot analysis of mutant HTT protein expression. (A) Detection of wild type HTT in KCL008-HD2, HFF feeders and positive control with the 2166 antibody. (B) Detection of mutant HTT in KCL008-HD2 and positive control with the MW1 antibody, but no detection in the HFF. Position indicated by the arrows.

6.3.10 Neuronal and astrocytic differentiation

To establish whether cell populations obtained with this protocol were a neuronal precursor population, further differentiation down the neuronal lineage was attempted. Neuronal differentiation was assessed by positive MAP2, PAX6 and TUJ1 expression. Astrocytic differentiation was assessed by GFAP, MSI1 and NES expression. Cells were cultured in triplicate in each condition with the aim of assessing the proportion of cells expressing each marker and analysing any differences in the behaviour of the two cell lines.

Following 14 d of culture without growth factor supplementation, KCL008-HD2 and KCL001 cells developed morphology suggestive of neuronal lineage differentiation. Cells were visible with long processes with multiple branches. Following 7 d of culture in 20% FCS without growth factor supplementation, the cells became bipolar as typical for astroglial cells. These morphological changes are shown in Figure 6.30.

Despite morphology indicative of neuronal cells as shown however, the cells were negative for TUJ1, PAX6 and MAP2, but positive for NES as shown in Figure 6.31. The differentiation protocol was repeated for 28 d but again no neuronal differentiation occurred.

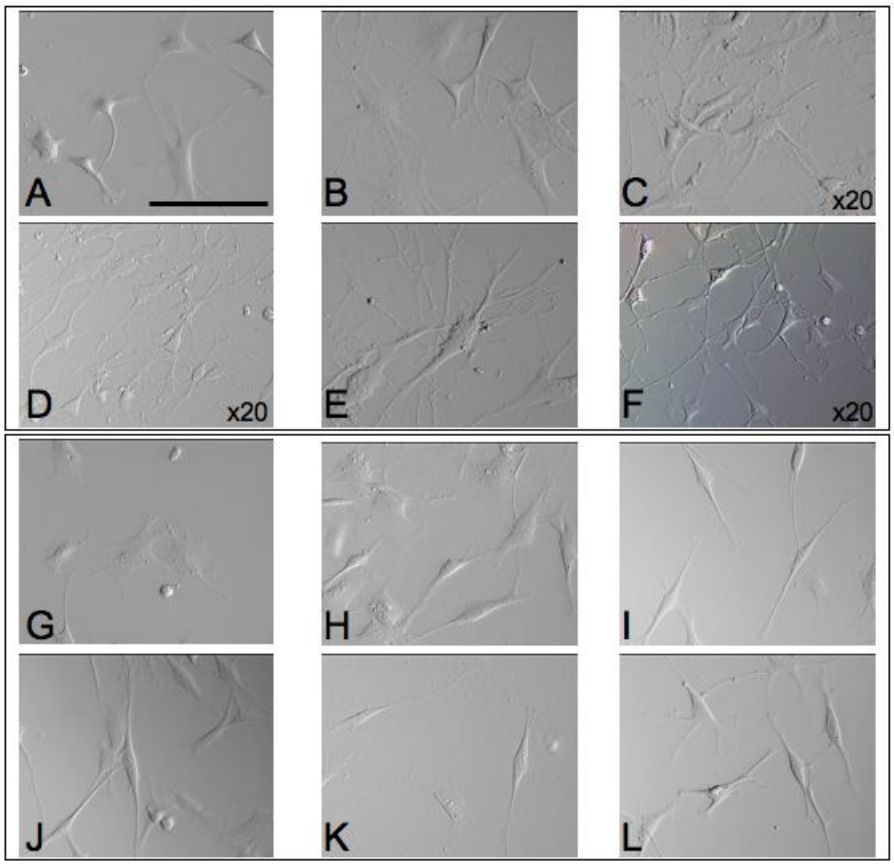

Figure 6.30: Morphology of KCL008-HD2 P12 POL cells in neuronal conditions without growth factor supplementation (A-F) and in astrocytic conditions with the addition of FCS (G-L). (A) Day 1 of growth factor withdrawal at 500 cells/cm^2. (B) Day 2. (C) Day 8. (D) Day 9. (E) Day 12 (F) Day 14. Cells developed multiple branched long extensions in this condition, characteristic of neuronal cells. (G) Day 1 of serum addition. (H) Day 2. (I,J) Day 6. (K,L) Day 7. Cells became bipolar, with two predominantly unbranched extensions, typical of astroglial cells. All images at x40 objective unless otherwise indicated. Scale bar indicates 50 μm at x40 objective.

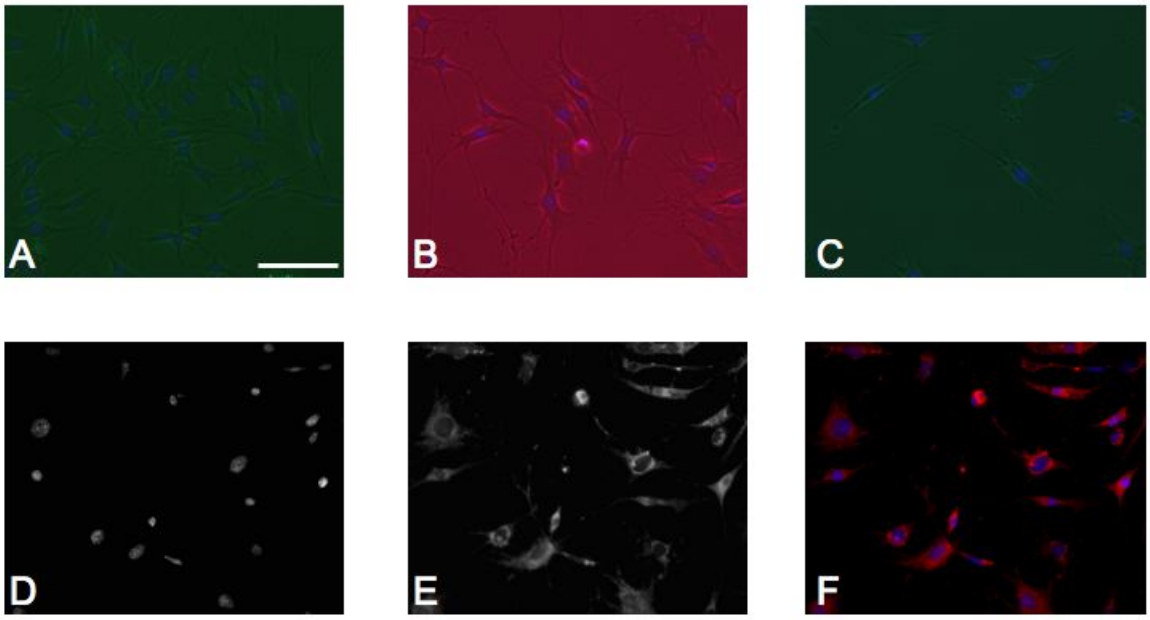

Figure 6.31: Failure of the neural cells to differentiate to the neuronal lineage was evidenced by negative expression of (A) TUJ1, (B) PAX6, (C) MAP2 and continued positive expression of NES (D) DAPI nuclei, (E) NES, (F) merged image. All images at x20 objective. Scale bar indicates 50 μm.

Following astroglial differentiation, the entire population of cells in all experiments were GFAP, MSI1 and NES positive, as shown in Figure 6.32.

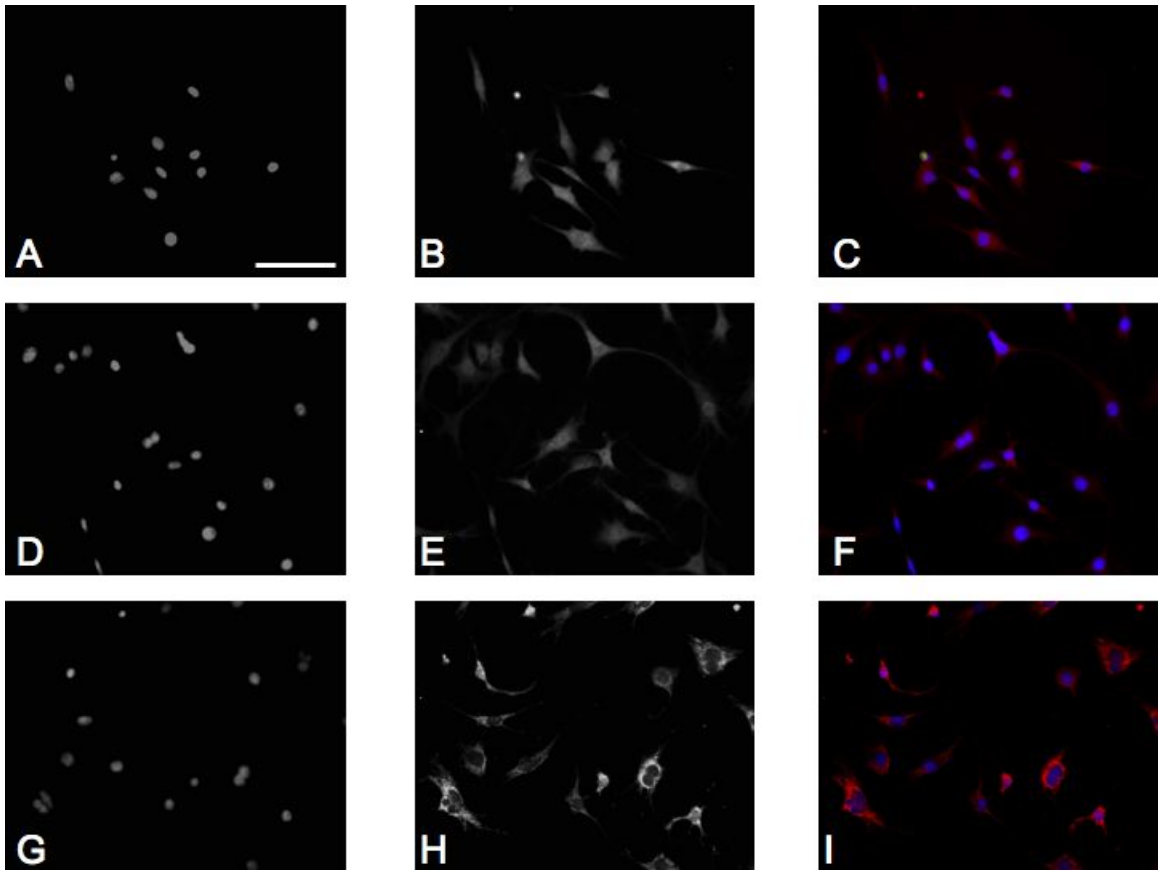

Figure 6.32: The astroglial phenotype of the KCL008-HD2 cells was evidenced by positive expression of (A-C) GFAP, (D-F) MSI1 and (G-I) NES. (A,D,G) DAPI nuclei. (B) GFAP, (C) merged image. (E) MSI1, (F) merged image. (H) NES, (I) merged image. All images at x20 objective. Scale bar indicates 50 μm.

6.4 Discussion

6.4.1 Early culture of KCL008-HD2

Difficulty with early culture and passage of hESC lines carrying HD has been experienced in other laboratories (personal communication, K. Sermon, Brussels). There is some evidence to suggest that wild-type HTT plays a role in intracellular trafficking of proteins required for construction of the extracellular matrix or involved in cellular adhesion (Strehlow *et al.*, 2007). This may ultimately affect the overall stability and ability of a cell to interact with its neighbours, and suggests a basis for the difficulty in the culture of KCL008-HD2. In addition, attempts to thaw and further culture KCL005-HD1 have been unsuccessful. Reports concerning the derivation of triploid lines make no mention of abnormal culture behaviour. One even describes faster doubling times in triploid verses diploid lines (Baharvand *et al.*, 2006). Taken together, these observations suggest that the early culture problems experienced with KCL008-HD2 seem likely to be as a result of the mutant HD gene not the triploid status.

6.4.2 Karyotype

Triploidy is one of the most frequent chromosomal abnormalities affecting human conception with a prevalence amongst all pregnancies of 1%-3% (Rosenbusch, 2008). The birth of a triploid child is rare, with death normally occurring in the early postnatal period. However, a few cases of unusually long survival have been reported (Iliopoulos *et al.*, 2005).

There have been a small number of reports of triploid hESC lines arising from both bi- and tri-pronucleate embryos (Baharvand *et al.*, 2006), and also from embryos donated at the blastocyst stage where information on the pronuclear status was not available (Heins *et al.*, 2004; Sun *et al.*, 2008). The triploid line from a binucleate embryo was reported as a 69,XXY mosaic, but no further analysis of the inheritance mechanism was discussed. Generally the *in vitro* behaviour, marker expression and morphology of the triploid lines were comparable to those of diploid lines, which is in agreement with the results presented here. However, *in vivo* differentiation may be impaired. The generation of only fluid-filled cysts upon injection of the cells into SCID mice has been reported (Heins *et al.*, 2004). However another

group successfully generated teratomas with all three germ layers from a triploid line (Sun *et al.*, 2008). Whilst the *in vitro* differentiation attempted here was successful, teratoma formation was not attempted.

Initial microsatellite results confirmed that the cell line was triploid, but diploid results were obtained for the biopsied cell, which was in agreement with the original PGH diagnosis. This, coupled with the presence of only two visible pronuclei at fertilisation, suggested that the embryo was mosaic. The origin of non-mosaic triploids generally arise from simple digyny or diandry, but the origin of mosaic triploids is more complex. Case reports of triploid/diploid mosaics are available with the most likely mechanisms including chimerism originating from fusion of diploid and triploid zygotes, delayed dispermy by incorporation of a second sperm pronucleus into an embryonic blastomere, postzygotic maldivision of a triploid or diploid zygote, or incorporation of the second polar body into one blastomere at the cleavage stage (Brems *et al.*, 2003; Daniel *et al.*, 2003; Muller *et al.*, 1993). The first two mechanisms could be disregarded in this case; the first because fertilisation and development took place *in vitro* in individual embryo culture, and the second because fertilisation was by ICSI and the line had a normal haploid paternal chromosome content. Postzygotic maldivision of a maternally derived triploid zygote would result in expected loss of both maternal and paternal chromosomes randomly which was not observed for the chromosomes investigated for KCL008-HD2. Incorporation of the second polar body into a cleavage blastomere could have occurred at any cleavage stage to give rise to a population of triploid cells. The predominance of these cells from very early passage of the stem cell line suggested that if this was the causal mechanism, incorporation was early in division. Although two structures resembling polar bodies were visible just before biopsy, they could have been cellular fragments. However, the relatively low frequency of reports of triploid/diploid mosaicism coupled with the inconclusive microsatellite data required further investigation of the cytogenetic status of the biopsied cell.

A panel of markers on chromosome one was subsequently used for analysis of the biopsied cell. The results revealed that the cell was in fact triploid - with a diploid maternal, and a normal haploid paternal contribution. Therefore the embryo was not mosiac; the triploidy must have arisen by a mechanism of digyny, but complicated by the presence of only two pronuclei at fertilisation. It is plausible that there was a

third pronucleus present but not visible, due to asynchronous formation of pronuclei following fertilisation (Staessen & Van Steirteghem, 1997). Non-mosaic triploid mechanisms were considered to elucidate the most likely origin of the triploidy.

Table 6.4 details the most common events that can give rise to a triploid chromosome content, and whether the inheritance of KCL008-HD2 could have arisen from each mechanism.

Table 6.4: Details of the causal mechanisms of non-mosiac triploidy, and whether they offer a suitable explanation for the karyotype of the embryo used to derive KCL008-HD2.

Event	**Possible mechanism of triploidy**
Diandry - two haploid sperm	No, diploid maternal complement
Diandry - one diploid sperm	No, diploid maternal complement
Digyny - nondisjunction at meiosis I	Yes
Digyny - nondisjunction at meiosis II	No, non-reduction of pericentromeric markers
Digyny - diploid (giant) oocyte	No, morphology was normal at ICSI
Digyny - endoreduplication	No, heterozygous maternal complement

Diandry could clearly be excluded due to the diploid maternal chromosome content. A diploid (giant) oocyte could be rejected as the oocyte appeared of normal size at the time of injection. Endoreduplication is defined as duplication of the genome without intervening mitosis or cell division. This would create a triploid zygote that cannot be detected by standard morphologic or cytologic criteria employed in IVF laboratories. However, if the maternal pronucleus had replicated in this case a homozygous diploid maternal complement would have resulted. The detection of three different alleles at multiple loci therefore excluded this mechanism.

Nondisjunction at meiosis I or II were considered the most likely events to have caused the triploid chromosome content. Nondisjunction at meiosis I with a failure of separation of the entire set of homologous chromosomes (perhaps excluding chromosome 6) could have occurred. A polar body was extruded as it was seen during ICSI, but this could have contained only one copy of chromosome 6. Recombination between homologous chromosomes and a normal meiosis II phase would result in a heterozygous diploid oocyte. If the sister chromatids separated during fertilisation,

then three haploid pronuclei and three polar bodies would have been visible (Rosenbusch *et al.*, 2002). If the female sister chromatids remained united, two pronuclei (one diploid) and two polar bodies would be visible at fertilisation - exactly as seen in the embryo used to derive KCL008-HD2.

Nondisjunction at meiosis II with failure of separation of the entire set of sister chromatids was also considered as a plausible mechanism. However, whilst recombination between sister chromatids would be possible at the distal end of the chromatids, it would be very unlikely to occur around the centromere (Zaragoza *et al.*, 2000). The pericentromeric or distal position of all the markers was considered to determine whether or not maternal heterozygosity at the centromere was maintained (non-reduction) or was reduced to homozygosity (reduction) in the triploid offspring (Zaragoza *et al.*, 2000). The majority of the markers were distal except for those on chromosome one. Markers D1S1656 and D1S2885 were pericentrometric and a heterozygous maternal complement was seen in both KCL008-HD2 and the biopsied cell, evidenced by the presence of two different maternal microsatellite sizes in the analysis. This non-reduction at the centromere made it unlikely that the triploidy arose from nondisjunction at meiosis II.

Therefore whilst the mechanism producing the triploidy could not be determined unequivocally, the most likely explanation from the available evidence was nondisjunction at meiosis I. The sister chromatids remaining united during fertilisation would have resulted in a zygote with two pronuclei (diploid maternal, haploid paternal) and two polar bodies, exactly as seen.

It is not surprising that the triploid status of the biopsied cell was not detected during PGH. Firstly, PGH is not quantitative, and not designed to pick up aneuploidy status in blastomeres. Secondly, the *HTT* gene is positioned at 4p16.3, at the end of chromosome 4. Recombination of the gene is likely, giving rise to a homozygous marker pattern which would not reveal triploidy. This was confirmed by the SNP analysis, where every SNP marker used around the HD gene was homozygous.

This inheritance pattern, with the cell line carrying two copies of normal and one copy of mutant *HTT*, might alter the effect or contribution of loss-of-function of normal *HTT* to the disease pathology and progression. Gain of toxic function of the mutant protein could then be studied in isolation. However, the confounding effect of the triploid karyotype, and any possible silencing/regulation effects from the two

normal copies of *HTT* should not be overlooked and might render the cells of very little use for transcriptional studies. However, the number of hESC lines carrying HD are few, and in some of the diploid lines other chromosomal abnormalites are present (personal communication, N. Lefort, I-Stem). Therefore this cell line provides a novel and useful source of cells for the study of biochemical characteristics of HD. In particular, the ease of culture and rapid proliferation of the cells greatly facilitates scale-up for experimentation; a significant advantage over the undifferentiated hESC stage.

6.4.3 CAG repeat analysis

Repeat size is a major determinant of the severity and pathology of hereditary neurodegenerative diseases; the longer the repeat, the more severe the symptoms, the earlier the age of onset, and the more widespread the pathology (Zoghbi & Orr, 2000; Zuhlke *et al.*, 1993). Elongation of the trinucleotide repeat expansion on transmission to the next generation is a common occurrence. It has been identified in HD, spinal and bulbar muscular atrophy, dentatorubral-pallidoluysian atrophy, Machado-Joseph disease, fragile X syndrome, myotonic dystrophy and Friedreich's ataxia. In HD, the expanded CAG repeats are unstable in both germline and somatic tissues, indicating both meiotic and mitotic instability.

The extent of germline instability has been shown to be dependent on the sex of the affected parent; paternal transmissions tend to be most unstable and increase in size upon parent-to-offspring transmissions. This then causes earlier manifestation of the clinical symptoms in subsequent generations, a phenomenon termed *anticipation*. Juvenile onset of HD is associated with paternal transmissions with large increases in repeat size (THsDCR, 1993). Juvenile-onset HD patients develop dystonia and seizures in addition to the classical phenotype of chorea and dementia seen in adult-onset patients. This suggests that the toxicity associated with large repeats is more widespread through certain neuronal subtypes which are normally unaffected when the repeat sizes are in the adult-onset range.

A timeframe for germline instability has been suggested by a study describing four pairs of HD monozygotic twins, two pairs of which inherited the disease from the mother and two from the father (MacDonald *et al.*, 1993). Each pair had identical CAG repeat lengths. The vast majority of HD transmissions involve measurable

changes in repeat length, thus, any repeat instability almost certainly occurred before the twinning event. This usually take place between days 2 and 5 of embryonic development. There is also evidence for mosaicism of repeat length in sperm samples (Telenius *et al.*, 1994). Together these observations indicate that germline instability occurs during gametogenesis. One possible explanation for the increased paternally inherited repeat instability is the greater number of cellular divisions that take place during spermatogenesis compared with oogenesis (Zoghbi & Orr, 2000). Other evidence suggests that replication may not be a causative mechanism, as discussed below for somatic instability. KCL008-HD2 was derived from an embryo with paternal inheritance of the mutant HD gene. A repeat increase of 2 units was observed in the cell line. Although not conclusive due to technical limitations of the analysis, this is likely to be a true anticipatory event. In a small cohort of embryos, elongation of the repeat expansion was observed in the majority of paternal transmissions, with the increase being between 1 and 8 repeat units (Sermon *et al.*, 1998). Surprisingly, as many embryos showed contractions (6 out of 20) or no change (4 out of 20) as further expansions (10 out of 20) in embryos where the father was affected. Maternal transmissions showed contractions or no change, but no elongations were observed in this small group. The study of a larger group of embryos is needed to draw conclusions regarding contractions of the CAG repeat, although this has been reported elsewhere. Of note is one case report of a contraction in a maternal transmission which changed the CAG repeat in the offspring from a penetrant size of 48 to a normal size of 34. This deletion of 14 CAG repeats is much larger than normally observed (Tang *et al.*, 2006).

In somatic tissues, the expanded alleles do not seem to show a sex bias (Gonitel *et al.*, 2008). The repeats are unstable with variable patterns of expansions and contractions in different tissues. For longer repeat lengths, somatic instability of the repeat size has been observed both in human cases at autopsy (Telenius *et al.*, 1994) and in transgenic mouse models (Mangiarini *et al.*, 1997). Interestingly it has been shown that somatic repeat instability is significant in the striatum of aged HD knock-in mice (Wheeler *et al.*, 1999). As striatal neurons are the most vulnerable cells in HD, it is conceivable that somatic repeat instability contributes to the selective loss of these neurons. Furthermore it may help explain why certain subsets of neurons degenerate in HD even though the mutant protein is widely expressed throughout

the brain. Similarly, the greatest somatic instability has been shown in the basal ganglia and cerebral cortex of postmortem human tissue (Telenius *et al.*, 1994), and both regions are affected in HD. The instability was greater in the brains of juvenile-onset samples, strengthening the relationship between mitotic instability and repeat size. This was also shown for germline transmission, following analysis of mosaicism in spermatozoa of affected patients (Telenius *et al.*, 1994). Apparent contradictory results which assert that somatic transmission is stable in HD have been reported (MacDonald *et al.*, 1993). However, careful inspection of the figures within the manuscript suggests a small but consistent increase in repeat size in the striatal tissue compared to lymphoblast for each patient analysed.

The molecular mechanisms underlying somatic CAG repeat instability are still largely unknown. It has been suggested that repeat instability arises via DNA replication slippage during cell division (Richards & Sutherland, 1994). However, in tissues such as the brain, which contain a large proportion of post-mitotic cells, a remarkable degree of instability has been shown (Gonitel *et al.*, 2008; Wheeler *et al.*, 1999). Furthermore the absence of extreme mosaicism in tissues with a high cell turnover such as the liver and bowel (Telenius *et al.*, 1994) suggest that replication does not play a major role in the regional differences of CAG repeat instability. Another suggestion is that multiple rounds of DNA damage and repair may mediate somatic instability in post-mitotic cells (Kennedy & Shelbourne, 2000; Wheeler *et al.*, 1999). This hypothesis is supported by evidence that a deficiency in the mismatch repair enzyme Msh2 prevents *in vivo* somatic instability of the CAG repeat in HD transgenic mice (Manley *et al.*, 1999; Pearson *et al.*, 1997).

In undifferentiated KCL008-HD2 cells the CAG repeat length of the mutant allele was stable at 46 repeats. However, in the differentiated precursor population there was a dramatic increase in CAG repeat units to 70. Given the extremely rapid proliferation of these cells (6000-fold in 22 days), these results suggest that replication may be somehow involved in instability in agreement with previously cited results. However an alternative explanation may lie with evidence that DNA repair mechanisms in mESC and hESC are superior to differentiated cells (Maynard *et al.*, 2008). Microarray analysis has shown that mRNA levels of several DNA repair genes are elevated in hESC. This enhanced repair system allows hESC to maintain genomic integrity and differentiation potential during multiple cell cycles. However

these multiple rounds of DNA repair could have led to increased somatic instability during the differentiation of KCL008-HD2 cells.

The cell line generated is a unique tool with which to study HD pathogenesis despite the abnormal karyotype. It is unlikely that a cell line with a juvenile-onset repeat number would be obtained directly from a HD patient, neither after PGD nor through iPS cell generation, as individuals with such a repeat length are unlikely to survive to reproductive age or capacity. Until now the only way of generating such large repeats was to use genetically manipulated mouse or cell models. As discussed, lines generated from PGD embryos are likely to be superior models as the mutant protein is expressed in its normal physiological context. In particular this line lends itself to the study of the little understood mechanisms of somatic instability.

6.4.4 Protein analysis

The CAG repeat portion of the HD gene is translated into polyglutamine in the HTT protein. This allows mutant and wildtype isoforms in HD heterozygotes to be differentiated by variation in electrophoretic behavior and immunoreactivity (Persichetti *et al.*, 1995).

Wildtype HTT was observed by western blot in all samples; the HFF, the positive control and differentiated KCL008-HD2 cells. Mutant HTT was visible in the positive control and as a faint band in the KCL008-HD2 cells. The relative migration of the protein varies with the length of the CAG stretch. Therefore the positive control band (150 repeats) was slightly higher on the gel than the KCL008-HD2 band (46 to 70 repeats). The gel was not run for long enough to distinguish between the mutant and wildtype isoforms in KCL008-HD2 by position, and therefore analysis was by differential immunoreactivity. The MAB2166 antibody recognises an epitope around amino acid 450 of the normal protein. Since this region is the same in the normal and mutant protein the antibody recognises both forms. MW1 only recognises expanded polyglutamine tracts and therefore will only bind to the mutant protein.

Several studies have suggested a reduction in expression of HTT from the mutant allele, with the difference accentuated in juvenile onset cases. Mutant HTT is often seen at a lower level in HD heterozygote lymphoblast or brain protein extracts than in its wild-type counterpart. This was thought to arise from reduced stability, thereby reduced activity, of HTT, which might be involved in the pathogenesis

of HD (Persichetti *et al.*, 1995, 1996; Trottier *et al.*, 1995). However, pulse-chase experiments failed to reveal an alteration in mutant HTT turnover or processing to smaller fragments (Persichetti *et al.*, 1996). There now exists a plethora of data to show that the pathological effects of mutant HTT are mainly due to toxic gain-of-function, not to loss-of-function as the reduced activity hypothesis implies. Thus, a mutant HD allele, even at reduced relative expression, must produce an amount of abnormal HTT that saturates the pathogenic mechanism and causes disease.

The decreased signal from the protein could therefore be due to either a difference in gene expression level or decreased binding to the antibody. The mutant protein misfolds which could either expose or hide epitopes to either enhance or hinder antibody binding. The marked difference in band intensity for KCL008-HD2 is complicated by the triploid status of the cells. The 2166 antibody would have detected HTT gene product from three alleles - two normal and one mutant. MW1 would have detected the protein product from only one allele. Nevertheless, the results confirmed that the differentiated KCL008-HD2 cells expressed mutant HTT at the protein level. Further experiments are planned to determine whether the protein is in a soluble or aggregated form in these cells.

6.4.5 Neural induction

The aim of the experiment was to establish whether hESC carrying genetic disease could be used as research models. A neural precursor population would be the most suitable cell type for study in HD. In two out of 19 experiments, a stable, highly proliferative and homogenous cell population was generated from KCL008-HD2, which could be easily cultured, expanded and successfully undergo freeze-thaw cycles. Alongside this, a very similar cell population was generated in one from 7 experiments with KCL001, providing a wild-type control line.

The first 14 days of the protocol were designed to prevent differentiation to mesodermal and endodermal lineages. This allowed spontaneous or perhaps default neuroectodermal differentiation. One mechanism of action of the stromal cells is ectodermal induction and stabilisation, which prevents mesoderm differentiation. Subsequently, stromal co-cultured cells adopt a default neural status unless they receive a sufficient level of appropriate signalling (Kawasaki *et al.*, 2000). The use of serum has been shown to be inhibitory to neural differentiation (Kawasaki *et al.*,

2000) and therefore serum replacement was used. From day 14 onwards, specific medium and supplementation were introduced to direct any neuroectodermal cells towards neural precursors or the neural lineage.

Growth factor supplementation encouraged the cells to differentiate to neural progenitors. The switch from serum-replacement to N2 and then N2B27 medium was designed to keep any such progenitors in proliferative conditions. N2 is a serum-free supplement (with transferrin, insulin, progesterone, putrescine and selenite) shown to promote neural progenitor formation by an increase in MSI1 expression (Dhara *et al.*, 2008). It also supports the growth of post-mitotic neurons. B27 is a serum-free medium supplement shown to increase neuronal survival in primary central nervous system (CNS) cultures (Svendsen *et al.*, 1995). The combination of these supplements in a neuralbasal medium has been used extensively in a variety of approaches to neuronal differentiation experiments (Barberi *et al.*, 2003; Conti *et al.*, 2005; Joannides *et al.*, 2007; Ying & Smith, 2003).

The addition of the growth factors was designed to complement the action of the stromal feeders. bFGF is a well-established mitogen for CNS-derived embryonic and adult neural stem cells. Multiple *in vivo* and *in vitro* studies have implicated both autocrine (Joannides *et al.*, 2007) and paracrine (Streit *et al.*, 2000) FGF signalling in neural induction. FGFs also play a supportive role in the proliferation of ESC-derived neural stem cells once established (Conti *et al.*, 2005). EGF has been suggested to maintain and to support self-renewal of neural progenitors with competence for neurogenesis. Its action is partly via the suppression of apoptosis (Conti *et al.*, 2005). *In vivo* BDNF promotes survival of neurons arising from the forebrain (Kirschenbaum & Goldman, 1995) and enhances neuronal differentiation of neurosphere cells (Ahmed *et al.*, 1995). The effects of the neurotrophic factors would have been complicated by the stromal cell co-culture in this system. Not until defined conditions are developed will the molecular mechanism(s) underlying the effects of neurotrophic factor signalling on neuroectodermal differentiation be determined. However the use of these factors for neural induction has been extensively reported (Conti *et al.*, 2005). Had the initial neural induction step generated neural rosettes, it would have been expected that N2 and BDNF only on POL would have generated neuronal lineage cells. However, the failure to generate rosettes and subsequent proliferation arrest of the cells plated in N2 on POL suggested that insufficient

support was available in this condition. The success of the supplemented N2B27 on POL condition implies that EGF and FGF, and perhaps B27, were required for continued differentiation and growth in these experiments.

The use of a POL surface was designed to further encourage differentiation into neural progenitors in combination with the use of neurotrophic factors and specialised medium. Polyornithine is a non-extracellular matrix, positively charged polymer and laminin is a purified extracellular matrix protein. Such matrices have been shown to enhance neural progenitor migration and expansion as well as differentiation into neurons and astrocytes (Flanagan *et al.*, 2006). Gelatin-coated dishes are commonly used for neural differentiation of mESC (Kim *et al.*, 2003; Ying & Smith, 2003; Ying *et al.*, 2003). This was attempted with the hESC, as gelatin is inexpensive and a simple substrate to prepare. However it was not supportive to growth of the cells. Very low attachment of hESC to gelatin coated dishes during neural differentiation has also been reported elsewhere (Gerrard *et al.*, 2005). The cells could not be cultured beyond P3, despite identical medium and supplementation as the third, and successful, condition when the cells were plated on POL.

Loss of pluripotency throughout the protocol was confirmed by a marked reduction of SSEA4 from around 80% in undifferentiated KCL008-HD2 cells to around 3% by P3 on POL. This was accompanied by induction of NCAM expression by around one fifth of the cells at day 14 to almost all cells by P3 on POL. The quality of the starting hESC population seemed significant to the successful production of neural derivatives. When cell populations used in the differentiation experiments were tested, variability of marker expression was observed. This could have contributed to the low efficiency of differentiation. The quality of MS-5 feeders was also likely to have had an effect on the outcome of the study. In those experiments that successfully generated the precursor populations, the pre-differentiation marker expression by the hESC was appropriate and the loss of SSEA4 and gain of NCAM expression was consistent of throughout the neural induction.

Characterisation of the cells was performed once a homogeneous, proliferative population of precursors had been obtained from the two hESC lines. No specific markers are available to unequivocally identify neural stem cells; their functional characteristics (self-renewal and multipotent differentiation into all neural lineages) provide the main features for their identification. However in experimental studies,

positive expression of a panel of neural markers is widely used to determine cell identity.

NCAM is expressed on most neuroectodermal derived cell lines, tissues and neoplasm and was used to monitor differentiation during the induction phase of the protocol. Although NCAM alone is not sufficient to prove neuroectoderm lineage, without this marker it is very unlikely that the cells belong to this lineage. To determine the status of the proliferative populations, staining was completed for NES, SOX2, MSI1, TUJ1 and GFAP.

Nestin is a class VI intermediate filament expressed in the developing CNS in early embryonic neuroepithelial stem cells, and was positively expressed by differentiated KCL008-HD2 cells. Although not an exclusive or unique marker, NES is widely used as a marker in neural progenitor studies (Dhara *et al.*, 2008; Hong *et al.*, 2008). Neural identity was further confirmed by positive expression of the progenitor marker MSI1 1 and cytoplasmic expression of SOX2. MSI1 is selectively expressed in neural stem cells, neuronal progenitor cells, astroglial progenitor cells and astrocytes, and is co-expressed with NES (Kaneko *et al.*, 2000). SOX2 is expressed in the nucleus and cytoplasm of ICM cells, but exclusively in the cytoplasm of the TE (Avilion *et al.*, 2003). Expression continues throughout early neural tube development (Wood & Episkopou, 1999). SOX2 functions to maintain the proliferative state of potential neural progenitor cells (Dhara *et al.*, 2008). Therefore the expression of SOX2 by these cells is consistent with both the neural identity and progenitor status. However, as the expression was cytoplasmic in these cells, this may suggest that the cells were no longer actively transcribing this factor. Alternatively SOX2, as shown for SOX10, may require nucleo-cytoplasmic shuttling for transactivation of target genes *in vitro* (Avilion *et al.*, 2003). Nevertheless, the majority of reports regarding SOX2 expression in neural stem cells show nuclear expression of the marker.

Initial investigation of βIII tubulin expression suggested co-expression of this marker with SOX2 and NES, which was unexpected. However, it was then realised that the antibody used was a general βIII tubulin. Tubulin is the major building block of microtubules and is present in almost all eukaryotic cells. When the cells were re-stained with the neural specific isoform (TUJ1) no expression was detected at the progenitor stage. The neuron-specific form was then used in the assessment of differentiation. GFAP is a member of the class III intermediate filament protein

family. It is heavily and specifically expressed in astroglial progenitor cells and other astroglia in the CNS. The differentiatied KCL008-HD2 cells were positive for GFAP. Proliferative capacity of the cells was confirmed by almost universal expression of KI67.

The expression of CD9 at the differentiated state was unexpected, as it was chosen to assess the level of undifferentiated cells at the beginning of the experiments. CD9 is a cell surface protein belonging to the tetraspanin superfamily. As well as being expressed on the surface of undifferentiated hESC (Adewumi *et al.*, 2007), it is implicated in intercellular signalling in selected cell types of the hematopoietic system and developing nervous system. Cd9 is present very early in specific cell types in the rat in both the central and peripheral nervous system, including embryonic spinal motorneurons (Tole & Patterson, 1993). In humans, CD9 is a positive marker for human neural progenitor cells (Klassen *et al.*, 2001). The tetraspanin family of proteins form complexes with components of various growth factor signalling pathways, including the EGF receptor. As discussed, EGF plays a key role in neural induction. Therefore the expression of CD9 by these cells was appropriate, and substantiated the identity of the population as neural progenitor cells.

Due to the close interaction of lineage decisions in differentiating hESC, it was necessary to prove that the cells did not express markers of other lineages. In the presence of N2B27 hESC can generate extra-embryonic endoderm-like cells (Gerrard *et al.*, 2005), so the cells were tested for the presence of AFP. Due to the close interaction between neural and vascular systems, mesodermal induction was assessed by analysis of brachyury by ICC and CD73 by FACS. Epithelial induction was assessed by KRT5, 14 and 18 expression. The differentiated cells were negative for all of these markers. The cell also no longer expressed POU5F1. Together this strengthened the evidence for successful differentiation of the cells to the neural lineage.

The experiments demonstrated that the cells positively expressed NCAM, NES, MSI1, SOX2, CD9 and GFAP, but were negative for TUJ1, AFP, brachyury, CD73, KRT5, 14 and 18 and POU5F1. This combination of markers is suggestive of astroglial progenitor cells. Figure 6.33 (adapted from Kaneko *et al.* (2000)) is a schematic representation of the relationships between neural cell markers, which was used to determine the most likely identity of the cell population generated. Fur-

ther differentiation studies were performed to attempt confirmation of this astroglial induction.

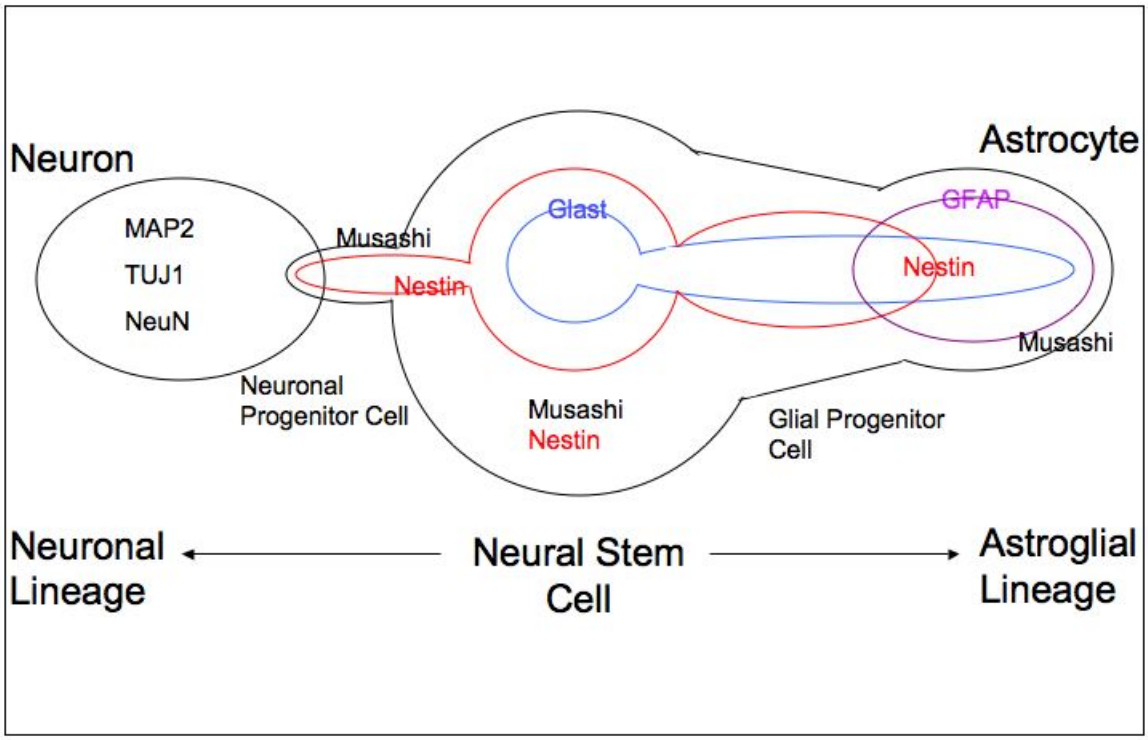

Figure 6.33: Schematic representation of the relationships between neural markers, and the panels of markers that distinguish between the neuronal and astoglial lineages. Adapted from Kaneko *et al.* (2000)

.

6.4.6 Neuronal and astrocytic differentiation

Growth factor withdrawal for 14 or 28 days generated cells with neuronal-like morphology. However these cells were negative for all early neuronal markers, and continued to be highly proliferative. Furthermore the cells remained positive for GFAP and NES. The addition of serum and withdrawal of growth factors did not change the expression of astroglial markers. The entire population of cells remained positive for NES, GFAP and MSI1. The morphology of the cells changed to the typical bipolar phenotype of astroglia. As the culture conditions were designed to induce differentiation into terminally differentiated astrocytes, subsequent loss of NES in

a sub-population of cells was expected (Figure 6.33). However, the cells retained their progenitor status with robust continued proliferation, suggesting that strong intercellular signalling maintained this cell state. The successful demonstration of astrocytic differentiation, but the failure to generate neurons, identified the cells as astroglial progenitors. As a result the cells were termed human ES-derived astroglial progenitors (hES-AGP). The cells originating from KCL008-HD2 were named hES-AGP-HD2.

hES-AGP-HD2 cells have the potential to be a valuable model of HD pathogenesis. Glial cells comprise 90% of the cells in the brain and provide neurons with nutrition, growth factors, and structural support. They also protect against excitotoxicity by removing excess excitatory neurotransmitters such as glutamate from the extracellular space (Maragakis & Rothstein, 2001). In normal astroglia, glutamate is converted to the nontoxic amino acid, glutamine, by glutamine synthetase. The glutamine is then transported to the neuron for conversion into glutamate for neurotransmission by glutaminase. However in HD brains, mutant *HTT* accumulates in glial nuclei and decreases the expression of glutamate transporters. Decreased mRNA levels of the major astroglial glutamate transporter (*GLT1*) in the striatum and cortex of R6 transgenic mice has been demonstrated (Lievens *et al.*, 2001), which was associated with a decrease in glutamate uptake and mRNA levels of glutamine synthetase. Striatal medium spiny neurons receive abundant glutamatergic input. Their vulnerability to excitotoxicity may be significantly influenced by the capacity of glial cells to remove extracellular glutamate. In a neuron-glia coculture system, wild-type glial cells protected neurons against mutant HTT-mediated neurotoxicity, whereas glial cells expressing mutant *HTT* increased neuronal vulnerability (Shin *et al.*, 2005). These findings suggest that decreased glutamate uptake caused by mutant HTT in glia may contribute to neuronal excitotoxicity and therefore to the phenotype and neuronal cell death in HD. The hES-AGP-HD2 cell population generated will provide a valuable human model in which to further study the effects of mutant HTT in astroglial cells and the causal mechanisms of excitotoxicity.

Of the 19 experiments initiated with KCL008-HD2 cells, three resulted in failed proliferation in N2 medium and three terminated with failed proliferation on gelatin. Of the remaining 13 experiments on POL in N2B27, two gave rise to progenitor cell populations. From the seven experiments with KCL001, four ended with failed

proliferation in N2 and on gelatin, and one progenitor line was obtained from the remaining three attempts on POL in N2B27. Due to ongoing modifications of the protocols, no conclusions can be drawn about the efficiency of the two lines in generating putative progenitor cells. However, the failure of the other attempts in the N2B27 and POL conditions was likely to be the result of the low number of cells and therefore low density plating onto the POL surface for both cell lines. Co-culture differentiation methods rely on unidentified cell-derived factors, generally of non-human origin, which can result in experimental variation and limit reproducibility. It was likely that this variability contributed both to the unpredictable success in generating a proliferative cell population between experiments, and for the occasional population of cells expressing inappropriate markers. Of the other most widely applied protocols for neural differentiation, spontaneous differentiation methods rely on high-density culture and the neural conversion efficiency is low, retinoic acid-based methods restrict progenitor diversity and therefore the range of terminal cells available, and conditioned medium protocols carry the same disadvantage as stromal co-culture.

However, the low reproducibility of the induction protocol, whether due to the feeders, the conditions or the cells themselves requires consideration. Although a homogeneous cell population was obtained for both cell lines, with extremely similar morphology, growth characteristics and marker expression, subtle differences may have been present in the populations due to the non-defined differentiation protocol used. Therefore differences or similarities in behaviour of the cell lines upon differentiation could be influenced by early events in induction. However, other comparisons have been made between hESC lines and between passages of the same line using this poorly-defined MS5 stromal co-culture (Hong *et al.*, 2008). Protocols that use only defined or human-derived qualified products are imperative for generating clinical standard neural stem cells or precursors. Achievements in work towards this goal have been reported (Dhara *et al.*, 2008; Joannides *et al.*, 2007).

Nevertheless, the present aim was to obtain a relevant precursor population with a hESC line carrying the mutant *HTT* gene, not to optimise an induction or differentiation protocol - work which is being rapidly advanced by more experienced neural research groups. The requirement when using PGD-derived lines will never be clinical therapy, rather, the generation of biologically and genetically relevant cell

populations to enable investigation of disease mechanisms. These results show that salient features of a disease can be replicated in hESC lines and validate the use of PGD-derived lines as disease models.

Chapter 7

General discussion and future work

As the field of human IVF celebrates four decades of clinical research and patient treatment, so the area of hESC research reaches the end of its first. The field of hESC biology emerged standing on the solid foundations of many years of *in vitro* embryo research, and its continued success is a result of cross-discipline collaboration and open sharing of expertise. With the formation and active meetings of societies such as the Human Embryonic Stem Cell Coordinator's (hESCCO) Network, the International Stem Cell Initiative (ISCI), ESTOOLS, the International Society for Stem Cell Research (ISSCR), the London Regenerative Medicine Network (LRMN) and the Human Embryonic Stem Cell Registry (hESCreg) to name but a few, the future of hESC research and application to regenerative medicine looks encouraging.

Despite exciting prospects, it is vital that expectations are handled appropriately to ensure the public have a realistic view on what can be achieved with hESC research, and over what time periods these achievements can be reasonably expected. Establishment of reliable and validated methods for the very basic technologies of deriving, growing, characterising and preserving hESC have yet to be achieved. Current hESC research therefore encompasses investigation into early embryo development, derivation and the basic biology of stem cells as well as the determination of optimum derivation and culture conditions. Furthermore complex biological questions have yet to be answered regarding robust and reliable differentiation of hESC to deliver products that may have real clinical potential. Research therefore focusses on the control of differentiation, mechanisms of karyotypic change, scale-up and delivery for therapy and the use of the cells as disease models. The over-arching challenge with all of this research is the ability to create and differentiate hESC efficiently in

fully defined conditions, using only qualified reagents, to GMP standards.

This thesis aimed to address several of these issues. By developing tailored derivation methods to the morphology of the blastocysts, the aim was to increase the efficiency of derivation and therefore reduce the number of embryos used in research. The derivation of multiple hESC lines then provided the tools with which to approach further questions. The analysis of the type of culture medium employed and also the source and suitability of novel feeder cell systems addressed the need to optimise culture conditions, but equally importantly to develop culture systems that qualify under GMP standards. Efforts to derive hESC from single blastomeres of cleavage embryos has contributed to the understanding of the earliest days of development and the pluripotent nature of these cells, which may ultimately enable derivation protocols to be better designed. Furthermore, the derivation and differentiation of hESC lines from PGD embryos has validated the use of these cells as disease models, with the generation of a line carrying HD that can be differentiated into cells of a relevant phenotype for the disease and which display salient features of HD pathophysiology. These studies, in turn, have raised a series of further questions warranting investigation.

7.1 Derivation and culture of human embryonic stem cell lines

In total seven hESC lines or putative lines were derived using four different methods depending on the morphology of the blastocyst. There was a correlation between the quality of the ICM and the success of derivation. However the overall derivation rates remained below pregnancy rates following IVF, implying that the culture methods currently in use are suboptimal. The work reported here suggests that this may be due, in part, to the use of inappropriate cell culture media in the first few days of derivation. The composition of in-house hESC CM, commercial KOSR and medium conditioned by both MEFs and HFFs was analysed, with the levels of the major metabolites and catabolites measured. Whilst KOSR was superior to hESC CM in terms of catabolite concentrations, the levels of substrate were in excess, and the serum replacement fraction not xeno-free. It is predicted that the design of a specific

derivation medium from physiological principles based on pre- and peri-implantation *in vivo* conditions may increase the efficiency of generation of hESC lines.

Two novel feeder cells were assessed for their suitability as replacement cells for MEFs. HFFs were comparable to MEFs as feeders for existing hESC. As a culture system they were superior given their robust proliferation and late senescence. AECs were similar to MEFs in proliferation and senescence, but with the potential to be isolated from a fully validated human source with complete details of provenance. Whilst there are both benefits and risks of using human feeder cells (Stacey *et al.*, 2006), qualified human feeder stocks are currently the best option available for hESC culture. The main disadvantage with human feeders is the risk of transmission of infectious agents. Appropriate history and routine screening of fibroblast donors for likely adventitious agent contamination, as applied to embryo donors, may shift the balance of risk to the same category as blood or tissue donation (Cobo *et al.*, 2005). Both AECs and HFFs supported the undifferentiated and pluripotent growth of existing hESC lines, but only AECs were able to support growth of the ICM. As stem-like cells were able to be cultured to P3 there is potential for AECs to support derivation. Future work will include laying down master cell banks of AECs and continued derivation attempts on these cells.

Each of the seven derivations was distinctive. Although the stage and morphology of the blastocysts were generally similar, the behaviour of the colonies was unpredictable; colony morphology and development was different with each attempt. Furthermore, as no two established hESC lines seem identical, either regarding pluripotent marker expression, transcriptional profiling, genetic stability or epigenetic stability (Allegrucci & Young, 2007; Skottman *et al.*, 2005), it is important to record all details of the derivation process and to share results between teams to try to elucidate the causes or mechanisms underlying these differences. However, without a clear minimum information convention for reporting derivation, understanding and comparing novel derivation methodologies and their potential impact on the resulting hESC line has been at best extremely difficult. The establishment of an internationally agreed standard for reporting derivation aimed to improve dissemination of results and promote collaboration in order to progress the derivation field as efficiently as possible. The collection of data from groups is ongoing and the aim of

future work is to publish a multi-author document, setting the baseline for derivation techniques and conditions (Stephenson *et al.*, 2007).

Although methods for deriving hESC lines were established with this work, and pluripotent and karyotypic characterisation performed, the quality of these lines remains an unknown. With the significant man-power and financial investment required to generate clinical-grade lines, it is important that the lines are of the best possible metabolic quality and functional competence. Whilst there is some evidence that culture at low oxygen tends to inhibit spontaneous differentiation of hESC in high passage colonies (Ezashi *et al.*, 2005) and significantly reduce the acquisition of spontaneous chromosomal abnormalities (Forsyth *et al.*, 2006), there is a lack of evidence about derivation efficiency and longevity at different oxygen tensions. Future work comparing derivation in conditions where reduced oxygen is used either only from the morula or blastocyst stage onwards (the usual stage that fresh embryos are received for research), or from thawed pronucleate embryos onwards, would reveal important information regarding the effect of oxygen on embryo development and subsequent derivation efficiency and differentiation capability. Some studies suggest that hESC with high degrees of oxidative metabolism survive in culture longer (Lonergan *et al.*, 2006), but the effect on the quality of, for example, derived myocytes or neurons is unknown. Measures of mitochondrial function, activity and turnover to assess the influence of the oxygen environment on the metabolic quality of the cells could also be used (Cho *et al.*, 2006; Lonergan *et al.*, 2006, 2007).

With the development of successful derivation methods compatible with GMP, future work will focus on ascertaining the best possible combination of media and feeder substrates that qualify under GMP criteria, and on deriving lines in clean-room facilities with appropriate qualification for submission to the UKSCB. Standard operating procedures and validation protocols must be written and assessed for reproducibility. Further proposed aims are to work with the UKSCB to develop a pack that can accompany lines intended for clinical use, in order for the information be added to the banking cell line master file which will be available to users. The pack will include data such as details of donor tissue procurement and consent, records of the cell line derivation environment, materials and reagents used and the environment used to establish the first frozen stocks of the line (Stacey & Hunt, 2008).

This information will be critical in the future regulatory process towards approving lines for clinical use.

The UK Stem Cell Bank is a vital resource to support the advance of research in this field. The deposit of cell lines enables the UKSCB to provide ethically sourced, high quality starting materials to facilitate the development of stem cell therapy and to disseminate best practice in hESC culture. The presence of the UKSCB should also reduce future demand for embryos for the development of hESC lines. However, there is still a need for multiple lines as the metabolic quality and differentiation potential differs between lines, and a bank of cells with a range of HLA identities is likely to be beneficial for future applications. Whilst the development of iPS cell technology has been hailed by some as the end of the hESC field and therefore could question the need for stem cell banks, this technology is at an early stage and many fundamental questions remain. The development of iPS cells would not have been possible without working with hESC, and while iPS cells and hESC share many characteristics they are not identical. Research with hESC, tissue-specific stem cells, and iPS cells needs to continue in parallel. It is this combined knowledge that will ultimately generate safe and effective therapies, as each cell type may be suited to particular applications over others.

7.2 Assessment of pluripotency and prepatterning in single human blastomeres

Derivation was attempted with single blastomeres of the early cleavage embryo, and the development of each blastomere was tracked so that the behaviour of sister cells could be compared. As differentiative divisions and an increased cell number at plating seem to have been beneficial for early culture, future work focussing on maximising such divisions may aid derivation, such as investigating the effect of laminin on blastomere polarity (Johnson, 2008). The development of a tailored medium for the first days of culture is also required as discussed for whole embryo derivation. The derivation from single cells rather than a heterogeneous ICM is a more attractive proposition for bioprocessing. The anecdotal evidence that hESC lines preferentially differentiate down one of the germ lineages could be ascribed the predominant genetic and epigenetic phenotype of the ICM cells on the day of

derivation. The generation of multiple lines from the single cells of the same embryo would remove the genetic variability between the lines and allow the study of other mechanisms that could be acting to promote preferential differentiation.

Whilst derivation was not successful within this time frame, while performing the work, successful derivation by two other groups was reported. However, neither group managed to derive from all sister blastomeres of the same embryo. Further work aiming to derive hESC lines from all sister blastomeres would show equivalent potential or plasticity of these cells and demonstrate that the regulative capacity of each human blastomere is able to compensate for severe cell loss and still generate pluripotent cell populations. Subtle expression differences between sister blastomeres may still exist however, and therefore further molecular work is needed. Global gene expression profiling studies by microarray have been reported for both mouse (Hamatani *et al.*, 2004, 2006) and human (Adjaye *et al.*, 2005) whole embryos. Whilst the timing of expression of lineage markers has been investigated in whole human embryos (Kimber *et al.*, 2008) no systematic analysis of the genes known to be involved in cell fate in normal, progressive, single human blastomeres, with a quantitative comparison between sister cells had been reported. The Fluidigm instrument was identified as a potential platform with sufficient sensitivity to study gene profiles in individual blastomeres. Whilst principle component analysis suggested that broad changes in gene expression were occurring with development stage, no consistent grouping structure for cells within embryos was observed, and no convincing pattern was seen when considering the individual embryo variance scores. The difficulty in analysing the sample data was due mostly to the highly significant chip, row and column effects on the data set.

The vast majority of knowledge regarding early lineage decisions in development is based on experiments with mouse embryos, which develop in a highly regular manner and are available in large numbers, together enabling statistically supported conclusions. This is not the case with human embryos, which are of limited supply and of variable developmental capacity. There are also fundamental differences between development of the two species, pertinently the activation of the embryonic genome at the 2-4 cell stage in the mouse and the reciprocal inhibition of lineage specific genes determining the differentiation between TE and ICM. The investigation of derivation potential and gene expression profiling was performed initially

with human embryos due to these species differences, but this was also a pragmatic approach as human but not murine embryos were immediately available. This allowed an initial assessment of the suitability of the technology for this experimental approach, therefore whether or not further studies with larger cohorts of mouse and human embryos were likely to yield robust results.

Although some patterns emerged from the data, further work is required to fully validate the methodological approach and determine whether the Fluidigm platform is suitable for this work. The most straightforward way to increase the power of the experiment requires that the work returns to the use of mouse embryos in order to provide the sample numbers needed to verify the use of the method, and to analyse if the differences in fate alluded to by multiple studies (Piotrowska-Nitsche *et al.*, 2005; Zernicka-Goetz, 2005) exist at the gene level. Should the method prove robust, to fully exploit the potential of the experiments, each cell position must be marked from the first cleavage division, and like compared with like between embryos of the same stage. This work could then be continued with human embryos to ascertain whether similar lineage-specific gene expression profiles exist in human and murine preimplantation development. Following this, the next step would include investigation of the cells of the morula and individual cells of the ICM.

7.3 Human embryonic stem cells as disease-in-a-dish models

Four lines were derived from patients entering the PGD program for HD diagnosis of embryos. However, two of these lines were from exclusion cases, and therefore the disease status of the lines is unknown, and must not be discovered, even inadvertently, as the donors do not wish to know their disease status. Therefore the cells cannot be banked for use by other researchers due to this risk. One line failed to survive the freeze-thaw, and continuation of the fresh cells in culture was not possible. Difficulty with early culture and passage of hESC lines carrying HD has been experienced in other laboratories, and the propagation of KCL008-HD2 was challenging until around passage 10-15. Stable, highly proliferative and homogenous cell populations with an astroglial phenotype were generated from neural induction of KCL008-HD2, which could be easily cultured, expanded and successfully undergo freeze-thaw cycles. The

CAG repeat length of the mutant allele in undifferentiated cells was stable at 46 repeats. However, in the differentiated precursor population there was a dramatic increase in CAG repeat units to 70. Somatic instability is seen clinically and thus these cells provide a unique source for research, as this large repeat is unlikely to be obtained directly from a HD patient. Mutant Huntingtin (HTT) was detected in the cells by western blot.

The suitability of hESC lines derived from PGD embryos as disease models has been verified within this thesis, at least in the context of HD. Cell populations can be obtained of a relevant phenotype and with salient behavioural characteristics, that are simple to culture and immensely suitable for scale up for experimentation. Functional analysis and characterisation of aggregate formation in the astroglial progenitor population in the context of neurotransmission in future work would be informative for determining underlying mechanisms in HD pathogenesis. It has been shown in the striatum of R6/2 transgenic mice that the proportion of glial cells showing intranuclear HTT aggregate staining increases with age, correlating with severity of disease phenotype in the mice (Shin *et al.*, 2005). The onset and conditions affecting the somatic instability of the CAG repeat can also be studied with this line.

Whilst this particular cell line is a valuable biochemical tool, the abnormal karyotype precludes useful transcriptional analysis of HD versus wild type cell lines. Therefore future work must aim to derive further HD lines that are stable, proliferative and karyotypically normal. Molecular, biochemical and immunocytochemical approaches to characterise the HD lines including HTT aggregates, transcriptional dysregulation, oxidative damage and cell death will be performed. Differentiation to the neural lineage can then be repeated and transcriptional analysis of the cells carried out. This would aim to highlight significant expression profile differences between wild-type and affected cells. Based on this eventual detailed analysis, HD lines will be available for development as high-throughput screening tools for appropriate targets. Future work must also focus on the derivation of hESC with other genetic disorders, such as SMA and DMD. These embryos are available through the Guy's PGD program, and collaborators with expertise in such diseases have already been identified, so that disease-specific investigation can begin as soon as the lines are established.

7.4 Concluding remarks

The use of stem cells for regenerative medicine has captured the imagination of the public, with media attention contributing to rising expectations of clinical benefit. Most biological medicines, such as vaccines and monoclonal antibodies, take decades to become established as accepted therapies. There is a clear need for ongoing public confidence in hESC research, particularly if early applications as therapies fail or cause unforeseen problems. Such confidence is fostered in the UK by appropriate and transparent ethical governance and regulation to match the permissive approach to embryo and stem cell research. Clinical therapy is not the only focus of hESC research, as these cells are unique tools with which to study early embryonic development and disease pathophysiology. Indeed some investigators no longer see cell therapy as the first goal of hESC research (Ben-Yosef *et al.*, 2008). Instead, it is considered that hESC from PGD embryos or iPS cells from patients serve as an excellent research tool to study the mechanism of disease. Human embryonic stem cells therefore offer a triad of potential: for clinical therapy, in disease research and as tools to study early embryonic development, and work in this thesis has focussed on each of these areas.

References

Abbott, A., Dennis, C., Ledford, H., & Smith, K. 2006. The lure of stem-cell lines. *Nature*, **442**(7101), 336–7.

Abe, H., & Hoshi, H. 2003. Evaluation of bovine embryos produced in high performance serum-free media. *J Reprod Dev*, **49**(3), 193–202.

Adams, G. B. 2008. Deconstructing the hematopoietic stem cell niche: revealing the therapeutic potential. *Regen Med*, **3**(4), 523–30.

Adewumi, O., Aflatoonian, B., Ahrlund-Richter, L., Amit, M., Andrews, P. W., Beighton, G., Bello, P. A., Benvenisty, N., Berry, L. S., Bevan, S., Blum, B., Brooking, J., Chen, K. G., Choo, A. B., Churchill, G. A., Corbel, M., Damjanov, I., Draper, J. S., Dvorak, P., Emanuelsson, K., Fleck, R. A., Ford, A., Gertow, K., Gertsenstein, M., Gokhale, P. J., Hamilton, R. S., Hampl, A., Healy, L. E., Hovatta, O., Hyllner, J., Imreh, M. P., Itskovitz-Eldor, J., Jackson, J., Johnson, J. L., Jones, M., Kee, K., King, B. L., Knowles, B. B., Lako, M., Lebrin, F., Mallon, B. S., Manning, D., Mayshar, Y., McKay, R. D., Michalska, A. E., Mikkola, M., Mileikovsky, M., Minger, S. L., Moore, H. D., Mummery, C. L., Nagy, A., Nakatsuji, N., O'Brien, C. M., Oh, S. K., Olsson, C., Otonkoski, T., Park, K. Y., Passier, R., Patel, H., Patel, M., Pedersen, R., Pera, M. F., Piekarczyk, M. S., Pera, R. A., Reubinoff, B. E., Robins, A. J., Rossant, J., Rugg-Gunn, P., Schulz, T. C., Semb, H., Sherrer, E. S., Siemen, H., Stacey, G. N., Stojkovic, M., Suemori, H., Szatkiewicz, J., Turetsky, T., Tuuri, T., van den Brink, S., Vintersten, K., Vuoristo, S., Ward, D., Weaver, T. A., Young, L. A., & Zhang, W. 2007. Characterization of human embryonic stem cell lines by the International Stem Cell Initiative. *Nat Biotechnol*, **25**(7), 803–16.

Adjaye, J., Huntriss, J., Herwig, R., BenKahla, A., Brink, T. C., Wierling, C., Hultschig, C., Groth, D., Yaspo, M. L., Picton, H. M., Gosden, R. G., & Lehrach, H. 2005. Primary differentiation in the human blastocyst: comparative molecular portraits of inner cell mass and trophectoderm cells. *Stem Cells*, **23**(10), 1514–25.

Ahmad, S., Stewart, R., Yung, S., Kolli, S., Armstrong, L., Stojkovic, M., Figueiredo, F., & Lako, M. 2007. Differentiation of human embryonic stem cells into corneal epithelial-like cells by in vitro replication of the corneal epithelial stem cell niche. *Stem Cells*, **25**(5), 1145–55.

Ahmed, S., Reynolds, B. A., & Weiss, S. 1995. BDNF enhances the differentiation but not the survival of CNS stem cell-derived neuronal precursors. *J Neurosci*, **15**(8), 5765–78.

Akle, C. A., Adinolfi, M., Welsh, K. I., Leibowitz, S., & McColl, I. 1981. Immunogenicity of human amniotic epithelial cells after transplantation into volunteers. *Lancet*, **2**(8254), 1003–5.

Alikani, M. 2007. The debate surrounding human embryonic stem cell research in the USA. *Reprod Biomed Online*, **15 Suppl 2**, 7–11.

Allegrucci, C., & Young, L. E. 2007. Differences between human embryonic stem cell lines. *Hum Reprod Update*, **13**(2), 103–20.

Allen, W. R., & Pashen, R. L. 1984. Production of monozygotic (identical) horse twins by embryo micromanipulation. *J Reprod Fertil*, **71**(2), 607–13.

Amariglio, N., Hirshberg, A., Scheithauer, B. W., Cohen, Y., Loewenthal, R., Trakhtenbrot, L., Paz, N., Koren-Michowitz, M., Waldman, D., Leider-Trejo, L., Toren, A., Constantini, S., & Rechavi, G. 2009. Donor-derived brain tumor following neural stem cell transplantation in an ataxia telangiectasia patient. *PLoS Med*, **6**(2), e1000029.

Amemiya, T. 1973. Regression analysis when the dependent variable is truncated Normal. *Econometrica*, **41**(6), 997–1016.

Amit, M., & Itskovitz-Eldor, J. 2002. Derivation and spontaneous differentiation of human embryonic stem cells. *J Anat*, **200**(Pt 3), 225–32.

Amit, M., Shariki, C., Margulets, V., & Itskovitz-Eldor, J. 2004. Feeder layer- and serum-free culture of human embryonic stem cells. *Biol Reprod*, **70**(3), 837–45.

Ammann, A. J., Cowan, M. J., Wara, D. W., Weintrub, P., Dritz, S., Goldman, H., & Perkins, H. A. 1983. Acquired immunodeficiency in an infant: possible transmission by means of blood products. *Lancet*, **1**(8331), 956–8.

Anderson, G. B., Behboodi, E., & Pacheco, T.V. 1992. Culture of inner cell masses from in vitro-derived bovine blastocysts. *Theriogenology*, **37**(1), 187.

Andrews, P. W., Benvenisty, N., McKay, R., Pera, M. F., Rossant, J., Semb, H., & Stacey, G. N. 2005. The International Stem Cell Initiative: toward benchmarks for human embryonic stem cell research. *Nat Biotechnol*, **23**(7), 795–7.

Antczak, M., & Van Blerkom, J. 1997. Oocyte influences on early development: the regulatory proteins leptin and STAT3 are polarized in mouse and human oocytes and differentially distributed within the cells of the preimplantation stage embryo. *Mol Hum Reprod*, **3**(12), 1067–86.

Antczak, M., & Van Blerkom, J. 1999. Temporal and spatial aspects of fragmentation in early human embryos: possible effects on developmental competence and association with the differential elimination of regulatory proteins from polarized domains. *Hum Reprod*, **14**(2), 429–47.

Aoi, T., Yae, K., Nakagawa, M., Ichisaka, T., Okita, K., Takahashi, K., Chiba, T., & Yamanaka, S. 2008. Generation of pluripotent stem cells from adult mouse liver and stomach cells. *Science*, **321**(5889), 699–702.

Armelin, H. A. 1973. Pituitary extracts and steroid hormones in the control of 3T3 cell growth. *Proc Natl Acad Sci U S A*, **70**(9), 2702–6.

Artley, J. K., Braude, P. R., & Johnson, M. H. 1992. Gene activity and cleavage arrest in human pre-embryos. *Hum Reprod*, **7**(7), 1014–21.

Ashton, R. S., Peltier, J., Fasano, C. A., O'Neill, A., Leonard, J., Temple, S., Schaffer, D. V., & Kane, R. S. 2007. High-throughput screening of gene function in stem cells using clonal microarrays. *Stem Cells*, **25**(11), 2928–35.

Atienza-Samols, S. B., & Sherman, M. I. 1978. Outgrowth promoting factor for the inner cell mass of the mouse blastocyst. *Dev Biol*, **66**(1), 220–31.

Atkinson, S., & Armstrong, L. 2008. Epigenetics in embryonic stem cells: regulation of pluripotency and differentiation. *Cell Tissue Res*, **331**(1), 23–9.

Austin, C. R. 1952. The capacitation of the mammalian sperm. *Nature*, **170**(4321), 326.

Avilion, A. A., Nicolis, S. K., Pevny, L. H., Perez, L., Vivian, N., & Lovell-Badge, R. 2003. Multipotent cell lineages in early mouse development depend on SOX2 function. *Genes Dev*, **17**(1), 126–40.

Bachoud-Levi, A. C., Remy, P., Nguyen, J. P., Brugieres, P., Lefaucheur, J. P., Bourdet, C., Baudic, S., Gaura, V., Maison, P., Haddad, B., Boisse, M. F., Grandmougin, T., Jeny, R., Bartolomeo, P., Dalla Barba, G., Degos, J. D., Lisovoski, F., Ergis, A. M., Pailhous, E., Cesaro, P., Hantraye, P., & Peschanski, M. 2000. Motor and cognitive improvements in patients with Huntington's disease after neural transplantation. *Lancet*, **356**(9246), 1975–9.

Baharvand, H., Ashtiani, S. K., Taee, A., Massumi, M., Valojerdi, M. R., Yazdi, P. E., Moradi, S. Z., & Farrokhi, A. 2006. Generation of new human embryonic stem cell lines with diploid and triploid karyotypes. *Dev Growth Differ*, **48**(2), 117–28.

Bahceci, M., Ciray, H. N., Karagenc, L., Ulug, U., & Bener, F. 2005. Effect of oxygen concentration during the incubation of embryos of women undergoing ICSI and embryo transfer: a prospective randomized study. *Reprod Biomed Online*, **11**(4), 438–43.

Bajada, S., Mazakova, I., Richardson, J. B., & Ashammakhi, N. 2008. Updates on stem cells and their applications in regenerative medicine. *J Tissue Eng Regen Med*, **2**(4), 169–83.

Balakier, H., & Cadesky, K. 1997. The frequency and developmental capability of human embryos containing multinucleated blastomeres. *Hum Reprod*, **12**(4), 800–4.

Barberi, T., Klivenyi, P., Calingasan, N. Y., Lee, H., Kawamata, H., Loonam, K., Perrier, A. L., Bruses, J., Rubio, M. E., Topf, N., Tabar, V., Harrison, N. L., Beal, M. F., Moore, M. A., & Studer, L. 2003. Neural subtype specification of fertilization and nuclear transfer embryonic stem cells and application in parkinsonian mice. *Nat Biotechnol*, **21**(10), 1200–7.

Barmat, L. I., Worrilow, K. C., & Paynton, B. V. 1997. Growth factor expression by human oviduct and buffalo rat liver coculture cells. *Fertil Steril*, **67**(4), 775–9.

Bates, G. P., & Hockly, E. 2003. Experimental therapeutics in Huntington's disease: are models useful for therapeutic trials? *Curr Opin Neurol*, **16**(4), 465–70.

Batt, P. A., Gardner, D. K., & Cameron, A. W. 1991. Oxygen concentration and protein source affect the development of preimplantation goat embryos in vitro. *Reprod Fertil Dev*, **3**(5), 601–7.

Bavister, B. D. 1992. Co-culture for embryo development: is it really necessary? *Hum Reprod*, **7**(10), 1339–41.

Bavister, B. D. 1995. Culture of preimplantation embryos: facts and artifacts. *Hum Reprod Update*, **1**(2), 91–148.

Bavister, B. D., & Poole, K. A. 2005. Duration and temperature of culture medium equilibration affect frequency of blastocyst development. *Reprod Biomed Online*, **10**(1), 124–9.

Beattie, G. M., Lopez, A. D., Bucay, N., Hinton, A., Firpo, M. T., King, C. C., & Hayek, A. 2005. Activin A maintains pluripotency of human embryonic stem cells in the absence of feeder layers. *Stem Cells*, **23**(4), 489–95.

Beck, F., Erler, T., Russell, A., & James, R. 1995. Expression of Cdx-2 in the mouse embryo and placenta: possible role in patterning of the extra-embryonic membranes. *Dev Dyn*, **204**(3), 219–27.

Beg, A. A., Sha, W. C., Bronson, R. T., Ghosh, S., & Baltimore, D. 1995. Embryonic lethality and liver degeneration in mice lacking the RelA component of NF-kappa B. *Nature*, **376**(6536), 167–70.

Beglinger, L. J., Paulsen, J. S., Watson, D. B., Wang, C., Duff, K., Langbehn, D. R., Moser, D. J., Paulson, H. L., Aylward, E. H., Carlozzi, N. E., Queller, S., & Stout, J. C. 2008. Obsessive and compulsive symptoms in prediagnosed huntington's disease. *J Clin Psychiatry*, **69**(11), 1758–1765.

Behr, B., Pool, T. B., Milki, A. A., Moore, D., Gebhardt, J., & Dasig, D. 1999. Preliminary clinical experience with human blastocyst development in vitro without co-culture. *Hum Reprod*, **14**(2), 454–7.

Ben-Yosef, D., Malcov, M., & Eiges, R. 2008. PGD-derived human embryonic stem cell lines as a powerful tool for the study of human genetic disorders. *Mol Cell Endocrinol*, **282**(1-2), 153–8.

Bendall, S. C., Stewart, M. H., Menendez, P., George, D., Vijayaragavan, K., Werbowetski-Ogilvie, T., Ramos-Mejia, V., Rouleau, A., Yang, J., Bosse, M., Lajoie, G., & Bhatia, M. 2007. IGF and FGF cooperatively establish the regulatory stem cell niche of pluripotent human cells in vitro. *Nature*, **448**(7157), 1015–21.

Bergstrom, J., Furst, P., Noree, L. O., & Vinnars, E. 1974. Intracellular free amino acid concentration in human muscle tissue. *J Appl Physiol*, **36**(6), 693–7.

Bianco, P., & Robey, P. G. 2001. Stem cells in tissue engineering. *Nature*, **414**(6859), 118–21.

Biggers, J. D. 2000. Ethical issues and the commercialization of embryo culture media. *Reprod Biomed Online*, **1**(3), 74–6.

Biggers, J. D., Whittingham, D. G., & Donahue, R. P. 1967. The pattern of energy metabolism in the mouse oocyte and zygote. *Proc Natl Acad Sci U S A*, **58**(2), 560–7.

Bloor, D. J., Metcalfe, A. D., Rutherford, A., Brison, D. R., & Kimber, S. J. 2002. Expression of cell adhesion molecules during human preimplantation embryo development. *Mol Hum Reprod*, **8**(3), 237–45.

Bodnar, M. S., Meneses, J. J., Rodriguez, R. T., & Firpo, M. T. 2004. Propagation and maintenance of undifferentiated human embryonic stem cells. *Stem Cells Dev*, **13**(3), 243–53.

Bolton, V. N., Hawes, S. M., Taylor, C. T., & Parsons, J. H. 1989. Development of spare human preimplantation embryos in vitro: an analysis of the correlations among gross morphology, cleavage rates, and development to the blastocyst. *J In Vitro Fert Embryo Transf*, **6**(1), 30–5.

Bongso, A., Ng, S. C., Sathananthan, H., Ng, P. L., Rauff, M., & Ratnam, S. S. 1989a. Establishment of human ampullary cell cultures. *Hum Reprod*, **4**(5), 486–94.

Bongso, A., Soon-Chye, N., Sathananthan, H., Lian, N. P., Rauff, M., & Ratnam, S. 1989b. Improved quality of human embryos when co-cultured with human ampullary cells. *Hum Reprod*, **4**(6), 706–13.

Bongso, A., Fong, C. Y., Ng, S. C., & Ratnam, S. 1994a. Human embryonic behavior in a sequential human oviduct-endometrial coculture system. *Fertil Steril*, **61**(5), 976–8.

Bongso, A., Fong, C. Y., Ng, S. C., & Ratnam, S. 1994b. Isolation and culture of inner cell mass cells from human blastocysts. *Hum Reprod*, **9**(11), 2110–7.

Bongso, A., Fong, C. Y., & Gauthaman, K. 2008. Taking stem cells to the clinic: Major challenges. *J Cell Biochem*, **105**(6), 1352–60.

Borland, R. M., Biggers, J. D., & Lechene, C. P. 1977. Studies on the composition and formation of mouse blastocoele fluid using electron probe microanalysis. *Dev Biol*, **55**(1), 1–8.

Borstlap, J., Kurtz, A., Stacey, G., Elstner, A., Damaschun, A., Aran, B., Gerlach, J., Izpisua, J., & Veiga, A. 2008. Development of a European human embryonic stem cell registry. *Regen Med*, **3**(6), 945–51.

Boyer, L. A., Lee, T. I., Cole, M. F., Johnstone, S. E., Levine, S. S., Zucker, J. P., Guenther, M. G., Kumar, R. M., Murray, H. L., Jenner, R. G., Gifford, D. K., Melton, D. A., Jaenisch, R., & Young, R. A. 2005. Core transcriptional regulatory circuitry in human embryonic stem cells. *Cell*, **122**(6), 947–56.

Bradley, A., Evans, M., Kaufman, M. H., & Robertson, E. 1984. Formation of germ-line chimaeras from embryo-derived teratocarcinoma cell lines. *Nature*, **309**(5965), 255–6.

Braude, P., Pelham, H., Flach, G., & Lobatto, R. 1979. Post-transcriptional control in the early mouse embryo. *Nature*, **282**(5734), 102–5.

Braude, P., Bolton, V., & Moore, S. 1988. Human gene expression first occurs between the four- and eight-cell stages of preimplantation development. *Nature*, **332**(6163), 459–61.

Braude, P., Pickering, S., Flinter, F., & Ogilvie, C. M. 2002. Preimplantation genetic diagnosis. *Nat Rev Genet*, **3**(12), 941–53.

Braude, P., Minger, S. L., & Warwick, R. M. 2005. Stem cell therapy: hope or hype? *BMJ*, **330**(7501), 1159–60.

Brazma, A., Hingamp, P., Quackenbush, J., Sherlock, G., Spellman, P., Stoeckert, C., Aach, J., Ansorge, W., Ball, C. A., Causton, H. C., Gaasterland, T., Glenisson, P., Holstege, F. C., Kim, I. F., Markowitz, V., Matese, J. C., Parkinson, H., Robinson, A., Sarkans, U., Schulze-Kremer, S., Stewart, J., Taylor, R., Vilo, J., & Vingron, M. 2001. Minimum information about a microarray experiment (MIAME)-toward standards for microarray data. *Nat Genet*, **29**(4), 365–71.

Brems, H., Vogels, A., Ribai, P., De Raedt, T., Fryns, J. P., & Legius, E. 2003. Second polar body inclusion results in diploid/triploid mixoploidy. *Genet Couns*, **14**(4), 425–9.

Brison, D. R., Hewitson, L. C., & Leese, H. J. 1993. Glucose, pyruvate, and lactate concentrations in the blastocoel cavity of rat and mouse embryos. *Mol Reprod Dev*, **35**(3), 227–32.

Brison, D. R., Houghton, F. D., Falconer, D., Roberts, S. A., Hawkhead, J., Humpherson, P. G., Lieberman, B. A., & Leese, H. J. 2004. Identification of viable embryos in IVF by non-invasive measurement of amino acid turnover. *Hum Reprod*, **19**(10), 2319–24.

Brockes, J. P. 1997. Amphibian limb regeneration: rebuilding a complex structure. *Science*, **276**(5309), 81–7.

Brons, I. G., Smithers, L. E., Trotter, M. W., Rugg-Gunn, P., Sun, B., Chuva de Sousa Lopes, S. M., Howlett, S. K., Clarkson, A., Ahrlund-Richter, L., Pedersen, R. A., & Vallier, L. 2007. Derivation of pluripotent epiblast stem cells from mammalian embryos. *Nature*, **448**(7150), 191–5.

Brooksbank, C., & Quackenbush, J. 2006. Data standards: a call to action. *Omics*, **10**(2), 94–9.

Burton, G. J., Hempstock, J., & Jauniaux, E. 2003. Oxygen, early embryonic metabolism and free radical-mediated embryopathies. *Reprod Biomed Online*, **6**(1), 84–96.

Butler, M, & Spier, R. E. 1984. The effects of glutamine utilisation and ammonia production on the growth of BHK cells in microcarrier cultures. *Journal of Biotechnology*, **1**(3-4), 187–196.

Cai, C., & Grabel, L. 2007. Directing the differentiation of embryonic stem cells to neural stem cells. *Dev Dyn*, **236**(12), 3255–66.

Catt, J. W., & Henman, M. 2000. Toxic effects of oxygen on human embryo development. *Hum Reprod*, **15 Suppl 2**, 199–206.

Cattaneo, E., Rigamonti, D., Goffredo, D., Zuccato, C., Squitieri, F., & Sipione, S. 2001. Loss of normal huntingtin function: new developments in Huntington's disease research. *Trends Neurosci*, **24**(3), 182–8.

Cauffman, G., Van de Velde, H., Liebaers, I., & Van Steirteghem, A. 2005a. DAZL expression in human oocytes, preimplantation embryos and embryonic stem cells. *Mol Hum Reprod*, **11**(6), 405–11.

Cauffman, G., Van de Velde, H., Liebaers, I., & Van Steirteghem, A. 2005b. Oct-4 mRNA and protein expression during human preimplantation development. *Mol Hum Reprod*, **11**(3), 173–81.

Cauffman, G., Liebaers, I., Van Steirteghem, A., & Van de Velde, H. 2006. POU5F1 isoforms show different expression patterns in human embryonic stem cells and preimplantation embryos. *Stem Cells*, **24**(12), 2685–91.

Cauffman, G., De Rycke, M., Sermon, K., Liebaers, I., & Van de Velde, H. 2009. Markers that define stemness in ESC are unable to identify the totipotent cells in human preimplantation embryos. *Hum Reprod*, **24**(1), 63–70.

Chan, A. W., Dominko, T., Luetjens, C. M., Neuber, E., Martinovich, C., Hewitson, L., Simerly, C. R., & Schatten, G. P. 2000. Clonal propagation of primate offspring by embryo splitting. *Science*, **287**(5451), 317–9.

Chang, M. C. 1951. Fertilizing capacity of spermatozoa deposited into the fallopian tubes. *Nature*, **168**(4277), 697–8.

Chang, M. C. 1959. Fertilization of rabbit ova in vitro. *Nature*, **184(Suppl 7)**, 466–7.

Chang, M. C. 1968. In vitro fertilization of mammalian eggs. *J Anim Sci*, **27 Suppl 1**, 15–26.

Chen, H., Qian, K., Hu, J., Liu, D., Lu, W., Yang, Y., Wang, D., Yan, H., Zhang, S., & Zhu, G. 2005. The derivation of two additional human embryonic stem cell lines from day 3 embryos with low morphological scores. *Hum Reprod*, **20**(8), 2201–6.

Chen, Y. T., Li, W., Hayashida, Y., He, H., Chen, S. Y., Tseng, D. Y., Kheirkhah, A., & Tseng, S. C. 2007. Human amniotic epithelial cells as novel feeder layers for promoting ex vivo expansion of limbal epithelial progenitor cells. *Stem Cells*, **25**(8), 1995–2005.

Chiba, S. 2006. Notch signaling in stem cell systems. *Stem Cells*, **24**(11), 2437–47.

Chin, A. C., Fong, W. J., Goh, L. T., Philp, R., Oh, S. K., & Choo, A. B. 2007. Identification of proteins from feeder conditioned medium that support human embryonic stem cells. *J Biotechnol*, **130**(3), 320–8.

Cho, Y. M., Kwon, S., Pak, Y. K., Seol, H. W., Choi, Y. M., Park do, J., Park, K. S., & Lee, H. K. 2006. Dynamic changes in mitochondrial biogenesis and antioxidant enzymes during the spontaneous differentiation of human embryonic stem cells. *Biochem Biophys Res Commun*, **348**(4), 1472–8.

Choo, A., Padmanabhan, J., Chin, A., Fong, W. J., & Oh, S. K. 2006. Immortalized feeders for the scale-up of human embryonic stem cells in feeder and feeder-free conditions. *J Biotechnol*, **122**(1), 130–41.

Chung, Y., Klimanskaya, I., Becker, S., Marh, J., Lu, S. J., Johnson, J., Meisner, L., & Lanza, R. 2006. Embryonic and extraembryonic stem cell lines derived from single mouse blastomeres. *Nature*, **439**(7073), 216–9.

Chung, Y., Klimanskaya, I., Becker, S., Li, T., Maserati, M., Lu, S. J., Zdravkovic, T., Ilic, D., Genbacev, O., Fisher, S., Krtolica, A., & Lanza, R. 2008. Human embryonic stem cell lines generated without embryo destruction. *Cell Stem Cell*, **2**(2), 113–7.

Ciemerych, M. A., Mesnard, D., & Zernicka-Goetz, M. 2000. Animal and vegetal poles of the mouse egg predict the polarity of the embryonic axis, yet are nonessential for development. *Development*, **127**(16), 3467–74.

Civin, C. I., & Rao, M. S. 2006. How many human embryonic stem cell lines are sufficient? A U.S. perspective. *Stem Cells*, **24**(4), 800–3.

Cobo, F., Stacey, G. N., Hunt, C., Cabrera, C., Nieto, A., Montes, R., Cortes, J. L., Catalina, P., Barnie, A., & Concha, A. 2005. Microbiological control in stem cell banks: approaches to standardisation. *Appl Microbiol Biotechnol*, **68**(4), 456–66.

Cohen, J., Trounson, A., Dawson, K., Jones, H., Hazekamp, J., Nygren, K. G., & Hamberger, L. 2005. The early days of IVF outside the UK. *Hum Reprod Update*, **11**(5), 439–59.

Cole, R. J., Edwards, R. G., & Paul, J. 1966. Cytodifferentiation and embryogenesis in cell colonies and tissue cultures derived from ova and blastocysts of the rabbit. *Dev Biol*, **13**(3), 385–407.

Conti, L., Pollard, S. M., Gorba, T., Reitano, E., Toselli, M., Biella, G., Sun, Y., Sanzone, S., Ying, Q. L., Cattaneo, E., & Smith, A. 2005. Niche-independent symmetrical self-renewal of a mammalian tissue stem cell. *PLoS Biol*, **3**(9), e283.

Cornwell, G. 2006. Ethical issues in deriving stem cells from embryos and eggs. *Br J Nurs*, **15**(12), 640–4.

Cowan, C. A., Klimanskaya, I., McMahon, J., Atienza, J., Witmyer, J., Zucker, J. P., Wang, S., Morton, C. C., McMahon, A. P., Powers, D., & Melton, D. A. 2004. Derivation of embryonic stem-cell lines from human blastocysts. *N Engl J Med*, **350**(13), 1353–6.

Criniti, A., Thyer, A., Chow, G., Lin, P., Klein, N., & Soules, M. 2005. Elective single blastocyst transfer reduces twin rates without compromising pregnancy rates. *Fertil Steril*, **84**(6), 1613–9.

Crook, J. M., Peura, T. T., Kravets, L., Bosman, A. G., Buzzard, J. J., Horne, R., Hentze, H., Dunn, N. R., Zweigerdt, R., Chua, F., Upshall, A., & Colman, A. 2007. The Generation of Six Clinical-Grade Human Embryonic Stem Cell Lines. *Cell Stem Cell*, **1**(5), 490–494.

Daar, A. S., & Greenwood, H. L. 2007. A proposed definition of regenerative medicine. *J Tissue Eng Regen Med*, **1**(3), 179–84.

Dadoune, J. P. 2007. New insights into male gametogenesis: what about the spermatogonial stem cell niche? *Folia Histochem Cytobiol*, **45**(3), 141–7.

Daheron, L., Opitz, S. L., Zaehres, H., Lensch, W. M., Andrews, P. W., Itskovitz-Eldor, J., & Daley, G. Q. 2004. LIF/STAT3 signaling fails to maintain self-renewal of human embryonic stem cells. *Stem Cells*, **22**(5), 770–8.

Daniel, A., Wu, Z., Darmanian, A., Collins, F., & Jackson, J. 2003. Three different origins for apparent triploid/diploid mosaics. *Prenat Diagn*, **23**(7), 529–34.

Davidson, E. H. 1989. Lineage-specific gene expression and the regulative capacities of the sea urchin embryo: a proposed mechanism. *Development*, **105**(3), 421–45.

Davies, S. W., Turmaine, M., Cozens, B. A., DiFiglia, M., Sharp, A. H., Ross, C. A., Scherzinger, E., Wanker, E. E., Mangiarini, L., & Bates, G. P. 1997. Formation of neuronal intranuclear inclusions underlies the neurological dysfunction in mice transgenic for the HD mutation. *Cell*, **90**(3), 537–48.

Davies, T. J., & Gardner, R. L. 2002. The plane of first cleavage is not related to the distribution of sperm components in the mouse. *Hum Reprod*, **17**(9), 2368–79.

Day, M. L., Winston, N., McConnell, J. L., Cook, D., & Johnson, M. H. 2001. tiK+ toK+: an embryonic clock? *Reprod Fertil Dev*, **13**(1), 69–79.

De Coppi, P., Bartsch, G., Jr., Siddiqui, M. M., Xu, T., Santos, C. C., Perin, L., Mostoslavsky, G., Serre, A. C., Snyder, E. Y., Yoo, J. J., Furth, M. E., Soker, S., & Atala, A. 2007. Isolation of amniotic stem cell lines with potential for therapy. *Nat Biotechnol*, **25**(1), 100–6.

De Hertogh, R., Vanderheyden, I., Pampfer, S., Robin, D., Dufrasne, E., & Delcourt, J. 1991. Stimulatory and inhibitory effects of glucose and insulin on rat blastocyst development in vitro. *Diabetes*, **40**(5), 641–7.

de Lamirande, E., Harakat, A., & Gagnon, C. 1998a. Human sperm capacitation induced by biological fluids and progesterone, but not by NADH or NADPH, is associated with the production of superoxide anion. *J Androl*, **19**(2), 215–25.

de Lamirande, E., Tsai, C., Harakat, A., & Gagnon, C. 1998b. Involvement of reactive oxygen species in human sperm acrosome reaction induced by A23187, lysophosphatidylcholine, and biological fluid ultrafiltrates. *J Androl*, **19**(5), 585–94.

De Laporte, L., & Shea, L. D. 2007. Matrices and scaffolds for DNA delivery in tissue engineering. *Adv Drug Deliv Rev*, **59**(4-5), 292–307.

De Rycke, M., Liebaers, I., & Van Steirteghem, A. 2002. Epigenetic risks related to assisted reproductive technologies: risk analysis and epigenetic inheritance. *Hum Reprod*, **17**(10), 2487–94.

De Sousa, P. A., Galea, G., & Turner, M. 2006. The road to providing human embryo stem cells for therapeutic use: the UK experience. *Reproduction*, **132**(5), 681–9.

Deb, K., Sivaguru, M., Yong, H. Y., & Roberts, R. M. 2006. Cdx2 gene expression and trophectoderm lineage specification in mouse embryos. *Science*, **311**(5763), 992–6.

Deech, R. 2008. 30 years: from IVF to stem cells. *Nature*, **454**(7202), 280–1.

Dhara, S. K., Hasneen, K., Machacek, D. W., Boyd, N. L., Rao, R. R., & Stice, S. L. 2008. Human neural progenitor cells derived from embryonic stem cells in feeder-free cultures. *Differentiation*, **76**(5), 454–64.

Di Maio, L., Squitieri, F., Napolitano, G., Campanella, G., Trofatter, J. A., & Conneally, P. M. 1993. Suicide risk in Huntington's disease. *J Med Genet*, **30**(4), 293–5.

Dietrich, J. E., & Hiiragi, T. 2007. Stochastic patterning in the mouse pre-implantation embryo. *Development*, **134**(23), 4219–31.

Dimos, J. T., Rodolfa, K. T., Niakan, K. K., Weisenthal, L. M., Mitsumoto, H., Chung, W., Croft, G. F., Saphier, G., Leibel, R., Goland, R., Wichterle, H., Henderson, C. E., & Eggan, K. 2008. Induced pluripotent stem cells generated from patients with ALS can be differentiated into motor neurons. *Science*, **321**(5893), 1218–21.

Doetschman, T., Williams, P., & Maeda, N. 1988. Establishment of hamster blastocyst-derived embryonic stem (ES) cells. *Dev Biol*, **127**(1), 224–7.

Dumoulin, J. C., Meijers, C. J., Bras, M., Coonen, E., Geraedts, J. P., & Evers, J. L. 1999. Effect of oxygen concentration on human in-vitro fertilization and embryo culture. *Hum Reprod*, **14**(2), 465–9.

Duval, C., Bouvet, P., Omilli, F., Roghi, C., Dorel, C., LeGuellec, R., Paris, J., & Osborne, H. B. 1990. Stability of maternal mRNA in Xenopus embryos: role of transcription and translation. *Mol Cell Biol*, **10**(8), 4123–9.

Edwards, R. G. 1965. Maturation in vitro of mouse, sheep, cow, pig, rhesus monkey and human ovarian oocytes. *Nature*, **208**(5008), 349–51.

Edwards, R. G., & Beard, H. K. 1997. Oocyte polarity and cell determination in early mammalian embryos. *Mol Hum Reprod*, **3**(10), 863–905.

Edwards, R. G., & Brody, S. A. 1995. *Principles of Assisted Human Reproduction*. W B Saunders Co.

Edwards, R. G., & Gardner, R. L. 1967. Sexing of live rabbit blastocysts. *Nature*, **214**(5088), 576–7.

Edwards, R. G., & Sharpe, D. J. 1971. Social values and research in human embryology. *Nature*, **231**(5298), 87–91.

Edwards, R. G., Bavister, B. D., & Steptoe, P. C. 1969. Early stages of fertilization in vitro of human oocytes matured in vitro. *Nature*, **221**(5181), 632–5.

Edwards, R. G., Steptoe, P. C., & Purdy, J. M. 1970. Fertilization and cleavage in vitro of preovulator human oocytes. *Nature*, **227**(5265), 1307–9.

Eiges, R., Schuldiner, M., Drukker, M., Yanuka, O., Itskovitz-Eldor, J., & Benvenisty, N. 2001. Establishment of human embryonic stem cell-transfected clones carrying a marker for undifferentiated cells. *Curr Biol*, **11**(7), 514–8.

El Mouatassim, S., Guerin, P., & Menezo, Y. 1999. Expression of genes encoding antioxidant enzymes in human and mouse oocytes during the final stages of maturation. *Mol Hum Reprod*, **5**(8), 720–5.

Ellerstrom, C., Strehl, R., Moya, K., Andersson, K., Bergh, C., Lundin, K., Hyllner, J., & Semb, H. 2006. Derivation of a xeno-free human embryonic stem cell line. *Stem Cells*, **24**(10), 2170–6.

Erbach, G. T., Lawitts, J. A., Papaioannou, V. E., & Biggers, J. D. 1994. Differential growth of the mouse preimplantation embryo in chemically defined media. *Biol Reprod*, **50**(5), 1027–33.

Evans, M. J., & Kaufman, M. H. 1981. Establishment in culture of pluripotential cells from mouse embryos. *Nature*, **292**(5819), 154–6.

Evans, M. J., Notarianni, E., Laurie, S., & Moor, R. M. 1990. Derivation and preliminary characterization of pluripotent cell lines from porcine and bovine blastocysts. *Theriogenology*, **33**(1), 125–8.

Ezashi, T., Das, P., & Roberts, R. M. 2005. Low O2 tensions and the prevention of differentiation of hES cells. *Proc Natl Acad Sci U S A*, **102**(13), 4783–8.

Falco, G., Stanghellini, I., & Ko, M. S. 2006. Use of Chuk as an internal standard suitable for quantitative RT-PCR in mouse preimplantation embryos. *Reprod Biomed Online*, **13**(3), 394–403.

Feki, A., Bosman, A., Dubuisson, J. B., Irion, O., Dahoun, S., Pelte, M. F., Hovatta, O., & Jaconi, M. E. 2008. Derivation of the first Swiss human embryonic stem cell line from a single blastomere of an arrested four-cell stage embryo. *Swiss Med Wkly*, **138**(37-38), 540–50.

Feng, H. L., Wen, X. H., & Presser, S. C. 1996. Effect of different co-culture systems in early human embryo development. *Hum Reprod*, **11**(7), 1525–8.

Ferrante, R. J., Andreassen, O. A., Dedeoglu, A., Ferrante, K. L., Jenkins, B. G., Hersch, S. M., & Beal, M. F. 2002. Therapeutic effects of coenzyme Q10 and remacemide in transgenic mouse models of Huntington's disease. *J Neurosci*, **22**(5), 1592–9.

Field, D., & Sansone, S. A. 2006. A special issue on data standards. *Omics*, **10**(2), 84–93.

Findikli, N., Kahraman, S., Akcin, O., Sertyel, S., & Candan, Z. 2005. Establishment and characterization of new human embryonic stem cell lines. *Reprod Biomed Online*, **10**(5), 617–27.

Fishel, S. B., Edwards, R. G., & Evans, C. J. 1984. Human chorionic gonadotropin secreted by preimplantation embryos cultured in vitro. *Science*, **223**(4638), 816–8.

Flach, G., Johnson, M. H., Braude, P. R., Taylor, R. A., & Bolton, V. N. 1982. The transition from maternal to embryonic control in the 2-cell mouse embryo. *Embo J*, **1**(6), 681–6.

Flanagan, L. A., Rebaza, L. M., Derzic, S., Schwartz, P. H., & Monuki, E. S. 2006. Regulation of human neural precursor cells by laminin and integrins. *J Neurosci Res*, **83**(5), 845–56.

Fleming, T. P. 1987. A quantitative analysis of cell allocation to trophectoderm and inner cell mass in the mouse blastocyst. *Dev Biol*, **119**(2), 520–31.

Fleming, T. P., & Pickering, S. J. 1985. Maturation and polarization of the endocytotic system in outside blastomeres during mouse preimplantation development. *J Embryol Exp Morphol*, **89**, 175–208.

Fleming, T. P., Pratt, H. P., & Braude, P. R. 1987. The use of mouse preimplantation embryos for quality control of culture reagents in human in vitro fertilization programs: a cautionary note. *Fertil Steril*, **47**(5), 858–60.

Fong, C. Y., Richards, M., & Bongso, A. 2006. Unsuccessful derivation of human embryonic stem cell lines from pairs of human blastomeres. *Reprod Biomed Online*, **13**(2), 295–300.

Forsyth, N. R., Musio, A., Vezzoni, P., Simpson, A. H., Noble, B. S., & McWhir, J. 2006. Physiologic oxygen enhances human embryonic stem cell clonal recovery and reduces chromosomal abnormalities. *Cloning Stem Cells*, **8**(1), 16–23.

Franklin, S. B., Hunt, C., Cornwell, G., Peddie, V., Desousa, P., Livie, M., Stephenson, E. L., & Braude, P. R. 2008. hESCCO: development of good practice models for hES cell derivation. *Regen Med*, **3**(1), 105–16.

Funston, R. N., Nauta, W. J., & Seidel, G. E., Jr. 1997. Culture of bovine embryos in buffalo rat liver cell-conditioned media or with leukemia inhibitory factor. *J Anim Sci*, **75**(5), 1332–6.

Furuya, S., Yamashiro, C., & Kato, Y. 2005. Morphological analysis of giant oocytes to assess their relevance for the origin of triploid zygote formation. *Fertil Steril*, **84**(Suppl. 1), S233.

Gage, F. H. 2000. Mammalian neural stem cells. *Science*, **287**(5457), 1433–8.

Garbutt, C. L., Johnson, M. H., & George, M. A. 1987. When and how does cell division order influence cell allocation to the inner cell mass of the mouse blastocyst? *Development*, **100**(2), 325–32.

Garcia-Gonzalo, F. R., & Belmonte, J. C. 2008. Albumin-associated lipids regulate human embryonic stem cell self-renewal. *PLoS ONE*, **3**(1), e1384.

Gardner, D. K., & Lane, M. 1993. Amino acids and ammonium regulate mouse embryo development in culture. *Biol Reprod*, **48**(2), 377–85.

Gardner, D. K., & Lane, M. 1996. Alleviation of the '2-cell block' and development to the blastocyst of CF1 mouse embryos: role of amino acids, EDTA and physical parameters. *Hum Reprod*, **11**(12), 2703–12.

Gardner, D. K., & Lane, M. 1997. Culture and selection of viable blastocysts: a feasible proposition for human IVF? *Hum Reprod Update*, **3**(4), 367–82.

Gardner, D. K., & Lane, M. 2002. *Principles of Cloning. Development of viable mammalian embryos in vitro: Evolution of sequential media*. 1 edn. Academic Press.

Gardner, D. K., & Lane, M. 2005. Ex vivo early embryo development and effects on gene expression and imprinting. *Reprod Fertil Dev*, **17**(3), 361–70.

Gardner, D. K., & Leese, H. J. 1988. The role of glucose and pyruvate transport in regulating nutrient utilization by preimplantation mouse embryos. *Development*, **104**(3), 423–9.

Gardner, D. K., Lane, M., Calderon, I., & Leeton, J. 1996. Environment of the preimplantation human embryo in vivo: metabolite analysis of oviduct and uterine fluids and metabolism of cumulus cells. *Fertil Steril*, **65**(2), 349–53.

Gardner, D. K., Lane, M., Johnson, J., Wagley, L., Stevens, J., & Schoolcraft, W. B. 1999. Reduced oxygen tension increases blastocysts development, differentiation, and viability. *Fertil Steril*, **72**(Suppl 1), O–079.

Gardner, D. K., Lane, M., Stevens, J., Schlenker, T., & Schoolcraft, W. B. 2000. Blastocyst score affects implantation and pregnancy outcome: towards a single blastocyst transfer. *Fertil Steril*, **73**(6), 1155–8.

Gardner, R. L. 1968. Mouse chimeras obtained by the injection of cells into the blastocyst. *Nature*, **220**(167), 596–7.

Gardner, R. L. 1997. The early blastocyst is bilaterally symmetrical and its axis of symmetry is aligned with the animal-vegetal axis of the zygote in the mouse. *Development*, **124**(2), 289–301.

Gardner, R. L. 2001. Specification of embryonic axes begins before cleavage in normal mouse development. *Development*, **128**(6), 839–47.

Gardner, R. L. 2002. Experimental analysis of second cleavage in the mouse. *Hum Reprod*, **17**(12), 3178–89.

Gardner, R. L. 2007. The axis of polarity of the mouse blastocyst is specified before blastulation and independently of the zona pellucida. *Hum Reprod*, **22**(3), 798–806.

Gardner, R. L., & Davies, T. J. 2006. An investigation of the origin and significance of bilateral symmetry of the pronuclear zygote in the mouse. *Hum Reprod*, **21**(2), 492–502.

Gavrilov, S., Papaioannou, V. E., & Landry, D. W. 2009. Alternative Strategies for the Derivation of Human Embryonic Stem Cell Lines and the Role of Dead Embryos. *Curr Stem Cell Res Ther*, **4**(1), 81–86.

Genbacev, O., Krtolica, A., Zdravkovic, T., Brunette, E., Powell, S., Nath, A., Caceres, E., McMaster, M., McDonagh, S., Li, Y., Mandalam, R., Lebkowski, J., & Fisher, S. J. 2005. Serum-free derivation of human embryonic stem cell lines on human placental fibroblast feeders. *Fertil Steril*, **83**(5), 1517–29.

Gerrard, L., Rodgers, L., & Cui, W. 2005. Differentiation of human embryonic stem cells to neural lineages in adherent culture by blocking bone morphogenetic protein signaling. *Stem Cells*, **23**(9), 1234–41.

Ghassemifar, M. R., Eckert, J. J., Houghton, F. D., Picton, H. M., Leese, H. J., & Fleming, T. P. 2003. Gene expression regulating epithelial intercellular junction biogenesis during human blastocyst development in vitro. *Mol Hum Reprod*, **9**(5), 245–52.

Gilligan, T., Schimmel, T., Esposito, B., & Cohen, J. 1997. Release of volatile organic compounds such as styrene by sterile petri dishes and flasks used for in-vitro fertilisation. *Fertil Steril*, **68 (Suppl. 1)**, S52–3.

Gonitel, R., Moffitt, H., Sathasivam, K., Woodman, B., Detloff, P. J., Faull, R. L., & Bates, G. P. 2008. DNA instability in postmitotic neurons. *Proc Natl Acad Sci U S A*, **105**(9), 3467–72.

Gorba, T., & Allsopp, T. E. 2003. Pharmacological potential of embryonic stem cells. *Pharmacol Res*, **47**(4), 269–78.

Gospodarowicz, D. 1974. Localisation of a fibroblast growth factor and its effect alone and with hydrocortisone on 3T3 cell growth. *Nature*, **249**(453), 123–7.

Goto, Y., Noda, Y., Mori, T., & Nakano, M. 1993. Increased generation of reactive oxygen species in embryos cultured in vitro. *Free Radic Biol Med*, **15**(1), 69–75.

Graham, J., Han, T., Porter, R., Levy, M., Stillman, R., & Tucker, M. J. 2000. Day 3 morphology is a poor predictor of blastocyst quality in extended culture. *Fertil Steril*, **74**(3), 495–7.

Greber, B., Lehrach, H., & Adjaye, J. 2007. Fibroblast growth factor 2 modulates transforming growth factor beta signaling in mouse embryonic fibroblasts and human ESCs (hESCs) to support hESC self-renewal. *Stem Cells*, **25**(2), 455–64.

Griveau, J. F., Grizard, G., Boucher, D., & Le Lannou, D. 1998. Influence of oxygen tension on function of isolated spermatozoa from ejaculates of oligozoospermic patients and normozoospermic fertile donors. *Hum Reprod*, **13**(11), 3108–13.

Gruen, L., & Grabel, L. 2006. Concise review: scientific and ethical roadblocks to human embryonic stem cell therapy. *Stem Cells*, **24**(10), 2162–9.

Guerin, P., El Mouatassim, S., & Menezo, Y. 2001. Oxidative stress and protection against reactive oxygen species in the pre-implantation embryo and its surroundings. *Hum Reprod Update*, **7**(2), 175–89.

Hamatani, T., Carter, M. G., Sharov, A. A., & Ko, M. S. 2004. Dynamics of global gene expression changes during mouse preimplantation development. *Dev Cell*, **6**(1), 117–31.

Hamatani, T., Ko, MSh, Yamada, M., Kuji, N., Mizusawa, Y., Shoji, M., Hada, T., Asada, H., Maruyama, T., & Yoshimura, Y. 2006. Global gene expression profiling of preimplantation embryos. *Hum Cell*, **19**(3), 98–117.

Handyside, A. H., Kontogianni, E. H., Hardy, K., & Winston, R. M. 1990. Pregnancies from biopsied human preimplantation embryos sexed by Y-specific DNA amplification. *Nature*, **344**(6268), 768–70.

Hanna, J., Wernig, M., Markoulaki, S., Sun, C. W., Meissner, A., Cassady, J. P., Beard, C., Brambrink, T., Wu, L. C., Townes, T. M., & Jaenisch, R. 2007. Treatment of sickle cell anemia mouse model with iPS cells generated from autologous skin. *Science*, **318**(5858), 1920–3.

Hansis, C., Grifo, J. A., & Krey, L. C. 2000. Oct-4 expression in inner cell mass and trophectoderm of human blastocysts. *Mol Hum Reprod*, **6**(11), 999–1004.

Hansis, C., Tang, Y. X., Grifo, J. A., & Krey, L. C. 2001. Analysis of Oct-4 expression and ploidy in individual human blastomeres. *Mol Hum Reprod*, **7**(2), 155–61.

Hansis, C., Grifo, J. A., Tang, Y., & Krey, L. C. 2002. Assessment of beta-HCG, beta-LH mRNA and ploidy in individual human blastomeres. *Reprod Biomed Online*, **5**(2), 156–61.

Hansis, C., Grifo, J. A., & Krey, L. C. 2004. Candidate lineage marker genes in human preimplantation embryos. *Reprod Biomed Online*, **8**(5), 577–83.

Hanson, C., & Caisander, G. 2005. Human embryonic stem cells and chromosome stability. *Apmis*, **113**(11-12), 751–5.

Hardarson, T., Caisander, G., Sjogren, A., Hanson, C., Hamberger, L., & Lundin, K. 2003. A morphological and chromosomal study of blastocysts developing from morphologically suboptimal human pre-embryos compared with control blastocysts. *Hum Reprod*, **18**(2), 399–407.

Hardy, K. 1999. Apoptosis in the human embryo. *Rev Reprod*, **4**(3), 125–34.

Harris, S. E., Gopichandran, N., Picton, H. M., Leese, H. J., & Orsi, N. M. 2005. Nutrient concentrations in murine follicular fluid and the female reproductive tract. *Theriogenology*, **64**(4), 992–1006.

Harvey, A. J., Kind, K. L., Pantaleon, M., Armstrong, D. T., & Thompson, J. G. 2004. Oxygen-regulated gene expression in bovine blastocysts. *Biol Reprod*, **71**(4), 1108–19.

Harvey, A. J., Navarrete Santos, A., Kirstein, M., Kind, K. L., Fischer, B., & Thompson, J. G. 2007a. Differential expression of oxygen-regulated genes in bovine blastocysts. *Mol Reprod Dev*, **74**(3), 290–9.

Harvey, A. J., Kind, K. L., & Thompson, J. G. 2007b. Regulation of gene expression in bovine blastocysts in response to oxygen and the iron chelator desferrioxamine. *Biol Reprod*, **77**(1), 93–101.

Harvey, M. B., Arcellana-Panlilio, M. Y., Zhang, X., Schultz, G. A., & Watson, A. J. 1995. Expression of genes encoding antioxidant enzymes in preimplantation mouse and cow embryos and primary bovine oviduct cultures employed for embryo coculture. *Biol Reprod*, **53**(3), 532–40.

Hassell, T., Gleave, S., & Butler, M. 1991. Growth inhibition in animal cell culture. The effect of lactate and ammonia. *Appl Biochem Biotechnol*, **30**(1), 29–41.

Heins, N., Englund, M. C., Sjoblom, C., Dahl, U., Tonning, A., Bergh, C., Lindahl, A., Hanson, C., & Semb, H. 2004. Derivation, characterization, and differentiation of human embryonic stem cells. *Stem Cells*, **22**(3), 367–76.

Heiser, V., Engemann, S., Brocker, W., Dunkel, I., Boeddrich, A., Waelter, S., Nordhoff, E., Lurz, R., Schugardt, N., Rautenberg, S., Herhaus, C., Barnickel, G., Bottcher, H., Lehrach, H., & Wanker, E. E. 2002. Identification of benzothiazoles as potential polyglutamine aggregation inhibitors of Huntington's disease by using an automated filter retardation assay. *Proc Natl Acad Sci U S A*, **99 Suppl 4**, 16400–6.

Herszfeld, D., Wolvetang, E., Langton-Bunker, E., Chung, T. L., Filipczyk, A. A., Houssami, S., Jamshidi, P., Koh, K., Laslett, A. L., Michalska, A., Nguyen, L., Reubinoff, B. E., Tellis, I., Auerbach, J. M., Ording, C. J., Looijenga, L. H., & Pera, M. F. 2006. CD30 is a survival factor and a biomarker for transformed human pluripotent stem cells. *Nat Biotechnol*, **24**(3), 351–7.

Hewitson, L. C., & Leese, H. J. 1993. Energy metabolism of the trophectoderm and inner cell mass of the mouse blastocyst. *J Exp Zool*, **267**(3), 337–43.

Hewitt, Z. A., Amps, K. J., & Moore, H. D. 2007. Derivation of GMP raw materials for use in regenerative medicine: hESC-based therapies, progress toward clinical application. *Clin Pharmacol Ther*, **82**(4), 448–52.

Hiiragi, T., & Solter, D. 2004. First cleavage plane of the mouse egg is not predetermined but defined by the topology of the two apposing pronuclei. *Nature*, **430**(6997), 360–4.

Hiiragi, T., Alarcon, V. B., Fujimori, T., Louvet-Vallee, S., Maleszewski, M., Marikawa, Y., Maro, B., & Solter, D. 2006. Where do we stand now? Mouse early embryo patterning meeting in Freiburg, Germany (2005). *Int J Dev Biol*, **50**(7), 581–6.

Hoffman, R. M. 2006. The pluripotency of hair follicle stem cells. *Cell Cycle*, **5**(3), 232–3.

Hogan, B., & Tilly, R. 1977. In vitro culture and differentiation on normal mouse blastocysts. *Nature*, **265**(5595), 626–9.

Hollands, P. 1987. Differentiation and grafting of haemopoietic stem cells from early postimplantation mouse embryos. *Development*, **99**(1), 69–76.

Hong, S., Kang, U. J., Isacson, O., & Kim, K. S. 2008. Neural precursors derived from human embryonic stem cells maintain long-term proliferation without losing the potential to differentiate into all three neural lineages, including dopaminergic neurons. *J Neurochem*, **104**(2), 316–24.

Houghton, F. D., Hawkhead, J. A., Humpherson, P. G., Hogg, J. E., Balen, A. H., Rutherford, A. J., & Leese, H. J. 2002. Non-invasive amino acid turnover predicts human embryo developmental capacity. *Hum Reprod*, **17**(4), 999–1005.

Hovatta, O., Mikkola, M., Gertow, K., Stromberg, A. M., Inzunza, J., Hreinsson, J., Rozell, B., Blennow, E., Andang, M., & Ahrlund-Richter, L. 2003. A culture system using human foreskin fibroblasts as feeder cells allows production of human embryonic stem cells. *Hum Reprod*, **18**(7), 1404–9.

Hu, Y., Maxson, W., Hoffman, D., Ory, S., Eager, S., Dupre, J., & Worrilow, K. 1998. Co-culture with assisted hatching of human embryos using Buffalo rat liver cells. *Hum Reprod*, **13**(1), 165–8.

Huntington, G. 1872. On chorea. *Med. surg. Reporter*, **26**, 317–321.

Huntriss, J., Hinkins, M., Oliver, B., Harris, S. E., Beazley, J. C., Rutherford, A. J., Gosden, R. G., Lanzendorf, S. E., & Picton, H. M. 2004. Expression of mRNAs for DNA methyltransferases and methyl-CpG-binding proteins in the human female germ line, preimplantation embryos, and embryonic stem cells. *Mol Reprod Dev*, **67**(3), 323–36.

Hyafil, F., Babinet, C., & Jacob, F. 1981. Cell-cell interactions in early embryogenesis: a molecular approach to the role of calcium. *Cell*, **26**(3 Pt 1), 447–54.

Hyslop, L., Stojkovic, M., Armstrong, L., Walter, T., Stojkovic, P., Przyborski, S., Herbert, M., Murdoch, A., Strachan, T., & Lako, M. 2005. Downregulation of NANOG induces differentiation of human embryonic stem cells to extraembryonic lineages. *Stem Cells*, **23**(8), 1035–43.

Iliopoulos, D., Vassiliou, G., Sekerli, E., Sidiropoulou, V., Tsiga, A., Dimopoulou, D., & Voyiatzis, N. 2005. Long survival in a 69,XXX triploid infant in Greece. *Genet Mol Res*, **4**(4), 755–9.

Illmensee, K., Kaskar, K., & Zavos, P. M. 2006. In-vitro developmental potential of individual mouse blastomeres cultured with and without zona pellucida: future implications for human assisted reproduction. *Reprod Biomed Online*, **13**(2), 284–94.

Inzunza, J., Gertow, K., Stromberg, M. A., Matilainen, E., Blennow, E., Skottman, H., Wolbank, S., Ahrlund-Richter, L., & Hovatta, O. 2005. Derivation of human embryonic stem cell lines in serum replacement medium using postnatal human fibroblasts as feeder cells. *Stem Cells*, **23**(4), 544–9.

Iwasaki, A., & Gagnon, C. 1992. Formation of reactive oxygen species in spermatozoa of infertile patients. *Fertil Steril*, **57**(2), 409–16.

Jeong, Y. J., Choi, H. W., Shin, H. S., Cui, X. S., Kim, N. H., Gerton, G. L., & Jun, J. H. 2005. Optimization of real time RT-PCR methods for the analysis of gene expression in mouse eggs and preimplantation embryos. *Mol Reprod Dev*, **71**(3), 284–9.

Jeyendran, R. S., Van der Ven, H. H., & Zaneveld, L. J. 1992. The hypoosmotic swelling test: an update. *Arch Androl*, **29**(2), 105–16.

Joannides, A., Fiore-Heriche, C., Westmore, K., Caldwell, M., Compston, A., Allen, N., & Chandran, S. 2006. Automated mechanical passaging: a novel and efficient method for human embryonic stem cell expansion. *Stem Cells*, **24**(2), 230–5.

Joannides, A. J., Fiore-Heriche, C., Battersby, A. A., Athauda-Arachchi, P., Bouhon, I. A., Williams, L., Westmore, K., Kemp, P. J., Compston, A., Allen, N. D., & Chandran, S. 2007. A scaleable and defined system for generating neural stem cells from human embryonic stem cells. *Stem Cells*, **25**(3), 731–7.

Johnson, M. H. 2003. So what exactly is the role of the spermatozoon in first cleavage? *Reprod Biomed Online*, **6**(2), 163–7.

Johnson, M. H. 2008. Human ES cells and a blastocyst from one embryo: exciting science but conflicting ethics? *Cell Stem Cell*, **2**(2), 103–4.

Johnson, M. H., & Day, M. L. 2000. Egg timers: how is developmental time measured in the early vertebrate embryo? *Bioessays*, **22**(1), 57–63.

Johnson, M. H., & Nasr-Esfahani, M. H. 1994. Radical solutions and cultural problems: could free oxygen radicals be responsible for the impaired development of preimplantation mammalian embryos in vitro? *Bioessays*, **16**(1), 31–8.

Johnson, M. H., & Ziomek, C. A. 1981a. The foundation of two distinct cell lineages within the mouse morula. *Cell*, **24**(1), 71–80.

Johnson, M. H., & Ziomek, C. A. 1981b. Induction of polarity in mouse 8-cell blastomeres: specificity, geometry, and stability. *J Cell Biol*, **91**(1), 303–8.

Johnson, M. H., Maro, B., & Takeichi, M. 1986. The role of cell adhesion in the synchronization and orientation of polarization in 8-cell mouse blastomeres. *J Embryol Exp Morphol*, **93**, 239–55.

Johnson, W. H., Loskutoff, N. M., Plante, Y., & Betteridge, K. J. 1995. Production of four identical calves by the separation of blastomeres from an in vitro derived four-cell embryo. *Vet Rec*, **137**(1), 15–6.

Jones, G. M., Trounson, A. O., Gardner, D. K., Kausche, A., Lolatgis, N., & Wood, C. 1998. Evolution of a culture protocol for successful blastocyst development and pregnancy. *Hum Reprod*, **13**(1), 169–77.

Jones, K. T. 2005. Mammalian egg activation: from Ca2+ spiking to cell cycle progression. *Reproduction*, **130**(6), 813–23.

Kanatsu-Shinohara, M., Miki, H., Inoue, K., Ogonuki, N., Toyokuni, S., Ogura, A., & Shinohara, T. 2005. Germline niche transplantation restores fertility in infertile mice. *Hum Reprod*, **20**(9), 2376–82.

Kaneko, Y., Sakakibara, S., Imai, T., Suzuki, A., Nakamura, Y., Sawamoto, K., Ogawa, Y., Toyama, Y., Miyata, T., & Okano, H. 2000. Musashi1: an evolutionally conserved marker for CNS progenitor cells including neural stem cells. *Dev Neurosci*, **22**(1-2), 139–53.

Karagenc, L., Sertkaya, Z., Ciray, N., Ulug, U., & Bahceci, M. 2004. Impact of oxygen concentration on embryonic development of mouse zygotes. *Reprod Biomed Online*, **9**(4), 409–17.

Kawasaki, H., Mizuseki, K., Nishikawa, S., Kaneko, S., Kuwana, Y., Nakanishi, S., Nishikawa, S. I., & Sasai, Y. 2000. Induction of midbrain dopaminergic neurons from ES cells by stromal cell-derived inducing activity. *Neuron*, **28**(1), 31–40.

Kehoe, P., Krawczak, M., Harper, P. S., Owen, M. J., & Jones, A. L. 1999. Age of onset in Huntington disease: sex specific influence of apolipoprotein E genotype and normal CAG repeat length. *J Med Genet*, **36**(2), 108–11.

Kennedy, L., & Shelbourne, P. F. 2000. Dramatic mutation instability in HD mouse striatum: does polyglutamine load contribute to cell-specific vulnerability in Huntington's disease? *Hum Mol Genet*, **9**(17), 2539–44.

Keski-Oja, J., Lehto, V. P., & Virtanen, I. 1981. Keratin filaments of mouse epithelial cells are rapidly affected by epidermal growth factor. *J Cell Biol*, **90**(2), 537–41.

Khalaf, Y., Taylor, A., & Braude, P. 2000. Low serum estradiol concentrations after five days of controlled ovarian hyperstimulation for in vitro fertilization are associated with poor outcome. *Fertil Steril*, **74**(1), 63–6.

Khalaf, Y., El-Toukhy, T., Coomarasamy, A., Kamal, A., Bolton, V., & Braude, P. 2008. Selective single blastocyst transfer reduces the multiple pregnancy rate and increases pregnancy rates: a pre- and postintervention study. *BJOG*, **115**(3), 385–90.

Kim, H. S., Oh, S. K., Park, Y. B., Ahn, H. J., Sung, K. C., Kang, M. J., Lee, L. A., Suh, C. S., Kim, S. H., Kim, D. W., & Moon, S. Y. 2005. Methods for derivation of human embryonic stem cells. *Stem Cells*, **23**(9), 1228–33.

Kim, J. H., Panchision, D., Kittappa, R., & McKay, R. 2003. Generating CNS neurons from embryonic, fetal, and adult stem cells. *Methods Enzymol*, **365**, 303–27.

Kimber, S. J., Sneddon, S. F., Bloor, D. J., El-Bareg, A. M., Hawkhead, J. A., Metcalfe, A. D., Houghton, F. D., Leese, H. J., Rutherford, A., Lieberman, B. A., & Brison, D. R. 2008. Expression of genes involved in early cell fate decisions in human embryos and their regulation by growth factors. *Reproduction*, **135**(5), 635–47.

Kind, K. L., Collett, R. A., Harvey, A. J., & Thompson, J. G. 2004. Oxygen-regulated expression of GLUT-1, GLUT-3, and VEGF in the mouse blastocyst. *Mol Reprod Dev*, **70**(1), 37–44.

Kirschenbaum, B., & Goldman, S. A. 1995. Brain-derived neurotrophic factor promotes the survival of neurons arising from the adult rat forebrain subependymal zone. *Proc Natl Acad Sci U S A*, **92**(1), 210–4.

Klassen, H., Schwartz, M. R., Bailey, A. H., & Young, M. J. 2001. Surface markers expressed by multipotent human and mouse neural progenitor cells include tetraspanins and non-protein epitopes. *Neurosci Lett*, **312**(3), 180–2.

Kleinsmith, L. J., & Pierce, G. B., Jr. 1964. Multipotentiality of Single Embryonal Carcinoma Cells. *Cancer Res*, **24**, 1544–51.

Klimanskaya, I., Chung, Y., Meisner, L., Johnson, J., West, M. D., & Lanza, R. 2005. Human embryonic stem cells derived without feeder cells. *Lancet*, **365**(9471), 1636–41.

Klimanskaya, I., Chung, Y., Becker, S., Lu, S. J., & Lanza, R. 2006. Human embryonic stem cell lines derived from single blastomeres. *Nature*, **444**(7118), 481–5.

Koivisto, H., Hyvarinen, M., Stromberg, A. M., Inzunza, J., Matilainen, E., Mikkola, M., Hovatta, O., & Teerijoki, H. 2004. Cultures of human embryonic stem cells: serum replacement medium or serum-containing media and the effect of basic fibroblast growth factor. *Reprod Biomed Online*, **9**(3), 330–7.

Koizumi, N. J., Inatomi, T. J., Sotozono, C. J., Fullwood, N. J., Quantock, A. J., & Kinoshita, S. 2000. Growth factor mRNA and protein in preserved human amniotic membrane. *Curr Eye Res*, **20**(3), 173–7.

Kojima, K., Kanzaki, H., Iwai, M., Hatayama, H., Fujimoto, M., Inoue, T., Horie, K., Nakayama, H., Fujita, J., & Mori, T. 1994. Expression of leukemia inhibitory factor in human endometrium and placenta. *Biol Reprod*, **50**(4), 882–7.

Koong, A. C., Chen, E. Y., & Giaccia, A. J. 1994. Hypoxia causes the activation of nuclear factor kappa B through the phosphorylation of I kappa B alpha on tyrosine residues. *Cancer Res*, **54**(6), 1425–30.

Kordower, J. H., Freeman, T. B., Snow, B. J., Vingerhoets, F. J., Mufson, E. J., Sanberg, P. R., Hauser, R. A., Smith, D. A., Nauert, G. M., Perl, D. P., & et al. 1995. Neuropathological evidence of graft survival and striatal reinnervation after the transplantation of fetal mesencephalic tissue in a patient with Parkinson's disease. *N Engl J Med*, **332**(17), 1118–24.

Koutsourakis, M., Langeveld, A., Patient, R., Beddington, R., & Grosveld, F. 1999. The transcription factor GATA6 is essential for early extraembryonic development. *Development*, **126**(9), 723–32.

Kowaltowski, A. J., & Vercesi, A. E. 1999. Mitochondrial damage induced by conditions of oxidative stress. *Free Radic Biol Med*, **26**(3-4), 463–71.

Kueh, J., Richards, M., Ng, S. W., Chan, W. K., & Bongso, A. 2006. The search for factors in human feeders that support the derivation and propagation of human embryonic stem cells: preliminary studies using transcriptome profiling by serial analysis of gene expression. *Fertil Steril*, **85**(6), 1843–6.

Kurotaki, Y., Hatta, K., Nakao, K., Nabeshima, Y., & Fujimori, T. 2007. Blastocyst axis is specified independently of early cell lineage but aligns with the ZP shape. *Science*, **316**(5825), 719–23.

Landis, J. R., & Koch, G. G. 1977. The measurement of observer agreement for categorical data. *Biometrics*, **33**(1), 159–74.

Lane, M., & Gardner, D. K. 1992. Effect of incubation volume and embryo density on the development and viability of mouse embryos in vitro. *Hum Reprod*, **7**(4), 558–62.

Lane, M., & Gardner, D. K. 1994. Increase in postimplantation development of cultured mouse embryos by amino acids and induction of fetal retardation and exencephaly by ammonium ions. *J Reprod Fertil*, **102**(2), 305–12.

Lane, M., & Gardner, D. K. 1995. Removal of embryo-toxic ammonium from the culture medium by in situ enzymatic conversion to glutamate. *J Exp Zool*, **271**(5), 356–63.

Lane, M., & Gardner, D. K. 1997. Differential regulation of mouse embryo development and viability by amino acids. *J Reprod Fertil*, **109**(1), 153–64.

Lane, M., & Gardner, D. K. 2003. Ammonium induces aberrant blastocyst differentiation, metabolism, pH regulation, gene expression and subsequently alters fetal development in the mouse. *Biol Reprod*, **69**(4), 1109–17.

Lee, J. B., Song, J. M., Lee, J. E., Park, J. H., Kim, S. J., Kang, S. M., Kwon, J. N., Kim, M. K., Roh, S. I., & Yoon, H. S. 2004. Available human feeder cells for the maintenance of human embryonic stem cells. *Reproduction*, **128**(6), 727–35.

Lee, J. B., Lee, J. E., Park, J. H., Kim, S. J., Kim, M. K., Roh, S. I., & Yoon, H. S. 2005. Establishment and maintenance of human embryonic stem cell lines on

human feeder cells derived from uterine endometrium under serum-free condition. *Biol Reprod*, **72**(1), 42–9.

Leese, H. J. 1988. The formation and function of oviduct fluid. *J Reprod Fertil*, **82**(2), 843–56.

Leese, H. J. 2002. Quiet please, do not disturb: a hypothesis of embryo metabolism and viability. *Bioessays*, **24**(9), 845–9.

Leese, H. J. 2003. What does an embryo need? *Hum Fertil (Camb)*, **6**(4), 180–5.

Leese, H. J., & Barton, A. M. 1984. Pyruvate and glucose uptake by mouse ova and preimplantation embryos. *J Reprod Fertil*, **72**(1), 9–13.

Leese, H. J., Conaghan, J., Martin, K. L., & Hardy, K. 1993. Early human embryo metabolism. *Bioessays*, **15**(4), 259–64.

Leese, H. J., Sturmey, R. G., Baumann, C. G., & McEvoy, T. G. 2007. Embryo viability and metabolism: obeying the quiet rules. *Hum Reprod*, **22**(12), 3047–50.

Lerou, P. H., Yabuuchi, A., Huo, H., Takeuchi, A., Shea, J., Cimini, T., Ince, T. A., Ginsburg, E., Racowsky, C., & Daley, G. Q. 2008. Human embryonic stem cell derivation from poor-quality embryos. *Nat Biotechnol*, **26**(2), 212–4.

Levenstein, M. E., Ludwig, T. E., Xu, R. H., Llanas, R. A., VanDenHeuvel-Kramer, K., Manning, D., & Thomson, J. A. 2006. Basic fibroblast growth factor support of human embryonic stem cell self-renewal. *Stem Cells*, **24**(3), 568–74.

Levenstein, M. E., Berggren, W. T., Lee, J. E., Conard, K. R., Llanas, R. A., Wagner, R. J., Smith, L. M., & Thomson, J. A. 2008. Secreted proteoglycans directly mediate human embryonic stem cell-basic fibroblast growth factor 2 interactions critical for proliferation. *Stem Cells*, **26**(12), 3099–107.

Lievens, J. C., Woodman, B., Mahal, A., Spasic-Boscovic, O., Samuel, D., Kerkerian-Le Goff, L., & Bates, G. P. 2001. Impaired glutamate uptake in the R6 Huntington's disease transgenic mice. *Neurobiol Dis*, **8**(5), 807–21.

Limb, G. A., & Daniels, J. T. 2008. Ocular regeneration by stem cells: present status and future prospects. *Br Med Bull*, **85**, 47–61.

Lippman, M. E. 2000. High-dose chemotherapy plus autologous bone marrow transplantation for metastatic breast cancer. *N Engl J Med*, **342**(15), 1119–20.

Llewelyn, C. A., Hewitt, P. E., Knight, R. S., Amar, K., Cousens, S., Mackenzie, J., & Will, R. G. 2004. Possible transmission of variant Creutzfeldt-Jakob disease by blood transfusion. *Lancet*, **363**(9407), 417–21.

Lonergan, T., Brenner, C., & Bavister, B. 2006. Differentiation-related changes in mitochondrial properties as indicators of stem cell competence. *J Cell Physiol*, **208**(1), 149–53.

Lonergan, T., Bavister, B., & Brenner, C. 2007. Mitochondria in stem cells. *Mitochondrion*, **7**(5), 289–96.

Lorincz, M. T., Detloff, P. J., Albin, R. L., & O'Shea, K. S. 2004. Embryonic stem cells expressing expanded CAG repeats undergo aberrant neuronal differentiation and have persistent Oct-4 and REST/NRSF expression. *Mol Cell Neurosci*, **26**(1), 135–43.

Lorthongpanich, C., Yang, S. H., Piotrowska-Nitsche, K., Parnpai, R., & Chan, A. W. 2008. Development of single mouse blastomeres into blastocysts, outgrowths and the establishment of embryonic stem cells. *Reproduction*, **135**(6), 805–13.

Lovell-Badge, R. 2001. The future for stem cell research. *Nature*, **414**(6859), 88–91.

Lowit, A., & van Teijlingen, E. R. 2005. Avoidance as a strategy of (not) coping: qualitative interviews with carers of Huntington's Disease patients. *BMC Fam Pract*, **6**, 38.

Ludwig, T. E., Levenstein, M. E., Jones, J. M., Berggren, W. T., Mitchen, E. R., Frane, J. L., Crandall, L. J., Daigh, C. A., Conard, K. R., Piekarczyk, M. S., Llanas, R. A., & Thomson, J. A. 2006. Derivation of human embryonic stem cells in defined conditions. *Nat Biotechnol*, **24**(2), 185–7.

Lundin, K., Bergh, C., & Hardarson, T. 2001. Early embryo cleavage is a strong indicator of embryo quality in human IVF. *Hum Reprod*, **16**(12), 2652–7.

Luthi-Carter, R., Strand, A., Peters, N. L., Solano, S. M., Hollingsworth, Z. R., Menon, A. S., Frey, A. S., Spektor, B. S., Penney, E. B., Schilling, G., Ross, C. A., Borchelt, D. R., Tapscott, S. J., Young, A. B., Cha, J. H., & Olson, J. M. 2000. Decreased expression of striatal signaling genes in a mouse model of Huntington's disease. *Hum Mol Genet*, **9**(9), 1259–71.

Lysdahl, H., Gabrielsen, A., Minger, S. L., Patel, M. J., Fink, T., Petersen, K., Ebbesen, P., & Zachar, V. 2006. Derivation and characterization of four new human embryonic stem cell lines: the Danish experience. *Reprod Biomed Online*, **12**(1), 119–26.

Macchiarini, P., Jungebluth, P., Go, T., Asnaghi, M. A., Rees, L. E., Cogan, T. A., Dodson, A., Martorell, J., Bellini, S., Parnigotto, P. P., Dickinson, S. C., Hollander, A. P., Mantero, S., Conconi, M. T., & Birchall, M. A. 2008. Clinical transplantation of a tissue-engineered airway. *Lancet*, **372**(9655), 2023–30.

MacDonald, M. E., Barnes, G., Srinidhi, J., Duyao, M. P., Ambrose, C. M., Myers, R. H., Gray, J., Conneally, P. M., Young, A., Penney, J., & et al. 1993. Gametic but not somatic instability of CAG repeat length in Huntington's disease. *J Med Genet*, **30**(12), 982–6.

Mackie Ogilvie, C., & Scriven, P. N. 2004. Preimplantation genetic diagnosis (PGD) for reciprocal translocations. *Prenat Diagn*, **24**(7), 553–5.

Maher, E. R., Afnan, M., & Barratt, C. L. 2003. Epigenetic risks related to assisted reproductive technologies: epigenetics, imprinting, ART and icebergs? *Hum Reprod*, **18**(12), 2508–11.

Mallon, B. S., Park, K. Y., Chen, K. G., Hamilton, R. S., & McKay, R. D. 2006. Toward xeno-free culture of human embryonic stem cells. *Int J Biochem Cell Biol*, **38**(7), 1063–75.

Mamo, S., Gal, A. B., Bodo, S., & Dinnyes, A. 2007. Quantitative evaluation and selection of reference genes in mouse oocytes and embryos cultured in vivo and in vitro. *BMC Dev Biol*, **7**, 14.

Mangiarini, L., Sathasivam, K., Seller, M., Cozens, B., Harper, A., Hetherington, C., Lawton, M., Trottier, Y., Lehrach, H., Davies, S. W., & Bates, G. P. 1996. Exon 1 of the HD gene with an expanded CAG repeat is sufficient to cause a progressive neurological phenotype in transgenic mice. *Cell*, **87**(3), 493–506.

Mangiarini, L., Sathasivam, K., Mahal, A., Mott, R., Seller, M., & Bates, G. P. 1997. Instability of highly expanded CAG repeats in mice transgenic for the Huntington's disease mutation. *Nat Genet*, **15**(2), 197–200.

Manley, K., Shirley, T. L., Flaherty, L., & Messer, A. 1999. Msh2 deficiency prevents in vivo somatic instability of the CAG repeat in Huntington disease transgenic mice. *Nat Genet*, **23**(4), 471–3.

Mann, K., Donaghue, C., Fox, S. P., Docherty, Z., & Ogilvie, C. M. 2004. Strategies for the rapid prenatal diagnosis of chromosome aneuploidy. *Eur J Hum Genet*, **12**(11), 907–15.

Maragakis, N. J., & Rothstein, J. D. 2001. Glutamate transporters in neurologic disease. *Arch Neurol*, **58**(3), 365–70.

Maro, B., Johnson, M. H., Pickering, S. J., & Louvard, D. 1985. Changes in the distribution of membranous organelles during mouse early development. *J Embryol Exp Morphol*, **90**, 287–309.

Martin, G. R. 1981. Isolation of a pluripotent cell line from early mouse embryos cultured in medium conditioned by teratocarcinoma stem cells. *Proc Natl Acad Sci U S A*, **78**(12), 7634–8.

Martin, G. R., & Evans, M. J. 1975. Differentiation of clonal lines of teratocarcinoma cells: formation of embryoid bodies in vitro. *Proc Natl Acad Sci U S A*, **72**(4), 1441–5.

Martin, J. B., & Gusella, J. F. 1986. Huntington's disease. Pathogenesis and management. *N Engl J Med*, **315**(20), 1267–76.

Martin, M. J., Muotri, A., Gage, F., & Varki, A. 2005. Human embryonic stem cells express an immunogenic nonhuman sialic acid. *Nat Med*, **11**(2), 228–32.

Massip, A., Mulnard, J., Vanderzwalmen, P., Hanzen, C., & Ectors, F. 1982. The behaviour of cow blastocyst in vitro: cinematographic and morphometric analysis. *J Anat*, **134**(Pt 2), 399–405.

Masui, S., Ohtsuka, S., Yagi, R., Takahashi, K., Ko, M. S., & Niwa, H. 2008. Rex1/Zfp42 is dispensable for pluripotency in mouse ES cells. *BMC Dev Biol*, **8**, 45–51.

Mateizel, I., De Temmerman, N., Ullmann, U., Cauffman, G., Sermon, K., Van de Velde, H., De Rycke, M., Degreef, E., Devroey, P., Liebaers, I., & Van Steirteghem, A. 2006. Derivation of human embryonic stem cell lines from embryos obtained after IVF and after PGD for monogenic disorders. *Hum Reprod*, **21**(2), 503–11.

Matsui, Y., Toksoz, D., Nishikawa, S., Nishikawa, S., Williams, D., Zsebo, K., & Hogan, B. L. 1991. Effect of Steel factor and leukaemia inhibitory factor on murine primordial germ cells in culture. *Nature*, **353**(6346), 750–2.

Matsumoto, K., Miyake, M., Utsumi, K., & Iritani, A. 1989. Production of identical twins by separating two-cell rat embryos. *Gamete Res*, **22**(3), 257–63.

Maynard, S., Swistowska, A. M., Lee, J. W., Liu, Y., Liu, S. T., Da Cruz, A. B., Rao, M., de Souza-Pinto, N. C., Zeng, X., & Bohr, V. A. 2008. Human embryonic stem cells have enhanced repair of multiple forms of DNA damage. *Stem Cells*, **26**(9), 2266–74.

McNeish, J. D. 2007. Stem cells as screening tools in drug discovery. *Curr Opin Pharmacol*, **7**(5), 515–20.

Meissner, A., & Jaenisch, R. 2006. Generation of nuclear transfer-derived pluripotent ES cells from cloned Cdx2-deficient blastocysts. *Nature*, **439**(7073), 212–5.

Menalled, L. B., & Chesselet, M. F. 2002. Mouse models of Huntington's disease. *Trends Pharmacol Sci*, **23**(1), 32–9.

Menezo, Y. J., Sakkas, D., & Janny, L. 1995. Co-culture of the early human embryo: factors affecting human blastocyst formation in vitro. *Microsc Res Tech*, **32**(1), 50–6.

Meng, G., Liu, S., Krawetz, R., Chan, M., Chernos, J., & Rancourt, D. E. 2008. A novel method for generating xeno-free human feeder cells for human embryonic stem cell culture. *Stem Cells Dev*, **17**(3), 413–22.

Meng, X. T., Chen, D., Dong, Z. Y., & Liu, J. M. 2007. Enhanced neural differentiation of neural stem cells and neurite growth by amniotic epithelial cell co-culture. *Cell Biol Int*, **31**(7), 691–8.

Mertes, H., Pennings, G., & Van Steirteghem, A. 2006. An ethical analysis of alternative methods to obtain pluripotent stem cells without destroying embryos. *Hum Reprod*, **21**(11), 2749–55.

Miki, T., Lehmann, T., Cai, H., Stolz, D. B., & Strom, S. C. 2005. Stem cell characteristics of amniotic epithelial cells. *Stem Cells*, **23**(10), 1549–59.

Miki, T., Mitamura, K., Ross, M. A., Stolz, D. B., & Strom, S. C. 2007. Identification of stem cell marker-positive cells by immunofluorescence in term human amnion. *J Reprod Immunol*, **75**(2), 91–6.

Miller, J. G., & Schultz, G. A. 1987. Amino acid content of preimplantation rabbit embryos and fluids of the reproductive tract. *Biol Reprod*, **36**(1), 125–9.

Mitalipov, S. M., Yeoman, R. R., Kuo, H. C., & Wolf, D. P. 2002. Monozygotic twinning in rhesus monkeys by manipulation of in vitro-derived embryos. *Biol Reprod*, **66**(5), 1449–55.

Mitalipov, S. M., Kuo, H. C., Hennebold, J. D., & Wolf, D. P. 2003. Oct-4 expression in pluripotent cells of the rhesus monkey. *Biol Reprod*, **69**(6), 1785–92.

Mitalipova, M., Calhoun, J., Shin, S., Wininger, D., Schulz, T., Noggle, S., Venable, A., Lyons, I., Robins, A., & Stice, S. 2003. Human embryonic stem cell lines derived from discarded embryos. *Stem Cells*, **21**(5), 521–6.

Mitalipova, M. M., Rao, R. R., Hoyer, D. M., Johnson, J. A., Meisner, L. F., Jones, K. L., Dalton, S., & Stice, S. L. 2005. Preserving the genetic integrity of human embryonic stem cells. *Nat Biotechnol*, **23**(1), 19–20.

Miyamoto, K., Hayashi, K., Suzuki, T., Ichihara, S., Yamada, T., Kano, Y., Yamabe, T., & Ito, Y. 2004. Human placenta feeder layers support undifferentiated growth of primate embryonic stem cells. *Stem Cells*, **22**(4), 433–40.

Moley, K. H., & Mueckler, M. M. 2000. Glucose transport and apoptosis. *Apoptosis*, **5**(2), 99–105.

Moricard, R. 1950. Penetration of the spermatozoon in vitro into the mammalian ovum oxydo potential level. *Nature*, **165**(4202), 763.

Motosugi, N., Bauer, T., Polanski, Z., Solter, D., & Hiiragi, T. 2005. Polarity of the mouse embryo is established at blastocyst and is not prepatterned. *Genes Dev*, **19**(9), 1081–92.

Muggleton-Harris, A. L., & Brown, J. J. 1988. Cytoplasmic factors influence mitochondrial reorganization and resumption of cleavage during culture of early mouse embryos. *Hum Reprod*, **3**(8), 1020–8.

Muller, U., Weber, J. L., Berry, P., & Kupke, K. G. 1993. Second polar body incorporation into a blastomere results in 46,XX/69,XXX mixoploidy. *J Med Genet*, **30**(7), 597–600.

Munne, S. 2006. Chromosome abnormalities and their relationship to morphology and development of human embryos. *Reprod Biomed Online*, **12**(2), 234–53.

Nagao, Y., Saeki, K., Hoshi, M., & Kainuma, H. 1994. Effects of oxygen concentration and oviductal epithelial tissue on the development of in vitro matured and fertilized bovine oocytes cultured in protein-free medium. *Theriogenology*, **41**(3), 681–7.

Nichols, J., Evans, E. P., & Smith, A. G. 1990. Establishment of germ-line-competent embryonic stem (ES) cells using differentiation inhibiting activity. *Development*, **110**(4), 1341–8.

Nichols, J., Zevnik, B., Anastassiadis, K., Niwa, H., Klewe-Nebenius, D., Chambers, I., Scholer, H., & Smith, A. 1998. Formation of pluripotent stem cells in the mammalian embryo depends on the POU transcription factor Oct4. *Cell*, **95**(3), 379–91.

Nikas, G., Ao, A., Winston, R. M., & Handyside, A. H. 1996. Compaction and surface polarity in the human embryo in vitro. *Biol Reprod*, **55**(1), 32–7.

Niwa, H., Miyazaki, J., & Smith, A. G. 2000. Quantitative expression of Oct-3/4 defines differentiation, dedifferentiation or self-renewal of ES cells. *Nat Genet*, **24**(4), 372–6.

Niwa, H., Toyooka, Y., Shimosato, D., Strumpf, D., Takahashi, K., Yagi, R., & Rossant, J. 2005. Interaction between Oct3/4 and Cdx2 determines trophectoderm differentiation. *Cell*, **123**(5), 917–29.

Noda, Y., Matsumoto, H., Umaoka, Y., Tatsumi, K., Kishi, J., & Mori, T. 1991. Involvement of superoxide radicals in the mouse two-cell block. *Mol Reprod Dev*, **28**(4), 356–60.

Nothias, J. Y., Majumder, S., Kaneko, K. J., & DePamphilis, M. L. 1995. Regulation of gene expression at the beginning of mammalian development. *J Biol Chem*, **270**(38), 22077–80.

Ohlsson, R., Larsson, E., Nilsson, O., Wahlstrom, T., & Sundstrom, P. 1989. Blastocyst implantation precedes induction of insulin-like growth factor II gene expression in human trophoblasts. *Development*, **106**(3), 555–9.

Okita, K., Ichisaka, T., & Yamanaka, S. 2007. Generation of germline-competent induced pluripotent stem cells. *Nature*, **448**(7151), 313–7.

Orsi, N. M., & Leese, H. J. 2004. Ammonium exposure and pyruvate affect the amino acid metabolism of bovine blastocysts in vitro. *Reproduction*, **127**(1), 131–40.

Orsi, N. M., & Reischl, J. B. 2007. Mammalian embryo co-culture: trials and tribulations of a misunderstood method. *Theriogenology*, **67**(3), 441–58.

Ottosen, L. D., Hindkaer, J., Husth, M., Petersen, D. E., Kirk, J., & Ingerslev, H. J. 2006. Observations on intrauterine oxygen tension measured by fibre-optic microsensors. *Reprod Biomed Online*, **13**(3), 380–5.

Palermo, G., Joris, H., Devroey, P., & Van Steirteghem, A. C. 1992. Pregnancies after intracytoplasmic injection of single spermatozoon into an oocyte. *Lancet*, **340**(8810), 17–8.

Palmieri, S. L., Peter, W., Hess, H., & Scholer, H. R. 1994. Oct-4 transcription factor is differentially expressed in the mouse embryo during establishment of the first two extraembryonic cell lineages involved in implantation. *Dev Biol*, **166**(1), 259–67.

Papaioannou, V. E., Mkandawire, J., & Biggers, J. D. 1989. Development and phenotypic variability of genetically identical half mouse embryos. *Development*, **106**(4), 817–27.

Paria, B. C., & Dey, S. K. 1990. Preimplantation embryo development in vitro: cooperative interactions among embryos and role of growth factors. *Proc Natl Acad Sci U S A*, **87**(12), 4756–60.

Park, I. H., Zhao, R., West, J. A., Yabuuchi, A., Huo, H., Ince, T. A., Lerou, P. H., Lensch, M. W., & Daley, G. Q. 2008. Reprogramming of human somatic cells to pluripotency with defined factors. *Nature*, **451**(7175), 141–6.

Park, J. H., Kim, S. J., Oh, E. J., Moon, S. Y., Roh, S. I., Kim, C. G., & Yoon, H. S. 2003. Establishment and maintenance of human embryonic stem cells on STO, a permanently growing cell line. *Biol Reprod*, **69**(6), 2007–14.

Parolini, O., Alviano, F., Bagnara, G. P., Bilic, G., Buhring, H. J., Evangelista, M., Hennerbichler, S., Liu, B., Magatti, M., Mao, N., Miki, T., Marongiu, F., Nakajima, H., Nikaido, T., Portmann-Lanz, C. B., Sankar, V., Soncini, M., Stadler, G., Surbek, D., Takahashi, T. A., Redl, H., Sakuragawa, N., Wolbank, S., Zeisberger, S., Zisch, A., & Strom, S. C. 2008. Concise review: isolation and characterization of cells from human term placenta: outcome of the first international Workshop on Placenta Derived Stem Cells. *Stem Cells*, **26**(2), 300–11.

Paulsen, J. S., Ready, R. E., Hamilton, J. M., Mega, M. S., & Cummings, J. L. 2001. Neuropsychiatric aspects of Huntington's disease. *J Neurol Neurosurg Psychiatry*, **71**(3), 310–4.

Pearson, C. E., Ewel, A., Acharya, S., Fishel, R. A., & Sinden, R. R. 1997. Human MSH2 binds to trinucleotide repeat DNA structures associated with neurodegenerative diseases. *Hum Mol Genet*, **6**(7), 1117–23.

Pearson, H. 2003. *http://www.nature.com/news/2003/030721/full/news030721-13.html (accessed 18/11/2008).*

Pedersen, R. A., & Spindle, A. I. 1980. Role of the blastocoele microenvironment in early mouse embryo differentiation. *Nature*, **284**(5756), 550–2.

Pellegrini, G., Traverso, C. E., Franzi, A. T., Zingirian, M., Cancedda, R., & De Luca, M. 1997. Long-term restoration of damaged corneal surfaces with autologous cultivated corneal epithelium. *Lancet*, **349**(9057), 990–3.

Pera, M. F. 2004. Unnatural selection of cultured human ES cells? *Nat Biotechnol*, **22**(1), 42–3.

Perrier, A. L., Tabar, V., Barberi, T., Rubio, M. E., Bruses, J., Topf, N., Harrison, N. L., & Studer, L. 2004. Derivation of midbrain dopamine neurons from human embryonic stem cells. *Proc Natl Acad Sci U S A*, **101**(34), 12543–8.

Persichetti, F., Ambrose, C. M., Ge, P., McNeil, S. M., Srinidhi, J., Anderson, M. A., Jenkins, B., Barnes, G. T., Duyao, M. P., Kanaley, L., & et al. 1995. Normal and expanded Huntington's disease gene alleles produce distinguishable proteins due to translation across the CAG repeat. *Mol Med*, **1**(4), 374–83.

Persichetti, F., Carlee, L., Faber, P. W., McNeil, S. M., Ambrose, C. M., Srinidhi, J., Anderson, M., Barnes, G. T., Gusella, J. F., & MacDonald, M. E. 1996. Differential expression of normal and mutant Huntington's disease gene alleles. *Neurobiol Dis*, **3**(3), 183–90.

Pesce, M., & Scholer, H. R. 2001. Oct-4: gatekeeper in the beginnings of mammalian development. *Stem Cells*, **19**(4), 271–8.

Peura, T., Bosman, A., Chami, O., Jansen, R. P., Texlova, K., & Stojanov, T. 2008. Karyotypically normal and abnormal human embryonic stem cell lines derived from PGD-analyzed embryos. *Cloning Stem Cells*, **10**(2), 203–16.

Pickering, S. J., Maro, B., Johnson, M. H., & Skepper, J. N. 1988. The influence of cell contact on the division of mouse 8-cell blastomeres. *Development*, **103**(2), 353–63.

Pickering, S. J., Braude, P. R., Patel, M., Burns, C. J., Trussler, J., Bolton, V., & Minger, S. 2003. Preimplantation genetic diagnosis as a novel source of embryos for stem cell research. *Reprod Biomed Online*, **7**(3), 353–64.

Pickering, S. J., Minger, S. L., Patel, M., Taylor, H., Black, C., Burns, C. J., Ekonomou, A., & Braude, P. R. 2005. Generation of a human embryonic stem cell line encoding the cystic fibrosis mutation deltaF508, using preimplantation genetic diagnosis. *Reprod Biomed Online*, **10**(3), 390–7.

Piedrahita, J. A., Anderson, G. B., & Bondurant, R. H. 1990. On the isolation of embryonic stem cells: Comparative behavior of murine, porcine and ovine embryos. *Theriogenology*, **34**(5), 879–901.

Pincus, G. 1930. Observations on the Living Eggs of the Rabbit. *Proceedings of the Royal Society of London. Series B, Containing Papers of a Biological Character*, **107**(749), 132–167.

Piotrowska, K., & Zernicka-Goetz, M. 2001. Role for sperm in spatial patterning of the early mouse embryo. *Nature*, **409**(6819), 517–21.

Piotrowska, K., & Zernicka-Goetz, M. 2002. Early patterning of the mouse embryo–contributions of sperm and egg. *Development*, **129**(24), 5803–13.

Piotrowska-Nitsche, K., Perea-Gomez, A., Haraguchi, S., & Zernicka-Goetz, M. 2005. Four-cell stage mouse blastomeres have different developmental properties. *Development*, **132**(3), 479–90.

Pittenger, M. F., Mackay, A. M., Beck, S. C., Jaiswal, R. K., Douglas, R., Mosca, J. D., Moorman, M. A., Simonetti, D. W., Craig, S., & Marshak, D. R. 1999. Multilineage potential of adult human mesenchymal stem cells. *Science*, **284**(5411), 143–7.

Plusa, B., Piotrowska, K., & Zernicka-Goetz, M. 2002. Sperm entry position provides a surface marker for the first cleavage plane of the mouse zygote. *Genesis*, **32**(3), 193–8.

Plusa, B., Hadjantonakis, A. K., Gray, D., Piotrowska-Nitsche, K., Jedrusik, A., Papaioannou, V. E., Glover, D. M., & Zernicka-Goetz, M. 2005. The first cleavage of the mouse zygote predicts the blastocyst axis. *Nature*, **434**(7031), 391–5.

Poueymirou, W. T., & Schultz, R. M. 1987. Differential effects of activators of cAMP-dependent protein kinase and protein kinase C on cleavage of one-cell mouse embryos and protein synthesis and phosphorylation in one- and two-cell embryos. *Dev Biol*, **121**(2), 489–98.

Pouton, C. W., & Haynes, J. M. 2007. Embryonic stem cells as a source of models for drug discovery. *Nat Rev Drug Discov*, **6**(8), 605–16.

Pratt, H. P., Chakraborty, J., & Surani, M. A. 1981. Molecular and morphological differentiation of the mouse blastocyst after manipulations of compaction with cytochalasin D. *Cell*, **26**(2 Pt 2), 279–92.

Pratt, H. P., Ziomek, C. A., Reeve, W. J., & Johnson, M. H. 1982. Compaction of the mouse embryo: an analysis of its components. *J Embryol Exp Morphol*, **70**, 113–32.

Price, P., Goldsborough, M., & Tilkins, M. 1998. Embryonic stem cell serum replacement. *International Patent Application*, **WO98/30679**.

Prowse, A. B., McQuade, L. R., Bryant, K. J., Van Dyk, D. D., Tuch, B. E., & Gray, P. P. 2005. A proteome analysis of conditioned media from human neonatal fibroblasts used in the maintenance of human embryonic stem cells. *Proteomics*, **5**(4), 978–89.

Pyle, A. D., Lock, L. F., & Donovan, P. J. 2006. Neurotrophins mediate human embryonic stem cell survival. *Nat Biotechnol*, **24**(3), 344–50.

Quinn, P. 1995. Enhanced results in mouse and human embryo culture using a modified human tubal fluid medium lacking glucose and phosphate. *J Assist Reprod Genet*, **12**(2), 97–105.

Quinn, P., Lydic, M. L., Ho, M., Bastuba, M., Hendee, F., & Brody, S. A. 1998. Confirmation of the beneficial effects of brief coincubation of gametes in human in vitro fertilization. *Fertil Steril*, **69**(3), 399–402.

Quint, W. G., Fetter, W. P., van Os, H. C., & Heijtink, R. A. 1994. Absence of hepatitis B virus (HBV) DNA in children born after exposure of their mothers to HBV during in vitro fertilization. *J Clin Microbiol*, **32**(4), 1099–100.

Rajala, K., Hakala, H., Panula, S., Aivio, S., Pihlajamaki, H., Suuronen, R., Hovatta, O., & Skottman, H. 2007. Testing of nine different xeno-free culture media for human embryonic stem cell cultures. *Hum Reprod*, **22**(5), 1231–8.

Ralston, A., & Rossant, J. 2005. Genetic regulation of stem cell origins in the mouse embryo. *Clin Genet*, **68**(2), 106–12.

Reddy, P. H., Williams, M., Charles, V., Garrett, L., Pike-Buchanan, L., Whetsell, W. O., Jr., Miller, G., & Tagle, D. A. 1998. Behavioural abnormalities and selective neuronal loss in HD transgenic mice expressing mutated full-length HD cDNA. *Nat Genet*, **20**(2), 198–202.

Reik, W., Dean, W., & Walter, J. 2001. Epigenetic reprogramming in mammalian development. *Science*, **293**(5532), 1089–93.

Reitzer, L. J., Wice, B. M., & Kennell, D. 1980. The pentose cycle. Control and essential function in HeLa cell nucleic acid synthesis. *J Biol Chem*, **255**(12), 5616–26.

Renwick, P. J., Trussler, J., Ostad-Saffari, E., Fassihi, H., Black, C., Braude, P., Ogilvie, C. M., & Abbs, S. 2006. Proof of principle and first cases using preimplantation genetic haplotyping–a paradigm shift for embryo diagnosis. *Reprod Biomed Online*, **13**(1), 110–9.

Resnick, J. L., Bixler, L. S., Cheng, L., & Donovan, P. J. 1992. Long-term proliferation of mouse primordial germ cells in culture. *Nature*, **359**(6395), 550–1.

Revazova, E. S., Turovets, N. A., Kochetkova, O. D., Kindarova, L. B., Kuzmichev, L. N., Janus, J. D., & Pryzhkova, M. V. 2007. Patient-specific stem cell lines derived from human parthenogenetic blastocysts. *Cloning Stem Cells*, **9**(3), 432–49.

Reya, T., Morrison, S. J., Clarke, M. F., & Weissman, I. L. 2001. Stem cells, cancer, and cancer stem cells. *Nature*, **414**(6859), 105–11.

Richards, M., Fong, C. Y., Chan, W. K., Wong, P. C., & Bongso, A. 2002. Human feeders support prolonged undifferentiated growth of human inner cell masses and embryonic stem cells. *Nat Biotechnol*, **20**(9), 933–6.

Richards, M., Tan, S., Fong, C. Y., Biswas, A., Chan, W. K., & Bongso, A. 2003. Comparative evaluation of various human feeders for prolonged undifferentiated growth of human embryonic stem cells. *Stem Cells*, **21**(5), 546–56.

Richards, R. I., & Sutherland, G. R. 1994. Simple repeat DNA is not replicated simply. *Nat Genet*, **6**(2), 114–6.

Rifkin, D. B., & Moscatelli, D. 1989. Recent developments in the cell biology of basic fibroblast growth factor. *J Cell Biol*, **109**(1), 1–6.

Rijnders, P. M., & Jansen, C. A. 1998. The predictive value of day 3 embryo morphology regarding blastocyst formation, pregnancy and implantation rate after day 5 transfer following in-vitro fertilization or intracytoplasmic sperm injection. *Hum Reprod*, **13**(1O), 2869–73.

Rinaudo, P. F., Giritharan, G., Talbi, S., Dobson, A. T., & Schultz, R. M. 2006. Effects of oxygen tension on gene expression in preimplantation mouse embryos. *Fertil Steril*, **86**(4 Suppl), 1252–65, 1265 e1–36.

Ringner, M. 2008. What is principal component analysis? *Nat Biotechnol*, **26**(3), 303–4.

Rodda, D. J., Chew, J. L., Lim, L. H., Loh, Y. H., Wang, B., Ng, H. H., & Robson, P. 2005. Transcriptional regulation of nanog by OCT4 and SOX2. *J Biol Chem*, **280**(26), 24731–7.

Roegiers, F., McDougall, A., & Sardet, C. 1995. The sperm entry point defines the orientation of the calcium-induced contraction wave that directs the first phase of cytoplasmic reorganization in the ascidian egg. *Development*, **121**(10), 3457–66.

Rogers, M. B., Hosler, B. A., & Gudas, L. J. 1991. Specific expression of a retinoic acid-regulated, zinc-finger gene, Rex-1, in preimplantation embryos, trophoblast and spermatocytes. *Development*, **113**(3), 815–24.

Rosenbusch, B., Schneider, M., Glaser, B., & Brucker, C. 2002. Cytogenetic analysis of giant oocytes and zygotes to assess their relevance for the development of digynic triploidy. *Hum Reprod*, **17**(9), 2388–93.

Rosenbusch, B. E. 2008. Mechanisms giving rise to triploid zygotes during assisted reproduction. *Fertil Steril*, **90**(1), 49–55.

Rosner, M. H., Vigano, M. A., Ozato, K., Timmons, P. M., Poirier, F., Rigby, P. W., & Staudt, L. M. 1990. A POU-domain transcription factor in early stem cells and germ cells of the mammalian embryo. *Nature*, **345**(6277), 686–92.

Rossant, J. 1976. Postimplantation development of blastomeres isolated from 4- and 8-cell mouse eggs. *J Embryol Exp Morphol*, **36**(2), 283–90.

Ruocco, H. H., Bonilha, L., Li, L. M., Lopes-Cendes, I., & Cendes, F. 2008. Longitudinal analysis of regional grey matter loss in Huntington disease: effects of the length of the expanded CAG repeat. *J Neurol Neurosurg Psychiatry*, **79**(2), 130–5.

Saito, S., & Niemann, H. 1991. Effects of extracellular matrices and growth factors on the development of isolated porcine blastomeres. *Biol Reprod*, **44**(5), 927–36.

Santana, A., Ensenat-Waser, R., Arribas, M. I., Reig, J. A., & Roche, E. 2006. Insulin-producing cells derived from stem cells: recent progress and future directions. *J Cell Mol Med*, **10**(4), 866–83.

Saxena, S., Hanwate, M., Deb, K., Sharma, V., & Totey, S. 2008. FGF2 secreting human fibroblast feeder cells: a novel culture system for human embryonic stem cells. *Mol Reprod Dev*, **75**(10), 1523–32.

Schini, S. A., & Bavister, B. D. 1988a. Development of golden hamster embryos through the two-cell block in chemically defined medium. *J Exp Zool*, **245**(1), 111–5.

Schini, S. A., & Bavister, B. D. 1988b. Two-cell block to development of cultured hamster embryos is caused by phosphate and glucose. *Biol Reprod*, **39**(5), 1183–92.

Schuldiner, M., Yanuka, O., Itskovitz-Eldor, J., Melton, D. A., & Benvenisty, N. 2000. Effects of eight growth factors on the differentiation of cells derived from human embryonic stem cells. *Proc Natl Acad Sci U S A*, **97**(21), 11307–12.

Schultz, R. M. 2005. From egg to embryo: a peripatetic journey. *Reproduction*, **130**(6), 825–8.

Sermon, K., Goossens, V., Seneca, S., Lissens, W., De Vos, A., Vandervorst, M., Van Steirteghem, A., & Liebaers, I. 1998. Preimplantation diagnosis for Huntington's disease (HD): clinical application and analysis of the HD expansion in affected embryos. *Prenat Diagn*, **18**(13), 1427–36.

Seshagiri, P. B., & Bavister, B. D. 1991. Glucose and phosphate inhibit respiration and oxidative metabolism in cultured hamster eight-cell embryos: evidence for the 'crabtree effect'. *Mol Reprod Dev*, **30**(2), 105–11.

Shamblott, M. J., Axelman, J., Wang, S., Bugg, E. M., Littlefield, J. W., Donovan, P. J., Blumenthal, P. D., Huggins, G. R., & Gearhart, J. D. 1998. Derivation of pluripotent stem cells from cultured human primordial germ cells. *Proc Natl Acad Sci U S A*, **95**(23), 13726–31.

Sharma, N., Liu, S., Tang, L., Irwin, J., Meng, G., & Rancourt, D. E. 2006. Implantation Serine Proteinases heterodimerize and are critical in hatching and implantation. *BMC Dev Biol*, **6**, 61.

Shelbourne, P. F., Killeen, N., Hevner, R. F., Johnston, H. M., Tecott, L., Lewandoski, M., Ennis, M., Ramirez, L., Li, Z., Iannicola, C., Littman, D. R., & Myers, R. M. 1999. A Huntington's disease CAG expansion at the murine Hdh locus is unstable and associated with behavioural abnormalities in mice. *Hum Mol Genet*, **8**(5), 763–74.

Sherman, M. I. 1975. Long term culture of cells derived from mouse blastocysts. *Differentiation*, **3**(1-3), 51–67.

Sheth, B., Fesenko, I., Collins, J. E., Moran, B., Wild, A. E., Anderson, J. M., & Fleming, T. P. 1997. Tight junction assembly during mouse blastocyst formation is regulated by late expression of ZO-1 alpha+ isoform. *Development*, **124**(10), 2027–37.

Shin, J. Y., Fang, Z. H., Yu, Z. X., Wang, C. E., Li, S. H., & Li, X. J. 2005. Expression of mutant huntingtin in glial cells contributes to neuronal excitotoxicity. *J Cell Biol*, **171**(6), 1001–12.

Sibley, C., Glazier, J., & D'Souza, S. 1997. Placental transporter activity and expression in relation to fetal growth. *Exp Physiol*, **82**(2), 389–402.

Simon-Sanchez, J., Scholz, S., Fung, H. C., Matarin, M., Hernandez, D., Gibbs, J. R., Britton, A., de Vrieze, F. W., Peckham, E., Gwinn-Hardy, K., Crawley, A., Keen, J. C., Nash, J., Borgaonkar, D., Hardy, J., & Singleton, A. 2007. Genome-wide SNP assay reveals structural genomic variation, extended homozygosity and cell-line induced alterations in normal individuals. *Hum Mol Genet*, **16**(1), 1–14.

Sjogren, A., Hardarson, T., Andersson, K., Caisander, G., Lundquist, M., Wikland, M., Semb, H., & Hamberger, L. 2004. Human blastocysts for the development of embryonic stem cells. *Reprod Biomed Online*, **9**(3), 326–9.

Skottman, H., Mikkola, M., Lundin, K., Olsson, C., Stromberg, A. M., Tuuri, T., Otonkoski, T., Hovatta, O., & Lahesmaa, R. 2005. Gene expression signatures of seven individual human embryonic stem cell lines. *Stem Cells*, **23**(9), 1343–56.

Skottman, H., Dilber, M. S., & Hovatta, O. 2006a. The derivation of clinical-grade human embryonic stem cell lines. *FEBS Lett*, **580**(12), 2875–8.

Skottman, H., Stromberg, A. M., Matilainen, E., Inzunza, J., Hovatta, O., & Lahesmaa, R. 2006b. Unique gene expression signature by human embryonic stem cells cultured under serum-free conditions correlates with their enhanced and prolonged growth in an undifferentiated stage. *Stem Cells*, **24**(1), 151–67.

Smith, A. G., & Hooper, M. L. 1987. Buffalo rat liver cells produce a diffusible activity which inhibits the differentiation of murine embryonal carcinoma and embryonic stem cells. *Dev Biol*, **121**(1), 1–9.

Solter, D., & Knowles, B. B. 1975. Immunosurgery of mouse blastocyst. *Proc Natl Acad Sci U S A*, **72**(12), 5099–102.

Spradling, A., Drummond-Barbosa, D., & Kai, T. 2001. Stem cells find their niche. *Nature*, **414**(6859), 98–104.

Spurgeon, S. L., Jones, R. C., & Ramakrishnan, R. 2008. High throughput gene expression measurement with real time PCR in a microfluidic dynamic array. *PLoS ONE*, **3**(2), e1662.

Squirrell, J. M., Lane, M., & Bavister, B. D. 2001. Altering intracellular pH disrupts development and cellular organization in preimplantation hamster embryos. *Biol Reprod*, **64**(6), 1845–54.

Stacey, G. N., & Hunt, C. J. 2008. *Advances in Tissue Engineering*. Imperial College Press.

Stacey, G. N., Cobo, F., Nieto, A., Talavera, P., Healy, L., & Concha, A. 2006. The development of 'feeder' cells for the preparation of clinical grade hES cell lines: challenges and solutions. *J Biotechnol*, **125**(4), 583–8.

Staessen, C., & Van Steirteghem, A. C. 1997. The chromosomal constitution of embryos developing from abnormally fertilized oocytes after intracytoplasmic sperm injection and conventional in-vitro fertilization. *Hum Reprod*, **12**(2), 321–7.

Steinhauer, J., & Kalderon, D. 2006. Microtubule polarity and axis formation in the Drosophila oocyte. *Dev Dyn*, **235**(6), 1455–68.

Stephenson, E. L., Braude, P. R., & Mason, C. 2007. International community consensus standard for reporting derivation of human embryonic stem cell lines. *Regen Med*, **2**(4), 349–62.

Stephenson, E. L., Mason, C., & Braude, P. R. 2009. Preimplantation genetic diagnosis as a source of human embryonic stem cells for disease research and drug discovery. *BJOG*, **116**(2), 158–65.

Stephenson, E.L., Braude, P.R., & Mason, C. 2006. Proposal for a universal minimum information convention for the reporting on the derivation of human embryonic stem cell lines. *Regenerative Medicine*, **1**(6), 739–750.

Steptoe, P. C., & Edwards, R. G. 1976. Reimplantation of a human embryo with subsequent tubal pregnancy. *Lancet*, **1**(7965), 880–2.

Steptoe, P. C., & Edwards, R. G. 1978. Birth after the reimplantation of a human embryo. *Lancet*, **2**(8085), 366.

Steptoe, P. C., Edwards, R. G., & Purdy, J. M. 1971. Human blastocysts grown in culture. *Nature*, **229**(5280), 132–3.

Stojkovic, M., Lako, M., Stojkovic, P., Stewart, R., Przyborski, S., Armstrong, L., Evans, J., Herbert, M., Hyslop, L., Ahmad, S., Murdoch, A., & Strachan, T. 2004. Derivation of human embryonic stem cells from day-8 blastocysts recovered after three-step in vitro culture. *Stem Cells*, **22**(5), 790–7.

Stojkovic, P., Lako, M., Stewart, R., Przyborski, S., Armstrong, L., Evans, J., Murdoch, A., Strachan, T., & Stojkovic, M. 2005. An autogeneic feeder cell system that efficiently supports growth of undifferentiated human embryonic stem cells. *Stem Cells*, **23**(3), 306–14.

Strehlow, A. N., Li, J. Z., & Myers, R. M. 2007. Wild-type huntingtin participates in protein trafficking between the Golgi and the extracellular space. *Hum Mol Genet*, **16**(4), 391–409.

Streiffer, R. 2008. Informed consent and federal funding for stem cell research. *Hastings Cent Rep*, **38**(3), 40–7.

Streit, A., Berliner, A. J., Papanayotou, C., Sirulnik, A., & Stern, C. D. 2000. Initiation of neural induction by FGF signalling before gastrulation. *Nature*, **406**(6791), 74–8.

Strelchenko, N., Verlinsky, O., Kukharenko, V., & Verlinsky, Y. 2004. Morula-derived human embryonic stem cells. *Reprod Biomed Online*, **9**(6), 623–9.

Strickland, S., Reich, E., & Sherman, M. I. 1976. Plasminogen activator in early embryogenesis: enzyme production by trophoblast and parietal endoderm. *Cell*, **9**(2), 231–40.

Strom, S., Inzunza, J., Grinnemo, K. H., Holmberg, K., Matilainen, E., Stromberg, A. M., Blennow, E., & Hovatta, O. 2007. Mechanical isolation of the inner cell mass is effective in derivation of new human embryonic stem cell lines. *Hum Reprod*, **22**(12), 3051–8.

Summers, M. C., & Biggers, J. D. 2003. Chemically defined media and the culture of mammalian preimplantation embryos: historical perspective and current issues. *Hum Reprod Update*, **9**(6), 557–82.

Sun, X., Long, X., Yin, Y., Jiang, Y., Chen, X., Liu, W., Zhang, W., Du, H., Li, S., Zheng, Y., Kong, S., Pang, Q., Shi, Y., Huang, Y., Huang, S., Liao, B., Xiao, G., & Wang, W. 2008. Similar biological characteristics of human embryonic stem cell lines with normal and abnormal karyotypes. *Hum Reprod*, **23**(10), 2185–93.

Surani, M. A. 2001. Reprogramming of genome function through epigenetic inheritance. *Nature*, **414**(6859), 122–8.

Surani, M. A., & Barton, S. C. 1984. Spatial distribution of blastomeres is dependent on cell division order and interactions in mouse morulae. *Dev Biol*, **102**(2), 335–43.

Surani, M. A., Barton, S. C., & Burling, A. 1980. Differentiation of 2-cell and 8-cell mouse embryos arrested by cytoskeletal inhibitors. *Exp Cell Res*, **125**(2), 275–86.

Suss-Toby, E., Gerecht-Nir, S., Amit, M., Manor, D., & Itskovitz-Eldor, J. 2004. Derivation of a diploid human embryonic stem cell line from a mononuclear zygote. *Hum Reprod*, **19**(3), 670–5.

Svendsen, C. N., Fawcett, J. W., Bentlage, C., & Dunnett, S. B. 1995. Increased survival of rat EGF-generated CNS precursor cells using B27 supplemented medium. *Exp Brain Res*, **102**(3), 407–14.

Swann, K., & Yu, Y. 2008. The dynamics of calcium oscillations that activate mammalian eggs. *Int J Dev Biol*, **52**(5-6), 585–94.

Swann, K., Larman, M. G., Saunders, C. M., & Lai, F. A. 2004. The cytosolic sperm factor that triggers Ca2+ oscillations and egg activation in mammals is a novel phospholipase C: PLCzeta. *Reproduction*, **127**(4), 431–9.

Taipale, J., & Beachy, P. A. 2001. The Hedgehog and Wnt signalling pathways in cancer. *Nature*, **411**(6835), 349–54.

Takahashi, K., Okita, K., Nakagawa, M., & Yamanaka, S. 2007. Induction of pluripotent stem cells from fibroblast cultures. *Nat Protoc*, **2**(12), 3081–9.

Takahashi, M., Nagai, T., Hamano, S., Kuwayama, M., Okamura, N., & Okano, A. 1993. Effect of thiol compounds on in vitro development and intracellular glutathione content of bovine embryos. *Biol Reprod*, **49**(2), 228–32.

Tang, Y., Wang, Y., Yang, P., Liu, Y., Wang, B., Podolsky, R., McIndoe, R., & Wang, C. Y. 2006. Intergeneration CAG expansion and contraction in a Chinese HD family. *Am J Med Genet B Neuropsychiatr Genet*, **141B**(3), 242–4.

Tarkowski, A. K. 1959. Experiments on the development of isolated blastomers of mouse eggs. *Nature*, **184**, 1286–7.

Tarkowski, A. K., & Wroblewska, J. 1967. Development of blastomeres of mouse eggs isolated at the 4- and 8-cell stage. *J Embryol Exp Morphol*, **18**(1), 155–80.

Tay, J. I., Rutherford, A. J., Killick, S. R., Maguiness, S. D., Partridge, R. J., & Leese, H. J. 1997. Human tubal fluid: production, nutrient composition and response to adrenergic agents. *Hum Reprod*, **12**(11), 2451–6.

Taylor, D. M., Handyside, A. H., Ray, P. F., Dibb, N. J., Winston, R. M., & Ao, A. 2001. Quantitative measurement of transcript levels throughout human preimplantation development: analysis of hypoxanthine phosphoribosyl transferase. *Mol Hum Reprod*, **7**(2), 147–54.

Telenius, H., Kremer, B., Goldberg, Y. P., Theilmann, J., Andrew, S. E., Zeisler, J., Adam, S., Greenberg, C., Ives, E. J., Clarke, L. A., & et al. 1994. Somatic and gonadal mosaicism of the Huntington disease gene CAG repeat in brain and sperm. *Nat Genet*, **6**(4), 409–14.

Temple, S. 2001. The development of neural stem cells. *Nature*, **414**(6859), 112–7.

Tesar, P. J., Chenoweth, J. G., Brook, F. A., Davies, T. J., Evans, E. P., Mack, D. L., Gardner, R. L., & McKay, R. D. 2007. New cell lines from mouse epiblast share defining features with human embryonic stem cells. *Nature*, **448**(7150), 196–9.

Thompson, J. G., Simpson, A. C., Pugh, P. A., Donnelly, P. E., & Tervit, H. R. 1990. Effect of oxygen concentration on in-vitro development of preimplantation sheep and cattle embryos. *J Reprod Fertil*, **89**(2), 573–8.

Thompson, J. G., Gardner, D. K., Pugh, P. A., McMillan, W. H., & Tervit, H. R. 1995. Lamb birth weight is affected by culture system utilized during in vitro pre-elongation development of ovine embryos. *Biol Reprod*, **53**(6), 1385–91.

Thompson, J. G., Kind, K. L., Roberts, C. T., Robertson, S. A., & Robinson, J. S. 2002. Epigenetic risks related to assisted reproductive technologies: short- and long-term consequences for the health of children conceived through assisted reproduction technology: more reason for caution? *Hum Reprod*, **17**(11), 2783–6.

Thomson, J. A., Kalishman, J., Golos, T. G., Durning, M., Harris, C. P., Becker, R. A., & Hearn, J. P. 1995. Isolation of a primate embryonic stem cell line. *Proc Natl Acad Sci U S A*, **92**(17), 7844–8.

Thomson, J. A., Itskovitz-Eldor, J., Shapiro, S. S., Waknitz, M. A., Swiergiel, J. J., Marshall, V. S., & Jones, J. M. 1998. Embryonic stem cell lines derived from human blastocysts. *Science*, **282**(5391), 1145–7.

THsDCR. 1993. A novel gene containing a trinucleotide repeat that is expanded and unstable on Huntington's disease chromosomes. The Huntington's Disease Collaborative Research Group. *Cell*, **72**(6), 971–83.

THsDCR. 2001. A randomized, placebo-controlled trial of coenzyme Q10 and remacemide in Huntington's disease. *Neurology*, **57**(3), 397–404.

Tole, S., & Patterson, P. H. 1993. Distribution of CD9 in the developing and mature rat nervous system. *Dev Dyn*, **197**(2), 94–106.

Torres-Padilla, M. E., Parfitt, D. E., Kouzarides, T., & Zernicka-Goetz, M. 2007. Histone arginine methylation regulates pluripotency in the early mouse embryo. *Nature*, **445**(7124), 214–8.

Trottier, Y., Devys, D., Imbert, G., Saudou, F., An, I., Lutz, Y., Weber, C., Agid, Y., Hirsch, E. C., & Mandel, J. L. 1995. Cellular localization of the Huntington's disease protein and discrimination of the normal and mutated form. *Nat Genet*, **10**(1), 104–10.

Trounson, A., & Mohr, L. 1983. Human pregnancy following cryopreservation, thawing and transfer of an eight-cell embryo. *Nature*, **305**(5936), 707–9.

Turetsky, T., Aizenman, E., Gil, Y., Weinberg, N., Shufaro, Y., Revel, A., Laufer, N., Simon, A., Abeliovich, D., & Reubinoff, B. E. 2008. Laser-assisted derivation of human embryonic stem cell lines from IVF embryos after preimplantation genetic diagnosis. *Hum Reprod*, **23**(1), 46–53.

Ueno, M., Matsumura, M., Watanabe, K., Nakamura, T., Osakada, F., Takahashi, M., Kawasaki, H., Kinoshita, S., & Sasai, Y. 2006. Neural conversion of ES cells by an inductive activity on human amniotic membrane matrix. *Proc Natl Acad Sci U S A*, **103**(25), 9554–9.

Unger, C., Skottman, H., Blomberg, P., Dilber, M. S., & Hovatta, O. 2008. Good manufacturing practice and clinical-grade human embryonic stem cell lines. *Hum Mol Genet*, **17**(R1), R48–53.

Unger, C., Gao, S., Cohen, M., Jaconi, M., Bergstrom, R., Holm, F., Galan, A., Sanchez, E., Irion, O., Dubuisson, J. B., Giry-Laterriere, M., Salmon, P., Simon, C., Hovatta, O., & Feki, A. 2009. Immortalized human skin fibroblast feeder cells support growth and maintenance of both human embryonic and induced pluripotent stem cells. *Hum Reprod*, **dep232v2-dep232**.

Urner, F., & Sakkas, D. 2003. Protein phosphorylation in mammalian spermatozoa. *Reproduction*, **125**(1), 17–26.

Vamos, M., Hambridge, J., Edwards, M., & Conaghan, J. 2007. The impact of Huntington's disease on family life. *Psychosomatics*, **48**(5), 400–4.

Van Blerkom, J. 1993. Development of human embryos to the hatched blastocyst stage in the presence or absence of a monolayer of Vero cells. *Hum Reprod*, **8**(9), 1525–39.

Van de Velde, H., Cauffman, G., Tournaye, H., Devroey, P., & Liebaers, I. 2008. The four blastomeres of a 4-cell stage human embryo are able to develop individually into blastocysts with inner cell mass and trophectoderm. *Hum Reprod*, **23**(8), 1742–7.

Van Laake, L. W., Van Hoof, D., & Mummery, C. L. 2005. Cardiomyocytes derived from stem cells. *Ann Med*, **37**(7), 499–512.

Van Landuyt, L., De Vos, A., Joris, H., Verheyen, G., Devroey, P., & Van Steirteghem, A. 2005. Blastocyst formation in in vitro fertilization versus intracytoplasmic sperm injection cycles: influence of the fertilization procedure. *Fertil Steril*, **83**(5), 1397–403.

Van Winkle, L. J., & Dickinson, H. R. 1995. Differences in amino acid content of preimplantation mouse embryos that develop in vitro versus in vivo: in vitro effects of five amino acids that are abundant in oviductal secretions. *Biol Reprod*, **52**(1), 96–104.

Vansteenbrugge, A., Van Langendonckt, A., Scutenaire, C., Massip, A., & Dessy, F. 1994. In vitro development of bovine embryos in Buffalo rat liver- or bovine oviduct-conditioned medium. *Theriogenology*, **42**(6), 931–40.

Veiga, A., Calderon, G., Barri, P. N., & Coroleu, B. 1987. Pregnancy after the replacement of a frozen-thawed embryo with less than 50% intact blastomeres. *Hum Reprod*, **2**(4), 321–3.

Verlinsky, Y., Strelchenko, N., Kukharenko, V., Rechitsky, S., Verlinsky, O., Galat, V., & Kuliev, A. 2005. Human embryonic stem cell lines with genetic disorders. *Reprod Biomed Online*, **10**(1), 105–10.

Villa-Diaz, L. G., Pacut, C., Slawny, N. A., Ding, J., O'Shea, K. S., & Smith, G. D. 2008. Analysis of the Factors That Limit the Ability of Feeder-Cells to Maintain the Undifferentiated State of Human Embryonic Stem Cells. *Stem Cells Dev.*

Voss, A. K., Thomas, T., Petrou, P., Anastassiadis, K., Scholer, H., & Gruss, P. 2000. Taube nuss is a novel gene essential for the survival of pluripotent cells of early mouse embryos. *Development*, **127**(24), 5449–61.

Wakayama, S., Hikichi, T., Suetsugu, R., Sakaide, Y., Bui, H. T., Mizutani, E., & Wakayama, T. 2007. Efficient establishment of mouse embryonic stem cell lines from single blastomeres and polar bodies. *Stem Cells*, **25**(4), 986–93.

Waldenstrom, U., Engstrom, A. B., Hellberg, D., & Nilsson, S. 2008. Low-oxygen compared with high-oxygen atmosphere in blastocyst culture, a prospective randomized study. *Fertil Steril*, **89**(6), 1677–1684.

Wang, D., Haviland, D. L., Burns, A. R., Zsigmond, E., & Wetsel, R. A. 2007. A pure population of lung alveolar epithelial type II cells derived from human embryonic stem cells. *Proc Natl Acad Sci U S A*, **104**(11), 4449–54.

Wang, Q., Fang, Z. F., Jin, F., Lu, Y., Gai, H., & Sheng, H. Z. 2005. Derivation and growing human embryonic stem cells on feeders derived from themselves. *Stem Cells*, **23**(9), 1221–7.

Wang, Y., Wang, F., Sun, T., Trostinskaia, A., Wygle, D., Puscheck, E., & Rappolee, D. A. 2004. Entire mitogen activated protein kinase (MAPK) pathway is present in preimplantation mouse embryos. *Dev Dyn*, **231**(1), 72–87.

Warnock, M. 1984. *Committee of Inquiry into Human Fertilisation and Embryology.*

Warnock, M. 2007. The ethical regulation of science. *Nature*, **450**(7170), 615.

Watase, K., & Zoghbi, H. Y. 2003. Modelling brain diseases in mice: the challenges of design and analysis. *Nat Rev Genet*, **4**(4), 296–307.

Watson, A. J. 1992. The cell biology of blastocyst development. *Mol Reprod Dev*, **33**(4), 492–504.

Watson, A. J., Watson, P. H., Warnes, D., Walker, S. K., Armstrong, D. T., & Seamark, R. F. 1994. Preimplantation development of in vitro-matured and in vitro-fertilized ovine zygotes: comparison between coculture on oviduct epithelial cell monolayers and culture under low oxygen atmosphere. *Biol Reprod*, **50**(4), 715–24.

Watson, A. J., Westhusin, M. E., De Sousa, P. A., Betts, D. H., & Barcroft, L. C. 1999. Gene expression regulating blastocyst formation. *Theriogenology*, **51**(1), 117–33.

Weber, R. J., Pedersen, R. A., Wianny, F., Evans, M. J., & Zernicka-Goetz, M. 1999. Polarity of the mouse embryo is anticipated before implantation. *Development*, **126**(24), 5591–8.

Wenger, R. H. 2000. Mammalian oxygen sensing, signalling and gene regulation. *J Exp Biol*, **203**(Pt 8), 1253–63.

Wheeler, V. C., Auerbach, W., White, J. K., Srinidhi, J., Auerbach, A., Ryan, A., Duyao, M. P., Vrbanac, V., Weaver, M., Gusella, J. F., Joyner, A. L., & MacDonald, M. E. 1999. Length-dependent gametic CAG repeat instability in the Huntington's disease knock-in mouse. *Hum Mol Genet*, **8**(1), 115–22.

Whitten, W.K. 1956. Culture of tubal ova. *Nature*, **177**, 96.

Whittingham, D. G. 1968. Fertilization of mouse eggs in vitro. *Nature*, **220**(5167), 592–3.

Wiemer, K. E., Dale, B., Hu, Y., Steuerwald, N., Maxson, W. S., & Hoffman, D. I. 1995. Blastocyst development in co-culture: development and morphological aspects. *Hum Reprod*, **10**(12), 3226–32.

Wiley, L. M., Spindle, A. I., & Pedersen, R. A. 1978. Morphology of isolated mouse inner cell masses developing in vitro. *Dev Biol*, **63**(1), 1–10.

Willadsen, S. M. 1979. A method for culture of micromanipulated sheep embryos and its use to produce monozygotic twins. *Nature*, **277**(5694), 298–300.

Willadsen, S. M., Lehn-Jensen, H., Fehilly, C. B., & Newcomb, R. 1981. The production of monozygotic twins of preselected parentage by micromanipulation of non-surgically collected cow embryos. *Theriogenology*, **15**(1), 23–9.

Wilson, P. G., Cherry, J. J., Schwamberger, S., Adams, A. M., Zhou, J., Shin, S., & Stice, S. L. 2007. An SMA project report: neural cell-based assays derived from human embryonic stem cells. *Stem Cells Dev*, **16**(6), 1027–41.

Wolff, P., Tanaka, A. M., Chenker, E., Cabrera-Crespo, J., Raw, I., & Ho, P. L. 1996. Purification of fibroblast growth factor-2 from human placenta using tri(n-butyl)phosphate and sodium cholate. *Biochimie*, **78**(3), 190–4.

Wood, H. B., & Episkopou, V. 1999. Comparative expression of the mouse Sox1, Sox2 and Sox3 genes from pre-gastrulation to early somite stages. *Mech Dev*, **86**(1-2), 197–201.

Xiao, L., Yuan, X., & Sharkis, S. J. 2006. Activin A maintains self-renewal and regulates fibroblast growth factor, Wnt, and bone morphogenic protein pathways in human embryonic stem cells. *Stem Cells*, **24**(6), 1476–86.

Xu, C., Inokuma, M. S., Denham, J., Golds, K., Kundu, P., Gold, J. D., & Carpenter, M. K. 2001. Feeder-free growth of undifferentiated human embryonic stem cells. *Nat Biotechnol*, **19**(10), 971–4.

Xu, C., Jiang, J., Sottile, V., McWhir, J., Lebkowski, J., & Carpenter, M. K. 2004. Immortalized fibroblast-like cells derived from human embryonic stem cells support undifferentiated cell growth. *Stem Cells*, **22**(6), 972–80.

Xu, C., Rosler, E., Jiang, J., Lebkowski, J. S., Gold, J. D., O'Sullivan, C., Delavan-Boorsma, K., Mok, M., Bronstein, A., & Carpenter, M. K. 2005. Basic fibroblast growth factor supports undifferentiated human embryonic stem cell growth without conditioned medium. *Stem Cells*, **23**(3), 315–23.

Xu, R. H., Chen, X., Li, D. S., Li, R., Addicks, G. C., Glennon, C., Zwaka, T. P., & Thomson, J. A. 2002. BMP4 initiates human embryonic stem cell differentiation to trophoblast. *Nat Biotechnol*, **20**(12), 1261–4.

Yanagimachi, R., & Chang, M. C. 1963. Fertilization of Hamster Eggs in Vitro. *Nature*, **200**, 281–2.

Yang, H. W., Hwang, K. J., Kwon, H. C., Kim, H. S., Choi, K. W., & Oh, K. S. 1998. Detection of reactive oxygen species (ROS) and apoptosis in human fragmented embryos. *Hum Reprod*, **13**(4), 998–1002.

Yang, J., Yamato, M., Nishida, K., Ohki, T., Kanzaki, M., Sekine, H., Shimizu, T., & Okano, T. 2006. Cell delivery in regenerative medicine: the cell sheet engineering approach. *J Control Release*, **116**(2), 193–203.

Yeom, Y. I., Fuhrmann, G., Ovitt, C. E., Brehm, A., Ohbo, K., Gross, M., Hubner, K., & Scholer, H. R. 1996. Germline regulatory element of Oct-4 specific for the totipotent cycle of embryonal cells. *Development*, **122**(3), 881–94.

Ying, Q. L., & Smith, A. G. 2003. Defined conditions for neural commitment and differentiation. *Methods Enzymol*, **365**, 327–41.

Ying, Q. L., Stavridis, M., Griffiths, D., Li, M., & Smith, A. 2003. Conversion of embryonic stem cells into neuroectodermal precursors in adherent monoculture. *Nat Biotechnol*, **21**(2), 183–6.

Yu, J., Vodyanik, M. A., Smuga-Otto, K., Antosiewicz-Bourget, J., Frane, J. L., Tian, S., Nie, J., Jonsdottir, G. A., Ruotti, V., Stewart, R., Slukvin, II, & Thomson, J. A. 2007. Induced pluripotent stem cell lines derived from human somatic cells. *Science*, **318**(5858), 1917–20.

Zaragoza, M. V., Surti, U., Redline, R. W., Millie, E., Chakravarti, A., & Hassold, T. J. 2000. Parental origin and phenotype of triploidy in spontaneous abortions: predominance of diandry and association with the partial hydatidiform mole. *Am J Hum Genet*, **66**(6), 1807–20.

Zernicka-Goetz, M. 2005. Developmental cell biology: cleavage pattern and emerging asymmetry of the mouse embryo. *Nat Rev Mol Cell Biol*, **6**(12), 919–28.

ZernickaGoetz, M. 1998. Fertile offspring derived from mammalian eggs lacking either animal or vegetal poles. *Development*, **125**(23), 4803–8.

Zhang, J., Tam, W. L., Tong, G. Q., Wu, Q., Chan, H. Y., Soh, B. S., Lou, Y., Yang, J., Ma, Y., Chai, L., Ng, H. H., Lufkin, T., Robson, P., & Lim, B. 2006. Sall4 modulates embryonic stem cell pluripotency and early embryonic development by the transcriptional regulation of Pou5f1. *Nat Cell Biol*, **8**(10), 1114–23.

Zhang, Y., Yang, Z., & Wu, J. 2007. Signaling pathways and preimplantation development of mammalian embryos. *Febs J*, **274**(17), 4349–59.

Ziomek, C. A., & Johnson, M. H. 1980. Cell surface interaction induces polarization of mouse 8-cell blastomeres at compaction. *Cell*, **21**(3), 935–42.

Zoghbi, H. Y., & Orr, H. T. 2000. Glutamine repeats and neurodegeneration. *Annu Rev Neurosci*, **23**, 217–47.

Zuhlke, C., Riess, O., Schroder, K., Siedlaczck, I., Epplen, J. T., Engel, W., & Thies, U. 1993. Expansion of the (CAG)n repeat causing Huntington's disease in 352 patients of German origin. *Hum Mol Genet*, **2**(9), 1467–9.